Title

Site Characterization Plan Vol. II, part A, Chapter 3,4 & 5 (entire document) (DOE/RW-0199)

Author

DOE

101402

Document Date

12/30/88

ERC Index number

05.09.446

Document Type

Other Tech. Resource

Box Number

1720-1

Recipients

DOE & Participants

DOE/RW-0199 Vol II

DUPLICATE

DOE/RW-0199 Vol I

Nuclear Waste Policy Act
(Section 113)

Site Characterization Plan

Yucca Mountain Site, Nevada Research and Development Area, Nevada

Volume II, Part A

Chapters 3, 4, and 5

December 1988

U. S. Department of Energy
Office of Civilian Radioactive Waste Management

DISCLAIMER

Printed in the United States of America

Available from:

U.S. Department of Energy
Office of Scientific and Technical Information
Post Office Box 62
Oak Ridge, TN 37831

DOCUMENT ORGANIZATION

DOCUMENT ORGANIZATION (continued)

DOE/RW-0199

DOE/RW-0199

Nuclear Waste Policy Act
(Section 113)

Site Characterization Plan

Yucca Mountain Site, Nevada Research and Development Area, Nevada

Volume II, Part A

Chapters 3, 4, and 5

December 1988

U. S. Department of Energy
Office of Civilian Radioactive Waste Management

DOCUMENT ORGANIZATION (continued)

VOLUME IX

TABLE OF CONTENTS

VOLUME II

TABLE OF CONTENTS (continued)

TABLE OF CONTENTS (continued)

TABLE OF CONTENTS (continued)

TABLE OF CONTENTS (continued)

TABLE OF CONTENTS (continued)

LIST OF FIGURES

VOLUME II

LIST OF FIGURES (continued)

LIST OF FIGURES (continued)

LIST OF FIGURES (continued)

LIST OF FIGURES (continued)

LIST OF FIGURES (continued)

LIST OF FIGURES (continued)

LIST OF TABLES

VOLUME II

LIST OF TABLES (continued)

LIST OF TABLES (continued)

LIST OF TABLES (continued)

LIST OF TABLES (continued)

DOE/RW-0199

Nuclear Waste Policy Act
(Section 113)

Site Characterization Plan

Yucca Mountain Site, Nevada Research and Development Area, Nevada

Volume II, Part A

Chapter 3, Hydrology

December 1988

U. S. Department of Energy
Office of Civilian Radioactive Waste Management

Chapter 3

HYDROLOGY

This chapter summarizes present knowledge of the regional and site hydrologic systems. The purpose of the information presented is to (1) describe the hydrology based on available literature and preliminary site-exploration activities that have been or are being performed and (2) provide information to be used to develop the hydrologic aspects of the planned site characterization program.

INTRODUCTION

An understanding of the hydrologic regime is required for many of the issues in the Yucca Mountain Project Issues Hierarchy (Section 8.2). In particular, the nine Performance Issues (1.1 through 1.9) of Key Issue 1 (related to the postclosure environment); the Characterization Programs 8.3.1.2 (geohydrology), 8.3.1.3 (geochemistry), and 8.3.1.9 (water resources); the Performance Issue (4.1) of Key Issue 4 (preclosure); and the Characterization Program 8.3.1.16 (hydrology) all pertain directly to hydrology. In addition, other programs are indirectly related to hydrology (e.g., Programs 8.3.1.5, 8.3.1.6, and 8.3.1.8 question the effects that climatic change, erosional processes, and tectonic processes exert on the hydrologic characteristics at the site). Furthermore, issues related to design (both in the preclosure and postclosure time frames) require a knowledge of the emplacement environment, a major component of which is moisture. Therefore, an understanding of the hydrologic system in and around Yucca Mountain is paramount to satisfying many of the issues in the issues hierarchy.

One of the primary advantages of the proposed Yucca Mountain repository site is that it is intended to be located in the unsaturated zone, approximately 300 m above the saturated zone. This chapter discusses in detail the present understanding of hydrologic conditions within the unsaturated zone, as well as conditions in the saturated zone and in the surface hydrologic systems; the last two act as boundaries to the unsaturated zone.

For convenience in describing the hydrologic regime, two types of study areas are defined in this chapter: (1) a hydrographic study area (Figure 3-1) that delineates the regional surface water system that encompasses

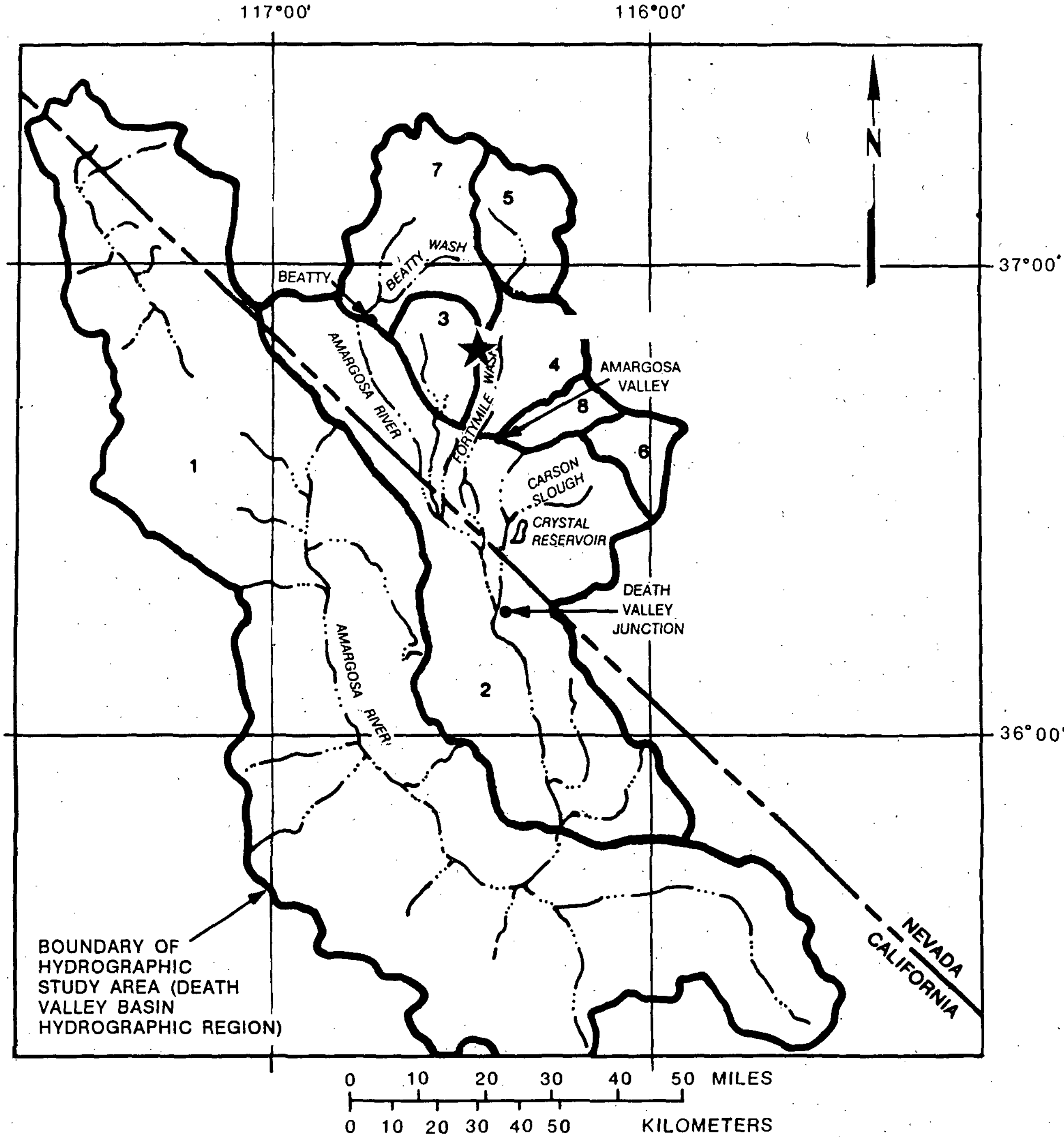

HYDROGRAPHIC AREAS

1 DEATH VALLEY AND LOWER AMARGOSA AREA
2 AMARGOSA DESERT AND UPPER AMARGOSA AREA
3 CRATER FLAT
4 FORTYMILE CANYON, JACKASS FLATS
5 FORTYMILE CANYON, BUCKBOARD MESA
6 MERCURY VALLEY
7 OASIS VALLEY
8 ROCK VALLEY

BOUNDARY OF HYDROGRAPHIC STUDY AREA

MAJOR STREAM CHANNELS

YUCCA MOUNTAIN SITE

Figure 3-1. Hydrographic study area, showing the eight hydrographic areas and major stream channels. Modi

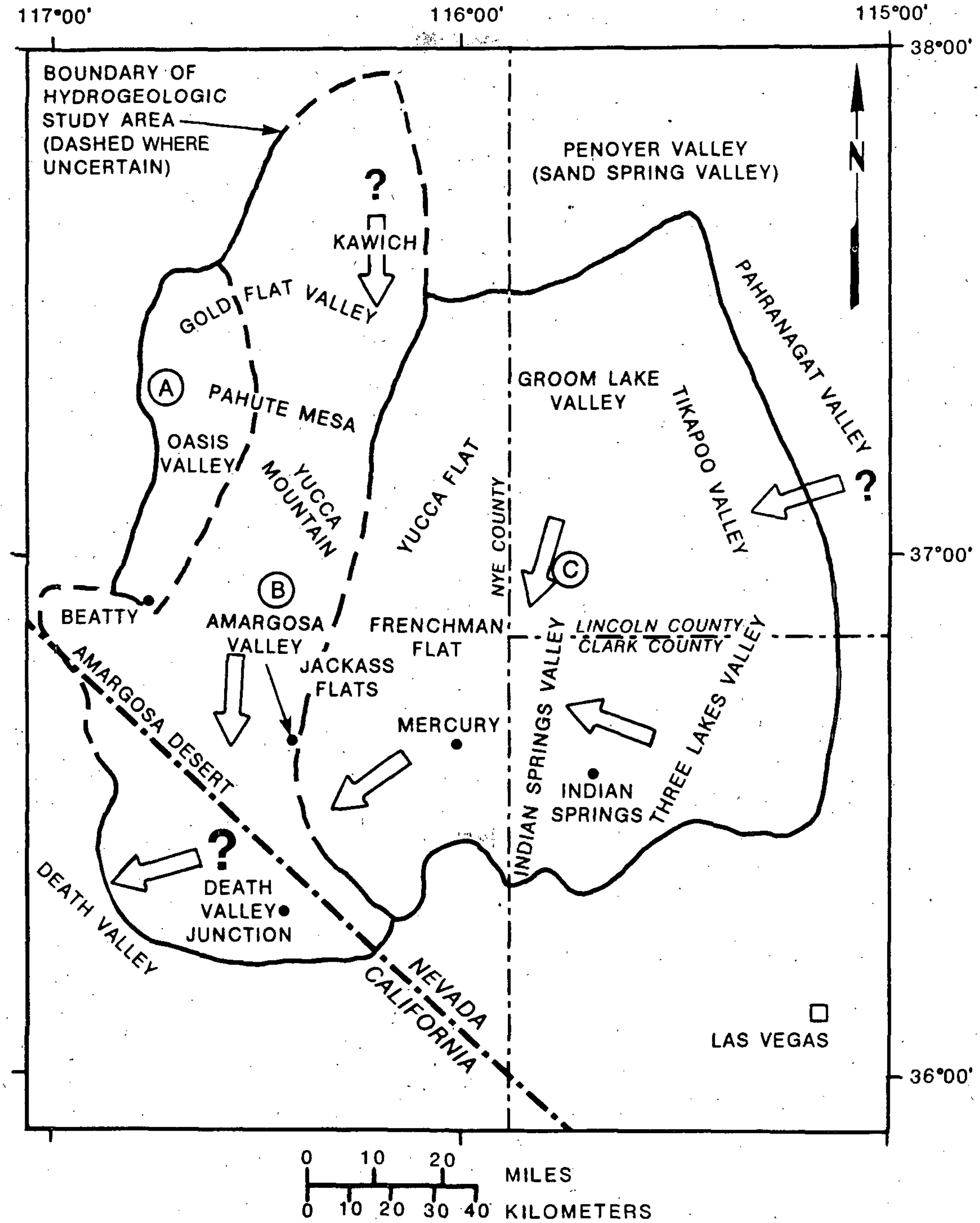

GENERAL DIRECTION OF REGIONAL GROUND WATER FLOW surface hydrology), 3.2 (floods), 3.3 (locations and distances to points of surface-water use), and 3.4 (chemical composition of adjacent watercourses). As these sections discuss, the occurrence of surface-water bodies is extremely limited in the vicinity of Yucca Mountain; their primary importance is in their relationship to the ground-water system, as discussed in Section 3.5 (points of ground-water discharge).

The hydrogeologic study area (Figure 3-2) consists of three ground-water subbasins that together form a part of the Death Valley ground-water basin (Waddell et al., 1984). These subbasins are the Oasis Valley subbasin, Alkali Flat-Furnace Creek Ranch subbasin, and the Ash Meadows subbasin. The division into and the approximate boundaries of these ground-water subbasins have been estimated from potentiometric levels, geologic controls of subsurface flow, discharge areas, and inferred flow paths (Rush, 1970; Blankennagel and Weir, 1973; Winograd and Thordarson, 1975; Dudley and Larson, 1976; Waddell, 1982; Waddell et al., 1984). In some areas, the boundaries are uncertain due to the lack of potentiometric data, the complexity of geologic structures, or the occurrence of interbasin flow of ground water through the lower carbonate aquifer (Winograd and Thordarson, 1975). Regional flow paths in the hydrogeologic study area vary in direction from southerly to southwesterly (Winograd and Thordarson, 1975; Waddell, 1982). Detailed discussions of the regional hydrogeology and regional flow systems are included in Sections 3.6 and 3.7. Detailed discussions of the site (Yucca Mountain) hydrogeology are included in Section 3.9. The discussions include aquifer-hydraulics information, water-balance calculations, and water-chemistry data for both the saturated and the unsaturated zones.

Most of the information on the regional hydrology is available in published reports from general ground-water studies made during the 1960s and 1970s by the Nevada Department of Conservation and Natural Resources or by the Department in cooperation with the U.S. Geological Survey (USGS). The studies were used principally for general water-resource appraisals of parts of Nevada. A few studies of surface hydrology were also made, but because [illegible]

very few data have been collected.

In 1957 the U.S. Atomic Energy Commission (later the Energy Research and Development Administration and presently the U.S. Department of Energy) began hydrology. Such possible future effects may be important to isolation of waste at Yucca Mountain.

In general, hydrogeologic data for the region are believed to be adequate for regional quantitative ground-water flow modeling, although there remain some hydrologic features that are not completely understood for the purposes of site characterization. Where it is important to resolve such questions (such as the potential for recharge near Fortymile Wash), plans have been developed for additional field studies as described in Section 8.3.1.2.1. Various hypotheses about the ground-water flow systems and probable present and future fluxes are continuing to be evaluated to improve general understanding and to determine probable error bounds for calculated quantities such as ground-water velocities and future water levels. These hypotheses are discussed in Sections 3.6, 3.7, and 3.9.

Most of the hydrologic information about the Yucca Mountain site has been obtained from studies conducted since 1978. During the first few years commonly taken: (1) the continuum approach in which the aquifer is modeled, both with respect to transport of water and solutes, as an equivalent porous medium; (2) the dual porosity approach in which the rock matrix and fractures are treated as coupled flow systems of highly differing properties; and (3) the discrete fracture approach in which flow through a regular geometric network of parallel-plate fractures is simulated using fluid-dynamics equations. Newer approaches involve the application of near-field stochastic analyses to predict far-field hydraulic and transport properties. Alternative approaches will be examined as the project develops and as the state of the modeling art is refined (Section 3.9).

In addition, multiple-well tests, some of which involve tagging ground water with tracers to evaluate the tests, will be conducted within the saturated zone. The purpose of these tests is to determine the nature and extent of the permeability contributed by fractures and to determine effective porosity.

Beginning in 1983, test holes were drilled to depths greater than 300 m within the unsaturated zone. The purposes of these boreholes were to obtain rock samples for the determination of hydrologic properties and to monitor ambient water saturation, potential, and flux in rocks above, below, and within the horizon proposed for the repository. Rock samples have been tested to determine effective porosities, ambient saturations and matric potentials, saturated matrix hydraulic conductivities, and water retention characteristics. Ambient water potentials have been monitored in one test well since 1983. The data from the rock samples show a wide variation in hydrologic property values between the various hydrogeologic units within the unsaturated zone. The in situ water potential data show considerable variability; however, the data are consistent with the supposition that the hydrogeologic units are vertically homogeneous and that steady-state vertical moisture flow occurs under unit vertical hydraulic gradients. The mechanisms of moisture flow and storage (as liquid water, water vapor, or both) at any location within the system depend largely upon the amount of water entering the system as net infiltration. The actual rate and distribution of net are independently or jointly characterized. These programs for site characterization are described in Section 8.3.1.2. Specific levels and types of existing uncertainties or data needs are discussed throughout Chapter 3.

In very general terms, the regional hydrology and hydrogeology are fairly well understood and their levels of uncertainty are relatively low. However, the unsaturated zone at the site has only recently come under data collected to this point and the limited amount of relevant information available in the open literature.

9. The conceptual model of ground-water flow through the unsaturated zone at the site has not been developed to a high confidence level as yet because of the limitations of the supporting data.

These and other areas of uncertainty will be significantly reduced through further data collection and through the application of multiple approaches that may produce corroborative results. These programs will be carried out during site characterization and are described in Section 8.3.1.2.

3.1 DESCRIPTION OF SURFACE HYDROLOGY

Characterization of surface hydrology is required to provide baseline data necessary to resolve several issues. Knowledge gained through the surface hydrology studies will be used to (1) evaluate the potential for erosion in the site area and any hazards that this may cause, (2) evaluate the potential for floods and the potential hazards to the surface facilities due to floods (Section 3.2), and (3) help evaluate the amount of infiltration and establish the relationship between surface runoff and ground-water recharge that occurs in the study area.

The hydrographic study area (Figure 3-1) is the same as the Death Valley Basin Hydrographic Region of California and Nevada, as defined by Rush (1968) and the USGS (1978). This study area consists of eight hydrographic areas. The boundary lines of the eight hydrographic areas within the hydrographic study area are drawn principally along topographic divides. These hydrographic areas serve as the basic morphologic unit of the surface-water hydrologic system. A listing of these areas is shown in Table 3-1.

The general configuration of surface drainage of the hydrographic areas is shown in Figure 3-1. The Yucca Mountain site proposed for waste disposal lies on the boundary between the Crater Flat and Fortymile Canyon-Jackass Flats hydrographic areas (Figure 3-1).

The eastern slopes of Yucca Mountain drain to Fortymile Wash and the northern slopes drain to Beatty Wash; these washes are major tributaries to the Amargosa River. The southern and western slopes of Yucca Mountain drain to the Amargosa River through a smaller unnamed drainage system.

There are no perennial streams in or near the Yucca Mountain area. However, the many ephemeral stream channels, including the large drainage systems of Fortymile Wash and the Amargosa River, flow following significant regional or local storms. Although the region that includes Yucca Mountain has a generally arid to semiarid climate that includes high annual average potential evaporation (about 1,500 to 1,700 mm/yr; Kohler et al., 1959), low average annual precipitation (about 150 mm; Quiring, 1983), and infrequent storms (Section 5.1.1.6), surface runoff does occur. Runoff results from regional storms that occur most commonly in winter and, occasionally in autumn and spring and from localized thunderstorms that occur mostly during

Table 3-1. Hydrographic areas in the hydrographic study area

Area number on Figure 3-1	Hydrographic area	State[a,b]	Approximate area (mi²)	Approximate area (km²)
1	Death Valley and Lower Amargosa area	Nevada	344	891
		California	5,019	13,000
2	Amargosa Desert and Upper Amargosa area	Nevada	896	2,321
		California	1,122	2,906
3	Crater Flat	Nevada	182	471
4	Fortymile Canyon, Jackass Flat	Nevada	279	723
5	Fortymile Canyon, Buckboard Mesa	Nevada	240	622
6	Mercury Valley	Nevada	110	285
7	Oasis Valley	Nevada	460	1,191
8	Rock Valley	Nevada	82	212

[a]Data for Nevada modified from Rush (1968).
[b]Data for California from U.S. Geological Survey (1978).

the summer. Rugged relief, abundant bedrock exposed at the land surface, and sparse vegetal cover promote runoff, particularly during intense rainstorms. The annual precipitation pattern usually follows a bimodal distribution, with greatest average amounts occurring during the winter storms and less during the summer (Quiring, 1983). Although runoff can result from severe winter storms, the scanty data available for the region suggests that peak discharges commonly result from summer storms (Table 3-2). These few streamflow data available for the general study area were collected to document flooding. Locations of the gaging sites are shown in Figure 3-3, and data collected at these sites summarized in Table 3-2. (These sites and data are also discussed later in Section 3.2.) No data are presently available that relate runoff to recharge (see studies planned for Fortymile Wash area, Section 8.3.1.2.1.3), and the data are insufficient to develop meaningful flood recurrence intervals.

Quantitative data on rainfall, runoff, and evaporation for the area are not yet adequate to determine rainfall-runoff-recharge relations for individual storms, seasons, or years. Therefore, only general knowledge of runoff parameters is available. Numerical simulations of rainfall-runoff relations

Table 3-2. Summary of peak streamflow data for selected crest-stage sites in hydrographic study area and adjacent areas[a] (page 1 of 2)

Site number[b]	Station number	Station name	Drainage area (mi^2)	Drainage area (km^2)	Period of record	Peak discharge (m^3/s)	Date of peak discharge	Discharge per unit area ($(m^3/s)/km^2$)
1	10247860	Penoyer Valley tributary near Tempiute, Nevada	1.48	3.83	1964-80	3.68	8/06/68	0.96
2	10248490	Indian Springs Valley tributary near Indian Springs, Nevada	29.0	75.1	1964-80	14.1	8/14/72	0.19
3	10251270	Amargosa River tributary near Mercury, Nevada	110.0	284.9	1963-80	97.1	8/04/68	0.34
4	10251271	Amargosa River tributary No. 1 near Johnnie, Nevada	2.21	5.72	1967-80	9.9	8/04/70	1.73
5	10251272	Amargosa River tributary No. 2 near Johnnie, Nevada	2.49	6.45	1968-80	3.54	8/01/68	0.55
6	10251220	Amargosa River near Beatty, Nevada	470.0	1,217.0	1964-79	453.0	2/24/69	0.37

Table 3-2. Summary of peak streamflow data for selected crest-stage sites in hydrographic study area and adjacent areas[a] (page 2 of 2)

Site number[b]	Station number	Station name	Drainage area (mi^2)	Drainage area (km^2)	Period of record	Peak discharge (m^3/s)	Date of peak discharge	Discharge per unit area $((m^3/s)/km^2)$
7	10249050	Sarcobatus Flat tributary near Springdale, Nevada	37.1	96.1	1961-80	1.78	9/09/80	0.02
8	10249850	Palmetto Wash tributary near Lida, Nevada	4.73	12.25	1967-80	5.46	7/07/69	0.45
9	10248970	Stonewall Flat tributary near Goldfield, Nevada	0.53	1.37	1964-79	4.25	6/16/69	3.10
10	10249680	Big Smoky Valley tributary near Blair Junction, Nevada	11.4	29.5	1961-79	4.81	10/02/76	0.16
11	10249135	San Antonio Wash tributary near Tonopah, Nevada	3.42	8.86	1965-80	18.7	8/13/72	2.10
12	10249180	Salsbury Wash Tonopah, Nevada	56.0	145.0	1962-80	9.62	3/27/69	0.07

[a]Source: Squires and Young (1984), and Waddell et al. (1984).
[b]Location of sites is shown in Figure 3-3.

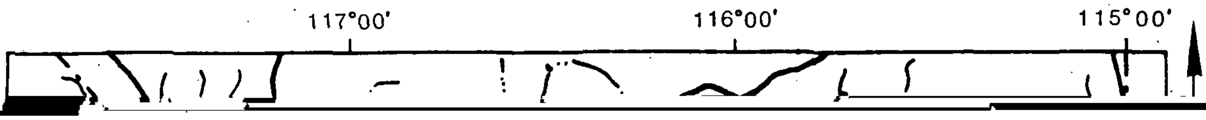
117°00'
116°00'
115°00'

are possible, but these models cannot be calibrated until more field data become available. See Section 3.2.1.1 for a discussion of investigations currently underway to improve the surface-water hydrologic data base at Yucca Mountain and surrounding areas. Plans for future investigations and analysis of surface-water flow in terms of precipitation, runoff, infiltration, evaporation and transpiration, and floods are given in Section 8.3.1.2.1.

Throughout the hydrographic study area, perennial surface water comes only from springs, and it is restricted to some short reaches of the Amargosa River, to source pools at some large springs, and to some marshes around the edge of the salt pan in Death Valley (Hunt et al., 1966). One small lake, locally known as Crystal Reservoir, with a storage capacity of 2.27 x 10^6 m^3 (Giampaoli, 1986), occurs in the Ash Meadows part of the Upper Amargosa hydrographic area (Figure 3-1). The water for the reservoir is supplied via a concrete flume from Crystal Pool (Giampaoli, 1986).

The Amargosa River originates in Oasis Valley and continues southeastward through the Amargosa Desert past Death Valley Junction then southward another 75 km, where it turns northwestward and terminates in Death Valley (Figure 3-1). The river carries floodwaters following cloudbursts or intense storms but is normally dry, except for a few short reaches that contain water from springs (Walker and Eakin, 1963), in Oasis Valley between Springdale and Beatty (Malmberg and Eakin, 1962), in Ash Meadows northeast of Death Valley Junction, and near Shoshone, about 40 km south of Death Valley Junction. Springs are discussed in greater detail in Sections 3.3 and 3.5. Base flow to these segments of the river is maintained by ground-water discharge during the winter, when evapotranspiration is at a minimum. During the summer, discharge from the springs is almost entirely lost by evapotranspiration. During winter, ground water discharges into the river south of Alkali Flat near Eagle Mountain about 10 km south of Death Valley Junction (Walker and Eakin, 1963).

Because of the ephemeral character of streamflow, specifically in the [illegible]

3.2 FLOODS

Because of limited streamflow data in the hydrographic study area, the flood history of individual drainages tributary to Death Valley is not well known. Analysis of the general character of flooding is based on scattered data from peak-flow stations located around the Yucca Mountain area and from quantitative measurements of flood-flow peaks in a five-state region that comprises Arizona, California, Nevada, New Mexico, and Utah.

Flood analyses at Yucca Mountain are needed to provide flood data for design and performance considerations. Flood data will also be used to help evaluate infiltration rates and long term erosion rates. Two hydraulic engineering studies of flood-prone areas at and near Yucca Mountain (Christensen and Spahr, 1980; Squires and Young, 1984) provided a basis for estimating the magnitudes of future floods with various recurrence intervals. The results of these investigations are presented in Section 3.2.1. Analytical methods other than those presented in ANSI/ANS 2.8-1981 (American Nuclear Standards Institute/American Nuclear Society) for estimating the potential for flooding of the site were used in these introductory studies; the reasons for applying alternate methods and a description of the procedures used are given in Section 3.2.1.

The measures that will be used to protect the site from floods are described in Section 3.2.2.

3.2.1 FLOOD HISTORY AND POTENTIAL FOR FUTURE FLOODING

Moderate to large floods in low-lying areas along the major drainages (drainage areas of several hundred square kilometers), such as the Amargosa River and Fortymile Wash, usually are the result of regional storm systems that most commonly occur during the winter and occasionally occur during autumn and spring. These extensive storm systems sometimes include areally restricted cells that discharge intense precipitation.

Flash floods of similar intensity and areal extent commonly occur as the result of summer thunderstorms. These summer floods usually do not cumulate to cause regional floods, but their intensive character renders them potentially destructive over limited areas. The summer storms are commonly the products of monsoonal air masses that invade southern Nevada and California from the general vicinity of the Gulf of California. The areally restricted storm cells are triggered by local convective lifting of the moist air or by cooler frontal systems that move through the region and intersect with the warmer monsoonal air mass. A detailed discussion on climatic conditions including precipitation, temperature, wind, and severe weather phenomena is given in Section 5.1.

In summary, although flooding can occur over an extensive area, intense floods are generally restricted to relatively small areas and occur as flash floods of short duration.

Flash floods constitute a hazard throughout the Great Basin (Chapter 1) and specifically in southern Nevada. These floods and associated debris flows are among the most important geomorphic processes currently active in the region and local area. They play a major role in the development of alluvial fans, denudation of mountainous landscapes, and the evolution of drainage-channel morphology. Flash-flood discharges range in character from water-dominated mixtures of sediments and water to debris flows. The hazards posed by debris movement associated with flash floods may be of equal or greater importance with regard to destructive potential than that of the mobilizing water. The intensive rainfall and runoff of flash flooding commonly promotes debris avalanching on steep slopes. Erosion scars caused by these debris avalanches are not uncommon in the Yucca Mountain area.

Data have been collected since the early 1960s on flooding and stream-flow in ephemeral stream channels throughout Nevada. A network of crest-stage gages has been operated for almost two decades. Crest-stage gages are simple devices that record evidence of the peak-flow stage of a stream at the specific site where they are located. They do not record the duration of flow associated with the peak stage; also, they are poor indicators of multiple-peak stages that can occur between visits to the site. Also, because the network of gages was not dense, only a small percentage of ephemeral stream channels throughout Nevada has been monitored. Individual gages were visited monthly during this data collection program to ascertain recent occurrences of stream flow at the gage sites. If evidence of recent streamflow was noted during a visit, an indirect measurement of the peak-flow discharge was made and recorded along with the stage of the peak flow. Additional site visits were made when knowledge of recent flooding or major flooding was available. The resultant data base is a reasonably reliable record of the magnitude and frequencies of peak flows at the crest-stage gaging sites during the tenure of operation of the gages.

Twelve crest-stage gaging sites that were part of the monitoring network are located in the general area of Yucca Mountain. Locations of these sites are shown in Figure 3-3, and data collected at the sites are summarized in Table 3-2. Data collection at these sites was discontinued in 1980 when the statewide network was reduced. Stations 2 through 6 (Figure 3-3) have been reactivated as part of ongoing studies (Section 3.2.1.1).

Table 3-2 indicates that maximum unit peak-flood discharges (peak discharge divided by stream drainage areas) measured at the 12 gaging stations near Mercury. This drainage basin has an area of 284.9 km^2; the basin terrain is also similar to that of Fortymile Wash.

Long-range flood predictions are difficult to make, even for drainages that have stream-flow records as long as 100 yr. Predictions are especially difficult for drainages with minimal stream-flow records, such as those in the hydrographic study area. Current flood-prediction methods for this area generally involve some form of statistical evaluation of available regional stream flow, precipitation, modeling, and channel morphology data. These evaluations will be supplemented by studies of paleoflood sediments in order to provide a history of major paleofloods in the area (Section 8.3.1.5.2).

Analyses of the effects of probable maximum floods near the surface sites of proposed repository facilities have been initiated. An analysis was made of the flood plain of Fortymile Wash and its southwestern tributaries that include ephemeral stream channels from the east flank of Yucca Mountain (Figure 3-4) (Squires and Young, 1984). An analysis also was made of flood plains of Topopah Wash, a sizable drainage from the Shoshone Mountain area into Jackass Flats, about 10 to 15 km east of Yucca Mountain (Christensen and Spahr, 1980). These studies of flooding potential of major desert washes are pertinent introductory investigations of flood potential at Yucca Mountain because of their close geographic and physiographic relations to that area.

Squires and Young (1984) estimate the magnitudes of the 100- and 500-yr flood peaks and the regional maximum peaks. The standard errors for the estimates of the 100- and 500-yr floods are relatively large. These relatively large errors result primarily from the short period of record (15 to 20 yr) and the extreme areal variability of floodflows in arid climates. However, the regression approach used by Squires and Young (1984), which is based on data from nearby streams, is believed to be the best available method for peak-discharge determinations. Other methods, such as rainfall-runoff modeling, may give results that are not qualified as to their statistical reliability. These other methods are not believed inherently better than the method used in the study of Squires and Young (1984), which allows a reliability evaluation and is based on nearby flood data. The estimated discharges for the 100- and 500-yr floods on Fortymile Wash and the three southwestern tributaries are considered accurate to no more than two significant figures (Squires and Young, 1984).

The estimates of regional maximum floods made by Squires and Young (1984) are based on a graphical boundary curve developed by Crippen and Bue (1977). The graph defines a boundary curve of maximum discharges that have occurred in drainages of varying sizes and is based on quantitative measurements of flood-flow peaks in a five-state region that includes Arizona, California, Nevada, New Mexico, and Utah. That graph is reproduced and modi-

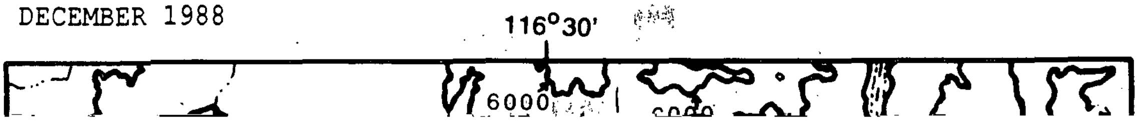
116°30'
6000

many speculations and assumptions would be needed to calculate the magnitudes of probable maximum floods in complex drainages the size of Fortymile Wash and Topopah Wash. Also, the lack of storm and runoff data throughout the hydrographic study area prevents checking the validity of the various assumptions used.

Because of data limitations just discussed, the methods for predicting extreme discharges of unusually large floods as used by Christensen and Spahr (1980) and Squires and Young (1984) were considered preferable to the methods presented in ANSI/ANS 2.8-1981 at the time the flood studies were conducted for Topopah and Fortymile washes. A preliminary study has been done to evaluate the clear-water probable maximum flood discharge for the Yucca Mountain site (Bullard, 1986). Results of this study will be analyzed to evaluate the flood potential of the site. Further studies are planned and discussed in Section 8.3.1.16.1.

Squires and Young (1984) determined flood magnitudes and frequencies less than the regional maximum by statistically manipulating the measured data collected at the 12 sites of Table 3-2. The study by Christensen and Spahr (1980) defined flood-prone areas of 100-yr, 500-yr, and maximum potential floods for Topopah Wash and its tributaries in the eastern part of Jackass Flats (Figure 3-4). Their maximum potential flood is essentially equivalent to the regional maximum flood of Squires and Young (1984). Christensen and Spahr (1980) reproduced the curve developed by Crippen and Bue (1977) for the region including Yucca Mountain as their basis for determination of the magnitude of their maximum potential flood.

From their investigation of Topopah Wash, Christensen and Spahr (1980) concluded the following:

1. The areas prone to 100-yr floods closely parallel most main channels, with few occurrences of out-of-bank flooding of the areas between the main channel and adjacent secondary channels. Out-of-bank flooding would result in a water depth of less than 0.6 m, with a mean velocity as high as 2 m/s occurring on the steeper slopes. Flood-water depth in the stream channels would range from 0.3 to 2.7 m, with mean velocities of 0.9 to 2.7 m/s.

2. The 500-yr flood would exceed the discharge capacity of all stream channels except Topopah Wash and some upstream reaches of a few tributaries. Out-of-bank flooding of areas between the adjacent channels would result in water depths as much as 0.9 m, with mean velocities greater than 2 m/s. Flood-water depth in the stream channels would range from 0.3 to 3.7 m, with mean velocities ranging from 0.9 to 4 m/s.

3. The maximum potential flood would inundate most of Jackass Flats. Out-of-bank flows in the areas between adjacent channels would have a depth as much as 1.5 m, with a mean velocity as high as 4 m/s. Flood water in the stream channels would have depths of 0.6 to 7 m, with velocities of 1.2 to 7.9 m/s.

Squires and Young (1984) studied the downstream part of Fortymile Wash. Within this area, Fortymile Wash has three tributaries that are informally designated from south to north as Busted Butte Wash, Drill Hole Wash, and Yucca Wash. Approximate flood-prone areas in these washes are shown on Figure 3-5. Squires and Young (1984) conclude the following:

1. Fortymile Wash, within the flood-study area, is a well-defined incised channel, with a cross section of 15 to 21 m depth and 300 to 450 m width. The estimated values of the 100-yr, 500-yr, and regional maximum floods indicate that the flow would stay within the confines of the wash. Estimated depths of flood water in the stream channel would range from 0.9 to 2.4 m for the 100-yr flood, from 1.8 to 3.3 m for the 500-yr flood, and 6.4 to 8.8 m for the regional maximum flood; corresponding mean velocities would be from 1.8 to 2.7 m/s for the 100-yr flood, 3.3 to 4.3 m/s for the 500-yr flood, and from 7.0 to 8.5 m/s for the regional maximum flood.

2. The drainage basin of Busted Butte Wash varies from a shallow valley with meandering ephemeral streams to a deeply incised canyon in the upstream reaches. Drill Hole Wash is characterized by deep canyons extending from Yucca Mountain to its mid-drainage area. Both washes would have estimated flood-water depths of from 0.3 to 1.2 m in the stream channel during the 100-yr flood, and the corresponding mean velocities would range from 1.2 to 2.4 m/s. The 500-yr flood would exceed bank capacities at several reaches of the washes. Depths and mean velocities would range from 0.9 to 3.0 m and 1.5 to 3.3 m/s. The regional maximum flood would inundate all central flat-fan areas in these two watersheds. Flood-water depths in the stream channels would range from 1.5 to 3.7 m, with mean velocities varying from 2.1 to 4.9 m/s.

3. Yucca Wash is contained within an incised channel that is about 14 m deep and 240 m wide at its confluence with Fortymile Wash. The 100-yr, 500-yr, and regional maximum floods would stay within the steep-side-slope stream banks that contain the flood plain. Flood-water depths in the stream channel would range from 0.9 to 1.5 m for the 100-yr flood, from 1.5 to 2.7 m for the 500-yr flood, and from 2.7 to 7 m for the regional maximum flood; corresponding mean velocities would vary from 1.5 to 2.7 m/s for the 100-yr flood, from 2.4 to 3.7 m/s for the 500-yr flood, and from 2.7 to 6.7 m/s for the regional maximum flood.

According to Squires and Young (1984), "Geomorphic studies on the Nevada Test Site have indicated that some of the alluvial surfaces along Fortymile Wash are thousands of years old. Such ages might imply that the surfaces have not been flooded since they were formed several thousand years ago. However, distinct high-water marks are observed along Fortymile Wash in the vicinity of cross-section FM-4" (Figure 3-5), indicating that the alluvial surfaces along Fortymile Wash were inundated. Survival of these alluvial surfaces may be explained by a previous observation in Colorado that a fine-grained alluvial surface overtopped by a flash flood was virtually unaffected (Squires and Young, 1984). They continue, "From these marks and from data on the cross-sectional area and channel slope, a peak flow of about 20,000 ft^3/s (570 m^3/s) is estimated. Documentation of similar flooding in nearby washes indicates that this flood peak probably occurred during February 1969." A discharge of 20,000 ft^3/s (570 m^3/s) for this section of stream channel is

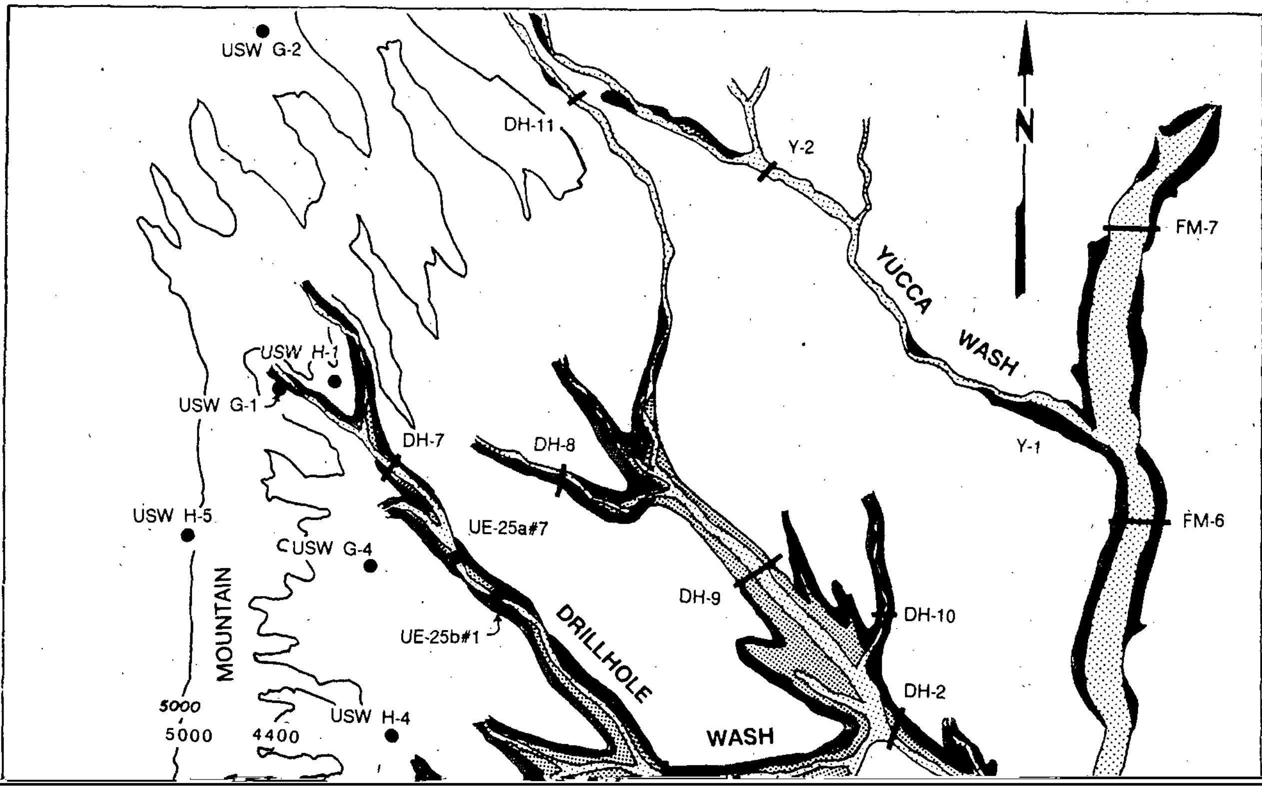
USW G-2
DH-11
Y-2
N
FM-7
YUCCA
WASH
USW H-1
USW G-1
DH-7
DH-8
Y-1
USW H-5
UE-25a#7
FM-6
USW G-4
MOUNTAIN
DH-9
DH-10
UE-25b#1
DRILLHOLE
DH-2
5000
5000
4400
USW H-4
WASH

greater than the estimated discharge for the 100-yr flood (12,000 ft^3/s (340 m^3/s)) but less than the estimated discharge for the 500-yr flood (57,000 ft^3/s (1,600 m^3/s)) (Squires and Young, 1984). Additional studies are planned to evaluate paleoflooding in the Yucca Mountain area through the use of geomorphic and geologic evidence. These studies are discussed in [redacted]

The extent of erosion and sediment movement caused by flood flow in Fortymile Wash and its tributaries that drain Yucca Mountain is not known quantitatively. Qualitatively, however, on the basis of knowledge of record major floods elsewhere in southern Nevada (Glancy and Harmsen, 1975; Katzer et al., 1976), erosion of or deposition in channels and flood plains probably would occur during the 100-yr, 500-yr, and regional maximum floods. While erosion or deposition due to an individual flood event cannot be quantified, average rates of stream incision over long periods of time can be evaluated. Section 1.1.3.3.2 discusses surficial processes, and Table 1-3 lists average rates of stream incision in the Yucca Mountain area.

Evidence of erosion and deposition was observed in some channels during field surveys. Channel erosion or aggradation in the existing streambeds could alter the flood-flow characteristics of cross-sectional area, width, mean velocity and maximum depth listed in the report by Squires and Young (1984). The effect of erosion or deposition on flood-flow characteristics would vary from place to place. Because velocities for the 100-yr, 500-yr, and regional maximum flood peaks are high, channel erosion and aggradation appear likely.

Because most of Yucca Mountain is well above expected flood levels of Fortymile Wash and its major tributaries, as assessed by Squires and Young (1984), numerous small ephemeral stream channels from the mountain to the major drainages were not included in their study. Flow in the ephemeral stream channels that may affect the Yucca Mountain site will be assessed in future studies (Section 8.3.1.2.1).

The sparseness of the historical data base on surface-water hydrology, including the movement of both water and debris inhibits accurate prediction of flood and debris hazards for the immediate future. Data needs, plans for future data collection, and data-collection methodologies are given in Section 8.3.1.16.1. Likewise, a deficient understanding of paleoclimates (Section 5.2.1) and past geomorphic processes (Section 1.1.3) limits the ability to predict climatic changes and their probable effects on flood-and-debris-hazards potential over the next several thousands of years. Plans for studies of future climates are discussed in Section 8.3.1.5.1.

Hydrologic conditions that have occurred during the Quaternary that have differed from present conditions, and the likelihood of recurrence over the next 10,000 yr, are described in Sections 3.7.4 and 3.9.8. Evidence for long term changes in hydrometeorology are discussed in Section 3.7.4. A more detailed discussion on past influences of glacial environments in the western United States and their effects on climate is given in Section 5.2. Hoover et al. (1981) describes a system for correlating and mapping surficial deposits in the Yucca Mountain area. The stratigraphic sequence of units, soils, and unconformities that has been observed indicates fluctuating climatic conditions.

3.2.1.1 Ongoing and future studies of flood and debris hazard potentials

Studies are planned to improve the surface-water hydrologic data base at Yucca Mountain and surrounding areas (Section 8.3.1.2.1). The minimal data on stream flow and insufficient knowledge of geomorphic parameters make predictions of flood and debris hazards very speculative. To rectify this deficiency, the Yucca Mountain Project plans to expand the streamflow (movement of water and debris) data base (Section 8.3.1.2.1). A network of stream-gaging stations near Yucca Mountain has been established to monitor and record modern stream flows. Four continuously recording stream gages and five peak-flow gages were installed. Locations of these gages are shown in Figure 3-4. Precipitation gages also installed at these stream gaging sites collect rainfall data. Also, five peak-flow gages at sites 2 through 6 (Table 3-2 and Figure 3-3) have been reactivated. Investigations of flooding also provide stream flow data at other miscellaneous ungaged sites when floods occur near Yucca Mountain or the surrounding region. These investigations also yield data on debris transport, particularly where debris avalanches or debris flows are part of the flooding process.

Investigations of paleofloods, including debris flows, have been initiated. Paleoflood studies involve analyses of sediment deposits of Quaternary floods and collection of evidence for mass movement of debris by these floods. These investigations are being conducted to improve understanding of Quaternary runoff events, develop a chronology of flooding, provide data on past geomorphic processes for comparison with modern processes, and aid in interpretation of paleoclimates. Plans for future investigations of, and data collection for, potential flood and debris hazards are described in Section 8.3.1.5.2.

Inasmuch as the Yucca Mountain area is located inland and has no significant surface-water bodies or water-control structures located near the site, there is no potential for events such as surges, seiches, tsunamis, dam failures, or ice jams that could affect the site, nor is there any potential for future dam development. The Yucca Mountain area was not glaciated during the Pleistocene (Section 5.2). No evidence for pluvial lakes has been found in the Yucca Mountain area (Mifflin and Wheat, 1979). This indicates that the potential for floods during maximum glaciation is minimal. Additional studies to evaluate the potential for climatic change and the effects of any change on the proposed site are discussed in Section 8.3.1.5.2. No evidence for past flooding induced by landslides in the vicinity of the site has been reported (USGS, 1984, and Section 1.1.3, geomorphic processes).

3.2.2 FLOOD PROTECTION

The rugged terrain at the Yucca Mountain site and local convective storms can cause intense flooding to occur periodically in the normally dry washes that drain Yucca Mountain ridge. Protection from this flooding was been compiled (Wu, 1985) of the Yucca Mountain area at a scale of 1:5,000 and a contour interval of 2 m (with 1-m supplemental contours). These will be used for some aspects of final design.

As described in Section 6.2.4.2 (flood protection) a preliminary analysis of the probable maximum flood (PMF), based on a study by Bullard (1986), has been performed for the men-and-materials shaft area because of the local rugged terrain and the proximity of the shaft area to the confluence of two washes that are tributary to the larger Drill Hole Wash. The purpose of the preliminary analysis was to evaluate the feasibility of locating the shaft and its supporting surface complex in such a rugged area. In the analysis, [illegible]

shaft area is benched, with the shaft entrance designed to be above the PMF [illegible]

3.3.1 PRESENT QUANTITY AND QUALITY OF SURFACE WATER EXTRACTED

Very little surface water exists in the vicinity of Yucca Mountain. The climate in the region is arid; no perennial streams are present except short reaches of the Amargosa River which are fed by springs (Figure 3-1) (Waddell et al., 1984). Other perennial sources of surface water are the small spring-fed ponds in Oasis Valley, the Amargosa Desert, and Death Valley (French et al., 1984; Waddell et al., 1984). Spring locations and their water chemistries are presented in Sections 3.5.1 and 3.7.3, respectively. Spring water use is discussed in Section 3.8.1.

Several small, man-made reservoirs used for agricultural, milling, and mining purposes are scattered throughout the southern portion of the hydrologic study area. The largest, a man-made reservoir, known locally as Crystal Reservoir, is located in the Ash Meadows area 52 km (32 mi) southeast of Yucca Mountain (Figure 3-1). This reservoir receives its water from Crystal Pool spring, located approximately 0.8 km (0.5 mi) to the north. Crystal Reservoir, which has a capacity of 1,840 acre-feet (2.27×10^6 m^3) is used for recreational purposes only. Another small reservoir (Clay Camp at NE 1/4, Section 1, T.18S., R.49E.) with a capacity of 43 acre-feet (53,000 m^3), is used for milling. This and many other reservoirs are fed by wells (Section 3.8.1). Other small reservoirs with capacities much less than 40 acre-feet (49,300 m^3) exist near Point of Rocks and Death Valley Junction (Giampaoli, 1986).

The Amargosa River (Section 3.1) is not used for water supply. The flow regime has been intermittent to ephemeral throughout historic times, except for the spring-fed reaches. As such, sufficient supplies for domestic, municipal, commercial, agricultural, or industrial supply have not been available (Walker and Eakin, 1963). The chemical composition of Amargosa River water is discussed in Section 3.4.

Hydroelectric power is generated at Hoover Dam near Boulder City, Nevada. Although Hoover Dam is located only 180 km southeast of Yucca Mountain, the hydrologic settings of the two areas are very different. The absence of a perennial river within the boundaries of the hydrographic study area precludes the development of hydroelectric power.

No other sources of surface water exist within the hydrographic study area. Frenchman Lake and Yucca Lake are playas that contain water only after rainstorms. Runoff to these playas serves to recharge the valley-fill aquifer (Claassen, 1985; Section 3.7.1). However, because of the sporadic precipitation and runoff and the excessive amounts of dissolved solids, playas are not considered as possible sources of water supply (Waddell et al., 1984). The virtual absence of perennial surface water has precluded its application for beneficial use in the hydrographic study area.

3.3.2 PROJECTED SURFACE-WATER USES

Arid conditions of the region and the absence of perennial streams and lakes make surface water an unlikely future water supply. Within the hydrographic study area, surface water serves two principal functions:

(1) recharge to the valley-fill aquifer and (2) maintenance of habitats for aquatic species. Surface-water use by man in the study area would probably increase only in the event of a change in climate to a wetter regime. Studies done to date indicate that such an event is possible, but not in the period of repository construction, operation, closure, and decommissioning (DOE, 1986). (See Section 5.2 for a complete discussion of climatic modeling and Section 8.3.1.5.1 for a discussion of planned studies.) Consequently, there are no known plans to construct dams or reservoirs in the vicinity of Yucca Mountain site.

3.4 CHEMICAL COMPOSITION OF ADJACENT WATERCOURSES

This section addresses the chemical composition of surface water at the Yucca Mountain site and vicinity. Classically, the section would include discussions of (1) seasonal cycles of physical and chemical limnological parameters, (2) bottom and shoreline configuration, (3) sedimentation rates, (4) sedimentation graduation analysis, and (5) sorption properties. However, because of the arid to semiarid climate of the region, these topics are not applicable. This section presents data required to address questions of the adequacy of the description of the present and expected hydrogeologic characteristics in order to provide the information required by the design and performance issues and the formation of a sufficient baseline against which to assess potential impacts.

The historical records and onsite monitoring of surface water composition is quite limited. Present data consist of two historic and six recent chemical analyses. The analyses are presented here along with discussions on trends and observations.

Within the hydrographic study area, the Amargosa River is the major surface-water source to the regional drainage sink of Death Valley. As described in Section 3.1, the Amargosa River is normally dry, except for short reaches that receive water discharging from the underlying ground-water flow system. Because of the ephemeral character of the Amargosa River only two water samples have been collected; one from a reach near Eagle Mountain and the other from Carson Slough, a major tributary that joins the Amargosa River near Alkali Flat (Figure 3-6). From the chemical analyses presented in Table 3-3, it can be seen that sodium and bicarbonate are the primary constituents. The high sulfate and chloride is indicative of ground-water interaction with playa deposits. The chemical composition of these two surface water samples is quite similar to that of the water from the tuffaceous valley fill aquifer (Section 3.7.3). This similarity suggests that the source of the water sampled is the tuffaceous valley fill. Hunt et al. (1966) indicate that ponding occurs where the shallow ground-water table in southern Amargosa Desert encounters a structural barrier north of Eagle Mountain.

Samples of surface water from the Yucca Mountain area were collected during period of runoff and flooding in July and August of 1984. Water samples were collected from the main stream channel of Fortymile Wash and from two of its principal tributaries, Drill Hole and Busted Butte washes (Figure 3-6). Results of analyses are shown in Table 3-3. All the samples

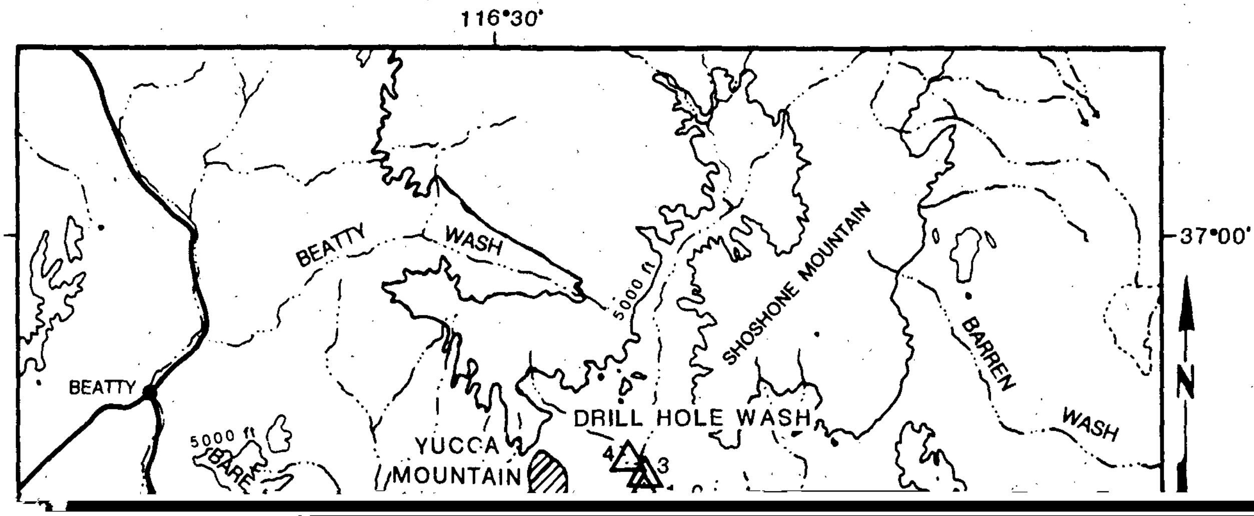
116°30'
37°00'
BEATTY
BEATTY WASH
5000 ft
5000 ft
SHOSHONE MOUNTAIN
BARREN WASH
DRILL HOLE WASH
YUCCA MOUNTAIN
4
3
N

Table 3-3. Chemical composition of watercourses adjacent to Yucca Mountain[a]

Parameter	1 Flood sample Fortymile Wash at road M[b]	2 Flood sample Fortymile Wash at road W[b]	3 Flood sample Fortymile Wash above Drill Hole Wash[b]	4 Flood sample Drill Hole Wash at mouth[b]	5 Flood sample Fortymile Wash at J-12[b]	6 Flood sample Busted Butte Wash[b]	7 Stream sample Carson Slough[c]	8 Stream sample Amargosa River near Eagle Mountain[c]
Laboratory sample number	4212602	4248608	4248604	4248605	4248607	428606	3060	3062
Latitude	36°49'07"	36°49'04"	36°49'08"	36°49'11"	36°49'51"	36°47'49"	≈36°25'	≈36°13'
Longitude	116°23'47"	116°23'47"	116°23'46"	116°23'52"	116°23'51"	116°23'51"	≈116°21'	116°22'50"
Site number on Figure 3-6	1	2	3	4	5	6	7	8
Date	7/22/84	8/15/84	8/14/84	8/14/84	8/14/84	8/14/84	1958	1958?
Specific conductance, field (microsiemens per cm at 25°C)	--[d]	170	70	100	59	120	937	1,860
Specific conductance, laboratory (microsiemens per cm at 25°C)	201	859	198	218	100	217	--	--
pH, field	--	8	8.4	8.3	8.2	8.3	8.5	8.8
pH, laboratory	7.4	7.4	7.5	7.8	7	7.8	--	--
Temperature (°C)	--	21.5	--	--	--	--	10	4.4
Calcium (Ca)	24	31	8.1	9.5	6.7	12	40	24
Magnesium (Mg)	3.3	2.9	0.9	1.3	0.7	1.8	26	29
Sodium (Na)	8.1	8.2	4.1	8.6	2.4	7	125	344
Potassium (K)	7.8	9.1	5.6	7.4	6.3	8.1	16	40
Bicarbonate (HCO_3)	--	--	--	--	--	--	362	542
Carbonate (CO_3)	--	--	--	--	--	--	10	33
Alkalinity as $CaCO_3$, lab	73	75	36	42	26	47	--	--
Chloride (Cl)	3.7	1.4	1.3	2.2	2	1.7	40	123
Sulfate (SO_4)	10	10	6.2	13	6.3	7.9	122	277
Fluoride (F)	0.2	0.2	<0.1	0.3	<0.1	0.3	2	2.8
Silica (SiO_2)	25	24	8.7	20	4.5	23	28	26
Arsenic (µg/L as As)	2	2	<1	2	<1	3	0.0	2
Iron (µg/L as Fe)	110	77	18	100	28	200	210	450
Manganese (µg/L as Mn)	3.3	5	11	6	22	10	0.0	0.0
Strontium (µg/L as Sr)	100	100	34	66	31	86	1,800	800
Lithium (µg/L as Li)	6	7	6	14	5	17	--	--
Iodide (I)	0.009	0.005	0.003	0.002	0.004	0.003	--	--
Bromide (Br)	0.049	<0.01	<0.01	<0.01	<0.01	<0.01	--	--
Boron (B)	--	--	--	--	--	--	0.68	2.1
Dissolved solids (sum)	127	122	57	92	45	100	566	1,140

[a]Values for chemical constituents are in milligrams per liter unless otherwise indicated. Analyses by U.S. Geological Survey, Denver, Colorado.
[b]Flood sample analyses (USGS) from WATSTORE files.
[c]Stream sample analyes from Hunt et al. (1966).
[d]-- indicates no data.

are dilute and are significantly lower in solutes than ground-water samples of the area (Section 3.7.3). However, samples 1 and 2 are noticeably more concentrated in calcium and dissolved solids than are samples 3 through 6. This difference is most likely attributed to the fact that samples 1 and 2 were collected on different days than samples 3 through 6, which means that they are not only from different locations but also from different rainfall events. Even with the last four samples showing remarkably similar compositions, any quantitative interpretation is unwarranted unless the following are known:

1. The compositional variability of storms throughout the year.

2. The compositional variability within a given storm.

3. The lithologic composition of the source areas for the drainage systems.

However, the data do provide information about the base level composition of recharge to the valley-fill aquifer along Fortymile Wash (Section 3.7.3).

Waddell et al. (1984) cite water chemistry data that indicate that washes may be the principal source of ground-water recharge beneath Yucca Mountain. Periodic temperature measurements made in wells in Drill Hole Wash during 1981 to 1983 revealed a pronounced increase in the temperature profile above a depth of 150 m in drillhole UE-25a#7. This occurrence of warmer water may be related to recharge from a major storm that occurred early in March, 1983 (Waddell et al., 1984). Furthermore, as discussed in Section 3.7.3.2, the high tritium concentration of water from well UE-29a#1 in Fortymile Wash (62 tritium units) indicates that precipitation containing bomb-test tritium has recharged the aquifer since the mid-1960s possibly correlating with the major flood in the winter of 1969 (Section 3.2.1). This evidence clearly establishes that modern rainfall and runoff contribute recharge to the shallow ground-water system in the tuffaceous valley-fill aquifer. The extent of this contribution, which probably is small, cannot be they were calculated are included in Section 3.7. Ground-water withdrawals from specific wells are listed in Section 3.8.1. A discussion of the potential for contamination of ground-water and surface-water supplies that might result from site characterization activities is also included.

Throughout this section, the term ground water refers to one of several classifications of water lying beneath the surface, including deep and shallow saturated zones, unsaturated zones, soil water and perched water. The particular usage depends on the topic of discussion and may be derived from the context.

The data presented in this section generally address the question of the isolation of radioactive waste from the accessible environment after closure of the mined geologic disposal system at Yucca Mountain (Key Issue 1). More specifically, data concerning the location and nature of points of ground-water discharge may be used to assist in the identification of paths of likely radionuclide travel and in the calculation of ground-water travel tim along those paths. Further, this information contributes to the descriptior and understanding of the hydrologic system (both the unsaturated and saturated zones) and to the prediction of potential impacts to the quality and availability of water resources in the vicinity of Yucca Mountain.

In general, definitive discharge data for the hydrogeologic study area are scanty. Walker and Eakin (1963) estimated discharge in the Amargosa Desert; Malmberg and Eakin (1962) made similar estimates for Oasis Valley. These estimates are summarized in Table 3-4. But, because in this instance it is not possible to separate all the various forms of discharge, the figures presented are intended for comparison purposes only and may not represent the actual conditions present in the two areas.

Evapotranspiration in the Amargosa Desert is approximately 1.4 times greater than spring discharge and 47 times greater than ground-water underflow. In Oasis Valley, evapotranspiration exceeds spring discharge and underflow by factors of 10 and 5, respectively. It is evident from these estimates that evapotranspiration is the primary mechanism for discharge of ground water in these areas and probably throughout the hydrogeologic study area. Surface discharge is not considered significant, because it is ephemeral (Malmberg and Eakin, 1962; Walker and Eakin, 1963). A further discussion is given in Section 3.1. However, the existing data are insufficient to quantify properly the surface-water component of the total discharge. To address this deficiency, site characterization activities will include measurements of overall runoff and the estimation of peak runoff, flood magnitudes, and recurrence intervals. The scope of work and timetable for these activities are discussed in Section 8.3.1.2.1. These plans allow for the ephemeral nature of desert runoff, including the possibility of no runoff events in any single year.

Several authors have used a variety of techniques to determine the average annual recharge rate for the area encompassing Yucca Mountain. Montazer and Wilson (1984) estimate the average annual recharge rate for Yucca Mountain to be between 0.5 and 4.5 mm/yr on the basis of various published estimates for the region. Using the analyses of Rush (1970), Czarnecki (1985) estimated recharge to be 0.7 mm/yr in a precipitation zone

Table 3-4. Ground-water discharge from the Amargosa Desert and Oasis Valley

Discharge category	Amargosa Desert[a]		Oasis Valley[b]	
	acre-ft/yr	m^3/s	acre-ft/yr	m^3/s
Average annual consumptive use				
[redacted]				
Total evapotranspiration	23,500	0.92	2,000	0.08
Surface-water runoff discharging from basin	ND	ND	ND	ND
Spring discharge	17,000[c]	0.66	200[e]	0.008
Ground-water underflow	500	0.02	200	0.008

[a]Source: Walker and Eakin (1963).
[b]Source: Malmberg and Eakin (1962).
[c]Total spring discharge, includes water becoming underflow, evapotranspiration, etc.

the saturated zone at less than 2.5 mm annually. However, Rice's (1984) model lacked sufficient detail to be used as an accurate representation of the conditions present at Yucca Mountain.

[redacted]

Yucca Mountain site. A regional hydrologic budget is one method of estimat-

[redacted]

hydrologic budget will be accomplished through hydrologic modeling as discussed in Section 8.3.1.2.1.

Although discharge through surface-water runoff and ground-water outflow are smaller components of the total discharge, they are equally important for proper quantification of the total discharge. However, the data for the study area are not sufficient to quantify inflow, outflow, and runoff, or to relate these to recharge. Net subsurface flux (outflow minus inflow) must be quantified for proper comparison of recharge versus outflow from the basin. Plans for these studies are discussed in Section 8.3.1.2.1. Surface runoff and ground-water outflow are discussed further in Section 3.1, 3.2, and 3.7.

Total evapotranspiration is the sum of several processes (Robinson, 1957).

$$Et = E_s + E_i + E_x + E_p + E_c + E_{sw} \quad (3\text{-}2)$$

where

Et = total evapotranspiration

E_s = evaporation from soil

E_i = evaporation of precipitation intercepted by foliage

E_x = transpiration by xerophytes

E_p = transpiration by phreatophytes

E_c = evaporation from capillary fringe

E_{sw} = evaporation from surface water.

Although evaporation from soil has not been sufficiently quantified in the study area, available studies indicate that losses due to evaporation from soil may be an important factor in the water budget. In a study by Nichols (1986), soil evaporation near Beatty was estimated to average

97 percent of the annual precipitation during the period 1961 to 1976.

Data concerning evaporation of intercepted precipitation are not available for the study area. Investigations of this process in Utah and Idaho (Hull and Klomp, 1974; West and Gifford, 1976) report average water-holding capacities for individual sagebrush plants of 1.5 mm. Within the study area, the limited plant density (average shrub coverage ranging from 16 to 29 percent depending on elevation (O'Farrell and Emery, 1976)) and small crown diameters indicate that this element of the water budget is relatively minor, but not insignificant, particularly compared with the average annual recharge estimate of 0.5 mm/yr made by Wilson (1985) for Yucca Mountain.

Data concerning transpiration by xerophytes is lacking for the area of study. Sammis and Gay (1979) estimated the transpiration by a large creosote bush to be 5 to 8 percent of precipitation. Since these plants do not draw water from the water table, it seems that their primary effect is to reduce infiltration from the soil zone to the unsaturated zone. This may be an important factor in the budget.

Phreatophytic transpiration, on the other hand, has been relatively well studied, and some data exist for the study area that can be used for quantification of this parameter; for example, some areas of phreatophytic growth are identified in the spring inventory in Section 3.5.1 and in Section 3.6. Included in the studies of phreatophytes are several attempts at formulating a general method for estimating transpiration based on empirical data (Decker and Wein, 1957; Hughes and McDonald, 1966; Robinson, 1970) and several methods for calculating evapotranspiration using meteorological or hydrologic data (Rantz, 1968; Hanson and Dawdy, 1976). Proper estimation of the rate of transpiration from the various plant types will depend on the availability of information detailing areal distributions and densities of vegetation throughout the area. Several studies have surveyed the biota in the area of the NTS (O'Farrell and Emery, 1976; Collins et al., 1982; O'Farrell and horizon will be evaluated in the infiltration studies discussed in Section 8.3.1.2.2.

Evaporation from those surface-water bodies identified in Section 3.1 can be estimated on the basis of their surface area and pan evaporation data for the area. Pan evaporation for the area is estimated to be over 250 cm/yr according to Dudley and Larson (1976) and Nichols (1986). However, this figure is the potential evaporation. The volume of actual evaporation is expected to be relatively low due to the very limited availability of surface water bodies in the area. Nonetheless, this form of discharge is believed to be an important factor in the water budget. Information concerning the surface areas of these bodies is lacking and plans to obtain this information during site characterization are described in Section 8.3.1.2. Estimates of evaporation during periods of inundation due to flooding could also be made based on the area and period of inundation and pan evaporation. Much of the data necessary for these calculations are available in the form of topographic maps and previous and planned flood studies. Plans for these activities are discussed in Section 8.3.1.2.1.

Planned studies at Franklin Lake playa (Section 8.3.1.2.1) will provide data related to total evapotranspiration. Several techniques will be used to provide information on discharge rates and quantities, soil-moisture, phreatophyte distribution, evapotranspiration rates, and other parameters.

In addition to evapotranspiration from natural sources, quantification of discharge through human-related activities is planned (Section 8.3.1.16). Water use projections are available for agriculture, livestock, and domestic users in publications such as Water for Nevada (Office of the State Engineer, 1974). Discussions of ground-water use are included in Section 3.8.

In summary, studies that have been performed to date indicate that all of the components of ground-water discharge are significant when compared with the estimated recharge rates. In general there is a paucity of site-specific data, and meaningful estimates of these components cannot be made at this time. Additional studies, which will provide the necessary data to quantify these parameters, are included in the site characterization plans discussed in Section 8.3.1.2.

3.5.1 SPRINGS, SEEPS, AND PHREATOPHYTE AREAS

Springs can be classified on the basis of their ground-water source, (i.e., water-table springs and perched springs). Water-table springs discharge where the land surface intersects the water table. Perched springs, however, flow from the intersection of the land surface with a local ground-water body that is separated from the main saturated zone below by a zone of relatively lower permeability and an unsaturated zone.

Seeps are springs with very low discharge rates, commonly so low as to preclude measurement. Similar to springs, seeps may be classified according to their ground-water source.

An inventory of springs, seeps, and phreatophyte areas in the hydrogeologic study area has been compiled and is presented in Table 3-5. This list is based on data from Thordarson and Robinson (1971), Malmberg and Eakin (1962), Pistrang and Kunkel (1964), Schoff and Moore (1964), Miller (1977), Winograd and Thordarson (1975), Dudley and Larson (1976), White (1979), and Waddell et al. (1984). The springs are grouped according to basin boundaries (Sections 3.7.1 and 3.7.2). Springs are located using latitude and longitude coordinates to the nearest second, when available, and township and range designation. Perched springs are noted in the comments column. Hydrostratigraphic unit information, when available, is derived from the reference(s) listed in the reference column.

Also included in the spring inventory are some areas of phreatophytic growth. These areas are responsible for considerable amounts of ground-water discharge through evapotranspiration. Playas and alkali flats have not been included in the spring inventory because of the lack of data concerning quantities of discharge and the locations of many of these areas. As stated previously, such hydrologic conditions do not occur within the immediate vicinity of Yucca Mountain. However, they are believed to be important sites for ground-water discharge and are planned to be identified and mapped during site characterization (Section 8.3.1.2.1).

Table 3-5. Springs, seeps, and phreatophyte areas in the hydrogeologic study area (page 1 of 12)

Latitude	Longitude	Township and range, spring location number	Name[a]	Aquifer[b]	Elevation ft	Elevation m	Discharge gpm	Discharge L/s	Temperature °F	Temperature °C	Use	Reference[c]	Comments
ALKALI FLAT-FURNACE CREEK RANCH SUBBASIN (CALIFORNIA)													
36 26 40	116 49 50	27N/01E-23R1	Travertine		400	122	305	19.2	92	33	ND	T&R, 71 P&K, 64	
36 26 30	116 49 40	27N/01E-26A2	Travertine		320	98	220	13.9	92	33	Irrigation	T&R, 71 P&K, 64	
36 26 30	116 49 50	27N/01E-26A5	Travertine		320	98	ND[d]	ND	95	35	Irrigation	T&R, 71 P&K, 64	
36 26 30	116 49 50	27N/01E-26A6	Travertine		330	100	270	17.0	94	34	Irrigation	T&R, 71 P&K, 64	
36 26 30	116 49 50	27N/01E-26A7	Travertine		330	100	ND	ND	85	29	Irrigation	T&R, 71 P&K, 64	
36 26 30	116 49 40	27N/01E-26A1	Travertine		330	100	103	6.5	82	28	Irrigation	T&R, 71 P&K, 64	Discharge value includes discharge from the two springs listed below
36 26 30	116 49 40	27N/01E-25D2	Travertine		400	122	ND	ND	92	33	Irrigation	T&R, 71 P&K, 64	Seep
36 26 30	116 49 40	27N/01E-25D1	Travertine		400	122	ND	ND	92	33	Irrigation	T&R, 71 P&K, 64	
36 26 30	116 49 50	27N/01E-26A3	Travertine		320	98	0.4	0.025	89	32	Irrigation	T&R, 71 P&K, 64	
36 26 30	116 49 50	27N/01E-26A4	Travertine		320	98	4	0.25	94	34	Irrigation	T&R, 71 P&K, 64	
36 30 30	116 49 10	28N/01E-36K1	Nevares		920	280	ND	ND	69	21	Domestic Public supply	M, 77 P&K, 64	Seep
36 30 30	116 49 40	28N/01E-36M2	Nevares		745	227	ND	ND	84	29	Domestic Public supply	M, 77 P&K, 64	
36 30 30	116 49 40	28N/01E-36M1	Nevares		720	220	31	1.96	78	26	Domestic Public supply	M, 77 P&K, 64	
36 30 40	116 49 10	28N/01E-36G2	Nevares		896	273	22	1.39	102	39	Domestic Public supply	M, 77 P&K, 64	

Table 3-5. Springs, seeps, and phreatophyte areas in the hydrogeologic study area (page 2 of 12)

Latitude	Longitude	Township and range, spring location number	Name[a]	Aquifer[b]	Elevation ft	Elevation m	Discharge gpm	Discharge L/s	Temperature °F	Temperature °C	Use	Reference[c]	Comments
ALKALI FLAT-FURNACE CREEK RANCH SUBBASIN (CALIFORNIA) (continued)													
ND	ND	28N/01E-36FS1			ND	ND	40	2.5	ND	ND	ND	M, 77 P.59	
36 30 40	116 49 10	28N/01E-36GS1	Nevares		937	286	269	16.97	104	40	Domestic Public supply	M, 77 P&K, 64	
36 29 40	116 51 20	27N/01E-03P1	Salt		0	0	4	0.25	73	23	Unused	P&K, 64	
36 29 40	116 51 20	27N/01E-03K1	Salt		100	30	ND	ND	ND	ND	NA[e]	P&K, 64	
36 27 10	116 51 00	27N/01E-22H1	Furnace Creek Inn Tunnel		50	15	148	9.34	92	33	Irrigation	P&K, 64	
36 26 30	116 49 40	27N/01E-26B1	South Travertine (Sump in Furnace Creek Wash)		280	85	566	35.7	92	33	Irrigation	M, 77 P&K, 64	
			Wash										
36 26 40	116 49 50	27N/01E-23B1	Texas Spring (Tunnel)		380	116	224	14.1	91	33	Irrigation and public	P&K, 64	

Table 3-5. Springs, seeps, and phreatophyte areas in the hydrogeologic study area (page 3 of 12)

Latitude	Longitude	Township and range, spring location number	Name[a]	Aquifer[b]	Elevation ft	Elevation m	Discharge gpm	Discharge L/s	Temperature °F	Temperature °C	Use	Reference[c]	Comments
ALKALI FLAT-FURNACE CREEK RANCH SUBBASIN (CALIFORNIA) *(continued)*													
		27N/01E-23J1			410	125	NA	NA	ND	ND	NA	P&K, 64	Phreatophyte area
		27N/01E-23J2			410	125	NA	NA	ND	ND	NA	P&K, 64	Phreatophyte area
36 27 00	116 50 10	27N/01E-23K1			410	125	NA	NA	ND	ND	NA	P&K, 64	Seep
36 27 00	116 50 10	27N/01E-23K2			400	122	4	0.25	ND	ND	ND	P&K, 64	
36 27 00	116 50 20	27N/01E-23L1			160	49	NA	NA	ND	ND	NA	P&K, 64	Seep
36 27 00	116 50 20	27N/01E-23L2			160	49	NA	NA	ND	ND	NA	P&K, 64	Phreatophyte area
36 27 00	116 50 20	27N/01E-23L3			160	49	NA	NA	ND	ND	NA	P&K, 64	Seep
36 26 40	116 50 10	27N/01E-23Q1			320	98	NA	NA	ND	ND	NA	P&K, 64	Seep
36 26 40	116 50 10	27N/01E-23Q2			320	98	NA	NA	ND	ND	NA	P&K, 64	Seep
36 26 40	116 50 10	27N/01E-23Q3			320	98	4	0.25	72	22	ND	P&K, 64	
36 26 40	116 50 10	27N/01E-23Q4			320	98	NA	NA	ND	ND	NA	P&K, 64	Seep
36 26 40	116 50 10	27N/01E-23Q5			320	98	NA	NA	ND	ND	NA	P&K, 64	Seep
36 26 40	116 50 10	27N/01E-23Q6			320	98	NA	NA	ND	ND	NA	P&K, 64	Seep
36 26 40	116 49 50	27N/01E-23R2			410	125	NA	NA	ND	ND	NA	P&K, 64	Phreatophyte area
36 26 40	116 49 50	27N/01E-23R3			410	125	NA	NA	ND	ND	NA	P&K, 64	Phreatophyte area
36 26 40	116 49 40	27N/01E-24N1			400	122	NA	NA	ND	ND	NA	P&K, 64	Seep
36 26 30	116 50 10	27N/01E-26B4			320	98	NA	NA	ND	ND	NA	P&K, 64	Seep
36 26 30	116 50 10	27N/01E-26B5			320	98	NA	NA	ND	ND	NA	P&K, 64	Seep
36 30 00	116 51 00	27N/01E-3A1	Cow		200	61	18	1.14	81	27	Unused	P&K, 64	
		27N/01E-3B1			240	73	NA	NA	ND	ND	NA	P&K, 64	Phreatophyte area
		28N/01E-34M1			0	0	NA	NA	ND	ND	NA	P&K, 64	Phreatophyte area

Table 3-5. Springs, seeps, and phreatophyte areas in the hydrogeologic study area (page 4 of 12)

Latitude	Longitude	Township and range, spring location number	Name[a]	Aquifer[b]	Elevation ft	Elevation m	Discharge gpm	Discharge L/s	Temperature °F	Temperature °C	Use	Reference[c]	Comments
ALKALI FLAT-FURNACE CREEK RANCH SUBBASIN (CALIFORNIA) (continued)													
36 30 10	116 51 50	28N/01E-34N1			10	3	NA	NA	74	23	NA	P&K, 64	Seep
36 30 10	116 51 50	28N/01E-34N2			80	24	NA	NA	ND	ND	NA	P&K, 64	Phreatophyte area
		28N/01E-34P1			100	30	NA	NA	ND	ND	NA	P&K, 64	Phreatophyte area
		28N/01E-35E1			380	116	NA	NA	ND	ND	NA	P&K, 64	Phreatophyte area
		28N/01E-35G1			500	152	NA	NA	ND	ND	NA	P&K, 64	Phreatophyte area
36 30 30	116 50 20	28N/01E-35K1			520	158	NA	NA	76	24	Unused	P&K, 64	Seep
		28N/01E-35N1			380	115	4	0.25	78	26	NA	P&K, 64	
		25N/02E-13GS1	Lemonade	Volcanic Rock	3,800	1,160	<1	<0.06	54	12	ND	USGS Map 1:250,000 Death Valley M,77	
		26N/02E-13FS1	Navel	Fanglomerate	2,080	634	ND	ND	73	23	ND	USGS Map 1:250,000 Death Valley M, 77	
36°39′	116°51′	29N/01E-15			1,800	360	ND	ND	ND	ND	ND	USGS Map 1:250,000 Death Valley M, 77	
36°37′	116°48′	29N/02E-30			2,000	610	ND	ND	ND	ND	ND	USGS Map 1:250,000 Death Valley M, 77	
ALKALI FLAT-FURNACE CREEK RANCH SUBBASIN (NEVADA)													
36 25 40	116 24 50	17S/49E-35d1	Ash Tree	ND	2,175	663	9	0.57	74	23	ND	T&R, 71 W&T, 75	
36 48 07	116 05 13	ND	Cane	Tertiary igneous	4,060	1,286	2	0.13	64	18	Unused	T&R, 71 W&T, 75	Perched (Wahmonie Formation) (W&T, 75)[c]
36 53 00	116 45 00	12S/47E-20bb1		ND	3,200	975	ND	ND	ND	ND	Irrigation	T&R, 71	
36 53 10	116 45 00	12S/47E-20bbb		ND	3,200	975	100	6.31	71	22	Irrigation	T&R, 71	

Latitude	Longitude	Township and range, spring location number	Name[a]	Aquifer[b]	Elevation ft	Elevation m	Discharge gpm	Discharge L/s	Temperature °F	Temperature °C	Use	Reference[c]	Comments
						OASIS VALLEY SUBBASIN (continued)							
36 57 00	116 47 50	11S/46E-26ca-1	Middle Indian	Tertiary igneous	4,150	1,265	ND	ND	60	16	Municipal	T&R, 71 M&E, 62	Perched (W et al., 84)[c]; Beatty Municipal Supply (Gram, 1985)
36 57 10	116 48 20	11S/46E-26cbb-1	Upper Indian	Tertiary igneous	4,200	1,280	5	0.32	80	27	Municipal	T&R, 71 M&E, 62	Perched (W et al., 84)[c]; Beatty Municipal Supply (Gram, 1985)
36 57 00	116 43 00	11S/47E-28dac-1		Tertiary-Quaternary alluvium	3,480	1,061	35	2.21	70	21	Irrigation	T&R, 71	
36 57 30	116 43 10	11S/47E-28aa-2	Ute	Quaternary alluvium	3,540	1,109	25	1.58	70	21	Irrigation	T&R, 71 W, 79	
36 57 50	116 43 20	11S/47E-21dbb-2		Tertiary-Quaternary alluvium	3,550	1,082	37	2.33	79	26	Domestic	T&R, 71	
36 58 20	116 43 10	11S/47E-21aba-2	(Hicks?) (Bailey?)	Tertiary alluvium	3,600	1,097	ND	ND	106	41	Public	T&R, 71	
36 58 30	116 43 20	11S/47E-16dcd-2	Burro Hot	Tertiary igneous	3,600	1,097	5	0.32	98	37	Public	T&R, 71 M&E, 62	
36 58 30	116 43 20	11S/47E-16dcd-1	Burro Hot	Tertiary igneous	3,600	1,097	ND	ND	98	37	Domestic	T&R, 71	
36 59 10	116 45 30	11S/47E-18acb	Crystal	Tertiary igneous	3,960	1,207	2	0.13	75	24	Domestic	T&R, 71 M&E, 62	
36 59 30	116 42 50	11S/47E-10ccb		Tertiary-Quaternary alluvium	3,650	1,113	ND	ND	70	21	Stock	T&R, 71	
36 59 30	116 42 50	11S/47E-10ccb		Tertiary igneous	3,680	1,122	ND	ND	65	18	Domestic	T&R, 71	
36 59 40	116 42 30	11S/47E-10bdd		Tertiary igneous	3,800	1,158	49	3.09	75	24	Irrigation	T&R, 71	
37 00 00	116 42 20	11S/47E-10ab-1	Goss	Tertiary igneous	3,800	1,158	50	3.15	71	22	Irrigation	T&R, 71	

Table 3-5. Springs, seeps, and phreatophyte areas in the hydrogeologic study area (page 7 of 12)

Latitude	Longitude	Township and range, spring location number	Name[a]	Aquifer[b]	Elevation		Discharge		Temperature		Use	Reference[c]	Comments
					ft	m	gpm	L/s	°F	°C			
					OASIS VALLEY SUBBASIN (continued)								
37 00 20	116 42 30	11S/47E-03cdb-1		Tertiary igneous	3,840	1,170	40	2.52	73	23	Irrigation	T&R, 71	
37 00 30	116 42 30	11S/47E-04cad		Tertiary-Quaternary alluvium	3,680	1,122	10	0.63	70	21	Irrigation	T&R, 71	
37 00 50	116 43 50	11S/47E-04bb-1		ND	3,720	1,134	7	0.44	65	18	Domestic	T&R, 71	
37 01 40	116 43 20	10S/47E-33abc		Tertiary igneous	3,680	1,122	255	16.09	72	22	Irrigation	T&R, 71	
37 01 50	116 45 10	10S/47E-31aab-1		Tertiary-Quaternary alluvium	3,840	1,170	11	0.69	67	19	Irrigation	T&R, 71	
37 02 00	116 45 20	10S/47E-30d-1		ND	3,850	1,173	25	1.58	58	14	Domestic	T&R, 71	
37 04 30	116 41 30	10S/47E-14bab		Tertiary-Quaternary alluvium	3,182	970	100	6.31	84	29	Irrigation	T&R, 71	
37 37 10	116 43 40	04S/47E-04ca	Antelope	Tertiary alluvium	6,220	1,896	0.4	0.025	53	12	Unused	T&R, 71	
36 59 40	116 51 20	11S/46E-08bdc	Mud	Tertiary-Quaternary alluvium	4,244	1,294	ND	ND	67	19	Stock	T&R, 71	
		12S/47E-20bb1		ND	ND	ND	ND	ND	ND	ND	Irrigation, domestic	M&E, 62	
		11S/47E-7dc1		ND	ND	ND	ND	ND	ND	ND	ND	M&E, 62	
		10S/47E-30d1		ND	ND	ND	25	1.58	58	14	Domestic, stock	M&E, 62	
		10S/47E-32dda		Quaternary alluvium	ND	ND	225	14.19	72	22	ND	W, 79	
					ASH MEADOWS SUBBASIN								
36 26 00	116 18 30	17S/50E-35a1		Lower carbonate aquifer	2,328	710	140	8.83	92	33	ND	T&R, 71 W&T, 75	Ash Meadows

Table 3-5. Springs, seeps, and phreatophyte areas in the hydrogeologic study area (page 8 of 12)

Latitude	Longitude	Township and range, spring location number	Name[a]	Aquifer[b]	Elevation ft	Elevation m	Discharge gpm	Discharge L/s	Temperature °F	Temperature °C	Use	Reference[c]	Comments
ASH MEADOWS SUBBASIN (continued)													
36 26 10	116 18 50	17S/50E-35b1		Lower carbonate aquifer	2,305	703	17	1.07	83	28	ND	T&R, 71 W&T, 75	Ash Meadows
36 27 50	116 19 00	17S/50E-23b1	(Five Springs Area ?)	Lower carbonate aquifer	2,345	715	193	12.18	94	34	ND	T&R, 71 D&L, 76 W&T, 75	Ash Meadows
36 28 00	116 19 30	17S/50E-22a1	Longstreet	Lower carbonate aquifer	2,305	703	1,042	65.74	82	28	ND	T&R, 71 W&T, 75	Ash Meadows
36 28 50	116 19 30	17S/50E-15a1	Rogers	Lower carbonate aquifer	2,270	692	736	46.43	92	33	ND	T&R, 71 W&T, 75	Ash Meadows
36 29 20	116 20 10	17S/50E-10c1	Bell (Soda)	Lower carbonate aquifer	2,272	693	79	4.98	73	23	ND	T&R, 71 W&T, 75	Ash Meadows
36 29 20	116 20 30	17S/50E-09a1	Fairbanks	Lower carbonate aquifer	2,280	695	1,715	108.2	81	27	ND	T&R, 71 W&T, 75	Ash Meadows
		17S/50E-22ac	McGillivary	Lower carbonate aquifer	2,300	701	See comments		ND	ND	ND	D&L, 76	Ash Meadows; flow reported in 1986 @ 155 gpm; no flow observed in 1971; water level 5 ft below outlet
		17S/50E-35acc	Scruggs	Lower aquifer	2,360	719	60	3.78	91	33	ND	D&L, 76	Ash Meadows
		17S/50E-35d1	School	Lower carbonate aquifer	2,360	719	6	0.38	94	34	ND	D&L, 76	Ash Meadows
		18S/50E-01ca	Collins	Lower carbonate aquifer	2,360	719	10	0.63	78	26	ND	D&L, 76	Ash Meadows

Table 3-5. Springs, seeps, and phreatophyte areas in the hydrogeologic study area (page 9 of 12)

Latitude	Longitude	Township and range, spring location number	Name[a]	Aquifer[b]	Elevation ft	Elevation m	Discharge gpm	Discharge L/s	Temperature °F	Temperature °C	Use	Reference[c]	Comments
ASH MEADOWS SUBBASIN (continued)													
		18S/50E-12dc	Sink	Lower carbonate aquifer	2,260	689	See comments		ND	ND	ND	D&L, 76	Ash Meadows; flow observed @ 25 gpm in 1986; no flow observed in 1971; water level 3 ft below outlet
ND	ND	17S/50E-21ac	Cold	Lower carbonate aquifer	ND	ND	73	4.60	67	20	ND	D&L, 76	Ash Meadows
36 25 10	116 19 20	18S/50E-03a	Crystal Pool	Lower carbonate aquifer	2,197	670	2,820	177.91	91	33	ND	W&T, 75 T&R, 71	Ash Meadows
36 24 50	115 44 20	18S/55E-01d	Cold Creek	Tertiary-Quaternary alluvium	6,220	1,896	690	43.53	ND	ND	Domestic	T&R, 71	
36 25 00	115 45 50	18S/55E-02a	Willow	Tertiary-Quaternary alluvium	5,990	1,826	340	21.45	ND	ND	ND	T&R, 71	
36 26 40	115 55 40	17S/54E-29d	Big Timber	Cambrian sedimentary	6,720	2,048	ND	ND	ND	ND	ND	T&R, 71	
36 18 30	115 41 10	19S/56E-10c	Three	Cambrian limestone	8,700	2,652	21	1.32	ND	ND	ND	T&R, 71	Spring Mountains
36 19 10	115 40 40	19S/56E-03c	Scout Canyon	Ordovician limestone	8,470	2,582	11	0.69	ND	ND	ND	T&R, 71	Spring Mountains
36 21 30	116 16 20	18S/51E-30d	Last Chance	Lower carbonate aquifer	2,253	687	1	0.063	68	20	ND	T&R, 71 W&T, 75	Ash Meadows
36 21 50	116 15 40	18S/51E-29b		Lower carbonate aquifer	2,275	693	1	0.063	72	22	ND	T&R, 71 W&T, 75	Ash Meadows
36 21 50	116 16 10	18S/51E-30a1	Bole	Lower carbonate aquifer	2,245	684	12	0.76	72	22	ND	T&R, 71 W&T, 75	Ash Meadows

Table 3-5. Springs, seeps, and phreatophyte areas in the hydrogeologic study area (page 10 of 12)

Latitude	Longitude	Township and range, spring location number	Name[a]	Aquifer[b]	Elevation ft	Elevation m	Discharge gpm	Discharge L/s	Temperature °F	Temperature °C	Use	Reference[c]	Comments
ASH MEADOWS SUBBASIN (continued)													
36 22 30	116 16 20	18S/51E-19a1	Big (Deep) (Ash Meadows)	Lower carbonate aquifer	2,239	682	1,036	65.36	83	28	ND	T&R, 71 W&T, 75	Ash Meadows
36 23 20	116 16 40	18S/51E-18b1	Jack Rabbit	Lower carbonate aquifer	2,270	692	587	37.03	82	28	ND	T&R, 71 W&T, 75	Ash Meadows
36 24 00	116 18 00	18S/50E-12c1		Lower carbonate aquifer	2,245	684	11	0.69	80	27	ND	T&R, 71 W&T, 75	Ash Meadows
36 24 00	116 18 10	18S/50E-11d3	Davis Ranch (Bradford)	Lower carbonate aquifer	2,242	683	30	1.89	72	22	ND	T&R, 71 W&T, 75	Ash Meadows
36 24 10	116 18 10	18S/50E-11d2	Davis Ranch (Bradford)	Lower carbonate aquifer	2,242	683	5	0.32	74	23	ND	T&R, 71 W&T, 75	Ash Meadows
36 24 00	116 18 10	18S/50E-11d1	Davis Ranch (Bradford)	Lower carbonate aquifer	2,242	683	397	25.05	77	25	ND	T&R, 71 W&T, 75	Ash Meadows
36 24 10	116 16 10	18S/51E-07d1	King Pool (Point of Rock)	Lower carbonate aquifer	2,325	709	1,078	68.01	90	32	ND	T&R, 71 W&T, 75	Ash Meadows
36 24 10	116 16 10	18S/51E-07d4	(Point of Rock)	Lower carbonate aquifer	2,325	709	19	1.20	93	34	ND	T&R, 71 W&T, 75	Ash Meadows
36 24 10	116 16 10	18S/51E-07d3	Indian Rock (Point of Rock)	Lower carbonate aquifer	2,325	709	379	23.91	92	33	ND	T&R, 71 W&T, 75	Ash Meadows
36 24 10	116 16 10	18S/51E-07d2	Indian Rock (Point of Rock)	Lower carbonate aquifer	2,325	709	22	1.83	92	33	ND	T&R, 71 W&T, 75	Ash Meadows
36 24 10	116 16 20	18S/51E-07d5	(Point of Rock)	Lower carbonate aquifer	2,310	704	2	0.13	93	34	ND	T&R, 71 W&T, 75	Ash Meadows

Table 3-5. Springs, seeps, and phreatophyte areas in the hydrogeologic study area (page 11 of 12)

Latitude	Longitude	Township and range, spring location number	Name[a]	Aquifer[b]	Elevation ft	Elevation m	Discharge gpm	Discharge L/s	Temperature °F	Temperature °C	Use	Reference[c]	Comments
ASH MEADOWS SUBBASIN (continued)													
36 25 30	116 17 30	17S/50E-36d1	Devils Hole	Lower carbonate aquifer	2,361	720	See comments		93	34	See comments	T&R, 71 D&L, 76 W&T, 75	Ash Meadows. No discharge as flow. Cyprinodon diabolis habitat
36 33 40	115 39 50	16S/56E-16b1	Indian	Tertiary-Quaternary alluvium	3,175	968	430	27.13	78	26	Domestic	T&R, 71	
36 34 30	115 43 40	16S/55E-11a	Cactus	Tertiary-Quaternary alluvium	3,238	987	0.5	0.031	ND	ND	Domestic	T&R, 71	
36 59 10	116 45 30	11S/57E	Quartz	ND	ND	ND	ND	ND	ND	ND	ND	T&R, 71	
37 10 09	116 10 07	ND	Captain Jack	Tertiary igneous	5,490	1,673	0.2	0.013	56	13	Unused	T&R, 71	Perched (S&M, 64)[c]
37 12 13	116 07 54	ND	Whiterock	Tertiary igneous	5,050	1,539	1.0	0.063	48	9	Unused	T&R, 71	Perched (S&M, 64)[c]
37 14 23	116 02 30	ND	Tubb	Tertiary igneous	5,190	1,582	ND	ND	52	11	Unused	T&R, 71	Perched (S&M, 64)[c]
37 14 41	116 04 24	ND	Oak	Tertiary igneous	5,800	1,768	0.1	0.0063	55	13	Unused	T&R, 71	Perched (S&M, 64)[c]
37 31 40	115 56 00	05S/54E-08bc	White Blotch	Tertiary igneous	5,960	1,817	0.2	0.013	42	6	Unused	T&R, 71	
36 27 50	115 57 40	17S/53E-24a	Gold	Cambrian sedimentary	6,780	2,067	ND	ND	ND	ND	ND	T&R, 71	
36 29 10	115 58 20	17S/53E-12c	Rock	Cambrian sedimentary	5,850	1,783	ND	ND	ND	ND	ND	T&R, 71	
36 29 10	115 59 00	17S/53E-11d	Jaybird	Cambrian sedimentary	6,280	1,914	ND	ND	ND	ND	ND	T&R, 71	
36 38 00	115 12 30	ND	Wiregrass	Ordovician dolomite	7,990	2,435	0.5	0.031	ND	ND	ND	T&R, 71	
36 38 50	115 13 50	ND	Pine	Ordovician dolomite	7,360	2,243	ND	ND	ND	ND	ND	T&R, 71	

Table 3-5. Springs, seeps, and phreatophyte areas in the hydrogeologic study area (page 12 of 12)

Latitude	Longitude	Township and range, spring location number	Name[a]	Aquifer[b]	Elevation ft	Elevation m	Discharge gpm	Discharge L/s	Temperature °F	Temperature °C	Use	Reference[c]	Comments
ASH MEADOWS SUBBASIN (continued)													
36 39 30	115 13 10	ND	Canyon	Ordovician dolomite	8,020	2,444	ND	ND	ND	ND	ND	T&R, 71	
36 40 50	115 10 40	ND	Sawmill	Ordovician dolomite	8,140	2,481	ND	ND	ND	ND	ND	T&R, 71	
36 41 30	115 12 30	ND	Basin	Ordovician dolomite	7,950	2,423	ND	ND	ND	ND	ND	T&R, 71	
36 42 20	115 00 50	ND	Perkins	Ordovician dolomite	7,900	2,408	ND	ND	ND	ND	ND	T&R, 71	
36 42 30	115 11 00	ND	Yellow Jacket	Ordovician dolomite	7,750	2,362	ND	ND	ND	ND	ND	T&R, 71	
36 42 30	115 14 20	ND	Whiterock	Ordovician dolomite	5,930	1,807	ND	ND	ND	ND	ND	T&R, 71	
36 42 50	115 10 50	ND	Shalecut	Ordovician dolomite	7,400	2,255	ND	ND	ND	ND	ND	T&R, 71	
36 43 00	115 10 50	ND	Bootleg	Ordovician dolomite	7,200	2,194	ND	ND	ND	ND	ND	T&R, 71	

[a]Blank means the area is not named.
[b]When the discharging aquifer could be determined, it is listed; otherwise only the lithology is shown. The main source of the ground water discharging in the Furnace Creek Ranch area is believed to be the lower carbonate aquifer (Waddell et al., 1984).
[c]P&K, 64 = Pistrang and Kunkel, 1964; M&E, 62 = Malmberg and Eakin, 1962; T&R, 71 = Thordarson and Robinson, 1971; W&T, 75 = Winograd and Thordarson, 1975; D&L, 76 = Dudley and Larson, 1976; M, 77 = Miller, 1977; W, 79 = White, 1979; W et al., 84 = Waddell et al., 1984; S&M, 64 = Schoff and Moore, 1964.
[d]ND = no data.
[e]NA = not applicable.

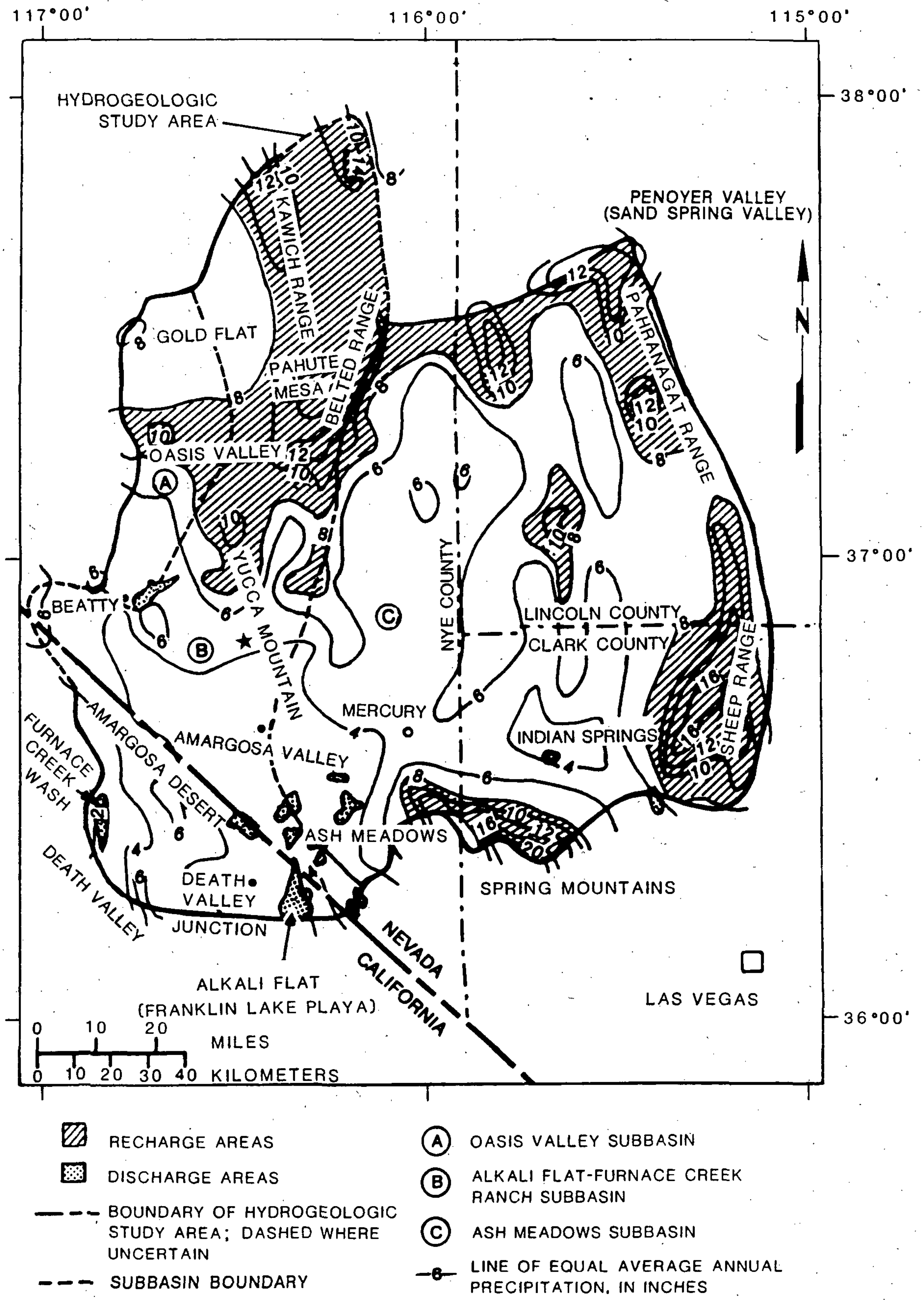

Figure 3-7. Hydrogeologic study area, showing precipitation, recharge areas, and discharge areas. Modified from Winograd and Thordarson (1975), Waddell (1982), and Waddell et al. (1984).

Table 3-6. Magnitude of springs in the hydrogeologic study area, based on Meinzer's[a] classification of spring discharge

Magnitude	Volume of discharge: English units	Volume of discharge: Metric units (L/s)	Number of springs in hydrogeologic study area
1	>100 ft^3/s	>2830	0
2	10-100 ft^3/s	283-2830	0
3	1-10 ft^3/s	28.3-283	9
4	100 gal/min to 1 ft^3/s	6.31-28.3	16
5	10-100 gal/min	0.631-6.31	29
6	1-10 gal/min	0.0631-0.631	20
7	1 pt/min to 1 gal/min	0.0079-0.0631	11
8	<1 pt/min	<0.0079	4

[a]Adapted from Meinzer (1923).

Storm runoff would, most probably, only be affected in the immediate vicinity of the site. For this reason, modification of surface runoff, either in quantity or in chemical quality, is expected to have minimal, if any, impact on vegetation or wildlife. Other potential sources of surface runoff, such as dust-control spraying, are not expected to contribute to either surface or ground waters (DOE, 1986).

Ground water in the hydrogeologic study area is not expected to be contaminated or affected during site characterization activities. Controls over site characterization activities discussed below are considered sufficient to minimize the potential for any contamination of the ground water (DOE, 1986).

No contact is to be made with the water table at Yucca Mountain during site characterization except through exploratory boreholes. All water used for construction of the exploratory shaft will be tagged with a suitable tracer for identification purposes (Whitfield, 1985). Tracers will be used according to accepted procedures (Bedmar, 1983; Rao, 1983). Waste water from surface facilities and the exploratory shaft will be disposed of away from the repository block at either the hypalon-lined waste rock pile, lined evaporative ponds, or through septic tanks. The exploratory shaft will be constructed using established mining techniques and a minimum of tagged water to prevent significant alteration of subsurface conditions. Subsurface construction techniques will be designed to reduce the effects on the hydraulic characteristics of the rock (Sections 2.8.3 and 3.6.4). It is recognized that drilling fluids used in exploratory boreholes will have an effect on the chemical and hydraulic nature of the subsurface environment, including any water samples taken from that hole. These effects have been studied and can be quantified and controlled to some degree (NRC, 1983; Brobst and Buszka, 1986). If drilling mud is used in the drilling of boreholes, waste fluids would be disposed of on the rock pile or in the evaporative ponds. Drilling mud may not be used where vacuum drilling is possible (Whitfield, 1985). This process will not only prevent contamination by drilling fluids but also allow for collection of uncontaminated rock and [illegible]

Table 3-7. Relation of stratigraphic units to hydrogeologic units in the hydrogeologic study area[a] (page 1 of 7)

System	Series	Stratigraphic unit	Major lithology	Maximum thickness (m)	Hydrogeologic unit (underlined) and hydrologic characteristics
Quaternary and Tertiary	Holocene, Pleistocene, and Pliocene deposits	Valley fill	Alluvial fan, fluvial, fanglomerate, lakebed, and mudflow deposits	600	VALLEY FILL AQUIFER Transmissivity ranges from 10 to 400 m^2/d average coefficient of interstitial hydraulic conductivity ranges from 0.21 to 2.9 m/d. Interstitial porosity controls flow of water.
Tertiary	Pliocene	Basalt of Kiwi Mesa	Basalt flows, dense and vesicular	75	LAVA-FLOW AQUIFER Water movement controlled by primary and secondary fractures and possibly by rubble between intercrystalline porosity and conductivity negligible; estimated transmissivity ranges from 4.2 to 1,200 m^2/d; saturated only beneath east-central Jackass Flats.
		Rhyolite of Shoshone Mountain	Rhyolite flows	600	
		Basalt of Skull Mountain	Basalt flows	75	
	?[b]	Thirsty Canyon Tuff	Ash-flow tuff, partially to densely welded; trachytic lava flows	230	No corresponding hydrologic unit. Generally unsaturated; present beneath Black Mountain, northwestern part of the basin.
	Miocene[c]	Piapi Canyon Group, Timber Mountain Tuff, Ammonia Tank Member	Ash-flow tuff, moderately to densely welded; thin ash-fall tuff at base	75	WELDED AND BEDDED TUFF AQUIFER Water movement controlled by primary and secondary joints in densely welded part of ash-flow tuff; transmissivity ranges from 1 to 1,200 m^2/d; intercrystalline porosity and conductivity negligible; nonwelded part of ash-flow tuff, where present, has relatively high
		Piapi Canyon Group, Timber Mountain Tuff, Rainier Mesa Member	Ash-flow tuff, nonwelded to densely welded; thin ash-fall tuff at base	175	

Table 3-7. Relation of stratigraphic units to hydrogeologic units in the hydrogeologic study area[a] (page 2 of 7)

System	Series	Stratigraphic unit		Major lithology	Maximum thickness (m)	Hydrogeologic unit (underlined) and hydrologic characteristics
Tertiary	Miocene	Piapi Canyon Group	Tiva Canyon Member	Ash-flow tuff, nonwelded to densely welded; thin ash-fall tuff near here	90-100	interstitial porosity (35 to 50%) and modest hydraulic conductivity (0.08 m/d) and may act as a leaky aquitard; saturated only beneath deeper parts of Yucca, Frenchman, and Jackass Flats.
		Paintbrush Tuff	Topopah Spring Member	Ash-flow tuff, nonwelded to densely welded; thin ash-fall tuff near base	275	
			Bedded tuff (informal unit)	Ash-flow tuff and fluvially reworked tuff	300	Transmissivity ranges from 2 to 10 m^2/d; saturated only beneath structurally deepest parts of Yucca, Frenchman, and Jackass Flats; occurs locally below ash-flow tuff members of Paintbrush Tuff and below Grouse Canyon Member of Belted Range Tuff.
				Lava-flow and interflow	1,200	LAVA-FLOW AND TUFF AQUITARD

Table 3-7. Relation of stratigraphic units to hydrogeologic units in the hydrogeologic study area[a] (page 3 of 7)

System	Series	Stratigraphic unit		Major lithology	Maximum thickness (m)	Hydrogeologic unit (underlined) and hydrologic characteristics
Tertiary	Miocene[c]	Salyer Formation		Breccia flow, lithic breccia, and tuff breccia, all interbedded with ash-fall tuff, sandstone, siltstone, claystone, matrix commonly clayey or zeolitic	600	fractures, interstitial conductivity probably controls regional ground-water movement; perches minor quantities of water beneath foothills flanking valleys; fully saturated only beneath structurally deepest parts of Yucca, Frenchman, and Jackass flats; Grouse Canyon and Tub Spring members of Belted Range Tuff may locally be aquifers in northern Yucca Flat.
		Belted Range Tuff	Grouse Canyon Member	Ash-flow tuff, densely welded	60	
			Tub Spring Member	Ash-flow tuff, nonwelded to welded	90	
		Local Informal Units		Ash-fall bedded tuff, nonwelded to semiwelded ash-flow tuff, tuffaceous sandstone. Siltstone, and claystone; all massively altered to zeolite or clay minerals; locally minor welded tuff near base; minor rhyolite and basalt.	600	

Table 3-7. Relation of stratigraphic units to hydrogeologic units in the hydrogeologic study area[a] (page 4 of 7)

System	Series	Stratigraphic unit	Major lithology	Maximum thickness (m)	Hydrogeologic unit (underlined) and hydrologic characteristics
Tertiary	Miocene[c]	Rhyolite flows and tuffaceous beds of Calico Hills	Rhyolite, nonwelded and welded ash flow, ash-fall tuff, tuff breccia, tuffaceous sandstone; hydrothermally altered at Calico Hills; matrix of tuff and sandstone commonly clayey or zeolitic	600	TUFF AQUIFER/AQUITARD Rhyolite lavas and ash flows may be transmissive. Bedded tuffs may be zeolitized or argillized and less transmissive. Beneath Yucca Mountain the tuffaceous beds of Calico Hills are mostly unsaturated.
		Crater Flat Tuff: Prow Pass Member, Bullfrog Member, Tram Member	Ash-flow tuff, nonwelded to moderately welded, interbedded with ash-fall bedded tuff; matrix commonly clayey or zeolitic	>600	TUFF AQUIFER/AQUITARD Transmissivity ranges from less than 0.1 to several hundred m^2/d. Interstitial hydraulic conductivity is small (8×10^{-4} to 3×10^{-1} m/d). At Yucca Mountain, unit commonly contains the water table.
		Lithic Ridge Tuff	Ash-flow tuff, partially to densely welded. Commonly argillized	300	TUFF AQUITARD Not well characterized. Transmissivity about 2×10^{-4} m^2/d. Interstitial hydraulic conductivity low (3×10^{-4} to 6×10^{-5} m/d).
Tertiary	Miocene (?) Oligocene (?)	Older tuffs and lavas beneath Yucca Mountain	Altered rhyolitic and quartz latitic lavas, and altered bedded and ash-flow tuffs	?	
	Miocene and Oligocene	*Rocks of Pavits Spring*	Tuffaceous sandstone and siltstone, claystone; fresh water limestone and conglomerate; minor gypsum; matrix commonly clayey, zeolitic, or calcerous	425	See Salyer Formation.

Table 3-7. Relation of stratigraphic units to hydrogeologic units in the hydrogeologic study area[a] (page 5 of 7)

System	Series	Stratigraphic unit	Major lithology	Maximum thickness (m)	Hydrogeologic unit (underlined) and hydrologic characteristics
Tertiary (continued)	Oligocene	Horse Spring Formation	Fresh-water limestone, conglomerate, tuff	300	See Salyer Formation
Cretaceous to Permian		Granitic stocks	Granodiorite and quartz monzonite in stocks, dikes and sills	--[d]	(A MINOR PLUTONIC-ROCK AQUITARD) Complexly fractured but nearly impermeable.
Permian and Pennsylvanian		Tippipah Limestone	Limestone	1,100	UPPER CARBONATE AQUIFER Complexly fractured aquifer; transmissivity estimated in range from 10 to 1,250 m^2/d; intercrystalline porosity and permeability negligible, saturated only beneath western one-third of Yucca Flat.
Mississippian and Devonian		Eleana Formation	Argilliate, quartzite, conglomerate, limestone	2,400	UPPER CLASTIC AQUITARD Complexly fractured but nearly impermeable; transmissivity estimated less than 5 m^2/d; interstitial permeability negligible but owing to poor hydraulic connection of fractures probably controls ground-water movement; saturated only beneath western Yucca and Jackass Flats; interstitial porosity ranges from 2.0 to 18%.

Table 3-7. Relation of stratigraphic units to hydrogeologic units in the hydrogeologic study area[a] (page 6 of 7)

System	Series	Stratigraphic unit	Major lithology	Maximum thickness (m)	Hydrogeologic unit (underlined) and hydrologic characteristics
Devonian	Upper	Devils Gate Limestone	Limestone, dolomite, minor	>425	LOWER CARBONATE AQUIFER
[illegible]	[illegible]	[illegible]	[illegible]	[illegible]	[illegible]
	---?---				out eastern Nevada; transmissivity ranges from 10 to 10,000 m^2/d; intercrystalline porosity, 0.4 to 12%; intercrystalline hydraulic conductivity, 9×10^{-7} to 4×10^{-3} m/d; solution caverns are present locally but regional ground-water movement is controlled by fracture transmissivity;
	Middle	Nevada Formation	Dolomite		
Devonian and Silurian		Undifferentiated	Dolomite	430	
	Upper	Ely Springs Dolomite	Dolomite	90	

Table 3-7. Relation of stratigraphic units to hydrogeologic units in the hydrogeologic study area[a] (page 7 of 7)

		Stratigraphic	Major	Maximum thickness	Hydrogeologic unit (underlined)
Cambrian	Middle	Bonanza King Formation			
		Banded Mountain Member	Limestone, dolomite, minor siltstone	750	
		Papoose Lake Member	Limestone, dolomite, minor siltstone	650	
	Lower	Carrara Formation	Siltstone, limestone, interbedded (upper part predominantly limestone; lower part predominantly siltstone	320 290	
Precambrian		Zabriskie Quartzite	Quartzite	70	LOWER CLASTIC AQUITARD Complexly fractured but nearly impermeable; supplies no major springs; transmissivity less than 10 m^2/d; interstitial porosity and permeability is negligible but probably controls ground-water movement owing to poor hydraulic connection of fractures; saturated
		Wood Canyon Formation	Quartzite, siltsone, shale minor dolomite	700	
		Stirling Quartzite	Quartzite, siltstone	1025	
		Johnnie Formation	Quartzite, sandstone, siltstone, minor limestone and dolomite	975	

area is sufficient to define regional hydrogeologic units and their general properties. No additional activities are designed to specifically refine the existing definition. However, the results of many of the planned activities will generate data that will help to further refine the level of knowledge about the regional hydrogeologic system.

3.6.1.1 <u>Definition</u>

A hydrogeologic unit (also referred to as a geohydrologic unit), as defined by Bates and Jackson (1980), is a geologic unit with consistent hydraulic properties such that the unit may be classified as an aquifer, confining layer (aquiclude or aquitard), or a combination of both, making up a framework for a reasonably distinct hydraulic system. The definition of a hydrogeologic unit is usually based on stratigraphic or lithologic characteristics, but as pointed out by Montazer and Wilson (1984), it may also be

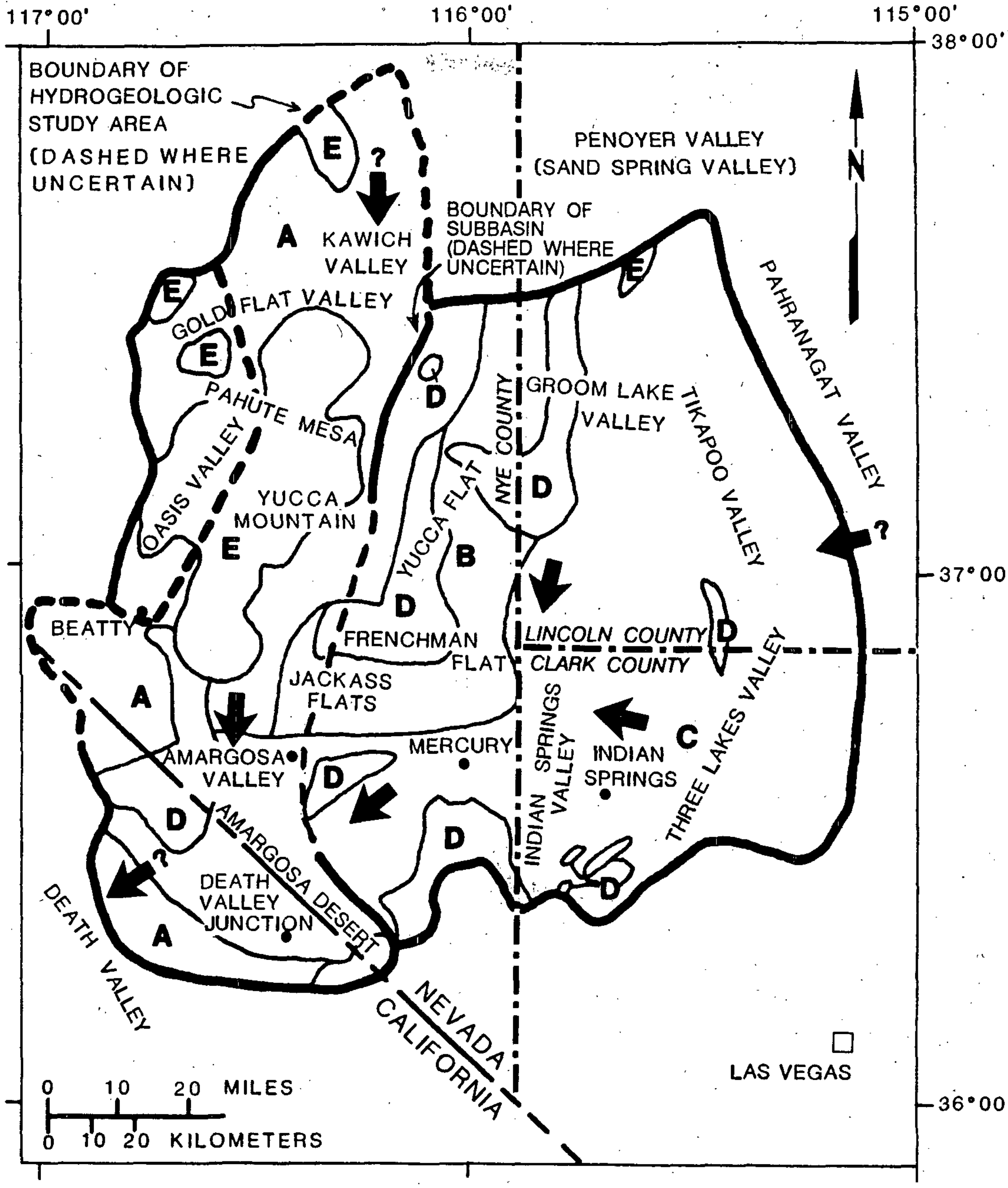

GENERAL DIRECTION OF REGIONAL GROUND-WATER FLOW (QUESTION MARK INDICATES UNCERTAINTY)

A. VOLCANIC ROCK AQUIFERS AND AQUITARDS OVERLYING CLASTIC AQUITARDS OR LOWER CARBONATE AQUIFER
B. VOLCANIC ROCK AQUIFERS AND AQUITARDS OVERLYING LOWER CARBONATE AQUIFER
C. LOWER CARBONATE AQUIFER
D. CLASTIC AQUITARDS
E. VOLCANIC ROCK AQUIFER AND AQUITARDS OF CALDERAS

NOTE: FOR CLARITY, VALLEY FILL AQUIFER NOT SHOWN

Figure 3-8. Generalized distribution of uppermost hydrogeologic units in the saturated zone of the region.

3.6.1.4 Volcanic rock aquifers and aquitards

Volcanic rocks that occur in the region are of Tertiary age and consist of nonwelded to welded ash-flow tuffs and basaltic and rhyolitic flows (Table 3-7). Because of the complex stratigraphy of these volcanics, individual rock types are not differentiated on a regional scale. The aggregate thickness of this unit is not known, but in places it exceeds several thousand meters. These volcanics form the uppermost water-bearing unit throughout most of the northwestern part of the hydrogeologic study area (Figure 3-8).

3.6.1.5 Upper carbonate aquifer

The Tippipah Limestone of Pennsylvanian and Permian age constitutes the upper carbonate aquifer (Table 3-7). Although this unit is as much as 1,100 m thick, it is of minor regional hydrologic significance because it probably is saturated only beneath western Yucca Flat.

3.6.1.6 Upper clastic aquitard

The Eleana Formation of Devonian and Mississippian age constitutes the upper clastic aquitard. This unit comprises primarily argillite with minor quartzite and limestone (Table 3-7). The upper clastic aquitard acts as a confining unit separating the upper carbonate aquifer from the lower carbonate aquifer beneath western Yucca Flat and northern Jackass Flats. In these areas, the upper clastic aquitard is more than 2,400 m thick.

3.6.1.7 Lower carbonate aquifer

The lower carbonate aquifer comprises limestone in the upper part of the Cambrian Carrara Formation and the overlying limestones and dolomites of Cambrian through Devonian age (Table 3-7). The limestones of this aquifer occur extensively in the eastern part of the hydrogeologic study area and are a major regional aquifer. In places the thickness of this aquifer exceeds 4,700 m.

3.6.1.8 Lower clastic aquitard

Siltstone, quartzite, shale, and sandstone of Precambrian through early Cambrian age comprise the lower clastic aquitard (Table 3-7). Thicknesses greater than 3,000 m of these rocks occur within the hydrogeologic study area. The lower clastic aquitard is an important regional unit because it probably significantly affects the distribution of hydraulic potential and the locations of ground-water discharge areas.

3.6.1.9 Spatial relationships of units

The spatial relationships of these units are primarily a result of the depositional history of the sedimentary rocks, the volcanic history of the area, and the complex structural evolution of the region. The rocks of the lower clastic aquitard and lower carbonate aquifer were deposited in a miogeocline in thick accumulations (Stewart and Poole, 1974). In middle Paleozoic time, a sequence composed of generally poor water-transmitting siliceous clastic rocks was thrust eastward about 150 km along the Roberts Mountains thrust. These rocks now overlie a sequence composed mostly of relatively soluble, water-transmitting carbonate rocks. Subsequent deposition of rocks forming the upper clastic aquitard and upper carbonate aquifer occurred, followed by additional structural activity. In the Tertiary, volcanic activity resulted in the formation of the volcanic rock aquifers and aquitards. More recent geomorphic processes resulted in the deposition of the valley fill aquifer and unsaturated valley fill over these rocks.

3.6.2 RELATIONSHIP AMONG HYDROGEOLOGIC UNITS

Because of the complex geologic history, ground-water flow relationships within and between the hydrogeologic units are also complex. Present data are sufficient only to allow preliminary generalizations of these relationships. The valley fill aquifer lacks lateral continuity. Ground water in the valley fill aquifer in the northeastern part of the hydrogeologic study area has a downward component of flow resulting in leakage of ground water into the underlying aquifers (Winograd and Thordarson, 1975).

Where several aquifers and aquitards are present, such as beneath Yucca Flat, hydraulic heads generally decrease with depth indicating downward leakage toward the lower carbonate aquifer (Winograd and Thordarson, 1975). Near Yucca Mountain, on the other hand, the reverse is true, and an upward hydraulic gradient occurs (Waddell et al., 1984). The upward gradient in this area is discussed in Section 3.9.3.

Although both upward and downward components of interunit flow occur, the primary component of ground-water flow, in a regional scale, is lateral. With respect to detailed characterization of the Yucca Mountain area, knowledge of the distribution of vertical hydraulic gradients is important. [illegible]

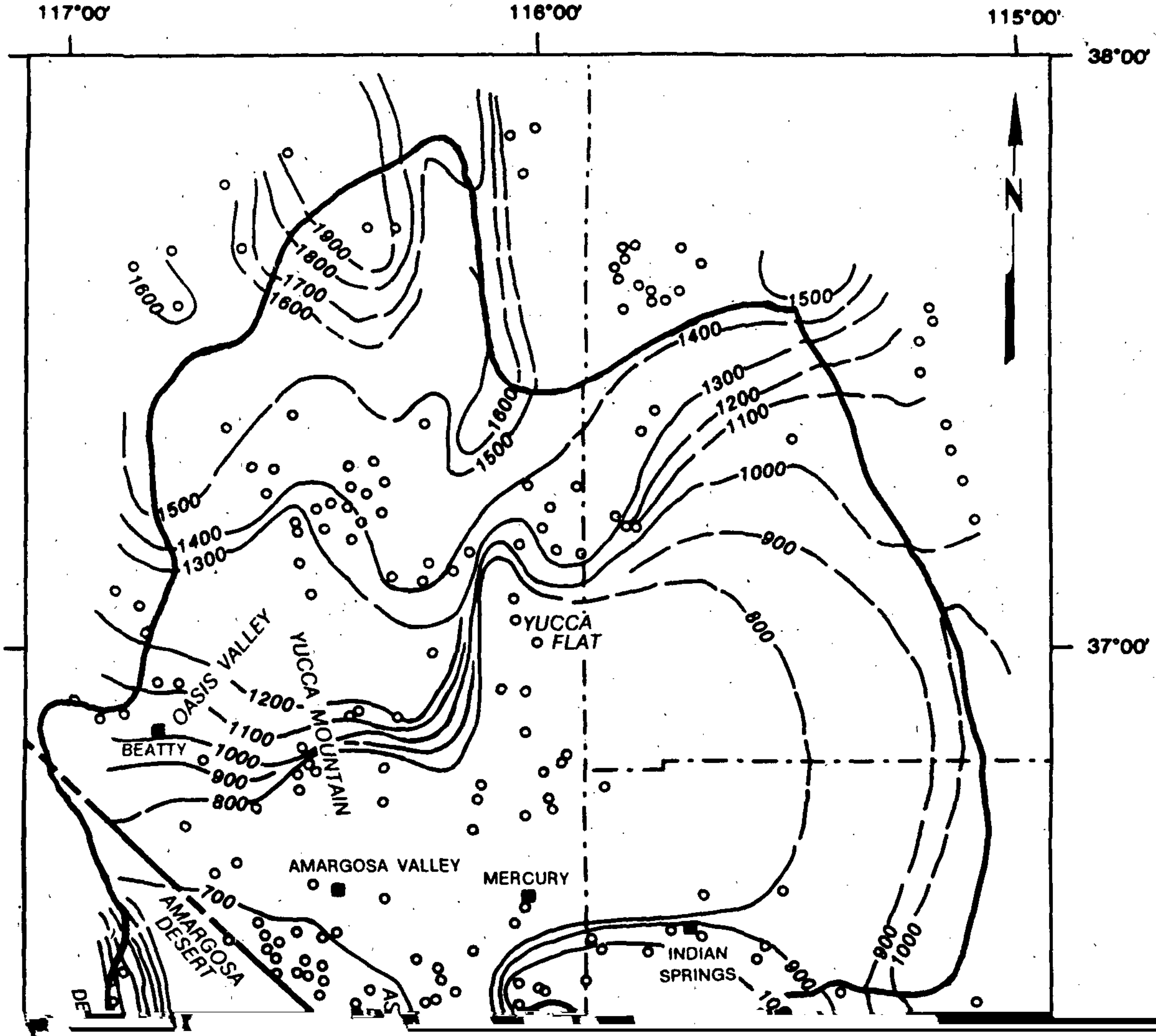
117°00'
116°00'
115°00'
38°00'
37°00'
N
1900
1800
1700
1600
1500
1400
1300
1200
1100
1000
900
800
700
OASIS VALLEY
YUCCA MOUNTAIN
YUCCA FLAT
BEATTY
AMARGOSA VALLEY
MERCURY
AMARGOSA DESERT
INDIAN SPRINGS

regional potentiometric surface. Sources of potentiometric data include Eakin et al. (1963), Malmberg (1967), Mifflin (1968), Winograd and Thordarson (1968), Rush (1970), Thordarson and Robinson (1971), Naff et al. (1974), Winograd and Thordarson (1975), Miller (1977), Harrill (1982), Waddell (1982), Czarnecki and Waddell (1984), and Robison (1984, 1986). Specific construction information for these wells is provided in the cited references and are not included here. The equipotential lines shown on Figure 3-9 are based upon composite water levels from several hydrogeologic units and are averages of the hydraulic heads in the boreholes.

The altitude of the potentiometric surface ranges from over 1,900 m above MSL in the northernmost part of the hydrogeologic study area to below sea level in Death Valley. Steep hydraulic gradients occur in several areas, including north of Yucca Mountain, near Death Valley, southeast of Mercury, and north of Yucca Flat. These steep gradients may be due to stratigraphic, structural, or hydraulic conditions, or to a combination of these conditions. Thermal conditions could also affect gradients, but preliminary analyses indicate that such effects probably are not significant influences on these steep gradients. The definition of areas of steep gradients and evaluation of the causes of these gradients are important considerations in determining ground-water flow paths and velocities. Additional syntheses and modeling of the regional hydrogeologic system will be performed as part of site characterization activities (Section 8.3.1.2.1.2). Two-dimensional and three-dimensional models of ground-water flow and sensitivity analyses performed during these studies will help to assess the relative importance of these steep gradients in the overall characterization of regional flow conditions.

The potentiometric data needed to establish temporal histories of variations in the potentiometric surface are available in selected areas, including Yucca Mountain, Amargosa Desert, Ash Meadows, and Franklin Lake playa. Collection of additional data is planned as part of the characterization of the regional ground-water flow system (Section 8.3.1.2.1.2). This data collection will include (1) regional potentiometric level studies to identify and compile additional data, (2) the expansion of the existing monitoring well network, and (3) local water-level monitoring.

3.6.4 HYDRAULIC CHARACTERISTICS OF PRINCIPAL HYDROGEOLOGIC UNITS

This section provides information on the hydraulic characteristics of the hydrogeologic units. The capability of the various regional hydrogeologic units to store and transmit ground water is a function of their hydraulic properties. Estimates of ground-water flow paths and velocities require that the hydraulic characteristics of each of the important hydrogeologic units be known. The principal hydraulic characteristics discussed are transmissivity, porosity, and both interstitial and fracture hydraulic conductivity.

Information on the hydraulic properties of the principal regional units is listed in Tables 3-7 and 3-8. These data are based on information published by Winograd (1962a,b), Blankennagel and Weir (1973), Winograd and Thordarson (1975), and Lin (1978). Transmissivity estimates are based upon aquifer testing. In many instances, transmissivity was estimated from

Table 3-8. Pumping-test data for aquifers in Nevada Test Site and vicinity[a] (page 1 of 4)

Stratigraphic	Depth interval	Thick- ness	penetration of aquifer	Hydraulic	to static water level	(L/s per meter of	from specific	from drawdown	from recovery

Table 3-8. Pumping-test data for aquifers in Nevada Test Site and vicinity[a] (page 2 of 4)

Well	Stratigraphic unit	Depth interval (m)	Thick-ness (m)	Estimated penetration of aquifer (%)	Hydraulic setting	Depth to static water level (m)	Specific capacity (L/s per meter of drawdown)[b]	Transmissivity (m^2/d) Estimated from specific capacity	Calculated from drawdown curve	Calculated from recovery curve	Remarks
73-66	Silurian (?) dolomite	956-1,036	80	<5	Confined	529	6.21±	740	--	--	Density changes in water column, due to anomalously high water temperature, completely masked water-level fluctuations due to pumping. Air-line measurements permitted approximation of specific capacity.
87-62	Devils Gate Limestone and Nevada Formation undifferentiated	1,128-1,280	172	<20	Confined	600	0.17	12	--	43	--
84-68d	Devonian (?) dolomite and calcareous quartzite	860-922	62	<5	Confined	596	0.08	9	30	--	--
					BEDDED-TUFF AQUIFER						
81-67	Bedded tuff (?) of Piapi Canyon Group	514-549	35	--	Confined	478	0.19	12	16	26	Aquifer is probably bedded tuff or nonwelded ash-flow tuff.
90-74	Bedded tuff (?) of Piapi Canyon Group	149-204	55	--	Unconfined (?)	149	0.08	2	--	--	Constant-rate pumping test not made; specific capacity based on measurements made after 90 min pumping; aquifer is probably bedded tuff or non-welded ash-flow tuff.
90-75	Bedded tuff (?) of Piapi Canyon Group	273-333	59	--	Unconfined (?)	273	0.12	5	--	--	Constant-rate pumping test not made; specific capacity reported after 30 min of pumping; aquifer is probably bedded tuff or nonwelded ash-flow tuff.

Table 3-8. Pumping-test data for aquifers in Nevada Test Site and vicinity[a] (page 3 of 4)

Well	Stratigraphic unit	Depth interval (m)	Thick-ness (m)	Estimated penetration of aquifer (%)	Hydraulic setting	Depth to static water level (m)	Specific capacity (L/s per meter of drawdown)[b]	Transmissivity (m^2/d) Estimated from specific capacity	Calculated from drawdown curve	Calculated from recovery curve	Remarks
					WELDED-TUFF AQUIFER						
75-58	Topopah Spring Member of Paintbrush Tuff	226-270	45	40	Confined (?)	226	11.6	1,240	See remarks	See remarks	Drawdown of 2.1 m measured with air line and test pressure gage in first 3 min of pumping test at rate of 24.4 L/s. Additional drawdown not detectable in subsequent 57 min of pumping test.
74-57	Topopah Spring Member of Paintbrush Tuff	283-444	161	100	Confined (?)	283	4.6	500	850	--	Step-drawdown analysis suggests considerable head losses at face of bore; losses are probably due to poor gun perforation of casing.
81-69	Topopah Spring Member of Paintbrush Tuff	459-511	51	100	Confined (?)	457	0.02	2.5	See remarks	0.6	Well tested by bailing.
					LAVA-FLOW AND WELDED-TUFF AQUIFERS						
74-61	Basalt of Kiwi Mesa	317-351	34	100	Unconfined	317	0.52	50	350	--	Combined test of lava-flow and welded-tuff aquifers. Mesurements made with test pressure gage and air line.
	Topopah Spring Member of Paintbrush Tuff	351-465	55	45	Confined	--	--	--	--	--	--
					VALLEY-FILL AQUIFER						
74-70b	Valley fill	210-366	156	60	Unconfined	210	0.35	12	30	31	Value of 21 m^2/d from recovery during 133-day shutdown; other values from 48-hour pumping test.

Table 3-8. Pumping-test data for aquifers in Nevada Test Site and vicinity[a] (page 4 of 4)

Well	Stratigraphic unit	Depth interval (m)	Thick-ness (m)	Estimated penetration of aquifer (%)	Hydraulic setting	Depth to static water level (m)	Specific capacity (L/s per meter of drawdown)[b]	Transmissivity (m^2/d) Estimated from specific capacity	Calculated from drawdown curve	Calculated from recovery curve	Remarks
74-70a	Valley fill	208-274	66	15	Unconfined	208	0.83	37	95	136	--
75-72	Valley fill	218-265	48	--	Unconfined	218	0.27	10	--	--	Specific capacity and static water level reported by driller.
83-68	Valley fill	489-570	80	80-100	Unconfined	185	0.39	12	160	150	--
91-74	Valley fill	33-113	80	100	Unconfined	33	2.48	120	--	400	Specific capacity after about 211 hours of pumping; driller's log indicates mostly clay below 71.9 m.
91-74a	Valley fill	35-165	130	100	Unconfined	35	6.21	370	--	--	Specific capacity and static water level reported by driller; driller's log suggests chief aquifer in depth interval 34.7-61.0 m.

[a]Modified from Winograd and Thordarson (1975).
[b]Specific capacity computed at 100 min of pumping.
[c]-- indicates no data.
[d]Time drawdown curves in Winograd and Thordarson (1975) indicate a positive boundary of very high transmissivity at 35 min; the "zone" of high transmissivity probably is that tapped by adjacent well 76-69a.
[e](?) indicates data uncertainty.

specific-capacity data from wells. In the absence of other aquifer test data, these estimates are useful to provide minimum values for transmissivity (Winograd and Thordarson, 1975). The porosity and hydraulic conductivity estimates are based upon laboratory studies, including measurements of grain and bulk densities, and mercury-injection and water-saturation methods.

Based upon the results of these tests, the most transmissive unit is the lower carbonate aquifer, which has transmissivity values as large as 900,000 gpd/ft (10,000 m^2/d) (Winograd and Thordarson, 1975). All other aquifers have transmissivities that are at least an order of magnitude smaller. By comparison, the aquitards all have listed values less than about 800 gpd/ft (10 m^2/day).

The transmissivity of the valley-fill aquifer ranges from about 800 gpd/ft to 34,000 gpd/ft (10 to 400 m^2/day) (Winograd and Thordarson, 1975). The saturated thickness data suggest that these transmissivities reflect interstitial hydraulic conductivity ranging from 5 to 70 gpd/ft^2 (0.21 to 2.9 m/day).

The volcanic rocks function locally as either aquifers or aquitards, depending on the presence or absence of open, unsealed fractures. The character of these units at Yucca Mountain, where most of the more recent hydraulic data have been collected, is described in Section 3.9.2.2. The

[illegible]

because the borehole penetrated 1,072 m of the aquitard and the cores resemble examined outcrop specimens. The total porosity of this unit averages about 4 percent and the effective porosity is about 2 percent.

The transmissivity values summarized above are based upon analyses that assume porous media rather than fracture flow conditions and which presume that the ground-water flow in the saturated rocks satisfies Darcy's law (i.e., the flow rate through porous media is proportional to the head loss and inversely proportional to the length of the flow path). For the purposes of regional characterization, such analyses are considered appropriate. However, their utility for calculation of ground-water flow paths and velocities over distances of a few kilometers or less is questionable. To determine the validity of the use of porous media solutions for flow through fractured media in the hydrogeologic study area, additional evaluations will be performed as part of the assessment of regional hydrogeologic data needs in the saturated zone.

3.7 REGIONAL GROUND-WATER FLOW SYSTEM

This section describes the general ground-water flow and principal flow paths in the hydrogeologic study area and its component subbasins. The system hydrochemistry is presented, the ages of ground water are estimated, and the system paleohydrology is described. Information about the regional ground-water flow system is required to define ground-water flow paths, to estimate the effects of climatic or tectonic induced changes on the water table altitude at the site, and to understand the ground-water flow system at the site.

Hydrologic conditions beneath Yucca Mountain are controlled in part by the regional ground-water flow system. Flow paths and water velocities beneath the site are determined by aquifer properties and hydraulic gradients. Because hydraulic gradients are affected by the regional distribution of permeability, and the locations and amounts of ground-water recharge and discharge, knowledge of the regional system is needed for assessment of hydrologic conditions at Yucca Mountain.

3.7.1 IDENTIFICATION OF RECHARGE AND DISCHARGE AREAS

This section presents information on the (1) location of areas of ground-water recharge to and discharge from the ground-water system, (2) modes of recharge and discharge, (3) residence time of ground water, (4) bulk rates of ground-water flow for specific hydrogeologic units, and (5) surface-water ground-water interrelations.

3.7.1.1 Location of ground-water recharge and discharge areas

The recharge and discharge areas in the ground-water basin shown in Figure 3-7 are taken from Winograd and Thordarson (1975), Waddell (1982), and

Waddell et al. (1984). The recharge areas shown are those areas of the basin that receive 200 mm or more average annual precipitation (Winograd and Thordarson, 1975) and are estimated to have relatively significant ground-water recharge, minor recharge probably occurs elsewhere in the basin, including Yucca Mountain. Surface-water runoff along major stream channels, such as Fortymile Wash, probably results in significant recharge, under both modern and post-pluvial conditions (Claassen, 1985; Czarnecki, 1985). Section 8.3.1.2.1 presents plans to evaluate the significance of this recharge present-day stream channels such as Fortymile Wash. Today this area receives an average precipitation of less than 200 mm/yr. Infrequent, small, and localized modern floods still occur in these channels, and some recharge from them probably does occur.

In his estimates of recharge in the Alkali Flat-Furnace Creek Ranch ground-water subbasin, Czarnecki (1985) assumed that recharge associated with annual precipitation rates of less than 76 mm/yr was minor. Further, in his closing remarks, he states that "additional work is needed to document recharge mechanisms and rates, and to establish analytical expressions between precipitation rates and associated ground-water recharge rates." This is particularly true for channels such as Fortymile Wash to the east of Yucca Mountain, where highly transmissive stream-channel sediments possibly focus recharge during flooding events. Little is known about the rate or distribution of deep infiltration there. Recharge through Fortymile Wash may affect the water-table altitude and gradient and flow-path directions beneath Yucca Mountain. Increased recharge through Fortymile Wash could result in a water table with higher altitudes and in modified gradients and ground-water flow rates (Czarnecki, 1985).

The amount of estimated average annual ground-water recharge from precipitation has been computed by Rush (1970) to be about 4.5×10^4 acre-ft (5.6×10^7 m^3) for a 16,000 km^2 area of the geohydrologic study area. This is equivalent to an average recharge rate of 3.5 mm/yr over the total area. Winograd and Friedman (1972) estimate that as much as 35 percent of the discharge at Ash Meadows in the southern Amargosa Desert (Figure 3-7) may be ground-water underflow from Pahranagat Valley. The springs at Ash Meadows flow about 2×10^7 m^3/yr (Walker and Eakin, 1963); therefore, the underflow from Pahranagat Valley may be on the order of 7×10^6 m^3/yr.

Although some uncertainty remains on the quantities and distributions of recharge over the region, the level of uncertainty does not appear significant in terms of affecting site-specific analyses and interpretations for Yucca Mountain. Nonetheless, additional work is planned through regional modeling and water balance measurements as described in Section 8.3.1.2.1.

Ground-water discharge from the ground-water basin is by (1) spring flow; (2) evapotranspiration from phreatophyte areas where depths to ground water are less than about 15 m; and (3) evaporation from bare soil areas such as playas, where depth to ground water is less than about 5 m (Rush, 1970), and to a lesser extent, well withdrawals. At the major discharge areas in the basin (Figure 3-7), discharge is by evapotranspiration by phreatophytes and by natural springs that flow at the land-surface contact between transmissive and less-transmissive hydrogeologic units. The less-transmissive units act as barriers to ground-water flow, causing ground water to flow upward to land surface (Winograd and Thordarson, 1975). Major ground-water discharge is summarized in Table 3-9. Modeling studies by Waddell (1982) and Czarnecki and Waddell (1984) have shown recharge to be a highly sensitive element of regional flow models and additional studies are planned to determine discharge rates (Section 8.3.1.2.1).

Table 3-9. Major ground-water discharge in the hydrogeologic study area

Area (see Figure 3-9)	Nature of discharge	Estimated average discharge (m^3/yr)	Reference
Southern Amargosa Desert	Springs, evaporation, and evapotranspiration	3.0×10^7	Rush (1970), Walker and Eakin (1963)
Death Valley	Springs	6.3×10^6	Waddell (1982)
Near Beatty in Oasis Valley	Springs and evapotranspiration	2.7×10^6	Malmberg and Eakin (1962)
Indian Springs Valley	Springs	9.8×10^5	Maxey and Jameson (1948)
Total discharge		4.0×10^7	

Production wells contribute to the total discharge of the system. Data presented in Table 3-9 and tables in Section 3.8 indicate that well production may represent one third of the total discharge (total discharge from wells is 1.9×10^7 m^3/yr).

The total discharge shown in Table 3-9 does not include diversion from the study area by wells; well discharge is described in Section 3.8. Flow paths of ground water between recharge and discharge areas and the controls on the flow paths are discussed in Section 3.7.2.

3.7.1.3 Residence times of the ground water

Residence time of water in the hydrogeologic units is dependent on two factors: (1) ground-water velocities and (2) travel distances. Each of these factors is controlled by the highly complex hydrogeologic characteristics of the ground-water system.

A commonly used method for determining ground-water age is carbon-14 dating, although the presence of carbonate rocks along the flow path has an effect on the apparent ages determined (Tamers, 1967; Section 3.7.4).

7 m/yr in the Amargosa Desert. Apparent carbon-14 ages from the tuff aquifers are probably not subject to much error, but apparent ages of the carbonate aquifers are assumed to require significant correction. Carbon-14 ground-water data and their interpretation for the Yucca Mountain vicinity are presented and discussed in more detail in Section 3.7.3.2, based on Claassen (1985) and Benson and McKinley (1985).

In a discussion of ground-water velocity, Winograd and Thordarson (1975) developed some estimates for residence and travel time for ground water beneath parts of the basin:

1. Beneath Yucca Flat, assuming an average saturated thickness of about 300 m and vertical movement, the time needed for a water particle to move from the top to the bottom of the tuff aquitard is about 6,000 to 2,000,000 yr, corresponding to velocities of 6×10^{-2} m/yr to 1.5×10^{-4} m/yr.

2. A carbon-14 date of water from the valley-fill aquifer beneath Frenchman Flat suggests that the age of the ground water in the tuff aquitard probably is in the range of several tens of thousands of years based on a sample with an apparent age of 13,000 yr. An age of several hundred thousand years is not beyond possibility for waters near the base of the tuff aquitard beneath Yucca or Frenchman flats, because vertical flow velocities through the underlying aquitard are likely to be very small, based on current rock-property data and recharge estimates.

3. Estimates of the velocity in the lower carbonate aquifer beneath central Yucca Flat range from about 6 to 600 mm/day, or from about 2 to 200 m/yr. Estimated average velocities beneath the Specter Range (15 km southwest of Mercury) are about 100 times larger than those for the lower carbonate aquifer beneath central Yucca Flat, or about 200 m to 20 km/yr and probably represent an upper limit of the

3.7.1.4 Bulk rates of ground-water flow

Bulk rates of ground-water flow for specific hydrogeologic units have not been determined; however, Waddell (1982), using a two-dimensional flow [redacted]

Czarnecki and Waddell (1984) used a two-dimensional ground-water flow model of an area approximately equivalent to the Alkali Flat-Furnace Creek Ranch subbasin to calculate vertically integrated specific fluxes ranging from about 3.6 m^2/yr to 2.9 x 10^3 m^2/yr. Although only limited field data were available to calibrate the model, the calculated flux rates are consistent with total water balance data, gradients, and hydraulic conductivity and transmissivity data.

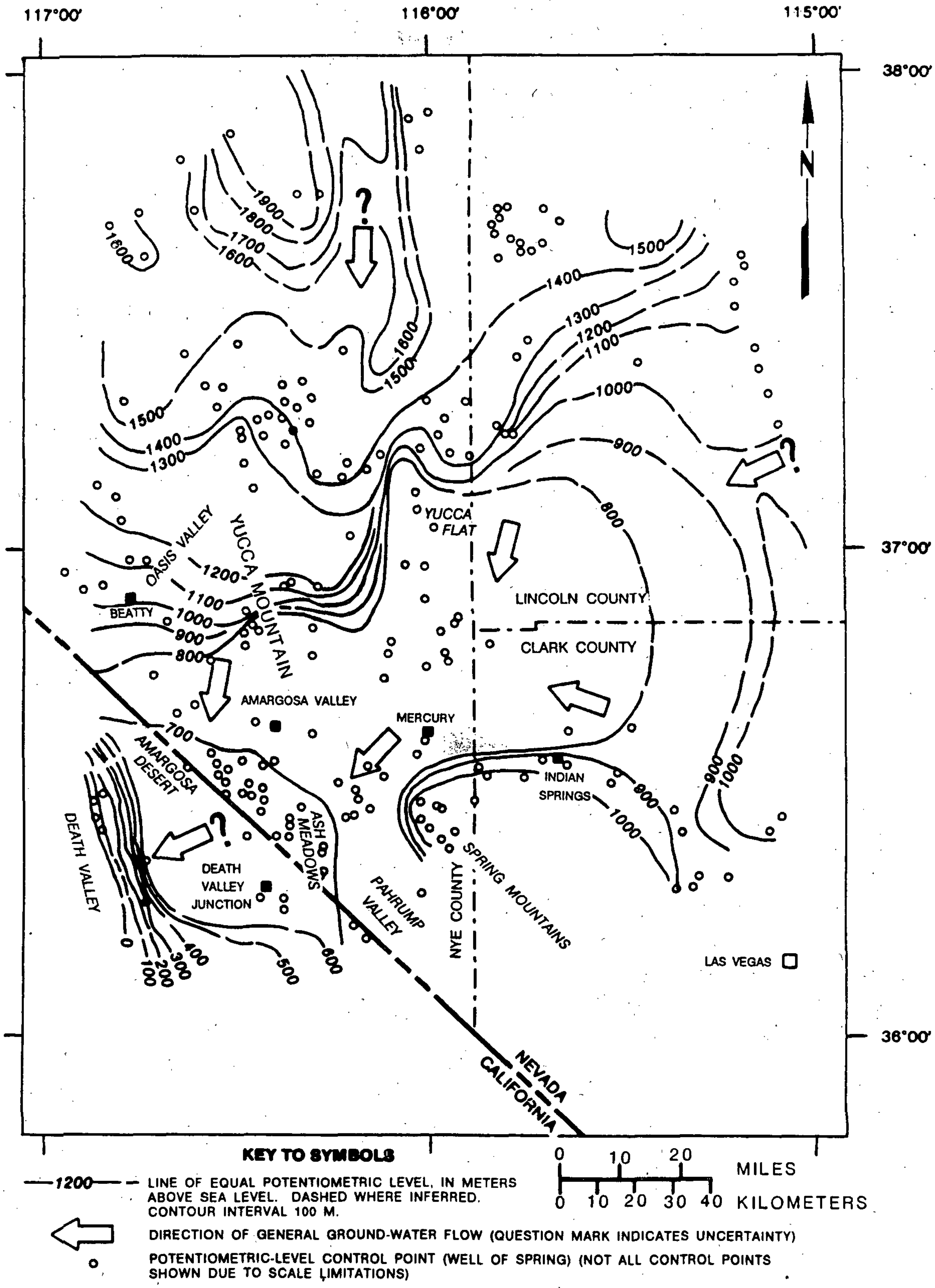

Figure 3-10. Regional ground-water flow paths. Modified from Waddell et al. (1984).

[redacted]

selected boreholes in the hydrogeologic study area and surrounding area (Sass and Lachenbruch, 1982). Sass and Lachenbruch have interpreted a large area of anomalously low heat flow in eastern Nevada, extending into the north-eastern part of the hydrogeologic study area. The area, called the Eureka Low, is interpreted to possibly have a downward component of ground-water flow on the order of a few millimeters per year, which is consistent with regional interpretations of recharge and discharge zones by Winograd and Thordarson (1975). The heat flow to land surface in the Eureka Low is less than 0.6 W/m^2. Elsewhere in the region, upward heat flow is higher and more typical of upward heat flow in the Great Basin (0.6 to 1.0 W/m^2, see Figure

Flow paths are from the principal recharge areas, mostly in the central part of the subbasin (Figure 3-7), southward to the discharge area near Beatty. This flow is principally through volcanic-rock aquifers to the valley-fill aquifer underlying the discharge area. It is not known whether the lower carbonate aquifer is present at considerable depth below parts of the subbasin (Figure 3-7). According to Waddell (1982), the valley fill aquifer is underlain by the lower clastic aquitard. Some of the spring discharge is warm, suggesting deep circulation. Ground water not discharged by evapotranspiration flows southward through the valley fill aquifer, past an alluvium-filled narrows, and into the Amargosa Desert.

3.7.2.2 <u>Ash Meadows subbasin</u>

and earlier parts of Section 3.7. Flow paths are determined by hydraulic head differences in open fractures in the lower carbonate aquifer.

Flow in the Ash Meadows subbasin is primarily in the lower carbonate aquifer. Hydraulic gradients are low (commonly less than 0.0002) because of high transmissivities of the soluble, fractured lower carbonate aquifer (Winograd and Thordarson, 1975). Distribution of head and direction of flow are greatly affected by permeability differences among the hydrogeologic units (Winograd and Thordarson, 1968).

According to Winograd and Thordarson (1975) spring discharge of 8.7×10^5 m^3/yr occurs at Indian Springs. It is probably fed by upward leakage of ground water from the lower carbonate aquifer by way of the valley fill aquifer. A major hydraulic barrier probably exists in the vicinity of the spring that causes the ground water to flow upward.

From northern Yucca Flat to Ash Meadows, ground water apparently flows downward through the valley fill aquifer and volcanic-rock hydrogeologic units into the underlying carbonate aquifers beneath Yucca Flat. The potentiometric level is as much as 43 m lower in the carbonate aquifer than in the overlying units (Winograd and Thordarson, 1975; Doty and Thordarson, 1983). Ground water from the overlying aquifers is drained by the more transmissive underlying carbonate aquifers. These interpretations are based primarily on data from two well locations. It may be desirable to confirm the interpretations with one or more additional wells with multidepth head measurements. Plans for collecting additional data on this type are discussed in Section 8.3.1.2.

The lower carbonate aquifer transmits most of the water in the subbasin, but other lithologies are locally important. Northeast of the Ash Meadows spring line, the saturated thickness of the valley fill aquifer probably is more than 100 m. Beneath Frenchman Flat, both valley fill and volcanic aquifers are saturated beneath the structurally deepest parts of the valley. Most of the valley-fill aquifer beneath Yucca Flat is unsaturated (Winograd and Thordarson, 1975).

Discharge from springs at Ash Meadows is estimated to be 2×10^7 m^3/yr (Walker and Eakin, 1963; Dudley and Larson, 1976). An additional unknown amount of ground water flows to the Alkali Flat-Furnace Creek Ranch subbasin to the west, some of which discharges by evapotranspiration (Winograd and Thordarson, 1975). A normal fault, downthrown to the southwest (Healey and Miller, 1971), probably juxtaposes a low-permeability lake bed aquitard or eolian deposits on the downthrown side of the fault against the lower carbonate aquifer across the fault, forcing flow upward (Dudley and Larson, 1976). Discharge is from springs in alluvium downgradient (southwest) of the fault. Regional transmissivities of about 40,000 m^2/d have been calculated (Winograd and Thordarson, 1975) for the lower carbonate aquifer in the area northeast of Ash Meadows using estimated values for discharge, hydraulic gradient, and width of the aquifer; this figure is six to nine times greater than that determined from aquifer tests (Waddell, 1982).

3.7.2.3 Alkali Flat-Furnace Creek Ranch subbasin

Winograd and Thordarson (1975) suggest evidence that ground water flows from the south-central Amargosa Desert, through the lower carbonate aquifer, discharging at springs and seeps at Furnace Creek Ranch. Evidence supporting this belief consisted of the following: (1) proximity of spring discharge to the lower carbonate aquifer, (2) temperature relations of spring waters that are similar to those at Ash Meadows, and (3) the chemical quality of Travertine, Texas, and Nevares Springs are nearly identical. Ground water in the lower carbonate aquifer beneath the south-central Amargosa Desert may be [redacted]

aquifer is extensive beneath the central Amargosa Desert), and downward leakage from the valley-fill aquifer beneath the central and south-central Amargosa Desert.

Table 3-10. Summary of fluxes into and out of the Alkali Flat-Furnace Creek Ranch subbasin[a,b]

Flux location	Rate[c] (m^3/d)	Percentage
Timber Mountain[d]	+31,446	57.3
Fortymile Wash	+22,140	40.3
Rock Valley	+1,079	2.0
Calico Hills	+158	0.3
Ash Meadows	+78	0.1
Western Amargosa Desert	+19	<0.01
Franklin Lake playa	-35,600	64.8
Furnace Creek Ranch, Death Valley	-19,320	35.2

[a]Source: Czarnecki and Waddell (1984).
[b]Flux calculated as a residual of the mass balance.
[c]+ indicates flow is into subbasin; - indicates flow is out of subbasin.
[d]Timber Mountain area was simulated as a constant head boundary in the model.

3.7.3 ISOTOPIC AND REGIONAL HYDROCHEMISTRY

This section describes the hydrochemical and isotopic nature of the ground water within the saturated zone in the hydrologic study area. Based on these data, estimates of ground-water age, origins, residence times, and travel times are presented. Discussions are provided regarding (1) the relative degree of circulation within the hydrogeologic units, (2) areas and modes of recharge and discharge, and (3) the delineation of regional hydrochemical facies. Figure 1-10 (Section 1.2.1) provides the distribution of rock types in the region, Figure 3-11 shows the location of many of the regional physiographic features, and Figure 3-2 shows the hydrogeologic subbasins.

3.7.3.1 Regional hydrochemistry

The chemical composition of ground water in the region is principally determined by (1) reactions with carbonate and volcanic rocks or rock fragments; (2) concentration of dissolved chemicals by evaporation; (3) formation of smectites, zeolites, and evaporite minerals; and (4) mixing of waters of different compositions. Because of a scarcity of shales, quartzites and granites, reactions with these rocks do not produce significant changes in the chemical composition of water in the region.

DECEMBER 1988

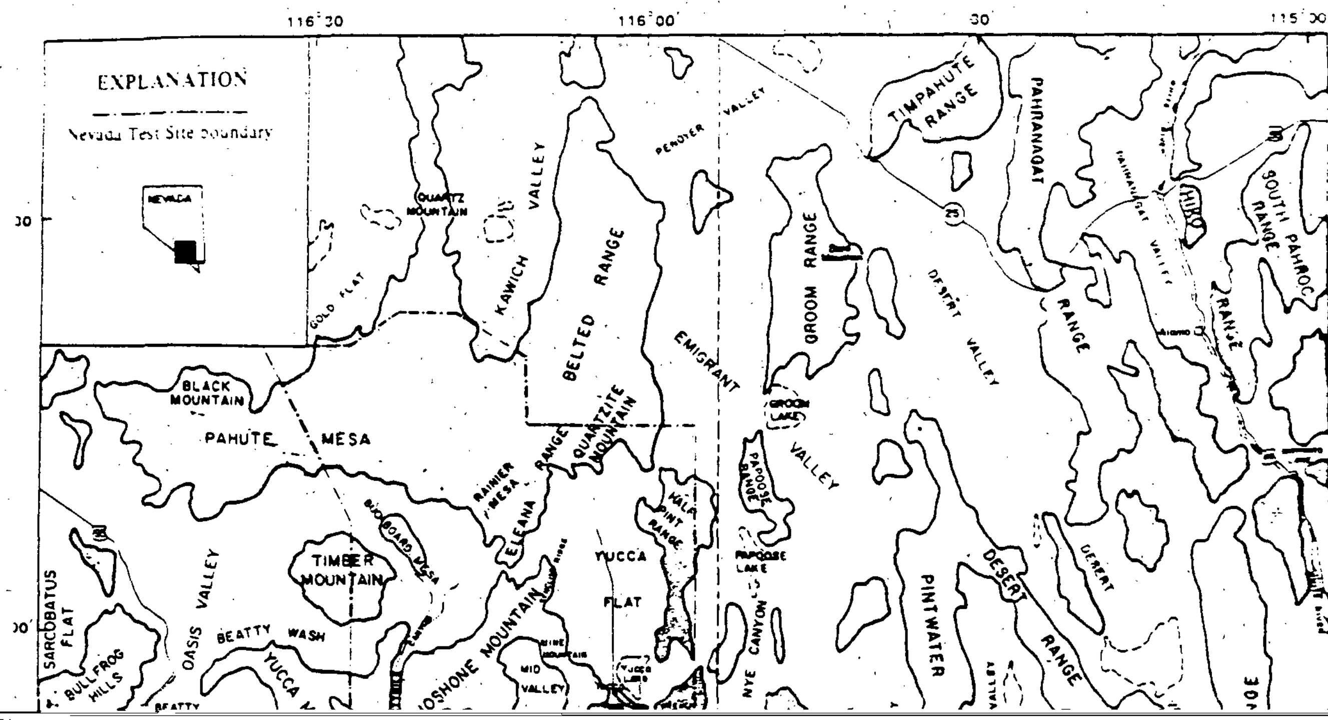

3.7.3.1.1 Chemical composition of ground water

The chemical composition of the ground water within the hydrogeologic study area is discussed in terms of the tuffaceous, lower carbonate, and valley fill aquifers. Plans to expand and improve the existing information base are described in Section 8.3.1.2.3.

Tuffaceous aquifer

The sodium bicarbonate water, which dominates the tuffaceous rocks, evolves principally by dissolution of rhyolitic volcanic glass and subsequent precipitation of various zeolites and smectite clays (Claassen and White, 1979; White, 1979; Claassen, 1985). White (1979) presents chemical analyses for 13 water samples from the tuffaceous aquifer northwest of Yucca Mountain in the Oasis Valley. The major cations are sodium (50 to 200 mg/L), calcium (0 to 36 mg/L), potassium (1.5 to 11 mg/L) and magnesium (0 to 5 mg/L). The dominance of sodium ions can be attributed to the incongruent dissolution and hydrolysis of volcanic glass. White et al. (1980) report that incongruent dissolution in the tuff beds within Rainier Mesa preferentially releases sodium, calcium, and magnesium while retaining potassium. Calcium and magnesium show progressive depletion relative to sodium, not by ion exchange but due to the effective removal of bivalent ions as clinoptilolite and montmorillonite are precipitated. Greater percentages of sodium ion are associated with larger clinoptilolite:montmorillonite precipitation ratios (Claassen, 1985). The 13 water samples taken from the tuffaceous rocks in Oasis Valley show that the dominant anion is bicarbonate (115 to 330 mg/L), with sulfate, chloride, and fluoride present in concentrations of 0 to 217 mg/L, 14 to 3 mg/L, and 0 to 10 mg/L, respectively. Since the occurrence of carbonate minerals in the tuffaceous rocks is minimal, the principal source and control of bicarbonate is the reaction of dissolved soil-zone carbon dioxide with various mineral phases (White, 1979). Chloride is leached preferentially relative to fluoride from the fresh, previously unreacted, glass phase (White and Claassen, 1980). Aqueous silica (SiO_2) concentrations remain constant, showing supersaturation with respect to cristobalite and quartz, and saturation with respect to silica gel (amorphous hydrated SiO_2). Excess silica is removed from the aqueous systems as silica gel, which is observed in fractures in the tuffaceous rocks of Oasis Valley (White, 1979). For the 13 water samples from Oasis Valley, the pH is reported as ranging from 7.6 to 8.7, and temperatures range from 18 to 41°C.

White et al. (1980) report chemical analyses for 55 water samples from the pores and fractures of the saturated tuffs of Rainier Mesa. The data show that the fracture water is predominantly a sodium bicarbonate. The interstitial water, however, shows much higher concentrations of chloride and sulfate relative to bicarbonate. Relative concentrations are similar to those specified in White (1979) for the Oasis Valley. However, actual concentrations are less with the dominant ions sodium, bicarbonate, and chloride having maximum concentrations of 71 mg/L, 220 mg/L, and 62 mg/L, respectively. The pH values reported range from 6.8 to 8.3.

Two wells drilled in rhyolites in Fortymile Canyon produced water containing predominantly sodium (39 to 44 mg/L) and bicarbonate (54.9 to 56.7 mg/L). Calcium and sulfate are the next dominant, with concentrations of 10 to 23 mg/L and 19 to 22 mg/L, respectively (Waddell, 1985). Measured temperatures were 19 and 20°C. Waddell reports that four samples at varying depths in one well have dissolved oxygen contents of 2 to 5 mg/L and pH values of 7.1 to 7.6.

Benson and McKinley (1985) report the chemical composition of 25 water samples obtained from 14 test wells in and near the exploratory block (Section 3.9.1.3 and Chapter 4). Again, sodium and bicarbonate ions predominate. Temperatures range from 22 to 56°C, and pH values are 6.6 to 9.2. Although plots of relative cation and anion concentrations indicate a general description of sodium bicarbonate water, the ground water at Yucca Mountain is not chemically homogeneous. The differences in ionic composition among the wells is outlined and the authors conclude that ground water from the wells in the Yucca Mountain area has a significant degree of lateral and vertical chemical variability.

Claassen (1973) reports chemical data from eight wells drawing water from the tuff strata in the north, southeast, and southwest areas of the NTS. The analyses are in good agreement with the previously reported data.

The chemical composition of 15 ground-water samples from Pahute Mesa were reported by Blankennagel and Weir (1973). As with other waters from the tuff aquifer, the ground water of Pahute Mesa is of a sodium potassium bicarbonate type. Sodium plus potassium ranged from 58 to 99 percent of the total cations, with 8 of the samples having the alkali ions present at more than 90 percent. Bicarbonate is the most abundant anion with bicarbonate plus carbonate making up more than 50 percent of the total anions in 12 of the samples. Water from the western side of the mesa has dissolved solids concentrations ranging from 206 to 336 mg/L, and averaging 280 mg/L. In the eastern part of the mesa, the dissolved solids range from 117 to 248 mg/L, and average 200 mg/L. Blankennagel and Weir (1973) consider that the lesser concentrated water in the east may be due to its nearness to areas of recharge.

Chemical analyses for 12 ground-water samples primarily from the northern area of the NTS are presented by Claassen (1985). Claassen (1985) recognized that some of the samples were atypical of the regional tuffaceous aquifer. These samples "all represent very young, generally perched ground water," thus not having evolved chemically to the extent of the waters representative of the regional aquifer. Specifically, the decrease in calcium relative to sodium is presumed to result from greater quantities of clinoptilolite precipitated from a ground-water composition evolved by reaction with vitric tuff and, therefore, represents a trend of increasing maturity of ground water.

Figure 3-12 provides a graphical description of water in the tuffaceous aquifer in the form of a Piper diagram.

Lower carbonate aquifer

Schoff and Moore (1964) recognized two varieties of water in the regional carbonate aquifer: a calcium magnesium bicarbonate type and a mixed type. Winograd and Pearson (1976) determined that the variation in composition corresponded to the distance from recharge area. The authors found that ground water in close proximity to the Spring Mountains recharge area was

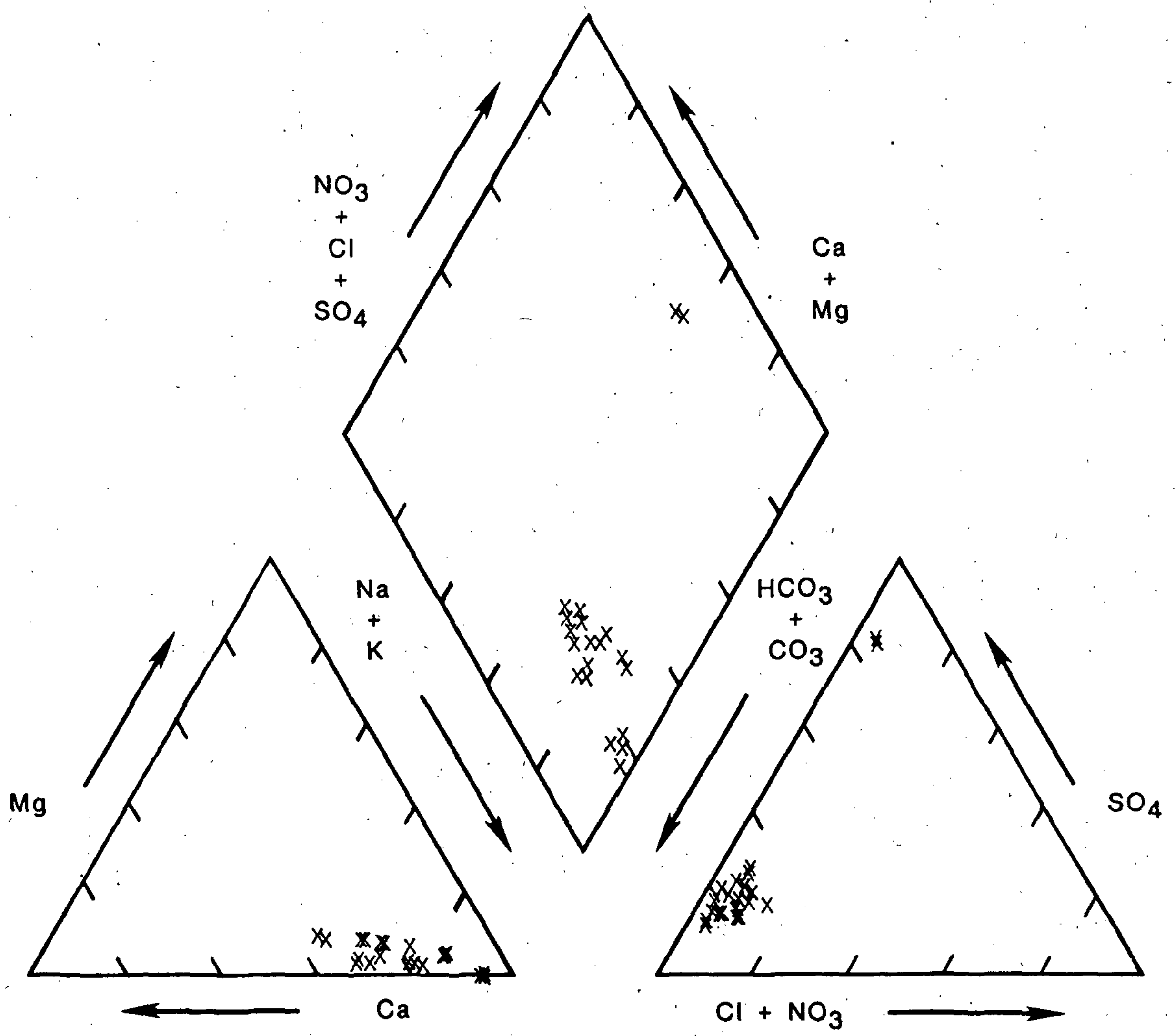

Figure 3-12. Piper diagram showing the regional sodium bicarbonate character of the tuff aquifer.

typical of water moving through an upland carbonate; that is, calcium (45 to 69 mg/L), magnesium (10 to 16 mg/L) and bicarbonate (180 to 290 mg/L) occurred as primary constituents, and sodium, potassium, chloride and sulfate were present in negligible quantities. Water that is primarily calcium magnesium bicarbonate is still found at intermediate points along the flow system; however, concentrations of sodium and sulfate are increased. Finally, near the Ash Meadows discharge area sodium, sulfate, and chloride are present as major ions with concentrations of 69 to 100 mg/L, 80 to 110 mg/L, and 21 to 27 mg/L, respectively. The mixed waters of Schoff and Moore are characterized by these last two types. Winograd and Thordarson (1975) attribute this increase in sodium, sulfate, and chloride to the downward leakage of sodium- and sulfate-rich water from the tuff aquitard. Temperatures are typically between 26 and 38°C, with outliers at 6.5 and 64°C; pH values vary insignificantly around 7.4.

The chemical composition of water from four wells tapping the carbonate aquifer on the eastern side of the NTS are reported in Claassen (1973). Three of the wells are in an area where the carbonate aquifer is directly overlain by tuff beds. As expected, the sodium concentration in these waters is high (up to 142 mg/L) relative to calcium (80 mg/L maximum concentration) and magnesium (33 mg/L). Bicarbonate and sulfate are present in concentrations up to 589 mg/L and 76 mg/L, respectively. The fourth well is in an area where the producing zone is separated from the tuff by 637 ft (190 m) of limestone and dolomite, thereby making sodium less dominant than calcium and magnesium. With the exception of one measurement of 9.9, pH values are between 7.0 and 8.3. Temperatures vary insignificantly around 34°C.

Water quality data for three samples from the lower carbonate aquifer in the southern portion of Ash Meadows ground-water subbasin (Claassen, 1985) are characteristic of the mixed water previously described.

Water from the lower carbonate aquifer is depicted graphically in Figure 3-13 in a Piper diagram.

Valley fill aquifer

Water in the tuffaceous valley fill has a composition similar to that of water in the tuffaceous aquifer shown in Figure 3-12. However, because of the shallowness of the water table in some areas, evapotranspiration results in an increased concentration. Analyses of 16 water samples from the tuffaceous alluvium in Oasis Valley (White, 1979) show sodium concentrations ranging between 100 and 315 mg/L and bicarbonate measuring between 207 and 512 mg/L. Chloride (68-100 mg/L) and sulfate (53-250 mg/L) also show a general increase. Other ions--calcium, magnesium, potassium and fluoride--are present in quantities less than 40 mg/L. Although some additional reaction may occur between the ground water and the tuffaceous detritus, White (1979) maintains that the principal mechanism for concentrating the sodium and bicarbonate is the decrease in volume of water due to the proximity of the water table to the atmosphere and soil zone. Temperatures vary between 18 and 31.5°C.

Claassen (1985) presented analyses for approximately 55 wells and springs tapping the valley fill in the Amargosa Desert. Many of the samples were differentiated as to tuffaceous or carbonate alluvium. All analyses

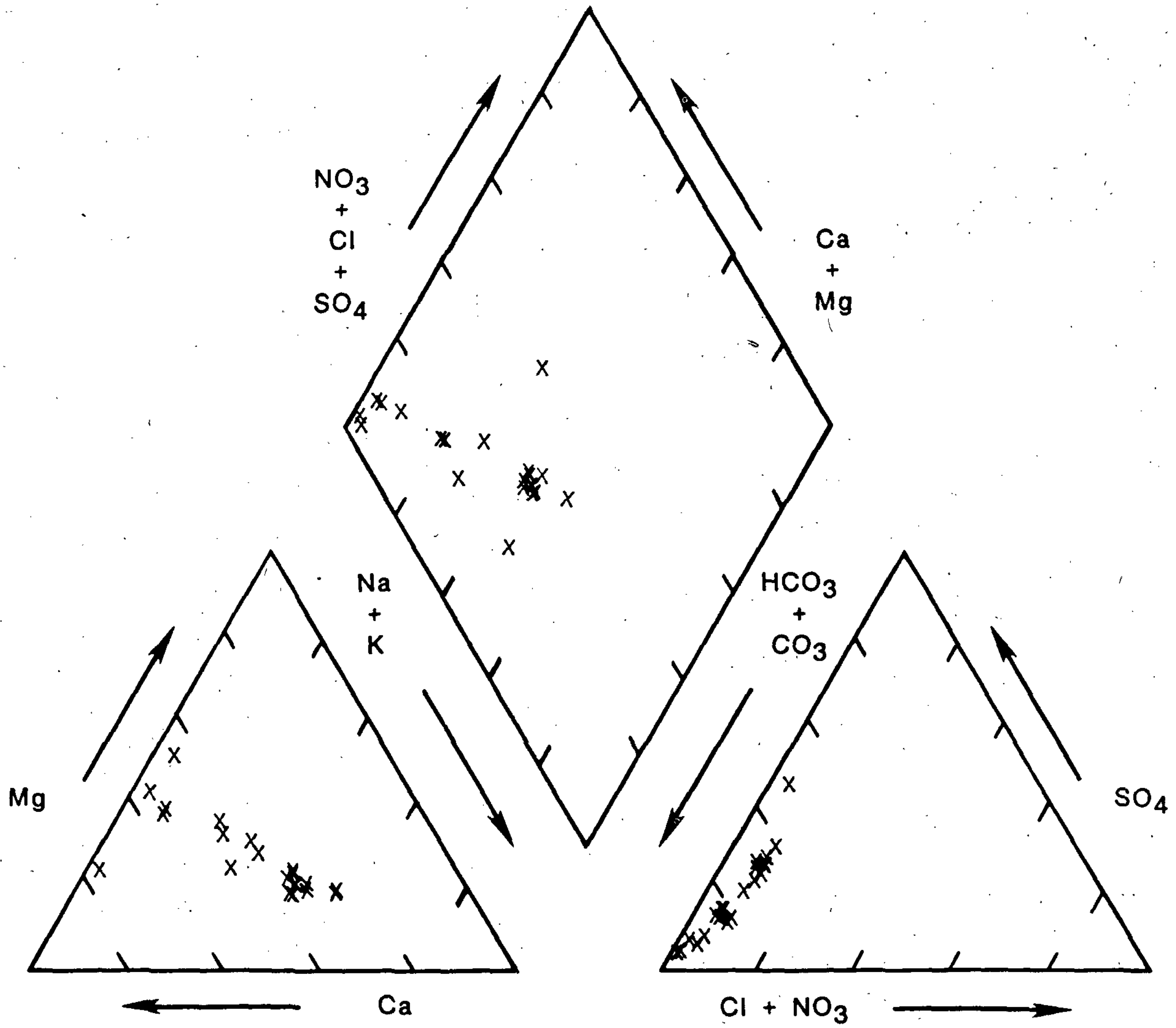

Figure 3-13. Piper diagram showing the regional mixed character of the lower carbonate aquifer.

show a wide range of concentrations for sodium (30 to 250 mg/L), calcium (0 to 66 mg/L), bicarbonate (116 to 437 mg/L) and sulfate (25 to 235 mg/L). The average temperature for water in seven wells completed in the valley fill aquifer was reported as 21°C.

There are instances where water from each of the above alluvial aquifers shows the effect of local playa deposits. These deposits tend to increase the concentrations of sulfate and chloride in associated ground water. Claassen (1985) reports that six wells in the Amargosa Desert drawing water associated with playas have sulfate and chloride compositions ranging from 89 to 186 mg/L and 24 to 70 mg/L, respectively. By contrast three nearby wells not associated with playa deposits have sulfate and chloride concentrations ranging from 27 to 35 mg/L and 6 to 10 mg/L, respectively.

The chemical composition of water in the valley fill is depicted graphically in Figure 3-14 in a Piper diagram.

3.7.3.1.2 Recharge and discharge mechanisms

Areas and modes of recharge and discharge for the aquifers are discussed in this section, based on the ground-water hydrochemistry.

Recharge to the tuff aquifer

The highlands of Pahute Mesa and Gold Flat serve as probable recharge areas for the tuff aquifer in Oasis Valley. White (1979) shows a linear trend for concentrations of bicarbonate and chloride plotted against sodium

for ground water in the tuffaceous aquifers of Oasis Valley, Pahute Mesa, and Gold Flat (Figures 3-15 and 3-16). Ground water from the latter two areas plots in the dilute portion of the trend while water from Oasis Valley plots along a more concentrated part of the line. The similarity in composition supports the suggestion of Blankennagel and Weir (1973) that water beneath Pahute Mesa is related to Oasis Valley ground water, and merely represents a less advanced stage in the chemical reaction sequence farther upgradient (White 1979).

Other parts of the tuff aquifer may be recharged differently. Winograd and Thordarson (1975), Claassen and White (1979), and White et al. (1980) discuss recharge at Rainier Mesa. Consideration of altitude and vegetation would include Timber Mountain as a potential recharge area also. One further, and perhaps critically important recharge area, may be Fortymile Canyon. This was first suggested by Winograd and Thordarson (1975); however, Claassen (1985) presents chemical and isotopic evidence to support the hypothesis that major amounts of ground water beneath and in the vicinity of the canyon were recharged by infiltration of surface runoff. This infiltra-

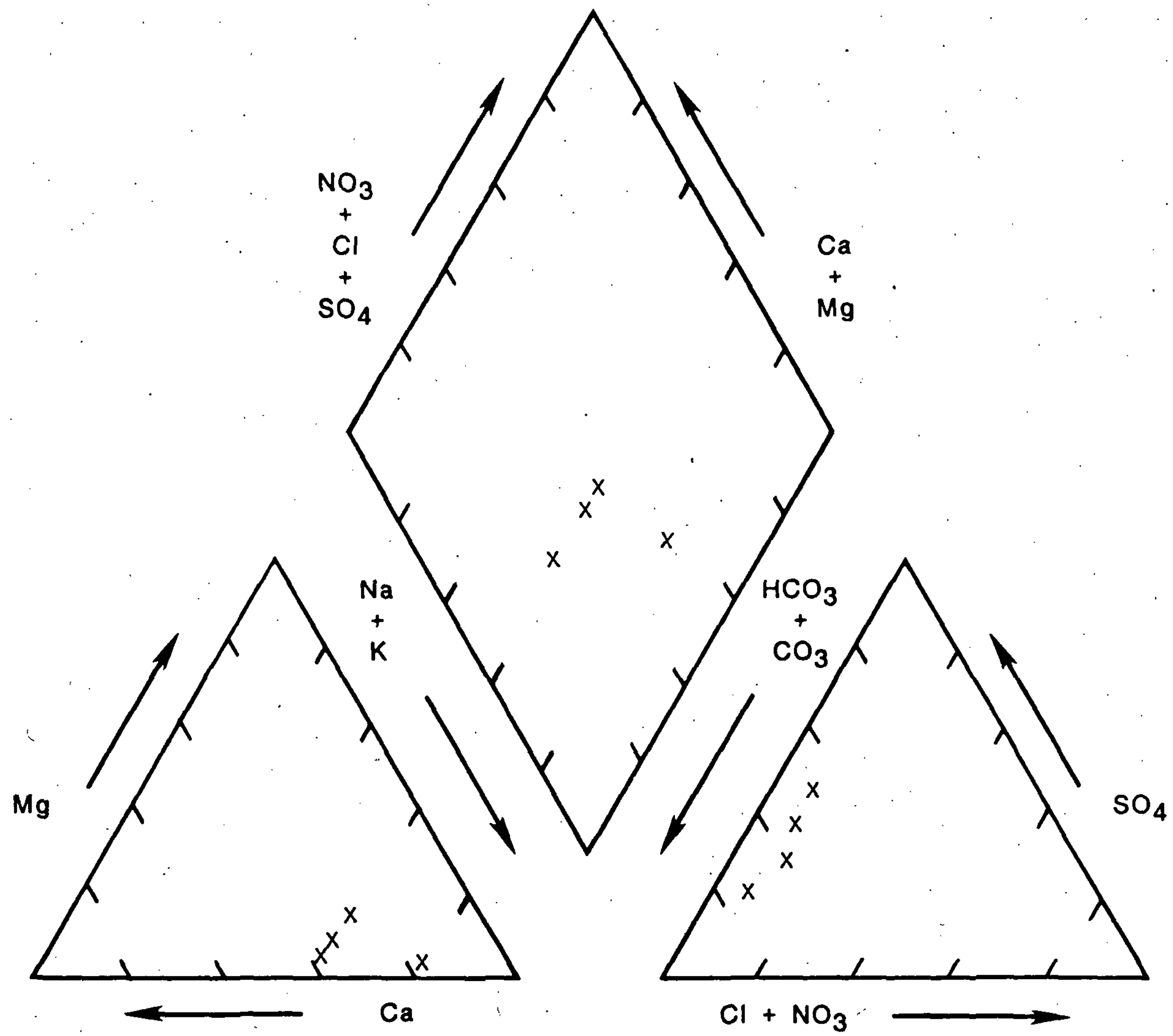

Figure 3-14. Piper diagram showing the regional character of the valley fill aquifer.

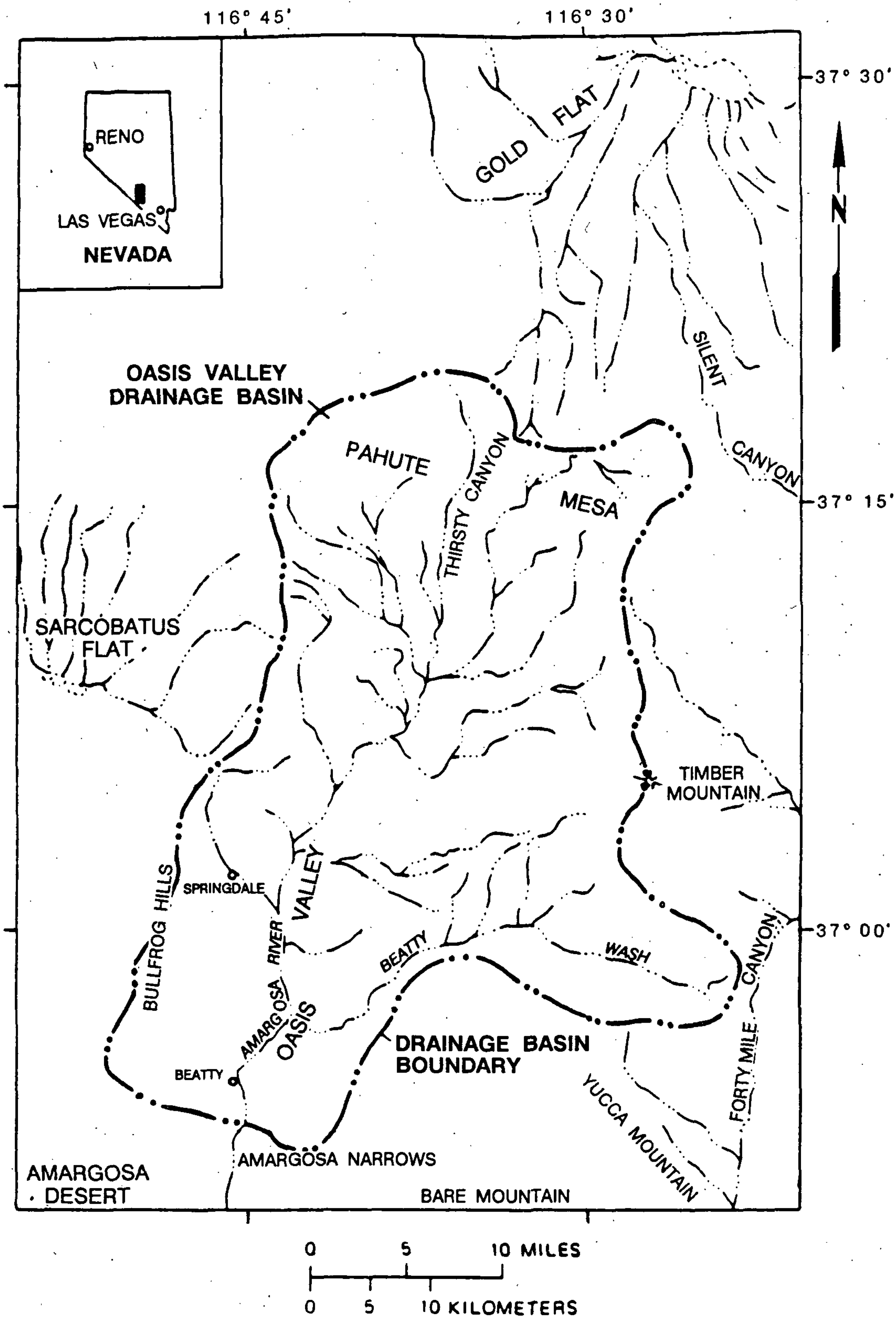

Figure 3-15. General location of Oasis Valley, Pahute Mesa, and Gold Flat ground-water sampling areas. Modified from White (1979).

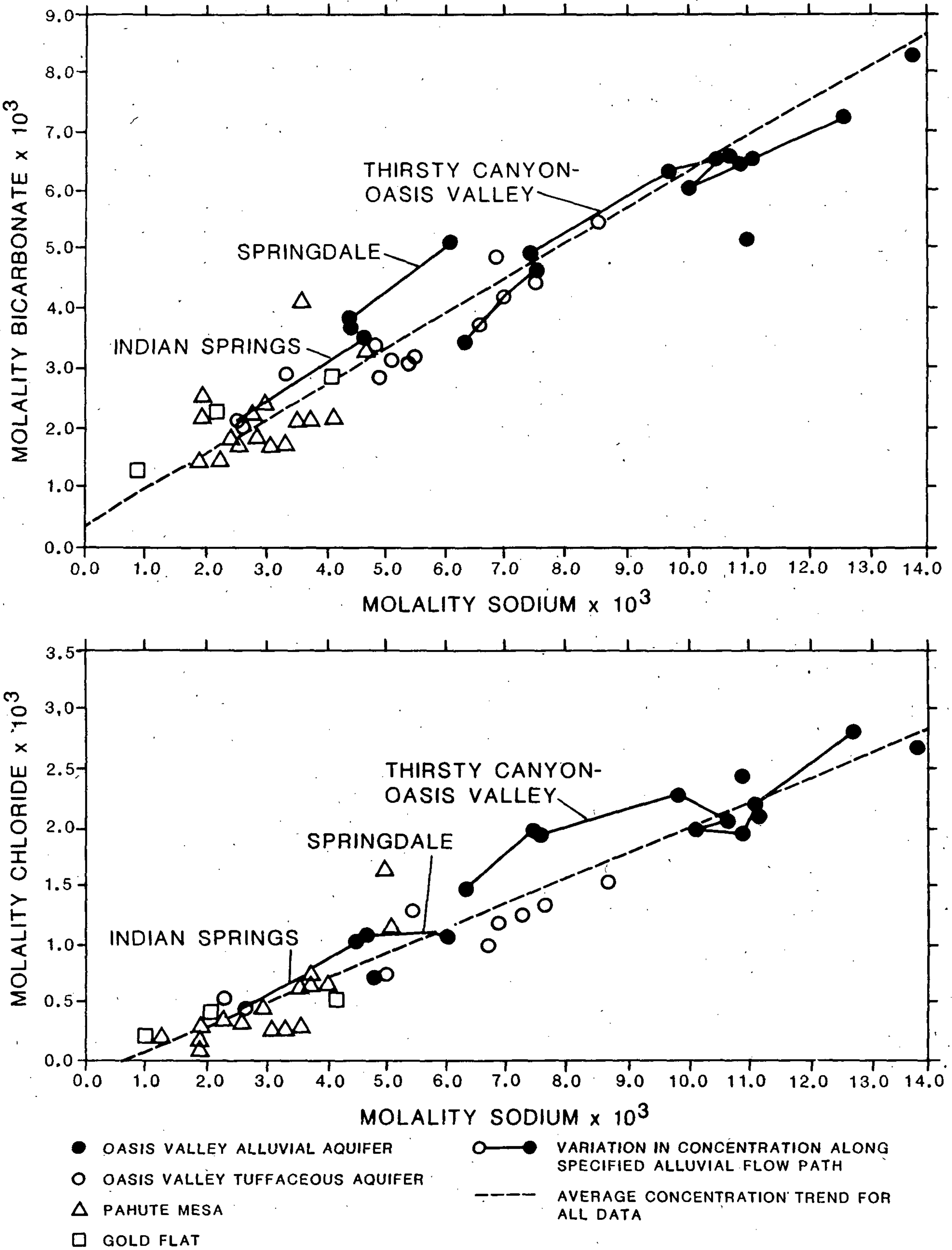

Figure 3-16. Concentration trends of sodium, bicarbonate, and chloride. Modified from White (1979).

Discharge from the tuff aquifer

There are three primary mechanisms for ground-water discharge from the tuffaceous aquifer in the vicinity of the NTS: (1) vertical leakage to the underlying lower carbonate aquifer, (2) subsurface flow infiltrating into the valley-fill aquifer, and (3) spring discharge. Hydrochemical evidence for the first mechanism is presented in the section addressing recharge to the lower carbonate aquifer. The second mechanism is supported by White (1979) where he showed that, through the effects of evapotranspiration, water in the tuffaceous alluvium could be produced from water in the tuff aquifer. White (1979) included data from the Oasis Valley alluvium on his plot of bicarbonate and chloride concentrations relative to sodium (Figure 3-16). Alluvial water compositions for specific flow paths ranged from the dilute region at the initial stages along the flow paths to considerably higher concentrations on the linear trend farther downgradient. White (1979) concluded that based on the linearity of the data, water in the alluvium could evolve from tuffaceous compositions by concentration increases due to evapotranspiration.

The third mechanism, direct spring discharge, is most likely to occur where fracture systems are saturated, broken by recent faulting, or intersect the land surface. White (1979) notes several locations in Oasis Valley where this is evidenced. Although a spring may be issuing directly from the tuff aquifer, Claassen (1985) found that the cation composition of tuffaceous spring water may not necessarily be consistent with that of the regional aquifer. Claassen (1985) explained that the spring discharge is young and generally perched ground water, and thus, has not had the opportunity to evolve to a similar chemical nature as the water from the regional aquifer. Claassen (1985) concludes that although the spring discharge may not be representative of the regional tuffaceous aquifer, it does represent a point in the evolution of the composition of waters in tuffs of southern Nevada.

Recharge to lower carbonate aquifer

The highlands of the Sheep Range, northwestern Spring Mountains, and southern Pahranagat Range are the primary source of recharge to the lower carbonate aquifer. To a lesser extent the Pintwater, Desert, and Spotted ranges also contribute to the recharge (Winograd and Thordarson, 1975). These are highly fractured Paleozoic carbonate rocks that yield ground water of the calcium-magnesium bicarbonate type. However, there are relatively few areas where the lower carbonate aquifer actually yields the calcium-magnesium water characteristic of the recharge areas. This is attributed to vertical leakage in the eastern and northeastern valleys; that is, sodium rich water from the tuff aquifer leaking vertically downward to mix with the calcium-magnesium water in the lower carbonate aquifer. On the basis that Frenchman Flat and Ash Meadows ground waters have nearly identical compositions, Winograd and Thordarson (1975) conclude that vertical leakage of high sodium water must be occurring in northern Indian Springs, northern Three Lakes, and eastern Emigrant and Desert valleys. There are, however, two areas where the carbonate water has had little opportunity to come in contact with tuff or tuffaceous alluvium. Water from these areas, the Spring Mountains and the Pahranagat Valley, show the untainted calcium magnesium chemistry that would result from precipitation in the eastern Paleozoic carbonate highlands.

A second source of recharge to the lower carbonate aquifer is downward leakage of water from the Cenozoic strata. Schoff and Moore (1964) concluded that based on the distribution of sodium, the water in the Paleozoic carbonate rocks underlying the NTS is being recharged by downward percolation through the tuff and tuffaceous alluvium. When added to the calcium magnesium water already in the carbonate rock, the sodium potassium water associated with these tuffaceous rocks yields the water of mixed chemical character, which is generally found downgradient in the Amargosa Desert. Naff et al. (1974) used a Piper diagram as chemical evidence supporting the idea of downward leakage from the tuff aquifer. Points on the Piper diagram representing downward leakage through the Tertiary aquitard and points representing water moving through a potentiometric trough in the carbonate aquifer just below Yucca and Frenchman flats virtually surround points representing spring water issuing from the carbonate aquifer in the Ash Meadows discharge area (Devils Hole). From this, the authors conclude that the chemical character of the discharge at Ash Meadows can be accounted for by ground water percolating downward across the Tertiary aquitard and mixing with water in the carbonate aquifer. Winograd and Thordarson (1975) used the differences and variations in chemical quality between the carbonate aquifer and the tuff aquitard to estimate that leakage across the aquitard probably

A third source of recharge to the lower carbonate aquifer, possibly contributing as much as 35 percent (Winograd and Friedman, 1972), is the underflow (i.e., trans-basin regional ground-water movement) into the basin from the northeast. Winograd and Thordarson (1975) found that the chemical centimeter at 25°C. Winograd and Thordarson (1975) cite as support for the

A temperature of 30.6°C was measured in only one of the aforementioned wells. This temperature is closer to temperatures measured in water from wells in the carbonate aquifer (27 to 30°C) than to temperatures measured in water from wells in the distal valley fills (21°C). Furthermore, at this same location the difference in hydraulic potential between the carbonate aquifer and the valley fill is just 6 m, almost the smallest difference observed in the west central Amargosa Desert. Claassen (1985) explains that the smaller potential difference and the presence of more permeable sand and gravel in the valley fill at this site supports the idea of significant upward leakage from the carbonate aquifer.

Recharge to the valley fill aquifer

There are three principal sources of recharge to the valley fill aquifer: (1) upward leakage from the tuff aquifer, (2) upward leakage from the lower carbonate aquifer, and (3) overland flow. All but the third have been previously discussed under sections relating to discharge from the tuff and lower carbonate aquifers. Surface runoff is considered the most likely recharge mechanism for tuffaceous alluvium in the west-central Amargosa Desert. Winograd and Thordarson (1975) suggested that the low dissolved solids content of water from six wells along Fortymile Wash reflected recharge primarily via infiltration along the arroyo rather than underflow from Pahute Mesa and Timber Mountain. Claassen (1985) found that sodium-calcium-magnesium concentrations of water in the tuffaceous valley fill in the Amargosa Desert were generally inconsistent with the composition of water in the bedrock aquifers to the north. The data showed that the sodium concentration for valley fill ground water was consistently less than that for bedrock aquifers, sometimes as much as 15 percent. Claassen (1985) concluded that valley fill recharge was primarily surface runoff from the tuffaceous highlands infiltrating along present day wash bottoms.

Discharge from the valley fill aquifer

The most likely mechanism for discharge from saturated valley fill is evapotranspiration. Because of the close proximity of the water table to the ground surface in some areas, Oasis Valley for instance, direct exchange with the atmosphere as well as transpiration occurs (White, 1979). White found that along a valley fill flow path, upgradient samples contained less than half the dissolved solids of the water in the alluvium at the lower end of the flow path (458 mg/L compared with 1,040 mg/L). White (1979) acknowledged that there may be some additional reaction between the ground water and tuffaceous alluvium but concluded that the principal reason for the increase in dissolved solids was a decrease in the volume of ground water due to direct evaporation and transpiration through the vegetative cover.

3.7.3.1.3 Hydrochemical facies

The major hydrochemical facies of the NTS and vicinity were delineated by Winograd and Thordarson (1975). These authors recognized the three types of water described by Schoff and Moore (1964) and suggested two additional facies. The hydrochemical nature of the NTS and vicinity can thus be characterized as follows:

DECEMBER 1988

1. A sodium potassium bicarbonate facies is present in western Emigrant

Discharge from the tuff aquifer occurs as (1) vertical leakage to the

Table 3-11. Environmental isotope data for ground-water samples from the samples from the tuff and tuffaceous valley fill aquifers in the region near Yucca Mountain[a]

Well designation[b]	Collection date	δD (o/oo SMOW)[c]	$\delta^{18}O$ (o/oo SMOW)[c]	$\delta^{13}C$ (o/oo PDB)[d]	^{14}C (pmc)[e]	HTO (TU)[f]
UE-29a#1[g]	01/29/82	-92.0	-12.4	-12.6[h]	75.3	62.0
UE-29a#2[g,i]	01/08/82	-93.5	-13.0	-12.6[h]	62.3	11.0
UE-29a#2[g,i]	01/15/82	-93.0	-13.1	-13.1[h]	60.0	11.0
J-12[j]	03/26/71	-97.5	-12.8	-7.9	32.2	<68.0
J-13[j]	03/26/71	-97.5	-13.0	-7.3	29.2	<68.0
UE-25c#1	09/30/83	-102	-13.5	-7.1	15.0	<0.3
UE-25c#2	03/13/84	-100	-13.4	-7.0	16.6	<0.6
UE-25c#3	05/09/84	-103	-13.5	-7.5	15.7	0.6
USW H-6	10/16/82	-106	-13.8	-7.5	16.3	<3.0
USW H-6	06/20/84	-105	-14.0	-7.3	10.0	1.2
USW H-6	07/06/84	-107	-14.0	-7.1	12.4	0.3
USW VH1[j]	02/11/81	-108	-14.2	-8.5	12.2	6.0
AM-4	03/04/74	-103	-13.2	-7.1	19.3	--
AM-9	03/01/74	-102	-12.6	--[k]	28.4	--
AM-11	03/05/74	-101	-13.1	--	20.8	--
AM-13	03/05/74	-102	-13.0	--	19.3	--
AM-15	03/05/74	-104	-13.0	--	18.4	--
AM-18	03/06/74	-102	-13.0	--	27.8	--
AM-20[l]	03/06/74	-102	-12.4	--	13.8	--
AM-21	06/25/74	-99	-13.2	-8.4	27.4	--
AM-23	03/31/71	-103	-13.4	-7.1	17.1	--
AM-25	03/31/71	-102	-13.4	-5.6	15.6	--
NTS#8[m]	03/24/71	-104	-13.0	-12.1	25.4	--

[a]Sources: Data from Benson and McKinley (1985) and as noted in footnotes. AM-samples from Claassen (1985).

[b]Well locations for UE-, J- and USW-holes are shown in Figure 3-22. Well locations for AM (Amargosa) wells are shown in Figure 3-16.

[c]δ deuterium and δ oxygen-18 are reported in parts per thousand relative to the standard mean ocean water (SMOW) standard.

[d]δ carbon-13 is reported in parts per thousand relative to the Peedee belemnite (PDB) carbonate standard.

[e]Carbon-14 activity is reported as a percent of the modern carbon (pmc) standard.

[f]HTO = tritium; reported in tritium units (TU).

[g]Waddell (1985).

[h]Value reported as positive in reference.

[i]Also reported by Benson and McKinley (1985).

[j]Also reported by Claassen (1985).

[k]-- indicates no data.

[l]Completion in tuffaceous material unsure.

[m]Claassen (1985).

therefore, probably currently recharge the shallow tuff aquifer at this location. Note that locations for the Amargosa Valley wells listed in Table 3-11 are shown in Figure 3-17.

Claassen (1985) shows that this tendency for the higher carbon-14 content waters in the tuff to occur along washes also prevails down hydraulic gradient from Yucca Mountain. Wells J-12, J-13, Amargosa-9, and Amargosa-18 are good examples. The recharge through wash bottoms need not be recent, as it has been in well UE-29a#2. Claassen (1985) demonstrates that low bicarbonate waters in the tuff having δ carbon-13 ($\delta^{13}C$) values near atmospheric (-7 parts per thousand with respect to the Peedee belemnite carbonate standard (PDB) have probably had minimal isotopic dilution of their original carbon-14 by carbon-12 from carbonate minerals and have not exchanged with

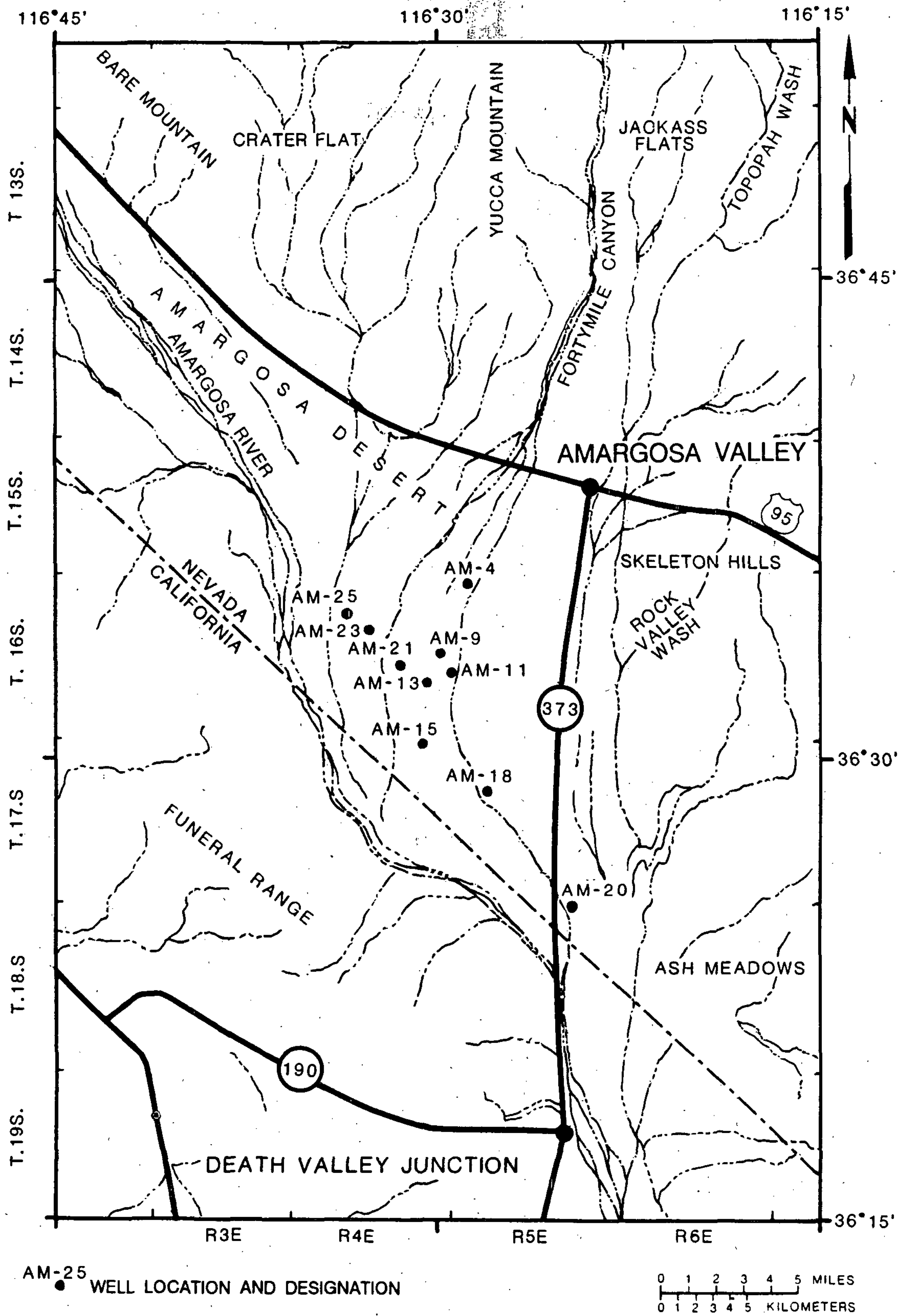

Figure 3-17. Location of Amargosa Valley (AM) ground-water sample wells.

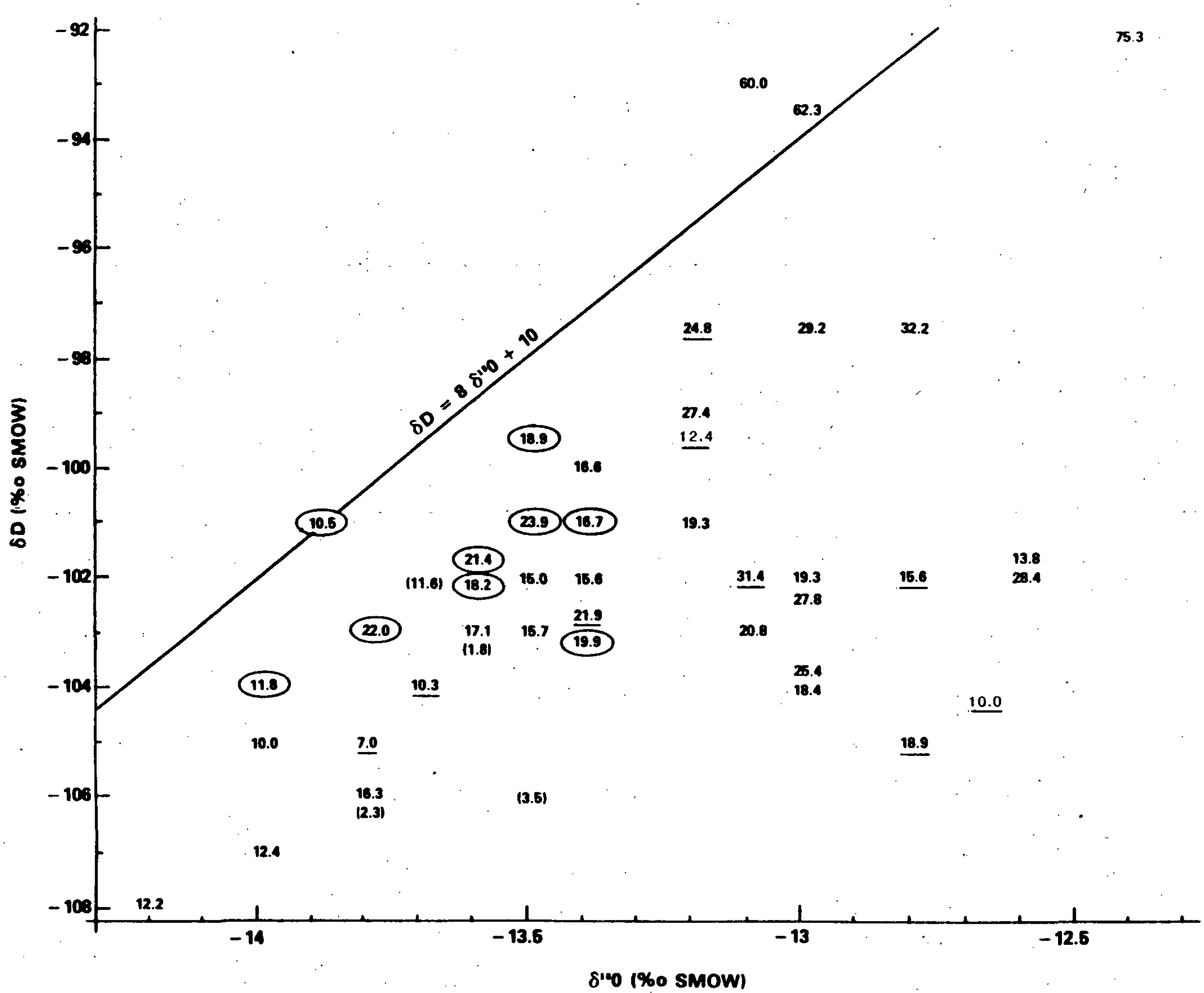

Figure 3-18. $\delta D - \delta^{18}O$ plot of waters from Yucca Mountain area, with radiocarbon content (in percent modern carbon (pmc) units) shown at the corresponding $\delta D - \delta^{18}O$ coordinate. Values in parentheses are from the lower carbonate aquifer. Underlined values are from mixed carbonate/tuff origin. The remaining values are from the tuff formations, with the Yucca Mountain samples circled.

Table 3-12. Environmental isotope data for ground-water samples from the carbonate aquifer and from mixed carbonate-tuff sources[a]

Well or spring designation	Collection date	δD o/oo SMOW[b]	$\delta^{18}O$ o/oo SMOW[b]	$\delta^{13}C$ o/oo PDB[c]	^{14}C (pmc)[d]	HTO (TU)[e]
			CARBONATE AQUIFER			
UE-25p#1[f,g]	02/09/83	-106	-13.5	-4.2	3.5	<3.1
UE-25p#1[f,h]	05/12/86	-106	-13.8	-2.3	2.3	3.1
16S/51E-23[i]	--[j]	--	-13.6	-4.6	1.8	--
Fairbanks Spring NE[k]	12/13/74	--	--	-5.2	2.2 ± 0.3	0.1 ± 0.2
Fairbanks Spring SW[k]	--	-103	-13.6	-4.9	1.8 ± 0.2	0.0 ± 0.4
Rogers Spring[k]	--	-102	--	-4.6	1.5 ± 0.3	0.0 ± 0.2
Longstreet Spring[k]	--	-103	--	-4.8	2.7 ± 0.4	0.0 ± 0.2
Scruggs Spring[k]	03/10/75[l]	-103	--	-4.7	1.1 ± 0.3	0.2 ± 0.2
Crystal Pool[k,m]	--	-102	-13.7	-5.0	11.6 ± 0.7	0.6 ± 0.4
Devils Hole[k]	--	--	-13.6	-5.0	2.8 ± 0.4	0.3 ± 0.2
King Spring[k,m]	--	-104	--	-4.7	1.7 ± 0.4	0.4 ± 0.2
Big Spring[k,m]	03/09/75	-102	--	-4.6	2.9 ± 0.4	0.3 ± 0.1
			MIXED SYSTEMS			
AM-3[n]	10/20/72	-102	-12.8	--	15.6	--
AM-5[n]	11/17/72	-99.5	-13.2	-6.8	12.4	--
AM-8[n]	03/01/74	-103	-13.4	-7.3	21.9	--
AM-10[n]	06/26/79	-97.5	-13.2	-5.2	24.8	--
AM-16[n]	03/01/74	-104	-12.7	--	10.0	--
AM-17[n]	03/01/74	-105	-12.8	--	18.9	--
AM-19[n]	03/06/74	--	--	--	40.3	--
AM-27[o]	08/18/62	-105	-13.8	-3.6	7.0	--
AM-29[p]	03/31/71	-105	-13.8	-3.4	--	--
AM-30[o]	06/24/79	-104	-13.7	-4.4	10.3	--
AM-47[o]	03/31/71	-102	-13.1	-6.2	31.4	--
AM-50[o]	06/25/79	-104	-13.6	-5.7	--	--
AM-60[p]	12/16/68	--	--	-5.9	28.8	--

[a]Data from Claassen (1985) unless otherwise indicated.
[b]δD and δ oxygen-18 ($\delta^{18}O$) are reported in parts per thousand relative to Standard Mean Ocean Water (SMOW) standard.
[c]Carbon-13 ($\delta^{13}C$) is reported in parts per thousand relative to the Peedee belemnite (PDB) carbonate standard.
[d]Carbon-14 (^{14}C) activity is reported as a percent of the modern carbon standard (pmc).
[e]HTO = tritium; T is reported in tritium units (TU).
[f]Benson and McKinley (1985).
[g]Sampled from the 381 to 1,197 m interval.
[h]Sampled from 1,297 to 1,805 m interval.
[i]Claassen (1985) reports this well as "Amargosa Tracer Well #2."
[j]Data from multiple collection dates.
[k]Winograd and Pearson (1976).
[l]Representative of multiple samplings.
[m]Similar values reported by Riggs (1984).
[n]Tuffaceous lithology, possible carbonate influence.
[o]Carbonate lithology, possible tuff influence.
[p]In both tuff and carbonate formations.

of this system. Plans for further sample collection are presented in Sections 8.3.1.2.3 and 8.3.1.12.

3.7.3.2.2 Carbonate aquifer

Environmental isotope data for ground-water samples from the carbonate aquifer and from mixed carbonate-tuff sources are listed in Table 3-12. Benson and McKinley (1985) have reported isotopic data for ground waters from the carbonate aquifer in the area around Yucca Mountain (drillhole UE-25p#1). Claassen (1985) reports two carbonate aquifer analyses and several analyses on mixed carbonate-tuff systems from the Amargosa Desert. Winograd and Pearson (1976) and Riggs (1984) report analyses of spring water from Ash Meadows, which drains primarily the area to the east of Yucca Mountain and the Amargosa Desert.

All samples from the carbonate aquifer show low carbon-14 contents (<4 pmc; except for Crystal Pool, which is discussed in the following paragraphs), as would be expected at the distal end of a regional carbonate aquifer system. The use of "apparent, uncorrected radiocarbon ages," which may be justified in the tuff aquifer is unsupportable in the carbonate system. The modeling of the carbon-14 content of the recharge waters is extremely complicated in a semiconfined carbonate aquifer system. The carbon-13 analyses show that interaction has occurred between the relatively carbon-14-free carbonate minerals of the aquifer and the flowing ground water. Small adjustments of the isotopic balance to account for this dilution process can greatly affect the resulting radiocarbon dates in such systems (Muller and Mayo, 1986). Without further modeling, these waters can only be taken to be "old," with 30,000 yr B.P. as the conservative upper limit. A very simple example can show why this is an upper limit. A pure carbonate water, one which derived half its carbon from active CO_2 gas and half from dead carbonate minerals, is one half-life younger than its apparent age. Thus, a ground water with an apparent age of 30,000 yr B.P. is probably around 24,000 yr old, if no isotopic dilution occurs as a result of precipitation/dissolution (i.e., isotopic exchange with the aquifer matrix).

The carbon-14 content of ground water at the center of a 16-km-long fault-controlled spring line at Ash Meadows is 5 times greater than that in water from other major springs along the lineament. Winograd and Pearson (1976) have examined the radiocarbon anomaly of Crystal Pool. They have shown it to probably be caused by megascale channeling, with water moving to this discharge point at velocities appreciably greater than those to adjacent springs. Such channeling is consistent with the known flow regime of karstic aquifers.

The data from Claassen (1985) for wells penetrating both tuff and carbonate lithologies show a variability in isotopic compositions expected in mixed systems (Table 3-12). Several of these wells are shallow, with waters also probably derived from valley fill sediments. There are insufficient data available to assess the extent and direction of mixing.

Few deuterium and oxygen-18 data are available for the carbonate aquifer (Figure 3-18 and Table 3-12). The waters show no hydrothermal fractionation and do not resemble expected modern precipitation. Additional stable isotopic data from the carbonate aquifer in the vicinity of Yucca Mountain is expected to provide further information on the interconnection of the tuff and carbonate aquifers. Plans for further data collection are presented in Section 8.3.1.2.3.

3.7.4 PALEOHYDROLOGY

The purpose of paleohydrologic studies is to determine hydrologic conditions during the Quaternary Period that have differed significantly from present conditions. This information will be used to evaluate the likelihood of episodic conditions recurring that may affect the regional ground-water-flow system over the next 100,000 yr. Of specific interest are (1) the maximum altitude of the water table during pluvial periods of the Quaternary Period, (2) the effects of pluvial water-table rises on shortening of ground-water flow paths to discharge areas, and (3) the magnitude of increases in recharge during pluvial periods. With such information, questions such as the following can be addressed: What is the possibility of the repository being flooded by a rising water table during a return of pluvial conditions? [illegible]

Evidence for former, higher water tables, changes in length of ground-water flow paths, and the presence and absence of pluvial lakes in the south-central Great Basin are discussed in the following sections. Although the period of major concern is the past 100,000 yr, the discussion will include paleohydrologic information extending into late Pliocene time.

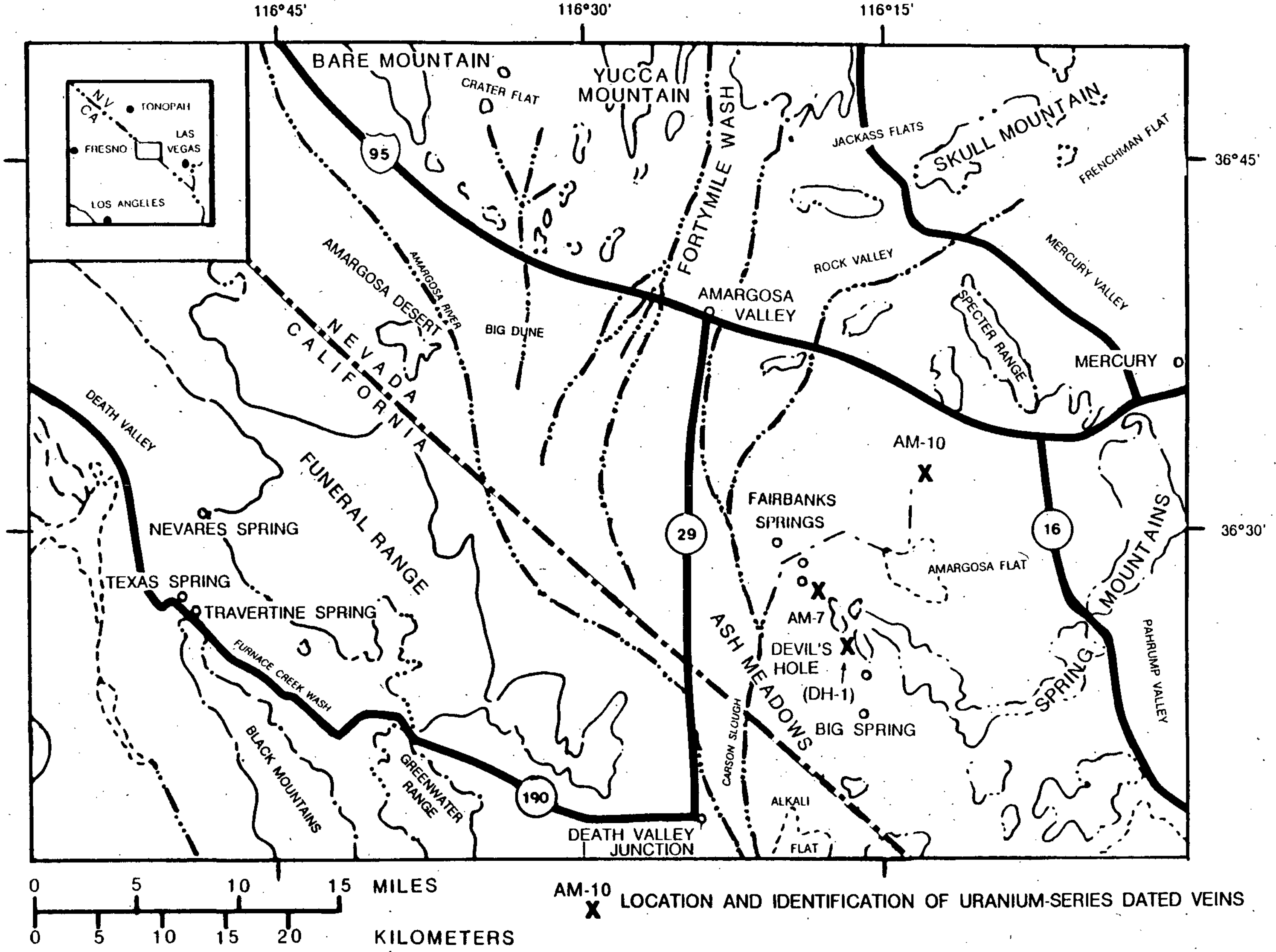
116°45'
116°30'
116°15'
36°45'
36°30'
NV
CA
TONOPAH
FRESNO
LAS VEGAS
LOS ANGELES
BARE MOUNTAIN
CRATER FLAT
YUCCA MOUNTAIN
FORTYMILE WASH
JACKASS FLATS
SKULL MOUNTAIN
FRENCHMAN FLAT
95
AMARGOSA DESERT
AMARGOSA RIVER
BIG DUNE
AMARGOSA VALLEY
ROCK VALLEY
MERCURY VALLEY
SPECTER RANGE
MERCURY
NEVADA
CALIFORNIA
DEATH VALLEY
FUNERAL RANGE
NEVARES SPRING
TEXAS SPRING
TRAVERTINE SPRING
FURNACE CREEK WASH
BLACK MOUNTAINS
GREENWATER RANGE
190
29
16
AM-10
FAIRBANKS SPRINGS
AMARGOSA FLAT
AM-7
DEVIL'S HOLE
(DH-1)
BIG SPRING
ASH MEADOWS
CARSON SLOUGH
ALKALI FLAT
SPRING MOUNTAINS
PAHRUMP VALLEY
DEATH VALLEY JUNCTION
N
0 5 10 15 MILES
0 5 10 15 20 KILOMETERS
AM-10 X LOCATION AND IDENTIFICATION OF URANIUM-SERIES DATED VEINS

(AM-7, AM-10, and DH-1 in Figure 3-19) show that the higher stands of water levels occurred during Pleistocene time, 1 million to 500,000 yr ago (Pexton, 1984; Winograd et al., 1985; and Winograd and Szabo, 1986).

Still higher and older ground-water levels are recorded throughout the central Amargosa Desert by widespread marsh deposits of ground-water origin. These deposits are described by Khoury et al. (1982) and Pexton (1984). The marsh deposits have been referred to as lacustrine or playa deposits (Walker and Eakin, 1963; Denny and Drewes, 1965; and Swadley, 1983). Hay et al. (1986) present evidence based on stratigraphy, mineral composition, fossil assemblages, and lithofacies relationships that these sediments were deposited in marshes or ponds fed by ground water rather than in lake or playa environments. In this report, they will be referred to as marsh deposits. The marsh deposits occur at altitudes as high as 790 m (Winograd and Doty, 1980) in Amargosa Flat in the east-central portion of the Amargosa Desert. This is about 70 m above the highest modern water level in Devils Hole (altitude 719 m).

A sample from the south end of Crater Flat described as nodular tufa spring deposits has been dated by the uranium-series method to approximately 30,000 yr B.P. (Szabo et al., 1981). Another sample described as seep-deposited tufa or calcrete from the south of Yucca Mountain was dated to 78,000 ± 5,000 yr B.P. (Szabo et al., 1981). These dates may not be correct, however, because this dating method is only considered accurate if the material is from a closed chemical system (Swadley et al., 1984; Bradley, 1985). Szabo et al. (1981) state that these types of deposits may form open systems. Studies to reexamine and redate the deposits are planned and discussed in Section 8.3.1.2. In the Ash Meadows area, these marsh deposits range in age from about 2 to 3 million years (Pexton, 1984) and presumably mark the altitude of regional ground-water discharge during late Pliocene and perhaps earliest Pleistocene time.

The occurrence of the various deposits, marking Quaternary water tables, at altitudes tens to over 100 m above the modern water table probably resulted from a combination of tectonism, water-table lowering due to increasing aridity since Pliocene time, and erosion. Winograd and Szabo (1986) believe that the altitude of the water-table-related deposits at Furnace Creek Wash (Figure 3-19) principally reflect uplift of the terrane, rather than an actual lowering of the water table. However, they infer that regionally the water table in the lower carbonate aquifer is likely to have lowered during the Quaternary Period. The following evidence is cited in support of their hypothesis:

1. The several-thousand-meter topographic relief in Death Valley dates largely from Pliocene and Pleistocene time (Hunt and Mabey, 1966; USGS, 1984), and the movement of the floor of Death Valley probably has been downward relative to sea level and to bordering areas (Hunt and Mabey, 1966).

2. Interbasin flow of ground water through Paleozoic carbonate rock and Tertiary welded-tuff aquifers toward Ash Meadows and Death Valley occurs today (Winograd and Thordarson, 1975). Interbasin flow of ground water toward Death Valley likely also occurred during the Quaternary Period in response to the lowering of ground-water dis-

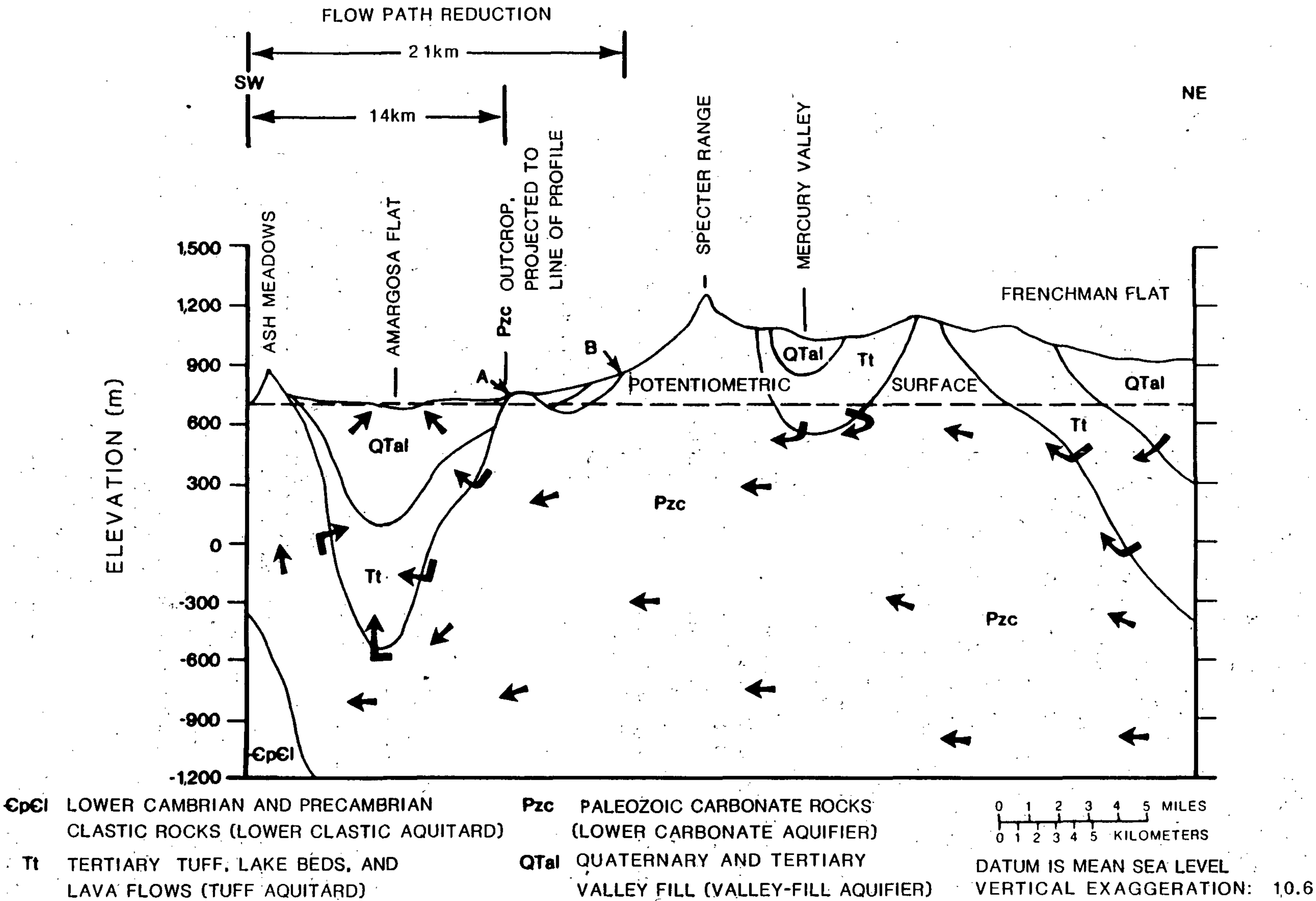

Figure 3-20. Diagrammatic section illustrating effects of possible past or future pluvial-related water-table rise on length of ground-water flow path from Frenchman Flat to points of natural discharge at Ash Meadows in the Amargosa Desert. Water-level rises of 40 and 150 m would initiate discharge from lower carbonate aquifer at points A and B, respectively 14 and 21 km northeast of modern spring lineament; arrows depict ground-water flow. Modified from Winograd and Doty (1980).

carbonate aquifer, either directly or indirectly via Tertiary aquitards. Like the calcitic veins, they occur as much as 14 km upgradient from Ash Meadows. West of Highway 29 and both north and south of Highway 95 the marsh deposits may reflect not only former discharge from the lower carbonate aquifer (which crops out in the west-central portion of the valley) but also from the Cenozoic welded-tuff and valley-fill aquifers. The marsh deposits in north-central Amargosa Desert are as much as 70 km from Alkali Flat, the modern discharge area in the southern Amargosa Desert.

3.7.4.3 Late Wisconsin lakes, marsh deposits, and ground-water levels

During the late Wisconsin, 21,000 to 10,000 yr ago, average annual precipitation is believed to have been as much as 100 percent greater than modern, with average annual temperature as much as 6°C cooler (Spaulding et al., 1984). Not unexpectedly, changes in climate from late Wisconsin to present conditions have (Section 5.2) produced major changes in the hydrology of the region.

Mifflin and Wheat (1979) discuss pluvial lakes of late Wisconsin age in Nevada. In southern Nevada, they examined Frenchman Flat, Yucca Flat, Gold Flat, Kawich Valley, Sarcobatus Flat, Stonewall Flat, Emigrant (Groom Lake) Valley, Papoose Lake Valley, Pahrump Valley, and Indian Springs Valley, which generally surround the Yucca Mountain area. Of these valleys, they reported shoreline development only in Gold Flat, Kawich Valley, and Emigrant Valley. They report marsh deposits in Indian Springs, Pahrump, and Sarcobatus valleys. Mifflin and Wheat (1979) conclude that "southern Nevada did not contain perennial lakes during the Wisconsinan pluvial," but that "there were likely a number of areas of marsh environments in southern Nevada due to concentrated ground water and spring discharge considerably in excess of present discharge. In south-central and southern Nevada significant differences in the amount and location of ground-water discharge seem apparent."

Hooke (1972) believed that a 90-m deep lake existed in Death Valley about 11,000 yr B.P. Smith and Street-Perrot (1983) agree that there was a lake between 12,000 and 21,000 yr B.P. but conclude that any lake or lakes were small and much shallower.

Quade (1986) reports marsh deposits in southern Indian Springs Valley. These deposits are assumed to be of late Wisconsin age, based on their stratigraphic and topographic similarity to dated deposits in northwestern Las Vegas Valley. They lie at a maximum altitude of 1,037 m, 20 to 50 m higher than the present water table in the valley-fill aquifer. If these deposits are of ground-water origin, as Quade believes, they may record a higher water table during late Wisconsin time. The marsh deposits occur above an inferred major hydraulic barrier (Winograd and Thordarson, 1975), and are 15 to 20 km downgradient from the Spring Mountains, a major recharge area. These factors may bear on the apparent water-table rise.

Mifflin and Wheat (1979) report marsh deposits, presumably of late Wisconsin age in Sarcobatus Flat and Pahrump Valley. They do not provide information on the location of these deposits so that we cannot compare their maximum altitudes with that of the preirrigation water table in these valleys.

Preliminary uranium-disequilibrium dating of calcitic cave deposits in Devils Hole, in central Ash Meadows suggests a 10-m rise in water level in the lower carbonate aquifer about 30,000 yr ago at Ash Meadows (Winograd and Szabo, 1986).

3.7.4.4 Estimation of future ground-water levels

Winograd and Doty (1980) using a variety of boundary conditions, suggest that during future pluvials, water levels in the regional carbonate aquifer at Ash Meadows and areas upgradient might be a few tens of meters higher than, or perhaps even lower than, modern levels. See Section 3.9.8 for estimation of possible future water levels in the Cenozoic volcanic rocks beneath Yucca Mountain and vicinity.

Winograd and Szabo (1986) concluded that there was a progressive lowering of the water table in the south-central Great Basin during the Quaternary. They noted that "a continued decline of the regional water table in the next 100,000 yr (and beyond?)" was likely (Section 3.9.8).

Craig (1984) makes a comprehensive statistical-climatologic analysis of climate conditions affecting the Death Valley drainage systems that existed during the last glacial maximum. In one analysis, Craig modeled full glacial conditions without assuming a major decrease in lake evaporation rates. In this instance, precipitation increased by 90 percent and pluvial lakes formed and Mabey (1966) also note that "The slight erosion and sedimentation record of Lake Manly may mean that the lake was of brief duration and its level may have fluctuated rapidly. Whatever the cause, this California lake left one of the least distinct and most incomplete records of any Pleistocene lake in the Great Basin." Thus, even if Lake Manly is of Wisconsin age, the climatic [redacted]

The paucity of geomorphic and sedimentologic evidence for Lake Manly makes it difficult to date the age of this major ancient lake in Death Valley. Resolving whether this lake is closer to 100,000 or 1 million years old would be of value to the paleohydrologic and paleoclimatologic analyses of Czarnecki (1985) and Craig (1984). Application of new or established methods, such as dating of desert varnish (Dorn, 1983) and uranium-series disequilibrium dating of lake-water cemented gravels, may hold some promise (Section 8.3.1.2.1). The reconnaissance (air photo) observations of Mifflin and Wheat (1979), regarding the absence of shorelines of late Pleistocene age in Yucca and Frenchman Flats and the presence of such shorelines in Gold Flat, Kawich Valley, and Emigrant Valley will be confirmed by more detailed study (Section 8.3.1.2.1).

3.7.4.5 Ground-water recharge during late Wisconsin time: carbon-14 evidence

Apparent ground-water ages determined from carbon-14 data (Benson and McKinley, 1985; Claassen, 1985) indicate that much of the ground water within the tuffaceous rocks in the vicinity of Yucca Mountain and within the valley fill aquifer beneath the central Amargosa Desert was recharged during late Wisconsin time, about 10,000 to 18,000 yr ago. Holocene-age (less than 10,000 yr) water occurs in Fortymile Canyon at well UE-29a#2 (4,000 yr B.P.) and at well J-12 (9,100 yr B.P.).

According to Claassen (1985), "little or no radiocarbon dilution probably occurred during the evolution of water in tuff or tuffaceous valley fill; therefore, the unadjusted ages are taken as true ages." He concluded that for ground waters that contain as much as 20 percent of carbonate-derived constituents unadjusted ages could be as much as 1,000 yr too old, and that for a higher percentage there could be a serious problem in determining true ages from carbon-14 data. Since expected ground-water flow paths of waters sampled from Cenozoic aquifers in the vicinity of Yucca Mountain involve little or no contact with carbonate rocks, carbon-14 ages probably are near

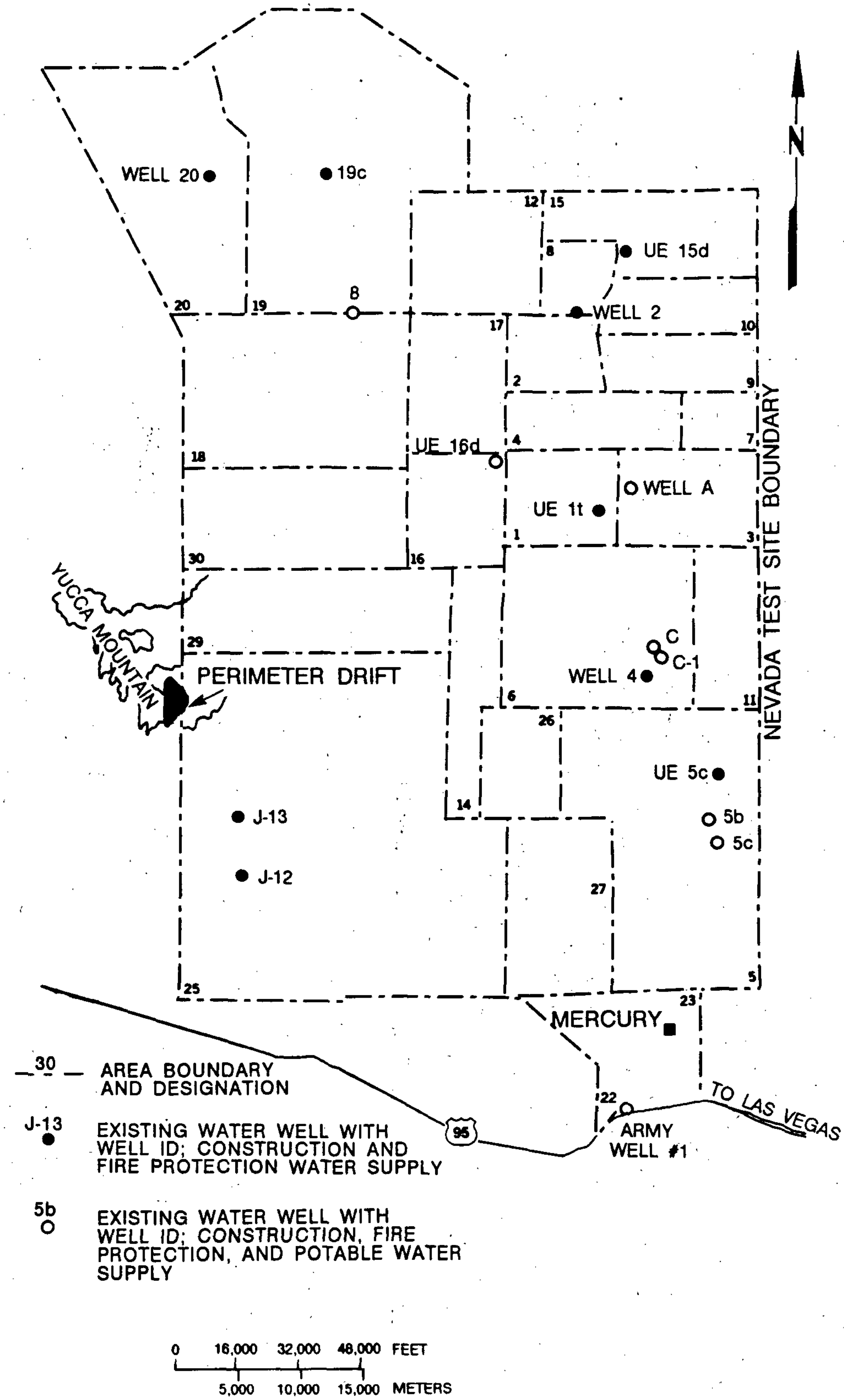

Figure 3-22. Index map showing water well locations and area boundaries at the Nevada Test Site. Modified from Witherill (1986).

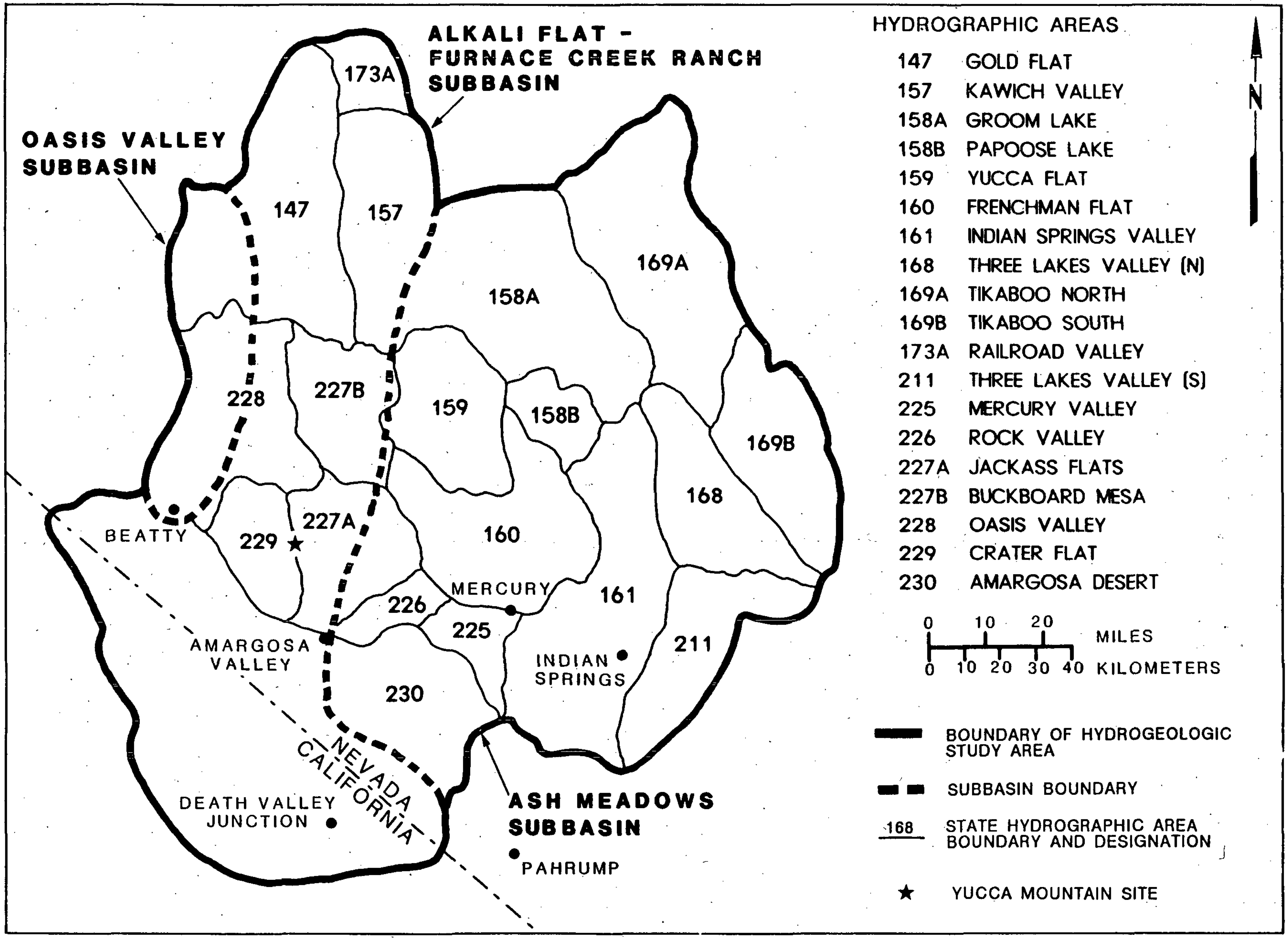

Figure 3-23. Location of Yucca Mountain with respect to the relevant hydrographic areas of Death Valley ground-water system and the hydrogeologic study area. Modified from Scott et al. (1971).

recharge from the Spring Mountains. Information presented in Harrill (1982) and Winograd and Thordarson (1975) suggests that site characterization activities and the possible subsequent development of a geologic repository in the Alkali Flat-Furnace Creek Ranch basin probably would not affect the Pahrump flow system.

3.8.1.1 Alkali Flat-Furnace Creek Ranch subbasin

The Yucca Mountain site is located within the Alkali Flat-Furnace Creek Ranch subbasin to the north of the Amargosa Desert (Figure 3-23). Very little ground water is withdrawn in the northern and central parts of this subbasin. In addition, very little ground water has been appropriated to the north of Yucca Mountain (upgradient) according to information filed with the Nevada State Engineer's Office.

The major ground-water users in the area, the town of Amargosa Valley and small rural communities of the northeastern Amargosa Desert, are located in the southwestern portion of the Alkali Flat-Furnace Creek Ranch subbasin (Figure 3-23) (French et al., 1984). Most of the water to these users is supplied by wells; however, there has been some spring development. Most residences rely on individual wells, while some trailer parks, public facilities, and commercial establishments are served by small, private water companies. Table 3-13 summarizes the public water suppliers in the area, the type of well used, and the population served. Table 3-14 identifies the total number of known water wells drilled in the Amargosa Desert according to their defined uses. All wells are completed in and produce from the valley-fill aquifer.

The only mineral production operation in the Amargosa Desert is owned by the American Borate Corporation. The operation, located between Amargosa Valley, Nevada, and Death Valley Junction, California (Figure 3-21), was decommissioned in July, 1986. The facility consisted of a large mineral processing plant and a housing development for its employees (French et al., 1984). Water for the community was pumped from a shallow well, having a capacity of 125 gpm (681 m^3/day). The water was treated by a reverse osmosis

Table 3-13. Public water suppliers in the community of Amargosa Valley[a,b]

Supplier	Type	Population served
American Borate Trailer Park	Community	300
Amargosa Water Company (IMV)	Community	45
Embrey's Trailer Park	Community	45
Mountain View Apartments and Shopping Center	Community	75
Amargosa Elementary School	Single user	(c)
Amargosa Senior Citizens' Center	Single user	(c)
Coach House Bar	Single user	(c)
Roadside Park 801NY	Single user	(c)
Water-N-Hole	Single user	(c)

[a]Source: SAIC (1986).

Table 3-15. Nevada Test Site water wells located in the Alkali Flat-Furnace Creek Ranch subbasin[a]

Area number[b]	Well	Pumping rate (gpm)[c]	Unit source[d]	Treatment required	Total withdrawals for 1985, in gal (acre-feet)[e]
18	8	400	Tuff	None	63,683,000 (195.4)
19	19	360	Tuff (?)[f]	None	114,467,200 (351.2)
20	U20a-2	340	Tuff	None	20,165,900 (61.9)
25	J-12	815	Tuff	None	25,049,800 (76.9)
25	J-13	680	Tuff	None	37,811,000 (116.0)

[a]Source: Witherill (1986) unless otherwise noted.
[b]Refer to Figure 3-22 for well locations.
[c]To convert to cubic meters per second, multiply by 6.31×10^{-5}.
[d]Based on information provided in Claassen (1973).
[e]To convert acre-feet to cubic meters, multiply by 1.23×10^{3}.
[f](?) = uncertain. Information regarding specific members is not available.

In addition to well production, a number of springs supply water to the region. The main concentration of springs is in Death Valley in the vicinity of Furnace Creek Ranch, approximately 50 to 60 km southwest of the Yucca Mountain site. Many points of ground-water discharge have been identified in

DECEMBER 1988

There are three resorts located within the boundaries of the Death Valley National Monument: the Stovepipe Wells Hotel, Furnace Creek Inn, and Furnace Creek Ranch. At Stovepipe Wells Hotel, northwest of Furnace Creek Ranch, potable water was trucked in for many years from a storage tank at Emigrant Ranger Station, 14 km (9 mi) southwest of the hotel. In 1973, the National Park Service constructed an underground storage tank in the alluvial

Table 3-16. Perennial yields, total appropriations, and actual water use for 1985 in the hydrographic

Hydrographic area[a]	Perennial	Total	Water use

only a fraction of the perennial yield that is available to those areas (Table 3-16).

3.8.1.2 Ash Meadows subbasin

Several small, unincorporated communities are located within the Ash Meadows subbasin. A large part of the NTS, including the community of Mercury, is also located within this subbasin. Very little water is withdrawn in this subbasin.

The Ash Meadows area is located 42 to 60 km (26 to 37.5 mi) southeast of Yucca Mountain (Figure 3-21). Water is pumped from the lower carbonate aquifer (Dudley and Larson, 1976). Virtually all irrigation withdrawals of ground water in this area currently are made by the Preferred Equities Corporation (Giampaoli, 1986). Water from eight major wells, supplemented by three small capacity wells, is used to irrigate more than 12 km^2 (4.6 mi^2) of cropland. Pumping peaked at a rate of approximately 1.2 million cubic meters per month during the years 1970 and 1971. Detailed pumping records were not maintained after 1971, while the land was controlled by the Spring Meadows,

with the planned development of a large agricultural enterprise caused a decline in the water level of the pool at Devils Hole (Dudley and Larson, 1976). This natural pool, formed from the collapse of the limestone bedrock, is the only remaining habitat of the endangered species, Devils Hole pupfish, Cyprinodon diabolis.

As a consequence of court action, ground-water withdrawals in this area are now restricted to a degree that is sufficient to maintain the water level in Devils Hole (Dudley and Larson, 1976). The land, which was previously owned by the Preferred Equities Corporation, was turned over to Nature Conservancy in 1986 and then transferred to the Federal Government (Giampaoli, 1986). Other springs in the Ash Meadows area are discussed in

Table 3-17. Nevada Test Site water wells located in the Ash Meadows subbasin[a]

Area number[b]	Well[b]	Pumping rate (gpm)[c]	Unit source[d]	Treatment required	Total withdrawals for 1985, in gal (acre-feet)[e]
1	UE1t	270	ND[f]	None	5,594,200 (17.2)
2	2	165	Lower carbonate aquifer(?)[g]	None	20,630,500 (63.3)
3	A	160	Valley fill	Chlorination	39,182,300 (120.2)
5	5b	240	Valley fill	None	6,107,800 (187.5)
5	5c	325	Valley fill	None	61,170,400 (187.7)
5	UE5C	350	ND	None	4,319,000 (13.3)
6	C	270	Lower carbonate aquifer(?)	None	26,162,900 (80.3)
6	C-1	280	Lower carbonate aquifer(?)	None	26,170,300 (80.3)
6	4	650	ND	None	41,815,300 (128.3)
15	UE15d	270	Tuff	Chlorination	ND
16	UE16d	194	ND	None	15,605,000 (47.9)
22	Army Well-1	530	Lower carbonate aquifer(?)	Chlorination	53,916,700 (165.4)

[a]Data from Witherill (1986) unless otherwise noted.
[b]Refer to Figure 3-22 for well locations.
[c]gpm = gallons per minute. To convert to cubic meters per second, multiply by 6.31×10^{-5}.
[d]Based on information provided in Claassen (1973), and Winograd and Thordarson (1975, plate 2b).
[e]To convert gallons to cubic meters, multiply by 3.785×10^{-3}.
[f]ND = No data.
[g](?) = uncertain.

53 water customers, including several trailer parks with multiple connections. The company has one well that is completed at the depth of 590 ft (180 m) and is capable of pumping at a rate of 550 gpm (2,998 m^3/day). The water from this well meets State drinking water standards and requires no chemical treatment. The water supply system is metered and is a separate system from that which supplies Indian Springs Air Force Base (French et al., 1984).

Approximately 80 other shallow, domestic wells in the Indian Springs area are in use. Information regarding water quality and quantity for these wells is unavailable. All wells in the area are probably completed in the valley-fill aquifer (Ciampoli, 1986), which is thought to be recharged

Table 3-18. Perennial yields, total appropriations, and actual water use for 1985 in the hydrographic areas making up the Ash Meadows subbasin (page 1 of 2)

Hydrographic area[a] Number	Hydrographic area[a] Name	Perennial yield (AFY)[b]	Existing appropriations (AFY)[c]	Water use in 1985 (AF)[d]	Comments
158A	Emigrant Valley (Groom Lake)	2,500	59.8	ND[e]	
158B	Emigrant Valley (Papoose Lake)	<10	0	0	
159	Yucca Flat	350	NA[f]	537.5	Nevada Test Site (NTS)
160	Frenchman Flat	100	NA	388.5	NTS
161	Indian Springs Valley	500	754.98	679.0[g]	
168	Three Lakes Valley (N)	4,000	11.48	ND	
169A	Tikaboo North	2,600	21.72	ND	
169B	Tikaboo South	4,000	ND	ND	
211	Three Lakes Valley (S)	5,000	ND	100[g,h]	

Table 3-18. Perennial yields, total appropriations, and actual water use for 1985 in the hydrographic areas making up the Ash Meadows subbasin (page 2 of 2)

Hydrographic area[a] Number	Name	Perennial yield (AFY)[b]	Existing appropriations (AFY)[c]	Water use in 1985 (AF)[d]	Comments
225	Mercury Valley	8,000	NA	165.4	NTS
226	Rock Valley	8,000	320.0	ND	
227A (East)	Fortymile Canyon (Jackass Flats)	2,000	NA	0	NTS
Subbasin totals		37,060	1,167.98	1,870.4	

[a]Hydrographic areas are shown on Figure 3-23.
[b]Data from Scott et al. (1971). AFY = acre-ft per year. To convert to cubic meters per year, multiply by 1.23×10^3.
[c]Tabulated from preliminary abstracts filed with the Office of the Nevada State Engineer.
[d]AF = acre-feet.
[e]ND = no data.
[f]NA = not applicable.
[g]Data from Giampaoli (1986).

3.8.1.3 Oasis Valley subbasin

The Oasis Valley subbasin encompasses the western parts of the Gold Flat and Oasis Valley hydrographic areas, 147 and 228 (Figure 3-23), respectively. Very little ground water is used in this area because of the low population density.

The unincorporated community of Beatty, Nevada (population 925), receives its water from the Beatty Water and Sanitation District. The water is supplied from four wells; three are located in town, and the fourth (Indian Springs Well) is approximately 6.4 km (4 mi) north of the town (Figure 3-21). The system supplies water to approximately 25 customers and the source capacity is about 500,000 gpd (1.9 x 10^3 m^3/day) (Gram, 1985). The water quality of the three wells in town, which produce from the valley fill aquifer (White, 1979), does not meet State drinking water standards because of excessive fluoride (water chemistry data are presented in Section 3.7.3). The EPA recently raised the maximum allowable fluoride content; if the State of Nevada raises its limits, the water from these three wells could meet the new standard with minimal treatment. The fourth well, located north of Beatty at Indian Springs (not to be confused with the community of Indian Springs, Nevada), is of higher quality and does meet the current State drinking water standards. This well is believed to produce from a perched tuff aquifer (White, 1979). Well production capacity from the Indian Springs well has recently decreased from 389 to 86 gpm (2.1 x 10^3 to 4.7 x 10^2 m^3/day) due to overpumping and subsequent dewatering of the aquifer (Gram, 1985). Five commercial establishments (Bailey's Hot Springs, Fran's Star Ranch, Ray's Last Stand, Scottie's Junction, and Cottontail) have water supplies and are available to the public. These establishments are all single-users and generally serve transient populations of 25 or fewer people per day. Outlying ranches in the area around Beatty have their own wells.

There are two gold mines operating in the Beatty area that require water for production purposes. The mines are owned by E. R. Fegert, Incorporated, and are located near Rhyolite and the boundary of the Death Valley National Monument. Water for production originates from two sources: One of these is a well owned by the company that produces 40 gpm (218 m^3/day). There are no data available to indicate the aquifer from which the well produces. An additional 483,000 gal (1,828 m^3) of water per month originates from one of the in-town wells operated by Beatty Water and Sanitation District (French et al., 1984). These mines are currently in the developmental phase; when planned future expansion is realized, peak employment will be approximately 100 persons. Another well is planned that will supplement the current water supplies (French et al., 1984).

Table 3-19 summarizes the known water use within the portions of Gold Flat and Oasis Valley basins (hydrographic areas 228 and 147 in Figure 3-23) that are located within the Oasis Valley subbasin. Note that although water use does not currently exceed the perennial yield in either basin, Oasis Valley (hydrographic area 228) has been designated. The designation of this area by the Nevada State Engineer was a protective measure to prevent the overappropriation.

Table 3-19. Perennial yields, total appropriations, and actual water use for 1985 in the hydrographic areas making up the Oasis Valley subbasin

Hydrographic area[a] Number	Name	Perennial yield (AFY)[b]	Total appropriations (AFY)[c]	Water use in 1985	Comments
147 (Southwest)	Gold Flat	1,900	NA[d]	ND[e]	Nevada Test Site
228 (West)	Oasis Valley	2,000	1528.72	Minor[f]	Designated
Subbasin totals		3,900	1528.72	Minor	

[a]Hydrographic areas are shown on Figure 3-23.
[b]Data from Scott et al. (1971). AFY = acre-feet per year.
[c]Tabulated from preliminary abstracts filed with the Office of the Nevada State Engineer.
[d]NA = not applicable.
[e]ND = no data.
[f]Data from Giampaoli (1986).

The water-supply problems that the community of Beatty is experiencing are not related to the designation of the basin (Section 3.8.2.2). A solution may now be imminent since the EPA raised the allowable limit of fluoride content in drinking water.

3.8.1.4 Proposed water use at Yucca Mountain

Water-use estimates for site characterization and subsequent repository construction and operation at Yucca Mountain are still in the early stages of development. The water-use figures presented in this section are preliminary and will probably change as more is learned about Yucca Mountain.

Wells J-12 and J-13, located along Fortymile Wash, supply water to the former Nuclear Research and Development Area facilities at the NTS (Young, 1972). Both of these wells are completed in and producing from the welded tuff aquifer (Section 3.6.4 for a description of aquifer characteristics). Well J-13 was in continuous service from 1962 to 1969 and caused only a slight decline in the water level (Thordarson, 1983; Section 3.9.7). By 1980, the static water level had recovered to within 0.1 m (0.3 ft) of its original elevation as water withdrawals became intermittent. A more detailed discussion of wells J-12 and J-13 appears in Section 3.9.7.

Test results by Young (1972), Claassen (1973), and Thordarson (1983),

Table 3-20. Estimated water use for exploratory shaft facilities at Yucca Mountain, Nevada[a,b]

Characterization phase	Amount of water needed (gal)	Amount of water needed (m^3)
PHASE I: SURFACE FACILITY CONSTRUCTION (30 WEEKS)		
Site preparation	15,376,000	5.8×10^4
Facilities construction	1,410,500	5.3×10^3
Pipe cleaning, flushing, testing, and filling	248,500	9.4×10^2
Fire suppression	90,000	3.4×10^2
Subtotal	17,125,000	6.46×10^4
PHASE II: SHAFT SINKING (107 WEEKS)		
Setup, collar, headframe	645,000	2.4×10^3
Shaft sinking and testing	4,962,350	1.9×10^4
Station construction and changeover	2,618,200	9.9×10^3
Raisebore second exploratory shaft	481,050	1.8×10^3
Subtotal	8,706,600	3.31×10^4
PHASE III: TEST CONSTRUCTION AND SUPPORT (174 WEEKS)		
Excavation	10,225,800	3.9×10^4
Construction	835,200	3.2×10^3
Test support	4,614,500	1.7×10^4
Subtotal	15,675,500	5.92×10^4
Total	41,507,100	1.57×10^5

[a]Source: Pedalino (1986).
[b]Includes water for personal use and consumption.

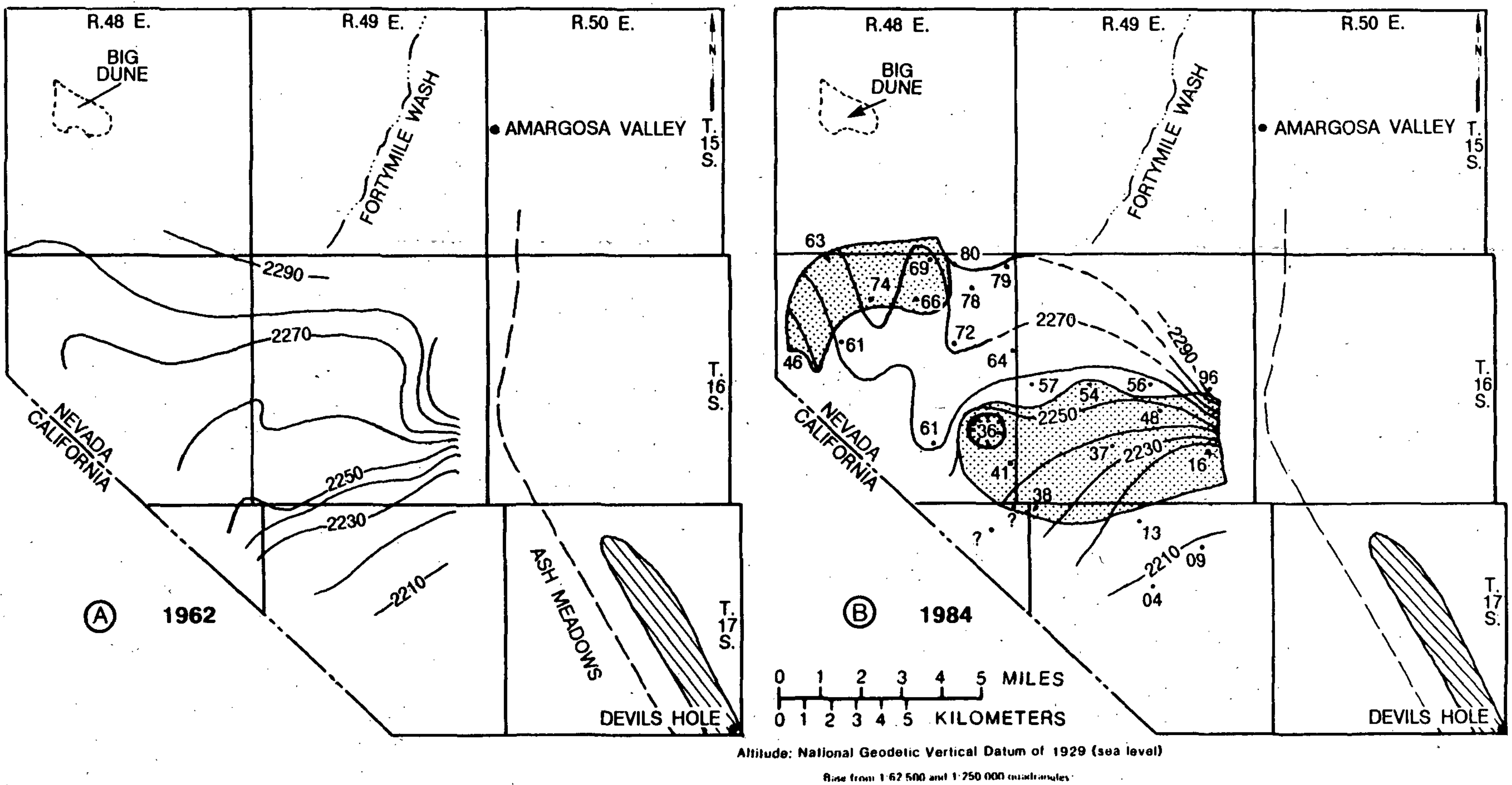

EXPLANATION

— — INFERRED FAULT -- From Winograd and Thordarson (1975, page C70, plate 1); delineated on basis of gravity survey

GENERALIZED AREA OF SPRING DISCHARGE

GENERALIZED AREA WHERE NET WATER-LEVEL DECLINE BETWEEN 1962 AND 1984 EXCEEDED 10 FEET

--2270-- WATER-LEVEL CONTOUR -- Shows altitude of ground-water level in valley-fill deposits. Dashed where approximately located. Contour interval 10 feet. Datum is sea level. Contours for 1962 from Walker and Eakin (1963, plate 3)

• 72 WELL -- Number is water-surface altitude, January 1984, in feet above 2,200 feet (question mark indicates lack of water-level measurement in 1984). Datum is sea level

Figure 3-24. Potentiometric maps of the Amargosa Desert (valley fill aquifer) based on the well data from (1962) (A) and (1984) (B). Modified from Nichols and Akers (1985).

The decline in water levels, and the formation of a depression cone, resulted from withdrawals made by 27 wells in the valley. Pumping rates for domestic wells range from 10 to 40 gpm while industrial wells produce from 100 to 800 gpm (including irrigation and mining wells) (Giampaoli, 1986). No other local potentiometric maps are published that show depression cones in areas of ground-water withdrawals, and no injection wells exist in the hydrogeologic study area. Plans for developing large-scale potentiometric maps of the hydrogeologic study area are presented in Section 8.3.1.2.1.

3.8.1.5 Water use for energy development

This section examines water use for the purpose of energy development in the hydrogeologic study area. Only geothermal resource development is considered, because it is the only form of ground-water-related energy development known to be present in southern Nevada.

The low-temperature geothermal resources located in the vicinity of Yucca Mountain have little potential for exploitation (refer to Section 1.7 for an evaluation of geothermal resources). The use of these resources for energy development is highly unlikely. Water temperatures measured in test holes in the vicinity of Yucca Mountain are in the range of 50 to 60°C at depths to 1,800 m (5,906 ft) (Craig and Robison, 1984). Current technology requires reservoir temperatures of at least 180°C for commercial power generation (White, 1973). Consequently, it is extremely unlikely that high temperature waters would be present at depths that are economically attractive. Should advances in technology make deeper geothermal resources economically attractive, many areas other than Yucca Mountain could be exploited (Garside and Schilling, 1979).

In summary, there currently is very little potential for geothermal energy resource development within the hydrogeologic study area.

3.8.2 REGIONAL GROUND-WATER MANAGEMENT PLANS

The first part of this section presents an overview of Nevada's philosophy of ground-water management and the measures that are taken to mitigate ground-water supply problems. Agencies involved in the appropriation of ground-water resources and programs or laws that govern ground-water use that might relate to activities at Yucca Mountain are identified. The second part of this section identifies the nearby communities that might be affected as a result of the proposed repository-related withdrawals. Site characterization activities and the construction and operation of a geologic repository at Yucca Mountain would increase the demand for water in the immediate vicinity of the site, as discussed in Section 3.8.1.4. Water use projections for the next 50- and 100-yr periods currently are not available. Data and information that are needed to assess the potential impacts are delineated. Plans for obtaining these data are presented in Section 8.3.1.16.2.

3.8.2.1 Ground-water management in Nevada

Most of the unincorporated communities located within the geohydrologic study area do not have municipal water supply systems. Water use is governed by the appropriate Board of County Commissioners. The State of Nevada, however, has responsibility for protecting its ground-water resources. Areas and communities examined in this section are Pahrump, Beatty, Amargosa Valley, and Area 25 (Figure 3-21) of the NTS; these areas are located proximal to the proposed repository site, or historically have experienced water supply problems. Estimated and projected water use figures for each community located within the hydrogeologic study area are presented in Table 3-21.

Water use in Nevada is governed by the Office of the State Engineer and the Division of Water Resources. Chapter 534 (Title 48-Water) of the Nevada Water Laws outlines and delineates the allowable uses of ground waters. Morros (1982a) presents the laws and statutes relating to all aspects of ground-water and geothermal resources, as described in Chapter 534 and Chapter 534A, respectively.

The State of Nevada uses a recharge-use philosophy in its management of ground-water resources. As previously discussed in Section 3.8.1, total annual ground-water withdrawals from any given basin may not exceed the perennial yield (Morros, 1982a). Unfortunately there are many difficulties inherent in determining the actual amount of recharge to an undeveloped basin where no pumping has occurred. In many instances, aquifer overdrafts occur before the perennial yield has been firmly established (Todd, 1980).

At the first indication of an aquifer overdraft, measures are taken to carefully regulate ground-water withdrawals. A provision of the Nevada Water Laws grants authority to the State Engineer to designate ground-water basin boundaries in areas where he deems that ground-water resources are being depleted. Such designation orders have been issued in four areas of consideration: (1) the Amargosa Desert ground-water basin, (2) the Pahrump Artesian Basin, (3) Oasis Valley West, and (4) Indian Springs Valley.

Table 3-21. Existing total water use in the communities located in the hydrogeologic study area

Community	Estimated population 1985[a]	Estimated existing water use (mg/d)[b]	Maximum population increase due to site characterization activities[c]	Projected increase in water use due to site characterization activities[c] (mg/d)
Indian Springs	912	0.8	85	0.07
Indian Springs Air Force Base	900	0.4	ND[d]	ND
Beatty	925[e]	0.8	2	0.002
Mercury	300	0.3	ND	ND
Pahrump	5,500	4.7	127	0.1
Ash Meadows	41	0.04	ND	ND
Johnnie	8	0.007	ND	ND
Amargosa Valley	1,905[f]	1.6	6	0.005
Crystal	65	0.06	ND	ND
Rhyolite	4	0.003	ND	ND
Death Valley Junction	20[g]	0.017	ND	ND
Totals	10,580	8.7	220	0.177

[a]Population data from Smith and Coogan (1984) except where otherwise noted.

[b]mg/d = million gallons per day. Maximum permissible water use in southern Nevada, is 1,800 gal per day per residential unit, or almost 2 acre-feet per year (assuming 2.1 residents per housing unit).

[c]Data from DOE (1986).

[d]ND = no data.

[e]Data from Gram (1985).

[f]Includes population of Amargosa Valley, American Borate Mill, American Borate Housing Complex, and the Spring Meadows area.

[g]Community distribution system. Water quality does not meet U.S. Environmental Protection Agency drinking water standards (French et al., 1984).

Although water use in Oasis Valley is currently considered minor (Giampaoli, 1986), the western portion of the Oasis Valley (hydrographic area 228) was designated in 1980 to prevent overappropriation. Recharge to the ground-water basin is estimated to be approximately 2,000 acre-feet per year (2.5×10^6 m^3/yr).

The community of Beatty may experience water supply shortages in the near future. Gram (1985) reported that the population growth rate from 1980 to 1985 was nearly 3 percent, while the demand for water had increased nearly 10 percent. Although a high-quality water source has not yet been developed, Gram (1985) has presented several recommendations that could alleviate future water supply problems.

The Indian Springs Valley (hydrographic area 161 in Figure 3-23) was designated in 1980. Water-level declines in the Indian Springs community caused a decrease in local spring discharge (Giampaoli, 1986). Although the amount of water appropriated is minor, total water withdrawals and natural discharge in the form of springs and evapotranspiration are in excess of the perennial yield.

The town of Pahrump, located approximately 100 km southeast of Yucca Mountain, has experienced ground-water overdraft problems in the past. Excessive agricultural withdrawals before 1970 caused a lowering of the water level in the valley fill aquifer. In 1970, the State Engineer ordered a moratorium on the issuance of water permits for irrigation from the Pahrump Artesian basin. Certificated appropriations and development permits for ground water in the Pahrump Valley totaled 90,790 acre-feet (112×10^6 m^3) in 1970, although in recent years actual water withdrawal has averaged approximately 39,720 acre-feet per year (49×10^6 m^3) (DOE, 1986). The repository project probably would not affect the water resources in the Pahrump Valley, since the proposed site is within a different subbasin of the Death Valley ground-water system (Figure 3-23) (Winograd and Thordarson, 1975; Harrill, 1982; French et al., 1984; Waddell et al., 1984).

3.9 SITE HYDROGEOLOGIC SYSTEM

In previous sections of Chapter 3, the regional hydrogeologic setting of Yucca Mountain was considered; this section focuses on the site hydrogeologic system in the immediate vicinity of Yucca Mountain (generally within a few kilometers of the outer boundary of the repository). The site at Yucca Mountain is unique among those being considered in that the repository is intended to be situated deep in the unsaturated zone, about 300 m below land surface and 250 m above the water table (Chapter 6).

The general concept of ground-water flow at Yucca Mountain assumes that a small fraction of the local precipitation enters the unsaturated zone as net infiltration below the surficial plant-root zone, to percolate generally downward and past the repository horizon, and eventually to reach the water table as recharge. However, downward moisture flow may be substantially reduced or even offset by upward flow of water vapor in fractures in welded tuff. Preliminary analyses indicate that temporal variations of net infiltration may be damped out within the uppermost few tens of meters within the unsaturated zone (Montazer and Wilson, 1984; Weeks and Wilson, 1984). Below these depths, moisture flow (net flux) may be under effectively steady-state conditions (Weeks and Wilson, 1984; Klavetter and Peters, 1986). Because net infiltration is irregularly distributed over the surface of Yucca Mountain and because the hydrologic properties within the unsaturated zone are heterogeneous, considerable spatial variability in flux probably occurs at any horizon within Yucca Mountain, including the repository horizon (Montazer and Wilson, 1984).

If any recharge occurs at Yucca Mountain the recharge will join and move laterally with the saturated-zone ground water. Most likely sources of recharge, however, are the mountainous highlands north of the site (although there may be some recharge that is more local; see Section 8.3.1.2.1 for plans to evaluate possible recharge along Fortymile Wash). Ground water arriving at the water table beneath Yucca Mountain probably mixes with ground water in the saturated zone only within the upper few hundred meters of saturated Tertiary tuffs, regardless of the particular hydrogeologic units along the flow path. This occurs because vertical hydraulic gradients within this interval generally are small, and potentiometric heads at greater depth in less permeable rocks of Tertiary and Paleozoic age are significantly greater than the water table, based on head movements at three sites. Although the reverse conditions are possible at the site, no evidence for this unlikely situation presently exists. At least within the upper part of the saturated zone, the water moves south or southeast from Yucca Mountain.

The rocks underlying Yucca Mountain through which the ground water moves are mostly fractured tuffs of Tertiary age; the major stratigraphic units are shown in a schematic geologic section in Figure 3-25. Because physical properties of the rocks that are believed to control movement of ground water in the unsaturated zone are not completely consistent with stratigraphic boundaries, hydrogeologic boundaries for the unsaturated zone have been defined and are shown in Table 3-22.

An understanding of the saturated-zone hydrologic system is required for waste isolation because this zone contains substantial portions of many pathways to the accessible environment. An understanding of saturated-zone hydrology is also needed in order to evaluate the hydrologic effects of future climate changes; these effects include potential rises in the water table and changes in gradients and paths of ground-water flow in the saturated zone. The distributions of critical parameters, such as effective porosity, are presently unknown and will be evaluated by future testing programs (Section 8.3.1.2.3).

This section describes monitoring networks, from which the following baseline hydrologic data are being obtained: potentiometric levels; hydraulic characteristics of the formations that may store and transmit water in the unsaturated and saturated zones; conceptual ideas of modes and flow paths of ground water, including recharge and discharge; hydrochemistry, ground-water age, and hydraulic parameters as indicators of ground-water velocity and travel times; local ground-water uses that could affect the natural flow system; and past hydrogeologic conditions, to the extent that an understanding of them may be helpful for prediction of future conditions.

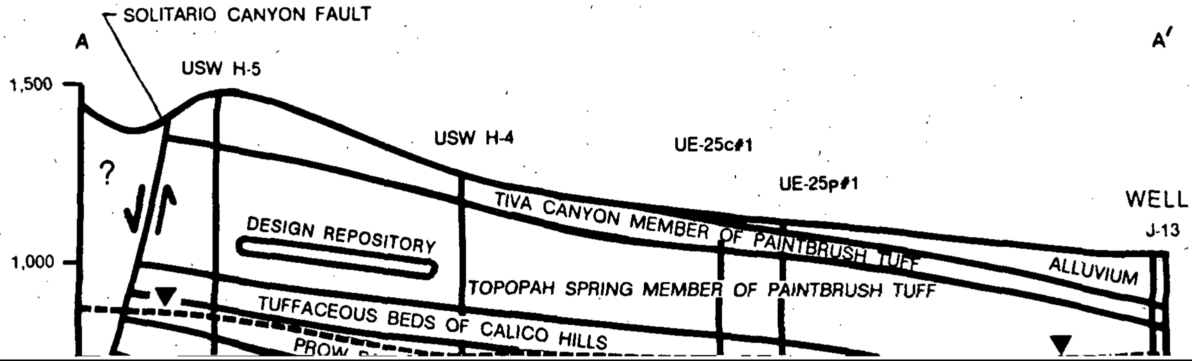
SOLITARIO CANYON FAULT
A
A′
USW H-5
1,500
1,000
USW H-4
UE-25c#1
UE-25p#1
WELL
J-13
?
DESIGN REPOSITORY
TIVA CANYON MEMBER OF PAINTBRUSH TUFF
ALLUVIUM
TOPOPAH SPRING MEMBER OF PAINTBRUSH TUFF
TUFFACEOUS BEDS OF CALICO HILLS

Table 3-22. Definition of unsaturated-zone hydrogeologic units and correlation with rock-stratigraphic units[a].

Rock-Stratigraphic Unit		Hydrogeologic Unit[b]	Approximate Range of Thickness (m)	Lithology[c]
Alluvium		QAL	0-30	Irregularly distributed surficial deposits of alluvium and colluvium
Paintbrush Tuff	Tiva Canyon Member	TCw	0-150	Moderately to densely welded, devitrified ash-flow tuff
Paintbrush Tuff	Yucca Mountain Member	PTn	20-100	Partially welded to nonwelded, vitric and occasionally divitrified tuffs
Paintbrush Tuff	Pah Canyon Member	PTn	20-100	Partially welded to nonwelded, vitric and occasionally divitrified tuffs
Paintbrush Tuff	Topopah Spring Member	TSw	290-360	Moderately to densely welded, devitrified ash-flow tuffs that are locally lithophysae-rich in the upper part, includes basal vitrophyre
Tuffaceous beds of Calico Hills		CHn: CHnv / CHnz	100-400	Nonwelded to partially welded ash-flow tuffs: Vitric / Zeolitized
Crater Flat Tuff	Prow Pass Member	CHn: CHnv / CHnz	100-400	Nonwelded to partially welded ash-flow tuffs: Vitric / Zeolitized
Crater Flat Tuff	Bullfrog Member	CFu	0-200	Undifferentiated, welded and nonwelded, vitric, devitrified, and zeolitized ash-flow and air-fall tuffs

[a]Sources: Montazer and Wilson (1984) except as noted.

[b]QAL = Quaternary Alluvium, TC_w = Tiva Canyon welded unit, PT_n = Paintbrush nonwelded unit, TS_w = Topopah Spring welded unit, CH_n = Calico Hills nonwelded unit, CH_{nv} = Calico Hills nonwelded vitric unit, CH_{nz} = Calico Hills nonwelded zeolitized unit, CF_u = Crater Flat undifferentiated unit.

[c]Lithology summarized from Ortiz et al. (1985).

Because of the need to emphasize the unsaturated zone at Yucca Mountain, hydrogeologic characterization of the site poses a dual problem. Specifically, it is necessary (1) to define the macroscopic hydrologic system within the unsaturated zone and (2) to describe this system in terms of the microscopic hydrologic processes that occur within the thick sequence of welded and nonwelded, fractured and unfractured tuffs that make up the unsaturated zone. The fundamental concepts and theory of moisture flow and storage within variably saturated natural media have been developed for specific application to problems of soil physics (Hillel, 1980), petroleum-reservoir engineering (Amyx et al., 1960) and geothermal resource evaluation (Faust and Mercer, 1977). The resultant generally considered theory may not be applicable to indurated tuffs that have low porosity and low permeability and that also may be highly fractured. Consequently, a complete characterization of the site hydrologic system must examine the mechanisms by which moisture can be stored and transported within the fractures and interstices of deeply buried tuffs. Only then can a set of hypotheses be developed to construct a macroscopic conceptualization within which these mechanisms act to determine the present, naturally occurring hydrologic system.

A major part of the site characterization program for the unsaturated zone, as described in Section 8.3.1.2.2, is devoted to field, laboratory, and theoretically based studies to test various concepts and hypotheses for moisture flow in fractured tuffs. These studies are to be combined with large-scale field and mathematical-modeling studies to further develop and test conceptualizations of the overall macroscopic hydrologic system. To establish an internally consistent conceptual framework and terminology, the conventional theory of moisture flow and storage in variably saturated porous media is reviewed in the following paragraphs, together with some of its potential limitations and inadequacies with respect to conditions thought to prevail at the Yucca Mountain site.

The term moisture is introduced here in a generic sense to include both liquid water and water vapor. Moisture flow and storage, thus, include the combined flow and storage of liquid water and water vapor. Under partially saturated conditions, water vapor will be present within the pore gas, regarded as a mixture of air and water vapor. Under most natural conditions, water vapor and liquid water will be in local thermodynamic phase equilibrium

1 micrometer (Peters et al., 1984) or less, while representative fracture spacings are of the order of 5 cm or more (Scott et al., 1983), a considerable difference may exist in the scale of (1) the bulk-rock volume appropriate for defining the rock-matrix hydrologic properties, which are averaged over the pore space, and (2) the volume containing many fractures that is required to define the bulk properties for the fractures. Under these conditions, the pores and fractures may effectively define two overlapping continuum systems, each regarded as an equivalent porous medium. Such a double-porosity model may be appropriate, for example, to describe a highly fractured but otherwise homogeneous tuff in which the fractures bound distinct rock-matrix blocks. At the opposite extreme, the fracture density may be so low that bulk fracture properties cannot be defined meaningfully, in which case the fractures that are present would have to be regarded as discrete entities. Such may be the case in an otherwise unfractured hydrogeologic unit that is transected by a fault.

Under partially saturated conditions, liquid water is bound to the solid within the pore and fracture openings either by surface-tension (capillary) forces or, at very low saturations, by physical or chemical adsorption. The strength of the bonding force is measured in terms of an equivalent negative pressure, or pressure head, here designated the matric potential. In a fractured medium, the matric potential within the fractures need not be equal to that within the enclosing rock matrix, although pressure equilibration will tend to be established over time. Large differences in matric potential between rock matrix and fractures may occur under transient conditions, for example, within and following an advancing infiltration front, and thus may affect significantly moisture movement under such conditions (Klavetter and Peters, 1986).

Matric potential is a function of liquid-water saturation, and an analytic or graphical representation of the functional relation defines the moisture-retention curve for the porous medium. Moisture-retention curves for most media are not unique; they display hysteresis in which the precise relation between matric potential and saturation depends on whether saturation is increasing (wetting curve) or decreasing (drying curve). Standard techniques, using mercury intrusion, pressure-plate apparatus, thermocouple psychrometers, and centrifuges have been developed (Hillel, 1980) by which to measure the moisture-retention curves for small soil or rock samples. The intact-fracture test within the exploratory shaft (Section 8.3.1.2.2) is designed, in part, to investigate the moisture-retention properties appropriate to discrete fractures.

The vector volumetric flux of liquid water moving under isothermal conditions through a partially saturated, natural hydrogeologic unit, regarded as an equivalent porous-medium continuum system, is generally presumed to be determined by the spatial gradients of matric and gravitational potentials and by the hydrologic properties. This functional dependence is expressed mathematically by the Darcy's law for unsaturated liquid-water flow, one version of which may be written as (Hillel, 1980):

$$q_l = -K_l \, K_R \text{ grad } (\psi_l + z), \tag{3-3}$$

where

q_l = volumetric flux of liquid water (L^3/L^2T)

K_l = saturated (liquid) hydraulic conductivity (L/T)

K_R = relative hydraulic conductivity (dimensionless)

ψ_l = capillary-pressure head (L)

z = vertical coordinate (positive upward) relative to a specified x- and y-coordinate plane (L)

grad = $i\frac{\partial}{\partial x} + j\frac{\partial}{\partial y} + k\frac{\partial}{\partial z}$, where i, j, and k are unit vectors aligned with the x-, y-, and z-coordinate axes, respectively (1/L).

In a fractured medium under the dual-porosity model, identical versions of Equation 3-3 would apply separately to the rock-matrix and fracture systems with q, ψ, K, and K defined appropriately for these two distinct systems.

The relative hydraulic conductivity, K_R, is defined as the ratio of hydraulic conductivity at a given matrix saturation to that at complete matrix saturation (K_1). The parameter, K_R, is of unit magnitude at complete saturation and, usually, decreases rapidly towards zero with decreasing saturation or, equivalently, matric potential. Because the functional dependence of K_R on S_1, or ψ_1, is difficult to determine through direct measurement, procedures have been developed for soils by which to infer closed-form analytic representations for this dependence from the corresponding moisture-retention curve (Brooks and Corey, 1964; Mualem, 1976; van Genuchten, 1980). It is not clear that these approximating representations are appropriate to indurated fractured tuffs, but they have been used in preliminary studies at Yucca Mountain (Klavetter and Peters, 1986; Rulon et al., 1986) in lieu of more fundamental data. That this approach is appropriate to describe the rock-matrix properties is supported indirectly in that the moisture-retention curves measured on individual samples of tuff can be fitted accurately, for example, by the analytic representation developed for soils by van Genuchten (1980). Fractured-rock systems introduce further complications that depend on the mechanisms by which moisture is transported in partially saturated fractures and define an area of current active research (Montazer and Harrold, 1985; Wang and Narasimhan, 1985). The bulk-permeability test to be conducted within the exploratory shaft (Section 8.3.1.2.2) is intended to obtain direct empirical data on the bulk hydrologic properties for the unsaturated, fractured Topopah Spring welded unit.

The moisture-retention curve together with the dependence of relative hydraulic conductivity on saturation or, equivalently, matric potential, constitute the set of moisture-characteristic relations for a particular porous medium under partially saturated conditions. Consequently, these relations must be supplied as part of the suite of hydrologic-property data for each hydrogeologic unit within the unsaturated zone at Yucca Mountain. A hydrogeologic unit, in this usage, is defined to be a functional unit composed of an interval or volume of rocks within which the mean hydrologic properties are effectively spatially invariant. A hydrogeologic unit may include, in whole or in part, one or more rock-stratigraphic units.

In addition to the storage and transport of moisture as liquid water within the unsaturated zone, moisture may be stored and transported as water vapor within the air-filled pore space. The bulk flow of air in pores and fractures probably is usually regarded to be Darcian in which the appropriate potential is the local pore-gas pressure. Gas flow is more complex, however, because the compressibility of the gas must be taken into account through an appropriate equation of state. Furthermore, in pores and fractures whose apertures are a few times the mean free path of pore-gas molecules, the gas will tend to slip past the pore and fracture walls to produce an effective increase of gas permeability k_g according to the law $k_g = k\ (1 + b/P)$ (Klinkenberg, 1941), where k is the (intrinsic) permeability of the medium, P is the ambient pore-gas pressure, and b is an empirical constant appropriate to the pore-gas system under consideration. For example, Reda (1985a) determined experimentally that the permeability with respect to nitrogen gas of a sample of the TSw unit was a strongly dependent function of pore-gas pressure for which the Klinkenberg constant b = 0.76 MPa.

Not only does bulk-gas flow and storage need to be considered in order to assess the efficacy of vapor-phase moisture transport within the unsaturated zone at Yucca Mountain; but also, air is a very convenient fluid medium to use in field determinations of permeability by monitoring both barometrically induced pressure changes with depth in wells (Weeks, 1978) and the response in observation wells due to air injection within packed-off zones in neighboring test wells. The monitoring and mathematical modeling of gas-tracer distribution and movement (using both environmental and introduced tracers) yield information on the overall pore-gas flow system from which inferences pertaining to the liquid-water system may be drawn (Section 3.9.1.3).

The division of the unsaturated zone at Yucca Mountain into hydrogeologic units is a first step in defining the macroscopic hydrologic system at the site. As described in Section 1.2.2, and depicted in Figure 3-26, Yucca Mountain is composed of a stratified sequence of Tertiary volcanic rocks consisting of ash flow and ash-fall tuffs that, at land surface, are overlain by irregularly distributed deposits of alluvium and colluvium. The division of this sequence into hydrogeologic units as described here is based on the divisions developed by Montazer and Wilson (1984) and by Ortiz et al. (1985) and is shown correlated with formal rock-stratigraphic units (Chapter 1) in Table 3-22. The hydrogeologic units are identified in Table 3-22 by symbols such as TSw, and these symbols are used to designate hydrogeologic units in subsequent discussions of the unsaturated zone to distinguish clearly between hydrogeologic and rock-stratigraphic units. The symbol QAL indicates alluvium, TCw indicates the Tiva Canyon welded (hydrogeologic) unit, PTn indicates the Paintbrush nonwelded unit, TSw indicates the Topopah Spring welded unit, CHn indicates the Calico Hills nonwelded unit (with "v" indicating the vitric facies and "z" indicating the zeolitic facies), and CFu indicating the Crater Flat undifferentiated unit.

Each of the individual hydrogeologic units listed in Table 3-22 belongs to one of three broadly based hydrogeologic rock types distinguished qualitatively as follows (the values given for saturated matrix hydraulic conductivity and for fracture density are taken from Section 3.9.2.1):

1. Densely to moderately welded tuffs that are highly fractured. This group includes units TCw and TSw of Table 3-22 and is characterized

DECEMBER 1988

hydraulic conductivity of about 10^{-11} m/s or less, a fracture density of 1 fracture/m^3 or less, and a matrix porosity of about 30 percent. A tuff sample need not be completely zeolitized to belong in this classification. The tuffs in CHnz range from partially to completely zeolitized but are grouped into this one rock type when their hydrologic properties are similar.

The hydrologic properties of the hydrogeologic units are discussed in greater detail in Section 3.9.2.1.

The formulation of a conceptual model of a natural process or phenomenon is the essence of scientific method that according to Russell (1948), "consists in inventing hypotheses which fit the (available) data, which are as simple as is compatible with this requirement, and which make it possible to draw inferences subsequently confirmed by observation." In general, the conceptual model of a natural hydrologic system considers the environmental setting and the internal geometry of the system together with the hydrologic and other related physical processes operating within the system. The development of a conceptual model is an ongoing, frequently iterative process of hypothesis testing; data analyses and interpretation; and numerical experimentation coupled with impartial, critical peer review.

Generalized conceptual models for the hydrologic system within the unsaturated zone at Yucca Mountain have been presented by Montazer and Wilson (1984) and Sinnock et al. (1986). The geologic framework underlying these conceptualizations is illustrated schematically in Figure 3-26, which depicts a generalized east-west cross section through the Yucca Mountain block at the repository site (Figure 3-25).

As depicted in Figure 3-26, the geologic framework for the hydrologic system within the unsaturated zone is defined by a block of layered, east-dipping hydrogeologic units that is bounded above by land surface, below by the water table, laterally on the west by a west-dipping normal fault, and laterally on the east by one or more west-dipping normal faults. In addition, the interior of the block may be transected by one or more high-angle faults (e.g., the Ghost Dance fault) across which hydrologic properties may change abruptly. In addition, the bounding and internal faults may act preferentially either as conduits for or as barriers against moisture flow. The processes of moisture flow that are envisioned to be occurring or that could occur under natural conditions within this macroscopic system are described and evaluated in terms of currently available data in Section 3.9.3.4.

3.9.1 BASELINE MONITORING

Baseline monitoring is an engineered system for continuing measurement of existing ground-water conditions that will serve as an historical data base for future observational comparison. Long-term monitoring of potentiometric levels and hydrochemistry may demonstrate the degree of stability of the geohydrologic system during the period required for waste isolation. In addition, water-level observations would record any changes of the water table that would affect the overall ground-water travel time in both the unsaturated and saturated zones beneath the repository.

Eight monitoring boreholes have been drilled into the unsaturated zone (Figure 3-27). Of these only one, drillhole USW UZ-1, located north of the Yucca Mountain site, is currently being monitored. Ten additional boreholes will be included in the unsaturated-zone monitoring network (Sec-

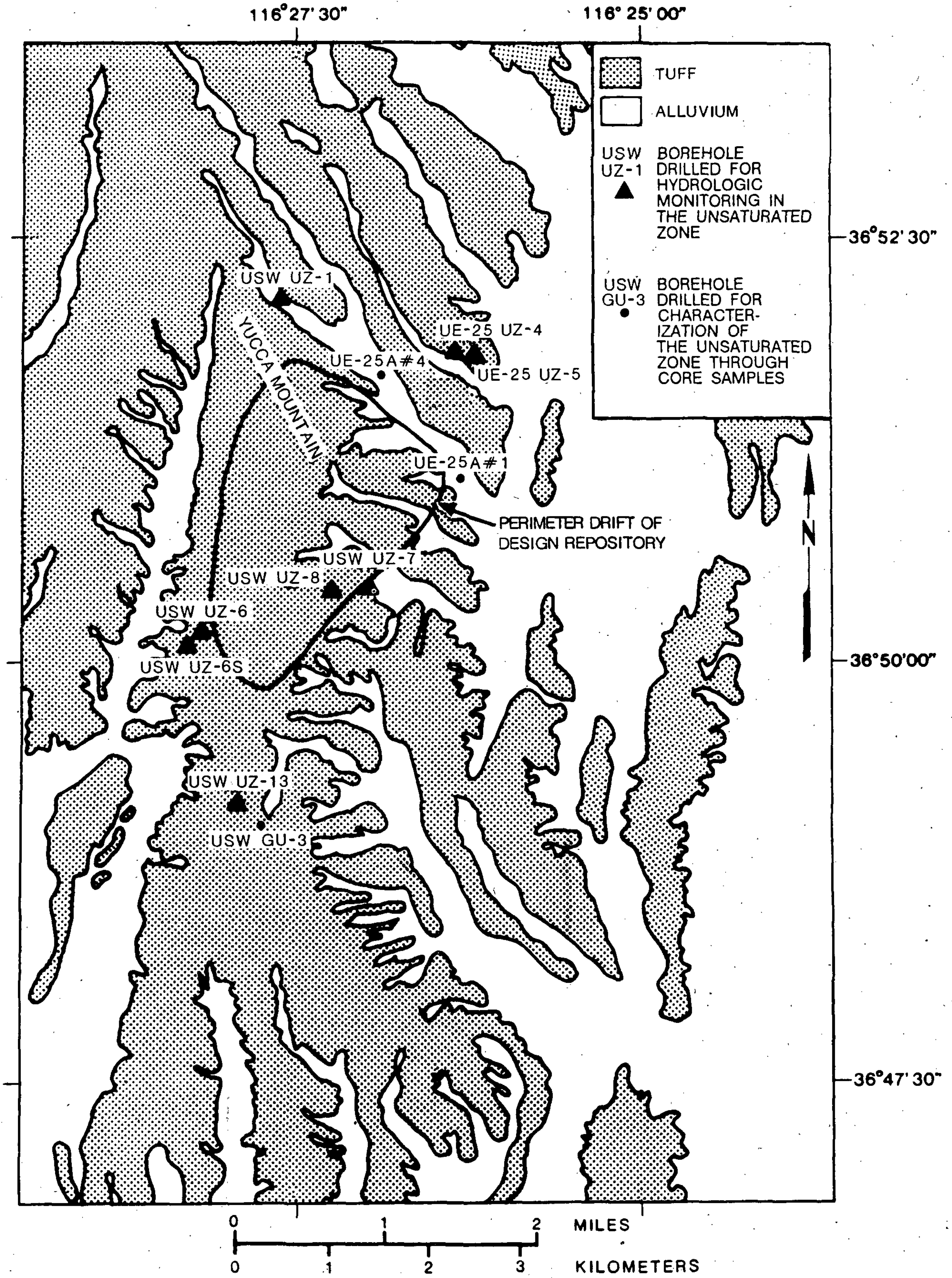

Figure 3-27. Locations of drilled monitoring boreholes and core sampling boreholes in the unsaturated zone at Yucca Mountain.

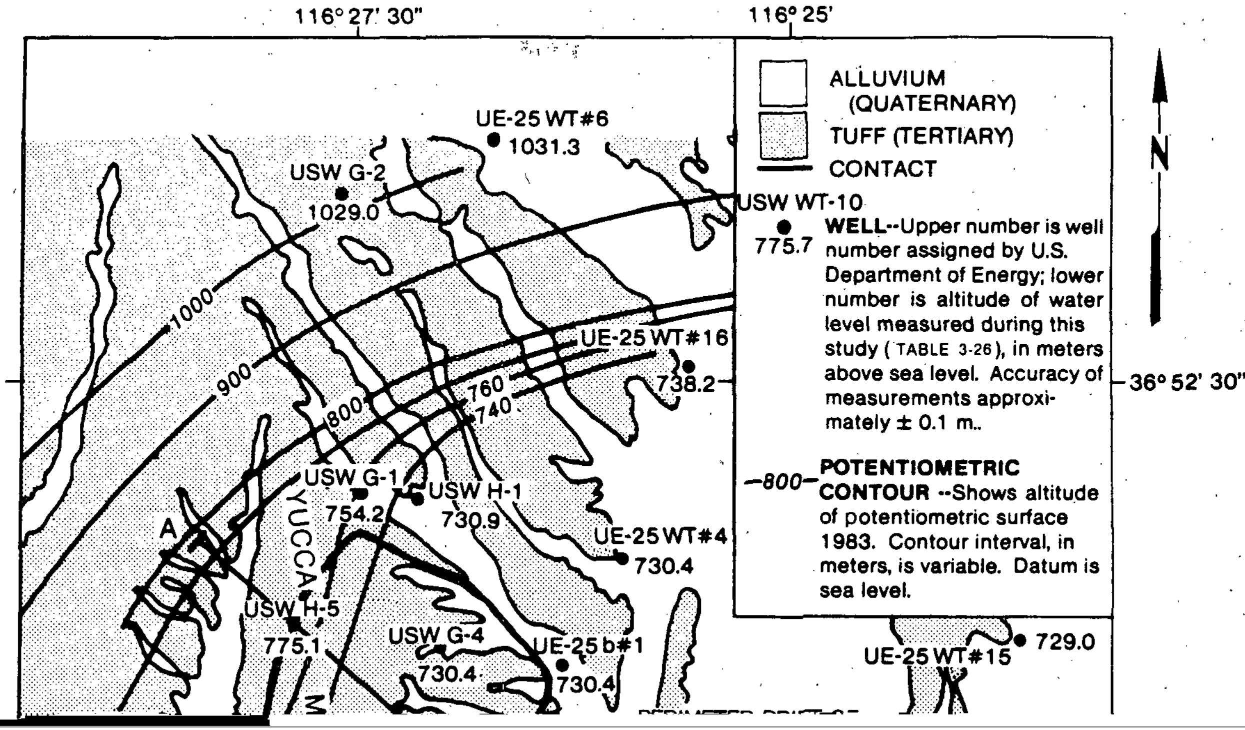
116° 27' 30"
116° 25'
36° 52' 30"
N
ALLUVIUM (QUATERNARY)
TUFF (TERTIARY)
CONTACT
USW WT-10
775.7
WELL--Upper number is well number assigned by U.S. Department of Energy; lower number is altitude of water level measured during this study (TABLE 3-26), in meters above sea level. Accuracy of measurements approximately ± 0.1 m..
—800— POTENTIOMETRIC CONTOUR --Shows altitude of potentiometric surface 1983. Contour interval, in meters, is variable. Datum is sea level.
UE-25 WT#6
1031.3
USW G-2
1029.0
1000
900
800
760
740
UE-25 WT#16
738.2
USW G-1
754.2
USW H-1
730.9
UE-25 WT#4
730.4
A
YUCCA
USW H-5
775.1
USW G-4
730.4
UE-25 b#1
730.4
UE-25 WT#15
729.0

characterization at Yucca Mountain. The monitoring program, both present and planned, is designed to quantify the energy status of the variably saturated rock-water system at Yucca Mountain. Moisture flux, whether under saturated or unsaturated flow conditions, cannot be measured directly and must be calculated from measured values of hydraulic conductivity and total potential gradient along the path of flow. Fluid potentials that govern variably saturated two-phase (liquid and gas) flow are as follows: (1) matric potential for the liquid phase; (2) gravitational potential; (3) gas-phase pressure, or pneumatic potential; (4) osmotic potential; and (5) thermal potential. In situ borehole monitoring at Yucca Mountain is designed to measure directly [illegible]

these potentials (except the gravitational potential, which is given directly by the height of the monitoring point above some arbitrarily selected datum). Laboratory testing of core and in situ pneumatic testing before instrumenting the boreholes are the means by which hydraulic conductivities (under various degrees of saturation) are obtained in order to calculate moisture and gas fluxes once the potential gradients are known. Plans for these testing programs are described in Section 8.3.1.2.2.

Hydrologic conditions within the unsaturated zone at Yucca Mountain are presently being monitored only in drillhole USW UZ-1 (Figure 3-27), which was completed in November 1983. This drillhole was drilled without water using a reverse air vacuum system to minimize disturbing local hydrologic conditions near the borehole (Whitfield, 1985). It was drilled to a total depth of 387 m, whereupon drilling was discontinued because an apparent perched-water zone was encountered. However, because the water was contaminated with the drilling-fluid polymer used to drill drillhole USW G-1, located 305 m from drillhole USW UZ-1, it was speculated that the perched-water horizon was not natural but a result of drilling drillhole USW G-1 (Whitfield, 1985). Following drilling and geophysical logging, drillhole USW UZ-1 was instrumented [illegible]

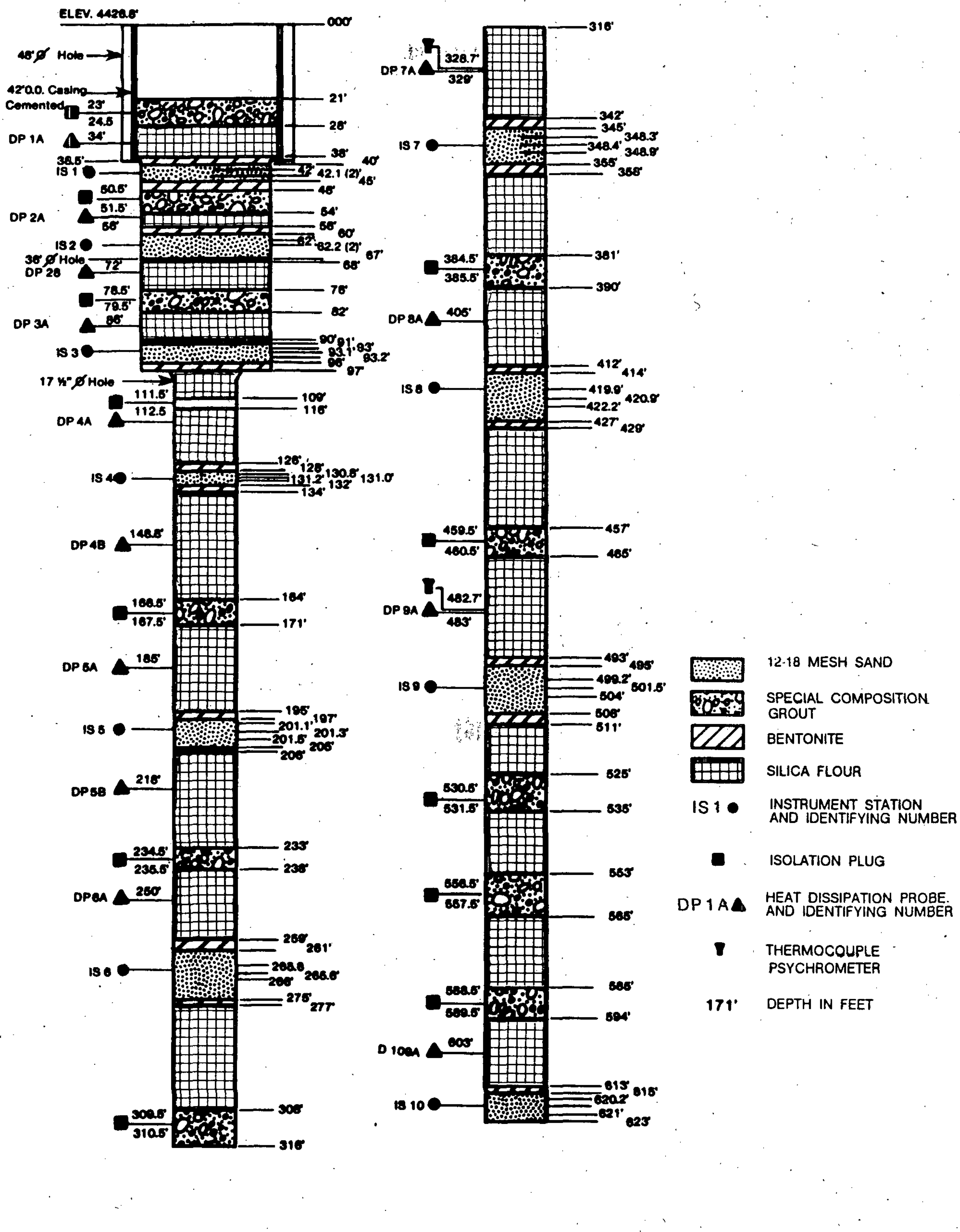

Figure 3-29a. Instrumentation of monitoring borehole USW UZ-1 (0- to 623-feet depth). Modified from Montazer et al. (1986).

DECEMBER 1988

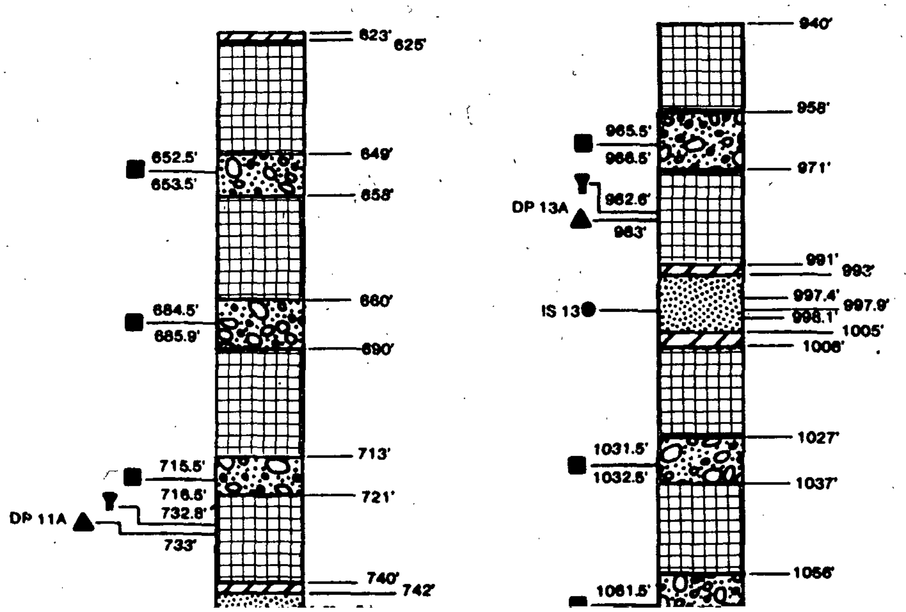

and thermocouples were sampled twice hourly during the first 90 days of operation and, subsequently, have been sampled every 2 h (Montazer et al., 1986).

The results of monitoring in borehole USW UZ-1 are described in a detailed report by Montazer et al. (1986). Preliminary findings indicated that after more than two years of regular monitoring, most of the instruments were still functioning and producing reasonable data.

Several operational problems were identified during the 2-yr trial monitoring period. These included possible long-term drift of the pressure transducers, long equilibration times for the thermocouple psychrometers placed in the dry, silica-flour columns, and frequency of failure of the heat-dissipation probes. Data from drillhole USW UZ-1 indicate that the gas-sampling program has had a positive effect on minimizing the equilibration time for psychrometers in screens equipped with gas sampling access tubes. Apparently, the periodic withdrawal of formation gas across the initially dry, coarse-sand columns decreased the time needed to establish moisture equilibrium between the instrument chamber and host formation. These equilibration problems will be addressed during site characterization (Section 8.3.1.2.2).

In addition to the continued matric-potential, gas-pressure, and gas-sampling monitoring at drillhole USW UZ-1, an expanded network of monitoring boreholes is planned (Section 8.3.1.2.2) to enlarge the areal and vertical coverage of ambient and changing hydrologic conditions within the unsaturated zone. Deep boreholes that penetrate the tuffaceous beds of Calico Hills are to be drilled north, east, south, and west of the repository block. The remaining boreholes are intended to penetrate the uppermost Topopah Spring Member of the Paintbrush Tuff and will be used to assess the rate and spatial distribution of net infiltration. Eight wells of this network have been drilled but not instrumented. These wells are listed in Table 3-23 and their locations shown in Figure 3-27.

3.9.1.1.2 Saturated zone

As indicated in Section 3.9.1, water-level measurements presently being made provide a foundation for a monitoring program. The monitored sites (most of those shown on Figure 3-28 are part of the monitoring program) include two geologic test holes, which were drilled as deep as 1,800 m to obtain data on lithology and stratigraphy; seven hydrologic test holes, in which pumping and other tests were performed to determine hydraulic characteristics of the formations; and 14 water-table holes, which were planned to penetrate the water table only a minimum amount. The water-table holes are areally distributed to enable definition of the potentiometric surface at Yucca Mountain so that gradients and probable flow paths can be determined. Additional water-table holes are planned to be drilled and monitored (Section 8.3.1.2.3.). The planned principal purpose of the drillholes now being observed was not for baseline monitoring, and there was no formal selection process for their locations or depths. However, they are situated for general coverage of the upper part of the saturated zone, through which ground-water flow paths from the repository are likely.

Table 3-23. Completion records of unsaturated-zone boreholes (page 1 of 2)

Borehole designation[a]	Drilling method	Total depth (m)	Diameter (cm)	Depth interval (m)	Casing inside diameter (cm)	Casing depth interval (m)	Rock-stratigraphic unit penetrated at total depth
USW UZ-1	Reverse vacuum	386.8	122 91 61 44.5	0-12.5 12.5-29.6 29.6-30.8 30.8-386.8	41	0-12.0	Topopah Spring Member (Paintbrush Tuff)
UE-25UZ-4	Odex/ cored	111.9	15 10.8	0-68.9 68.9-111.9	13	0-17.7	Topopah Spring Member (Paintbrush Tuff)
UE-25UZ-5	Odex	111.3	15	0-111.3	13	0-5.2	Topopah Spring Member (Paintbrush Tuff)
USW UZ-6	Reverse vacuum	575.2	76 61 44	0-12.2 12.2-103.9 103.9-575.2	66 48	0-12.2 0-98.8	Prow Pass Member (Crater Flat Tuff)
USW UZ-6S	Odex	158.2	22 18	0-150.9 150.9-158.2	10	0-0.91	Topopah Spring Member (Paintbrush Tuff)
USW UZ-7	Odex	63	15.2	0-63	12.7	0-6	Topopah Spring Member (Paintbrush Tuff)

Table 3-23 Completion records of unsaturated zone boreholes (page 2 of 2)

Borehole designation[a]	Drilling method	Total depth (m)	Diameter (cm)	Depth interval (m)	Casing inside diameter (cm)	Casing depth interval (m)	Rock-stratigraphic unit penetrated at total depth
USW UZ-8	Odex	107	21.6	(b)			Topopah Spring Member (Paintbrush Tuff)
USW UZ-13	Odex/ cored	131	15.2 10	0-125 125-131	12.7	0-101	Topopah Spring Member (Paintbrush Tuff)

[a]Location of boreholes shown on Figure 3-27.
[b]Drilling incomplete.

The construction of the geologic and hydrologic series of test holes was such that the first early measurements of head were composites, reflecting averages of all the members of the Paintbrush and Crater Flat Tuffs that were penetrated below the water table. Subsequent to initial completion, four piezometers of varying lengths were installed in one drillhole (drillhole USW H-1) in order to measure heads in each of four zones (water levels for the upper three intervals are very similar; water level in the deepest interval is about 54 m higher; refer to Table 3-24 and Robison, 1986). A single semipermanent packer was installed between permeable zones in each of five hydrologic holes (drillholes UE-25b#1, USW H-3, USW H-4, USW H-5, and USW H-6), enabling comparison of head in the zones above and below the depth of the packer setting. Potentiometric heads in the Tertiary rocks penetrated

Table 3-24. Ground-water levels, Yucca Mountain area[a] (page 1 of 3)

Hole or well number	Location[b] North (ft)	Location[b] East (ft)	Hole depth[c] (m)	Land surface altitude[d] (m)	Depth correction[e] (m)	Date measured[f]	Geologic unit[g]	Water level (corrected) Interval[h] (m)	Depth to water[i] (m)	Altitude[j] (m)
UE-25b#1	765,243	566,416	1,220	1,200.7	0.25	12/03/83	Th/Tlr	Composite	470.6	730.9
						08/01/83	Th/Tct	471-1199	470.3	730.4
						08/01/83	Tct/Tlr	1199-1220	472.2	728.5
UE-25c#1	757,095	569,680	914	1,130.6	0.06	11/07/83	Tpt/Tct	Composite	400.3	730.3
UE-25p#1	756,171	571,485	1,805	1,114.2	0.06	02/83	Th/Tcp	383-500	383.9	730.1
						11/07/83	Pz/Pz	1297-1805	364.7	749.4
USW G-1	770,500	561,000	1,829	1,325.9	0.67	03/23/82	Tcp/Tof	Composite	571.7	754.2
USW G-2	778,824	560,504	1,831	1,553.9	0.16	09/17/82	Tpt/Tof	Composite	524.9	1,029.0
USW G-3	752,780	558,483	1,533	1,480.5	0.57	11/30/83	Tcb/Tof	Composite	750.3	730.2
USW G-4	765,807	563,082	915	1,269.5	1.53	04/27/83	Tcp/Tct	Composite	539.5	730.0
USW H-1	770,254	562,388	1,829	1,303.0	0.19	02/25/82	Tcp/Tof	Composite	572.1	730.9
						11/01/83	Tcp/Tcp	572-673	572.4	730.7
						11/01/83	Tcb/Tcb	716-765	572.4	730.7
						11/01/83	Tct/Tct	1097-1123	571.7	731.4
						11/01/83	Tof/Tof	1783-1814	518.2	784.9
USW H-3	756,542	558,452	1,219	1,483.2	0.08	11/19/82	Tcb/Tlr	Composite	570.8	732.4
						11/03/83	Tcb/Tlr	751-1190	750.8	732.3
						11/03/83	Tlr/Tlr	1190-1219	729.0	754.0
USW H-4	761,643	563,911	1,219	1,248.5	0.45	12/30/82	Tcp/Tlr	Composite	518.7	729.8
						06/16/83	Tcp/Tlr	518-1181	518.2	730.3
						06/16/83	Tlr/Tlr	1181-1219	518.1	730.4
USW H-5	766,634	558,909	1,219	1,478.9	0.08	12/22/83	Tcb/Tl	Composite	704.2	774.7
						11/07/83	Tcb/Tl	704-1091	703.8	775.1
						11/07/83	Tl/Tl	1091-1219	703.8	775.1
USW H-6	763,299	554,075	1,220	1,301.7	0.05	12/15/82	Tcp/Tlr	Composite	526.6	775.1
						10/24/83	Tcp/Tcb	526-1187	526.1	775.6
						10/24/83	Tct/Tlr	1187-1220	524.7	777.0
USW WT#1	753,941	563,739	515	1,201.4	0.33	10/31/83	Th/Tcb	Composite	471.0	730.4
USW WT#2	760,661	561,924	628	1,301.3	0.53	11/01/83	Tcp/Tcp	Composite	571.0	730.3
UE-25 WT#3	745,995	573,384	348	1,030.0	0.27	10/31/83	Tcb/Tcb	Composite	300.5	729.5
UE-25 WT#4	768,512	568,040	482	1,169.2	0.46	11/01/83	Th/Th	Composite	438.9	730.4
UE-25 WT#6	780,576	567,524	383	1,314.8	0.24	10/31/83	Th/Th	Composite	283.8	1,031.3

Table 3-24. Ground-water levels, Yucca Mountain area[a] (page 2 of 3)

Hole or	Location[b]	Hole	Land surface	Depth	Water level (corrected) Depth to

Table 3-24. Ground-water levels, Yucca Mountain area[a] (page 3 of 3)

Footnotes (continued)

[h]Interval: depth interval of the hole represented by the water-level measurement. Composite levels represent mixed hydraulic heads of the entire interval between the water table or the lower end of the casing and the bottom of the hole. Where a specific interval is indicated, the zone was isolated using a single packer installed to determine hydraulic head differences above and below the packer.

[i]Depth to water: depth based on direct measurement of water levels using downhole wireline equipment, adjusted for depth correction, where available. Accuracy of measurements is approximately ±0.1 m. Depth in USW VH-2 estimated from geophysical logs.

[j]Altitude: computed altitude of water level above sea level, based on land surface altitude and measured depth to water (corrected). Where more than one altitude is reported, the value used on the map (Figure 3-28) is underscored in the table.

[k]-- indicates no data.

period between calibrations. This process will be part of the continuing monitoring program, as described in Section 8.3.1.2.3.

Ground-water flow direction and travel time are, in part, a function of hydraulic gradient, which is determined from water levels in wells. At Yucca Mountain, high accuracy and precision are needed because in parts of the area (Figure 3-28) the water table is nearly flat and calculation of the gradient is sensitive to small errors in water-level measurements. For comparison of levels among wells, true depths must be calculated, which involves a correction for hole deviation from vertical. To calculate water-level altitudes, highly precise altitudes of the measuring points at land surface are needed.

A further complicating factor that may affect the water levels measured in the saturated zone relates to density effects. However, effects on water levels caused by water-density differences due to differences in ground-water temperatures among wells probably are small. In addition, since the water in most of the wells in the eastern and southeastern areas of Yucca Mountain have similar chemistries and temperatures, density differences probably have little if any effect on the hydraulic gradient within that area.

3.9.1.2 Potentiometric levels

This section provides data on matric potentials obtained from drillhole USW UZ-1 in the unsaturated zone. In addition, data on potentiometric levels from wells in the saturated zone are presented and discussed, as well as an assessment of the possibility of short-term changes in these levels.

3.9.1.2.1 Unsaturated zone

In situ measurements of matric potential within the unsaturated zone at Yucca Mountain have been attempted only at the 33 instrumentation stations that are arrayed vertically within the prototype monitoring borehole USW UZ-1. A preliminary analysis and interpretation of data collected in drillhole USW UZ-1 over a 2-yr period following completion of the borehole are presented by Montazer et al. (1986). As described in Section 3.9.1.1.1, matric potentials in the borehole are being measured both by heat-dissipation

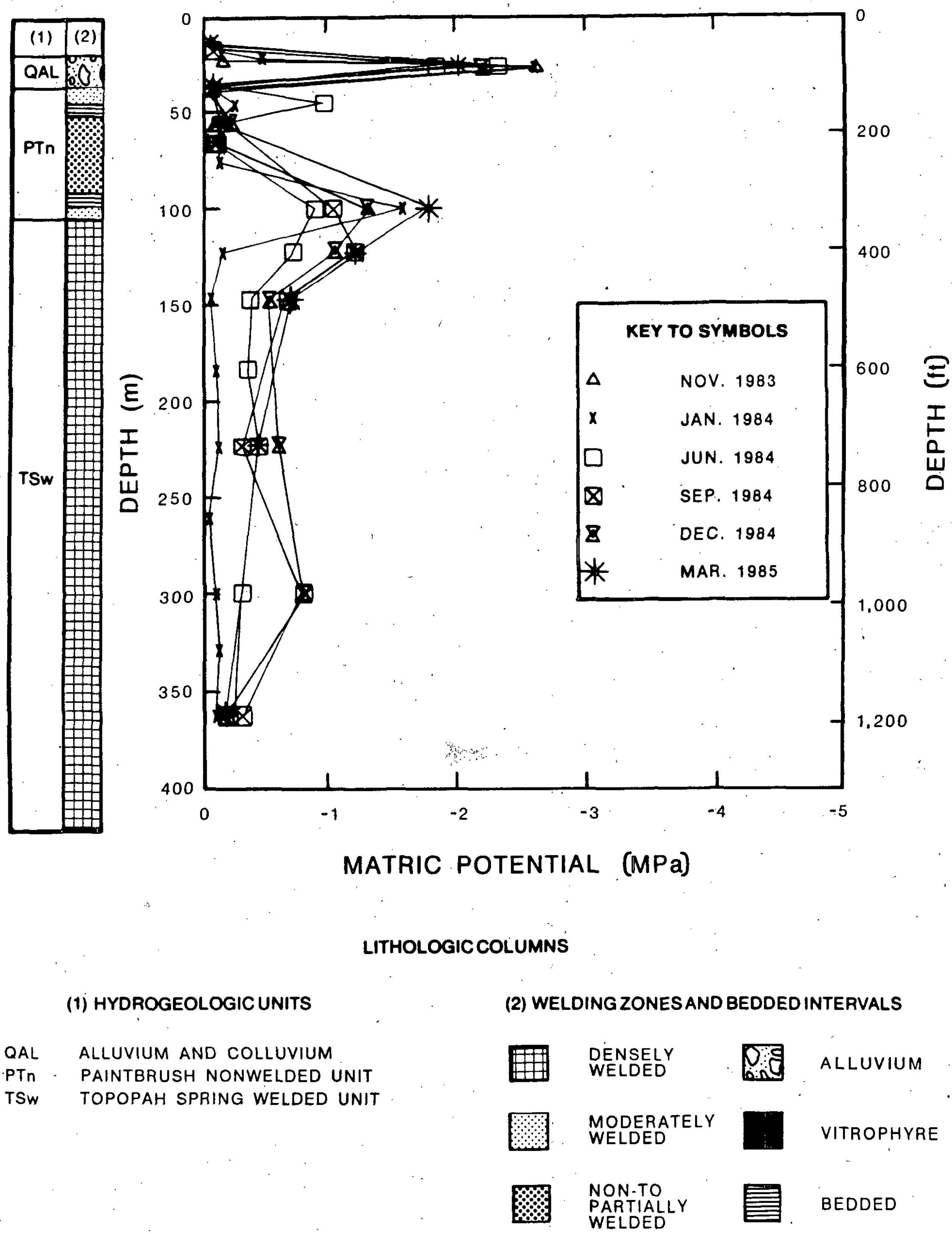

Figure 3-30. Matric-potential profiles for selected dates at monitoring borehole USW UZ-1 based on data from heat-dissipation probes. Modified from Montazer et al. (1986).

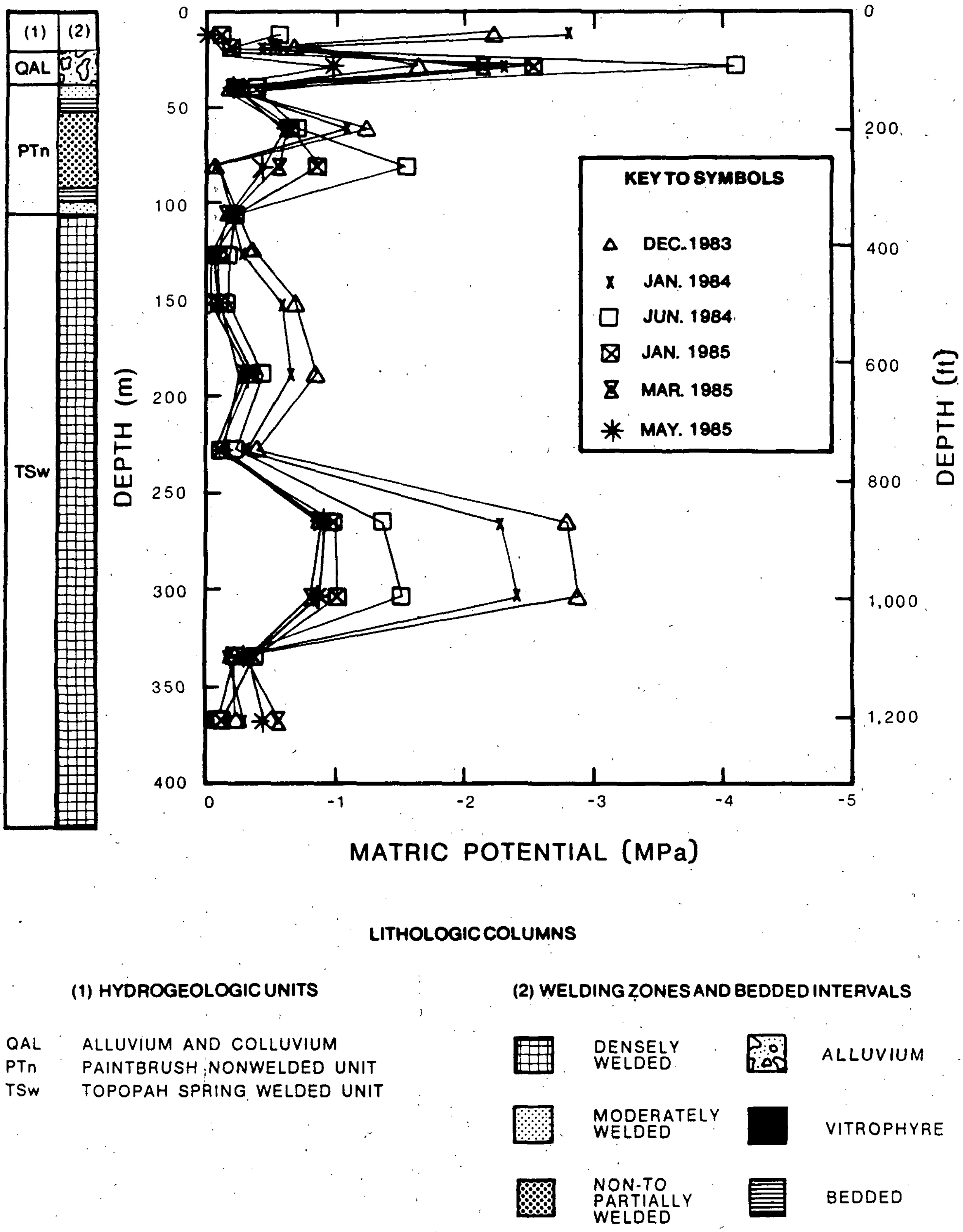

Figure 3-31. Matric-potential profiles for selected dates at monitoring borehole USW UZ-1 based on data from thermocouple psychrometers. Modified from Montazer et al. (1986).

the thermocouple psychrometers were emplaced under differing initial conditions in different backfill materials of different hydrologic properties, there is a considerable range of values of matric potential measured simultaneously by different instruments at the same level within the borehole. By May 1985, however, most of the instruments appeared to have stabilized sufficiently to yield a matric-potential profile that probably is indicative of ambient conditions within the host rock (Montazer et al., 1986).

Presuming conditions within the borehole to have equilibrated with those in the host rock, the data of Figures 3-30 and 3-31 indicate that matric potentials within the PTn hydrogeologic unit at drillhole USW UZ-1 range from -10 to -1 bars (-1 to -0.1 MPa) with a mean value of about -5 bars (-0.5 MPa) over the thickness of the unit. The matric potentials within the TSw unit range from -10 to -1 bars (-1.0 to -0.1 MPa), with an approximately constant mean value of about -3 bars (-0.3 MPa) over the thickness of the unit. Montazer et al. (1986) concluded that downward moisture flux within the TSw unit occurs predominantly as liquid-water flow within the rock matrix of the unit, with little or no liquid-water flow within the fractures. Assuming that the nearly constant matric potential over the depth interval from 122 to 224 m in drillhole drillhole USW UZ-1 (Figure 3-31) implied unit vertical hydraulic gradient, Montazer et al. (1986) estimated that the downward liquid-water flux within the TSw unit at drillhole USW UZ-1 probably is within the range from 0.1 to 0.5 mm/yr.

Pneumatic potentials (pore-gas pressures) are being monitored by downhole pressure transducers emplaced in borehole USW UZ-1 and have been measured within a piezometer nest installed in borehole UE-25a#4, about 1.6 km southeast of drillhole USW UZ-1. Diurnal and barometrically induced fluctuations of gas pressure of about 0.25 kPa (Montazer et al., 1986) have been observed in these boreholes to depths of about 30 m. Such fluctuations are apparently damped out below this depth, although seasonally induced pressure variations are observed to occur at greater depths (Montazer et al., 1986). The pneumatic data were used by Montazer et al. (1986) to make preliminary estimates of air permeability in the uppermost units penetrated by these boreholes but have not been interpreted in terms of the overall bulk-gas flow system within the unsaturated zone.

3.9.1.2.2 Saturated zone

The present monitoring program consists of measuring water levels and observing their variations with time. Selected water levels in the vicinity of Yucca Mountain are shown in Figure 3-28 and Table 3-24. The figure and table are modified from Robison (1986), the most recent source of published data; however, the figure and table contain revisions based on resurveying in 1984 of land-surface altitudes at most of the well sites. The water levels range in altitude from about 1,030 to 730 m above sea level and generally represent water-table or unconfined conditions. Within the level of available precision, potentiometric levels show little variation with depth in the upper part of the saturated zone (Table 3-24). In the deeper part of the saturated zone (drillhole USW H-1, in the older Tertiary rocks; drillhole UE-25p#1, in the Paleozoic carbonate rocks), potentiometric heads are higher than in the overlying rocks (Table 3-24).

Figure 3-25 a simplified section through Yucca Mountain (location shown on Figure 3-28, shows the general relationship of stratigraphic units and the water table. For clarity, only the Solitario Canyon fault is shown, although the section is known to include numerous steeply dipping normal faults.

In the Yucca Mountain area, the potentiometric surface occurs principally in members of the Paintbrush Tuff and underlying Crater Flat Tuff (the geologic units, not the hydrostratigraphic units defined for the unsaturated hydrologic zone). Slope of the potentiometric surface at Yucca Mountain, based on gradients indicated by the contours, is south to southeast, similar to the regional topographic slope.

The gradient in the north is relatively steep compared with that in the south. Water-level altitudes in Figure 3-28 are highest to the north at drillholes USW G-2 and UE-25 WT#6; however, it is not known whether the southward slope toward drillhole USW H-1 is uniform, or if there are abrupt flections. The cause for this steep slope is not known yet; it may be that southward movement of ground water is inhibited in this area by a low-permeability formation, such as the tuffaceous beds of Calico Hills, or by a fault or other unknown structural control. Test drilling to resolve these, and possible alternative, hypotheses is planned (Section 8.3.1.2.3).

West of the crest of Yucca Mountain, in drillholes USW H-6, USW WT-7, and USW WT-10 and also in USW H-5 on the crest, the water levels are about 775 m above sea level. Water levels are as much as 45 m lower at drillholes USW G-3 and USW H-3, just east of drillhole USW WT-7. A fault in Solitario Canyon may itself be poorly permeable and restrict eastward movement of ground water, or the fault may juxtapose permeable zones against less permeable zones and thereby restrict movement. Pumping tests in existing or proposed drillholes are expected to be used to determine the hydraulic effects of the fault (Section 8.3.1.2.3.1).

From the eastern edge and southern end of Yucca Mountain to western Jackass Flats, the potentiometric surface ranges from about 728 to 730 m in altitude with a general southeastward slope (Figure 3-28; Robison, 1986).

Hydrographs of water-level data are not presented, for the reasons given in Section 3.9.1.1.2. In regions where precipitation is greater and water levels are shallower, there is typically a well-defined seasonal or annual correlation between precipitation and ground-water levels. At Yucca Mountain, however, ground-water levels are not expected to show short-term or seasonal fluctuations that can be correlated with precipitation. This is because of extremely low rates of net infiltration and recharge attributable to local precipitation, the great depths to the water table, and ground-water travel times through the unsaturated zone that may be many thousands of years. Long-term precipitation data are not available for the site, although precipitation stations have been established recently in the Yucca Mountain area as part of a study to determine rainfall-infiltration relationships (Section 8.3.1.2.1).

Well J-13, 8 km from the site, and well J-12, 12 km from the site, (Figure 3-22) are in service for water supply; their production is discussed in Section 3.9.7.

3.9.1.3 Hydrochemistry

This section presents the hydrochemical information obtained from the baseline monitoring program of the site and its immediate surroundings. Hydrochemical data have not been collected at the site long enough for reliable time series to be developed. Therefore, temporal trends, if they exist, cannot be directly identified from the available data at this time. Some indirect information about changes in the hydrochemical conditions at the site over time can be obtained from understanding the hydrochemical evolution of the waters interacting with their host-rock environment. Their interaction is discussed in detail in Sections 4.1.1.4, 4.1.2.9, and 4.4.2. On the basis of this discussion, there is no reason to believe that while the existing climatic conditions prevail, the natural hydrochemical conditions at the site will not remain very similar to those currently observed.

Chapter 4 presents in detail the current knowledge of site ground-water temperature (4.1.2.8), major chemical composition (4.1.2.2), dissolved gas concentrations (4.1.2.5), pH and Eh (Tables 4-6 and 4-7 respectively), background radioactivity (4.1.2.6) and organic content (4.1.2.4), which will not be repeated here.

[redacted]

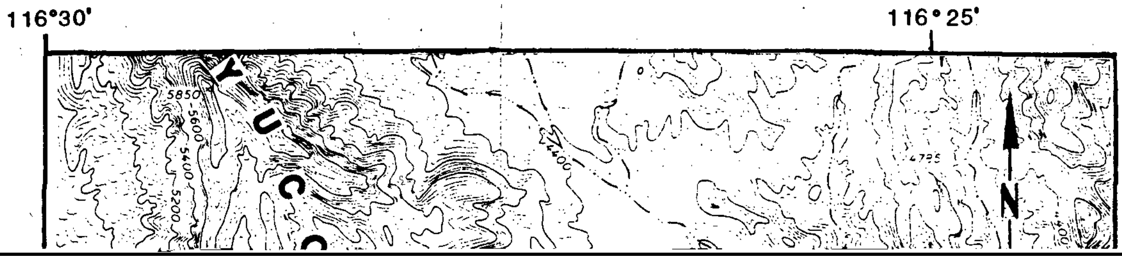
116°30'
116°25'
5850
5600
5400
5200
N

Table 3-25. *Environmental isotope data for ground-water samples from the tuff aquifers under the exploratory block and its immediate area*[a]

Well designation[b]	Collection date	δD (o/oo SMOW)[c]	$\delta^{18}O$ (o/oo SMOW)[c]	$\delta^{13}C$ (o/oo PDB)[d]	^{14}C (pmc)[e]	HTO (TU)[f]
UE-25b#1	08/07/81	-99.5	-13.4	-10.7	--[g]	--
UE-25b#1	09/09/81	-101.0	-13.4	-10.7	16.7	<62.0
UE-25b#1	07/20/82	-99.5	-13.5	-8.6	18.9	0.6
USW G-4	12/09/82	-103.0	-13.8	-9.1	22.0	--
USW H-1	10/20/80	-103.0	-13.4	--	19.9	<6.0
USW H-1	12/08/80	-101.0	-13.5	-11.4	23.9	<6.0
USW H-3	03/14/84	-101.0	-13.9	-4.9	10.5	0.6
USW H-4	05/17/82	-104.0	-14.0	-7.4	11.8	<3.0
USW H-5	07/03/82	-102.0	-13.6	-10.3	18.2	<62.0
USW H-5	07/26/82	-102.0	-13.6	-10.3	21.4	<62.0

[a]Source: Benson and McKinley (1985).
[b]Well locations indicated in Figure 3-32.
[c]δD and $\delta^{18}O$ are reported in parts per thousand relative to Standard Mean Ocean Water (SMOW) standard.
[d]$\delta^{13}C$ is reported in parts per thousand relative to Peedee belemnite carbonate (PDB) standard.
[e]^{14}C activity is reported as a percent of the modern carbon (pmc) standard.
[f]T is reported in tritium units (TU).
[g]-- indicates no data.

than samples from the other, more northerly drillholes (mean value 20.1 percent modern carbon) (Table 3-25). The significance of this difference cannot be fully assessed without carbon-14 modeling. Nevertheless, ground-water residence times of the southern samples may be on the order of 5,000 yr greater than the northern samples. Because significant amounts of carbonate minerals do not occur in the tuff or in tuffaceous valley fill with which these ground waters have come into contact, minimal radiocarbon dilution may have occurred from such contact and apparent ages may be more realistic than at other sites.

The δ carbon-13 ($\delta^{13}C$) values may show a spatial variability similar to those of the carbon-14. The values are consistent with recharge under very poorly vegetated conditions. The $\delta^{13}C$ value reported for sample USW H-3 is above the mean atmospheric value for carbon dioxide. The explanation of this unusual phenomenon could shed light on the differences in radiocarbon content between this sample and the northern ones. The $\delta^{13}C$ values below about -10 parts per thousand in dilute waters suggest that little carbonate rock/water and soil gas/water exchange has occurred (Section 3.7.3).

The three tritium values of <62 TU in Table 3-25 serve only to indicate that no large amounts of bomb-test tritium have reached the aquifer at those points. The other samples, which were analyzed by a more sensitive method to give a more precise result, are consistent with trace tritium contamination of samples of very old water (very old, in the context of tritium dating implies several hundred years or more). Such contamination is common and not unexpected at Yucca Mountain.

The deuterium and oxygen-18 data in Table 3-25 plot on and below the meteoric line (Section 3.9.1.3), occurring between a deuterium excess of +10 (mean continental meteoric water) to +5. Such a small deviation from the world-wide average meteoric deuterium excess is within expected local continental variation. The water is extremely depleted in heavy isotopes of both oxygen and hydrogen, consistent with high altitude, cold (winter) continental recharge or snow-melt. No evaporative enrichment or thermal alteration is observed. No complete hydrochemical or isotopic analyses are available for water from the unsaturated zone at the site. Methods (triaxial compression, high-speed centrifuge and vacuum distillation) are currently under development for extracting uncontaminated samples upon which to perform these analyses. Yang (1986) has reported some preliminary calcium and sodium concentration data, showing that calcium is elevated in the pore water relative to the ground water, to the extent that it dominates over sodium. Complete chemical and isotopic characterization of the infiltrating pore water is needed (1) to develop an understanding of the hydrochemical nature of the water that may contact a waste package and (2) to isotopically trace the movement of these waters through the unsaturated zone. The plans for collecting these data as a function of depth are presented in Section 8.3.1.2.3.

The carbon-14 and carbon-13 composition of the unsaturated zone $CO_2(g)$ phase has been determined by Yang et al. (1985) on samples obtained by the new methods developed by Haas et al. (1983). Radiocarbon from bomb-test fallout was observed to a depth of 12.2 m in borehole UZ-1 on the exploration block. Radiocarbon activity decreased to below 100 percent modern carbon below 18.3 m, which may indicate that downward gas-phase transport from the surface has not occurred beyond this depth since the mid-1960. Improvements in sample collection methods and the interpretation of these results with pore-water hydrochemical data as outlined in Section 8.3.1.2.3 will enhance the understanding of two-phase transport in the unsaturated zone at the site.

3.9.2 HYDRAULIC CHARACTERISTICS

This section presents information on the hydraulic characteristics of the unsaturated and the saturated zones. The hydraulic characteristics of the unsaturated zone include fracture characteristics, porosity, saturated matrix hydraulic conductivity, and moisture characteristic relations. For the saturated zone, values for hydraulic conductivity, transmissivity, porosity, and storage coefficient are presented and discussed.

3.9.2.1 Hydraulic characteristics of the unsaturated zone

Mean values of hydrologic properties for most of the hydrogeologic units defined in Table 3-22 are presented in Table 3-26. The compilation of Montazer and Wilson (1984) included data from several sources. The data of Peters et al. (1984) were based on analyses of core samples from test wells USW G-1, USW G-4, and USW GU-3; the data of Tien et al. (1985) includes data from wells USW H-1, USW G-1, J-13, UE-25a#1, and USW GU-3; and the data reported by Weeks and Wilson (1984) were obtained from core samples from well USW H-1. The range of mean values among the references cited for each property within each hydrogeologic unit reflects the effects of lateral and vertical spatial heterogeneity within each unit. Table 3-26 provides only values typical of the samples tested for hydrologic properties. These data are based, in general, on too few samples (several score for the entire unsaturated zone at Yucca Mountain) to permit meaningful statistical analyses to be performed for each hydrogeologic unit. An indication of the variance within and between sample sets is shown by the saturated matrix hydraulic conductivity, whose values listed in Table 3-26 range over two orders of magnitude.

The discrepancy in the values reported in Table 3-26 for saturated matrix hydraulic conductivity for hydrogeologic unit CHnv reflects, in part, the current uncertainty in the position of hydrogeologic unit contacts and, in part, the heterogeneity of the units. Rock-sample collection for the measurement of hydrologic properties is to be done through the program of surface-based borehole drilling and coring and of sampling within the exploratory shaft, as described in Section 8.3.1.4. Plans to define the hydrogeologic framework are described in Section 8.3.1.2.

The hydrologic property data of Table 3-26 must be supplemented by developing sets of moisture-characteristic curves, that is the functional dependence of liquid-water saturation and relative hydraulic conductivity on the liquid-water potential within the rock matrix and fractures appropriate for each hydrogeologic unit. In unfractured rocks, these relations refer to the storage and movement of liquid water within and through the interstitial pore space. In fractured rocks, allowance must be made for the storage and

Table 3-26. Summary of compilations of hydrogeologic properties of hydrogeologic units within the unsaturated zone, Yucca Mountain

Hydro-geologic unit[a]	Source of data	Range of thickness (m)	Grain density (kg/m^3)[b]	Fracture density ($no./m^3$)[c]	Porosity[b]	Saturated matrix hydraulic conductivity (m/s)
TCw	(d)	0-150	ND[f]	10-20	0.12	2×10^{-11}
	(e)	ND	2,490	ND	0.08	9.7×10^{-12}
PTn	(d)	20-100	ND	1	0.46	1×10^{-7}
	(e)	ND	2,350	ND	0.40	3.9×10^{-7}
TSw	(d)	290-360	ND	8-40	0.14	3.5×10^{-11}
	(e)	ND	2,580	ND	0.11	1.9×10^{-11}
CHnv	(d)	100-400	ND	2-3	0.37	5×10^{-8}
	(e)	ND	2,370	ND	0.46	2.7×10^{-7}
CHnz	(d)	100-400	ND	2-3	0.31	9×10^{-11}
	(e)	ND	2,230	ND	0.28	2.0×10^{-11}

[a]Hydrogeologic units are defined in Table 3-22.
[b]See Chapter 2 for more data.
[c]Scott et al. (1983).
[d]Montazer and Wilson (1984).
[e]Peters et al. (1984) and Peters et al. (1986).
[f]ND = no data.

movement of water within the interconnected fracture openings as well as for the movement of water between the fracture openings and the rock-matrix pore space. Standard mercury-intrusion (Gregg and Sing, 1967), centrifugal (Russell and Richards, 1938; Hassler and Brunner, 1945), pressure plate (Hillel, 1980) and psychrometric (Papendick and Campbell, 1981) techniques are available for the laboratory determination of the relation between matric potential and saturation in soil and unfractured rock samples. Saturated hydraulic conductivities are measured using standard permeametry techniques (Hillel, 1980). The saturated matrix hydraulic conductivity measurements reported in Table 3-26 were generally made using a constant-head permeametry technique on samples from drillhole core.

Hydraulic conductivity may vary within a given hydrogeologic unit because of differences in pore and fracture size and distributions. Tectonic stresses may also have an influence that varies areally. This effect may also vary with time, as stress fields change.

Techniques for the measurement of relative hydraulic conductivity values are available (Amyx et al., 1960) but are generally limited in applicability to consolidated rocks with permeabilities much larger than the values for welded tuff or zeolitic tuff samples. Techniques for the measurement of relative hydraulic conductivity on very low permeability tuffs, such as welded tuff matrix material from TSw, are under development, and theoretically based methods have been formulated to estimate relative hydraulic conductivity in unconsolidated porous media from matric potential, saturation, and pore-size-distribution data (Brooks and Corey, 1964; Mualem, 1976).

A set of moisture-retention curves under drainage conditions relating matric-potential and saturation is shown in Figure 3-33 and was developed by Peters et al. (1984) for the matrix properties of most of the hydrogeologic units listed in Table 3-22. These curves were obtained by fitting the van Genuchten (1978) analytic representation to laboratory psychrometric data obtained for unfractured samples extracted from cores from test wells USW G-4 and USW GU-3. Because psychrometric techniques are appropriate only for matric potentials less than about -3 bars (-0.3 MPa), the moisture-retention curves reported by Peters et al. (1984) are not well determined for matric potentials that exceed this value. In lieu of direct measurements, the van Genuchten (1978) representation can also be used to estimate matrix relative hydraulic conductivity for these units. Such estimates must be regarded as highly tentative, however, because it is not known to what extent this analytic representation for relative hydraulic conductivity is appropriate for the tuffs at Yucca Mountain (Section 8.3.1.2.2). Furthermore, the curves in Figure 3-33 are based on laboratory determinations on small sample sets from only two locations, and therefore, the curves may not be representative of the units at Yucca Mountain as a whole.

Standard field and laboratory methods are not yet available by which to determine the moisture-characteristic relations for variably saturated fractures and fractured rocks. Prototype testing to develop such methods will be conducted on welded tuffs from G-Tunnel which are similar to those [illegible]

expected to be encountered in the exploratory shaft facility. The benefits of this testing are twofold: first, the program will permit development of quality level 1 methods and procedures for ESF testing, and second, the results of the tests will provide preliminary data regarding the hydrologic behavior of fractured, welded tuff. Thus, preliminary assessment of the appropriateness of the models of flow processes will be possible.

Liquid-water storage within fractures probably is insignificant, but the flow of liquid water within and across fractures is not yet well understood. Theoretical models for liquid-water flow in single fractures have been developed (Montazer and Harrold, 1985; Wang and Narasimhan, 1985) but have not yet been field or laboratory tested. The intact-fracture test to be

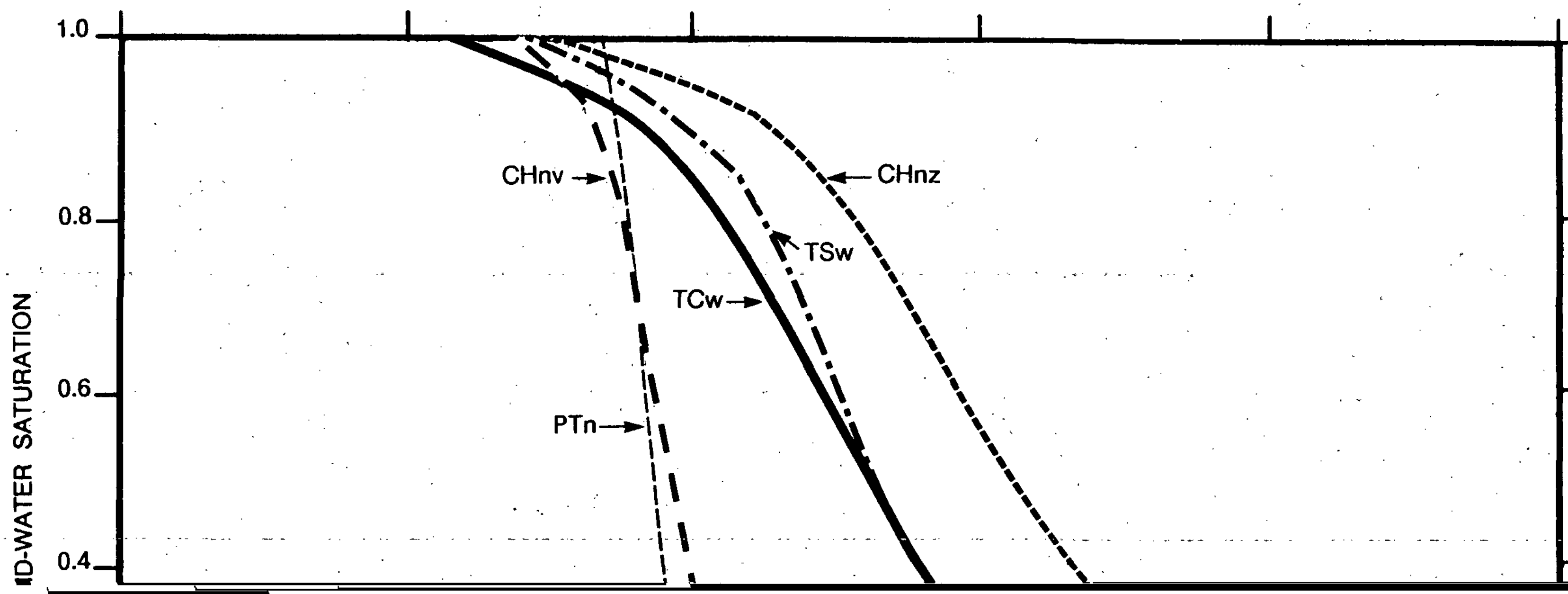
1.0
0.8
0.6
0.4
ID-WATER SATURATION
CHnv
CHnz
TSw
TCw
PTn

matrix saturation (Montazer and Wilson, 1984; and Klavetter and Peters, 1986). Consequently, at high matrix saturations the fracture systems within the densely welded, fractured hydrogeologic units (e.g., the TCw and TSw units) and within the fault zones may become highly efficient pathways for liquid-water flow. Liquid-water flow within the fractures may be Darcian with an appropriately defined potential and hydraulic conductivity (for example, under the parallel-plate, cubic-law approximation for flow in single fractures), but, as pointed out previously, the potential in the fractures need not be equal to the matrix potential in the rock matrix, especially under highly transient conditions (Klavetter and Peters, 1986).

Considerable attention must be given to the problem of how best to represent the hydrologic properties and hydrologic response of a highly fractured porous medium. Separate treatment of the matrix and the individual fractures is not practical. In the first place, no way is known to generate a complete set of fracture location and geometry data. Secondly, if the Topopah Spring welded unit has a mean fracture density of 20 fractures/m^3 and has a mean thickness of 300 m over the approximately 7×10^6 m^2 area of the central Yucca Mountain block, then one would have to consider flow in approximately 4×10^{10} discrete fractures. Consequently, the practical alternative is to regard the matrix and fractures as constituting either separate but overlapping continuum systems or as a single composite continuum system. These approaches assume that the matrix and fracture properties can be represented as spatial averages over rock mass volumes whose linear dimensions are very much smaller than the thickness of the hydrogeologic unit but sufficiently large to include a representative, statistical sample of hydraulically connected fractures. The rock mass volume over which the averaging is performed is commonly designated as a representative elementary volume (REV) (Bear, 1972). The macroscopic continuum approach for fractures and rock matrix has been examined theoretically by Klavetter and Peters (1986), who conclude that it appears to be applicable to the unsaturated, fractured tuffs at Yucca Mountain. Specifically, they consider a "composite-porosity" model which describes fluid movement in a single continuum composed of both matrix material and fractures. This approach would not be applicable to sparsely fractured media or to media in which the mean fracture apertures exceeded a few millimeters and, thus, for which the medium would cease to be approximated by a bundle of capillary tubes. One principal objective of the bulk-permeability test, which is to be performed within the exploratory shaft as described in Section 8.3.1.2.2.4, is to field-test the REV hypothesis as it may apply to the fractured Topopah Spring welded unit at the potential repository horizon.

Preliminary results based on a dual-porosity, porous-medium-equivalent representation for fractured hydrogeologic units have been reported by Montazer and Wilson (1984), Wang and Narasimham (1985), and Klavetter and Peters (1986). The dependence of relative hydraulic conductivity on liquid-water potential in a fractured porous medium under the composite continuum hypothesis may be expected to exhibit the qualitative appearance shown in Figure 3-34. At low matrix saturations, little or no water moves longitudinally within the fracture openings, and the effective hydraulic conductivity is controlled by that of the fracture-bounded matrix blocks. As the matrix approaches complete saturation, however, the movement of water within and along the fracture aperture rapidly becomes more efficient so that at complete saturation the fractures may be dominant contributors to the net

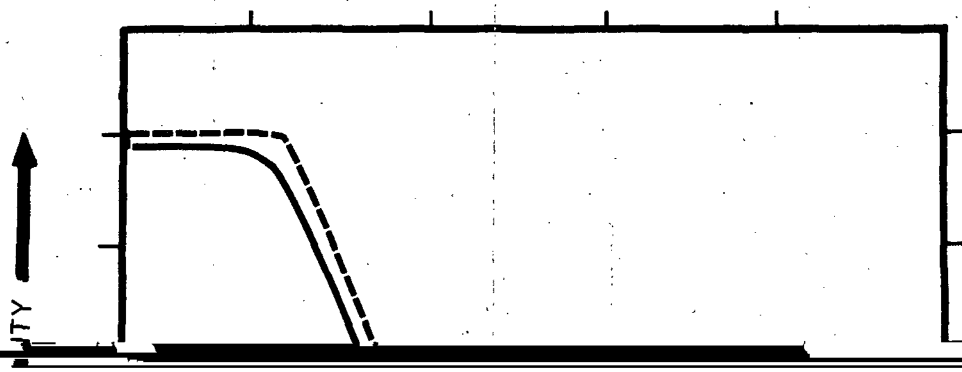

hydraulic conductivity. The relative contributions of fractures and matrix to the net effective hydraulic conductivity depend on the fracture frequency, aperture-size distribution, and degree of interconnectivity. The hydrogeologic unit TSw exemplifies the extremes that may be encountered. This unit has a matrix saturated hydraulic conductivity of about 10^{-11} m/s and a fracture density of 8 to 40 fractures/m^3 (Table 3-26). In well J-13, the Topopah Spring unit is fully saturated. It is the major source of water to the well and has an estimated net bulk, presumably fracture-controlled, hydraulic conductivity of about 8 x 10^{-6} m/s (Thordarson, 1983).

A further complication arises inasmuch as the hydrogeologic units may be anisotropic with respect to hydraulic conductivity. Data are presently insufficient to perform an adequate assessment. Because chemical alteration can be expected to destroy preferred orientations of rock properties, the matrix properties of the altered, zeolitized CHnz unit probably are largely isotropic. The fracture and fault systems within the densely welded units, however, probably introduce an inherent anisotropy wherever they are present and contribute significantly to moisture or pore-gas flow. Two principal fracture sets have been identified within the Yucca Mountain block (Scott et al., 1983). One set strikes north-northwest and the other strikes north-northeast, and both fracture sets exhibit steep to vertical dips. Most of the faults bounding and within the Yucca Mountain block are typical Basin and Range style high-angle normal faults that dip to the west, strike to the north, and exhibit small individual displacements (2 to 5 m). The Solitario Canyon fault, which bounds Yucca Mountain on the west, is a northward-striking high-angle normal fault that dips to the west and has a displacement ranging from 20 to 200 m along its trace. The Ghost Dance fault within the Yucca Mountain block is likewise a west-dipping, north-striking normal fault with a displacement of about 25 m. These faults and their associated fracture zones in the more competent hydrogeologic units probably introduce a fundamental preferential directional control on moisture movement, whether these fault zones act as conduits for or barriers to flow. Quantitative data by which to characterize rock-matrix and fracture-induced anisotropy is currently lacking but will be examined by field testing in surface-based boreholes and in the exploratory shaft and by laboratory measurements on

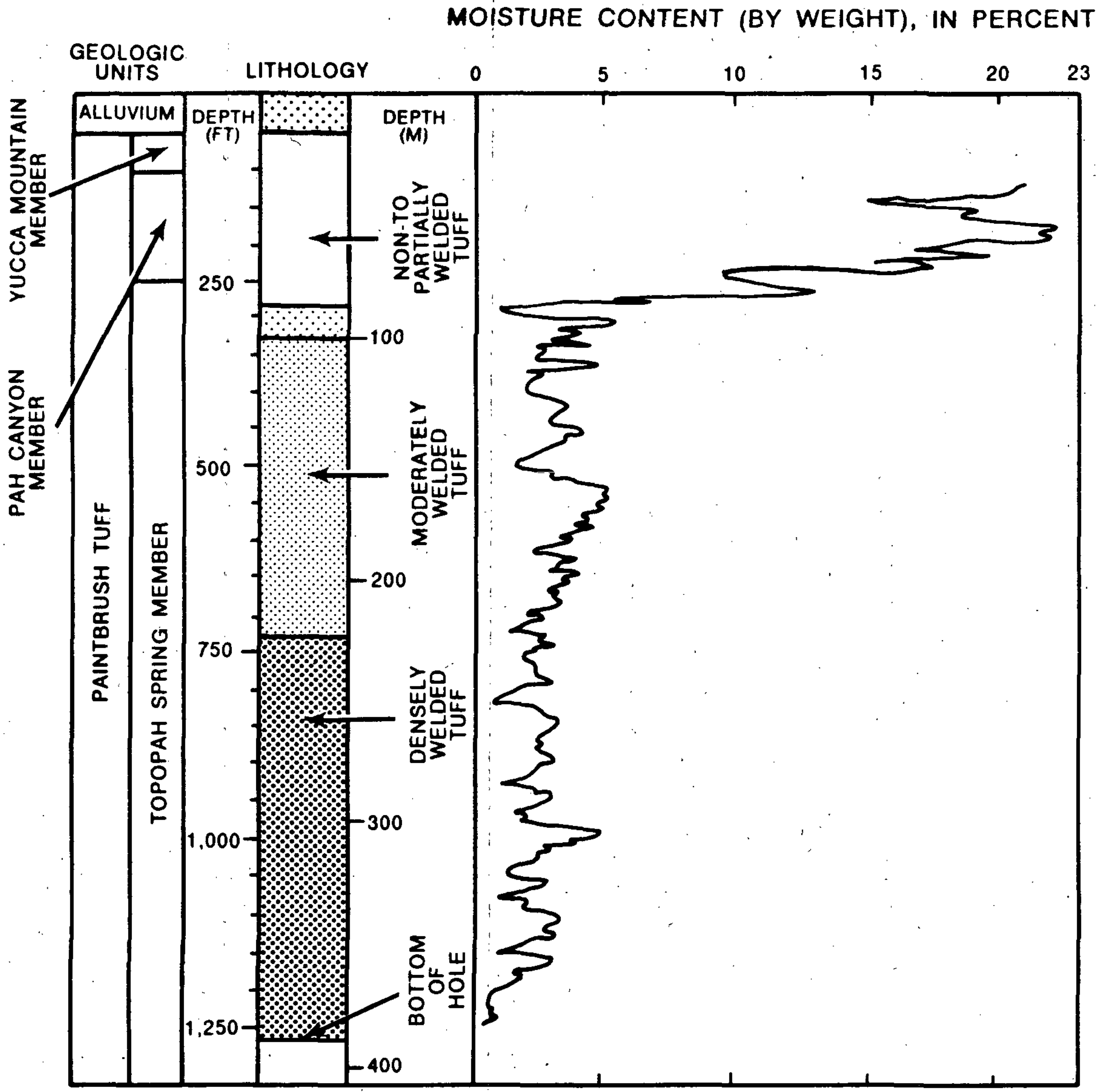

Figure 3-35. Moisture content of drill cuttings from borehole USW UZ-1. Modified from Whitfield (1985).

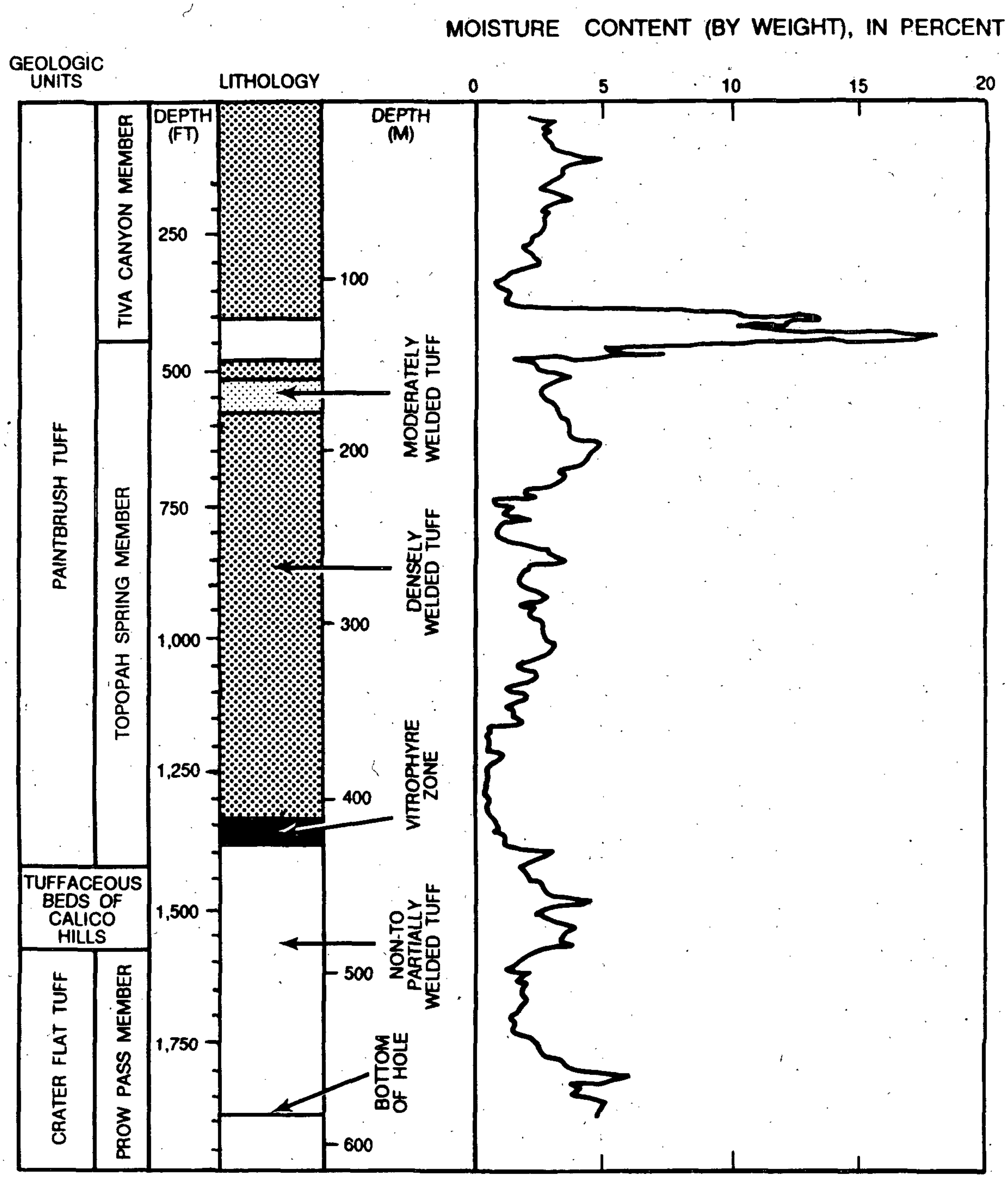

Figure 3-36. Moisture content of drill cuttings from borehole USW UZ-6. Modified from Whitfield (1985)

yields a mean saturation of about 0.6 for this unit. The interval of the Tiva Canyon welded (TCw) unit penetrated in drillhole USW UZ-6 has a mean moisture content of about 0.025 kg/kg, which, with a mean porosity of 0.1 and a mean grain density of about 2,500 kg/m^3 (Table 3-26), yields a mean saturation for this unit of about 0.6. The Topopah Spring welded (TSw) hydrogeologic unit has a mean moisture content of about 0.025 kg/kg in drillhole USW UZ-1 and about 0.02 kg/kg in drillhole USW UZ-6. Using a mean porosity of 0.12 and a grain density of about 2,600 kg/m^3 for this unit (Table 3-26), a mean saturation is obtained for the TSw unit of about 0.5 in drillhole USW UZ-1 and about 0.4 in drillhole USW UZ-6. These very tentative results generally are consistent with the ambient mean saturations of 0.61 for the PTn unit, 0.67 for the TCw unit, and 0.65 for the TSw unit reported by Montazer and Wilson (1984).

Using the moisture-retention curves shown in Figure 3-33, these estimates of in situ saturations may be converted into corresponding matric potentials. For example, if the saturation in the PTn unit is 0.6, the curve in Figure 3-33 for this unit implies a matric potential of about -0.75 MPa, a value that is compatible with the range of matric potentials for this unit implied by the matric-potential data obtained to date from drillhole USW UZ-1 (Figures 3-30 and 3-31). However, if the saturation in the TSw unit is 0.5, the curve for this unit in Figure 3-33 implies a corresponding matric potential of about -7 MPa, a value quite different from the mean of about -0.3 MPa for the TSw unit implied by from the matric-potential data in drillhole USW UZ-1 (Figures 3-30 and 3-31). This apparent discrepancy emphasizes the need for continued monitoring of ambient hydrologic conditions within the unsaturated zone at Yucca Mountain, as well as for the direct laboratory measurement of the hydrologic properties for statistically large samples of cores, drill cuttings, and bulk-rock samples taken from within each of the hydrogeologic units at numerous locations within Yucca Mountain.

Under transient moisture-flow conditions, moisture may be taken into or released from storage within the system, and parameters describing the moisture-storage properties of the system must be supplied as part of the hydrologic properties. Storativity is defined by Bear (1972) to be the change in volume of liquid water storage per unit volume of bulk rock mass upon unit change of liquid-water potential. The rate at which the quantity of water held in storage changes with time is equal to the product of storativity and the time rate of change of liquid-water potential. In partially saturated media, storativity depends upon (1) the relations between ambient matrix and fracture saturations and the liquid-water potential in the matrix and fractures; (2) the liquid-water compressibility; and (3) the effective bulk compressibility appropriate to the rock matrix and the fractures.

Consequently, specification of moisture storage and movement within the unsaturated zone requires the availability of hydro-mechanical-thermal properties and their spatial variation for each hydrogeologic unit. These data are to be determined through field, laboratory, and theoretical studies described in Sections 8.3.1.2 and 8.3.1.15. Thermomechanical data presently available for the rocks composing the hydrogeologic units at Yucca Mountain have been compiled and summarized in Section 2.4.

Capacitance is a measure of the amount of water stored in a partially saturated medium and depends both on the local value of pressure head and the thermomechanical properties of the medium. Using approximate values for the rock-matrix and fracture mechanical properties, Klavetter and Peters (1986) have performed a preliminary analysis of capacitance for the hydrogeologic units in the unsaturated zone at Yucca Mountain. They regarded each fractured unit to be represented as a composite porous medium in which the matric potential in the fractures is equal to that in the rock matrix. Their results, calculated for the TSw unit, are shown in Figure 3-37, which shows the contributions to the total capacitance due to a number of independent storage mechanisms. Under the assumed conditions, the results plotted in Figure 3-37, which are typical of those for the other hydrogeologic units, indicate that changing fracture and rock-matrix saturations dominate storage capacity with decreasing matric potential while the bulk rock-matrix compressibility becomes the dominant contributor near complete saturation.

Fundamental hydrologic-property data for the bulk-gas flow system within the unsaturated zone are presently lacking. Highly preliminary estimates of in situ air permeability in the TCw and PTn units at boreholes USW UZ-1 and USW UE-25a#4 have been reported by Montazer et al. (1986). Downhole pore-gas pressures are being monitored at regular intervals in borehole USW UZ-1 (Montazer et al., 1986; Section 3.9.1.1.1), and the results of pore-gas sampling and chemical analyses have been reported by Yang et al. (1985) (Section 3.9.1.3). An extensive program of gas-phase monitoring, chemical sampling, gas-tracer studies and pneumatic-property determinations is planned as part of the surface-based, exploratory shaft, and laboratory investigations of the unsaturated zone and are described in Section 8.3.1.2.2.

3.9.2.2 Hydraulic characteristics of the saturated zone

This section presents values for and discusses the following hydraulic characteristics for each hydrogeologic unit within the saturated zone: hydraulic conductivity, transmissivity, porosity, and storage coefficient.

3.9.2.2.1 Hydraulic conductivity and fractures

Analytical approaches to the determination of hydraulic conductivity of rocks in the saturated zone for the Yucca Mountain site have involved variations of Theis equations, which are based on Darcian flow, and assumptions of nonsteady discharge of water from wells. The specific or detailed nature of data from each test hole has varied; pumping responses have varied because of variations of hydraulic conditions among well sites; and conceptual ideas of the nature of the systems have evolved as experience has been gained, although analysis of the data for each well site has been based on assumptions that are generally common to each:

1. The tested rock has primary matrix porosity and is homogeneous and isotropic.

2. The secondary porosity is controlled by fractures. The fractures generally are vertical or very steep within the saturated zone. The

Table 3-29. Comparison of hydraulic-conductivity values from in situ tests with core-sample analyses (continued)

Stratigraphic unit	Selected depth interval from Table 3-28 (m)	Average hydraulic conductivity (m/d)	
		Total, from in situ tests (Table 3-28)	Matrix, from core analyses[a]
Bullfrog and Tram members	811-926	4×10^{-5}	[c]4×10^{-5}
Tram Member and flow breccia	926-1200	$<7 \times 10^{-6}$	[e]2×10^{-4}

[a]Core-sample analyses from Rush et al. (1984).
[b]Average for three core-sample analyses.
[c]Average for four core-sample analyses.
[d]Average for five core-sample analyses.
[e]Average for six core-sample analyses.

well J-13 that range from 2×10^{-4} to 8×10^{-7} m/day; however, the Topopah Spring Member is fractured, has an average in situ hydraulic conductivity of 0.7 m/day, and is the most productive unit penetrated by the well.

The tuffaceous beds of Calico Hills are above the water table in most hydrologic test holes near Yucca Mountain. In drillhole UE-25p#1 the unit is mostly saturated but poorly permeable; during a pumping test, a borehole-flow survey indicated the unit yielded less than 2 percent of the total amount pumped. Hydraulic conductivity of the unit was not separately determined by straddle tests; however, Craig and Robison (1984) concluded that the 41 m of saturated Calico Hills penetrated by UE-25p#1 has a transmissivity of about 0.5 m^2/day. In contrasts in drillhole UE-25b#1, the tuffaceous beds of Calico Hills yielded 32 percent of the production (Figure 3-38) during pumping of the entire hole (Lahoud et al., 1984). In the vicinity of UE-25b#1, the unit is zeolitized and would have low matrix hydraulic conductivity; therefore, the relatively high values determined from in situ tests (Table 3-27) probably are due to nearby normal faults or shear fractures (Waddell et al., 1984).

The Prow Pass and Bullfrog members of the Crater Flat Tuff are generally similar in hydrologic properties and are commonly the most productive ones penetrated by drillholes in the vicinity of Yucca Mountain (Figures 3-38 and 3-39). Their in situ bulk hydraulic conductivity is controlled largely by fractures (Waddell et al., 1984). Results from in situ tests and core analyses for drillhole USW H-1 are shown in Table 3-29 (Rush et al., 1984).

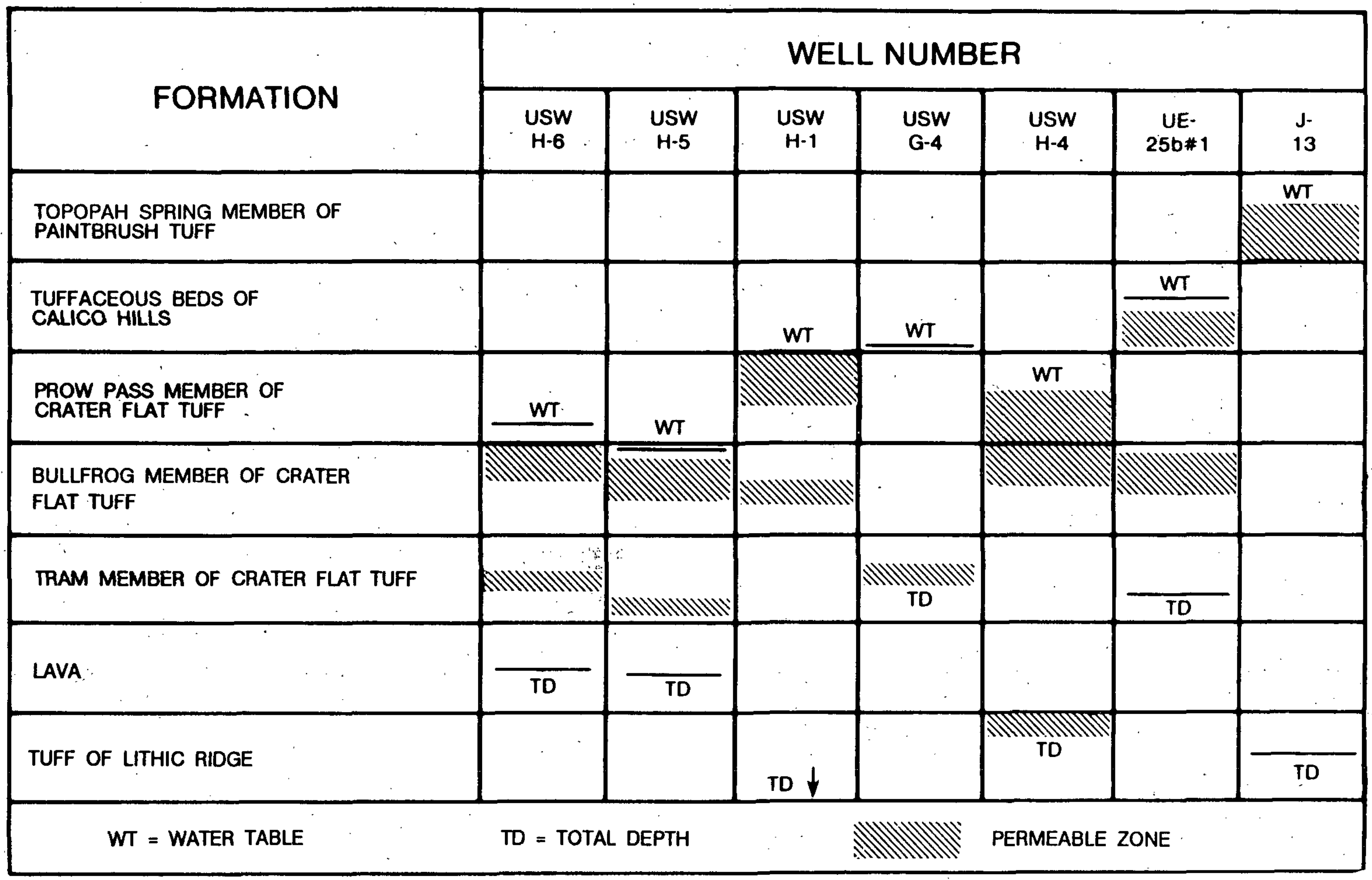

Figure 3-39. Vertical distribution of permeable zones in selected wells in the Yucca Mountain area. Modified from Benson et al. (1983).

The Tram Member of the Crater Flat Tuff generally is much less permeable than any of the overlying saturated units; at drillhole UE-25b#1, for example, the Tram yielded no measurable production during pumping of the entire

3.9.3 GROUND-WATER FLOW SYSTEM CONCEPTUAL MODEL

As indicated in the remarks prefacing Section 3.9, a conceptual model of a ground-water flow system uses available hydrogeologic data for the system to synthesize a general understanding of the overall (macroscopic) hydrologic system in terms of the specific (microscopic) hydrologic processes that are expected to operate within it. The macroscopic elements of the conceptual model include the hydrogeologic framework, a set of hydrologic boundary conditions (including the direction and magnitude of moisture or ground-water flux across the boundaries), and a knowledge of the present (initial) hydrologic state of the system, that is, the spatial distribution of hydraulic head in the saturated zone and of matric potential or saturation in the unsaturated zone. The microscopic elements are supplied by or developed from the fundamental concepts describing liquid and gaseous flow and storage in permeable media. Because it is usually abstracted from an incomplete set of

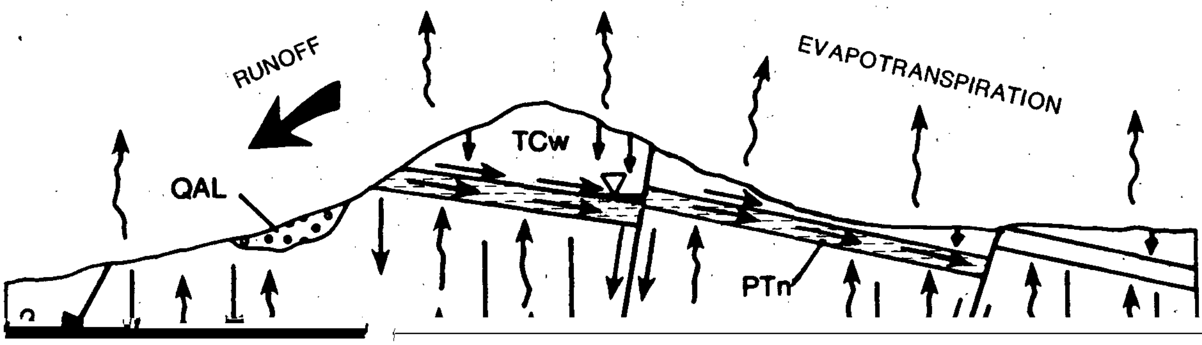
RUNOFF
EVAPOTRANSPIRATION
QAL
TCw
PTn

high-angle normal faults. The upper hydrologic boundary consists of the land surface, across which water enters the unsaturated zone as infiltration directly from precipitation or from runoff. The lower hydrologic boundary is

the water table, whose configuration is presumed to be known. Steady-state unit may produce lateral flow as well as vertical flow where the low-conductivity CHn unit underlies the TSw unit.

6. Flow in both the CHnv and CHnz units is predominantly vertical through the matrix (although a lateral component may occur parallel to the bedding within the vitric CHnv unit) and continues directly to the water table wherever the latter transects the CHn unit. Where the CHn unit lies above the water table, flow is presumed to proceed vertically downward to the water table through the Crater Flat undifferentiated unit (CFu).

7. The nearly vertically oriented fault zones and their associated fracturing may be highly effective pathways for vertical moisture flow, especially in the competent TCw and TSw units. But faults may impede lateral flow and may thus produce perched-water bodies where the faults transect zones or horizons of significant lateral flow.

8. Temperature-driven moisture transport may occur, especially within the highly fractured TSw unit. This could be expected to occur by molecular diffusion if local thermodynamic phase equilibrium is maintained between liquid water and water vapor within the system, which would produce a water-vapor concentration gradient along the natural geothermal gradient. Of greater importance may be the advective transport of water vapor accompanying thermally or barometrically driven upward bulk-gas flow within the fractures of the TSw unit. Under steady-state conditions, the upward movement of water vapor in the air-filled fracture openings would be compensated by downward return flow of liquid water within the rock matrix.

9. Moisture flow within the deep unsaturated zone at Yucca Mountain may be occurring under essentially steady-state conditions. The steady-state hypothesis implies that moisture flow within the natural system is occurring predominantly as vertically downward liquid-water flow within the rock matrix of the hydrogeologic units with possible water-vapor movement within the air-filled pore and

A general geohydrologic conceptual model for saturated ground-water flow near Yucca Mountain is based upon division of the Tertiary stratigraphic units into (1) moderately and densely welded tuff and (2) nonwelded and bedded tuffs, as a result of the different hydrologic properties of these materials. The moderately and densely welded tuffs are characterized by relatively low porosities, abundant fractures, and low matrix permeability. In nonwelded and bedded tuffs, porosities are greater and fractures are fewer, although fractures do occur. Unless the rock contains clays or zeolites, matrix conductivities are generally larger than in the welded tuffs (Waddell et al., 1984).

This model provides a basis for predicting saturated hydraulic properties near Yucca Mountain, provided that the welding characteristics and extent of secondary mineralization of units are known. The Paintbrush Tuff is mostly unsaturated; the Topopah Spring Member, which is unsaturated in the repository block, but saturated east of Yucca Mountain (Figures 3-25 and 3-28), consists mostly of moderately to densely welded tuffs. The Crater Flat Tuff (Prow Pass, Bullfrog, and Tram members) consists of partially to moderately welded tuffs. The tuffaceous beds of Calico Hills and Lithic Ridge Tuff are predominantly nonwelded and bedded tuffs. In addition, bedded tuffs commonly separate the major ash-flow tuff units.

Partial alteration of vitric tuffs to zeolites or clays reduces their permeability substantially. Thickness of the zeolitic facies of the tuffaceous beds of Calico Hills increases from southwest to northeast (Figure 3-41), and the entire unit is altered beneath the northern and northeastern parts of the Yucca Mountain repository block (Montazer and Wilson, 1984) (Section 3.9.2.1).

All the Tertiary stratigraphic units just discussed are within the regional "tuff aquitard" considered by Winograd and Thordarson (1975). Beneath Yucca Mountain are Paleozoic carbonate rocks, equivalent to the regional "lower carbonate aquifer" of Winograd and Thordarson (1975). These

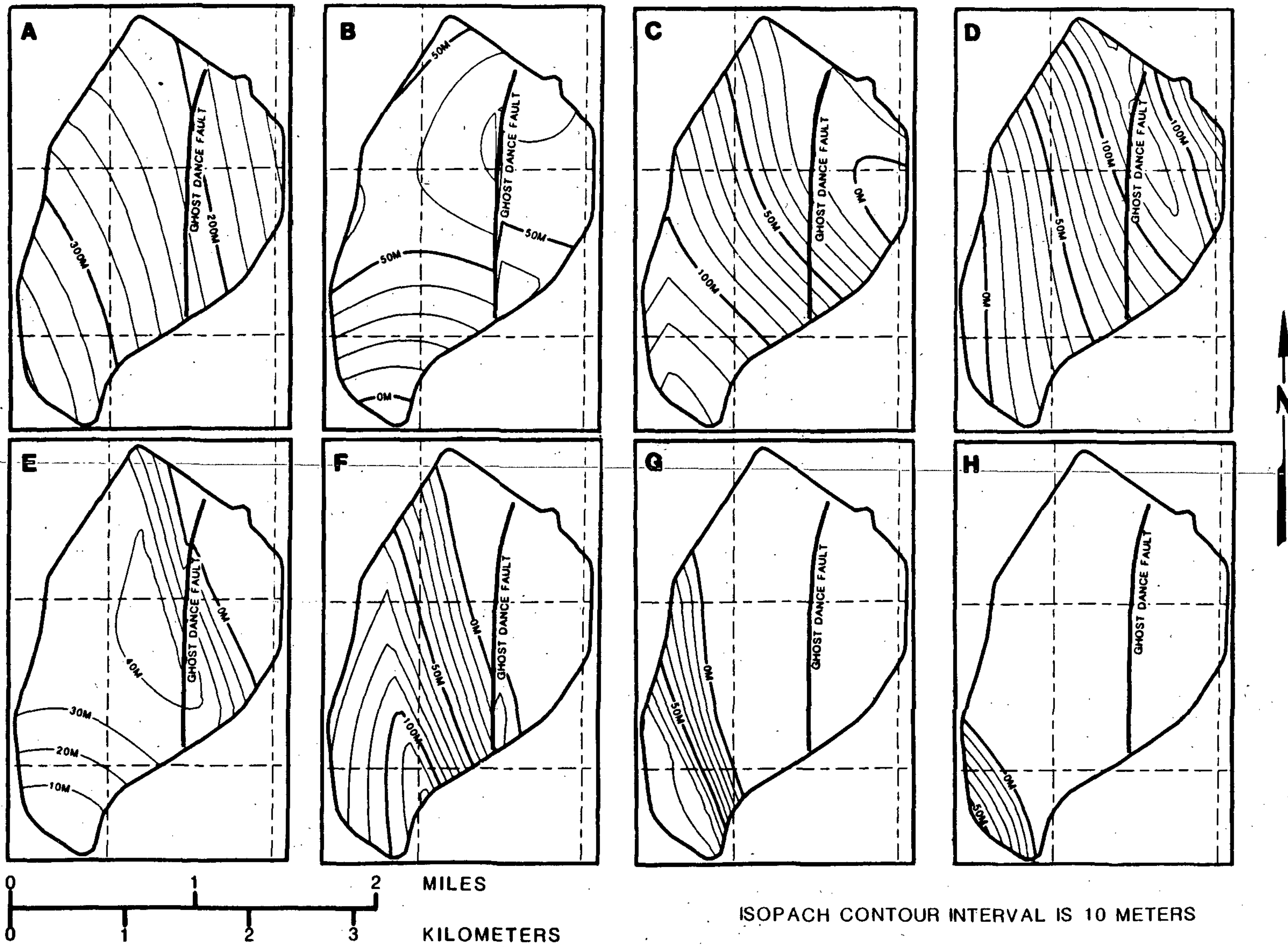

Figure 3-41. Isopach contour maps within the repository block: (A) Total thickness from disturbed zone to the water table; (B) Thickness of undisturbed Topopah Spring welded unit TSw; (C) Thickness of the Calico Hills nonwelded vitric unit, CHnv; (D) Thickness of the Calico Hills nonwelded zeolitic unit CHnz; (E) Thickness of the Prow Pass welded unit, PPw; (F) Thickness of the Prow Pass nonwelded unit, PPn, (G) Thickness of the Bullfrog welded unit. Modified from Sinnock et al. (1986).

(Rush et al., 1983), which minimized possible moisture uptake by the core samples. Mercury intrusion techniques were used to develop moisture-retention curves for each of the samples from which ambient matric potentials were inferred (Weeks and Wilson, 1984). Analytic representations of Peters et al. (1984) are shown in Figure 3-33, and were based on psychrometric measurements made over a range of matric potentials much less than the minimum value of about -0.20 MPa that could be measured by Weeks and Wilson (1984). Only one sample was available from the PTn hydrogeologic unit at a depth of 33.5 m below land surface; it had a matric potential of -0.15 MPa at an ambient saturation of 0.51. Sixteen samples were available for the TSw unit spanning a vertical interval of 278 m within the unit. The lowest saturation measured within this sample set was 0.47, the highest was 0.89, and the mean was 0.65. There was a poorly defined indication within the sample set for saturation to increase with depth. The matric potentials inferred from the measured saturations for the samples were highly variable, ranging from -0.07 to more than -0.25 MPa with a mean of -0.18 MPa and a standard deviation of -0.06 MPa. Two samples were available from the CHn unit at a depth of 530 m and both indicated complete matrix saturations. Because of the considerable scatter within the set of data, the matric-potential and saturation values for the samples from the TSw unit do not define a unique, representative moisture-retention curve for this unit. It is not known to what extent this scatter may be attributed to intrinsic heterogeneity of properties and conditions within the TSw unit or is due to undetermined experimental errors of measurement. Consequently, these data from drillhole USW H-1 probably are best interpreted as indications only of the hydrologic conditions that may be expected to be encountered within the hydrogeologic units of the unsaturated zone at Yucca Mountain.

As described in Section 3.9.1.1.1, test well USW UZ-1 (Figure 3-27) has been drilled to a total depth of 387 m within the unsaturated zone at Yucca Mountain and instrumented with thermocouple psychrometers and heat-dissipation probes to monitor in situ matric potentials at 33 selected depths within the TCw, PTn, and TSw hydrogeologic units (Montazer et al., 1986). Data from two years of continued monitoring indicate that hydrologic conditions within the borehole may be in approximate equilibrium with ambient conditions in the surrounding units. The data available to date are shown in Figures 3-30 and 3-31. Although the data show considerable variability, there is no well-defined systematic variation of matric potential with depth within hydrogeologic units, which is consistent with the supposition that the individual hydrogeologic units are relatively homogeneous in the vertical direction and that steady-state vertical moisture flow occurs under unit vertical hydraulic gradient. The trend with time, if interpreted as the approach to equilibrium between the well and its surroundings, indicates that present ambient matric potentials generally are greater than -1 MPa, and that the mean matric potential over the total depth of the borehole is about -0.3 MPa. These data from borehole USW UZ-1 are consistent with the range of values of matric potential inferred by Weeks and Wilson (1984) to be representative of conditions within the interval of the unsaturated zone penetrated by borehole USW H-1. As described in Section 8.3.1.2.2, additional test holes in the unsaturated zone will be drilled and instrumented to better define the distribution of matric potentials and fluxes.

3.9.3.2.2 Saturated zone

Measured head values used to construct the saturated-zone potentiometric map (Figure 3-28) are mostly composite heads, reflecting heads similar to those in the zones of higher transmissivity.

The hydraulic gradient is low in western Jackass Flats (Fortymile Wash area) and in the Amargosa Desert; the gradient is high in volcanic rocks north of Yucca Mountain and across northern Yucca Mountain. Low-permeability rocks likely occur where the gradients are steep, but the steep gradients may be caused by poorly-permeable faults. In areas where it may be important to know the cause of steep gradients, additional drilling or hydrologic testing is planned (Section 8.3.1.2.3).

Significant vertical hydraulic gradients have been observed in only a few drillholes: in drillhole UE-25p#1, the head in Paleozoic carbonate rocks that occur below a depth of 1.2 km is about 19 m higher than in the shallow zone; in drillhole USW H-1 the head is about 54 m higher in the older tuffs of Tertiary age, at a depth of 1.8 km; and preliminary data from drillhole USW H-3 suggest that the head below 0.8 km (Tram Member of Crater Flat Tuff) is about 40 m higher. These higher heads occur only within or below intervals of low permeability. Semipermanent packers are installed in lower sections of several drillholes (UE-25b#1, USW H-3, USW H-4, USW H-5, and USW H-6) to enable comparison of water levels above and below the packers. Except in drillhole USW H-3, vertical differences of head within the Paintbrush and Crater Flat tuffs have been less than a meter.

The upward component of ground-water flow that is indicated by higher heads in the deeper part of the saturated zone may be the result of the position of Yucca Mountain within the regional ground-water flow system. Simple models of ground-water basins consist of an area where recharge occurs (vertical flow is downward), and where discharge occurs (vertical flow is upward). In intermediate areas, flow is transitional from downward, to strictly horizontal, to upward (Figure 3-42). Although the Alkali Flat-Furnace Creek Ranch subbasin (of which Yucca Mountain is a part) is not simple, these concepts generally apply. Thus, Yucca Mountain is in an area where local vertical flow may be either up or down (Waddell et al., 1984). Erickson and Waddell (1985) observed slight upward and downward movement among different intervals of the same drillhole (USW H-4). This upward and downward movement may also be due to differences in horizontal and vertical hydraulic conductivity beneath Yucca Mountain.

3.9.3.3 Recharge-discharge and leakage

The ultimate source of moisture in the unsaturated zone at Yucca Mountain is by net infiltration from precipitation on the mountain, and the quantity of precipitation is used by some techniques to estimate net infiltration and, subsequently, recharge. Net infiltration refers to the rate and quantity of water entering the unsaturated zone below the plant-root zone and represents moisture that is effectively inaccessible for direct return to the atmosphere by evapotranspiration. Recharge is the rate and quantity of water entering the saturated zone from the unsaturated zone (the term specifically

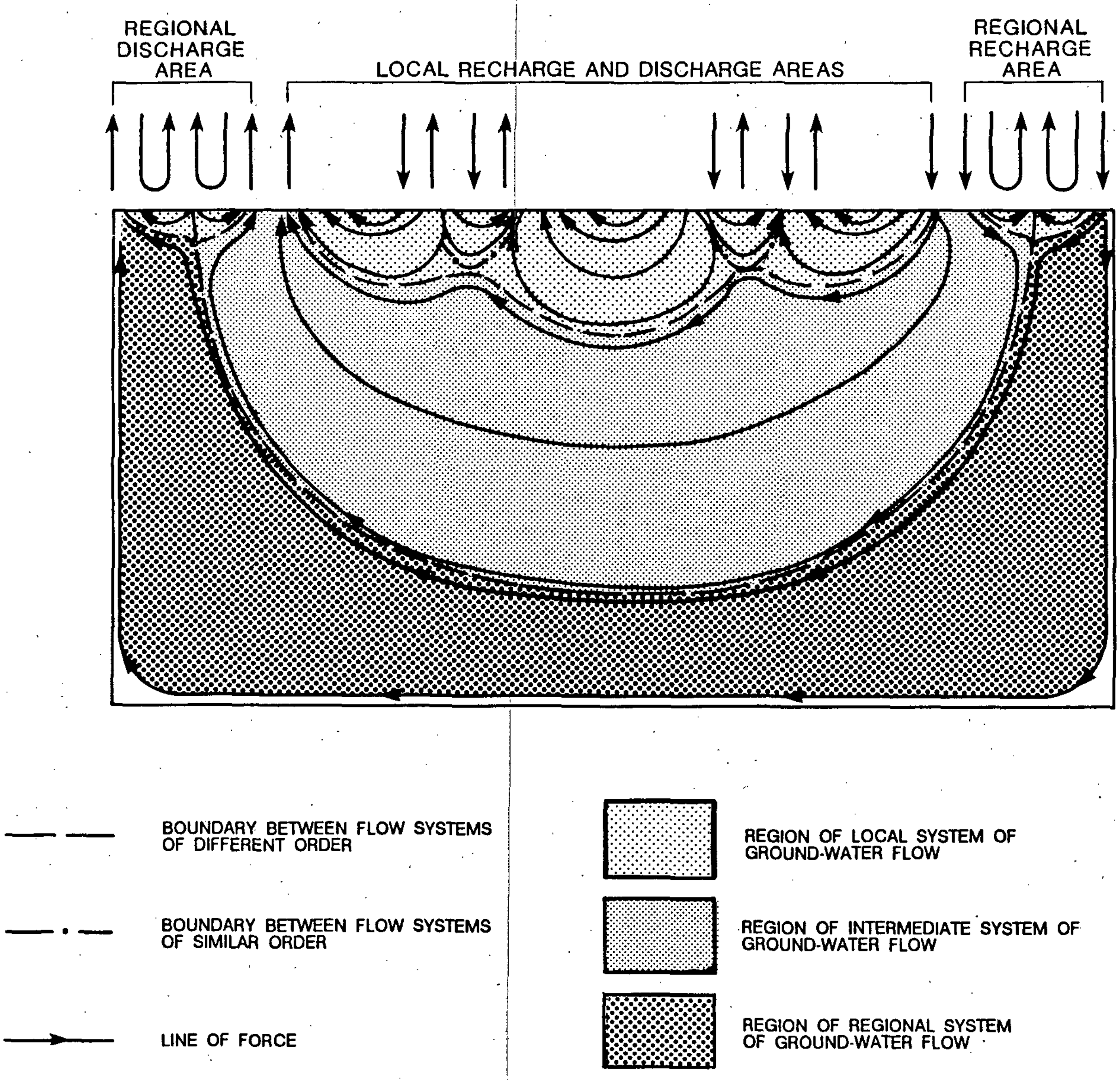

Figure 3-42. Standard theoretical flow pattern and boundaries between different flow systems. Modified from Toth (1963).

excludes underflow into or out of the region of interest; recharge to adjacent areas subsequently may enter the region of interest as underflow). Direct measurements of precipitation at Yucca Mountain have been initiated, but too recently to provide reliable annual average values (Section 5.1). However, precipitation at the site has been estimated from the regional distribution of precipitation or from relationships established between altitude and precipitation. From a regional map of precipitation presented by Winograd and Thordarson (1975), precipitation at Yucca Mountain is estimated to be about 100 to 150 mm/yr (Section 5.1). Quiring (1983) established local relationships between altitude and precipitation for 1964-81 at the NTS. Quiring's (1983) data included limited data outside the NTS and data from 13 stations within the NTS that range in altitude from 3,000 to 7,490 ft (914 to 2,283 m). From a map showing precipitation-to-altitude ratios (Quiring, 1983), precipitation for the approximate range of altitudes at Yucca Mountain (about 1,220 to 1,465 m) is estimated to be 138 to 166 mm/yr, or an areal average of about 150 mm/yr (Montazer and Wilson, 1984). Quiring's (1983) data indicate that about 73 percent of this quantity falls

Recharge to the saturated zone and the deep aquifers has been estimated within the region surrounding Yucca Mountain. For example, recharge to the regional carbonate aquifer, which underlies much of the NTS and vicinity, was estimated to be 3 percent of the precipitation falling on upland outcrops of this aquifer on the basis of measured spring discharge at Ash Meadows (Winograd and Thordarson, 1975). Applying this percentage to average precipitation at Yucca Mountain (150 mm/yr) would imply a recharge rate of about 4.5 mm/yr. In addition, Waddell et al. (1984), using data from Winograd (1981), estimated a moisture flux of about 0.5 mm/yr through the alluvium in Yucca Flat, which, however, being 40 km northeast of Yucca Mountain, probably is not typical of the Yucca Mountain site. Also, Case et al. (1984) determined a typical value of pore velocity of "about one-third centimeter per year" (under unsaturated conditions) in Frenchman Flat, 40 km east of Yucca Mountain. This is equivalent to a flux of 1 mm/yr if an effective porosity of 30 percent is assumed for the soil at Frenchman Flat. None of these studies provides a reliable basis for estimating recharge at Yucca Mountain. As at all sites, the actual value of recharge at Yucca Mountain depends on site-specific, local microclimatic, soil, vegetative, topographic, and hydrogeologic conditions.

Methods for estimating recharge for ground-water basins in Nevada were developed by Maxey and Eakin (1949) and refined by Eakin et al. (1951) and Malmberg and Eakin (1962). The resulting Maxey-Eakin method uses regional relationships among recharge, altitude zones, and precipitation but it does not account for a number of factors, such as runoff during intense storms, local rainfall distribution, temperature, and vegetative cover. Rush (1970)

Wilson (1985) reviewed available site and regional hydrogeologic data in order to set conservative upper limits on the present, net vertically downward moisture flux below the repository horizon at Yucca Mountain and on the present rate of net recharge to the saturated zone in the vicinity of Yucca Mountain. Wilson (1985) concludes (1) that the liquid-water percolation flux, directed vertically downward in the matrix of the TSw unit below the repository horizon, probably is less than 0.2 mm/yr and (2) that the areally averaged rate of net recharge to the saturated zone in the vicinity of Yucca Mountain probably is less than 0.5 mm/yr. Although Wilson (1985) considered

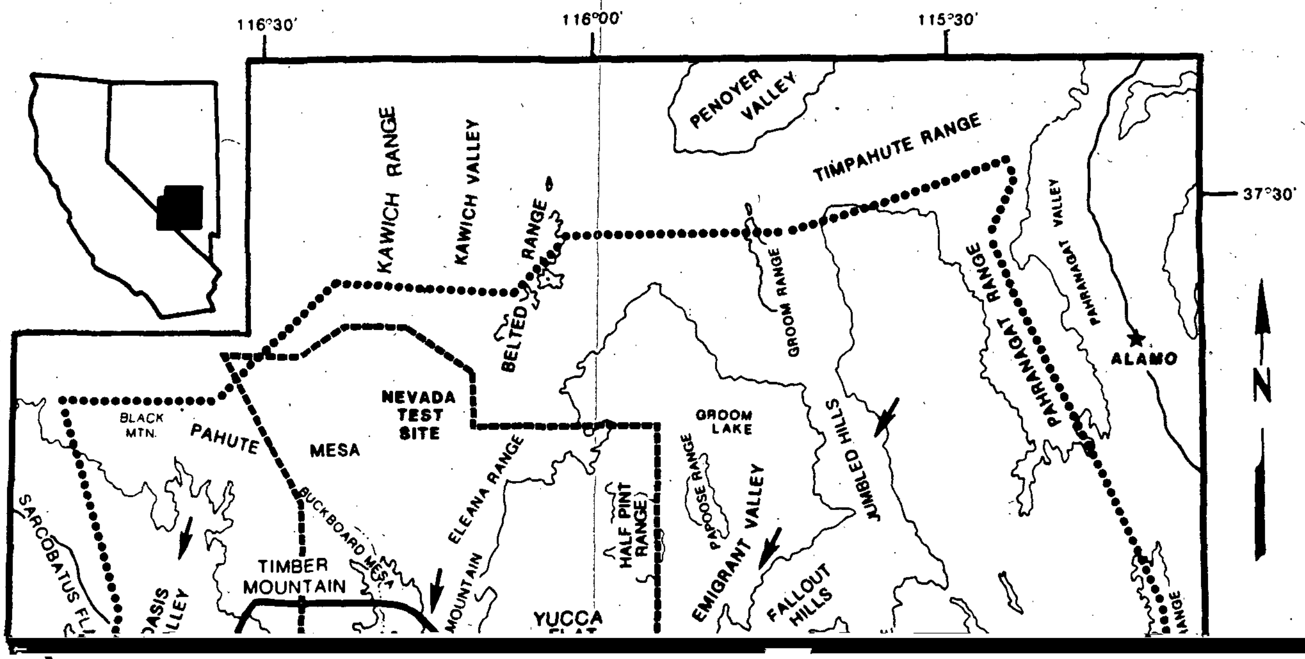

[redacted]

[redacted]

[redacted]

[redacted]

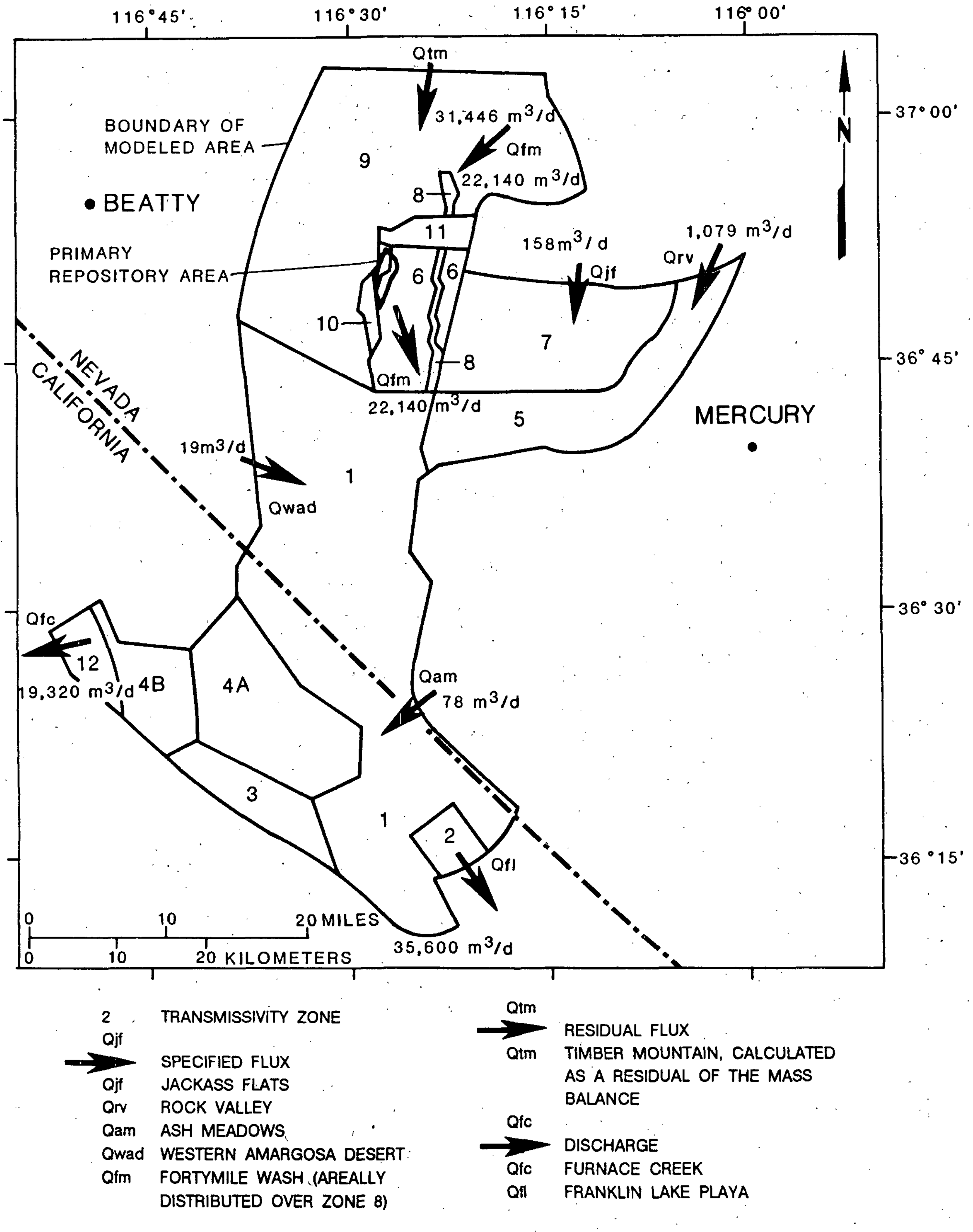

Figure 3-44. Locations and estimates of ground-water flow into and out of the Alkali Flat-Furnace Creek Ranch subbasin. Modified from Czarnecki and Waddell (1984).

3.9.3.4 Unsaturated-zone relationships

The factors controlling land-surface infiltration and the subsequent delivery of net infiltration as recharge to the water table are discussed in Section 3.9.3.3. The spatial distribution of net infiltration is one factor that controls moisture fluxes within the deep unsaturated zone beneath Yucca Mountain. No direct measurements of net infiltration have been made at Yucca Mountain and thus neither its magnitude nor its spatial and temporal distribution over the surface of Yucca Mountain are known. Montazer and Wilson (1984) estimate that the present average rate of net infiltration over the Yucca Mountain block may be expected to range from about 0.5 to no more than 4.5 mm/yr. As discussed in Section 3.9.3.3, Wilson (1985), in reviewing and analyzing available data, concluded that a value of 0.5 mm/yr may be a conservative upper bound for the mean vertical-downward percolation flux of water across the repository horizon. Net infiltration is expected to be episodic and unevenly distributed over the surface of Yucca Mountain. These irregularities, however, probably are smoothed rapidly with depth (Weeks and Wilson, 1984) so that the mean percolation rate at depth within Yucca Mountain is affected significantly only by large-scale climatic changes. If these changes occur sufficiently slowly in time, then the hydrologic system within the unsaturated zone can be presumed to adjust continuously to these changes so that an overall steady-state flow system may approximately exist at any point in time.

If, as is implied by the data obtained from test wells USW H-1, USW UZ-1, and USW UZ-6, the ambient liquid-water saturation within the repository TSw unit is within the range from about 0.5 to 0.7, then liquid-water percolation through the unit probably is matrix dominated (Klavetter and Peters, 1986; Peters et al., 1986) with little or no flow of water within fractures. Laboratory data (Table 3-26) indicate that the saturated hydraulic conductivity for the matrix of the TSw unit is about 3.5 x 10^{-11} m/s which, under a unit vertical hydraulic gradient, corresponds to a maximum vertical liquid-water flux through the matrix of about 0.8 mm/yr. At matrix saturations less than 1.0, this maximum flux within the TSw matrix would be reduced by the relative hydraulic conductivity appropriate to the matrix pore geometry and the ambient saturation. The relation between relative hydraulic conductivity and saturation for the TSw unit matrix material is not known. The van Genuchten (1980) representation used by Peters et al. (1984), however, would suggest a relative hydraulic conductivity factor of the order of 10^{-2} to 10^{-3} to be appropriate. Hence, the vertical percolation flux through the TSw unit, and by implication across the repository horizon within the unit, may well be about or much less than the 0.5 mm/yr maximum value estimated by Wilson (1985). This finding is consistent with the range of values from 0.1 to 0.5 mm/yr estimated by Montazer et al. (1986) from data obtained from borehole USW UZ-1 (Section 3.9.1.2.1). It must be emphasized that these analyses are very preliminary and approximate and presume that the TSw unit is laterally and vertically homogeneous and isotropic and that steady-state flow conditions prevail. In fact, however, conditions probably vary spatially, and the possibility exists that localized transient moisture flow occurs in fractures. This possibility will be evaluated as described in Section 8.3.1.2.2.

As described in Section 8.3.1.2.2, hydrologic data from the unsaturated shaft test facility and from a relatively small number of surface-based boreholes. Consequently, it will be necessary to rely on indirect methods, such as numerical flow and solute-transport modeling and geostatistical techniques, to infer the state of the presently existing natural hydrologic system by interpolating within and extrapolating from a somewhat incomplete set of field data (Section 8.3.1.2.2). Using data that are presently available for the site, several investigators have used these methods to perform rudimentary analyses and develop preliminary interpretations. These investigations have been directed in part towards examining some of the hypotheses underlying the conceptual model presented in Section 3.9.3 and contribute especially to identifying specific problems that will need to be resolved as part of the site-characterization program. These initial assessments, therefore, not only provide insight into the conceptualization of unsaturated-zone relationships at Yucca Mountain but also define specific data needs to be met by subsequent data acquisition at the site.

Peters et al. (1986) used a one-dimensional model to simulate liquid-water flow in an idealized but representative vertical column through the unsaturated zone at Yucca Mountain. They investigated the mode of liquid-water flow for a set of prescribed percolation fluxes within the column. The column was simulated to be 530.2 m in height and consisted of a basal CHnz or CHnv unit overlain by an upward succession of the units TSw, PTn, and TCw. The mean hydrologic properties for these units were taken from Peters et al. (1984). The results of these simulations indicate that virtually completely saturated conditions would be expected to occur within the TSw and TCw units for percolation fluxes exceeding about 0.5 mm/yr. This conclusion results from the values of the saturated matrix hydraulic conductivity for the TSw and TCw units that were used in the numerical simulations. The mean matrix conductivity values used for those two units were about 0.5 mm/yr. In a steady-state simulation, the value of percolation flux which induces saturated-matrix conditions in a particular hydrogeologic unit is directly proportional to its value of saturated matrix hydraulic conductivity. The results of the numerical simulations also predict that the time for the unsaturated system to return to steady state after a small change (a few tenths of a millimeter per year) in the steady percolation flux is on the order of tens or hundreds of thousands of years. These results suggest that the response time of the percolation flux at depth to changes in the net infiltration rate is very long. Greater percolation fluxes under this model would be expected to induce increasing volumes of flow within the fractures of the TSw and TCw units. However, the applicability of these results to Yucca Mountain is uncertain, because of (1) the limitations of one-dimensional modeling, which does not account for lateral heterogeneity, boundary conditions, and flow and (2) the uncertainty in the representativeness of the hydrologic properties. None the less, these results, together with the moisture-content data from boreholes USW UZ-1, USW UZ-6, and USW H-1, which indicate that the rock matrix of the penetrated units is not saturated, support the empirically based estimates of Wilson (1985) and Montazer et al. (1986) that the average percolation flux within much of the TSw unit probably is less than about 0.5 mm/yr.

Sinnock et al. (1986) used one-dimensional modeling techniques to calculate probable ground-water travel times from the repository horizon to the water table (Section 3.9.4). These calculations assumed that steady-state moisture-flow conditions prevail within the unsaturated zone at Yucca

Mountain and considered steady-state percolation fluxes of 0.1, 0.5, and 1.0 mm/yr. By varying flow-model parameters and using a Monte Carlo approach, probabilistic distributions for the ground-water travel time were developed. Although these calculations demonstrate the utility of the methodology, the quantitative results were sensitive to hydrologic-property input data that are as yet highly uncertain. Sinnock et al. (1986) emphasize the need for obtaining reliable field and laboratory hydrologic-property data for all of the hydrogeologic units that affect the travel-time calculations. In addition, they recommend that, to the extent that the sparse distribution of data-gathering sites will allow, geostatistical techniques be used to estimate the spatial correlation of hydrologic properties within and between hydrogeologic units. Geostatistical methods are also essential for the description of the unsaturated zone and the estimation of its hydraulic properties from the limited empirical data set that will be available from the Yucca Mountain site characterization studies.

Rulon et al. (1986) modeled multidimensional liquid-water flow within the unsaturated zone at Yucca Mountain by constructing a two-dimensional, vertical cross-sectional flow model to investigate: (1) the difference in steady-state flow patterns and moisture distributions that could result under the extremes of matrix-dominated or fracture-dominated liquid-water flow within the TCw and TSw units and (2) the likelihood for the occurrence of

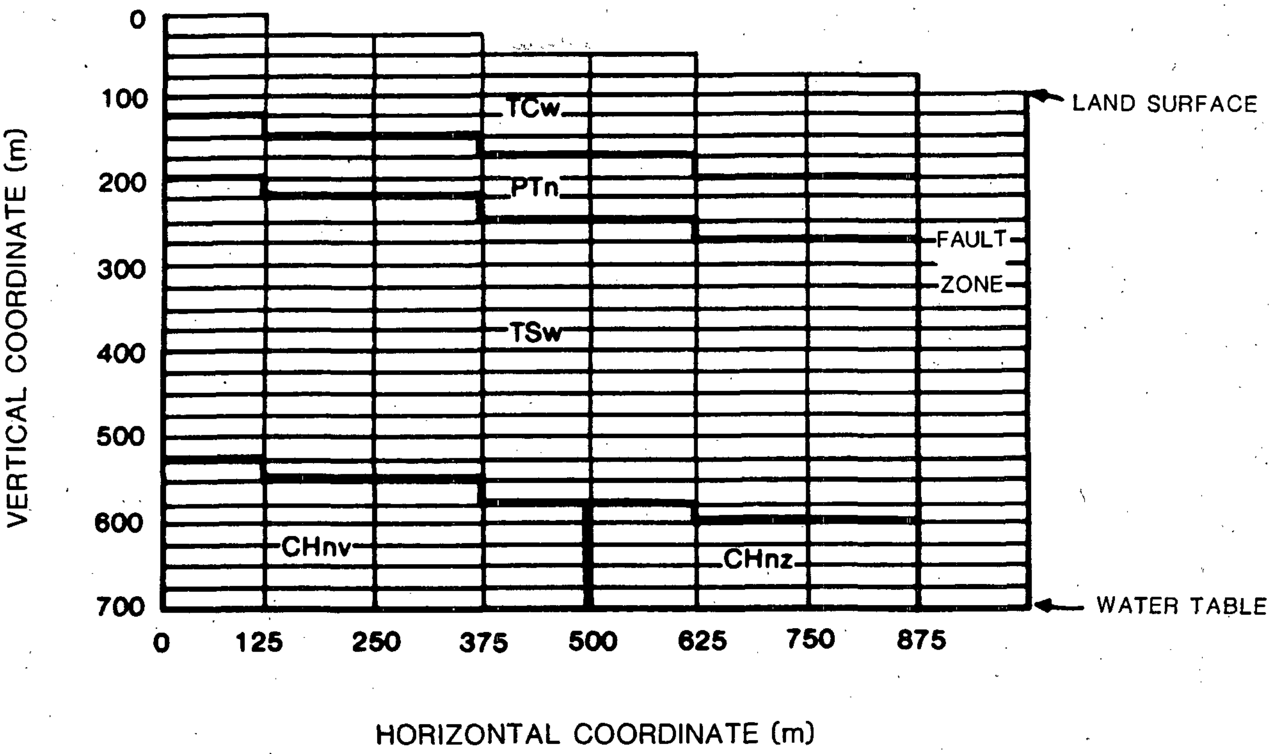

TCw	TIVA CANYON WELDED UNIT
PTn	PAINTBRUSH NONWELDED UNIT
TSw	TOPOPAH SPRING WELDED UNIT
CHnv	CALICO HILLS NONWELDED VITRIC UNIT
CHnz	CALICO HILLS NONWELDED ZEOLITIC UNIT

Figure 3-45. Numerical grid used in the two-dimensional flow simulations Modified from Rulon et al. (1986).

differed quantitatively from those computed by Peters et al. (1984). Both sets of model calculations, however, predicted that steady net infiltration rates (or percolation fluxes) exceeding values in the range from 0.5 to 1.0 mm/yr would produce complete matrix saturation in the TSw and TCw units after the mountain equilibrates to the change in flux. These conditions could lead to liquid-water flow within the fractures of these units. Both sets of calculations are consistent with the hypothesis that the present net percolation flux in the TSw unit is less than about 0.5 mm/yr (Wilson, 1985; Montazer et al., 1986), and that the flux is transmitted predominantly within the rock matrix of the TSw unit under conditions of less than complete matrix saturation.

Although the representation depicted in Figure 3-45 of inclined hydrogeologic units abutting a vertical fault zone is crude, the model results of Rulon et al. (1986) suggest that there is the potential for significant lateral flow above the repository TSw unit. At a high rate of net infiltration (4.5 mm/yr), significant lateral flow was predicted to occur within fractures of the uppermost TCw unit. At lower infiltration rates, significant lateral diversion of vertical flux was predicted to occur within the high matrix-conductivity PTn unit above its contact with the underlying TSw unit. Because these model calculations, as well as those of Peters et al. (1986), are based on highly idealized representations of the physical system, use a coarse grid size, and use hydrologic-property data that are preliminary and with unknown limits of uncertainty, the model results may not be quantitatively reliable. One of the major tasks to be accomplished through the data-acquisition program at the site, as detailed in Section 8.3.1.2, is to

DECEMBER 1988

The numerical modeling results reported here are preliminary but are zone. If the gas were saturated with respect to water vapor, such upward flow would produce an upward advective moisture flux of about 0.025 to 0.05 mm/yr under present conditions. Gas-pressure monitoring in test well USW UZ-1 shows a well-defined barometric response. It is unknown whether gas pressure variations at depths appropriate to the repository TSw unit would be sufficient to induce significant bulk gas flow. Nevertheless, the analysis of the hydrologic system within the unsaturated zone at Yucca Mountain, especially under nonisothermal, barometrically varying conditions, must consider the simultaneous, coupled flow of gas and moisture, the latter occurring both as liquid water and water vapor. Field measurements in surface-based boreholes, experiments in the exploratory shaft, and theoretically based modeling studies, as described in Section 8.3.1.2.2, are intended to address these issues.

3.9.4 GROUND-WATER VELOCITY AND TRAVEL TIME

Issue 1.6 of the issues hierarchy (discussed in the introduction to this document) addresses the performance objective defined in 10 CFR 60.113(a)(2): "The geologic repository shall be located so that pre-waste-emplacement ground-water travel time along the fastest path of likely radionuclide travel from the disturbed zone to the accessible environment shall be at least 1,000 years." The following discussion addresses this issue, focusing on that portion of the hydrogeologic system extending from the disturbed zone to the accessible environment. The components of this system which must be considered include: (1) the hydraulic properties of the formations through which the water will flow, (2) the present hydrologic conditions in the vicinity of the proposed repository, and (3) the locations and lengths of the flow paths between the disturbed zone and the accessible environment. The data and information required to assess the influences of these components on ground-water velocity and travel times are presently limited, and will be supplemented by the hydrologic investigations discussed in Section 8.3.1.2. The preliminary estimates of ground-water velocities and travel times presented here are based on sparse data and qualitative observations of hydrologic processes from limited field investigations.

Issue 1.6 addresses ground-water flow from the edge of the disturbed zone to the accessible environment. Based on the NRC Draft Generic Technical Position Paper on the Disturbed Zone (NRC, 1986b) the edge of the disturbed zone will be assumed conservatively to be 50 m below the repository level for this preliminary analysis. The actual extent of the disturbed zone will be determined during site characterization (Section 8.3.5.12.5). Based on the proposed amendments (NRC, 1986a) to 10 CFR Part 60, the accessible environment is located beyond 5 km from the outer boundary of the repository

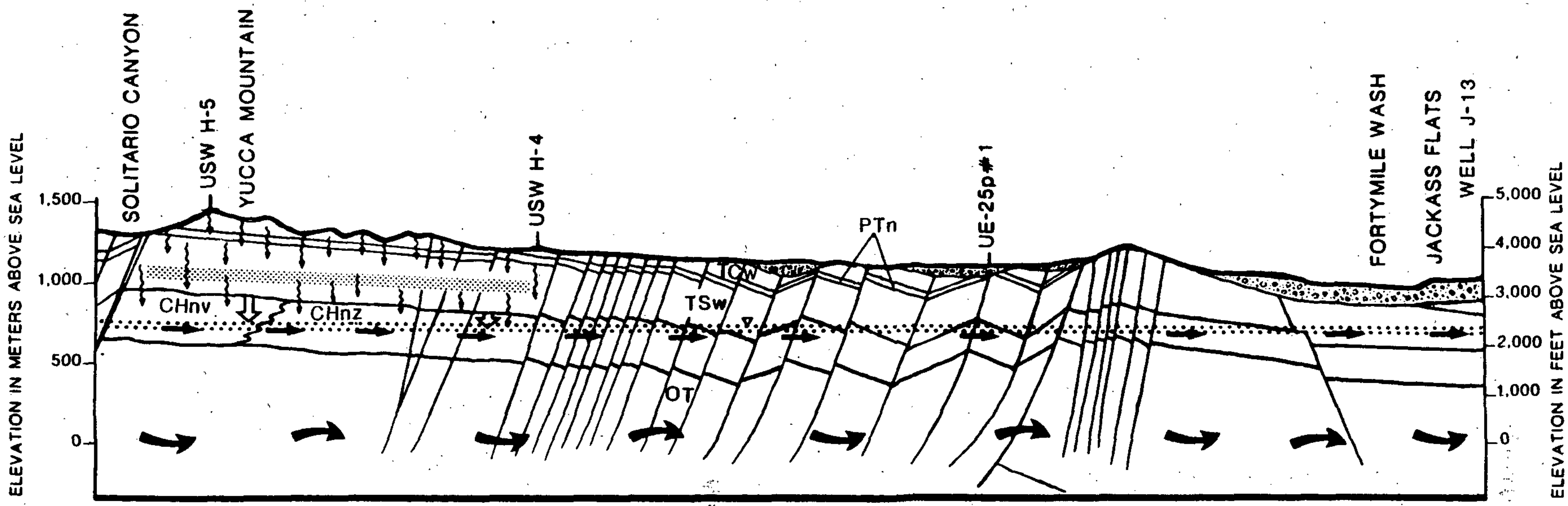

ALLUVIUM & TIMBER MOUNTAIN TUFF

DESIGN REPOSITORY (THICKNESS EXAGGERATED)

WATER TABLE

FLUX THROUGH THE UNSATURATED ZONE

UNSATURATED-ZONE FLOW PATHS USED FOR TRAVEL TIME CALCULATIONS

SATURATED-ZONE FLOW PATH FOR WATER THAT HAS PASSED THROUGH THE REPOSITORY LEVEL

DEEP SATURATED-ZONE FLOW PATHS FOR WATER THAT HAS NOT PASSED THROUGH THE REPOSITORY LEVEL

TCw	TIVA CANYON WELDED UNIT
PTn	PAINTBRUSH NONWELDED UNIT
TSw	TOPOPAH SPRING WELDED UNIT
CHnv	CALICO HILLS NONWELDED VITRIC UNIT
CHnz	CALICO HILL NONWELDED ZEOLITIC UNIT
OT	OLDER TUFF UNIT

0 0.5 1 MILES

0 0.5 1 KILOMETERS

Figure 3-46. Conceptual hydrogeologic section from Solitario Canyon northwest of the site, to well J-13 in Jackass Flats. Modified from Scott and Bonk (1984).

hydraulic gradient and the properties of the fractured medium. It is expected that flow to the accessible environment will be generally down gradient, with some directional variability induced by the anisotropy of the fractured rock matrix. The travel time estimates made below are based on this model, because it appears to be the most reasonable based on present understanding of the flow system and the present limited data base. As more

[illegible]

Table 3-30. Parameters used in travel-time calculations for the unsaturated zone[a] (page 1 of 2)

Parameter	Hydrogeologic unit[b] TSw	CHnv	CHnz	PPw	PPn	BFw	BFn[c]	Remarks
Vertical hydraulic gradient, i	1.0	1.0	1.0	1.0	1.0	1.0	1.0	i = grad (Ψ + z), where Ψ is the pressure head and z the elevation head. If |grad Ψ| << 1, $i_x \approx i_y \approx 0$ and $i_z \approx 1$. This implies vertical gravity flow.
Geometric mean saturated-matrix hydraulic conductivity	0.72	107	0.54	88	22	118	22	$\overline{K}_s = \exp(\text{mean} [\ln (K_s)])$

Table 3-30. Parameters used in travel-time calculations for the unsaturated zone[a] (page 2 of 2)

Parameter	Hydrogeologic unit[b] TSw	CHnv	CHnz	PPw	PPn	BFw	BFn[c]	Remarks
Range of thicknesses (continued)								within the design repository boundaries.
(m)[f]	(98.5)	(95.3)	(94.5)	(83.2)	(63.1)	(25.6)	(7.5)	Values in parentheses are percentages of total repository area underlain by the units.
Empirical constant ε	5.9	4.2	7.0	4.0	5.2	4.6	5.2	Empirical constant that represents the effects of the relationship between pore-size distribution and saturation on the amount of the effective porosity, n_e, available for flow; the effect of the empirical constant is to reduce flow area and thus increase particle velocity relative to values calculated using q/n_e.

[a]Source: Sinnock et al. (1986).

[b]TSw = Topopah Spring welded unit; CHnv = Calico Hills vitric unit; CHnz = Calico Hills zeolitic unit; PPw = Prow Pass welded unit; PPn = Prow Pass nonwelded unit; BFw = Bullfrog welded unit; BFn = Bullfrog nonwelded unit.

[c]Assumed to be hydrologically identical to PPn.

[d]Saturated conductivity and effective-porosity data are from Sandia National Laboratories Tuff Data Base (SNL, 1985).

[e]NA = not available.

[f]Range of thickness, Sandia National Laboratories Interactive Graphics Information System (IGIS) (SNL, 1985).

Table 3-31. Summary of unsaturated zone travel time for vertical flux of 0.5 mm/yr[a]

Travel path[b]	Travel time (yr)
Minimum	9,345
Mean	43,265
Maximum	80,095

[a]Source: Sinnock et al. (1986).
[b]Travel paths are from the repository horizon to the water table and are based on multiple modeling scenarios as discussed in Sinnock et al. (1986).

time through the unsaturated zone of more than 9,000 yr greatly exceeds the 1,000 yr required to satisfy the issue.

In an attempt to assess the sensitivity of the travel time to variations in flux, Sinnock et al. (1986) used an initial flux of 1 mm/yr, double the bounding value estimated by Wilson (1985). This analysis resulted in a minimum travel time of about 3,700 yr, still greater than the amount of time required to satisfy the issue.

The analysis presented here and discussed in detail in Sinnock et al. (1986) and DOE (1986) is considered preliminary. However, the modeling effort has attempted to use the best available data, and it is believed that the results obtained are realistic. Plans to develop this model further and to extend the data base are presented in Section 8.3.1.2.2.

3.9.4.2 Ground-water travel time in the saturated zone

For the saturated zone, the assumed flow path extends from the eastern edge of the primary repository area southeastward for 5 km to the accessible environment (Figures 3-28 and 3-25) through the tuffaceous beds of Calico Hills and the welded Topopah Spring Member or the welded Crater Flat Tuff (Prow Pass or Bullfrog Member). Estimates for ground-water travel times along this travel path have been made using the following assumptions (DOE, 1986):

1. Darcian flow applies.

2. Flow paths are parallel to the hydraulic gradient and are nearly horizontal.

3. The water-level measurements shown in Figure 3-28 (Robison, 1986) provide a reasonable estimate for the hydraulic gradient along the flow path.

4. The system is isotropic within each unit, and hydraulic conductivity values obtained from hydraulic tests of wells in the southeastern part of the Yucca Mountain area are representative of the values along the flow path.

5. Calculated effective porosities from Sinnock et al. (1984) are of a magnitude that will tend to result in minimum travel times calculated for flow in the saturated tuffaceous beds of Calico Hills.

The hydraulic gradient has been estimated using water-level altitudes of 730.4 m at drillhole UE-25b#1 and 728.3 m at well J-13 (Figure 3-28). An examination of the data for well UE-25p#1 (Craig and Robison, 1984) suggests that the water table is located approximately at the interface between the Calico Hills and the Topopah Spring units at this point (approximately 3,000 m from both the edge of the repository and well J-13). Using the principle of conservation of mass, hydraulic gradients have been estimated for each of the units as shown in Table 3-32. Uncertainties in these estimates include the following components: (1) with very low gradients, small errors in the measurements of water levels can have significant effects on the value of the gradient; (2) the measured water level at well J-13 could be expected to be lower than the static water level because of pumping, thereby resulting in a steeper estimated gradient; and (3) vertical components of flow may be present. Because vertical flow would have the effect of lengthening the flow path, the assumption of horizontal flow probably is conservative, although Waddell et al. (1984) indicate the controls on vertical and horizontal flow at Yucca Mountain are variable and generally unknown.

Table 3-32 shows these values and provides estimates for travel times through the Calico Hills and the Topopah Spring units. On the basis of these estimates, the cumulative travel time through the saturated zone is about 170 yr. This value is different from that presented in DOE (1986), due to the use of well UE-25b#1 instead of USW H-4; the former was chosen in this analysis as being more representative of regional trends in the hydraulic gradient (Figure 3-28).

This estimate of travel time is considered to be conservative, based on the assumptions mentioned above and on the fracture effective porosities reported by Sinnock et al. (1984). These effective porosities were calculated by multiplying the fracture density from Scott et al. (1983) by the effective aperture calculated from a relationship provided by Freeze and Cherry (1979). The resulting effective porosities are considered to be reasonable estimates for fracture flow in the saturated zone. However,

Table 3-32. Estimates for ground-water travel times through the saturated zone

Parameter	Unit: Tuffaceous beds of Calico Hills	Unit: Topopah Spring Member
Length of path (m)	3,000	2,000
Hydraulic conductivity (m/yr)[a]	69	365
Hydraulic gradient[b]	5.9×10^{-4}	1.1×10^{-4}
Darcy velocity (m/yr)[c]	4.1×10^{-2}	4.0×10^{-2}
Calculated bulk effective fracture porosity[d]	4×10^{-4}	2.8×10^{-3}
Particle velocity (m/yr)[e]	100	14
Travel time (yr)[f]	30	140

[a]Hydraulic conductivity for Calico Hills from Lahoud et al. (1984) and Thordarson (1983); Topopah Spring from Thordarson (1983).

[b]Based on water levels at drillhole UE-25b#1 and at well J-13 (Figure 3-28). The estimates for the hydraulic gradient for each of the units has been based on conservation of mass between drillhole UE-25b#1 and well J-13.

[c]Darcy velocity = (hydraulic conductivity) x (hydraulic gradient).

[d]Data from Sinnock et al. (1984).

[e]Particle velocity = (Darcy velocity)/(bulk effective porosity).

[f]Travel time = (length of path)/(particle velocity).

3.9.4.3 Retardation and thermal effects

The ground-water travel times estimated for the saturated and unsaturated zones at Yucca Mountain are presently based on Darcy's law and Richard's equation. In fact, ground-water flow through fractured unsaturated media tends to be dominated by the matrix hydraulic conductivity. Water moving through a fractured system may travel into and out of the matrix from the fractures as it moves down gradient (DOE, 1986). This is due to the differences in matric, osmotic, thermal, and pressure potentials across the fracture-matrix interface. This leads to a lengthening of the ground-water travel path for individual ground-water molecules, thereby increasing ground-water travel times.

Other factors may affect ground-water travel time, including dispersion, the existence of faults or impermeable zones along the travel path, the vertical movement of water in the saturated zone, and the upward movement of moisture in the unsaturated zone. At this time it is uncertain whether some

Section 3.9.1.3 for the site. As discussed in Section 3.9.1.3, only limited data exist in the immediate vicinity of Yucca Mountain, and those data tend to be mainly radiocarbon data. This section elaborates on the difficulties in interpreting ground-water velocities from radiocarbon data which have not been adequately modeled for initial carbon-14 activity. Plans for obtaining additional hydrochemical data are presented in Sections 8.3.1.2.2 for the unsaturated zone and 8.3.1.2.3 for the saturated zone.

The reported radiocarbon dates of ground water at Yucca Mountain have been uncorrected and represent apparent ages (Section 3.7.3.2.1) (Benson and McKinley, 1985; Claassen, 1986). Given a series of assumptions examined in more detail below, such ages may represent the time since ground water was isolated from the CO_2 gas reservoir of the atmosphere or the unsaturated zone (i.e., the time since the water entered the water table beneath Yucca Mountain). Uncorrected ages are realistic when no carbon-12 dilution has occurred to the initial carbon-14 by the dissolution of carbon-14-free carbonate minerals. Claassen (1985) indicates that this is the case in the tuffaceous aquifer, since these formations are virtually carbonate-free. If such dilution occurs, the apparent radiocarbon ages may be an upper limit of the ground-water age (Section 3.7.3.2.2).

The other major assumption underlying the apparent ages relates to the initial carbon-14 composition of the infiltrating water. Uncorrected ages assume that this water was in isotopic equilibrium with a gaseous reservoir at 100 percent modern carbon (pmc). This is generally valid, since both the atmosphere (before nuclear weapons testing) and soil gas (gas in the unsaturated zone in a well mixed or low CO_2 gas-residence-time system) have this composition. In a poorly mixed system with long CO_2 gas residence times where the carbon-14 in the CO_2 gas has decayed, the radiocarbon reservoir is at less than 100 pmc. In such a case, the apparent age of the ground water is greater than the time it has been in the aquifer (by an amount proportional to the difference between 100 pmc and the carbon-14 concentration in the equilibrating CO_2 gas).

Yang et al. (1985) have shown that the carbon-14 concentration of the CO_2 gas in the soil zone can be as low as 34.2 (±1.5) pmc in the unsaturated zone at 368 m below the surface. The apparent age of a ground-water sample equilibrated with such gas is really equal to the age of the gas in the unsaturated zone (without isotopic mixing) plus the residence time of the ground water in the aquifer since equilibration (without isotopic dilution). The apparent age is thus older than the true ground water residence time. Since isotopic reequilibration with CO_2 gas can occur throughout the unsaturated zone, apparent ages of the unsaturated zone water (time since precipitation) are not reliable.

Well documented and tested models of initial ground-water carbon-14 activity exist. Some of these models (Mook, 1976, 1980; Fountes and Garnier, 1979) are particularly well suited for modeling waters which equilibrate with CO_2 gas in the unsaturated zone and then enter the water table. Such models can be used to examine the apparent difficulties in interpreting carbon-14 data from Yucca Mountain (Section 8.3.1.2 for plans for their use). Such models, which are said to give corrected ages, do not actually perform corrections of an error, but rather, they simply do not ignore the hydrochemical processes which control carbon-14 behavior.

Kerrisk (1987) has pointed out that at Yucca Mountain, gaseous CO_2 from the unsaturated zone may be added to or exchange with the carbonate of the saturated zone water. This process could lead to apparent ages that are younger than the true ages of the water in the saturated zone.

An accurate knowledge of initial carbon-14 activity is less important in calculating relative ground-water ages or velocities than it is in determining absolute chronologies. Ground-water velocities can be estimated by dividing the distance between two points along a hydrologic flow line by the carbon-14 age difference of the water at the two points. Consistent errors in estimating initial activity tend to cancel, resulting in relative ages which are more accurate than are the individual absolute ages. This is not the case when calculating the velocity of water to a point where the carbon-14 age is known from the assumed point of present day recharge (absolute age zero). Mixing (i.e., the two points are not actually on the same hydrodynamic flow line or the line has moved during the transit of the parcel of water) is also not considered in this calculation. These two difficulties apply to the results of Claassen (1985) who states, "For example, assume recharge near the head of Fortymile Canyon occurred 17,000 years ago and flowed to the lower end of the Canyon, where it is sampled. The velocity that is calculated, 7 m/yr, must be a maximum. Because recharge may occur anywhere but not necessarily everywhere along surface drainageways, no probable minimum velocity can be calculated. The absence of water older than about (apparent age) 10,000 yr. B.P. even near the head of Fortymile Canyon, would favor velocities slower than 4 m/yr." The planned use of initial carbon-14 modeling and relative dating along flow paths to resolve apparent difficulties of interpretation is described in Section 8.3.1.2.3.

3.9.6 MONITORING AND VERIFICATION

This section discusses the monitoring and verification program designed to assess hydrologic conditions at and near Yucca Mountain. The program will also provide an historical background to permit detection of changes in baseline conditions during repository construction, operation, and following closure.

Data from the existing monitoring program are included in Section 3.9.1. The current program consists of 25 boreholes which penetrate the saturated zone and a single instrumented hole in the unsaturated zone. Details of the construction, instrumentation, and monitoring of these holes is discussed in Section 3.9.1.

The primary functions of the program are to provide a data base against which future observations may be compared, to provide information for verification of ground-water models, to evaluate parameters for use in travel-time calculations, and to collect data for the construction of a potentiometric-surface map and determination of ground-water flow directions. The current program provides this information and will be continued. However, additional data are required to provide the level of detail necessary for a thorough understanding of the hydrologic system at Yucca Mountain. Additional data on ground-water geochemistry, water potential temperature variations, etc., will be collected to fulfill the data requirements of the various conceptual models proposed for the site (Sections 8.3.1.2.2 and 8.3.1.2.3).

In order to provide an expanded data base, additional test holes will be added to the monitoring network during site characterization. The new holes will be used for various types of data acquisition, including determination of the hydraulic nature of structural features, measurement of the hydraulic gradient, estimation of ground-water flowpaths, and calculation of various hydraulic parameters in both the saturated and unsaturated zones. Detailed plans for these holes are included in Section 8.3.1.2 along with specific plans for monitoring and use of the resultant data.

3.9.7 LOCAL GROUND-WATER USERS

This section identifies all production wells that are located near the Yucca Mountain site. It is possible that withdrawals from these wells could affect the local flow system. Available pumping information that will aid in identifying these effects is presented. These data, in conjunction with results from planned modeling and field studies will be used to quantify and qualify any potential changes to the local flow system. Plans for further studies are presented in Section 8.3.1.2.

There are two wells located proximally to the Yucca Mountain site that withdraw water on a regular basis. Wells J-12 and J-13, located approximately 12 km and 8 km southeast of the Yucca Mountain site, respectively, are utilized and controlled by the DOE to support activities in the southwestern part of the Nevada Test Site (refer to Section 3.8.1 for a discussion of regional ground-water users).

Water from wells J-12 and J-13 is produced from the Topopah Spring Member of the Paintbrush Tuff, which constitutes the lower portion of the welded tuff aquifer (Section 3.6.1). The Topopah Spring Member occurs at a depth of approximately 180 to 347.2 m at well J-12 and 207.3 to 449.6 m at well J-13 (Thordarson et al., 1967; Claassen, 1973). Pumping-test and water-level data for both wells are shown in Table 3-33. Well-construction information can be found in Thordarson et al. (1967), Young (1972), Claassen (1973), and Thordarson (1983). Table 3-34 summarizes water production for wells J-12 and J-13 from 1983 through 1985. Water-quality data are presented in Section 4.1.2.2 of Chapter 4.

Wells J-12 and J-13 have been pumped intermittently since their completion. Before 1968, well J-12 was pumped at rates in excess of 2,000 m^3/day. After the wellbore was cleaned and deepened in 1968, production capabilities exceeded 4,500 m^3/day. Well J-13 has been shown to be capable of producing in excess of 3,500 m^3/day of water (Claassen, 1973). The specific capacity of the well underwent a slight decline in 1964 shortly after completion. Claassen (1973) hypothesized that the well was not fully developed during the 1964 tests. Subsequent pumping tests performed in 1969 support this hypothesis, and the specific capacity of 540 m^3/day/m is considered the most reliable measurement.

Table 3-33. Pumping test and water-level data for wells J-12 and J-13 from 1960 through 1969[a]

Date of pumping test	Water level (m) Datum: MSL[b]	Specific capacity ((m³/d)/m)	Pumping rate (m³/d)	Draw-down (m)	Duration of test (h)
		WELL J-12			
01/27/60	727.6	--[c]	--	--	--
11/01/60	--	1,700	2,080	1.2	2
08/22/62	726.7	1,000	2,110	2.10	1
07/27/65	--	2,800	2,020	0.73	83
07/25/68	727.0	220	4,250	19.54	1
08/24/68[d]	727.3	850	4,880	5.78	5
04/21/69	727.3	1,600	4,850	3.02	4
		WELL J-13			
02/18/64	728.5	420	3,800	9.11	3
02/18/64	727.9	310	2,800	12.31	96
03/31/64	729.4	--	--	--	--
04/21/69	728.2	540	3,640	6.77	4

[a]Modified from Claassen (1973).
[b]MSL = mean sea level.
[c]-- indicates no data.
[d]Well bore cleaned and deepened to 347.2 m. Test data indicated downhole sloughing, resulting in decreased hydraulic conductivity. Original total depth: 270.4 m.

Table 3-34. Water production from wells J-12 and J-13 from 1983 through 1985[a,b]

Well	1983 Gallons	1983 Acre-feet[c]	1984 Gallons	1984 Acre-feet	1985 Gallons	1985 Acre-feet
J-12	25,498,500	78.2	26,058,400	80.0	25,049,800	76.9
J-13	42,148,700	129.3	40,349,300	123.8	37,811,000	116.0
Total	67,647,200	207.5	66,407,700	203.8	62,860,800	192.9

[a]Production figures are for water year, October 1 through September 30.
[b]Source: Witherill (1986).
[c]To convert from acre-feet to cubic meters, multiply by 1233.489.

Pumping tests performed after 1968 on well J-13 produced drawdowns of less than 7 m with pumping rates in excess of 3,500 m^3/day (Table 3-33). Figure 3-47 indicates that even with well J-13 in continuous service, declines in the water level have been minimal. This suggests that the short-[illegible]

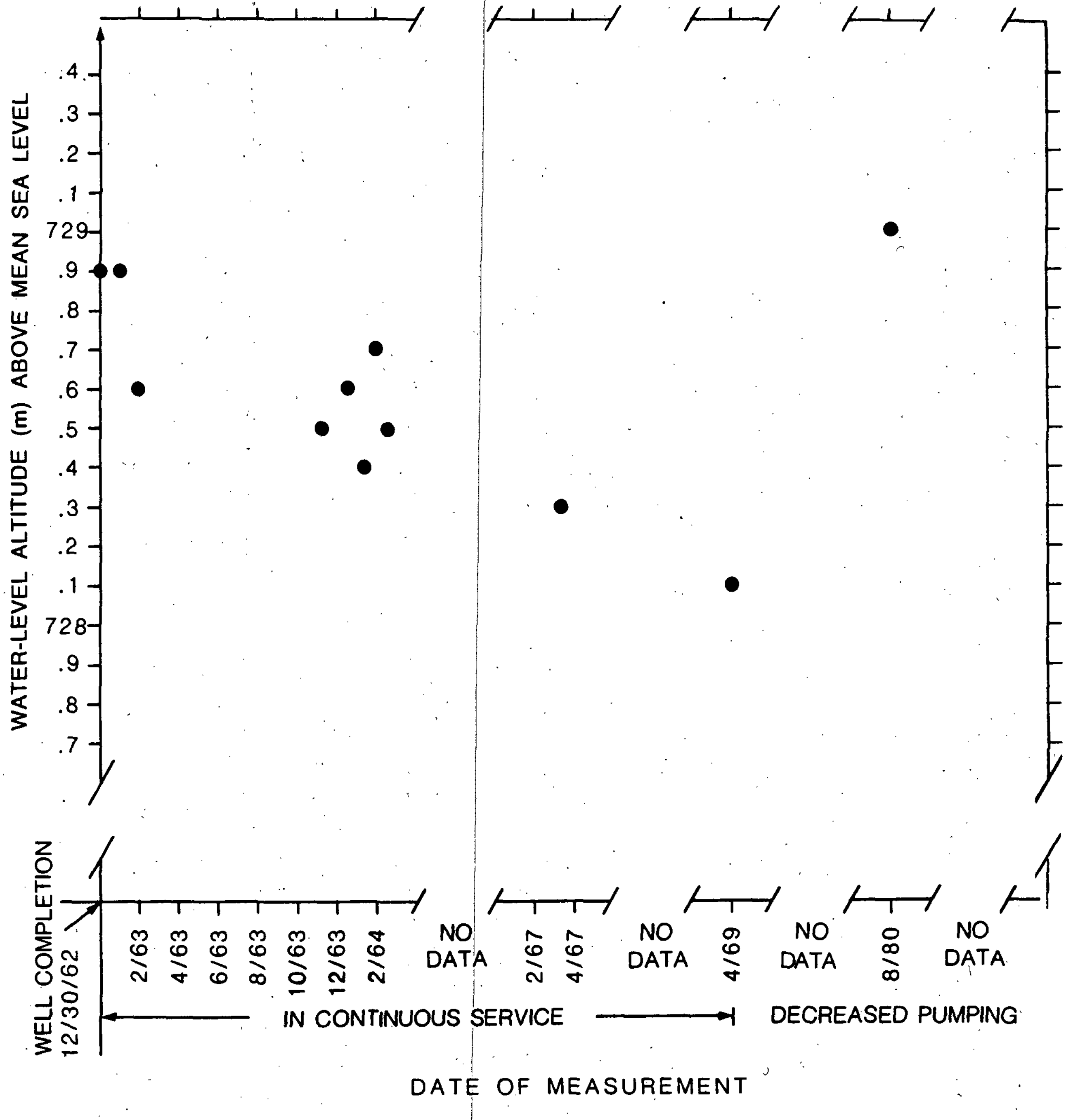

Figure 3-47. Water levels in well J-13 since completion Modified from Thordarson (1983)

Mountain is the alteration of vitric tuff of Calico Hills and lower Topopah Spring Member." The observations by Bish and Vaniman (1985) suggest that past water levels beneath Yucca Mountain may never have been more than 100 m higher than the modern water levels.

To help assess the implication in Bish and Vaniman (1985) that the lowest position of vitric nonwelded tuff might be related to a stand of a paleowater table, a contour map of the base of the lower vitric nonwelded tuff (in both the Topopah Spring Member and in the tuffaceous beds of the Calico Hills) will be prepared and contrasted with the modern water table. If such a contour map indicates (1) a relatively smooth surface at the base of the vitric nonwelded tuff, (2) a surface that locally cross-cuts stratigraphic horizons in the tuffs, and (3) a surface that climbs sharply to the north as does the modern water table beneath Yucca Mountain, then it is possible that the porous nonwelded vitric tuffs have indeed been altered below a paleowater table, as suggested by Bish and Vaniman (1985). Such a contour map would then presumably mark the stand of water table at the time or times of alteration of the tuffs. The occurrence of such a stand probably could not be dated, but might have occurred several million years ago. Even in the absence of a date for the alteration, the base of the nonwelded vitric tuff shown on Bish and Vaniman's cross sections (1985) is tens of meters to more than 100 m below the base of the proposed repository horizon. Thus, if the previously discussed work demonstrates the likelihood of a relationship of the paleowater table to the lowest occurrence of vitric tuff, a possible maximum (though undated) water-table stand would have been identified that is significantly lower than the repository horizon under consideration. Section 8.3.1.3 discusses the investigations planned to characterize the mineralogy of Yucca Mountain.

Czarnecki (1985) addressed the issue of possible past, and by implication, future pluvial-related water-table rises beneath Yucca Mountain with a two-dimensional finite element ground-water flow model of the region, together with assumptions about pluvial recharge on, and underflow into and from the region. He calculated a maximum increase in water-table altitude of about 130 m beneath the site of the proposed repository. Inundation of any part of the planned repository would require a water-table rise of more than 200 m. His analysis also suggests a past shortening by two-thirds of ground-water flow paths from Yucca Mountain to discharge areas in the southern Amargosa Desert. These discharge areas are still beyond the boundary of the accessible environment.

The analysis by Czarnecki (1985) may be considered conservative for

Other considerations were noted by Czarnecki (1985) that might have resulted in a greater simulated water-table rise. Recharge into Fortymile Wash was limited to the main stream channel near Yucca Mountain. If recharge had been included along the full length of Fortymile Wash and its distributaries, which extend beyond the town of Amargosa Valley, then a greater water-table rise would have been simulated. Simulated development of discharge areas southeast of the town of Amargosa Valley helped to limit the water-table rise beneath the primary repository area. If this discharge were decreased because of the possible existence of marsh deposits or eolian silts or because of a greatly decreased ratio of vertical hydraulic conductivity to horizontal hydraulic conductivity, then the simulated water-table rise might be greater. The model used by Czarnecki (1985) derived its parameters from a model presented in Czarnecki and Waddell (1984), which assumed that the ground-water system was in steady-state conditions. If the ground-water system was still equilibrating to recharge that may have occurred 10,000 to 20,000 yr before present, then the values of transmissivity used in the model in Czarnecki (1985) might be too high. Large transmissivities used in recharge simulations would produce less water-table rise than if smaller transmissivities were used.

Extensive investigations are planned to better quantify the parameters of the hydrologic system in the Yucca Mountain region. These parameters will be used to model the hydrologic system more effectively and any variations induced by climatic or tectonic changes. Plans for these studies are discussed in Sections 8.3.1.2.1 and 8.3.1.2.2.

During pluvial periods of the Pleistocene, perched springs and seeps could have occurred along the flanks of Yucca Mountain and these might have resulted from recharge along the exposed up-dip portion of tuff units, with water moving down-dip to discharge sites along the flank of the mountain. No conclusive evidence for former springs has been observed, but additional investigations are planned, as outlined in Section 8.3.1.5.2.

Deposits along fault zones may provide additional evidence for changed hydrologic conditions. Along portions of the Bow Ridge fault, 1 km east of the eastern boundary of the proposed repository, Trench 14 has exposed deposits of carbonate, opal, and minor amounts of sepiolite (Vaniman et al., 1985; Taylor and Huckins, 1986; Voegele, 1986a,b). These deposits are discussed more extensively in Section 1.2.2.2.10. The origin of these deposits is under study, and the following hypotheses are being considered:

1. The deposits are the result of ground-water discharge along the fault, from the deep regional flow system and reflect former higher water levels, tectonic uplift of the deposits, or a combination of both.

2. The deposits are the result of discharge along the fault zone from a shallow ground-water flow system along the flank of Yucca Mountain.

3. The deposits are shallow soil features that resulted from rain water that moved downslope from the top of a nearby low hill, along the contact between the soil zone and bedrock, and accumulated at the fault zone. The water would have evaporated slowly, leaving precipitates of the minerals that were dissolved in the water.

Present evidence from studies discussed in Section 1.2.2.2.10 supports this hypothesis (Vaniman et al., 1985; Taylor and Huckins, 1986; Voegele, 1986a).

Further investigations designed to determine the nature and origin of these deposits are discussed in Section 8.3.1.5.2.

3.10 SUMMARY

Chapter 3 discusses the data that are available and additional data that exist is restricted to short spring-fed reaches of the Amargosa River, small pools at some large springs, and some large springs and marshes in Alkali Flat and Death Valley. However, arroyos occasionally flood during convective rainstorms. Long-term flood records as a basis for predictions are few, but occasional flash floods and debris flows are anticipated. Erosion and deposition from flash floods and associated debris flows are among the most active geomorphic processes in the region, and they have a major role in the development of alluvial fans, denudation of mountainous landscapes, and the evolution of drainage-channel morphology.

Gages and other instrumentation are planned to be installed and operated in order to correlate streamflow events with precipitation. Streamflow and its characteristics will be studied in order to determine inundation, sediment transport, and erosion in the vicinity of the proposed repository surface facilities (Section 8.3.1.2.1).

Two hydraulic-engineering studies of flood-prone areas near Yucca Mountain provide a basis for estimating magnitudes and recurrence intervals of future floods (Section 3.2). Further studies will determine the magnitudes of probable maximum floods near the surface sites of proposed repository facilities (Section 8.3.1.16.1).

The nature and quantities of present and future infiltration or recharge need to be known better, especially at the site, including Fortymile Wash.

The hydraulic conductivity of rock in the hydrogeologic study area is controlled by fractures, joints, faults, vapor-phase cavities, interstitial spaces, and bedding planes. The aquitards have low fracture hydraulic conductivity and negligible interstitial hydraulic conductivity. Where fractures and faults are present, open, and unsealed with rock material, hydraulic interconnection among the hydrogeologic units is effective in transmitting water if hydraulic gradients of sufficient magnitude are present. Ground water in transit within the system and beneath Yucca Mountain has been estimated to be 10,000 to 20,000 yr old.

An initial conceptual model for ground-water flow in the saturated zone in the vicinity of Yucca Mountain has been developed and is based on the following assumptions: (1) the rock containing the primary matrix porosity is homogeneous and isotropic; (2) secondary porosity is controlled mostly by fractures; the volume of water stored in them is relatively small in comparison to that stored in the matrix; (3) hydraulic conductivity of fractures is several orders of magnitude larger than the conductivity of the matrix; (4) distances between fractures are small in comparison with the dimensions of the ground-water basin; and (5) on a large scale, the orientation of fractures may be assumed random so that the system appears isotropic, (i.e., a slightly different form of a porous medium with equivalent porous-media properties). The model is expected to evolve as new data become available and alternative concepts are tested.

Estimated average annual ground-water recharge from precipitation for the hydrogeologic study area is 5.6×10^7 m^3 (Rush, 1970). The largest natural discharge point in the study area is the southeastern Amargosa Desert, where estimated average annual ground-water discharge is 3.0×10^7 m^3 (Walker and Ekin, 1963; Rush, 1970). The remaining discharge is distributed among several smaller discharge areas. At Yucca Mountain the specific fluxes based on a two-dimensional flow model range from 3.6 m^2/yr to 1.1×10^6 m^2/yr.

Major-ion chemistry of ground water in the region has been summarized but enough water chemistry data are not yet available to develop a hydrochemical model to support conceptual-flow models, or to verify suggested ground-water flow paths (Section 3.7.3).

There is evidence for former, higher levels of the water table in the study area during the Plio-Pleistocene probably because increasing aridity associated with uplift of the Sierra Nevada resulted in lower precipitation with the Great Basin, which in turn has lead to a lowering of the water table. Also, flow-path lengths of ground water may have been shorter during the Plio-Pleistocene. However, current data based on climatic trends or evidence for past hydrologic conditions are insufficient to make reliable projections of future hydrologic conditions (Section 3.7.4). Section 8.3.1.5.2 discusses plans to evaluate further the potential effect of future climatic conditions on the hydrologic system at Yucca Mountain.

At the Yucca Mountain site, the water table is about 250 m below the proposed repository horizon. The proposed repository horizon is in turn, about 300 m below land surface. It is not known at this time under what circumstances the water table might be expected to rise sufficiently to saturate an underground facility at the repository horizon. As discussed in

Sections 3.7.4 and 3.9.8, there is no evidence that water levels were more than 100 m higher during the Quaternary Period, but evidence indicates that water levels may have declined during that time. The results of preliminary regional ground-water flow modeling studies indicate that the climatic regime is unlikely to produce water table rises over the next 10,000 yr that could inundate the repository. This unlikely scenario is to be examined further, as described in Section 8.3.1.5.2.

The preliminary information presented in Section 3.8.1 and 3.8.2 suggests that siting a mined geologic disposal system at Yucca Mountain will not adversely affect local ground-water users or the ground-water system. As discussed in Section 3.8.1, the Amargosa Desert, located within the Alkali Flat-Furnace Creek Ranch subbasin, currently is experiencing overdraft problems. Repository-related ground-water withdrawals probably will not

The unsaturated zone at Yucca Mountain consists of a stratified sequence of welded and nonwelded, fractured and unfractured tuffs that comprise a fault-bounded, eastward-tilted block extending from 300 to 750 m above the water table (Section 3.9.3.4). The rock-stratigraphic units have been measuring most matrix hydrologic properties for small rock samples and cores with the possible exceptions of measuring saturated hydraulic conductivity for welded and zeolitized tuff samples. Similar techniques are lacking, however, for single fractures and fracture systems. In fractured media, the scale of measurement must be large compared to the mean fracture aperture and spacing. Hence, the direct empirical determination of the bulk hydrologic properties of the fractured units must rely strongly on hydrologic testing in surface-based boreholes and within the exploratory shaft, as described in Section 8.3.1.2.2. Sufficient data need to be collected to permit statistical analyses of the limits of uncertainty of these data. Uncertainties may be introduced by random errors of measurement, as well as by inherent heterogeneities within the hydrogeologic units. The resulting statistical distributions are needed to provide the requisite input data to stochastic models from which the overall uncertainty of quantitative predictions, such as ground-water travel times, can be assessed.

Ambient hydrologic conditions within the unsaturated zone at Yucca Mountain remain poorly known, although, as described in Chapter 8.3.1.2.2 considerable data on these conditions will be obtained during monitoring in surface-based boreholes and within the exploratory shaft. Preliminary data and inference from test wells USW UZ-1, USW UZ-6, and USW H-1 indicate ambient rock-matrix saturations in the range from 0.4 to 0.65 and ambient matric potentials of about -0.3 MPa in the repository TSw unit. These data are consistent with the estimated value of 0.5 mm/yr or less for the present flux through this unit. It may be concluded from these conditions: (1) that the vertical flux of water within the repository TSw unit probably is low; (2) that the flow is restricted largely to the rock matrix with probably little significant flow within fractures; and (3) that the flux may be nearly constant, occurring under unit vertical hydraulic gradient. These conclusions are only indicative of existing conditions; considerably more data need to be acquired before they can be confirmed or refuted with sufficient certainty. Similar conclusions apply for the PTn and TCw units overlying the repository TSw unit; however, for these units, the paucity of reliable data precludes establishing little more than upper limits on possible fluxes based on estimates of the likely rate of net infiltration.

Because of the presence of the natural geothermal gradient, there is the potential for the upward movement of moisture as water vapor within the unsaturated zone. This potential probably is greatest within the fractured TSw unit in which vapor movement is envisioned to occur principally in the partially saturated fractures. Water-vapor movement may occur either as advection superimposed on an underlying bulk-gas flow or as diffusion along the water-vapor concentration gradient that would be coincident with the geothermal gradient if water vapor is in local thermodynamic phase equilibto the gas-phase hydrologic system, these data are to be collected through gas-phase testing and sampling within surface-based boreholes and the exploratory shaft as described in Chapter 8.3.1.2.2.

Velocity of ground-water flow and resulting travel time in the unsaturated zone strongly depend on effective porosity and hydraulic conductivity of fractures and rock matrix. Based on an upper-bound flux of 0.5 mm/yr, ground-water travel time within the unsaturated zone from the proposed repository to the water table is estimated to range from about 9,000 to 80,000 yr.

The lateral direction of ground-water movement in the saturated zone near the Yucca Mountain site probably is to the southeast. Hydraulic gradient is variable, and southeast of the repository block it is nearly flat. Hydraulic conductivity and effective porosity, two of the parameters that determine ground-water velocities and travel times, are not adequately known yet. Calculations based on conservative values of the controlling parameters indicate that saturated zone ground-water travel time, from the repository block to the accessible environment, may be about 200 yr (Section 3.9.4).

Based on these estimates for travel times, the minimum ground-water travel time from the edge of the repository to the accessible environment under present conditions is approximately 9,200 yr, well in excess of the 1,000 yr limits required by 10 CFR Part 60.113(a)(2).

Sections 3.2.2 and 6.2.4 discuss the potential for flooding at the Yucca Mountain site surface facilities. Preliminary investigations discussed in these sections indicate that the surface facilities are located above the level of the probable maximum flood. Further studies are discussed in Section 8.3.1.16. In addition, flood protection measures are included in the design to prevent surficial sheet flow affecting the surface facilities.

The proposed repository at Yucca Mountain is situated in the unsaturated zone. Therefore, it is unlikely that any significant bodies of water would be encountered in the development of the repository. The possibility of the occurrence of perched-water bodies exists; this will be examined during site characterization, particularly through the development of the exploratory shaft. However, it is considered unlikely that even if perched-water bodies do exist between the surface and the repository horizon at Yucca Mountain, they will present a major concern in repository development.

The waste emplacement package environment is one of the more important aspects considered in the design of waste containers. The potential interaction between the container walls and moisture in the emplacement holes is a consideration in estimating the lifetime of the canisters. This aspect is discussed further in Chapter 7, and additional plans for further analyses are presented in Sections 8.3.4 and 8.3.5.

3.10.3 IDENTIFICATION OF INFORMATION NEEDS

As mentioned in the introduction to Chapter 3, the hydrologic system in the vicinity of Yucca Mountain is one of the more important aspects that affects the postclosure and preclosure performance of the proposed repository. In particular, hydrology directly relates to the nine performance issues and associated information needs of Key Issue 1, namely:

<u>Short titles</u>

<u>Issue 1.1</u>: Total system performance (Section 8.3.5.13)

- 1.1.1 Site information needed for calculations (Section 8.3.5.13.1)
- 1.1.3 Calculational models for release scenario classes (Section 8.3.5.13.3)

<u>Short titles</u>

- 1.1.4 Radionuclide releases for scenario classes (Section 8.3.5.13.4)
- 1.1.5 Probabilistic release estimates (Section 8.3.5.13.5)

<u>Issue 1.2</u>: Individual protection (Section 8.3.5.14)

Issue 1.3: Ground-water protection (Section 8.3.5.15)

1.3.1 Class I or special sources of ground water (Section 8.3.5.15.1)

Issue 1.4: Containment by waste package (Section 8.3.5.9)

1.4.1 Waste package design features needed (Section 8.3.5.9.1)

1.4.3 Scenarios and models needed (Section 8.3.5.9.3)

1.4.4 Containment barrier degradation (Section 8.3.5.9.4)

1.4.5 Time to loss of containment (Section 8.3.5.9.5)

Issue 1.5: Engineered barrier system release rates (Section 8.3.5.10)

1.5.1 Waste package design features (Section 8.3.5.10.1)

1.5.3 Scenarios and models (Section 8.3.5.10.3)

1.5.4 Release rates from waste package and engineered barrier system

Issue 1.10: Waste package characteristics (postclosure) (Section 8.3.4.2)

1.10.4 Near-field environment (Section 8.3.4.2.4)

Issue 1.11: Configuration of underground facilities (postclosure) (Section 8.3.2.2)

1.11.6 Thermal loading and thermomechanical rock response (Section 8.3.2.2.6)

For the postclosure situation, most of the hydrologic information required to satisfy the performance and design issues identified above will be collected by the geohydrology program (Section 8.3.1.2) and its associated investigations:

SCP section	Short title
8.3.1.2.1	Regional hydrology system
8.3.1.2.2	Site unsaturated zone hydrologic system
8.3.1.2.3	Site saturated zone hydrologic system

In addition, Investigation 8.3.1.3.1 will provide information about water chemistry within the potential emplacement horizon and along potential flow paths, and Investigations 8.3.1.5, 8.3.1.6, and 8.3.1.8 will evaluate the potential effects of future climatic conditions, erosion, and igneous and tectonic activity on hydrologic characteristics, respectively.

Investigations 8.3.1.9 and 8.3.1.9.3 provide information on the present and future value of ground-water resources, and the potential effects of exploiting natural resources on the hydrologic characteristics in the vicinity of the Yucca Mountain site.

In the preclosure timeframe, Issues 4.1 and 4.4, along with the hydrology program (8.3.1.16), are associated with hydrologic characteristics, The hydrologic information will be provided by the following sections:

SCP section	Short title
8.3.1.16.1	Flooding recurrence intervals
8.3.1.16.2	Water supplies
8.3.1.16.3	Ground-water conditions

The plans to collect this information and the methods that will be used to evaluate the effects of the hydrologic regime on performance and design are presented in Section 8.3. The details of each study and activity are presented under each investigation, together with listings of parameters to be collected or that are required, and associated technical procedures and

DOE/RW-0199

Nuclear Waste Policy Act
(Section 113)

Site Characterization Plan

Yucca Mountain Site, Nevada Research and Development Area, Nevada

Volume II, Part A

Chapter 3 References

December 1988

U. S. Department of Energy
Office of Civilian Radioactive Waste Management

REFERENCES FOR CHAPTER 3

ANSI/ANS (American National Standard Institute/American Nuclear Society), 1981. "American National Standard for Determining Design Basis Flooding at Power Reactor Sites," ANSI/ANS-2.8-1981, American Nuclear Society, La

Blankennagel, R. K., and J. E. Weir, Jr., 1973. Geohydrology of the Eastern Part of Pahute Mesa, Nevada Test Site, Nye County, Nevada, U.S. Geological Survey Professional Paper 712-B, U.S. Goverment Printing Office, Washington, D.C.

Bradley, R. S., 1985. Quaternary Paleoclimatology, Methods of Paleoclimatic Reconstruction, Allen & Unwin, Boston, Mass., pp. 72-78.

Bredehoeft, J. D., and I. S. Papadopulos, 1965. "Rates of Vertical Groundwater Movement Estimated from the Earth's Thermal Profile," Water Resources Research, Vol. 1, No. 2, pp. 325-328.

Brobst, R. B., and P. M. Buszka, 1986. "The Effect of Three Drilling Fluids on Ground Water Sample Chemistry," Ground Water Monitoring Review, Vol. 6, No. 1, pp. 62-70.

Brooks, R. H., and A. T. Corey, 1964. Hydraulic Properties of Porous Media, Hydrology Paper No. 3, Colorado State University, Fort Collins, Colo.

Bullard, K. L., 1986. PMF (Probable Maximum Flood) Study for Nevada Nuclear Waste Storage Investigations Project, GR-87-8, U.S. Department of the Interior, Bureau of Reclamation, Washington, D.C.

Carr, W. J., 1974. Summary of Tectonic and Structural Evidence for Stress Orientation at the Nevada Test Site, USGS-OFR-74-176, Open-File Report, U.S. Geological Survey.

Case, C. M., M. Kautsky, P. M. Kearl, D. M. Nork, T. F. Panian, and S. L. Raker, 1984. "Unsaturated Flow Through the Alluvium at the Nevada Test Site," Geological Society of America Abstracts with Programs, Vol. 16, No. 6, p. 465.

Christensen, R. C., and N. E. Spahr, 1980. Flood Potential of Topopah Wash and Tributaries, Eastern Part of Jackass Flats, Nevada Test Site, Southern Nevada, USGS-OFR-80-963, Open File Report, U.S. Geological Survey, 22 p.

Claassen, H. C., 1973. Water Quality and Physical Characteristics of Nevada Test Site Water-Supply Wells, USGS-474-158, U.S. Geological Survey.

Claassen, H. C., 1985. Sources and Mechanisms of Recharge for Ground Water in the West-Central Amargosa Desert, Nevada--A Geochemical Interpretation, U.S. Geological Survey Professional Paper 712-F, U.S. Government Printing Office, Washington, D.C.

Claassen, H. C., 1986. "Late-Wisconsin Paleohydrology of the West-Central Amargosa Desert, Nevada, U.S.A.," Chemical Geology (Isotope Geoscience Section), Vol. 58, pp. 311-323.

Claassen, H. C., and A. F. White, 1979. "Application of Geochemical Kinetic Data to Ground-water Systems, A Tuffaceous-Rock System in Southern Nevada," Symposium on Chemical Modeling in Aqueous Systems, Speciation, Sorption, Solubility, and Kinetics, E. A. Jenne (ed.), Symposium Series Book 93, American Chemical Society, Washington, D.C., pp. 771-793.

Coache, R., 1986. "Amargosa Valley Basin 230-1985 Groundwater Pumpage Inventory," tabular material on water use, State of Nevada, Department of Conservation and Natural Resources, Water Resources Division, Las Vegas, Nev.

Collins, E., and T. P. O'Farrell, 1985. 1984 Biotic Studies of Yucca

Denny, C. S., and H. Drewes, 1965. Geology of the Ash Meadows Quadrangle, Nevada-California, Geological Survey Bulletin 1181-L, U.S. Government Printing Office, Washington, D.C.

Dettinger, M. D., and J. L. Wilson, 1981. "First Order Analysis of Uncertainty in Numerical Models of Groundwater Flow, Part 1, Mathematical Development," Water Resources Research, Vol. 17, No. 1, pp. 149-161.

Dorn, R. I., 1983. "Cation-Ratio Dating: A New Rock Varnish Age-Determination Technique," Quaternary Research, Vol. 20, pp. 49-73.

Doty, G. C., and W. Thordarson, 1983. Water Table in Rocks of Cenozoic and Paleozoic Age, 1980, Yucca Flat, Nevada Test Site, Nevada, USGS-WRI-83-4067, Water Resources Investigations Report, U.S. Geological Survey.

Dudley, W. W., Jr., and J. D. Larson, 1976. Effect of Irrigation Pumping on Desert Pupfish Habitats in Ash Meadows, Nye County, Nevada, U.S. Geological Survey Professional Paper 927, U.S. Goverment Printing Office, Washington, D.C.

Eakin, T. E., G. B. Maxey, T. W. Robinson, J. C. Fredericks, and O. J. Loeltz, 1951. Contributions to the Hydrology of Eastern Nevada, Water Resources Bulletin No. 12, Office of the State Engineer, State of Nevada, Carson City. 171 p.

Eakin, T. E., S. L. Schoff, and P. Cohen, 1963. Regional Hydrology of a Part of Southern Nevada: A Reconnaissance, USGS-TEI-833, Trace-Elements Investigations Report, U.S. Geological Survey.

Erickson, J. R., and R. K. Waddell, 1985. Identification and Characterization of Hydrologic Properties of Fractured Tuff using Hydraulic and Tracer Tests--Test Well USW H-4, Yucca Mountain, Nye County, Nevada, USGS-WRI-85-4066, Water-Resources Investigations Report, U.S. Geological Survey.

Faust, C. R., and J. W. Mercer, 1977. Theoretical Analysis of Fluid Flow and Energy Transport in Hydrothermal Systems, USGS-OFR-77-60, Open-File Report, U.S. Geological Survey.

Fetter, C. W., Jr., 1980. Applied Hydrogeology, Charles E. Merrill Publishing Co., Columbus, Ohio., p. 381.

Fontes, J-C., and J-M. Garnier, 1979. "Determination of the Initial 14-C Activity of the Total Dissolved Carbon: A Review of the Existing Models and a New Approach," Water Resources Research, Vol. 15, No. 2, pp. 399-413.

Freeze, R. A., and J. A. Cherry, 1979. Groundwater, Prentice-Hall, Inc., Englewood Cliffs, New Jersey, pp. 389-390, 551-552

French, R. H., A. Elzeftawy, J. Bird, and B. Elliot, 1984. Hydrology and Water Resources Overview for the Nevada Nuclear Waste Storage Investigations, Nevada Test Site, Nye County, Nevada, NVO-284, Desert Research Institute, Las Vegas, Nev.

Garside, L. J., and J. H. Schilling, 1979. Thermal Waters of Nevada, Nevada Bureau of Mines & Geology Bulletin 91, University of Nevada, Reno.

Giampaoli, M. C., 1986. Trip Report: Hydrologic Field Reconnaissance Led by Robert Coache, Water Resources Division, Nevada Department of Conservation

Heath, R. C., 1984. Ground-Water Regions of the United States, Geological Survey Water Supply Paper 2242, U.S. Geological Survey.

Hillel, D., 1980. Fundamentals of Soil Physics, Academic Press, Inc., New York, 413 p.

Hooke, R. L., 1972. "Geomorphic Evidence for Late-Wisconsin and Holocene Tectonic Deformation, Death Valley, California," Geological Society of America Bulletin, Vol. 83, No. 7, pp. 2073-2098.

Hoover, D. L., 1968. "Genesis of Zeolites, Nevada Test Site," Nevada Test Site, E. B. Eckel (ed.), Geological Society of America Memoir 110, pp. 275-284.

Hoover, D. L., W C Swadley, and A. J. Gordon, 1981. Correlation Characteristics of Surficial Deposits with a Description of Surficial Stratigraphy in the Nevada Test Site Region, USGS-OFR-81-512, Open-File Report, U.S. Geological Survey.

Huber, N. K., 1981. Amount and Timing of Late Cenozoic Uplift and Tilt of the Central Sierra Nevada, California--Evidence from the Upper San Joaquin River Basin, U.S. Geological Survey Professional Paper 1197, U.S. Goverment Printing Office, Washington, D.C.

Hughes, G. H., and C. C. McDonald, 1966. "Determination of Water Use by Phreatophytes and Hydrophytes," in Journal of the Hydraulics Division, Proceedings of the American Society of Civil Engineers, Vol. 92, No. HY2, pp. 63-81.

Hull, A. C., Jr., and G. J. Klomp, 1974. Yield of Crested Wheatgrass Under Four Densities of Big Sagebrush in Southern Idaho, Technical Bulletin No. 1483, U.S. Department of Agriculture, Washington, D.C.

Hunt, C. B., and D. R. Mabey, 1966. Stratigraphy and Structure, Death Valley, California, General Geology of Death Valley, California, U.S. Geological Survey Professional Paper 494-A, U.S. Goverment Printing Office, Washington, D.C.

Hunt, C. B., T. W. Robinson, W. A. Bowles, and A. L. Washburn, 1966. Hydrologic Basin, Death Valley, California, U.S. Geological Survey Professional Paper 494-B, U.S. Goverment Printing Office, Washington, D.C.

IAEA (International Atomic Energy Agency), 1983. "Radiocarbon (14-C)," Isotope Techniques in the Hydrogeological Assessment of Potential Sites for the Disposal of High-Level Radioactive Wastes, Technical Reports Series No. 228, Vienna, Austria, pp. 70-87.

Katzer, T. L., P. A. Glancy, and L. Harmsen, 1976. A Brief Hydrologic Appraisal of the July 3-4, 1975, Flash Flood in Las Vegas Valley, Nevada, Clark County Flood Control Division, Department of Public Works, Las Vegas, Nev.

Kerrisk, J. F., 1987. Groundwater Chemistry at Yucca Mountain, Nevada, and Vicinity, LA-10929-MS, Los Alamos National Laboratory, Los Alamos, N. Mex.

Khoury, H. N., D. D. Eberl, and B. F. Jones, 1982. "Origin of Magnesium Clays from the Amargosa Desert, Nevada," Clays and Clay Minerals, Vol. 30, No. 5, The Clay Minerals Society, pp. 327-336.

Klavetter, E. A., and R. R. Peters, 1986. Fluid Flow in a Fractured Rock Mass, SAND85-0855, Sandia National Laboratories, Albuquerque, N. Mex.

Klinkenberg, L. J., 1941. "The Permeability of Porous Media to Liquids and Gases," Drilling and Production Practice, American Petroleum Institute, pp. 200-213.

Kohler, M. A., T. J. Nordenson, and D. R. Baker, 1959. Evaporation Maps for the United States, U.S. Weather Service, U.S. Department of Commerce, Technical Paper No. 37, U.S. Government Printing Office, Washington, D.C.

Lahoud, R. G., D. H. Lobmeyer, and M. S. Whitfield, Jr., 1984. Geohydrology of Volcanic Tuff Penetrated by Test Well UE-25b#1, Yucca Mountain, Nye County, Nevada, USGS-WRI-84-4253, Water-Resources Investigations Report, U.S. Geological Survey.

Lin, W., 1978. Measuring the Permeability of Eleana Argillite from Area 17, Nevada Test Site, Using the Transient Method, UCRL-52604, Lawrence Livermore National Laboratory, Livermore, Calif.

Loeltz, O. J., 1960. "Source of Water Issuing from Springs in Ash Meadow Valley, Nye County, Nevada," Geological Society of America Bulletin, Vol. 71, No. 12, Part 2, pp. 1917-1918.

Malmberg, G. T., 1967. Hydrology of the Valley-Fill and Carbonate-Rock Reservoirs, Pahrump Valley, Nevada-California, Geological Survey Water-Supply Paper, USGS-WSP-1832, U.S. Government Printing Office, Washington, D.C.

Malmberg, G. T., and T. E. Eakin, 1962. Ground-Water Appraisal of Sarcobatus Flat and Oasis Valley, Nye and Esmeralda Counties, Nevada, Department of Conservation and Natural Resources Ground-Water Resources Reconnaissance Series Report 10, State of Nevada, Carson City.

Maxey, G. B., and T. E. Eakin, 1949. Ground Water in White River Valley, White Pine, Nye, and Lincoln Counties, Nevada, Water Resources Bulletin No. 8, State of Nevada, Office of the State Engineer, Carson City.

Maxey, G. B., and C. H. Jameson, 1948. Geology and Water Resources of Las Vegas, Pahrump, and Indian Spring Valleys, Clark and Nye Counties, Nevada, Office of the State Engineer Water Resources Bulletin No. 5, State of Nevada, Carson City.

Meinzer, O. E., 1923. Outline of Ground-Water Hydrology with Definitions, U.S. Geological Survey Water-Supply Paper 494, Government Printing Office, Washington, D.C., 71 p.

Mifflin, M. D., 1968. Delineation of Ground-Water Flow Systems in Nevada, Technical Report Series H-W Hydrology and Water Resources Publication No. 4, Desert Research Institute, Reno, Nev.

Mifflin, M. D., and M. M. Wheat, 1979. Pluvial Lakes and Estimated Pluvial Climates of Nevada, Nevada Bureau of Mines & Geology Bulletin 94, University of Nevada, Reno.

Miller, G. A., 1977. Appraisal of the Water Resources of Death Valley, California-Nevada, USGS-OFR-77-728, Open-File Report, U.S. Geological Survey.

Moench, A. F., 1984. "Double-Porosity Models for a Fissured Groundwater Reservoir with Fracture Skin," Water Resources Research, Vol. 20, No. 7, pp. 831-846.

Montazer, P., and P. E. Harrold, 1985. "Theoretical Calculation of Hydraulic Properties of Unsaturated Fractures from Roughness Profiles," Transactions of the American Geophysical Union, Abstract H12C-05, Vol. 66, No. 46, p. 883.

Montazer, P., and W. E. Wilson, 1984. Conceptual Hydrologic Model of Flow in the Unsaturated Zone, Yucca Mountain, Nevada, USGS-WRI-84-4345, Water-Resources Investigations Report, U.S. Geological Survey.

Montazer, P., E. P. Weeks, F. Thamir, S. N. Yard, and P. B. Hofrichter, 1986. "Monitoring the Vadose Zone in Fractured Tuff, Yucca Mountain, Nevada," in Proceedings of the NWWA Conference on Characterization and Monitoring of the Vadose (Unsaturated) Zone, November 19-21, 1985, Denver, Colo., National Water Well Association, Worthington, Ohio, pp. 439-469.

Mook, W. G., 1976. "The Dissolution-Exchange Model for Dating Groundwater with 14-C," in Interpretation of Environmental Isotope and Hydrochemical Data in Groundwater Hydrology, Proceedings of an Advisory Group Meeting Organized by the IAEA, Vienna, January 27-31, 1975, International Atomic Energy Agency, Vienna, Austria, pp. 213-225.

Mook, W. G., 1980. Handbook of Environmental Isotope Geochemistry, Vol. 1, P. Fritz and J. C. Fontes (eds.), Chapter 2, Elsevier Scientific Publishing Co., New York, pp. 49-74.

NRC (U.S. Nuclear Regulatory Commission), 1983. Draft Site Characterization Analysis of the Site Characterization Report for the Basalt Waste Isolation Project, NUREG-0960, Vol. 2, Appendices F and I, Washington, D.C., pp. F1-F17, I1-I4.

NRC (U.S. Nuclear Regulatory Commission), 1986a. "Disposal of High-Level Radioactive Wastes in Geologic Repositories; Conforming Amendments," Federal Register, Vol. 51, Washington, D.C., pp. 22288-22300.

NRC (U.S. Nuclear Regulatory Commission), 1986b. Draft Generic Technical Position: Interpretation and Identification of the Extent of the Disturbed Zone in the High-Level Waste Rule (10 CFR 60), M. Gordon, N. Tanious, J. Bradbury, L. Kovack and R. Codell (eds.), Washington, D.C.

NRC (U.S. Nuclear Regulatory Commission), 1987. Standard Format and Content of Site Characterization Plans for High-Level-Waste Geological Repositories, Regulatory Guide 4.17, Washington, D.C.

Naff, R. L., G. B. Maxey, and R. F. Kaufmann, 1974. Interbasin Ground-Water Flow in Southern Nevada, Nevada Bureau of Mines & Geology Report 20, University of Nevada, Reno.

Nichols, W. D., 1986. Geohydrology of the Unsaturated Zone at the Burial Site for Low-Level Radioactive Waste Near Beatty, Nye County, Nevada, USGS-OFR-85-198, Open-File Report, U.S. Geological Survey.

Nichols, W. D., and J. P. Akers, 1985. Water-Level Declines in the Amargosa Valley Area, Nye County, Nevada, 1962-84, USGS-WRI-85-4273, Water Resources Investigations Report, U.S. Geological Survey.

O'Farrell, T. P., and E. Collins, 1983. 1982 Biotic Survey of Yucca Mountain, Nevada Test Site, Nye County, Nevada, EGG-10282-2004, EG&G, Inc., Goleta, Calif.

O'Farrell, T. P., and E. Collins, 1984. 1983 Biotic Studies of Yucca Mountain, Nevada Test Site, Nye County, Nevada, EGG-10282-2031, EG&G, Inc., Goleta, Calif.

O'Farrell, T. P., and L. A. Emery, 1976. Ecology of the Nevada Test Site: A Narrative Summary and Annotated Bibliography, NVO-167, U.S. Department of Energy, Nevada Operations Office, Las Vegas, Nev.

Office of the State Engineer, 1974. Water for Nevada, Forecasts for the Future, Agriculture, Water Planning Report No. 8, Department of Conservation and Natural Resources, State of Nevada, Carson City.

Ortiz, T. S., R. L. Williams, F. B. Nimick, B. C. Whittet, and D. L. South, 1985. A Three-Dimensional Model of Reference Thermal/Mechanical and Hydrological Stratigraphy at Yucca Mountain, Southern Nevada, SAND84-1076, Sandia National Laboratories, Albuquerque, N. Mex.

Pahrump Valley Times-Star, 1986. "ABC to Close Mine April 12, Mill in June." March 14, 1986, Pahrump, Nev., pp. 1, 4.

Papendick, R. I., and G. S. Campbell, 1981. "Theory and Measurement of Water Potential," Water Potential Relations in Soils Microbiology, SSSA Special Publication No. 9, Soil Science Society of America, Madison, Wis., pp. 1-22.

Pedalino, J. P., 1986. Letter from J. D. Pedalino (H&N) to M. C. Giampaoli (SAIC), NTS:TPO:86-128, December 5, 1986; regarding request for support on the NNWSI Project Site Characterization Plan for Yucca Mountain.

Peters, R. R., E. A. Klavetter, I. J. Hall, S. C. Blair, P. R. Heller and G. W. Gee, 1984. Fracture and Matrix Hydrologic Characteristics of Tuffaceous Materials from Yucca Mountain, Nye County, Nevada, SAND84-1471, Sandia National Laboratories, Albuquerque, N. Mex.

Peters, R. R., J. H. Gauthier, and A. L. Dudley, 1986. The Effect of Percolation Rate on Water-Travel Time in Deep, Partially Saturated Zones, SAND85-0854, Sandia National Laboratories, Albuquerque, N. Mex.

Pexton, R. E., 1984. Geology and Paleohydrology of a Part of the Amargosa Desert, Nevada, unpublished Master's thesis, University of California, Berkeley.

Pistrang, M. A., and F. Kunkel, 1964. A Brief Geologic and Hydrologic Reconnaissance of the Furnace Creek Wash Area, Death Valley National Monument, California, USGS-WSP-1779-Y, Water-Supply Paper, U.S. Geological Survey.

Quade, J., 1986. "Late Quaternary Environmental Changes in the Upper Las Vegas Valley, Nevada," Quaternary Research, Vol. 26, pp. 340-357.

Quiring, R. F., 1983. Precipitation Climatology of the Nevada Test Site, WSNSO 351-88, National Weather Service, U.S. Department of Commerce, Las

Reda, D. C., 1985b. Liquid Permeability Measurements on Densely Welded Tuff Over the Temperature Range 25 deg. to 90 deg. C, SAND85-2482, Sandia National Laboratories, Albuquerque, N. Mex.

Rice, W. A., 1984. Preliminary Two-Dimensional Regional Hydrologic Model of the Nevada Test Site and Vicinity, SAND83-7466, Sandia National Laboratories, Albuquerque, N. Mex.

Riggs, A. C., 1984. "Major Carbon-14 Deficiency in Modern Snail Shells from Southern Nevada Springs," Science, Vol. 224, pp. 58-61.

Ripple, C. D., J. Rubin, and T. E. A. van Hylckama, 1972. Estimating Steady-State Evaporation Rates from Bare Soils Under Conditions of High Water Table, USGS-WSP-2019-A, Water-Supply Paper, U.S. Geological Survey.

Robinson, T. W., 1957. "The Phreatophyte Problem," Symposium on Phraetophytes, Pacific Southwest Regional Meeting, American Geophysical Union, Sacramento, California, February 14, 15, 1957, Phreatophyte Subcommittee of Pacific Southwest Inter-Agency Committee, American Geophysical Union, Sacramento, Calif. pp. 1-11.

Robinson, T. W., 1970. Evapotranspiration by Woody Phreatophytes in the Humbolt River Valley Near Winnemucca, Nevada, U.S. Geological Survey Professional Paper 491-D, U.S. Government Printing Office, Washington, D.C.

Robison, J. H., 1984. Ground-Water Level Data and Preliminary Potentiometric-Surface Maps, Yucca Mountain and Vicinity, Nye County, Nevada, USGS-WRI-84-4197, Water-Resources Investigations Report, U.S. Geological Survey.

Robison, J. H., 1986. Letter from J. H. Robison (USGS) to D. L. Vieth (DOE/NVO), September 17, 1986; regarding revisions of Yucca Mountain water

Rush, F. E., W. Thordarson, and L. Bruckheimer, 1983. Geohydrologic and Drill-Hole Data for Test Well USW H-1, Adjacent to Nevada Test Site, Nye County, Nevada, USGS-OFR-83-141, Open-File Report, U.S. Geological Survey.

Rush, F. E., W. Thordarson, and D. G. Pyles, 1984. Geohydrology of Test Well USW H-1, Yucca Mountain, Nye County, Nevada, USGS-WRI-84-4032, Water-Resources Investigations Report, U.S. Geological Survey.

Russell, B., 1948. Human Knowledge, Its Scope and Limits, Simon and Schuster, New York, p. 311.

Russell, M. B., and L. A. Richards, 1938. "The Determination of Soil Moisture Energy Relations by Centrifugation," in Proceedings of the Soil Science Society of America, Washington, D.C., November 16-18, 1938, Morgantown, West Va., pp. 65-69.

SAIC (Science Application International Corporation), 1986. Preliminary Socioeconomic Profile of Nye County, Nevada: Community Services, DOE/NV/10270-3, Las Vegas, Nev.

SNL (Sandia National Laboratories), 1985. System 2000 Tuff Data Base, Version 11,002, Sandia National Laboratories, Department 6310, Albuquerque, N. Mex.

Sammis, T. W., and L. W. Gay, 1979. "Evapotranspiration from an Arid Zone Plant Community," Journal of Arid Environments, Vol. 2, pp. 313-321.

Sass, J. H., and A. H. Lachenbruch, 1982. Preliminary Interpretation of Thermal Data from the Nevada Test Site, USGS-OFR-82-973, Open-File Report, U.S. Geological Survey.

Sass, J. H., A. H. Lachenbruch, and C. W. Mase, 1980. Analysis of Thermal Data from Drill Holes UE24a-3 and UE25a-1, Calico Hills and Yucca Mountain, Nevada Test Site, USGS-OFR-80-826, Open-File Report, U.S. Geological Survey.

Schoff, S. L., and J. E. Moore (comps.), 1964. Chemistry and Movement of Ground Water, Nevada Test Site, USGS-TEI-838, Trace-Elements Investigations Report, U.S. Geological Survey.

Scott, B. R., T. J. Smales, F. E. Rush, and A. S. Van Denburgh, 1971. Water for Nevada, Water Planning Report 3, Nevada Department of Conservation and Natural Resources, Division of Water Resources, Carson City, Nev.

Scott, R. B., and J. Bonk, 1984. Preliminary Geologic Map of Yucca Mountain, Nye County, Nevada, with Geologic Sections, USGS-OFR-84-494, Open-File Report, U.S. Geological Survey.

Scott, R. B., R. W. Spengler, S. Diehl, A. R. Lappin, and M. P. Chornak, 1983. "Geologic Character of Tuffs in the Unsaturated Zone at Yucca Mountain, Southern Nevada," Role of the Unsaturated Zone in Radioactive and Hazardous Waste Disposal, J. W. Mercer, P. S. C. Rao, and I. W. Marine (eds.), Ann Arbor Science Publishers, Ann Arbor, Mich., pp. 289-335.

Sinnock, S., Y. T. Lin, and J. P. Brannen, 1984. Preliminary Bounds on the Expected Postclosure Performance of the Yucca Mountain Repository Site, Southern Nevada, SAND84-1492, Sandia National Laboratories, Albuquerque, N. Mex.

Sinnock, S. (ed.), Y. T. Lin, and M. S. Tierney, 1986. Preliminary Estimates

Tamers, M. A., 1967. "Surface-Water Infiltration and Groundwater Movement in Arid Zones of Venezuela," in Isotopes in Hydrology, Proceedings of the Symposium on Isotopes in Hydrology, Vienna, 14-18 November, 1966, International Atomic Energy Agency, Vienna, Austria, pp. 339-353.

Taylor, E. M., and H. E. Huckins, 1986. "Carbonate and Opaline Silica Fault-Filling on the Bow Ridge Fault, Yucca Mountain, Nevada--Deposition from Pedogenic Processes or Upwelling Ground Water?," Geological Society of America, Abstracts with Programs, Vol. 18, No. 5, p. 418.

Taylor, E. M., and R. R. Shroba, 1986. "Morphology of Secondary Carbonate and Opaline Silica in Soils of Different Ages at the Nevada Test Site, Nye County, Nevada," Geological Society of America, Abstracts with Programs, Vol. 18, No. 6, p. 769.

Thamir, F., and C. M. McBride, 1985. "Measurements of Matric and Water Potentials in Unsaturated Tuff at Yucca Mountain, Nevada," in Proceedings of the NWWA Conference on Characterization and Monitoring of the Vadose (Unsaturated) Zone, National Water Well Association, Dublin, Ohio, pp. 470-487.

Thordarson, W., 1983. Geohydrologic Data and Test Results from Well J-13, Nevada Test Site, Nye County, Nevada, USGS-WRI-83-4171, Water-Resources Investigations Report, U.S. Geological Survey.

Thordarson, W., and B. P. Robinson, 1971. Wells and Springs in California and Nevada within 100 Miles of the Point 37 deg. 15 min. N., 116 deg., 25 min. W., on Nevada Test Site, USGS-474-85, U.S. Geological Survey.

Thordarson, W., R. A. Young, and I. J. Winograd, 1967. Records of Wells and Test Holes in the Nevada Test Site and Vicinity (through December, 1966), USGS-TEI-872, Trace-Elements Investigations Report, U.S. Geological Survey.

Thordarson, W., F. E. Rush, R. W. Spengler, and S. J. Waddell, 1984. Geohydrologic and Drill-Hole Data for Test Well USW H-3, Yucca Mountain, Nye County, Nevada, USGS-OFR-84-149, Open-File Report, U.S. Geological Survey, 28 p.

Thordarson, W., F. E. Rush, and S. J. Waddell, 1985. Geohydrology of Test Well USW H-3, Yucca Mountain, Nye County, Nevada, USGS-WRI-84-4272, Water-Resources Investigations Report, U.S. Geological Survey.

Tien, P-L, M. D. Siegel, C. D. Updegraff, K. K. Wahi, and R. V. Guzowski, 1985. Repository Site Data Report For Unsaturated Tuff, Yucca Mountain, Nevada, NUREG/CR-4110, U.S. Nuclear Regulatory Commission, Washington, D.C.

Todd, D. K., 1980. Groundwater Hydrology, Second Edition, John Wiley & Sons, New York. pp. 362-368.

Toth, J. A., 1963. "A Theoretical Analysis of Ground-Water Flow in Small Drainage Basins," Journal of Geophysical Research, Vol. 68, No. 16, pp. 4795-4812.

Travis, B. J., 1986. Stochastic Methodology, Milestone Report - R368, (Mimeo), Los Alamos National Laboratory, Los Alamos, N. Mex.

USGS (U.S. Geological Survey), 1978. Hydrologic Unit Map, 1978, State of California, Scale 1:500,000, U.S. Water Resources Council, Reston, Va.

USGS (U.S. Geological Survey) (comp.), 1984. A Summary of Geologic Studies through January 1, 1983, of a Potential High-Level Radioactive Waste Repository Site at Yucca Mountain, Southern Nye County, Nevada, USGS-OFR-84-792, Open-File Report, U.S. Geological Survey.

van Genuchten, M. Th., 1980. "A Closed-Form Equation for Predicting the Hydraulic Conductivity of Unsaturated Soils," Soil Science Society of America Journal, Vol. 44, No. 4, pp. 892-898.

Wang, J. S. Y., and T. N. Narasimhan, 1984. Hydrologic Mechanisms Governing Fluid Flow in Partially Saturated, Fractured, Porous Tuff at Yucca Mountain, LBL-18473, Lawrence Berkeley Laboratory, Berkeley, Calif.

Wang, J. S. Y., and T. N. Narasimhan, 1985. Hydrologic Mechanisms Governing Fluid Flow in Partially Saturated, Fractured Porous Tuff at Yucca Mountain, SAND84-7202, Sandia National Laboratories, Albuquerque, N. Mex.

Wang, J. S. Y., and T. N. Narasimhan, 1986. Hydrologic Mechanisms Governing Partially Saturated Fluid Flow in Fractured Welded Units and Porous Non-Welded Units at Yucca Mountain, SAND85-7114, Sandia National Laboratories, Albuquerque, N. Mex.

Watson, P., P. Sinclair, and R. Waggoner, 1976. "Quantitative Evaluation of a Method for Estimating Recharge to the Desert Basins of Nevada," Journal of Hydrology, Vol. 31, Elsevier Scientific Publishng Co., Amsterdam, pp. 335-357.

Weeks, E. P., 1978. Field Determination of Vertical Permeability to Air in the Unsaturated Zone, Geological Survey Professional Paper 1051, U.S. Government Printing Office, Washington, D.C.

Weeks, E. P., and W. E. Wilson, 1984. Preliminary Evaluation of Hydrologic Properties of Cores of Unsaturated Tuff, Test Well USW H-1, Yucca Mountain, Nevada, USGS-WRI-84-4193, Water-Resources Investigations Report, Wilson, W. E., 1985. Letter from W. E. Wilson (USGS) to D. L. Vieth (DOE/NVO), December 24, 1985; regarding unsaturated zone flux.

Winograd, I. J., 1962a. Interbasin Movement of Ground Water at the Nevada Test Site, USGS-TEI-807, Trace-Elements Investigations Report, U.S. Geological Survey.

Winograd, I. J., 1962b. "Interbasin Movement of Ground Water of the Site, Nevada," Geological Survey Research 1962, U.S. Geological Survey Professional Paper 450-C, U.S. Geological Survey.

Winograd, I. J., 1981. "Radioactive Waste Disposal in Thick Unsaturated Zones," Science, Vol. 212, No. 4502, pp. 1457-1464.

Winograd, I. J., and G. C. Doty, 1980. Paleohydrology of the Southern Great Basin, with Special Reference to Water Table Fluctuations Beneath the Nevada Test Site during the Late(?) Pleistocene, USGS-OFR-80-569, Open-File Report, U.S. Geological Survey.

Winograd, I. J., and I. Friedman, 1972. "Deuterium as a Tracer of Regional Ground-water Flow, Southern Great Basin, Nevada and California," Geological Society of America Bulletin, Vol. 83, No. 12, pp. 3691-3708.

Winograd, I. J., and F. J. Pearson, Jr., 1976. "Major Carbon-14 Anomaly in a Regional Carbonate Aquifer: Possible Evidence for Megascale Channeling, South Central Great Basin," Water Resources Research, Vol. 12, No. 6, pp. 1125-1143.

Winograd, I. J. and A. C. Riggs, 1984. "Recharge to the Spring Mountains, Nevada: Isotopic Evidence," Geological Society of America, Abstracts with Programs, Vol. 16, No. 6, p. 698.

Winograd, I. J., and B. J. Szabo, 1986. Water-Table Decline in the South-Central Great Basin during the Quaternary Period: Implications for Toxic-Waste Disposal, USGS-OFR-85-697, Open-File Report, U.S. Geological Survey.

Winograd, I. J., and W. Thordarson, 1968. "Structural Control of Ground-Water Movement in Miogeosynclinal Rocks of South-Central Nevada," Nevada Test Site, E. B. Eckel (ed.), Geological Society of America Memoir 110, pp. 35-48.

Winograd, I. J., and W. Thordarson, 1975. Hydrogeologic and Hydrochemical Framework, South-Central Great Basin, Nevada-California, with Special Reference to the Nevada Test Site, U.S. Geological Survey Professional Paper 712-C, U.S. Geological Survey, pp. C1-C126.

Winograd, I. J., B. J. Szabo, T. B. Coplen, A. C. Riggs, and P. T. Kolesar, 1985. "Two-Million-Year Record of Deuterium Depletion in Great Basin Ground Waters," Science, Vol. 227, pp. 519-522.

Witherill, V., 1986. Letter from V. F. Witherill (DOE/NTS) to M. D. Tuebner (SAIC), June 4, 1986, DOE/NTSO-8450; regarding water supply information for the Nevada Test Site.

Wu, S. S. C., 1985. Topographic Maps of Yucca Mountain Area, Nye County, Nevada, USGS-OFR-85-620, Open-File Report, Scale 1:5,000, U.S. Geological Survey.

Yang, A., 1986. Summary of Progress Report, Unsaturated Zone Hydrochemistry, February 12, 1986, U.S. Geological Survey.

Yang, I. C., H. H. Haas, E. P. Weeks, and D. C. Thorstenson, 1985. "Analysis of Gaseous-Phase Stable and Radioactive Isotopes in the Unsaturated Zone, Yucca Mountain, Nevada," in Proceedings of the NWWA Conference on Characterization and Monitoring of the Vadose (Unsaturated) Zone, National Water Well Association, Dublin, Ohio, pp. 488-506.

Young, R. A., 1972. Water Supply for the Nuclear Rocket Development Station at the U.S. Atomic Energy Commission's Nevada Test Site, USGS-WSP-1938, Water-Supply Paper, U.S. Geological Survey.

CODES AND REGULATIONS

10 CFR Part 60 (Code of Federal Regulations), 1987. Title 10, "Energy," Part 60, "Disposal of High-Level Radioactive Wastes in Geologic Repositories," U.S. Government Printing Office, Washington, D.C., pp. 627-658.

DOE/RW-0199

Nuclear Waste Policy Act
(Section 113)

Site Characterization Plan

Yucca Mountain Site, Nevada Research and Development Area, Nevada

Volume II, Part A

Chapter 4, Geochemistry

December 1988

U. S. Department of Energy
Office of Civilian Radioactive Waste Management

Chapter 4

GEOCHEMISTRY

INTRODUCTION

This chapter contains geochemical information about the Yucca Mountain site. The chapter references plans for continued collection of geochemical data as part of the site characterization program. Details of these plans are contained in Section 8.3.1.3.

This section provides a brief introduction to the geochemistry chapter. It contains discussions about the following: (1) the concerns that drive the collection of geochemical data, (2) the methods by which data presently available have been collected, (3) concepts of the site that influence geochemical data collection, and (4) the status of present data and models.

In addition to the discussions in this chapter, the following related concerns are addressed in Chapter 7:

1. Anticipated interactions among the waste form, engineered barriers, and environment.

2. The chemical composition and form of the waste.

3. The solubility of the waste form in ground water.

4. The radionuclide species released by leaching from the waste form.

5. Anticipated chemical and mineralogical compositions of natural and engineered barriers.

6. Anticipated interactions among the waste form, water, vapor, gas, and rock.

ISSUES

Geochemical information generated during the characterization of the Yucca Mountain site will play an important role in resolving questions about the ability of the site to isolate radioactive wastes from the accessible environment. This issue is addressed by Key Issue 1 (Will the mined geologic disposal system at Yucca Mountain isolate the radioactive waste from the accessible environment after closure in accordance with the requirements set forth in 40 CFR Part 191, 10 CFR Part 60, and 10 CFR Part 960?) (Section 8.2). Geochemical information is specifically addressed by Characterization Program 8.3.1.3 (geochemistry).

In addition, geochemical data will be used to evaluate the Yucca Mountain site in terms of the siting guidelines outlined in 10 CFR Part 960 and the siting criteria in 10 CFR Part 60. In particular, two issues will require site characterization data for their resolution: Issue 1.8 (Can the demonstrations for favorable and potentially adverse conditions be made as required by 10 CFR 60.122?) (Section 8.3.5.17) and Issue 1.9 (Can the higher level findings required by 10 CFR Part 960 be made for qualifying conditions on the postclosure system guideline and the disqualifying and qualifying conditions on the technical guidelines for geohydrology, geochemistry, rock characteristics, climate changes, erosion, dissolution, tectonics, and human interference; and can the comparative evaluations be made by 10 CFR 960.3-1-5?) (Section 8.3.5.18).

Specific to the geochemistry task are three favorable conditions and four potentially adverse conditions (10 CFR 60.122):

Favorable conditions:

1. The nature and rates of tectonic, hydrogeologic, geochemical, and geomorphic processes (or any of such processes) operating within the geologic setting during the Quaternary Period, when projected, would not affect or would favorably affect the ability of the geologic repository to isolate the waste.

2. Geochemical conditions that

   a. Promote precipitation or sorption of radionuclides.

   b. Inhibit the formation of particulates, colloids, and inorganic and organic complexes that increase the mobility of radionuclides.

   c. Inhibit the transport of radionuclides by particulates, colloids, and complexes.

3. Mineral assemblages that, when subjected to anticipated thermal loading, will remain unaltered or alter to mineral assemblages having equal or increased capacity to inhibit radionuclide

[illegible]

1. Ground-water conditions in the host rock, including chemical composition, high ionic strength or ranges of Eh-pH, that could

[illegible]

DECEMBER 1988

PAST DATA COLLECTION

The Yucca Mountain site was one of a number of sites on and near the

CONCEPTS OF THE SITE THAT INFLUENCE GEOCHEMICAL DATA COLLECTION

A definition of geochemical data needs depends on an understanding of the geochemical processes that affect radionuclide transport from the repository toward the accessible environment. A brief description of the present concepts of the site and of radionuclide transport processes that have influenced data collection is presented here to help orient the reader. (Alternative hypotheses which are consistent with available data have been identified and are listed in Table 8.3.1.3-2.)

The Yucca Mountain site is composed mostly of ash-flow and ash-fall tuffs in a number of distinct cooling units (Section 4.1.1). The resulting mineralogy primarily reflects the original bulk chemical composition, the extent of devitrification and welding of individual units, and the variable interaction with water during alteration. Where water has contacted vitric tuff, secondary minerals such as zeolites and clays have generally formed from the alteration of glass. Ground water at and near the site is mainly a dilute, near-neutral, sodium-bicarbonate water (Section 4.1.2).

The potential repository location is in the unsaturated zone, in the lower welded and devitrified part of the Topopah Spring Member of the Paintbrush Tuff (Chapter 1). The most likely transport path for radionuclides either in solution or as particulates is in water that might move through the repository and toward the accessible environment. In the presently preferred conceptual model (Montazer and Wilson, 1984), water in the

the repository in both the gas phase and the aqueous phase. Exchanges between the gas phase and the aqueous phase present in the rock pores may provide an effective retardation mechanism, and is a topic of investigation (Section 4.1.3.6).

The solubility of waste elements can influence their transport by limiting the concentrations of the elements dissolved in water. Solubility depends primarily on the chemistry of the specific element and the local water chemistry. Solubility measurements under conditions characteristic of the Yucca Mountain site, in combination with chemical equilibrium modeling, are being used to characterize waste element solubility (Section 4.1.3.4). In addition to being dissolved in water, waste elements can also exist as particulates (colloids) or be sorbed onto particulates that are present in the water. The formation of natural colloids of waste elements is discussed in Section 4.1.3.4; plans to study particulate material that is naturally present in the water from Yucca Mountain and sorption of radionuclides on particulate material are outlined in Section 8.3.1.3.4.

The relative importance of physical processes, such as diffusion, dispersion, or filtration of particulates in the water, that influence radionuclide transport by retarding the radionuclides is also strongly dependent on local flow conditions. As previously noted, the relative importance of matrix flow versus fracture flow is still somewhat uncertain (Section 3.9). Physical processes associated with both matrix and fracture flow are being studied (Section 4.1.3). Matrix diffusion, in which radionuclides being transported by water in fractures can diffuse into water in the surrounding porous rock matrix, is one of the physical processes being given special attention (Section 4.1.3.5). This retardation mechanism may be important if fracture flow is significant along portions of the flow paths.

The concepts presented above will be formalized into a number of conceptual models as data are collected that confirm the physical and chemical descriptions of the site and the operation of the various geochemical processes. The detailed plans for this work are described in Section 8.3.1.3. In particular, geochemical models of the unsaturated and saturated zones

Notwithstanding present uncertainties, there are a number of general comments that can be made about the present state of geochemical data and models for the site:

1. The water chemistry in the saturated zone has been well characterized, but ground-water samples are needed from the unsaturated zone. They will be obtained during construction of the exploratory shaft. A qualitative understanding exists of the mineralogical controls on ground-water composition.

2. The mineralogy and petrology, based on data from the existing drillholes, have been well characterized. Future work during construction of the exploratory shaft will provide additional data. However, characterization along flow paths away from the repository is not complete because flow-path definitions are uncertain and because there are few exploratory borings along potential pathways.

3. A conceptual model of mineral evolution is being developed. It must provide credible explanations of the present mineral distribution and must be capable of predicting future mineral evolution due to natural processes and the thermal loading of the repository.

4. Sorption data have been collected using representative ground water and tuffs. An understanding of the chemistry that controls sorption exists in some cases but is uncertain for many waste elements, such as the actinides, which have complex aqueous chemistry.

5. Solubility data appropriate to Yucca Mountain are being collected. Chemical equilibrium modeling is being done but it is uncertain whether equilibrium models will be adequate. If not, kinetic models will be required.

6. Physical processes (i.e., dispersion, diffusion, advective processes) that affect radionuclide transport are understood qualitatively, but quantitative data are lacking. Radionuclide transport depends strongly on local ground-water flow characteristics, which are presently not well understood.

7. Radionuclide retardation by all processes along the flow paths to the accessible environment is being assessed by performing integrated transport calculations. This includes an analysis of significant interactions among thermal, hydrologic, chemical, and mechanical processes that could have an impact on the geochemistry of the site and the transport of radionuclides as particulates, pseudocolloids, and colloids at Yucca Mountain.

8. The potential for gaseous transport needs to be assessed. No quantitative assessment has been made yet and the mechanism for isotopic exchange and gas and liquid-solid exchange is uncertain at this time.

Experimental methods and measurement techniques used to obtain the data in this chapter are discussed in detail in the references from which the data were taken. Data quality and related data uncertainty are also discussed in the references. The types of data collected range from mineral types and *distribution to specific measurements (e.g., sorption ratios and solubility measurements)*. In the case of measured sorption ratios, the experimental data uncertainty is included in the data tables.

4.1 GEOCHEMISTRY OF THE HOST ROCK AND SURROUNDING UNITS

4.1.1 MINERALOGY AND PETROLOGY

The mineralogic and petrologic characteristics of Yucca Mountain are important for defining the site conditions existing before repository construction and operation, and for predicting the site response to disruption. Mineral distributions as a function of depth and distance from the potential repository are also important for calculating overall radionuclide retardation by sorption. Because sorptive behavior and ground-water chemistry depend on mineralogy, this chapter begins with a description of the site mineralogy (Sections 4.1.1.1 to 4.1.1.3). Section 4.1.1.4 describes mineral stability at the site.

4.1.1.1 General description of the host rock and surrounding units

The most abundant rock type at Yucca Mountain is ash-flow tuff. The mineralogy of an ash-flow tuff is developed in several episodes of crystal-units occur where eruptive origins are more complex and the welding relations are not so simple; the proposed host rock for the repository in Yucca Mountain is within a compound cooling unit (Lipman et al., 1966). Even within this compound cooling unit, however, the general relationship is preserved in which the core of the cooling unit is more densely welded and the top, bottom, and distal edges of the ash flow are poorly welded or nonwelded. Immediately after the emplacement of an ash-flow tuff, primary glass in the more densely welded interiors of the cooling unit commonly devitrifies to intergrowths of silica minerals and alkali feldspars. The poorly welded or nonwelded margins of the cooling unit, however, often do not devitrify but remain glassy after the ash flow has lost its original heat. It is from the glass in these zones that the most significant intervals of secondary zeolites are formed. Thus, the zeolite intervals at Yucca Mountain (Section 4.1.1.3.2), are roughly correlated with the once vitric stratigraphic intervals that are at the margins of devitrified ash-flows (Vaniman et al., 1984).

Glass, feldspar, and mafic silicates may alter to smectites either within the feldspathic devitrified cores of cooling units or in their glassy margins. It might be expected, therefore, that smectites should occur throughout the tuff cooling units of Yucca Mountain, and in general this is true. In detail, however, the smectite abundances are lower in some zeolitized intervals than in adjacent nonzeolitized intervals; this is particularly true around the zeolitized tuff of Calico Hills (Caporuscio et al., 1982). This relationship is of interest in that the pH and ion concentrations during the hydrous alteration of glass are generally too low for zeolite formation unless the glass alters first to smectite (Hay and Sheppard, 1977). The negative correlation between clay and zeolite abundances at Yucca Mountain suggests that zeolite growth displaces smectite development soon after glass

Finally, it is important to note that although tuff mineralogy is closely related to cooling-unit petrology, the alteration of tuff to hydrous minerals is coupled with the availability of water. The minerals formed from altered tuff vary with depth. The transition from clinoptilolite to analcime to albite with depth is well documented at Yucca Mountain (Bish et al., 1981) trenches at Yucca Mountain. Standard optical petrography techniques were used in the study of thin sections made from these samples. Thin sections were used to determine textural relations, the degree of welding, and mineral growth distributions, with emphasis on the potential host rock in the Topopah Spring Member. Percentages of various textures and of phenocrysts were used to determine the stratigraphic position in the Topopah Spring Member (Byers, 1985).

Mineral occurrences and abundances are more generally determined by quantitative X-ray diffraction. The methods used for quantitative XRD analysis are described by Bish and Vaniman (1985). When estimating the uncertainties of values determined by quantitative XRD, errors due to peak integration, crystalline solution, sample-standard variability, and peak overlap are considered. Relatively high precision is obtained for quartz, calcite, and analcime data (<5 to 10 percent of amount present). Smectite, mica, alkali feldspar, clinoptilolite, and mordenite analyses have precisions that are lower (< 10 to 20 percent of the amount present). Representative XRD tables can be found in Bish and Vaniman (1985). A new deconvolution technique is being developed to allow greater precision in the feldspar, cristobalite, and tridymite analyses, although feldspar data will still be limited by large amounts of crystalline solution and sample-to-standard data are focused on their usefulness in indicating stratigraphic position and

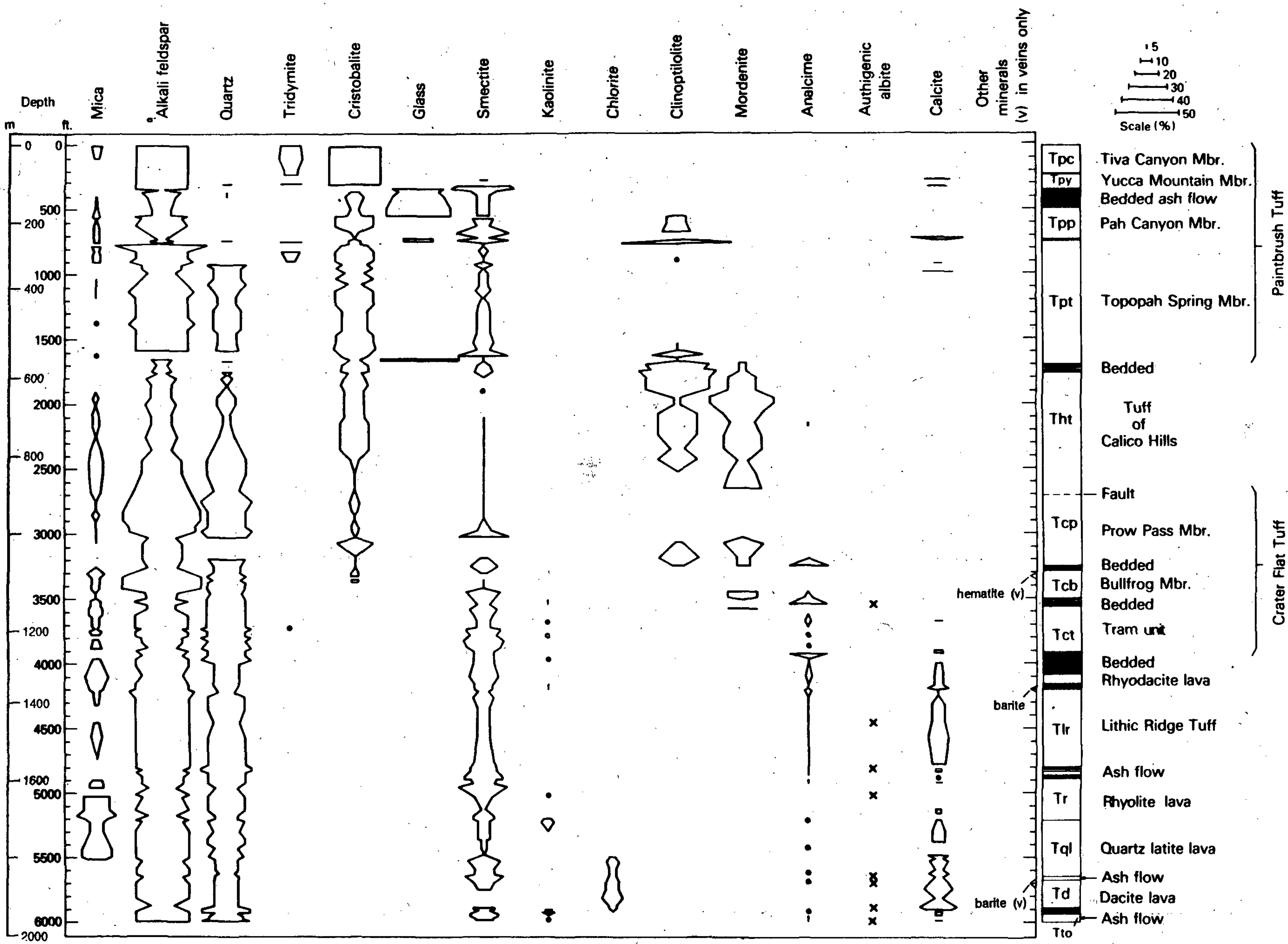

Figure 4-1. Abundance of minerals as a function of depth from surface; determined by x-ray diffraction for core samples from drillhole USW G-2. Modified from Caporuscio et al. (1982).

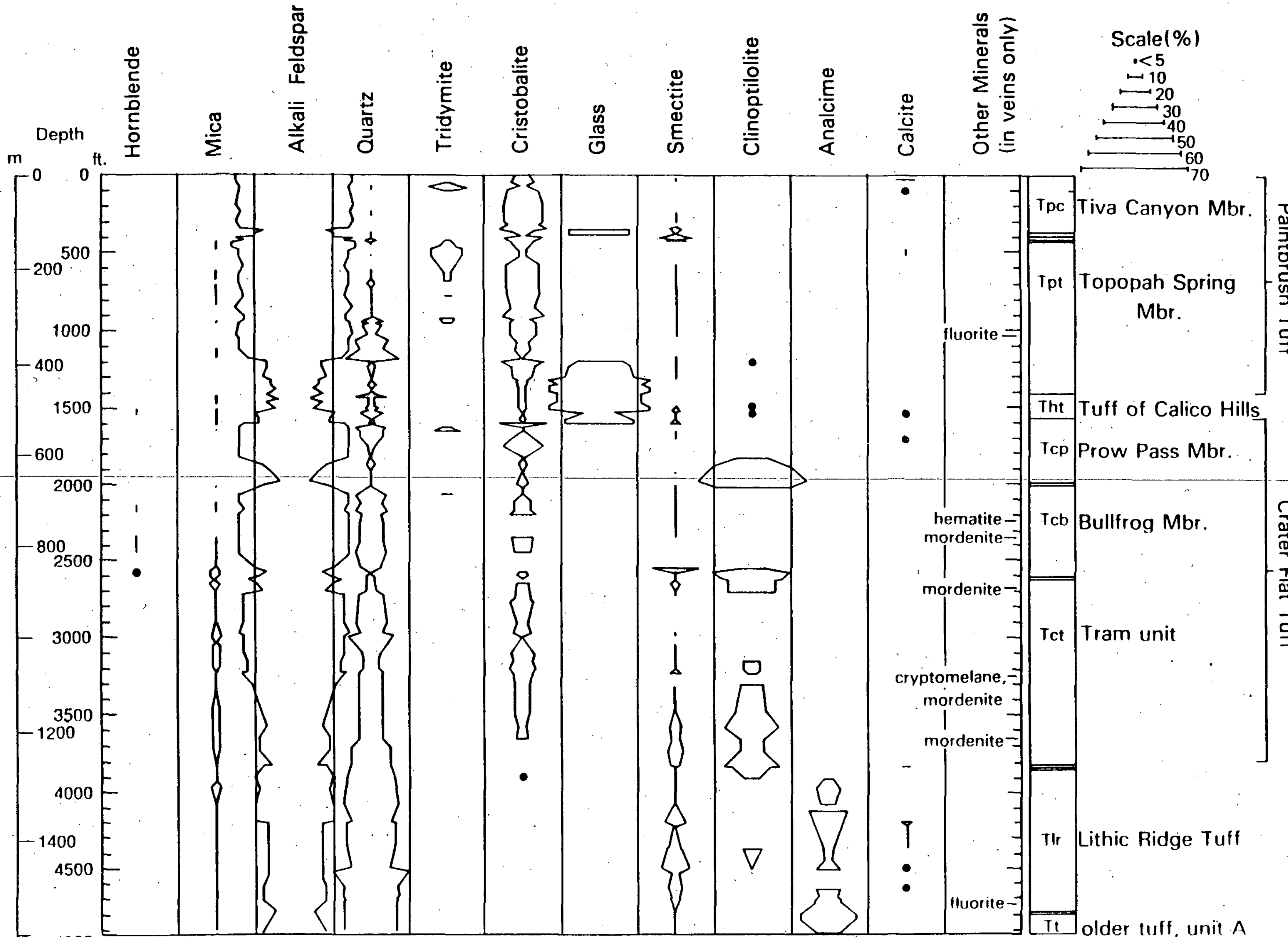

Figure 4-2. Abundance of minerals as a function of depth from surface; determined by x-ray diffraction for core samples from drillholes USW GU-3 and USW G-3. Modified from Vaniman et al. (1984).

Section 8.3.1.3. The studies planned will also cover the limits of mineralogic variability in the host rock to help interpret the results of in situ experiments and to help determine the stratigraphic position during repository construction.

4.1.1.3.1.2 Mineralogy of fractures in the host rock

Detailed studies of fracture mineralogy have recently been completed on samples taken from above the static water level (SWL) in drillhole USW G-4 (Carlos, 1985). (The SWL approximates the position of the present-day water table, although it is a composite level affected by differences of hydraulic

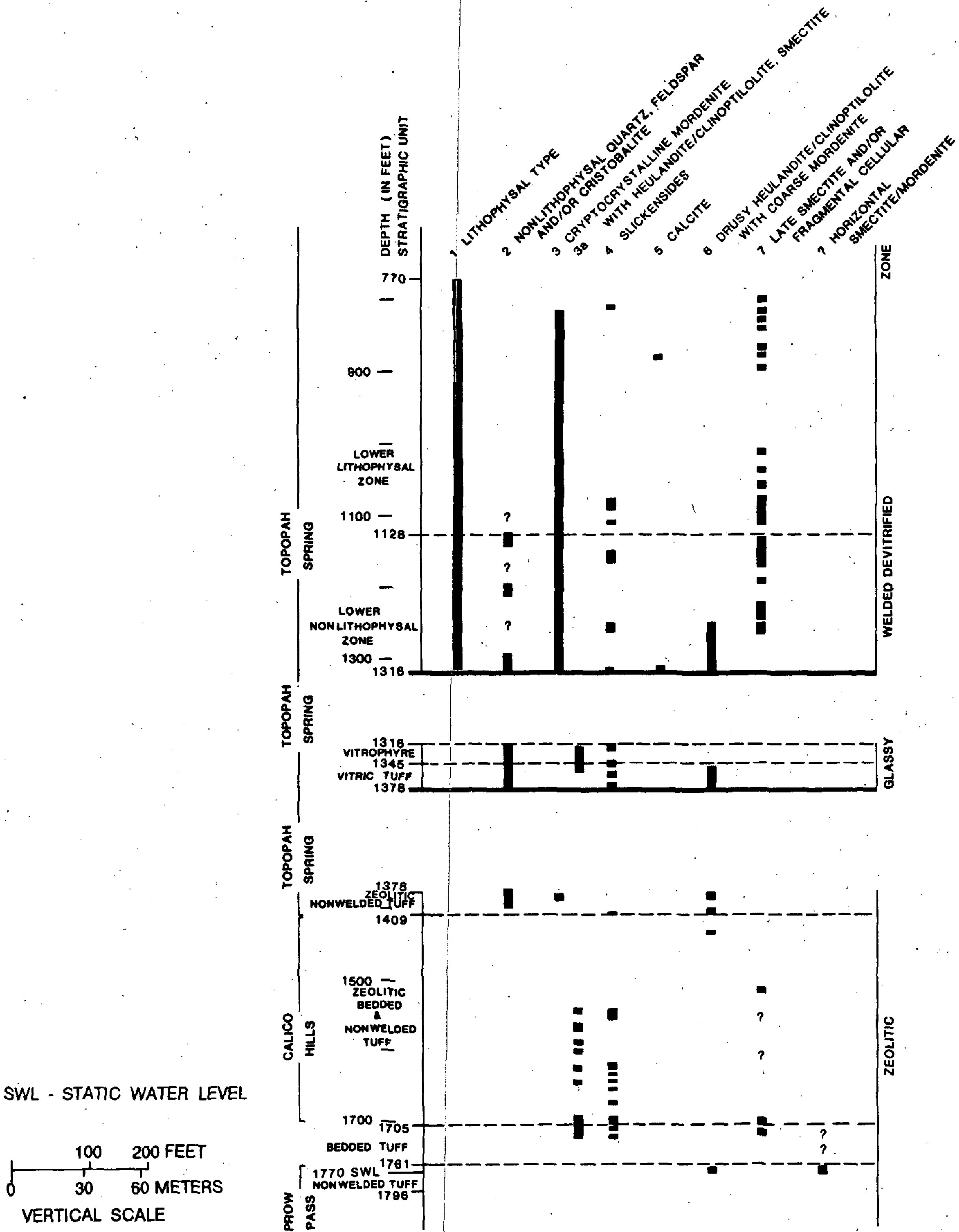

Figure 4-3. Sequence of fracture coatings in the unsaturated zone of drillhole USW G-4. Modified from Carlos (1985). Numbers across the top indicate inferred sequence of mineral growth, determined from overgrowth or cross-cutting relationships. Along the right side of the figure, major lithologic variations in the host rock (welded-devitrified, glassy, and zeolitic) are identified.

of secondary-mineral formation at Yucca Mountain (Section 8.3.1.3) and models of the mineralogy along potential radionuclide transport paths.

4.1.1.3.2 Surrounding units

The Topopah Spring Member is overlain and underlain by other silicic volcanic units. The mineralogy of these bounding units is summarized briefly below. The stratigraphic framework is discussed in Section 1.2.2.

Above the Topopah Spring Member, the younger members of the Paintbrush Tuff include the Pah Canyon, the Yucca Mountain, and the Tiva Canyon members in order of decreasing age. The Pah Canyon and Yucca Mountain members form thin units (less than 71 m) at the site and are absent throughout much of the exploration block; the Tiva Canyon, however, is about 70 to 150 m thick and forms most of the outcrops on the eastern dip slope of Yucca Mountain (Section 1.2.2.2). These upper members are described in Chapter 1; more detailed descriptions are given by Orkild (1965), Lipman et al. (1966), Byers et al. (1976), and Scott et al. (1983). The mineral constituents and petrography of the upper members are summarized in Section 1.2.2.2.6. Electron-microprobe analyses of phenocrysts are summarized by Broxton et al. (1982), and the compositions of glasses and zeolites are described by Caporuscio et al. (1982). Chemical analyses are yet to be completed (Section 8.3.1.3.2).

The mineralogic compositions of the Topopah Spring Member and of the underlying units are summarized by Warren et al. (1984) and by Bish and Vaniman (1985). Detailed descriptions are published for samples from well J-13 (Heiken and Bevier, 1979; Byers and Warren, 1983; Bish and Chippera, 1986), drillhole UE-25a#1 (Sykes et al., 1979; Carroll et al., 1981; Bish and Chippera, 1986) drillhole USW G-1 (Bish et al., 1981; Bish and Chippera, 1986), drillholes USW G-2 and UE-25b-1H (Broxton et al., 1982; Caporuscio et al., 1982), and drillholes USW GU-3 and USW G-3 (Vaniman et al., 1984). Selected whole-rock compositions are summarized by Zielinski (1983) and cover the range of quartz latitic to rhyolitic tuffs that characterize the volcanic sequence at Yucca Mountain, plus the less common dacitic lavas or flow breccias. Additional chemical data will be obtained during site characterization (Section 8.3.1.3.2).

The petrography and petrology of the Topopah Spring Member were mentioned in Section 4.1.1.3.1 and described in Chapter 1. The symbols used for petrologic units are given in Table 4-1. The petrography of units underlying the Topopah Spring Member is summarized in Table 4-2 based on samples from drillhole USW G-1, and in Table 4-3, which is based on this drillhole and surrounding localities (Warren et al., 1984). Drillhole USW G-1 is centrally located within the site, as shown in Figure 4-4. The tables show that two feldspars, plagioclase and sanidine, plus quartz predominate in the phenocryst assemblages, with biotite forming the most common mafic phenocryst (but note the exceptionally high orthopyroxene content of the Prow Pass Member of the Crater Flat Tuff). Warren et al. (1984) conclude that these petrographic features vary slightly within a given unit, although at the southern end of the site, the tuffaceous beds of Calico Hills contain amphibole, orthopyroxene, and clinopyroxene (Vaniman et al., 1984).

Table 4-1. Symbols used for petrologic units, rock types, alteration, and minerals listed in Table 4-2[a]

Unit, rock type, alteration, or mineral	Symbol
PETROLOGIC UNIT	
Paintbrush Tuff	TP
Topopah Spring Member	
Upper, mafic-rich portion	TPTu
Lower, mafic-rich portion	TPTl
Tuffaceous beds of Calico Hills	
Upper, mafic-poor portion	TH1
Lower, mafic-poor portion	TH2
Crater Flat Tuff	TC
Prow Pass Member	TCP
Bedded tuff	TCBa
Bullfrog Member	TCB
Upper portion, 2,152 to 2,317.4-ft depth, drillhole USW G-1	TCBu
Middle portion, 2,317.4 to 2,425-ft depth, drillhole USW G-1	TCBm
Lower portion, 2,425 to 2,601.6-ft depth, drillhole USW G-1	TCBl
Bedded tuff	TCTa
Tram Member	TCT
Upper portion, 2,601.6 to 3,083.0-ft depth, drillhole USW G-1	TCTu
Lower portion, 3,083.0 to 3,522.0-ft depth, drillhole USW G-1	TCTl
Flow breccia of drillhole USW G-1	TFB
Rhyodacite lava of drillhole USW G-2	TRD
Bedded tuff between the flow breccia of USW G-1 and the Lithic Ridge Tuff	TLRa
Lithic Ridge Tuff	TLR
Upper portion, 3,920.0 to ≈ 4,365-ft depth, drillhole USW G-1	TLRu
Lower portion, ≈ 4,365 to 4,940.2-ft depth, drillhole USW G-1	TLRl
Older tuffs of drillhole USW G-1	TT
Unit A	TTA
Unit B	TTB
Unit C	TTC

Table 4-1. Symbols used for petrologic units, rock types, alteration, and minerals listed in Table 4-2[a] (continued)

Unit, rock type, alteration, or mineral	Symbol
ROCK TYPE	
Tuff	tf
Bedded tuff	b
Ash-flow tuff	t
Nonwelded	nwt
Partially welded	pwt
Moderately welded	mwt
Densely welded	dwt
Vitrophyric	vt
Lava	l
Intermediate-composition lava (groundmass plagioclase present)	intl
Lava-flow breccia	fb
Tuff breccia	tb
Argillite	ar
Granitoid	gr
ALTERATION[b]	
None	
Vitric	gl
Low temperature (secondary)	
Opaline	O
Argillite	Ar
Zeolitic	Z
Clinoptilolite	Zc
Analcime	Za
Calcite	cc
Pyritic	py
Silicic (Chalcedony)	Q
High temperature (secondary)	
Albitic	Ab
High temperature (primary)	
Vapor phase	VP
Granophyric	Gr
Spherulite	Sp
Axiolitic	Ax

Table 4-1. Symbols used for petrologic units, rock types, alteration, and minerals listed in Table 4-2[a] (continued)

Unit, rock type, alteration, or mineral	Symbol
MINERALS[c]	
Felsic phenocrysts	
Quartz	Q
Sanidine (+ anorthoclase, if present)	K
Plagioclase	P
Mafic phenocrysts	
Biotite	Biot
Hornblende	Hbld
Clinopyroxene	Cpx
Orthopyroxene	Opx
Accessory minerals	
Sphene	Sph
Allanite	All
Perrierite/cherkinite	Per
Apatite	Ap
Zircon	Zr

[a]Source: Warren et al. (1984). To convert feet to meters, multiply by 0.328.

[b]The symbols m (minor) and μ (micro) are used as modifiers on the alteration symbols.

[c]The mineral volume abundances listed for most samples are for unaltered or partly altered phenocrysts. In some samples, phenocrysts are partly or completely altered. In these samples, the symbol "A" indicates that the accompanying concentration is for partly altered grains only, and the symbol "ps" indicates that the accompanying concentration is based entirely on completely altered (pseudomorphic) forms.

Table 4-2. Summary of petrography for core samples from drillhole USW G-1, determined by point count of glass-covered thin section[a,b] (page 1 of 2)

Sample depth (ft)[c]	Unit	Rock type	Alteration	Points counted	Major components (volume %) Lithics	Felsics	Felsic phenocrysts (relative %) Q	K	P	Mafic phenocrysts (ppmV) Biot	Hbld	Cpx	Opx	Fe-Ti oxide (ppmV)	Accessory minerals (grains identified) Sph	All	Ap	Zr
1,561.8	TH1	nwt	Zc	3,750	2.8	2.2	43	16	41	270	0	0	0	0	0	0	0	0
1,689.5	TH1	nwt	Zc	8,000	1.8	2.0	51	24	25	375	0	0	0	125	0	0	0	4
1,811.7	TCP	pwt		3,600	0.14	6.2	15	53	32	<280	0 (ps)	0	1,900 (ps)	560	0	0	0	4
1,943.4	TCP	mwt	VP	3,300	0.45	14.4	13	39	48	<280	0	0	910 (ps)	610	0	0	0	8
2,009.8	TCP	pwt		3,750	2.6	7.9	15	47	38	<280	<280	0	2,100 (ps)	530	0	1	Rare	5
2,124.7	TCP	nwt		3,600	0.6	8.8	6	50	44	280	0 (ps)	0	0	1,100	0	2	Rare	7
2,231.0	TCBu	pwt		3,700	0.03	12.2	22	36	42	2,700	1,300 (ps)	0	0	810	0	0	Rare	9
2,246.0	TCBu	p-mwt		3,000	0.00	11.8	19	45	36	4,300	1,000 (ps?)[d]	0	0	1,700	0	0	Gone	7
2,300.4	TCBu	pwt		3,750	0.00	13.6	24	31	45	1,600	2,400 (ps)	0	0	1,600	0	0	Rare	13
2,354.6	TCBm	mwt	Gr	3,750	0.03	14.6	27	30	43	3,500	2,400 (ps)	0	0	1,900	0	0	Rare	10
2,397	TCBm	pwt	VP	3,750	0.2	13.0	23	32	45	5,300	1,300 (ps)	0	0	530	0	0	Rare	7
2,461.5	TCBl	mwt	VP	3,650	0.9	7.1	5	44	51	2,200	1,600 (ps)	0	0	550	0	0	Rare	8
2,470.6	TCBl	pwt	VP	3,700	1.6	8.3	18	29	53	4,900	1,100 (ps)	0	0	1,300	0	0	Rare	10
2,478.3	TCBl	pwt	VP	3,750	0.5	10.0	14	39	47	4,000	530 (ps)	0	0	270	0	0	Rare	5
2,507	TCBl	mwt		3,700	1.2	9.6	13	36	51	4,100	3,200 (ps)	0	0	2,400	0	0	Rare-sparse	12
2,555	TCBl	mwt	Zc	3,520	0.8	9.9	9	40	51	2,300	2,300	-----280 (ps?)----		280	0	0	Shot?	5
2,594.2	TCBl	pwt		3,750	2.2	7.1	17	32	51	4,300	270 (ps)	0	0	800	0	4	Rare	10
2,678.0	TCTu	pwt		3,980	1.3	7.5	15	34	51	7,300	0	0	0	1,000	2	1	Sparse	6
2,772.6	TCTu	pwt		3,800	2.1	10.2	29	34	37	5,800	---------1,600 (ps?)---------			530	0	0	Sparse	5
2,851.7	TCTu	mwt		3,900	4.5	13.6	41	37	22	4,400	0	0	0	1,800	0	0	Rare	11
2,869	TCTu	m-dwt		3,360	3.8	12.1	41	35	24	6,000	0	0	0	890	0	0		7
2,931.4	TCTu	m-dwt		4,000	3.3	12.8	37	32	31	7,000	0	0	0	500	0	0		9
3,013.9	TCTu	pwt		3,500	12.3	12.9	27	44	29	4,900	(ps)	0	0	860	0	10		>2
3,192.8	TCTl	pwt		3,600	23.8	9.4	33	30	37	4,200	0	0	0	280	0	0	Many	3
3,197	TCTl	mwt		3,460	22.3	7.4	38	29	33	3,200	0	0	0	<280	0	0	?	3
3,284.5	TCTl	pwt	Ar,cc	3,600	9.0	8.6	35	31	34	3,300	0 (ps)	0	0	1,700 (py)	0	4	Alt.	>8
3,515.1	TCTl	pwt		3,800	25.8	8.3	34	22	44	2,900	260 (ps)	0	0	1,300 (py)	0	1	Present	Present
3,724.0	TFB	fb	Gl,O	3,700	0.00	8.8	0.0	0.0	100	0	11,100	---15,100 (ps)---		8,100	0	0	Large	0
3,908.2	TFB	fb	Gl	3,150	0.00	10.0	0.0	0.0	100	0	7,900	2,500	8,200 (ps)	5,700	0	0	Large	0
3,956.9	TLR	pwt	Ar	0	0	0	0	0	0					2	2		Present	Present
3,969.9	TLR	mwt	Ar	3,300	9.0	17.5	2	34	64	5,500	0 (ps?)	0	0	2,400	11	3	Present	Present
3,992	TLR	pwt		3,500	26.5	11.3	4	31	65	9,700	0	0	0	2,000	12	1	Present	Present
4,150.4	TLR	pwt		3,400	13.8	8.5	2	35	63	1,200	0	0	0	600	6	1	Rare	8
4,222.1	TLR	pwt		3,200	42.7	6.1	7	40	53	1,600	0	0	0	1,600	6	0	Sparse	5
4,408.4	TLR	pwt		1,800	11.8	9.2	1	37	62	5,000	0	0	0	1,100	1	1	Rare	7

Table 4-2. Summary of petrography for core samples from drillhole USW G-1, determined by point count of glass-covered thin section[a,b] (page 2 of 2)

Sample depth (ft)[c]	Unit	Rock type	Alteration	Points counted	Major components (volume %) Lithics	Felsics	Felsic phenocrysts (relative %) Q	K	P	Mafic phenocrysts (ppmV) Biot	Hbld	Cpx	Opx	Fe-Ti oxide (ppmV)	Accessory minerals (grains identified) Sph	All	Ap	Zr
4,471.0	TLR	pwt		3,600	26.4	5.1	7	36	57	3,600	0	0	0	560	8(ps)	1	Present	12
4,578.2	TLR	pwt		3,800	23.8	7.6	5	39	56	2,600	0	0	0	530	2(ps)	2	Sparse	9
4,758.4	TLR	pwt		3,900	19.0	9.2	9	38	53	2,600	0	0	0	1,500	6(5ps)	0	Sparse	10
4,849.0	TLR	pwt		3,900	13.0	8.9	10	35	55	3,300	0	0	0	1,000	7(ps)	0	Shot	10
4,917.0	TLR	nwt		3,800	5.9	5.6	14	51	35	3,200	0	0	0	1,800	11(ps)	3	Present	12
4,946.4	TTA	nwt		3,450	4.4	9.8	20	58	22	3,000	0	0	0	300	4(ps)	2	0	12
4,969.0	TTA	pwt		3,700	3.1	11.9	24	31	45	4,900	0	0	0	2,700	5(ps)	0	Partly shot	10
5,002.3	TTA	nwt		3,700	2.5	17.0	32	31	37	5,100	0	0	0	2,400	3(ps)	3	Rare	13
5,045.0	TTA	mwt		3,700	8.9	19.9	28	43	29	4,100	0	0	0	1,900	2(1ps)	0	1 ph	19
5,097.9	TTA	mwt		3,600	0.58	17.4	28	41	31	2,200	0	0	0	2,000	1(ps)	3	Rare	10
5,115.5	TTA	mwt		3,750	3.1	18.3	24	42	34	4,800	0	0	0	1,900	2	11	Sparse	20
5,141.5	TTA	mwt		3,700	9.2	14.1	27	33	40	2,100	0	0	0	1,200	4	4	Sparse	15
5,142.2	TTA	pwt		3,750	2.2	19.4	28	36	36	3,700	<270	0	0	1,900	7	5	Present	13
5,187.0	TTA	nwt		3,650	2.1	17.6	24	38	38	1,600	270	0	0	2,200	6	7	Sparse	17
5,265.6	TTA	pwt		3,400	5.4	17.4	35	31	34	2,400	590	0	0	1,800	6	8	Sparse	17
5,316.0	TTA	b		3,600	2.4	21.6	33	36	31	1,400	0	0	0	2,800	4	12	Rare	13
5,373.7	TTB	pwt		3,650	0.69	11.3	13	26	61	9,000	0	0	0	3,300	15	1	Sparse	20
5,400.0	TTB	pwt		3,800	2.3	13.6	12	30	58	4,500	0	0	0	3,200	8	1	Sparse	24
5,416.6	TTB	pwt		3,700	12.8	11.2	11	27	62	2,700	0(ps?)	0	0	3,200	5	1	Rare, shot	20
5,438.2	TTC	pwt		3,900	0.74	12.9	1	3	96	12,000	0	0	0	4,600	0	1	Present	50
5,454.1	TTC	b		3,800	1.9	14.9	16	18	66	7,100	0	0	0	5,000	9	9	Sparse	42
5,496.1	TTC	pwt		3,900	7.5	10.1	1	4	95	21,000	0	0	0	4,900	8	3	Sparse	21
5,517.3	TTC	pwt		3,600	10.3	11.8	2	9	89	11,400	0	0	0	4,500	9	2	Sparse	20
5,540.0	TTC	pwt		3,700	8.5	13.5	0.4	0.0	99.6	19,200	810(ps)	0	0	4,300	1	0	Sparse-common	29
5,558.7	TTC	pwt		3,600	0.64	19.1	4	4	92	16,400	1,100(ps)	0	0	5,300	12	3	Sparse (large)	20
5,600.0	TTC	mwt		3,750	8.4	14.8	5	7	88	10,100	800(ps)	0	0	6,400	16	4	Sparse	24
5,642.0	TTC	mwt		3,300	5.8	15.4	2	4	94	21,500	1,500(ps)	0	0	5,800	12	3	Sparse	22
5,728.0	TTC	mwt		1,650	21.1	21.6	0.0	1	99	18,200	0(ps)	0	0	7,900	4	3	Sparse (large)	24
5,841.0	TTC	mwt		1,650	10.8	18.0	0.0	4	96	12,100	600(ps?)	0	0	8,500	3	1	Sparse-common	26
5,894.3	TTC	mwt		1,650	7.2	15.5	0.0	4	96	6,100	6,100	0	0	3,600	6	1	Sparse	14
5,929.8	TTC	mwt		1,650	5.9	18.2	4	4	92	13,300	5,500(ps)	0	0	6,100	7	8	Sparse-common	24
5,944.9	TTC	m-dwt		1,600	6.3	21.6	1	6	93	6,900	7,500(ps)	0(ps)	0	5,000	8	5	Sparse-common	24
5,980.0	TTC	m-dwt		1,650	3.3	20.9	0.0	0.3	99.7	24,200	7,300(ps)	1,800(ps)	0	7,300	4	1	Sparse-common	24
5,984.7	TTC	m-dwt		1,650	2.3	25.3	0.0	0.0	100	27,2000	8,500(ps)	1,200(ps)	0	9,700	1	3	Sparse-common	25

[a]Source: Warren et al. (1984).
[b]ppmv = parts per million in volume. Other symbols are defined in Table 4-1.
[c]To convert feet to meters, multiply by 0.328.
[d]Question marks indicate uncertainty.

Table 4-3. Statistical modes[a] for compositional parameters of phenocrysts for the lower Topopah Spring Member and for underlying units

Unit symbol[b]	Number of samples	Sanidine[c] Or + Cn (mole%)	Sanidine[c] BaO (wt%)	Plagioclase[d] Rim (mole%An)	Plagioclase[d] Core (mole%An)	Mafic minerals[e] Biot (Molecular Mg/(Mg + Fe))	Mafic minerals[e] Hbld	Mafic minerals[e] Opx	Mafic minerals[e] Cpx
TPT1	5	59	0.00	15	17	0.43	--[f]	--	--
TH1	3	68	0.18	19	21	0.37	--	--	--
TH2	1	73	1.0	--	37	0.45	--	--	--
TCP	14	53	0.14	11	11	0.42	--	0.29	--
TCB	22	61	0.56	15	16	0.40	0.44	--	--
TCT	18	67	0.55	21	21	0.42	--	--	--
TFB	4	--	--	61	61	--	0.66	0.70	0.73
TLR	15	65	0.67	18	19	0.59	--	--	--
TTA	8	64	0.55	17	19	0.55	--	--	--
TTB	2	66	0.96	23	29	0.59	--	--	--
TTC	6	72	3.4	29	32	0.62	--	--	--

[a]The median value very closely approximates the statistical mode for compositional parameters of sanidine and mafic minerals and is the value given for these minerals. Sample locations are shown in Warren et al. (1984).

[b]Unit symbols are defined in Table 4-1.

[c]Or = potassium feldspar; Cn = celsian; BaO = barium oxide.

[d]An = anorthite.

[e]Biot = biotite; Hbld = hornblende; Opx = orthopyroxene; Cpx = clinopyroxene.

[f]-- = not present.

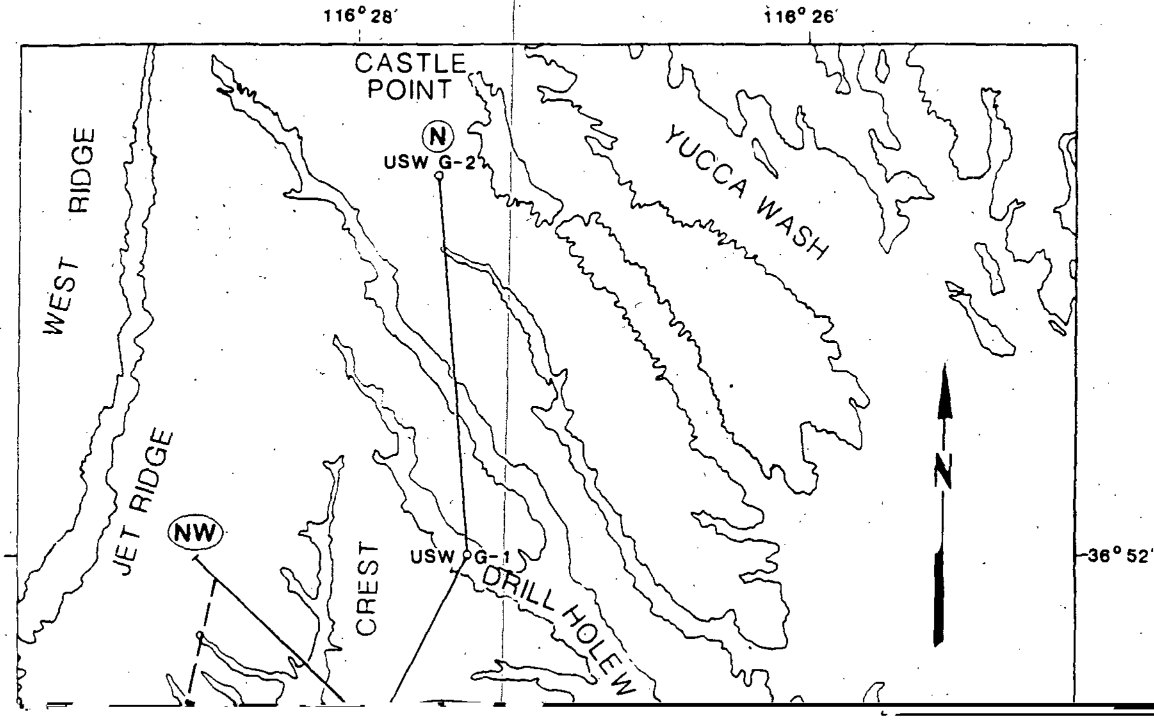
116° 28′
116° 26′
CASTLE POINT
N
USW G-2
YUCCA WASH
WEST RIDGE
JET RIDGE
NW
CREST
USW G-1
DRILL HOLE W
36° 52′
N

Table 4-3 is a concise summary of the major phenocryst compositions (excluding quartz) in the Topopah Spring Member and in the underlying units. The anorthite content of plagioclase and the potassium and barium content of sanidine have been found to be distinctive for particular units (Warren et al., 1984).

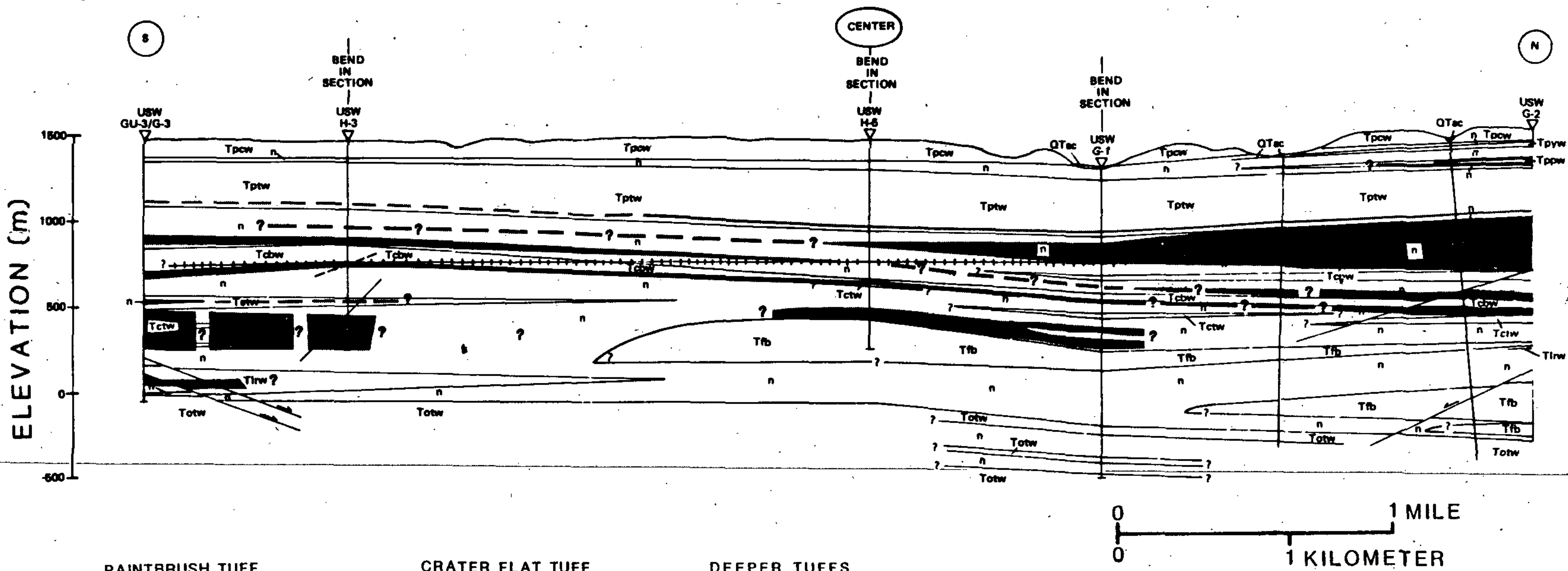

PAINTBRUSH TUFF	CRATER FLAT TUFF	DEEPER TUFFS	
Tpcw - TIVA CANYON MEMBER	Tcpw - PROW PASS MEMBER	Tlrw - WELDED LITHIC RIDGE TUFF	QTac - ALLUVIUM AND COLLUVIUM
Tpyw - YUCCA MEMBER	Tcbw - BULLFROG MEMBER	Totw - WELDED ZONES OF OLDER TUFFS	Tfb - LAVAS AND FLOW BRECCIAS
Tppw - PAH MEMBER	Tctw - TRAM MEMBER		n - NONWELDED TUFF ZONES
Tptw - TOPOPAH MEMBER			+++ - STATIC WATER LEVEL

Figure 4-5. Major zeolite distributions (Bish and Vaniman, 1985), north-south cross section, shown as a dark pattern overlying the stratigraphic cross section of Scott and Bonk (1984). Location of cross section is shown on Figure 4-4. Unit designations follow the usage of Scott and Bonk (1984). Tpcw, Tpyw, Tppw, and Tptw represent the welded zones of the Tiva Canyon, Yucca Mountain, Pah Canyon, and Topopah Spring members of the Paintbrush Tuff; Tcpw, Tcbw, and Tctw represent the welded zones of the Prow Pass, Bullfrog, and Tram members of the Crater Flat Tuff; Tfb represents lavas and flow breccias; the Totw represents the welded zones of older tuffs. The symbol n is used for all nonwelded tuff zones. The subhorizontal barred line indicates the water table as inferred from static water levels in the drillholes.

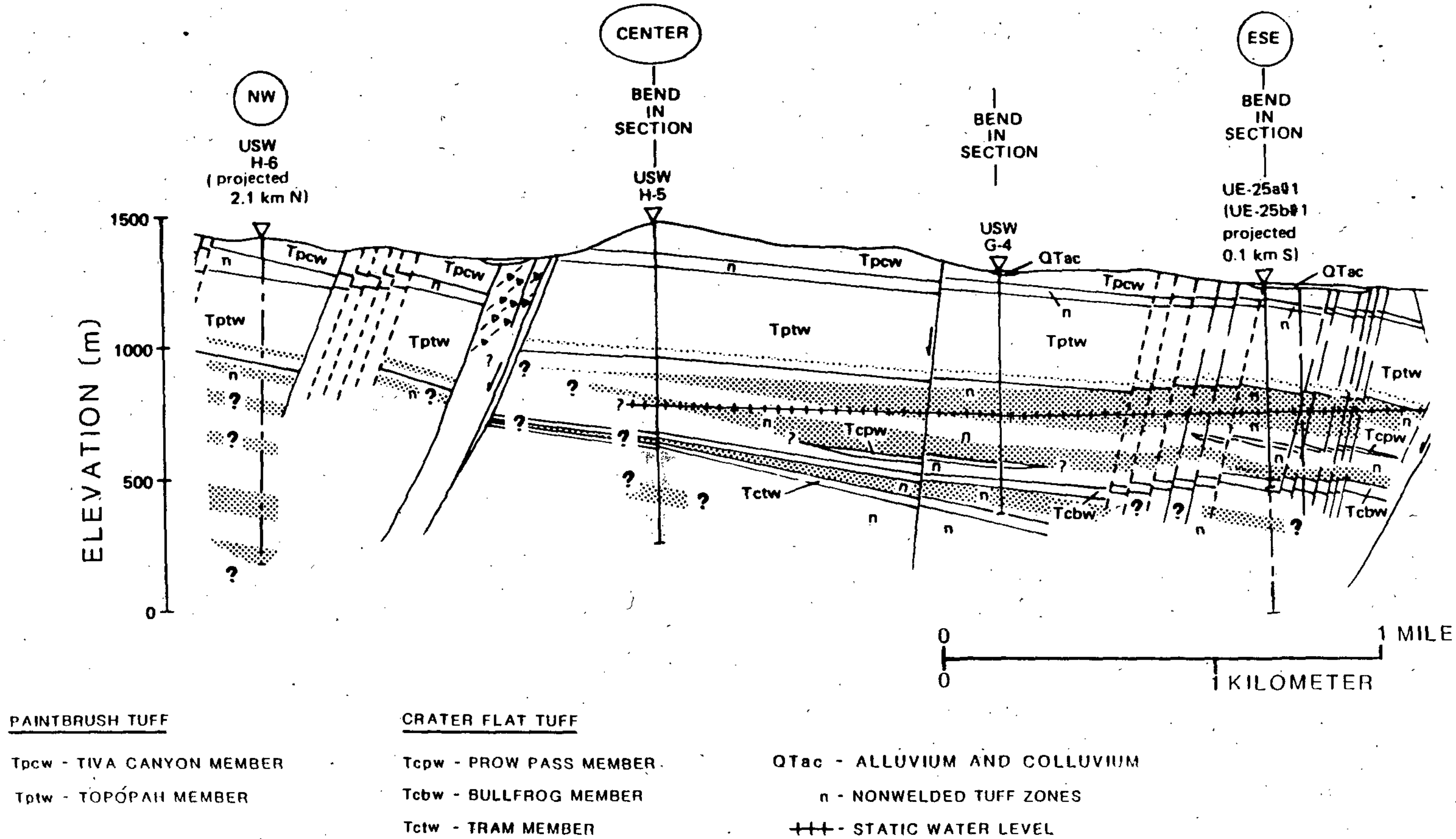

Figure 4-6. Major clinoptilolite-mordenite distributions (Bish and Vaniman, 1985), northwest-southeast cross section. Location of cross section is shown on Figure 4-4. Information on drillhole USW H-5 below 760 m is from Bentley et al. (1983), and information on the central part of the drillhole USW H-6 is from Craig et al. (1983).

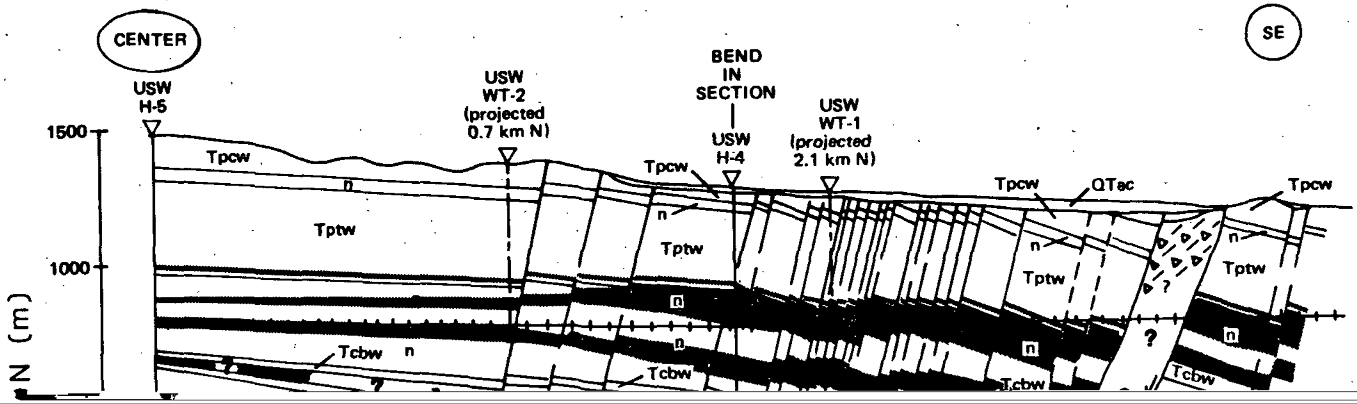
CENTER
SE
USW
H-5
USW
WT-2
(projected
0.7 km N)
BEND
IN
SECTION
USW
H-4
USW
WT-1
(projected
2.1 km N)
1500
1000
N (m)
Tpcw
Tptw
Tcbw
QTac
n

is consistently zeolitized throughout Yucca Mountain in the vicinity of the exploration block (Vaniman et al., 1984). In Figures 4-5, 4-6, and 4-7, it can generally be traced within the "n" unit between Tcpw and Tcbw.

4. Interval IV. This interval contains the poorly welded and bedded tuffs at the base of the Bullfrog Member compound cooling unit and at the top of an underlying cooling unit within the uppermost Tram Member. This interval also consists of clinoptilolite plus mordenite. In Figures 4-5, 4-6, and 4-7, it can generally be traced within the "n" unit below the Tcbw.

The weight percentages of zeolites in the rock in these intervals and the interval thicknesses are summarized in Table 4-4 for drillholes USW G-1, USW H-3, USW H-4, USW H-5, USW GU-3, USW G-3, USW G-4, UE-25a#1, and UE-25b#1

Table 4-4. Zeolitized intervals for Yucca Mountain[a,b]

Interval	USW G-1 SWL=577 m	UE-25a#1 UE-25b#1 SWL=471 m	USW G-4 SWL=541 m	USW H-4 SWL=519 m	USW H-5 SWL=704 m	USW H-3 SWL=754 m	USW GU-3 USW G-3 SWL=754 m
I: Above the lower Topopah Spring vitrophyre	Depth: 392-393 m (1 m thick) 15% cpt	Depth: 385-398 m (3 m thick) 7% cpt	Depth: 396-401 m (5 m thick) 10% (±12) cpt	Depth: 357-361 m (5 m thick) No samples	Depth: 485 m 10% cpt	Depth: 367-371 m (4 m thick) No samples	Depth: 360-364 m (4 m thick) Trace cpt
II: Base of the Topopah Spring unit, tuff of Calico Hills	Depth: 425-565 m (140 m thick) 52% (±17) cpt	Depth: 404-556 m (152 m thick) 67% (±6) cpt 17% (±20) mord	Depth: 420-545 m (125 m thick) 50% (±19) cpt 5% (±7) mord	Depth: 400-504 m (104 m thick) 63% (±13) cpt 8% (±12) mord	Depth: 584-594 m (10 m thick) 37%	Vitric (nonzeolitized)	Vitric (nonzeolitized)
III: Between the Prow Pass and the Bullfrog units	Depth: 622-706 m (84 m thick) 45% (±12) cpt 18% (±18) mord	Depth: 636-710 m (74 m thick) 60% cpt & mord	Depth: 600-682 m (82 m thick) 32% (±12) cpt 19% (±10) mord	Depth: 596-698 m (102 m thick) No samples	Depth: 665-689 m (34 m thick) 60% cpt	Depth: 549-610 m (61 m thick) 68% cpt	Depth: 557-613 m (56 m thick) 58% (±18) cpt
IV: Between the Bullfrog and the Tram units	Depth: 779-823 m (44 m thick) 37% (±6) cpt 15% (±11) mord	Depth: 863-890 m (27 m thick) 4% (±4) cpt 16% (±10) mord	Depth: 828-860 m (32 m thick) 9% (±9) cpt 35% (±33) mord	Depth: 765-774 m (9 m thick) No samples	No samples	Depth: 732-760 m (28 m thick) 52% (±17) cpt 18% (±13) mord	Depth: 776-822 m (46 m thick) 36% (±8) cpt

[a]Source: Vaniman et al. (1984).
[b]cpt = clinoptilolite and heulandite; mord = mordenite; and SWL = static water level (given in depth below surface). Percentages represent weight.

Present data on compositional variations in Yucca Mountain zeolites and clay minerals as a function of depth are summarized in the discussion that follows. The discussion includes consideration of the effects these variations in composition will have on rock properties. The zeolitized intervals I through IV, described earlier in this section and in Table 4-4, are used in the summary of sorptive zeolite compositions.

Sorptive zeolites (clinoptilolite, heulandite, mordenite). Representative compositions for the clinoptilolite-heulandite group minerals from Yucca Mountain are given in Table 4-5. Histograms showing the distribution of silicon-to-aluminum ratios in these minerals are presented in Figure 4-8; consistency in silicon-to-aluminum ratios may be one measure of consistency in sorptive behavior (Rundberg et al., 1985). Triangular plots showing vertical and lateral variations in exchangeable-cation ratios are presented in Figures 4-9 and 4-10. In zeolitized interval I, clinoptilolite and heulandite are calcium rich and have silicon-to-aluminum ratios ranging from 4.0 to 5.0 (Figure 4-8 shows some examples). The magnesium content of these zeolites is generally high, ranging from 0.6 to 1.5 percent magnesium oxide by weight. Using the thermal stability criteria of Mumpton (1960), Levy (1984a) determined that at least some of the calcium-rich clinoptilolite group minerals that occur at the top of the Topopah Spring vitrophyre belong to the heulandite structural group. Clinoptilolite-group zeolites from zeolitized intervals II through IV show more chemical diversity than those in interval I. In these deeper intervals, clinoptilolite compositions are subdivided into an eastern calcic suite of samples and a western alkalic suite of samples based on their exchangeable-cation contents (Figure 4-10). A transitional zone, found in drillholes USW G-4 and USW H-4, has characteristics intermediate between the eastern and western suites. The eastern clinoptilolites show a strong trend toward calcium enrichment with depth. In contrast, the western clinoptilolites become more sodium rich with depth. Silicon-to-aluminum ratios for both suites are similar (Rundberg et al., 1985), falling mostly between 4.0 and 5.2 and clustering around 4.6 (Figure 4-8). However, the silicon-to-aluminum ratios in eastern clinoptilolites have a bimodal distribution with a smaller population of ratios ranging from 2.8 to 3.6. This smaller population of low silicon-to-aluminum ratios correlates with the most calcic clinoptilolite compositions (approximately 70 mole percent calcium plus magnesium) in interval IV.

The other major zeolite type at Yucca Mountain is mordenite. Its chemistry is poorly known because individual mordenite crystals are fine grained and intergrown with other authigenic phases so that analysis by electron-microprobe and mineral-separation techniques is not feasible. The determination of mordenite compositions by bulk-rock techniques is difficult because monomineralic beds of mordenite are extremely rare at Yucca Mountain. In drillhole USW G-4, a bulk-rock sample containing more than 80 percent mordenite contains relatively equal amounts of sodium, potassium, and calcium (Broxton et al., 1986). These mordenites appear to be somewhat more sodic and less calcic than coexisting clinoptilolites.

The data from drillholes (Broxton et al., 1986) show that the first clinoptilolite-heulandites encountered below the repository horizon contain major amounts of calcium and minor amounts of potassium and sodium. Clinoptilolites of this composition will undergo cation exchange more readily than the potassium-rich clinoptilolites below in zeolitized interval II.

Table 4-5. Representative clinoptilolite analyses for Yucca Mountain[a] (page 1 of 2)

Mineral	Interval I		Intervals II, III, and IV and deeper occurring clinoptilolite: Calcic Suite, Eastern Yucca Mountain				Intervals II, III, and IV and deeper occurring clinoptilolite: Alkalic Suite, Western Yucca Mountain				
	Pah Canyon Member (G2-584)	Topopah Spring Member (H5-1666)	Tuff of Calico Hills (25p1-1250)	Prow Pass Member (25p1-1700)	Bullfrog Member (25b1-2879)	Tuff of Lithic Ridge (25p1-3330)	Tuff of Calico Hills (G1-1774)	Prow Pass Member (G3-1874)	Bullfrog Member (G3-2615)	Tram Member (G3-3589)	Tuff of Lithic Ridge (G3-4423)
	CONCENTRATION (WT%)										
SiO_2	65.6	65.5	68.6	67.1	56.1	60.6	68.1	68.2	63.9	65.1	65.3
TiO_2	0.00	0.02	0.00	0.00	0.00	0.00	0.00	0.00	0.00	0.00	0.00
Al_2O_3	13.8	13.3	12.4	12.9	16.9	16.0	12.2	11.9	11.7	11.4	12.6
[b]Fe_2O_3	0.00	0.00	0.00	0.00	0.05	0.00	0.00	0.00	0.00	0.51	0.12
MgO	1.47	0.86	0.07	0.32	0.22	0.08	0.09	0.00	0.00	0.12	0.22

Table 4-5. Representative clinoptilolite analyses for Yucca Mountain[a] (page 2 of 2)

	Interval I		Intervals II, III, and IV and IV and deeper occurring clinoptilolite								
			Calcic Suite, Eastern Yucca Mountain				Alkalic Suite, Western Yucca Mountain				
Mineral	Pah Canyon Member (G2-584)	Spring Member (H5-1666)	Calico Hills (25p1-1250)	Prow Pass Member (25p1-1700)	Bullfrog Member (25b1-2879)	Lithic Ridge (25p1-3330)	Calico Hills (G1-1774)	Prow Pass Member (G3-1874)	Bullfrog Member (G3-2615)	Tram Member (G3-3589)	Lithic Ridge (G3-4423)
(Al + Fe)/(2Mg + 2Ca + 2Ba + Na + K)											
	1.07	1.10	1.05	1.02	1.05	1.05	1.06	1.00	1.11	1.01	1.10
Si/(Al + Fe)											
	4.03	4.18	4.69	4.42	2.82	3.20	4.73	4.86	4.63	4.71	4.35
RELATIVE ABUNDANCE OF EXCHANGEABLE CATIONS (MOLE %)											
K	16	4	38	16	16	5	44	55	32	57	14
Na	4	4	22	31	16	17	45	27	52	35	59
Ca+Mg	80	92	40	53	68	78	11	18	16	8	27

[redacted]

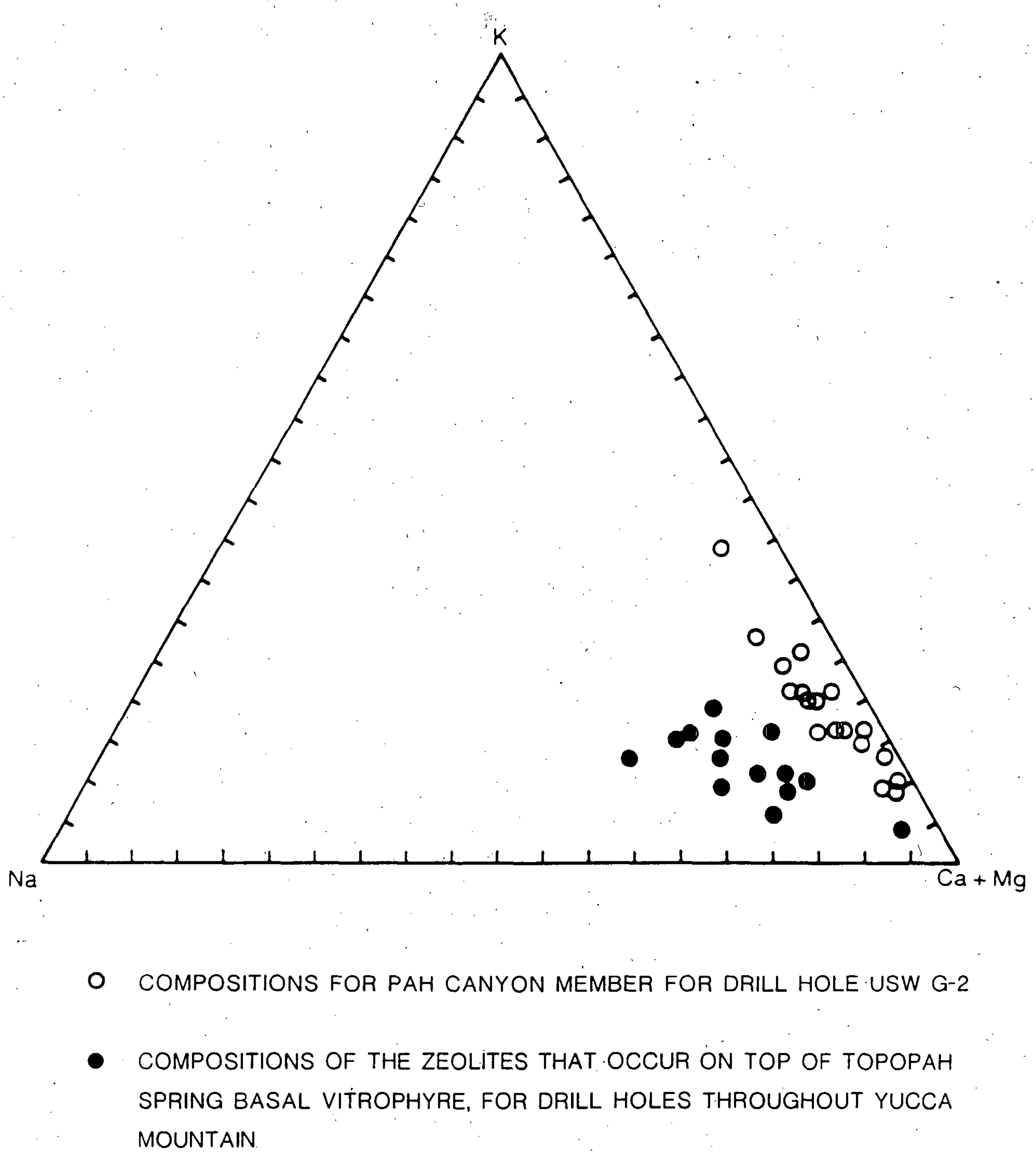

Figure 4-9. Triangular diagram showing the exchangeable-cation ratios in calcic-clinoptilolite and heulandite from zeolitized interval I at Yucca Mountain. Data plotted are in weight percent. Modified from Broxton et al. (1986).

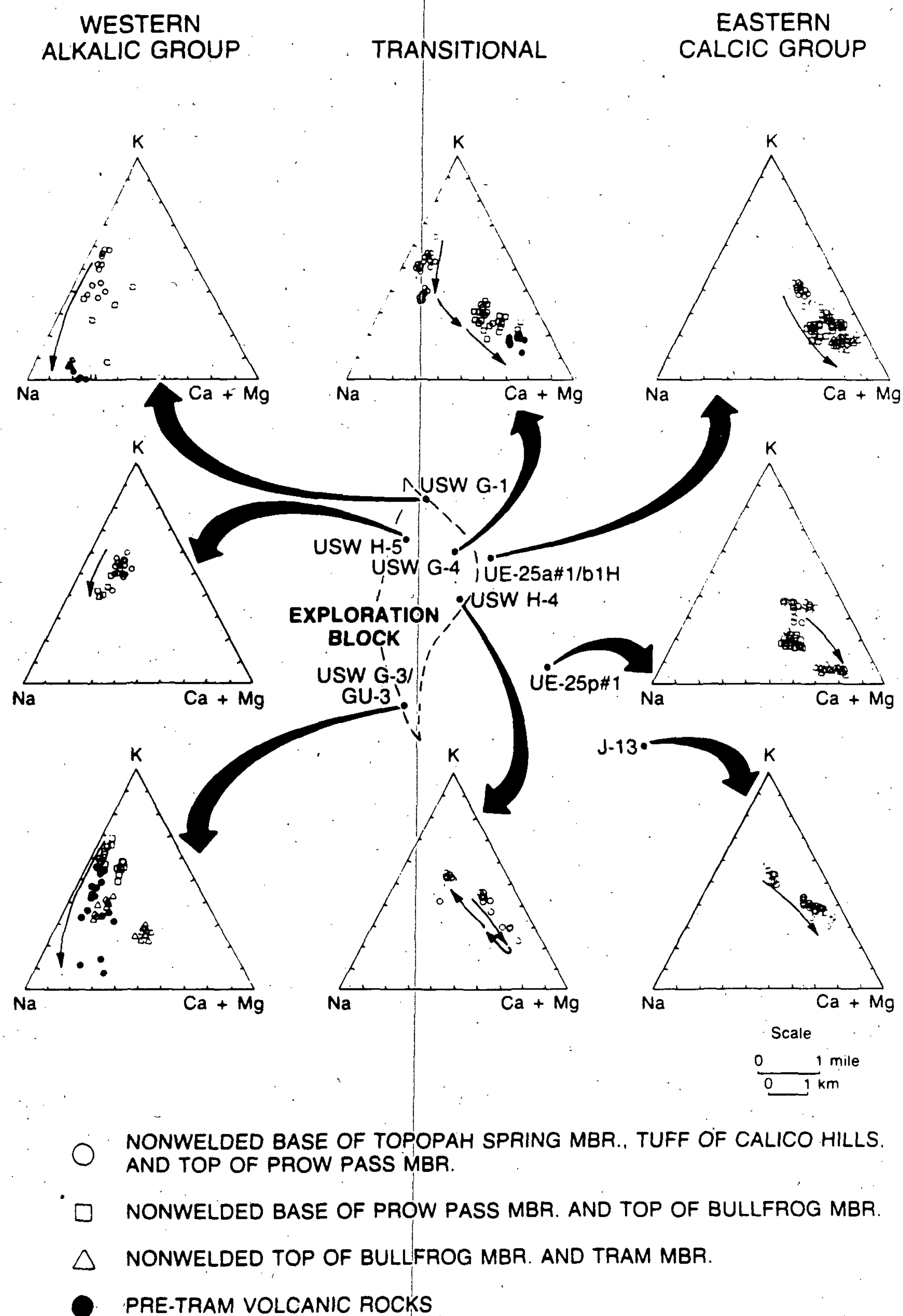
WESTERN ALKALIC GROUP
TRANSITIONAL
EASTERN CALCIC GROUP
K
Na
Ca + Mg
USW G-1
USW H-5
USW G-4
UE-25a#1/b1H
USW H-4
EXPLORATION BLOCK
USW G-3/ GU-3
UE-25p#1
J-13
Scale
0 1 mile
0 1 km
NONWELDED BASE OF TOPOPAH SPRING MBR., TUFF OF CALICO HILLS, AND TOP OF PROW PASS MBR.
NONWELDED BASE OF PROW PASS MBR. AND TOP OF BULLFROG MBR.
NONWELDED TOP OF BULLFROG MBR. AND TRAM MBR.
PRE-TRAM VOLCANIC ROCKS

In addition, the calcic clinoptilolites close to the repository will contract less at elevated temperatures than the deeper sodium-rich zeolites (Section 4.2.2), and fewer rock mechanical problems and permeability changes will be encountered because of this. Below the lower Topopah Spring vitrophyre, in the nonwelded base of the Topopah Spring Member and in the tuffaceous beds of Calico Hills, clinoptilolites contain subequal amounts of potassium and calcium. Below the Prow Pass Member the clinoptilolites are generally sodium rich, and sodium is more easily exchanged than calcium or potassium. Sodium-rich clinoptilolites contract appreciably when temperatures are elevated (Bish, 1985), but these zeolites only occur beyond the anticipated thermally disturbed zone and should pose no mechanical problems. Plans to test this are discussed in Section 8.3.1.3.2.

Smectites. Smectites are widespread throughout the units underlying the Topopah Spring Member (Bish, 1987) and, therefore, occur along possible flow paths. Although smectite abundances are typically 1 to 10 percent, amounts as high as 50 percent occur in some units (Figures 4-1 through 4-3). The sorption properties of smectites are not as strong a function of composition as they are for zeolites, but smectite dehydration under slightly elevated temperatures (up to 100°C) is determined largely by composition (Bish, 1981). In addition, information on geologic processes in the past can be obtained from data on smectite compositions and structures (Bish, 1987). This information can aid in the prediction and understanding of the effects of future elevated temperatures.

Smectites in the host rock unit and along flow paths into the saturated zone have mixed potassic, sodic, and calcic interlayers. These cations are easily exchanged by many small and large cations and complexes. There is a minor increase in the potassium content of smectites with depth throughout most of the exploration block (Caporuscio et al., 1982). However, potassium contents of the smectites between the host rock and the Tram Member are still low enough so that the sorptive properties of the smectites should not significantly differ from the smectites at shallower depths. Clays below the Tram Member include a higher content of illite, which will be less sorptive. Only in the deepest rocks at the northern end of the repository block (drillhole USW G-2) are the smectites significantly transformed to illite (Caporuscio et al., 1982; Bish, 1987). In the bulk of the repository block, the smectites retain their highly sorptive nature. As a result of their minor compositional variations, the smectite sorptive properties should not vary significantly near a Yucca Mountain repository. Plans to test this are discussed in Section 8.3.1.3.

(drillhole USW G-3) do not show evidence of this alteration and remain fully

(1982), Vaniman et al. (1984), Bish and Vaniman (1985), and Broxton et al. (1986). Glass exists in the vitrophyre in the lower Topopah Spring Member and in parts of the tuffaceous beds of Calico Hills (Figures 4-1 and 4-2). Alteration of the glass originally present in the tuffaceous beds of Calico Hills in the northeastern part of Yucca Mountain has led to the extensive development of clinoptilolite (Section 4.1.1.3). The persistence of glass in the southwest area of Yucca Mountain may be due to the lack of water for hydration because the glasses are above the water table. However, since considerable pore water is present, the general lack of clinoptilolite formation may also be due to lack of reaction because of low temperature. There is a possibility that glass would react to form appreciable clinoptilolite in response to moderate heating from the repository, or to increased hydration that would result from a rise in the water table. Future glass stability studies are outlined in Section 8.3.1.3.3.

4.1.2 GROUND-WATER CHEMISTRY

The composition of water in the Yucca Mountain exploration block is an important parameter for evaluating the suitability of the site for the containment and isolation of radioactive waste. The water composition will affect the rate at which the waste containers corrode, the leach rate of the waste form, and the rate of radionuclide transport to the accessible environment. A reference ground water (i.e., water from well J-13) similar in composition to the water of Yucca Mountain is needed to conduct transport and retardation experiments.

Because the composition of ground water is controlled by a number of variables both internal and external to the repository horizon, it is necessary to define the range of ground-water compositions, in both the saturated and the unsaturated zones, from the exploratory block to the accessible environment. In addition, it is necessary to identify the main factors that would determine how changes in the natural (e.g., increased recharge) and man-induced conditions would affect the ground-water compositions.

At present, the only water available for chemical analysis has come from saturated-zone wells on and near Yucca Mountain. When the exploratory shafts are constructed, water from the pores in unsaturated tuff, any water flowing in fractures in unsaturated tuff, and water from any perched water zones in Yucca Mountain will be sampled, where possible, and analyzed. Plans for further analyses of the saturated-zone ground water can be found in Section 8.3.1.2. The remainder of this section discusses ground water from the saturated zone. Plans for studying the unsaturated-zone water chemistry can be found in Section 8.3.1.2.2.

4.1.2.1 <u>General description of the hydrochemistry</u>

Analyses of ground water from drillholes that penetrate the host rock and surrounding units in the area of the exploration block indicate that they are principally sodium bicarbonate waters (Benson et al., 1983; Ogard and Kerrisk, 1984) with low contents of total dissolved solids (200 to 400 mg/L).

However, water from the carbonate aquifer (drillhole UE-25p#1) contains over 1,000 mg/L total dissolved solids. Tables 4-6 and 4-7 summarize the geochemical data reported on ground-water samples from Yucca Mountain and its vicinity. The data are consistent with the data reported in Section 3.9.1.3, but include additional species (dissolved iron, manganese, aluminum, nitrite, nitrate, and oxygen) not reported there. The analytical techniques and sampling procedures by which these data were obtained are reported by Ogard and Kerrisk (1984). The locations of wells are shown in Figure 4-11.

4.1.2.2 <u>Major inorganic content</u>

The content of major and minor inorganic constituents of ground water from Yucca Mountain and vicinity are listed in Tables 4-6 and 4-7 and are discussed in the following paragraphs.

The data presented in Tables 4-6 and 4-7 are representative of the chemistry of the ground waters at Yucca Mountain. Kerrisk (1987) is a more recent review of the water chemistry at Yucca Mountain and in the surrounding area. This report references and compiles hundreds of analyses representing [illegible] suggests that the aqueous silica activity in a particular horizon will remain high until most, if not all, of the cristobalite has converted to quartz. The silica-activity evolution is of particular concern because silica activity appears to be important in controlling the stability of clinoptilolite (Keith et al., 1978).

Clays are present in small quantities in the host rock and occur throughout Yucca Mountain as late-stage alteration minerals (Caporuscio et al., 1982). Clays are also observed as alteration products of Topopah Spring tuff in hydrothermal experiments (Section 7.4.1.3). On the basis of these observations and on reaction-path studies of glass alteration (Kerrisk, 1983) it seems possible that clays may be continuing to crystallize in Yucca Mountain. The stability of clays is of concern because they are highly sorptive minerals. At present it seems likely that the amount of clays will remain constant or increase in Yucca Mountain. The possibility of clay dehydration or breakdown due to repository-induced heating is discussed in Section 4.2.2.

The smectites at or above the stratigraphic level of the Tram Member in Yucca Mountain have interlayer water that can be driven out with minor temperature increases or with minor changes in the partial pressure of water, causing a decrease in volume (Bish, 1981). This volume reduction is reversible at low temperatures. The implications of irreversible collapse are discussed in Section 4.2.2.

Below the host-rock horizon, successive zones of glass, heulandite and smectite, clinoptilolite, analcime, and authigenic albite are found in addition to devitrified zones dominated by alkali feldspar and silica phases. The stability of clinoptilolite is of particular concern because it has been identified as an important sorptive phase (Section 4.1.3.3).

Smyth (1982) has summarized the diagenetic zones beneath Yucca Mountain. This diagenesis begins with unaltered glass. Unaltered glass occurs in many rocks above the water table, including the vitrophyre of the host rock (where devitrification is not extensive). The next zone contains clinoptilolite or mordenite or both (Calico Hills and the upper zeolitic Crater Flat Tuff). Below these zeolites, analcime occurs, replacing clinoptilolite and mordenite. Finally, authigenic albite is typical of the deepest tuff units examined. This generalized zonation can be seen in Figures 4-1 and 4-2.

There are varying hypotheses to explain this diagenetic zonation. Smyth and Caporuscio (1981) give a plot of sodium-ion concentration versus temperature appropriate for the zeolite transition in this diagenetic sequence. Increases in sodium concentration appear to decrease the temperatures at which these reactions occur. Because the present ground water has a low sodium content (37 to 171 mg/L, Ogard and Kerrisk, 1984), the analysis of Smyth (1982) would predict that the clinoptilolite-to-analcime transformation, if it occurred, would be expected at temperatures of about 100 to 120°C.

There are, however, other factors that must be considered in this analysis. First, the stoichiometry of clinoptilolite and analcime does not suggest that the concentration of the sodium ion should affect the relative stability of the two phases. Second, the transition from clinoptilolite to analcime is also characterized by the disappearance of cristobalite, which suggests that silica activity with analcime is lower than that with clinoptilolite. Because silica evolves in the transformation of clinoptilolite to analcime, a lowering of the silica activity would move the system toward analcime stability relative to clinoptilolite. Reaction-path modeling for temperatures up to 175°C (Kerrisk 1983) indicates that increase in temperature alone does not account for the transition from clinoptilolite to analcime; rather, this transition can probably be accounted for by the change in silica activity that occurs with the change from cristobalite to quartz saturation. Field observations (Keith et al., 1978) also indicate that silica activity, rather than temperature, may be a factor controlling the transformation of clinoptilolite to analcime. Keith et al. (1978) observed clinoptilolite and analcime in drillhole Y-8 in Yellowstone National Park. Clinoptilolite was observed in a temperature interval from about 70°C to slightly above 150°C. However, throughout this interval, clinoptilolite zones were interlayered with analcime-bearing zones, indicating that temperature was not a controlling factor in determining whether clinoptilolite or analcime was present. There was, however, an excellent correlation between the presence of clinoptilolite and that of cristobalite and between analcime and quartz (Figure 4-1), suggesting that silica activity was the controlling variable in determining the presence of clinoptilolite or analcime.

The observations on which the conclusions of Smyth (1982) were based probably reflect the effects of temperature on the kinetics of the transition from cristobalite to quartz more than an equilibrium temperature for the transformation of clinoptilolite to analcime. The apparent dependence of transition temperature on the sodium content of the solution may arise from two sources. The generally higher pH high-sodium solutions may increase the rate of transition from cristobalite to quartz. Also, as the sodium concentration increases, the activity of water is lowered by the increasing salinity of a solution, which would favor formation of the less hydrous phase, analcime.

Thus, it seems likely that the stability of clinoptilolite in Yucca Mountain is determined largely by the silica activity. If that activity in a particular horizon is at or above cristobalite saturation, the clinoptilolite is probably stable to at least 150°C. If clinoptilolite breaks down after the emplacement of waste in a repository at Yucca Mountain, it will probably be because repository heating will have increased the rate of cristobalite conversion to quartz. Plans to obtain the information to assess the likelihood of cristobalite transformation are discussed in Section 8.3.1.3.

The effects of composition on thermal expansion and thermal stability have been determined for several cation-exchanged clinoptilolites (Bish, 1984). It is known that sodium- and potassium-rich clinoptilolites are stable to higher temperatures than the calcium-rich clinoptilolites (Shepard and Starkey, 1966) that commonly occur above the basal vitrophyre in the Topopah Spring Member. However, the potassium-rich clinoptilolites in the base of and slightly below the Topopah Spring Member contract less with increased temperature than do the sodium-rich clinoptilolites farther along flow paths (Bish, 1984).

Glass is another phase in Yucca Mountain that is certainly metastable. The distribution and compositions of glass are discussed by Caporuscio et al.

Table 4-6. Element concentrations in ground water from the vicinity of Yucca Mountain

Well[b]	Field pH	Concentrations[a] (mg/L)								
		Ca	Mg	Na	K	Li	Fe	Mn	Al	Si
USW VH-1[c]	7.5	10	1.5	80	1.9	0.090	--[d]	--	--	23
USW H-6	7.4	5.5	0.22	74	2.1	0.10	0.12	0.04	0.12	20.0
USW H-3	9.4	0.8	0.01	124	1.5	0.22	0.13	0.01	0.51	16.9
USW H-5	7.1	1.1	0.03	54	2.3	0.04	0.01	--	0.17	17.4
USW G-4	7.1	9.2	0.15	56	2.5	0.08	0.04	0.02	0.02	19.6
USW H-1[c]	7.5	6.2	<0.1	51	1.6	0.04	--	--	--	19
USW H-4	7.4	10.8	0.19	84	2.6	0.16	0.03	0.005	0.04	25.9
UE-25b#1	7.7	19.7	0.68	56	3.3	0.28	0.04	0.004	0.03	31.5
UE-25b#1[e]	7.2	18.4	0.68	46	2.5	0.30	0.69	0.36	0.04	28.7
UE-25b#1[f]	7.3	17.9	0.66	37	3.0	0.17	0.08	0.07	0.06	28.8
J-13	6.9	11.5	1.76	45	5.3	0.06	0.04	0.001	0.03	30.0
UE-29a#2	7.0	11.1	0.34	51	1.2	0.10	0.05	0.03	0.04	25.8
J-12[c]	7.1	14	2.1	38	5.1	-	-	-	-	25
UE-25p#1[g]	6.7	87.8	31.9	171	13.4	0.32	<0.1	<0.01	0.1	30

[a]Concentrations from Ogard and Kerrisk (1984) unless otherwise noted. All samples are integral water samples unless otherwise noted.
[b]See Figure 4-11 for locations.
[c]Data from Benson et al. (1983).
[d]--indicates the element was not detected.
[e]Bullfrog zone, 4th day of pumping.
[f]Bullfrog zone, 28th day of pumping.
[g]From carbonate aquifer.

Table 4-7. Anion concentrations and other measurements for ground water from the vicinity of Yucca Mountain

Well[b]	Concentrations[a] (mg/L)								
	F^-	Cl^-	SO_4^{2-}	HCO_3^-	NO_2^-	NO_3^-	O_2	Detergent	Eh[c]
USW VH-1[d]	2.7	11	44	167	--	--	--	--	--
USW H-6	4.1	7.7	27.5	--	--[e]	5.3	5.6	--	395
USW H-3	5.4	8.3	31.2	245	<0.10	0.2	<0.1	<0.02	-123
USW H-5	1.3	5.7	14.6	--	--	8.6	6.3	<0.005	353
USW G-4	2.4	5.5	15.7	--	--	5.5	6.4	--	402
USW H-1[d]	1.0	5.8	19	122	--	--	--	--	--
USW H-4	4.5	6.2	23.9	--	--	4.7	5.8	>2	216
UE-25b#1	1.2	7.1	20.6	--	--	0.6	1.8	--	220
UE-25b#1[f]	1.5	9.8	21.0	--	0.5	2.2	<0.1	2.7	-18
UE-25b#1[g]	1.2	6.6	20.3	--	--	4.5	1.8	0.02	160
J-13	2.1	6.4	18.1	143	--	10.1	5.7	--	--
UE-29a#2	0.56	8.3	22.7	--	--	18.7	5.7	--	305
J-12[d]	2.1	7.3	22	119	--	--	--	--	--
UE-25p#1[h]	3.5	37	129	698	--	<0.1	--	<0.2	360

[a]Concentrations from Ogard and Kerrisk (1984) unless otherwise noted. All samples are integral samples unless otherwise noted.
[b]See Figure 4-11 for location.
[c]mV versus H_2 electrode.
[d]Data from Benson et al. (1983).
[e]--indicates the element was not detected.
[f]Bullfrog zone, 4th day of pumping.
[g]Bullfrog zone, 28th day of pumping.
[h]From carbonate aquifer.

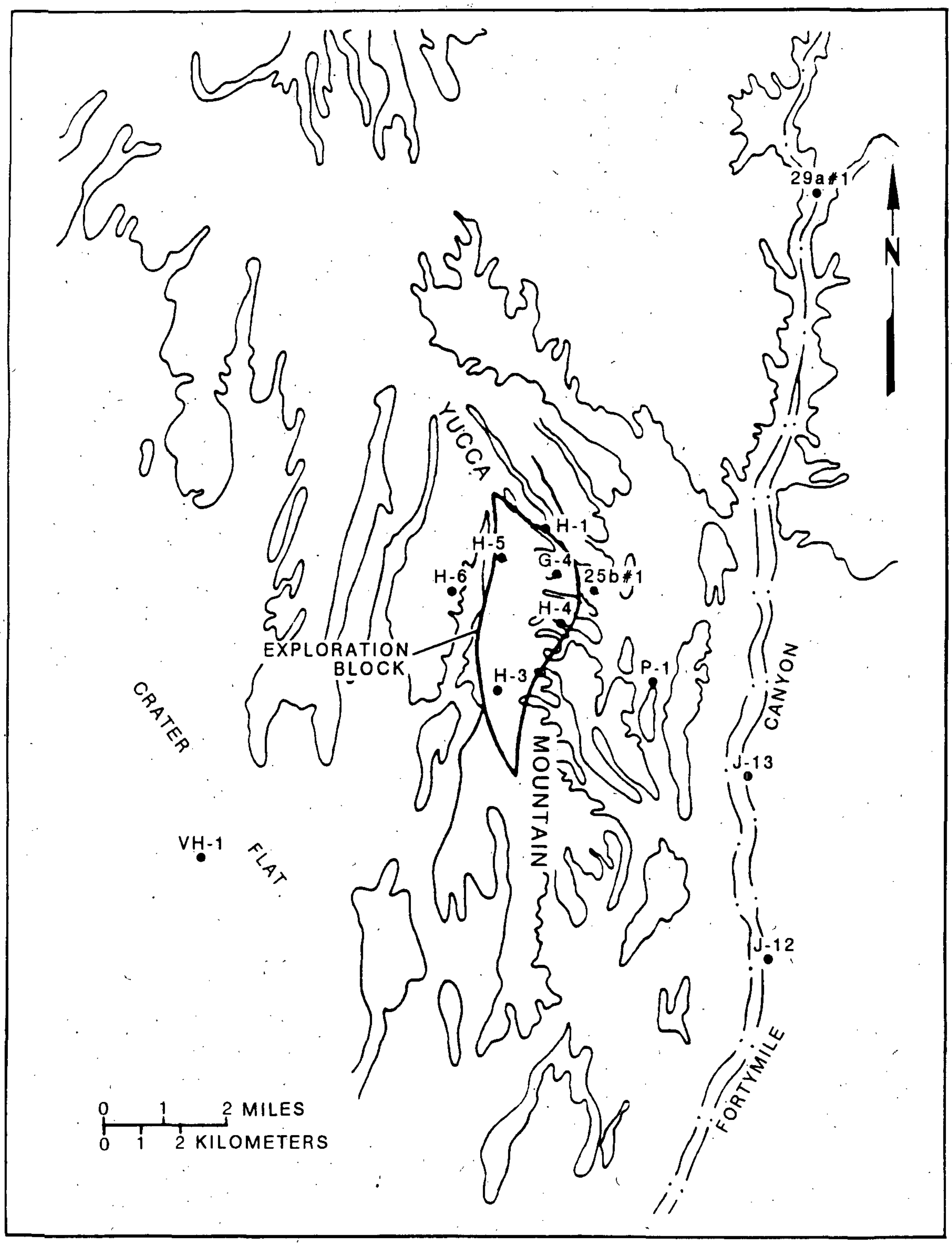

Figure 4-11. Selected drillhole and well locations on and near Yucca Mountain exploration block (the names of the wells and drillholes have been shortened for clarity; for example, drillhole USW H-6 is listed as H-6 and drillhole UE-25p#1 as P-1, etc.). Modified from Ogard and Kerrisk (1984).

[redacted]

The concentrations of iron and manganese are generally low (Table 4-6). The elevated concentrations in drillhole UE-25b#1 after the fourth day of pumping may reflect contaminants from the drilling operation because the concentrations dropped down to more typical values after 28 days. Both iron(III)/iron(II) and manganese(IV)/manganese(II) as well as nitrate/nitrite have been considered as oxidation-reduction (redox) couples that reflect the redox potential of the ground waters (Rundberg et al., 1985). Analytical data are available only for the nitrate/nitrite couple in drillhole UE-25b#1 water. The redox potential, Eh, calculated from these data (100 to 400 mV) is substantially different from the Eh measured in this water with a platinum electrode (80 to 170 mV) (Rundberg et al., 1985). Such differences are commonly observed in ground water (Lindberg and Runnells, 1984) and may indicate a lack of equilibrium due to slow reaction kinetics among the redox couples in the water. The positive Eh values and dissolved-oxygen content of waters listed in Table 4-7 indicate that most of the waters are oxidizing. The reducing character of the drillhole UE-25b#1 water collected on the fourth day after pumping was initiated probably reflects an initial disturbance of the producing horizon due to completion of the drillhole. The reducing character of the drillhole USW H-3 water has not been fully explained but may reflect a reduction of recharge waters by organics during the last pluvial (Ogard and Kerrisk, 1984).

The anionic constituents of the ground water show a relatively uniform distribution in all the wells, with about 80 percent bicarbonate and the remainder as sulfate and chloride (usually present in nearly equal molar concentrations) and fluoride (in varying concentrations). The carbonate ion is a major complexing agent for the actinide elements, with the hydroxide ion (Section 4.1.3.4) and the fluoride ion being of less importance under oxidizing conditions (Ogard and Kerrisk, 1984).

Spatial variations in ground-water composition are implicit in Tables 4-6 and 4-7 because the ground waters listed are from wells surrounding the repository block. Overall, there is only minor variation in ground-water compositions in and adjacent to Yucca Mountain.

4.1.2.3 Trace elements

The trace elements detected in Yucca Mountain ground water are barium, bromine, lithium, phosphorus, strontium, titanium, and vanadium. The observed ranges in concentration (in mg/L) are less than 0.001 to 0.011 for barium, less than 0.2 to 14.5 for bromine, 0.04 to 0.95 for lithium, less than 1.2 for phosphorus, less than 0.001 to 0.07 for strontium, less than 0.012 to 0.03 for titanium, and less than 0.004 to 0.03 for vanadium (Daniels et al., 1983; Ogard et al., 1983b).

Because lithium was added to the drilling fluid as a tracer to monitor contamination of ground water by the fluid (Daniels et al., 1983), the high

4.1.2.4 Organic content

The in situ organic contents of the waters from drillhole UE-25b#1 and well J-13 were measured by Means et al. (1983). The total organic carbon contents were 0.14 ± 0.05 mg/L in well J-13 water and 0.58 ± 0.06 mg/L in drillhole UE-25b#1 water, respectively. The lower carbon content in well J-13 water is probably representative of the in situ content because the well is a producing well for the Nevada Test Site and all drilling fluids have been removed by extensive pumping. Because of the low concentrations, little can be said about the individual organic compounds other than that organics with high molecular weight (higher than 1,000) constitute 50 percent of the organics present in J-13 water and 33 percent in UE-25b#1 water. The low organic content in the saturated zone suggests that complexing of waste elements americium, neptunium, plutonium, and uranium with naturally occurring organic ligands will be insignificant.

4.1.2.5 Dissolved gas

Measurements of the concentrations of dissolved gases in Yucca Mountain ground waters are very limited. The presence of carbon dioxide in saturated-zone water is indicated by the change in pH (from 7 to 8.5) of ground water that is pumped from deep wells and allowed to stand at atmospheric pressure. A change in dissolved carbon dioxide from $10^{-2.5}$ to the normal $10^{-3.5}$ atmospheres would explain this shift in pH (Daniels et al., 1982). A direct measurement of the carbon dioxide content of the lowest zone of well UE-25p#1

Table 4-8. Background radioactivity[a]

Number of samples analyzed	Radionuclide	Radioactivity concentration 10^{-9} µCi/ml Maximum	Minimum	Average
5	H-3	8	<7	<8
1	Sr-89	<2	<2	<2
1	Sr-90	<0.9	<0.9	<0.9
1	Ra-226	0.067	0.067	0.067
1	U-234	1.7	1.7	1.7
1	U-235	<0.02	<0.02	<0.02
1	U-238	0.22	0.22	0.22
1	Pu-238	<0.03	<0.03	<0.03
1	Pu-239	<0.04	<0.04	<0.04

[a]Data extracted from Table 8, EPA (1976) for five water samples collected

of radionuclides on colloids and particulates are outlined in Section 8.3.1.3.4.

4.1.2.8 Temperature and pressure

The temperatures in drillholes and wells on and near Yucca Mountain are shown in Figure 4-13. The temperature gradient varies between approximately 20 and 40°C/km at depths of less than or equal to 3 km. The variance suggests that the temperature in the repository horizon should be 25 to 35°C and it also provides a baseline range of temperatures for modeling the perturbation of the temperature gradient produced by the emplacement of the waste. This topic is discussed in Section 1.7 and the discussion here is taken from Sass and Lachenbruch (1982).

Because the repository horizon is in the unsaturated zone, the pressure on ground water in this horizon will be close to atmospheric at the appropriate elevation above sea level. Below the water table and along pathways to the accessible environment, the pressure of the ground water will correspond roughly to depth below the water table.

4.1.2.9 Mineralogical controls on water composition

The composition of ground water in the exploratory block and between the repository block and the accessible environment is determined by various factors, including the composition of water infiltrating from the surface, the composition of saturated zone water upgradient from the repository block, and interactions between ground water and the rocks through which it may flow. Ground-water interactions with rock and models describing these interactions are discussed in this section. These interactions between ground water and rock consist primarily of the dissolution of primary silicate phases contained in the volcanic rocks, the precipitation of secondary phases, and sorption and ion-exchange reactions with primary and secondary phases. Primary silicate phases include volcanic glass and various mineral types formed at high temperatures (higher than 500°C). Secondary phases include minerals such as clays, carbonates, and zeolites as well as amorphous solids such as amorphous silica and semiamorphous oxides (e.g., manganese-iron, oxyhydroxides). The models describing ground-water interactions with rock have not considered precipitation and ion-exchange reactions with these minerals.

Because reactions between ground water and silicate phases are generally slow at the temperatures and water-flow rates likely to prevail in rocks between the repository block and the accessible environment, models that assume chemical equilibrium between ground waters and host rocks may not be appropriate. Models of ground-water interactions with rock must incorporate reaction with rock kinetics. Because reaction kinetics cannot be reliably predicted on the basis of theoretical considerations alone, experimental data on the kinetics of appropriate interacting systems (ground water and rock) are required (Chapter 7 and Section 8.3.1.3.3).

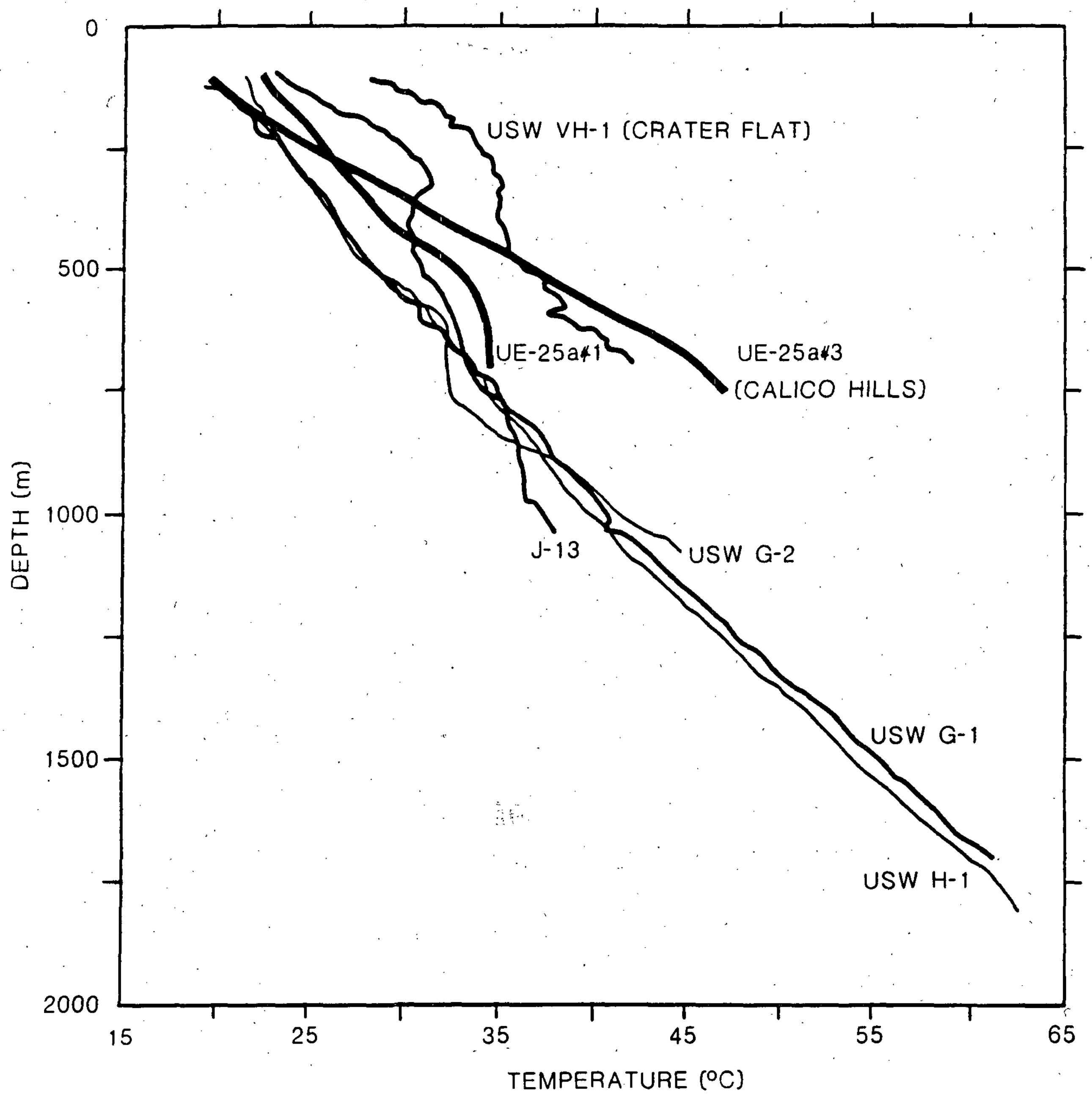

Figure 4-13. Plot of temperature versus depth in drillholes deeper than 600 m for Yucca Mountain and nearby areas. Modified from Sass and Lachenbruch (1982).

White and Claassen (1979; 1980) have presented experimental data and discussed mechanisms for the dissolution of volcanic glass by water. Their glass samples were obtained from the Timber Mountain Tuff exposed on Rainier Mesa at the Nevada Test Site. White et al. (1980) presented experimental data on the dissolution of glassy and nonglassy tuffs from Rainier Mesa. Using the data, they derived rate constants that were used to extrapolate the experimental results to longer time scales. White et al. (1980) concluded that the composition of interstitial and fracture waters obtained from the Rainier Mesa area could be explained on the basis of a glass-dissolution model. However, the model does not explain all the water compositions obtained by White et al. (1980), such as the highly sodic waters. In addition, the model does not attempt to explain the detailed variations in the pH and the Eh of the ground water. These two parameters are particularly important to radionuclide-transport calculations. Nonetheless, two important aspects of these studies are clear: (1) water composition varies with stratigraphic position in the tuffs of Rainier Mesa, suggesting local control, and (2) experimental data suggest that the variations are the result of dissolution of the tuffs through which the water flows.

The overall similarity of the rock types and alteration minerals in Yucca Mountain and Rainier Mesa (Byers et al., 1976) suggests that the controls on ground-water compositions in these two areas might be similar. This is supported by the overlap in the relative cation concentrations of Rainier Mesa and Yucca Mountain ground waters shown in Figure 4-12. Note that the overlap does not extend to ground water from the Paleozoic carbonate aquifer (drillhole UE-25p#1) beneath Yucca Mountain (Figure 4-12). The concentrations of other cations, anions, and uncharged species in Yucca Mountain waters also overlap those in Rainier Mesa waters.

Although the work of White and Claassen (1979, 1980) has provided important data on the possible influence of glass dissolution on ground-water compositions in tuffaceous aquifers, further work is required to adequately understand the controls on the composition of Yucca Mountain saturated- and unsaturated-zone waters. This additional work is discussed in Section 8.3.1.3.

4.1.2.10 Reference ground-water composition

Many of the processes taking place in the transport and retardation of waste elements along pathways from the repository to the accessible environment will be investigated in a laboratory and then the results will be used in modeling the entire pathway. To conduct such experiments, a reference ground water or ground waters that will represent ground-water conditions that will be experienced along such a pathway is needed. The reference ground water for the Yucca Mountain Project was chosen on the basis of meeting the following criteria:

1. It should be readily available because many laboratory experiments will use the reference ground water.

2. It should have a composition that is representative of compositions estimated for the interstitial and fracture waters in the Topopah

Spring Member tuff in the unsaturated zone (the potential repository horizon).

3. It should have a composition that is representative of ground waters along the potential flow paths away from the repository.

4. It should be a natural ground water rather than synthetic water.

The ground water from well J-13 has been chosen as best meeting these requirements.

Well J-13 is a producing well located in Jackass Flats southeast of the Yucca Mountain site (Figure 4-11) which has been pumped since 1962. Because of the large amount of water produced to date, the well should be clear of any drilling fluids that may have been used in the original drilling. The main producing zone in well J-13 is in the Topopah Spring Member of the Paintbrush Tuff, which corresponds to the potential repository horizon at Yucca Mountain. This aspect of well J-13 water makes it a useful reference water.

suction. Much of the smallest diameter porosity is intracrystalline pore space in the zeolites and clay minerals. This is particularly true in the nonwelded zeolitic tuff. The intracrystalline porosity of the zeolite clinoptilolite is about 36 percent based on the crystallographic structure. Zeolitic tuff, with 80 to 90 percent clinoptilolite, has a total porosity of 40 to 50 percent, and hence, in zeolitic tuff more than half the porosity is

Sorptive mineral phases, particularly zeolites and clays, along potential flow paths are expected to delay the rate at which radionuclides are released to the accessible environment. Flow paths from the repository to the saturated zone are through bedded tuff at the bottom of the Topopah Spring Member and through the tuffaceous beds of Calico Hills, both of which contain significant quantities of zeolites and clays (Section 4.1.1.3). Other formations that might be part of the flow path are the Prow Pass, the Bullfrog, and the Tram members of the Crater Flat Tuff; zones containing zeolites and clays in variable abundances are present in these units (Section 4.1.1.3).

Precipitation processes (i.e., solubility) will limit the concentration of radionuclides in water that moves from the repository toward the accessible environment. Solubility depends on the composition of the solution; that is, formation of complexes can retain species in solution in greater amounts than would otherwise exist. Yucca Mountain ground water is primarily a sodium-bicarbonate water (Section 4.1.2.1); carbonate, bicarbonate, and hydroxyl are the most prevalent anions that form complexes with radionuclide effects that would be analogous to matrix diffusion and fracture flow. The columns are run at flow rates that do not exceed mass transfer kinetics and under chemical conditions (i.e., controlled pH, complexing agents, etc.) which ensure well-behaved adsorption. Thus, for column chromatography the coupling between chemistry and flow is simple and can be successfully modeled. The transport of tracers in geohydrologic systems, however, is not simple and simplifying assumptions must be tested by laboratory and field

A general criterion for the importance of the various radionuclides in waste in terms of the EPA standards can be obtained from the ratio of the quantity of the radionuclide in the waste to the EPA release limit for that radionuclide, where both are expressed in curies per 1,000 MTHM. Tables 4-9 through 4-11 list radionuclides ordered by this ratio along with the ratios for PWR spent fuel, PWR HLW, and DHLW, respectively (Kerrisk, 1985). Radionuclides near the top of the lists in the tables have larger values of this ratio. Thus, larger fractions of these radionuclides must be contained by the repository to meet the EPA standard. At 100 yr after discharge from the reactor, isotopes of cesium, strontium, americium, and plutonium head the lists. In the 1,000- to 10,000-yr range, isotopes of the actinides (americium, plutonium, neptunium, and uranium) head the lists. By 100,000 yr after discharge, the lists are headed by actinides as well as radionuclides in the actinide decay chains, but a few other radionuclides, such as isotopes of nickel (present in subassembly hardware) and zirconium (present as a fission product and cladding activation product), are near the top.

Table 4-9. Radionuclides ordered by ratio of inventory to U.S. Environmental Protection Agency limit for pressurized water reactor spent fuel for various decay times[a]

1×10^2 yr		1×10^3 yr		1×10^4 yr		1×10^5 yr	
Am-241	3.8×10^4	Am-241	9.0×10^3	Pu-239	2.4×10^3	Pu-239	1.8×10^2
Pu-238	1.1×10^4	Pu-240	4.8×10^3	Pu-240	1.8×10^3	Th-230	1.0×10^2
Cs-137	1.0×10^4	Pu-239	3.1×10^3	Am-243	6.7×10^1	U-234	1.6×10^1
[b]Ba-137m	9.8×10^3	Am-243	1.6×10^2	U-234	1.9×10^1	Pu-242	1.5×10^1
Sr-90	6.8×10^3	U-234	2.0×10^1	Pu-242	1.7×10^1	Np-237	1.1×10^1
[c]Y-90	6.8×10^3	Pu-242	1.8×10^1	Th-230	1.7×10^1	[d]Ra-226	1.0×10^1
Pu-240	5.3×10^3	[e]Np-239	1.6×10^1	Np-237	1.2×10^1	U-233	4.1
Pu-239	3.1×10^3	C-14	1.4×10^1	[e]Np-239	6.7	U-236	4.0
Pu-241	1.0×10^3	Np-237	1.0×10^1	Ni-59	4.8	Th-229	3.7
Cm-244	3.3×10^2	Pu-238	9.7	C-14	4.6	U-238	3.2

Table 4-9. Radionuclides ordered by ratio of inventory to U.S. Environmental Protection Agency limit for pressurized water reactor spent fuel for various decay times[a] (continued)

1×10^2 yr		1×10^3 yr		1×10^4 yr		1×10^5 yr	
Ni-63	3.1×10^2	Ni-59	5.2	U-236	3.5	Ni-59	2.2
Am-243	1.7×10^2	U-238	3.2	U-238	3.2	Zr-93	1.9

[a]Source: Kerrisk (1985).
[b]Short-lived daughter of Cs-137.
[c]Short-lived daughter of Sr-90.
[d]Decay products of Ra-226 are in secular equilibrium. Each alpha emitter in the decay chain has the same ratio of inventory to EPA limit; others have a ratio that is 10 times lower. The Ra-226 decay products are generally short-lived.
[e]Short-lived daughter of Am-243.

Two of the most important retardation mechanisms available in a geologic

Table 4-10. Radionuclides ordered by ratio of inventory to the U.S. Environmental Protection Agency limit for high-level waste from pressurized water reactors for various decay times[a]

1 x 10^2 yr		1 x 10^3 yr		1 x 10^4 yr		1 x 10^5 yr	
Cs-137	1.0×10^4	Am-241	1.8×10^3	Am-243	1.6×10^2	Pu-239	5.1
[b]Ba-137m	9.8×10^3	Am-243	1.7×10^2	Pu-239	4.0×10^1	Np-237	3.4
Sr-90	6.8×10^3	Pu-240	6.3×10^1	Pu-240	2.4×10^1	Th-230	2.4
[c]Y-90	6.8×10^3	Pu-239	2.1×10^1	[d]Np-239	6.7	Ni-59	2.2
Am-241	2.0×10^3	[d]Np-239	1.6×10^1	Ni-59	4.8	Zr-93	1.7
Pu-238	5.2×10^2	C-14	1.4×10^1	C-14	4.6	[e]Nb-93m	1.6
Cm-244	3.3×10^2	Ni-59	5.1	Np-237	3.5	U-233	1.2
Ni-63	3.1×10^2	Np-237	3.5	Zr-93	1.8	[f]Th-229	1.1
Am-243	1.7×10^2	Zr-93	1.8	[e]Nb-93m	1.7	Tc-99	9.4×10^{-1}
Sm-151	1.7×10^2	[e]Nb-93m	1.7	Tc-99	1.3	Sn-126	3.9×10^{-1}
Pu-240	6.8×10^1	Tc-99	1.3	Nb-94	9.1×10^{-1}	U-234	3.6×10^{-1}
Cm-242	2.0×10^1	Nb-94	1.2	Sn-126	7.3×10^{-1}	[g]Pa-233	3.4×10^{-1}

[a]Source: Kerrisk (1985).
[b]Short-lived daughter of Cs-137.
[c]Short-lived daughter of Sr-90.
[d]Short-lived daughter of Am-243.
[e]Short-lived daughter of Zr-93.
[f]Decay products of Th-229 are in secular equilibrium. Each alpha emitter in the decay chain has the same ratio of inventory to EPA limit; others have a ratio that is 10 times lower. The Th-229 decay products are generally short lived.
[g]Short-lived daughter of Np-237.

Table 4-11. Radionuclides ordered by ratio of inventory to the U.S. Environmental Protection Agency limit for defense high-level waste for various decay times[a]

1×10^2 yr		1×10^3 yr		1×10^4 yr		1×10^5 yr	
Pu-238	8.7×10^3	Am-241	1.9×10^2	Pu-239	1.3×10^2	Th-230	7.5×10^1
Sr-90	7.8×10^3	Pu-239	1.7×10^2	Pu-240	3.8×10^1	U-234	1.1×10^1
[b]Y-90	7.8×10^3	Pu-240	9.9×10^1	U-234	1.4×10^1	Pu-239	9.7
Cs-137	7.4×10^3	U-234	1.5×10^1	Th-230	1.3×10^1	[c]Ra-226	7.4
[d]Ba-137m	7.0×10^3	Pu-238	7.1	Ni-59	3.3	Zr-93	1.9
Am-241	7.8×10^2	Ni-59	3.5	Zr-93	2.0	[e]Nb-93m	1.9
Ni-63	4.3×10^2	Zr-93	2.0	[e]Nb-93m	2.0[c]	Ni-59	1.4
Sm-151	2.1×10^2	[e]Nb-93m	2.0	[c]Ra-226	9.7×10^{-1}	U-236	6.3×10^{-1}
Pu-239	1.7×10^2	Th-230	1.2	U-236	6.2×10^{-1}	Np-237	2.6×10^{-1}
Pu-240	1.1×10^2	U-236	6.0×10^{-1}	Tc-99	3.3×10^{-1}	Tc-99	2.4×10^{-1}
Pu-241	2.4×10^1	Tc-99	3.4×10^{-1}	Np-237	2.7×10^{-1}	U-238	1.5×10^{-1}

[a]Source: Kerrisk (1985).
[b]Short-lived daughter of Sr-90.
[c]Decay products of Ra-226 are in secular equilibrium. Each alpha emitter in the decay chain has the same ratio of inventory to EPA limit; others have a ratio that is 10 times lower. The Ra-226 decay products are generally short lived.
[d]Short-lived daughter of Cs-137.
[e]Short-lived daughter of Zr-93.

waste elements, an exchange between the gas, aqueous, and solid phase may be possible.

On the basis of the quantity of radionuclides in the waste, the EPA release limits, solubility, sorption, the potential for vapor transport, and the potential for colloid transport, the following radionuclides should be considered important (Kerrisk, 1985):

1. Isotopes of the elements americium, plutonium, neptunium, and uranium are the most important because they are present in the largest quantities in waste relative to their EPA release limits and because of their potential for colloid transport. Solubility and sorption measurements for these elements should be of utmost importance.

2. Isotopes of the elements carbon, nickel, zirconium, technetium, thorium, radium (barium used as an analog), and tin are present in lesser amounts at most times, but are also important for solubility and for their transport potential.

3. Isotopes of the elements carbon, technetium, and iodine are important because these elements appear to have high solubility and low sorption at Yucca Mountain. This should be confirmed experimentally by determining their transport potential.

4. Isotopes of the elements carbon and iodine are important because they could be transported in the gas phase at Yucca Mountain. Studies of gas-phase transport should concentrate on these elements. Detailed discussions of the various retardation processes and the radionuclides considered for these processes are contained in Sections 4.1.3.3 through 4.1.3.8.

4.1.3.2 Analytical techniques

This section discusses the methods and procedures used to investigate geochemical retardation in the experiments reported here. (Results are reported in Sections 4.1.3.3. through 4.1.3.5.) The discussion emphasizes the retardation mechanism of sorption, but it also provides basic dynamic-characterize the sorptive properties. The limitations of the distribution-coefficient approach to geologic investigations are as follows:

1. The assumption of a linear sorption isotherm. The terms "sorption isotherm," "Freundlich isotherm," or "Langmuir isotherm" are generally used to define the relationships between sorption and the concentration of the element being sorbed at a constant temperature.

2. The distribution between the solid phase and the aqueous phase may include precipitation or irreversible reaction or both.

3. The aqueous-phase species are not well known for many of the important radionuclides.

4. The assumption of equilibrium (i.e., rapid kinetics).

pitfalls. To ensure that discrepancies between laboratory experiments are not due to experimental errors, the following must be carefully controlled:

1. Phase separation. When distribution coefficients (K_d) are high, the experiments are susceptible to contamination of the aqueous phase with colloidal material containing radionuclides leading to erroneously low K_d values.

2. Water composition. Comparison between experiments using radically different water compositions leads to large discrepancies.

3. Crushing and sieving. The rock must not be crushed below mineral crystal size. The samples should be sieved to ensure uniformity.

4. Mineral fractionation. This can occur either in the process of sieving or in the course of an experiment, such as a crushed tuff column, because the adsorption minerals (clays and zeolites) in tuff generally have small crystal sizes that will enrich in the smaller size fractions.

5. Speciation. The results of experiments where the complexing agents or oxidation-reduction conditions are not identical will show discrepancies for some radionuclides.

The above parameters must be controlled to study the distribution of geochemical properties in the geologic system. Where these parameters cannot be made to coincide exactly with the conditions in the field, compromises are made in a conservative direction for the purpose of applying the result to predictions in the field. For example, the smallest-size fractions are discarded, oxidizing conditions are used, etc. To systematically study which simplifying assumption may be valid and to experimentally examine the coupling of adsorption to dynamic processes the following types of experiments have been performed:

1. Crushed-tuff columns. The experiments allow the comparison of batch to transport through nearly identical material; they allow the study of kinetic effects, speciation, and other physical and chemical effects, such as anion exclusion. The advantage in using crushed tuff is that the results are free of ambiguities in the interpreta-

4. Fractured-tuff columns. The experiments represent the most complex transport system that can be simulated in the laboratory.

5. Diffusion in solid tuff. The experiments are ancillary to the fractured-tuff columns but provide fundamental data for modeling diffusion in the tuff matrix. The experiments will also provide some kinetic data.

6. Solubility. The experiments are primarily directed toward understanding actinide solution chemistry in near-neutral solution. The understanding of actinide chemistry under near-neutral conditions is growing at a very slow pace because the low solubility of these elements does not allow the direct determination of oxidation state and molecular structure at present. Without a firm knowledge of the aqueous chemical species, the interpretation of the above transport experiments is hampered.

The major isotopes chosen for study come from the EPA critical element list. Additional radionuclides have been investigated when warranted (Section 4.1.3.3.1).

4.1.3.2.1 Preparation of ground-water samples for use in laboratory experiments

Before use, reference ground water from well J-13 is pretreated by putting it in contact with samples of tuff from individual strata in the vicinity of Yucca Mountain to obtain water chemistries representative of steady-state equilibrium for each tuff sample. After contact for at least 2 wk, the water is filtered through 0.05 micrometer Nuclepore membranes. Then, the water is analyzed and used in the sorption experiments. In general during pretreatment, sodium increases up to 50 percent and magnesium decreases by 50 percent probably due to ion exchange; chloride, fluoride, and sulfate remain unchanged; and the pH (8.1 to 8.4) increases slightly. The changes, however, do not greatly affect sorption.

The spiked-feed solutions for each tuff sample were prepared by adding measured concentrations of radionuclide tracers to the pretreated water. Spiked-feed solutions are prepared as described by Daniels et al. (1982) for separate radionuclides. The final concentrations of the feed solutions generally range from 10^{-6} to 10^{-9} M; plutonium concentrations as low as 10^{-11} M have been studied.

4.1.3.2.2 Batch sorption methods

In batch measurements of sorptive properties, the distribution of a radionuclide is measured between ground water and crushed tuff as a function of contact time, the concentration of sorbing species, particle size, temperature, oxidation-reduction conditions, ground-water components, and lithology. In the batch procedure, a 1-g sample of crushed tuff is pretreated by contact with 20 ml of well J-13 ground water for at least 2 wk. The ground water used to prepare the solution containing radionuclides (spiked-feed solution) is also pretreated by contact for at least 2 wk with a crushed-tuff sample from the same section of core. The solids are separated from the liquid by centrifuging after the pretreatment period.

A sorption measurement starts when 20 ml of spiked-feed solution is added to the 1-g sample of tuff treated with ground water. The concentration of the spiked element ranges from 10^{-6} to 10^{-13} M, except in isotherm measurements where concentrations approaching the solubility limit are investigated. Care is taken to ensure that the spike concentration is well below predicted solubility limits in standard experiments. Except for the highest concentrations used in the isotherm studies (generally greater than 10^{-4} M), no significant change in sorption ratio has been observed with changing spike concentrations covering six to seven orders of magnitude (Wolfsberg et al., 1981; Daniels et al., 1982; Rundberg et al., 1985). Next, the two phases are thoroughly mixed and the sample is placed in a shaker to be agitated at about 200 rpm for selected times. At the end of the sorption period, the sample is removed from the shaker and the solids are separated by centrifuge. Tracer (spike) activity in the separated solid and liquid phases then is determined and the pH of the liquid is measured. The analytical techniques for each element are discussed by Daniels et al. (1982), who also discussed the technique used to completely separate the solids from the aqueous phase and to calculate the sorption ratios. The standard sorption and desorption times were 6 wk each. The data in Appendix A of Daniels et al. (1982) show that sorption either increases with time or remains unchanged. The choice of 6 weeks (or a total of 12 wk for both sorption and desorption measurements) was a compromise between reaching equilibrium, if

4.1.3.2.3 Crushed-tuff column method

The transport behavior of nuclides in columns of crushed tuff has been studied to characterize retardation in a flowing system. The column method is sensitive to speciation and also to reaction kinetics. The method will enable improvements to the transport model or empirical adjustments to the retardation data base so that the calculated bounds will encompass any

J-13 water, the pressure of carbon dioxide over the water was also controlled. Solids that precipitated were identified by x-ray diffraction; some of the solids were amorphous and could not be identified in this manner (Section 4.1.3.4.2; Nitsche and Edelstein, 1985). At this time there is a lack of firm knowledge of aqueous chemical species (actinides) under near-neutral conditions. Further work is planned in Section 8.3.1.3.

4.1.3.3 Sorption

Ion exchange and sorption (chemical or physical) are surface processes by which ions or other solution species can be removed from ground water by rock. The measured sorption ratios (defined in Section 4.1.3.2.2) are primary data for the assessment of retardation along the flow path. An understanding of these processes may permit extrapolation of laboratory data to field experiments and will aid in estimates of uncertainty limits. Plans for obtaining the additional information required are outlined in Section 8.3.1.3.4. The sorption of radionuclides on colloidal material will be studied as discussed in Section 8.3.1.3.4.

Several parameters directly affect sorption measurements as they relate to Yucca Mountain. Among these are the composition of the ground water used in the sorption experiments, the cation-exchange capacity of the minerals, the pH, the temperature, the oxidation-reduction conditions, the waste element being sorbed, and the concentration of the waste element. Additionally, three primary experimental methods (batch, crushed-rock column, or circulating systems) are used for measuring sorption coefficients as discussed in Sections 4.1.3.2.2 through 4.1.3.2.4. Relevant data that characterize the ion-exchange and sorption capacities of the tuff at Yucca Mountain are taken primarily from Daniels et al. (1982).

4.1.3.3.1 Sorption data for tuff

Daniels et al. (1982, 1983), Ogard et al. (1983b), Wolfsberg et al. (1983), Wolfsberg and Vaniman (1984), Crowe and Vaniman (1985), Ogard and Vaniman (1985), Rundberg et al. (1985) present data concerning sorption on tuff and list the results of all previous experiments. These sorption data were obtained from samples representative of Yucca Mountain strata from well J-13 (JA samples) and drillholes UE-25a#1 (YM samples), USW G-1 (G1 samples), USW G-2, and USW GU-3. Variables include time, temperature, particle size, oxidation-reduction conditions, element concentration, ground-water composition, and test method (batch, column, or circulating system). The radionuclides investigated were americium, cesium, neptunium, plutonium, uranium, thorium, strontium, technetium, tin, barium, radium, cerium, europium, and selenium. Strontium and cesium, while being shorter lived than many potentially hazardous waste elements, were studied first because of their relatively simple sorption behavior. These elements continue to be used to help validate the experimental techniques because their behavior can be predicted fairly well. Barium is included as a chemical analog for radium to reduce the number of experiments with radium. A great deal of care must be taken in radon-222 which could contaminate low-level counting facilities. Uranium and thorium are long-lived parents of radium; cerium and europium have been studied as analogs of rare-earth radionuclides. Selenium was studied as a potentially important waste element.

4.1.3.3.2 Sorption data from batch experiments

Average sorption ratios (R_d) from batch sorption and desorption experiments on tuff samples for strontium, cesium, barium, radium, cerium, europium, americium, plutonium, uranium, selenium, technetium, and neptunium are given in Tables 4-12a, 4-12b, 4-13a, and 4-13b. Each sample is assigned a depth equivalent in drillhole USW G-1 on the basis of the relative position of the sample in the major stratigraphic units so that sorption results on samples from one drillhole can be compared with samples from another. Data are for contact times greater than one week and particle sizes greater than 75 micrometers in an air environment at 25°C unless otherwise noted. Mineral abundance data determined by x-ray diffraction and petrologic characterization of these samples (as well as for finer fractions) are given in Table 4-14.

The R_d values from sorption experiments are often significantly lower than those from desorption experiments. Although the differences in R_d are unexplained at present, they suggest that, at least for some elements, sorption is not readily reversible. The sorption of cesium, strontium, and barium, which are noncomplexed cations that probably sorb by ion exchange, appears reversible because the R_d values from sorption and desorption experiments generally agree within a factor of 2. The R_d values from desorption experiments for technetium, the lanthanides, and the actinides are as much as 10 times greater than R_d values from sorption experiments. The latter elements all have multivalent species, some of which are sparingly soluble, hydrated, or form colloids and complexes (Section 4.1.3.4.1), which can alter the sorption processes. Differences in sorptive behavior may be caused by differences in aqueous speciation or sorption reactions with the solid phases. Further studies are described in Section 8.3.1.3.4.

Only limited data are available on the effect of elevated temperature on sorption behavior in tuff. Data obtained at 70 and 85°C (Table XVII, Ogard et al., 1983b) suggest that higher temperatures will generally increase slightly the sorptive capacity of the tuff samples for all elements studied (Daniels et al., 1982; Ogard et al., 1983a). Samples studied for temperature effects were Topopah Spring Member tuffs containing equal amounts of cristobalite and alkali feldspar; Topopah Spring Member tuff largely composed of

Table 4-12a. Average sorption ratios from batch sorption experiments on crushed tuff for strontium.

Table 4-12a. Average sorption ratios from batch sorption experiments on crushed tuff for strontium, cesium, barium, radium, cerium, and europium[a,b] (page 2 of 2)
(See footnotes at the end of Table 4-12b)

Strati-graphic unit[c]	Sample	Depth (ft)	Sorption ratios (ml/g)					
			Strontium	Cesium	Barium	Radium	Cerium	Europium
Tcb	JA-28	2,001	94(20)	1,640(210)	820(50)			2,100(1,000)
	G1-2233	2,233	48,000(3,000)[f]	13,500(800)	250,000(30,000)		1,400(300)	900(200)
	G1-2289	2,289	7,300(500)	37,000(13,000)	66,000(9,000)	46,000(20,000)		797(10)
	YM-54	2,491	62(12)	180(40)	400(150)		150(40)	470(40)
	G1-2333	2,333	180(20)	1,400(130)	1,500(200)			2,300(400)
	G1-2363	2,363	64(3)	470(40)	235(9)	540(60)		730(50)
	G1-2410	2,410	169(1)	1,250(50)	1,780			440(80)
	JA-32	2,533	57(3)	123(4)	380(30)		82(14)	90(20)
	G1-2476	2,476	41(1)	700(40)	385(11)			3,200(100)
Tct	G1-2698	2,698	42,000(3,000)[f]	7,700(400)[f]	63,000(5,000)[f]		240(30)[f]	200(30)[f]
	G1-2840	2,840	860(1)	2,200(200)	2,070(70)			4,900(400)
	G1-2854	2,854	94(1)	1,080(120)	1,000(50)			1,300(200)
	G1-2901	2,901	68(1)[f]	1,290(110)[f]	1,600(200)[f]		42,000(3,000)[f]	160,000(50,000)[f]
	G1-3116	3,116	2,400(17)[f]	6,600(500)[f]	12,000(4,000)[f]		100(10)[f]	760(60)[f]
	JA-37	3,497	287(14)	610(40)	760(150)			6,000(800)
Tl	G1-3658	3,658	13,000(0)	4,950(50)	13,500(500)		1,000(200)[f]	530(40)
Tba	G2-3933	3,933	240(60)[f]	2,500(1,000)[f]	1,700(500)[f]			1,500(700)[f]

Table 4-12b. Average sorption ratios from batch sorption experiments on crushed tuff for americium, plutonium, uranium, selenium, technetium, and neptunium[a,b] (page 1 of 3)

Strati-graphic unit[c]	Sample	Depth (ft)	Sorption ratios (ml/g)					
			Americium	Plutonium	Uranium	Selenium	Technetium	Neptunium
Tpc	JA-8	606						
	YM-5	251						
Tpp	G2-547	547	13,000(110)[f]	1,200(120)	9.4(0.1)	2(2)	0[f]	
	G2-723	723	890,000(40,000)	>4,500	2.4(0.6)	19(2)	0[f]	
	GU3-433	433	3,400(200)[d]	330(60)[g]	0	15(3)	0	7.9(0.1)
	GU3-855	855			10.0(0.7)	10(0.4)		
Tpt	YM-22	848	1,200(130)[d,e]	64(20)[d]	1.8(0.2)[d]		0.3(0.14)[d]	7.0
	GU3-1203	1,203	1,100(120)[g]	360(40)[g]	0	(1)	0	2.7(0.1)
	G1-1292	1,292						
	GU3-1301	1,301	1,800(160)[g]	290(40)[g]	0	7(2)	0.03(0.001)	5.0(0.1)
	YM-30	1,264						
	JA-18	1,420	180(30)	120(20)	2.5(0.4)			
Th	G1-1436	1,436						
	G2-1952	1,952	1,700(70)[f]	66(6)[f]	0	2(1)		2.7(0.1)
	GU3-1436	1,436			20.0(2)	3(10)		
Bt	GU3-1531	1,531			54.0(9)	5(1)		
	YM-38	1,504	14,600(1,000)	140(30)	5.3(0.2)			11.0
	YM-42	1,824						

Table 4-12b. Average sorption ratios from batch sorption experiments on crushed tuff for americium, plutonium, uranium, selenium, technetium, and neptunium[a,b] (page 2 of 3)

Strati-graphic unit[c]	Sample	Depth (ft)	Sorption ratios (ml/g)					
			Americium	Plutonium	Uranium	Selenium	Technetium	Neptunium
Tcp	G1-1854	1,854						
	YM-45	1,930						
	G1-1883	1,883	470(300)					
	YM-46	2,002		77(11)				6.4
	G1-1982	1,982						
	YM-48	2,114						
	YM-49	2,221	4,300(1,400)				0.15(0.02)	
	JA-26	1,995		230(50)[e]			0.21(0.02)	9.0(3)
Tcb	JA-28	2,001						
	G1-2233	2,233						
	G1-2289	2,289				9(1)		
	YM-54	2,491	153(6)	80(20)	1.3(0.3)		4.2(0.5)[h]	
	G1-2333	2,333						
	G1-2363	2,363		110		25(5)		
	G1-2410	2,410			2.2(0.9)			
	JA-32	2,533	130(30)					
	G1-2476	2,476						
Tct	G1-2698	2,698						
	G1-2840	2,840						
	G1-2854	2,854						
	G1-2901	2,901		400(70)[e]	4.6(0.3)			
	G1-3116	3,116						
	JA-37	3,497	28,000(10,000)[e]					24

Table 4-12b. Average sorption ratios from batch sorption experiments on crushed tuff for americium, plutonium, uranium, selenium, technetium, and neptunium[a,b] (page 3 of 3)

Stratigraphic unit[c]	Sample	Depth (ft)	Sorption ratios (ml/g)					
			Americium	Plutonium	Uranium	Selenium	Technetium	Neptunium
Tl	G1-3658	3,658						
Tba	G2-3933	3,923	6,600(400)		1,600.0(30)	0	0.0(1)	0.1(0.006)

[a]Sources: Daniels et al. (1982); Ogard et al. (1983b); Wolfsberg et al. (1983). If no footnote is indicated, the sorption ratio in parentheses represents the standard deviation of the mean.

[b]Ambient conditions, air, 20 ± 4°C; fractions do not contain particles smaller than 75 micrometers in diameter except in fractions designated by footnote (f). Sorption times greater than 1 week.

[c]Stratigraphic units are as follows: Tpc = Tiva Canyon Member; Tpp = Pah Canyon Member; Tpt = Topopah Spring Member; Th = tuffaceous beds of Calico Hills; Bt = bedded tuff; Tcp = Prow Pass Member; Tcb = Bullfrog Member; Tct = Tram Member; Tl = older tuffs; Tba = bedded tuff.

[d]Nonweighted average; value in parentheses is the standard deviation of the mean.

[e]Some data were rejected in averaging.

[f]Average of data for the fraction with particles smaller than 500 micrometers in diameter (contains some particles smaller than 75 micrometers).

[g]Nonweighted average of samples taken in two different positions.

[h]Performed under controlled atmospheric conditions of nitrogen with less than or equal to 0.2 parts per million O_2 and less than or equal to 20 parts per million CO_2.

Table 4-13a. Average sorption ratios from batch desorption experiments on crushed tuff for strontium, cesium, barium, cerium, and europium[a,b] (page 1 of 2)
(See footnotes at the end of Table 4-13b)

Stratigraphic unit[c]	Sample	Depth (ft)	Sorption ratios (ml/g)				
			Strontium	Cesium	Barium	Cerium	Europium
Tpc	JA-8	606	311(3)	4,600(400)	480(50)		10,000(3,000)
	YM-5	251	320(30)[d]	8,900(600)[d]	1,200(120)[d]	31,000(30,000)[d]	36,000(14,000)
Tpp	G2-547	547	210(10)[f]	8,700(550)[f]	2,900(200)[f]		1,700(600)[f]
	GS-723	723	330(4)[f]	4,300(4)[f]	4,200(10)[f]		>10,000[f]
	GU3-433	433	40(10)[g]	520(20)[g]	460(20)[g]		140(10)[g]
Tpt	YM-22	848	59(2)	365(7)	830(100)	6,500(800)	3,500(200)
	GU3-1203	1,203	47(1)	340(10)	720(30)		650(50)
	G1-1292	1,292	120(5)[f]	510(20)[f]	1,500(100)	600(200)[f]	600(70)
	GU3-1301	1,301	80(20)[g]	185(20)[g]	675(60)[g]		100(20)[g]
	YM-30	1,264	210(30)	1,500(100)	3,100(600)	170,000(15,000)	11,000(700)
	JA-18	1,420	15,000(2,000)	17,500(700)	280,000(50,000)	1,600(500)[e]	2,400(300)[e]
Th	G1-1436	1,436	87,000(12,000)	24,000(2,000)	340,000(90,000)	6,700(600)	5,300(600)
	G2-1952	1,952	4,200(200)[f]	46,000(1,400)[f]	40,000(1,000)[f]		1,600(200)
	YM-38	1,540	22,000	13,000	260,000	2,600	7,300
	YM-42	1,842	4,100(1,000)	21,000(2,000)	90,000(30,000)	44,000(5,000)	64,000(3,000)
Tcp	G1-1854	1,854	72,000(13,000)[e]	14,000(2,000)	150,000(40,000)		4,800(700)
	YM-45	1,930	210(20)	620(110)	1,310(60)	5,800(600)	7,300(900)
	G1-1883	1,883	59(1)[f]	430(4)	440(10)[f]	2,200(100)[f]	1,350(50)[f]
	YM-46	2,002	260(20)	1,800(300)	210,000(3,000)	300,000(50,000)	31,000(2,000)
	G1-1982	1,982	322(8)[f]	2,300(200)[f]	2,780(120)[f]	7,000(800)[f]	6,370(130)[f]
	YM-48	2,114	2,700(200)	27,000(4,000)	34,000(7,000)	128,000(300)	8,100(1,200)
	YM-49	2,221	4,400(100)	39,000(1,000)	65,000(7,000)	1,040(40)	2,100(500)
	JA-26	1,995	39(3)	1,580(90)	450(13)		2,900(200)

Table 4-13a. Average sorption ratios from batch desorption experiments on crushed tuff for strontium, cesium, barium, cerium, and europium[a,b] (page 2 of 2)
(See footnotes at the end of Table 4-13b)

Strati-graphic unit[c]	Sample	Depth (ft)	Sorption ratios (ml/g)				
			Strontium	Cesium	Barium	Cerium	Europium
Tcb	JA-28	2,001	114(3)	2,400(100)	1,160(20)		12,300(500)
	G1-2233	2,233	90,000(40,000)[f]	23,000(6,000)[f]	40,000(80,000)[f]	20,000(13,000)[e]	5,000(2,000)[f]
	G1-2289	2,289					
	YM-54	2,491	97(9)	310(20)	660(20)	1,000(200)	1,840(110)
	G1-2333	2,333	140(13)	1,230(100)	1,460(130)		9,900(1,200)
	G1-2363	2,363	150(6)[f]	1,200(30)[f]	820(20)	130,000(6,000)[f]	6,100(300)
	G1-2410	2,410	140(14)	1,120(100)	1,760(150)		6,000(3,000)
	JA-32	2,533	53(3)	175(11)	490(40)	530(120)	850(130)
	G1-2476	2,476	200(4)	1,520(0)			
Tct	G1-2698	2,698	210,000(50,000)	17,000(1,100)	190,000(80,000)[f]	2,000(400)[f]	
	G1-2840	2,840	1,540	2,300(130)	2,500(200)		9,000(1,100)
	G1-2854	2,854	96(1)	1,160(20)	1,300(0)		5,000(200)
	G1-2901	2,901	67(1)[e,f]	1,380(30)[f]	1,980(30)	39,000(1,000)[f]	210,000(50,000)
	G1-3116	3,116	24,000(13,000)[f]	11,000(3,000)[f]	160,000(80,000)	3,000(1,000)[f]	8,000(3,000)[f]
	JA-37	3,497	312(9)	850(50)	920(40)		11,000(2,000)
Tl	G1-3658	3,658	12,000(3,000)[f]	12,000(2,000)[f]	10,000(4,000)	9,000(4,000)[f]	9,000(3,000)[f]
Tba	G2-3933	3,933	140(20)[f]	1,400(350)[f]	1,100(200)[f]		3,000(1,100)[f]

Table 4-13b. Average sorption ratios from batch desorption experiments on crushed tuff for americium, plutonium, uranium, technetium, and neptunium[a,b] (page 1 of 3)

Stratigraphic unit[c]	Sample	Depth (ft)	Sorption ratios (ml/g)				
			Americium	Plutonium	Uranium	Technetium	Neptunium
Tpc	JA-8	606					
	YM-5	521					
Tpp	G2-547	547	17,000(1,400)	1,200(170)[f]			
	G2-743	723	2.8×10^6 (2.6×10^4)	>47,000			
	GU3-433	433	9,300(1,780)[g]	920(40)[g]			
Tpt	YM-22	848	2,500(400)[d]	1,330(140)[d]	5(2)[d]	1.2(0.3)[d]	33(5)[d]
	GU3-1203	1,203	1,300(200)[g]	920(15)[g]			
	G1-1292	1,292					
	GU3-1301	1,301	2,500(600)[g]	1,300(460)[g]			
	YM-30	1,264					
	JA-18	1,420	1,100(300)	350(140)	9.4(1.4)		
Tht	G1-1436	1,436					
	G2-1952	1,952	5,800(1,100)[g]	350(45)[g]			
	YM-38	1,540	7,100(1,200)	1,600(300)	14.8(1.0)		24(2)
	YM-42	1,824					

Table 4-13b. Average sorption ratios from batch desorption experiments on crushed tuff for americium, plutonium, uranium, technetium, and neptunium[a,b] (page 2 of 3)

Strati-graphic unit[c]	Sample	Depth (ft)	Sorption ratios (ml/g)				
			Americium	Plutonium	Uranium	Technetium	Neptunium
Tcp	G1-1854	1,854					
	YM-45	1,930					
	G1-1883	1,883	7,200(900)	890(60) = (61-1883)			36(10)
	YM-46	2,002					
	G1-1982	1,982					
	YM-48	2,114				1.6(0.2)	
	YM-49	2,221	3,400(400)[e]	720(90)		2.0(0.3)	12(4)
	JA-26	1,995					
Tcb	JA-28	2,001					
	G1-2233	2,233					
	G1-2289	2,289					
	YM-54	2,491	550(80)	720(40)	12(8)	38(-)[h]	
	G1-2333	2,333					
	G1-2363	2,363					
	G1-2410	2,410			8(2)		
	JA-32	2,533	2,200(600)				
	G1-2476	2,476					
Tct	G1-2698	2,698					
	G1-2840	2,840					
	G1-2854	2,854					
	G1-2901	2,901					
	G1-3116	3,116					
	JA-37	3,497	32,000(10,000)	1,400(300)	9.9(0.4)		170(50)

Table 4-13b. Average sorption ratios from batch desorption experiments on crushed tuff for americium, plutonium, uranium, technetium, and neptunium[a,b] (page 3 of 3)

Strati-graphic unit[c]	Sample	Depth (ft)	Sorption ratios (ml/g)				
			Americium	Plutonium	Uranium	Technetium	Neptunium
Tl	G1-3658	3,658					
Tba	G2-3933	3,933	1,200(410)	530(130)			

[a]Sources: Daniels et al. (1982); Ogard et al. (1983b); Wolfsberg et al. (1983). If no footnote is indicated, the sorption ratio in parentheses represents the standard deviation of the mean.

[b]Ambient conditions, air, 20 ± 4°C; fractions do not contain particles smaller than 75 micrometers in diameter except in fractions designated by footnote f. Sorption times greater than 1 week.

[c]Stratigraphic units are as follows: Tpc = Tiva Canyon Member; Tpp = Pah Canyon Member; Tpt = Topopah Spring Member; Th = tuffaceous beds of Calico Hills; Tcp = Prow Pass Member; Tcb = Bullfrog Member; Tct = Tram Member; Tl = older tuffs; Tba = bedded tuff.

[d]Nonweighted average; value in parentheses is the standard deviation of the mean.

[e]Some data were rejected in averaging.

[f]Average of data for the fraction with particles smaller than 500 micrometers in diameter (contains some particles smaller than 75 micrometers).

[g]Nonweighted average of samples taken in two different positions.

[h]Performed under controlled atmospheric conditions of nitrogen with less than or equal to 0.2 ppm O_2 and less than or equal to 20 ppm CO_2.

Table 4-14. Petrologic characterization of tuff samples from drillholes J-13, UE-25a#1, USW G-1, USW G-2, and USW GU-3[a] (page 1 of 4)

Unit[b]	Sample	Depth (ft)	USW G-1 depth (ft)[c]	Particle size (μm)	Abundance (weight %) Smectite	Illite Muscovite	Clinop-tilolite	Quartz	Cristob-alite	Alkali feldspar	Glass	Other[d]	Degree of welding[e]	Oxidation state[f]	Crystals (%)	Lithics (%)
Tpt	JA-8	606	172	All[g]	25-50	--[h]	--	--	10-20	tr[h]	25-50	--	M	(h)	8.9	6.7
Tpt	JA-8	606	172	75-500	30-60	--	--	<5	10-20	--	20-50	--				
Tpt	JA-8	606	172	75	30-60	--	--	--	10-20	--	30-60	--				
Tpc	YM-5	251	221	All	10	--	--	<5	<5	10-20	70	--	M		10.9	4.3
Tpp	G-2-547	547		<500	5-15	<5	--	--	5-15	10-20	40-60	--				
Tpp	G-2-547	547		75-500	14-84	--	--	3-7	2-8	43-63	--	6-16T				
Tpp	G-2-723	723		<500	5-15	<5	--	--	<5	5-10	15-30	30-70C				
Tpp	G-2-723	723		75-500	2-8	1-5	--	--	1-5	15-35	9-21	40-60C				
Tpt	GU-3-433	433	245	75-500	--	2-6	--	2-6	8-16	60-100	--	--				
Tpt	GU-3-855	855	758	<500	1-3	--	--	16-24	4-10	50-90	--	--				
Tpt	YM-22	480	868	All	5-10	--	--	40-60	--	40-60	--	--	O	C6(2-7)	1.0	0.4
Tpt	VII-22	848	868	106-500	<5	<2	--	30-50	--	30-50	--	--				
Tpt	VII-22	848	868	38-106	<2	tr	--	30-50	--	30-50	--	--				
Tpt	VII-22	848	868	<38	<5	<2	--	30-50	--	30-50	--	--				
Tpt	GG-3420[i]	1.000	1.100	75-500	1	1	--	2-7	8-16	35-55	20-60	000				
Tpt	G1-1292	1,292	1,292	All	tr	--	--	--	5-10	10-20	80-90	--	V	C1		
Tpt	G1-1292	1,292	1,292	75-500	--	--	--	--	15-30	10-20	10-60	--				
Tpt	GU-3-1201	1,201	1,298	75-500	1-3	2-6	--	4-8	9-21	15-55	20-60	--				
Tpt	YM-30	1,264	1,318	All	5-10	5	5-10	40-60	5-15	30-50	--	--	O	C5(2-7)	2.1	21.6
Tpt	YM-30	1,264	1,318	75-100	--	--	15	30	20	35	--	--				
Tpt	YM-30	1,264	1,318	<75	--	--	15	30	20	35	--	--				
Tpt	JA-18	1,420	1,339	All	5	5	5-10	--	15-25	15-25	50	--	N	C3(2-5)	1.8	11.9
Tpt	JA-18	1,420	1,339	355-500	5	--	10-20	--	30-50	30-50	40	--				
Tpt	JA-18	1,420	1,339	106-150	5	5	10-20	--	30-50	30-50	40	--				
Tht	G1-1436	1,436	1,436	75-500	<5	<5	75-90	5-10	--	5	--	--		C6(5-7)	5.2	3.2
Tht	G2-1952	1,952	1,493	<500	--	1	25-45	3-7	3-7	20-40	--	15-35	M			
Tht	G2-1952	1,952	1,493	75-500	--	1	10-30	5-9	5-11	26-46	--	20-40				
Tht	G43-1436	1,436	1,504[j]	<500[k]	--	1	--	2-6	3-9	30-70	20-60	--				
Tht	YM-3d	1,504	1,538	106-500	5-10	<2	30-50	15-30	10-20	5-15	--	A,tr	N	C5(4-6)	4.0	7.7
Tht	YM-3d	1,504	1,538	38-106	5-10	<5	40-60	2-10	10-20	5-15	--	--				
Tht	YM-3d	1,504	1,538	<38	5-15	<5	40-60	2-10	10-20	10-10	--	A,tr				
Tht	VII-42	1,824	1,802	75-500	tr	<5	20	35-40	--	40	--	--			15.6	46.6
Tht	V14-42	1,824	1,802	<75	tr	tr	20	40	--	40	--	--				
Tba	GU3-1531	1,531		<500[k]	--	3-7	--	15-25	3-9	20-60	10-50	--				

Table 4-14. Petrologic characterization of tuff samples from drillholes J-13, UE-25a#1, USW G-1, USW G-2, and USW GU-3[a] (page 2 of 4)

Unit[b]	Sample	Depth (ft)	USW G-1 depth (ft)[c]	Particle size (μm)	Abundance (weight %): Smectite	Illite Muscovite	Clinop-tilolite	Quartz	Cristob-alite	Alkali feldspar	Glass	Other[d]	Degree of welding[e]	Oxidation state[f]	Crystals (%)	Lithics (%)
Tcp	G1-1854	1,854	1,854	75-500	5-10	--	30-50	5-15	15-30	20-40	--	--				
Tcp	G1-1854	1,854	1,854	<75	5-10	--	40-60	20-40	15-30	10-30	--	--				
Tcp	YM-45	1,930	1,873	All	1-5	--	--	40-60	tr	30-50	--		M	C4(3-5)	13.5	0.6
Tcp	G1-1883	1,883	1,883	75-500	<2	<5	--	30-50	--	50-70	--	--	P	C4(3-5)	16.6	1.0
Tcp	G1-1883	1,883	1,883	106-500	<2	<2	--	20-40	0-10	40-60	--	--				
Tcp	G1-1883	1,883	1,883	38-106	<2	<5	--	30-50	0-10	30-50	--	--				
Tcp	G1-1883	1,883	1,883	<38	2-5	<2	--	20-40	0-10	40-60	--	--				
Tcp	VII-46	2,002	1,926	All	<5	<5	--	40-60	--	35-55	--	--	O		12.7	0.3
Tcp	G1-1982	1,982	1,982	All	tr	<5	--	5-15	40-60	30-50	--	--	N	C2	13.2	0.4
Tcp	G1-1982	1,982	1,982	75-500	5-10	<2	--	--	--	70-90	--	--				
Tcp	G1-1982	1,982	1,982	38-106	<2	--	--	--	40-60	40-60	--	--				
Tcp	G1-1982	1,982	1,982	<38	10-20	--	--	--	30-40	20-40	--	C.<2				
Tcp	YM-48	2,114	2,019	All	tr	--	10-20	--	--	20-30	40-60	--				
Tcp	YM-48	2,114	2,019	106-500	<2	--	20-40	5-10	5-15	20-40	10-30	--				
Tcp	YM-49	2,221	2,090	All	tr	tr	10-20	--	--	20-30	40-60	--	P	C6(5-7)	8.0	1.4
Tcp	JA-26	1,995	2,173	All	--	--	tr	30-50	tr	10-20	--	A,30-50	N		18.3	1.0
Tcb	JA-28	2,001	2,178	All	tr	2.5	--	30-50	--	10-20	--	A,30-50			20	5
Tcb	G1-2233	2,233	2,233	<500	<5	<5	20-40	11-20	10-20	10-20	--	H,20-40	N	C6(6-7)	15.4	0.4
Tcb	G1-2233	2,233	2,233	75-500	<5	5-15	15-30	5-10	--	40-60	--	H,<5				
Tcb	G1-2233	2,233	2,233	38-106	<5	5	20-40	15-30	10-20	10-20	--	H,20-40				
Tcb	G1-2289	2,289	2,289	75-500	--	5-10	30-50	<5	--	30-50	--	H,10-20	N	C6(5-7)	15.8	1.0
Tcb	YM-54	2,491	2,330	All	tr	tr	--	50-70	--	20-40	--	--	W	C5(4-7)	17.8	0
Tcb	YM-54	2,491	2,330	106-500	5-10	2-5	--	30-50	--	25-45	--	--				
Tcb	YM-54	2,491	2,330	38-106	5-10	5-10	--	30-50	--	30-50	--	--	M	C6(5-7)	20.4	0.2
Tcb	YM-54	2,491	2,330	<38	5-10	2-10	--	15-30	--	40-60	--	--				
Tcb	G1-2333	2,333	2,333	75-500	2-5	2-5	--	15-30	10-30	50-70	--	--				
Tcb	G1-2333	2,333	2,333	<75	5-10	<5	--	15-30	20-40	20-40	--	--				
Tcb	G1-2363	2,363	2,363	All	10-20	5-10	--	30-50	--	30-50	--	--				
Tcb	G1-2363	2,363	2,363	106-500	5	<2	--	30-50	0-10	30-50	--	--				
Tcb	G1-2363	2,363	2,363	38-106	5	<2	--	30-50	0-10	30-50	--	--				
Tcb	G1-2363	2,363	2,363	<38	5-10	<2	--	20-40	0-10	40-60	--	--				

Table 4-14. Petrologic characterization of tuff samples from drillholes J-13, UE-25a#1, USW G-1, USW G-2, and USW GU-3[a] (page 3 of 4)

					Abundance (weight %)											
Unit[b]	Sample	Depth (ft)	USW G-1 depth (ft)[c]	Particle size (μm)	Smectite	Illite Muscovite	Clinop-tilolite	Quartz	Cristob-alite	Alkali feldspar	Glass	Other[d]	Degree of welding[e]	Oxidation state[f]	Crystals (%)	Lithics (%)
Tcb	G1-2410	2,410	2,410	75-500	5-10	<2	--	20-40	0-10	30-50	--	--				
Tcb	G1-2410	2,410	2,410	<75	5-10	<5	--	20-40	5-15	30-50	--	--				
Tcb	JA-32	2,533	2,467	106-500	<5	5-15	--	30-50	--	30-50	--	--				
Tcb	JA-32	2,533	2,467	355-500	--	5-10	--	40-50	--	30-40	--	--				
Tcb	JA-32	2,533	2,467	150-180	--	10-15	--	35-50	--	40-65	--	--				
Tcb	JA-32	2,533	2,467	106-150	<5	5-15	--	30-50	--	30-50	--	--				
Tcb	JA-32	2,533	2,467	38-106	<2	tr	--	30-50	--	30-50	--	--				
Tcb	JA-32	2,533	2,467	<38	5-10	--	--	20-40	--	40-60	--	A, tr				
Tcb	G1-2476	2,476	2,476	75-500	<2	2	--	30-50	5-15	40-60	--	--				
Tcb	G1-2476	2,476	2,476	<75	2-5	2	--	30-50	5-15	40-60	--	--				
Tct	G1-2698	2,698	2,698	All	<5	10-15	30-50	<5	--	30-50	--	H, 5	M	C6(5-7)	S13.2	1
Tct	G1-2840	2,840	2,840	75-500	2-5	2-5	--	40-60	0-10	30-50	--	--				
Tct	G1-2840	2,840	2,840	<75	2-5	2-5	--	40-60	0-10	30-50	--	--				
Tct	G1-2854	2,854	2,854	75-500	<2	5-10	--	30-50	0-10	30-50	--	--				
Tct	G1-2854	2,854	2,854	<75	<2	5-10	--	30-50	0-10	30-50	--	--				
Tct	G1-2901	2,901	2,901	All	5-10	5-10	--	20-40	--	40-60	--	--	W	C6(6-7)	4.0	21.4
Tct	G1-3116	3,116	3,116	All	5-10	5-10	5-15	20-40	--	20-40	--	A,10-30				
Tct	JA-37	3,497	3,286	All	20-40	5	5	30-60	--	15-30	--	--				
Tct	JA-37	3,497	3,286	355-500	10-15	--	tr	40-50	--	30-40	--	C,tr				
Tct	JA-37	3,497	3,286	106-150	5-10	--	--	40-50	--	30-40	--	C,tr				
TI	G1-3658	3,658	3,658	75-500	40-60	--	--	--	--	40-60				C3	23.4	0
TI	G1-3658	3,658	3,658	106-500	40-60	--	--	--	--	40-60						
TI	G1-3658	3,658	3,658	38-106	30-50	--	--	--	--	50-70						
TI	G1-3658	3,658	3,658	<38	50-70	--	--	--	--	30-50						

Table 4-14. Petrologic characterization of tuff samples from drillholes J-13, UE-25a#1, USW G-1, USW G-2, and USW GU-3[a] (page 4 of 4)

					Abundance (weight %)												
Unit[b]	Sample	Depth (ft)	USW G-1 depth (ft)[c]	Particle size (µm)	Smectite	Illite Muscovite	Clinoptilolite	Quartz	Cristobalite	Alkali feldspar	Glass	Other[d]	Degree of welding[e]	Oxidation state[f]	Crystals (%)	Lithics (%)
Tba	G2-3933	3,933		<500	10-20	--	--	20-40	--	20-40	--	10-40,A				
Tba	G2-3933	3,933		75-500	40-10	--	--	29-39	--	34-54	--	10-20,A				

[a]Analyses were performed by ESS division of the Los Alamos National Laboratory; methods are discussed in Caporuscio et al., (1982). Data from Daniels et al., (1982). To convert from feet to meters, multiply by 0.328.

[b]Tpc = Tiva Canyon Member of the Paintbrush Tuff; Tpt = Topopah Spring Member of the Paintbrush Tuff; Tht = tuffaceous beds of Calico Hills; Tcp = Prow Pass Member of the Crater Flats Tuff; Tcb = Bullfrog Member of the Crater Flat Tuff; Tct = Tram unit of the Crater Flat Tuff; TI = lava flow and flow breccia; Tba = bedded tuff; and Tpp = Pah Canyon Member.

[c]Equivalent depth in drillhole USW G-1 according to relative position in stratigraphic unit. The thickness of the Bullfrog and Tram units in drillholes UE-25a#1 and J-13, respectively, are assumed to be of the same thickness as the corresponding units in drillhole USW G-1.

[d]A = analcime; C = calcite; M = mordenite; and T = tridymite.

[e]N = nonwelded; P = partly welded; M = moderately welded; O = densely welded; V = very densely welded (vitrophyre); and W = intermediately welded.

[f]The empirical stage of oxidation of iron-titanium exsolution oxide phases; C1 denotes unoxidized and C7 denotes completely oxidized. See Caporuscio for a discussion of oxide mineral alteration trends.

[g]Starting with whole rock.

[h]A blank indicates that an analysis was not performed; dashes indicate that the mineral was not detected, and tr = trace (<1%).

[i]Topopah Spring vitrophyre.

[j]Mineralogy in Tht in USW GU-3 is not similar to that in Tht in USW G-1. Stratigraphic equivalence is not valid.

[k]Sorption work was done with 75-500 µm fraction. Analysis still in progress.

million (ppm) oxygen and less than 20 ppm carbon dioxide. These conditions are somewhat different from those in deep geologic environments because of the low carbon dioxide content in the laboratory experiment and the possible (n = 0.71 to 0.92) for the coarse size fraction of sample YM-22 (welded tuff) and for sample G1-2840, both of which are nonzeolitized tuffs. With the possible exception of strontium (n = 0.87), a linear isotherm (n = 0.98 to 1.1) is indicated for the coarse-size fraction of sample YM-38 (zeolitized tuff). This latter result is expected because the sorption of these elements on zeolitized material should occur predominantly by ion exchange. The results of this study indicate that isotherms can be used to interpret the

4.1.3.3.4 Sorption data from circulating-system experiments

Average sorption ratios determined by both the batch and the circulating-system methods are shown in Table 4-15 for strontium, cesium, barium, americium, and plutonium. Considering the spread of experimental values, the agreement between the two methods is acceptable. In most cases the results fall within the spread of individual experimental values reported by Daniels et al. (1982).

Devitrified tuffs give slightly higher sorption ratios in the batch method than in the circulating-system method. The R_d values for the smectite-bearing devitrified tuff and for the zeolite-bearing vitric tuff show no consistent pattern.

Table 4-15. Average sorption ratios from batch, circulating-system, and crushed-tuff column sorption measurements at room temperature[a]

Element	Sample	Petrologic character[b]	Sorption ratio (ml/g)		
			Batch[c]	Circulating system	Column
Sr	YM-22	D	53 (3)[d]	27 (2)[c]	22
	YM-54	D	62 (12)	45 (3)	43
	JA-37	D + S	287 (14)	390 (10)	123
Cs	YM-22	D	290 (30)	490 (50)	363
	YM-54	D	180 (40)	120 (10)	130
	JA-37	D + S	610 (40)	1,800 (10)	1390
Ba	YM-22	D	900 (30)	120 (10)	137
	YM-54	D	410 (150)	130 (10)	149
	JA-37	D + S	760 (150)	860 (40)	--[e]
Am	YM-49	V + Z	4,300 (1,400)	2,200 (300)	--
	JA-37	D + S	28,000 (10,000)	3,400 (600)	--
	G1-1883	D	4,700 (300)	3,300 (100)	--
Pu	YM-49	V + Z	230 (50)	570 (170)	--
	JA-37	D + S	400 (70)	290 (170)	--
	G1-1883	D	77 (11)	56 (11)	--

[a]Sources: Daniels et al. (1982); Treher and Raybold (1982).
[b]D = devitrified, V = vitric, S = contains smectite, Z = contains zeolite.
[c]From Tables 4-12 and 4-13.
[d]Value in parentheses is the absolute-value standard deviation of the means of duplicate measurements.
[e]-- = no data.

4.1.3.3.5 Comparison of sorption ratios from batch, circulating system, and column measurements

Batch and both types of column experiments on various tuffs with the same particle-size distribution yield sorption ratios for strontium, barium, cesium, americium, and plutonium that are within a factor of 2 (americium on sample JA-37, a devitrified tuff containing smectite, was an exception). This agreement means that self-grinding of the tuff in batch experiments is probably not a problem. The experiments with crushed-tuff columns show that

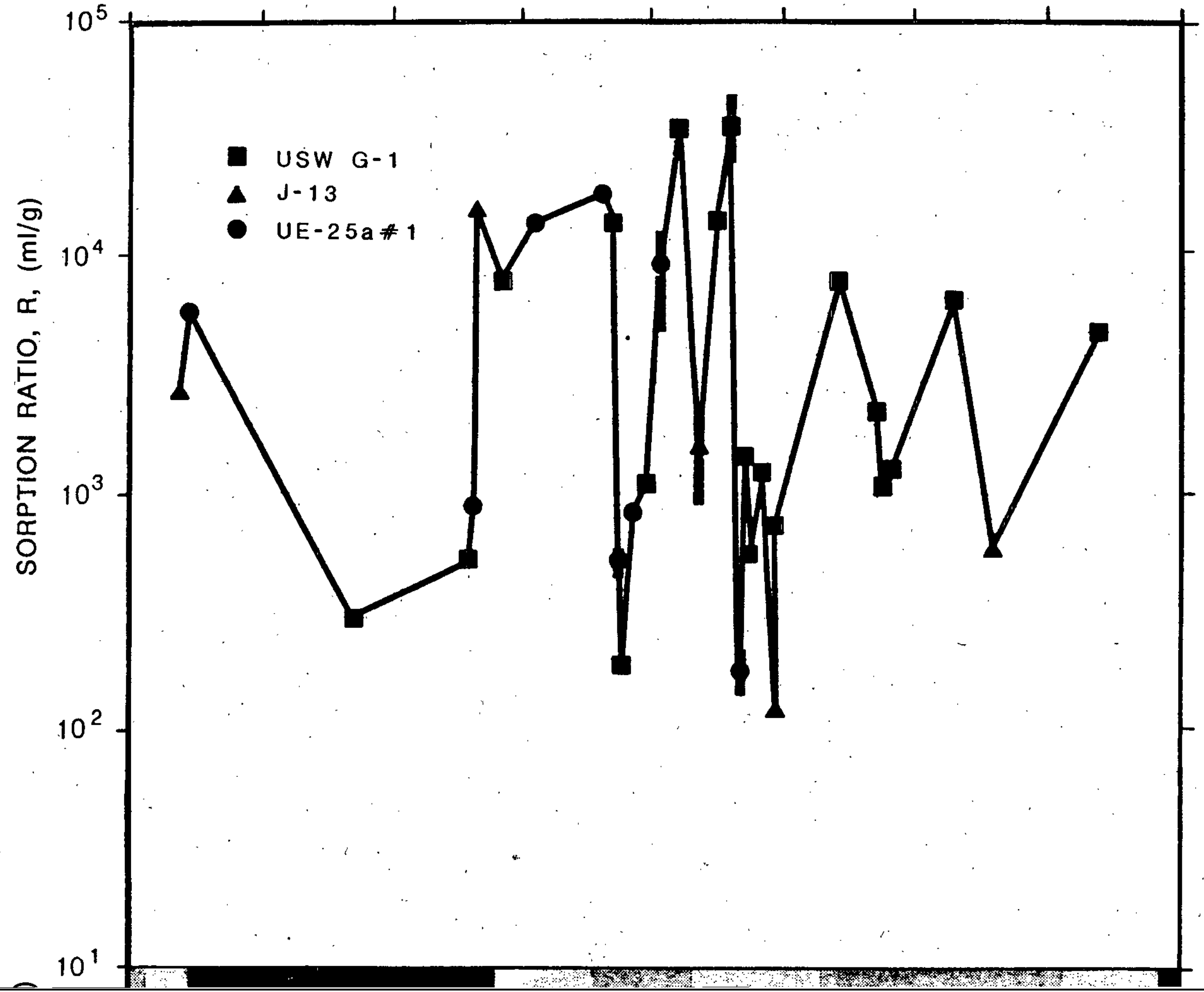

10^5
10^4
10^3
10^2
10^1
SORPTION RATIO, R, (ml/g)
USW G-1
J-13
UE-25a#1

strontium, and barium (and vice versa). The difference may be explained by mineralogic differences and will be investigated on that basis (Section 8.3.1.3). It may be difficult to correlate statistically this difference with

As described in Section 8.3.1.3, current studies will provide a more complete understanding of the sorption of the radionuclides listed in 40 CFR Part 191, Appendix A, including technetium, tin, and neptunium. Uranium and thorium are also being studied because they are the parents of radium. Regression analysis is being employed to determine the correlation of sorption with tuff mineralogy.

Because tuff samples may be composed of more than one sorbing mineral, a method has been developed to predict sorption ratios for samples of known mineralogy by combining the effects of several minerals. The combined effect is tentatively defined as a weighted sum called the SMC. Thus,

$$SMC = \Sigma W_i X_i, \quad (4-4)$$

where W_i is the weighting factor for each mineral phase relative to that of clinoptilolite and X_i is the abundance in percent of each phase. Further details are given in Daniels et al. (1982). Studies of sorption on pure minerals and selected core samples will be performed to quantify expected sorption along transport pathways using the SMC concept (Section 8.3.1.3.4).

The following correlations of mineralogy with sorptive behavior of radionuclides have been identified and can be summarized as follows:

1. The sorption of alkali metals (e.g., cesium) and alkaline earths (strontium, barium, and radium), which probably exist in ground water as uncomplexed ions (Section 4.1.3.4.2) and probably sorb by ion exchange, is directly related to the presence of minerals with exchangeable cations: the zeolite clinoptilolite and potentially the smectite clays. The sorption ratios on these minerals are from 1,000 to higher than 10,000 ml/g. Because of the large quantities of the zeolite clinoptilolite in the Calico Hills and Prow Pass units lying below the repository horizon, the waste elements cesium, strontium, and radium would be strongly sorbed and their movement greatly retarded if the flow path is through these units.

2. The correlation of sorption of cerium, europium, plutonium, and americium with mineralogy also exists, but the relation is not as clear as for the alkali metals. However, sorption ratios are high for the elements previously listed (from 100 to higher than 1,000 ml/g) and, therefore, the lack of correlation is not critical. The sorption of these elements, though, is undoubtedly influenced by the formation of hydroxyl and carbonate complexes.

3. It appears that sorption on tuff will not offer much retardation for such anionic species as oxidized technetium species (i.e., TcO^{4-}).

4.1.3.3.7 Sorptive behavior as a function of ground-water composition

The composition of the ground water and matrix mineralogy controls the oxidation state and speciation of radionuclides as well as their solubility, while at the same time providing competing ion and species for sorption sites, all of which can affect sorption of the radionuclides by tuff.

Because ground-water composition may vary between the repository and the accessible environment, studies have been performed to determine what effect changes in ground-water composition have on measured sorption ratios.

Three ground waters are being investigated: water from well J-13, located in Jackass Flats; water from drillhole UE-25p#1 and from drillhole USW H-3, both of which are located on Yucca Mountain. Water from well J-13 has been used as the reference ground-water composition partly because the approximate production region of the well is the Topopah Spring Member; which, at Yucca Mountain, lies in the unsaturated zone and is the proposed repository horizon, and because, at the time studies on ground water began, well J-13 was the nearest producing well to Yucca Mountain. Comparisons are now being made of sorption ratios obtained with J-13 water to those from drillholes UE-25p#1 and USW H-3. The composition of these waters is given in Tables 4-7 and 4-8. Water from drillhole UE-25p#1 has the highest ionic strength, whereas drillhole USW H-3 water has the highest pH measured thus far at Yucca Mountain and was measured as slightly reducing in the field. A thorough discussion of water chemistry at Yucca Mountain is contained in Ogard and Kerrisk (1984). Distilled water was also studied (in some instances) as a representative of an extreme in ground-water composition.

Elements studied thus far include strontium, cesium, barium, europium, and tin. Plans for studying the sorption of actinides as a function of ground-water chemistry is found in Section 8.3.1.3.4. The selection of tuff samples used was based on their predominant mineralogy. Sample GU3-1301 is a vitric tuff from the Topopah Spring Member; G1-2233 is a zeolitized tuff from the Bullfrog Member; G4-1504 is a zeolitized tuff from the Calico Hills; and G1-2901 is a devitrified tuff from the Tram Member. Sorption ratios were measured using standard batch technique (Section 4.1.3.2.2).

Tables 4-16a and 4-16b give the results obtained for well J-13, drillhole UE-25p#1, and distilled water (where available). Data from drillhole USW H-3 have not yet been published. For those elements presumed to sorb by an ion exchange mechanism (such as strontium, barium, and cesium), the lower ionic strength waters gave the highest sorption ratios. This is probably due

Table 4-16a. Sorption ratios for cesium and strontium in different waters[a,b,c]

Core[d]		Cesium			Strontium		
		J-13	UE-25p#1	Distilled water	J-13	UE-25p#1	Distilled water
GU3-1301 (vitric)	Sorption	160(35)	46(5)	NA[e]	32(8)	10(2)	NA
	Desorption	180(40)	55(4)	NA	90(20)	32(1)	NA
G1-2233 (zeolitized)	Sorption	13,500(800)	7,500(1,100)	13,000(1,600)	48,000(3,000)	2,000(330)	56,000
	Desorption	23,000(6,000)	8,800(900)	8,700(3,400)	90,000(40,000)	3,000(500)	21,000(12,000)
G1-2901 (devitrified)	Sorption	1,290(110)	900(250)	3,350(170)	68(1)	44(13)	136(1)
	Desorption	1,380(30)	850(76)	3,800(670)	67(1)	35(4)	105(13)
G4-1502 (zeolitized)	Sorption	ND[g]	ND	ND	ND	ND	ND
	Desorption	ND	ND	ND	ND	ND	ND
G1-2840	Sorption	ND	ND	ND	ND	ND	ND
	Desorption	ND	ND	ND	ND	ND	ND

[a]Sorption ratios in ml/g.
[b]Numbers in parentheses represent the standard deviation of the mean.
[c]Crowe and Vaniman (1985); Daniels et al. (1982); Ogard and Vaniman (1985); and Rundberg et al. (1985).
[d]The cores are described in the text.
[e]NA = not applicable.
[f]Particle size was <500 μm rather than the standard 75 to 500 μm.
[g]ND = no data.

Table 4-16b. Sorption ratios for barium, europium and tin[a,b,c]

Core[d]		Barium J-13	Barium UE-25p#1	Barium Distilled water	Europium J-13	Europium UE-25p#1	Europium Distilled water	Tin J-13	Tin UE-25p#1
GU3-1301	Sorption	570(60)	82(18)	NA[e]	75(12)	>17,000	NA	160(8)	4,000(520)
(vitric)	Desorption	660(100)	140(30)	NA	110(40)	>20,000	NA	1,280(180)	6,750[h]
G1-2233	Sorption	250,000(30,000)[f]	41,000(6,300)	55,000(5,300)	900(200)	>5,600	516(100)	ND[g]	ND
(zeolitized)	Desorption	240,000(80,000)[f]	59,000(6,000)	34,000(23,000)	5,000(2,000)	>7,900	1,400(600)	ND	ND
G1-2901	Sorption	1,600(200)	1,400(520)	7,200(100)	160,000(50,000)	38,000(16,000)	37,000(400)	22,000(5,000)	35,800(900)
(devitrified)	Desorption	1,980(30)	1,100(90)	6,100(900)	210,000(50,000)	69,000(20,000)	27,500(6,200)	38,000(8,000)	52,500(1,900)
G4-1502	Sorption	ND	ND	ND	ND	ND	ND	215(56	800(110)
(zeolitized)	Desorption	ND	ND	ND	ND	ND	ND	500(8)	300(130)
G1-2840	Sorption	ND	ND	ND	ND	ND	ND	283(160)	20,000(2,700)
	Desorption	ND	ND	ND	ND	ND	ND	780(130)	18,400(6,900)

[a]Sorption ratios in ml/g.
[b]Numbers in parentheses represent the standard deviation of the mean.
[c]Crowe and Vaniman (1985); Daniels et al. (1982); Ogard and Vaniman (1985); and Rundberg et al. (1985).
[d]The cores are described in the text.
[e]NA = not applicable.
[f]Particle size was <500 μm rather than the standard 75 to 500 μm.
[g]ND = no data.
[h]Only one measurement.

4.1.3.4 Processes affecting radionuclide concentrations and speciation solution

The solubility of the waste elements can influence their transport by limiting the maximum concentration of the elements dissolved in the aqueous phase. Speciation, defined as the formation of various complexes and oxidation states in the aqueous phase, in turn affects the solubility. Speciation and solubility of individual waste elements depend on the chemical properties of the waste element, on the state of the local water (composition, pH, oxidation state, and temperature), and, if nonequilibrium processes are important, on factors such as precipitation and dissolution kinetics, oxidation-reduction kinetics, the identity of the solids present, water-flow conditions, and colloid formation. The following discussion of solubility and speciation is in terms of waste elements rather than radionuclides because these processes are controlled by the total concentration of an element in solution--that is, the sum of the concentrations of all its isotopes. The concentrations of individual radionuclides depend on the isotopic composition of the element.

At this time it is possible to estimate the solubilities of many important waste elements under repository conditions. The estimates are primarily based on literature data interpreted in terms of a chemical-equilibrium model. However, solubility calculations alone will not be sufficient for determining the concentration limits of waste elements (NRC, 1984). For this reason, solubility data for important waste elements have

Solubility generally increases as the variety and concentration of complexes of an element increase; thus, the solubility is influenced by the tendency of a given element to form complexes and the concentrations of species with which it can complex. Sorptive behavior depends on the size and charge of the sorbing species; both of these quantities vary among the complexes of a given element. Thus, speciation can influence sorption. Aqueous species can be experimentally detected in solution by a number of techniques; spectroscopy is most commonly used (Rossotti and Rossotti, 1961). However, concentrations of aqueous species are normally calculated from a knowledge of the overall composition of the solution (total concentrations of the elements in solution) and the formation constants of possible aqueous species using equilibrium thermodynamic methods. Equilibrium thermodynamic methods work well (given the proper data) for the various complexes of a particular oxidation state, but may yield inaccurate results for the distribution of the element among possible oxidation states (Lindberg and Runnells, 1984).

4.1.3.4.1.2 Precipitation

Solubility, like speciation, depends on the composition, pH, and temperature of the water (Garrels and Christ, 1965; Sposito, 1981; Stumm and Morgan, 1981). If an element can also exist in various oxidation states, variables that control oxidation-reduction behavior also influence solutibility. Unlike complex formation, which is essentially always an equilibrium process, precipitation processes are often not in equilibrium or in metastable equilibrium (Stumm and Morgan, 1981). If dissolution and precipitation kinetics are fast on the time scale of interest, equilibrium behavior can be assumed. If kinetics are very slow, a metastable equilibrium may exist where the aqueous phase is in metastable equilibrium with some solid other than the most stable (least soluble) one. In some intermediate cases, the dissolution or precipitation rates may be comparable to the time scale of interest; for these cases, kinetic data are required to accurately describe aqueous concentrations.

Coprecipitation refers to a group of processes whereby more than one compound precipitates at one time (Sposito, 1981). Three examples are mixed-solid formation, adsorption during precipitation, and inclusion during precipitation. The importance of coprecipitation for waste-element solubility at Yucca Mountain is uncertain at this time.

4.1.3.4.1.3 Natural-colloid formation

A number of actinides, plutonium in particular, can form natural colloids under certain conditions (Avogadro and DeMarsily, 1984; Kim et al., 1984a; Olofsson et al., 1984). The questions of primary importance for a waste repository are whether natural colloids can form under the conditions expected at the repository or along flow paths to the environment--and whether the colloids would be transported by the aqueous phase. This section addresses only the question of natural-colloid formation; colloid transport is discussed in Section 4.1.3.6. Related, but different phenomena, the sorption of waste elements on particulate material normally present in the water and colloid formation during waste-form or waste-package dissolution, are discussed in Sections 4.1.2 and 4.1.3.3, and Section 7.4, respectively.

Plutonium(IV) readily forms colloids under conditions that are similar to Yucca Mountain water (Olofsson et al., 1984) near-neutral solutions of low ionic strength (about 10^{-3} mole/L) (Newton and Rundberg, 1984). These colloids are solution like sols that are optically clear, show a characteristic absorption spectrum, and do not settle out of solution. Colloidal plutonium shows x-ray diffraction patterns similar to crystalline plutonium dioxide; higher-order lines are missing, indicating small crystalline size (20 to 30 angstroms). There is also some indication that americium(III) may form colloids under similar conditions (Olofsson et al., 1984). Neither element has been studied to the extent that colloid properties (particle size and stability) can be predicted for known solution conditions. Colloid properties are, however, being examined. Plans for obtaining this information are outlined in Section 8.3.1.3.5.

4.1.3.4.1.4 Radiolysis

Radiation can affect the solubility of waste elements by altering the composition of the water or by influencing the crystallinity of the solids that form (Ausloos, 1969). The primary effect of gamma radiation will be a reduction of water pH and a trend toward more oxidizing conditions as long as air is present; secondary effects will be the production of nitrate (or nitrite) anions. Gamma radiation will be most important early in the life of these conditions. This section describes data that can be used to estimate waste element solubilities at Yucca Mountain.

4.1.3.4.2.1 Solubility of americium, plutonium, and neptunium in well J-13 water

Preliminary measurements of the solubility of americium, plutonium, and neptunium in a neutral electrolyte and in water from well J-13 have been completed (Nitsche and Edelstein, 1985). The measurements were made from oversaturation at 25°C and a pH of 7. For plutonium and neptunium, measurements were started with different oxidation states that might exist under natural conditions. Table 4-17 summarizes the results.

Under the conditions of the measurements, neptunium(V) was the only oxidation state finally observed in the aqueous phase, for neptunium(V) or neptunium(VI) as the initial aqueous oxidation state. Measurements were done starting with plutonium(IV), plutonium(V), and plutonium(VI) aqueous species; the final aqueous species were predominantly plutonium(V) plus plutonium(VI) (over 90 percent), with plutonium(V) ranging from about 40 to 80 percent. Some difficulties were encountered in identifying the solid phases that precipitated in the experiments. For americium solubility in well J-13 water, both americium(III) hydroxy carbonate ($AmOHCO_3$) and americium (III) carbonate-2-hydrate ($Am_2(CO_3)_3 2H_2O$) were found. For neptunium in well J-13 water, sodium neptunyl carbonate-n-hydrate ($Na_3NpO_2(CO_3)_2 \cdot nH_2O$) was tentatively identified as the solid. For plutonium, the solids could not be identified.

The results from these experiments are being reviewed in terms of a chemical equilibrium model of solubility. They will be incorporated into the solubility models for Yucca Mountain.

4.1.3.4.2.2 Solid waste dissolution experiments

In addition to direct solubility measurements, dissolution experiments on spent fuel and other high-level waste forms such as borosilicate glass are also being performed. The measurements are described in Section 7.4.3 (Bazan and Rego, 1985; Wilson and Oversby, 1985). The experiments expose bare spent fuel or glass to well J-13 water and other water compositions and essentially approach steady state from undersaturation. Many of the experiments contain other materials such as zircaloy cladding, stainless steel, or tuff. Thus, the experimental data may be more difficult to interpret in terms of fundamental mechanisms than simple solubility experiments.

Waste-dissolution experiments under conditions characteristic of Yucca

Table 4-17. Analytical results of solutions in equilibrium with their solid phase (supersaturated starting conditions) in 0.1 M $NaClO_4$ and well J-13 ground water at pH = 7.0 ± 0.1, 25 ± 1°C

Test no.	Initial species	Solubility (M)		Final oxidation state of soluble species[a]		Solid	
		$NaClO_4$	Well J-13	$NaClO_4$	Well J-13	$NaClO_4$	Well J-13
1	NpO_2^+	$(4.4 \pm 0.1) \times 10^{-4}$	$(1.6 \pm 0.6) \times 10^{-3}$	+V = 100%	+V = 100%	Amorphous	Crystalline $Na_3NpO_2(CO_3)_2 \times nH_2O$
2	NpO_2^{2+}	$(3.5 \pm 0.1) \times 10^{-4}$	$(7.2 \pm 0.7) \times 10^{-4}$	+V = 100%	+V = 100%	Crystalline unidentified	Crystalline unidentified
3	Am^{3+}	$(3.0 \pm 0.1) \times 10^{-4}$	$(1.1 \pm 0.2) \times 10^{-6}$	+III = 100%	+III = 100%	Mostly amorphous	Crystalline $Am_2(CO_3)_3 \times 2H_2O/AmOHCO_3$
4	Pu^{4+}	$(3 \pm 2) \times 10^{-8}$	$(1.6 \pm 0.2) \times 10^{-6}$	III + IV + p = 3 ± 2% V + VI = 95 ± 4% V = 68 ± 9%	III + IV + p = 2 ± 3% V + IV = 98 ± 3% V = 40 ± 5%	Amorphous	Amorphous
5	PuO_2^+	$(2 \pm 1) \times 10^{-8}$	$(8 \pm 3) \times 10^{-6}$	III + IV + p = 5 ± 4% + VI = 95 ± 4% V = 70 ± 17%	III + IV + p = 0 ± 2% V + VI = 100 ± 2% V = 64 ± 6%	Amorphous	Crystalline unidentified
6	PuO_2^{2+}	$(1.0 \pm 0.5) \times 10^{-7}$	$(3 \pm 2) \times 10^{-5}$	III + IV + p = 3 ± 2% V + VI = 97 ± 2% V = 82 ± 16%	III + IV + p = 2 ± 2% V + VI = 98 ± 2% V = 67 ± 6%	Amorphous	Crystalline unidentified

[a]p = Pu(IV) polymer (Nitsche and Edelstein, 1985).

4.1.3.4.2.3 Literature data for waste elements

The measurement of solubilities and other thermodynamic properties of important waste elements is an active field of study. Thus, the literature contains data that are useful for understanding and modeling solubility and speciation. Although these data were not obtained under conditions that are characteristic of a Yucca Mountain repository, solubility models for repository conditions can be tested and validated using literature data.

Americium. The behavior of americium in natural waters is somewhat simpler than that of the other actinides (e.g., plutonium or uranium) because americium(III) is the only stable oxidation state observed under these conditions. There have been a number of recent measurements of the solubility of americium(III) in a neutral electrolyte and with carbonate present (Rai et al., 1983; Silva and Nitsche, 1983; Bernkopf and Kim, 1984; Kim et al., 1984b; Rai and Ryan, 1984; Nitsche and Edelstein, 1985). The studies have also been used to define or support formation constant data for a number of important americium(III) complexes. Experiments by Lundquist (1982) and total plutonium concentrations in solution at pH 7 are in the range of 10^{-6} to 10^{-8} M.

From solubility measurements with carbonate present, Kim et al. (1984b) have proposed the existence of solid plutonium(IV) dihydroxide carbonate ($Pu(OH)_2\ CO_3$) and a very stable complex, plutonium(IV) carbonate ion ($PuCO_3^+$). Their value of the formation constant for the reaction $Pu^{4+} + CO_3^{-} = PuCO_3^+$, is log(K) = 47.1. This is similar to a value of log(K) of 41 or less at 25°C for the same reaction reported by Lemire and Tremaine (1980). If the formation constant of the plutonium(IV) carbonate ion ($PuCO_3^+$) is this large, the solubility of plutonium in water from Yucca Mountain could be quite high (Wolfsberg et al., 1982a). However, estimates of the formation and thus these data are not indicative of uranium solubility at Yucca Mountain. They are, however, useful for testing solubility models with carbonate present.

Experiments on spent fuel dissolution in well J-13 water showed uranium concentrations in solution that are less than about 2 x 10^{-5} mole/L (Wilson and Oversby, 1985). At present it is not clear what solid phase is controlling uranium solubility at this concentration. Although the test solutions are exposed to air, uranium in spent fuel is primarily as uranium(IV), that is as uranium dioxide; thus, it is possible that a uranium solid other than schoepite controls solubility. This measured concentration limit is about a factor of 100 below the calculated solubility of uranium in well J-13 water assuming schoepite as the controlling solid (Ogard and Kerrisk, 1984). The calculations indicate that one polynuclear complex, uranyl(VI) trihydroxide carbonate ion $((UO_2)_2 CO_3(OH)_3)^-$, incorporates almost all the aqueous uranium. An experimental determination of uranium solubility in well J-13 water may be needed to resolve this difference. Plans for obtaining the information are outlined in Section 8.3.1.3.5.

Thermodynamic data for uranium(VI) have recently been reviewed by Tripathi (1984). The thermodynamic data base for EQ3/6 is being updated using this review as a basis.

Neptunium. Solubility data for neptunium were discussed in Section 4.1.3.2.1 and in the work of Nitsche and Edelstein (1985). Other literature data on the solubility of neptunium under oxidizing conditions will be reviewed as part of the incorporation of neptunium data. Plans for the work are outlined in Section 8.3.1.3.5.

Other waste elements. A number of waste elements are likely to have high solubilities in water from Yucca Mountain. They include carbon, cesium, iodine, and technetium (Rai and Serne, 1978; Allard and Torstenfelt, 1983; Apps et al., 1983; Ogard and Kerrisk, 1984). The solubility of technetium, which can exist in a number of oxidation states, should be high because of

Mountain water (Apps et al., 1983); solubility measurements are planned for these elements because they are in large quantities and because they are considered as important radionuclides (Section 4.1.3.1.1). Radioisotopes of nickel are present as waste elements in subassembly hardware from light water reactors and in defense high-level waste glass. No solubility data were found for nickel that could be applied to water from Yucca Mountain; solubility measurements are planned as outlined in Section 8.3.1.3.5.

4.1.3.4.3 Solubility modeling

A program to model solubility and speciation data is an important part of any effort to assess the concentration limits of elements in solution. It is necessary to model experimental data in terms of some theoretical framehigher than the calculated solubility. For uranium, Table 4-18 shows the value calculated by Ogard and Kerrisk (1984) for uranium(VI). This solubility is about 100 times higher than measured uranium concentrations in the same water over spent fuel (Section 7.4.3 and Wilson and Oversby, 1985). The reason for this difference is uncertain. At this time there are no other direct measurements of waste-element solubilities in well J-13 water.

Ogard and Kerrisk (1984) also reported calculated solubilities of the same six elements in waters from two other drillholes in the vicinity of Yucca Mountain (UE-25p#1 and USW H-3). The water from these drillholes has somewhat different compositions than water from well J-13 (Tables 4-6 and 4-7); the calculated solubilities were significantly different in a number of cases. Particularly, the water from drillhole USW H-3 was assumed to be reducing. No waste element solubility measurements have yet been made in waters from drillholes UE-25p#1 and USW H-3. Future experimental solubility measurements are described in Section 8.3.1.3.5.

Table 4-18. Solubility of waste elements in well J-13 water[a]

Waste element	Solubility (moles/L)	Source of data
Americium	1×10^{-6}	
Plutonium	1×10^{-5}	Nitsche and Edelstein, 1985
Neptunium	1×10^{-3}	Nitsche and Edelstein, 1985
Uranium	4×10^{-3}	Ogard and Kerrisk, 1984
Curium	[b]1×10^{-6}	Apps et al.1983
Thorium	[b]1×10^{-9}	Apps et al. 1983
Strontium	8×10^{-4}	Ogard and Kerrisk, 1984
Radium	3×10^{-7}	Ogard and Kerrisk, 1984
Carbon	High[b,c]	Kerrisk, 1984b
Cesium	High[b,c]	Rai and Serne, 1978
Technetium	High[b,c]	Ogard and Kerrisk, 1984
Iodine	High[b,c]	Apps et al. 1983
Tin	[b]1×10^{-9}	Apps et al. 1983
Zirconium	[b]1×10^{-10}	Rai and Serne, 1978

Table 4-18. Solubility of waste elements in well J-13 water[a] (continued)

Waste element	Solubility (moles/L)	Source of data
Samarium	[b]2×10^{-9}	Benson and Teague, 1980
Nickel	[b]1×10^{-2}	Benson and Teague, 1980

[a]At pH of 7, 25°C, and oxidizing conditions.
[b]Estimated data.
[c]Solubility of these waste elements is expected to be high enough so that solubility will not limit concentration at a Yucca Mountain site.

4.1.3.5 Matrix diffusion

Moving ground water would provide the principal means of transporting radionuclides from the repository. Consequently, an understanding of water movement through tuff formations is vital. The diffusion of radionuclides from fracture water into the pore water in the rock matrix is important for retarding the transport of dissolved radionuclides through fractures in tuff, particularly for nonsorbing or low-sorbing soluble species. The apparent diffusion coefficient for a given radionuclide in tuff matrix depends on properties that are intrinsic to the chemical species (e.g., ion mobility) and properties of the tuff (such as porosity, tortuosity, and sorption ratio). It is, therefore, necessary to measure the diffusion coefficient of waste-element species in various unsaturated and saturated fractured tuff units. Preliminary results from experiments on radionuclide diffusion in tuff matrix are described in detail by Daniels et al. (1982). The information presented here is based on that report. Further work on the dynamic transport of radionuclides is planned in Section 8.3.1.3.6. This work will encompass diffusion studies in saturated and unsaturated fractured tuff.

4.1.3.5.1 Diffusion into the rock matrix

In the current conceptual model of the hydrology of Yucca Mountain, water is believed to flow predominantly in the matrix of the tuffs in the unsaturated zone, and predominantly in the fracture networks of the tuffs in the saturated zone. The effective diffusion coefficient of a dissolved species in the tuff matrices is an important quantity in determining the rates at which that species is transported through the rock units of either zone. If the flux through unsaturated rocks is small (less than 0.05 mm/yr), ordinary diffusion will be the dominant transport mechanism, and measurements of the effective diffusion coefficient will be needed in order to model the transport of radionuclide-bearing compounds to the accessible environment. For the flows through the fracture networks of the saturated zones, the effective diffusion coefficient in the matrix is one of several quantities that determine the rate at which radionuclides dissolved in rapidly flowing fracture water can enter the pore water of the matrix, where chemical retardation is generally most pronounced; this is the "matrix diffusion" mechanism alluded to earlier in this section. Thus, the effectiveness of

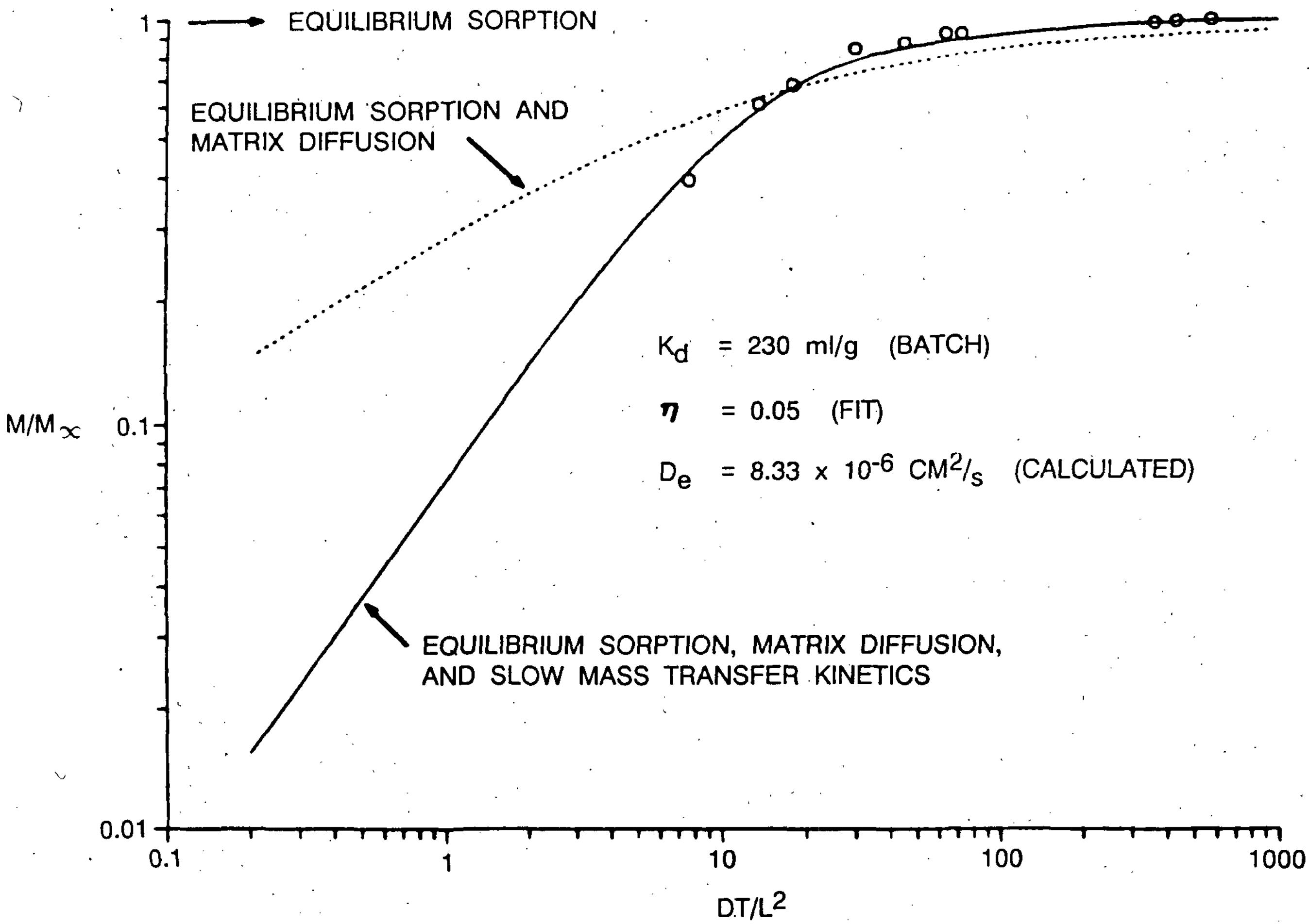

M/M_∞ = MASS OF SOLID OVER TIME (T) / MASS OF SOLID (∞)

DT/L^2 = DIMENSIONLESS TIME WHERE D = EFFECTIVE POROSITY, T = TIME, AND L = THICKNESS OF TUFF WAFER

K_d = DISTRIBUTION COEFFICIENT (ASSUMED TO BE EQUAL TO R_d (SORPTION RATIO))

η = REACTION RATE OF DESORPTION/DIFFUSIVITY

D_e = DIFFUSION COEFFICIENT

Figure 4-15. Cesium diffusion with slow sorption (tuff sample number G1-1883). Modified from Rundberg (1985).

the experimental uptake. At early times, the discrepancy between the slow kinetics and the conventional treatment becomes quite large.

The rate constants for the sorption of cesium-137, strontium-85, and barium-133 are summarized in Table 4-19 with the diffusion coefficients determined by fitting the data to the Crank (1975) solution. The diffusion coefficients are all smaller than the ionic diffusion coefficient calculated from ionic mobilities. This is as expected because the pores in the tuff matrix represent a tortuous path that also may have constrictions to slow the diffusion of ions through the matrix. Details of the above analysis are given by Rundberg (1985). Plans for obtaining additional information are outlined in Section 8.3.1.3.6.

Table 4-19. Sorption rate constants for tuff from drillhole USW G-1[a,b]

Tuff sample	Radionuclide	kd (ml/g)	k_1 (s^{-1})	k_2 (s^{-1})	D (cm^2/s)
G1-1436	Cesium	7,790	6.3×10^{0}	1.4×10^{-4}	2.78×10^{-6}
	Strontium	36,300	3.5×10^{0}	2.0×10^{-5}	2.11×10^{-6}
	Barium	148,000	1.2×10^{1}	1.7×10^{-5}	3.38×10^{-7}
G1-1883	Cesium	230	5.9×10^{-2}	4.2×10^{-5}	1.33×10^{-6}
	Strontium	27	1.1×10^{-3}	6.7×10^{-6}	1.33×10^{-5}
	Barium	210	5.7×10^{-2}	4.4×10^{-5}	8.89×10^{-6}
G1-1982	Cesium	1,000	4.0×10^{-1}	4.7×10^{-5}	9.44×10^{-6}
	Strontium	88	9.5×10^{-3}	1.4×10^{-5}	1.37×10^{-5}
	Barium	800	2.6×10^{-1}	4.4×10^{-5}	8.89×10^{-6}

[a]Source: Rundberg (1985).
[b]K_d = retardation coefficient; k_1 = rate constant for forward reaction; k_2 = rate constant for reverse reaction; D = diffusion coefficients.

The experiments employed artificial fractures induced in tuff and granite core samples. Artificial fractures are hydraulically smooth; thus, the pieces mate well and do not have fracture-fill material that would complicate the surface chemistry and diffusion process. Experiments were performed on

Other factors include:

1. Chemical species in the water flowing in fractures diffuse into the water contained in rock pores.

2. The negative charge that is present on many rock surfaces can restrict the approach of anions. The exclusion may limit the diffusion of anions into the matrix thereby allowing the anions to move at the higher velocity of the water flowing in the center of the fractures, or channels, away from the surface film. The same phenomenon can restrict the entry of anions into the smaller pores.

3. A somewhat similar effect, called hydrodynamic chromatography, can result in particles flowing along pores at velocities somewhat greater than the average water velocity. Filtration in rock pores, however, can remove or retard the flow of suspended particulates.

4. Dispersion can result from diffusion, channeling, and turbulent flow, but dispersion by itself does not affect the average rate at which the transported material moves.

Gaseous phase transport is another means of transporting radionuclides. Volatile elements such as iodine-129 and carbon-14 can be transported in the gaseous phase in the unsaturated zone.

Previous portions of Section 4.1.3 have discussed radionuclide transport in terms of the retardation processes of sorption, precipitation, and diffusion. The remainder of this section will discuss radionuclide transport by suspended solids and by gaseous transport.

4.1.3.6.1 Transport of suspended solids

A possible mode of transport involves the movement of radioactive particles suspended in the ground water. Colloidal particles (less than a few micrometers in diameter) remain suspended for long periods and hence may migrate with the ground water. As the solid waste form is leached, particles containing radionuclides may form by the sorption of dissolved radionuclides on nonradioactive particles. At this time it is believed that plutonium and americium are likely to contribute most to transport as colloids.

To estimate the amount of radionuclides that could be transported by colloidal suspension, it is necessary to determine whether colloidal-sized particles that could be sorption sites for waste elements exist in the ground water of Yucca Mountain. Then, the sorption ratios for waste elements on these particles must be measured or estimated from the composition of the particles. In addition, the conditions under which colloids could form from the waste elements or from the waste and their stability after formation must be determined (Section 4.1.3.4.1). Finally, the conditions necessary for filtration of the particles by the tuff itself must be defined.

Matter in the colloidal state has a large surface area (300 m^2/g), thus it is not surprising that the most important properties of colloids are those that depend on surface interactions, such as adsorption. Drever (1982) discusses the nature and geochemistry of colloids, with emphasis on the charge surrounding colloids and its effect on suspension stability.

Olofsson et al. (1981, 1982a,b) classify radiocolloids (colloids containing radionuclides) as true colloids or pseudocolloids depending on their formation process. True colloids are formed by condensation of molecules or ions as a result of hydrolytic or precipitation processes. Colloids consist mostly of hydroxides or polymers formed by hydrolysis, and they have a very rapid formation rate. Pseudocolloids, on the other hand, are formed as a result of adsorption on impurities in the solution and tend to be much larger than true colloids (up to 5,000 angstroms). Pseudocolloids can be of two types, reversible and irreversible. The formation rate of pseudocolloids is basically determined by the sorption rate on colloidal impurities (Olofsson et al., 1982a,b).

In the event of a repository failure, radiocolloids are believed to be a significant factor for the transport of radionuclides, and might actually accelerate their transport away from the repository (Avogadro and Lanza, 1982; Avogadro and De Marsily, 1984). Radiocolloids may arise from a variety of sources. The corrosion of canister material can lead to the formation of absorbent colloids. Degradation of engineered backfills at the end of a repository's active life may also lead to colloid formation. If the waste form is leached by ground water, naturally occurring colloids derived from smectites, vermiculites, illites, kaolinite, and chlorite present in ground water may also adsorb radionuclides. Champ et al. (1982) have demonstrated experimentally the existence and rapid transport of plutonium colloids using core samples and ground water. Fried et al. (1975), in their 1975 laboratory studies, observed a fast migrating form of plutonium in their column experiments on Bandelier Tuff. Retardation of this polymeric form of plutonium was only one-tenth of the ionic form. A discussion of radiocolloid formation is found in Section 4.1.3.4.1.3.

Transport of particulates in geologic media will depend on aqueous flow rate, on pore and fracture size in the rock, on ions carried with the water, and on the nature of the particulate matter. Several mechanisms may remove colloidal particulates from ground water such as mechanical filtration by the rock matrix, sorption on the surface of rock pores (van der Waals), and neutralization of the repulsive charges on the colloids thus allowing them to coagulate.

Filtration will be an effective barrier to transport in the tuff matrix. Pore size is an important element in filtration. Pseudocolloids will not flow through pores that are smaller than the pseudocolloid carrier particles. In very small pores, true colloids will have a high probability of entering boundary layers around matrix particles, where they can be captured in the small pores. Pore-size distributions have been measured (Daniels et al., 1982) for several Yucca Mountain tuff samples. Mercury porosimetry data on a sample of Topopah Spring tuff show that most of the pores are less than 1.0 micrometer in diameter. There is a small percentage larger than 1.0 micrometer, but they should be dry because the amount of Topopah Spring saturation is less than 90 percent. More than 50 percent of the pore volume is made up of pores 0.1 micrometer in diameter or smaller. For samples from the Calico Hills, 50 percent of the pores are smaller than 0.05 micrometer, but there are somewhat more of the largest pores (4 micrometers). The data indicate that to pass through pores in the tuff matrix, colloids must be on the order of 0.1 micrometer or less.

Pore-water velocities, assuming matrix flow, are estimated to be less than 1.0 cm/yr (Travis and Nuttall, 1987). It is not clear whether such low velocities can provide sufficient momentum to allow bulk colloid movement. If fracture flow is significant, then colloid transport may be likely. If fracture flow is dominant in the Topopah Spring tuff, the average fracture-flow rate would be roughly 2 m/yr (Travis and Nuttall, 1987); this is still only on the order of transfer rates by molecular diffusion. If fracture flow is episodic, corresponding to a few intense rainfalls per year, flow rates in fractures might be much larger (tens of meters per year) but of shorter duration.

In addition, colloids will be subject to gravitational settling (Travis and Nuttall, 1987) for particles larger than about 0.1 micrometer. The transporting ability of very small colloids will be diminished by diffusion of radionuclides out of the carrier particles. Diffusion in solid phases is small, but not zero. Solid phase diffusion for some radionuclides on several Yucca Mountain minerals has been measured at about 10^{-16} to 5×10^{-13} cm^2/s (Rundberg, 1985). A characteristic diffusion time (T) from 0.1 micrometer diameter particles is given by

$$D \approx \frac{R^2}{T} \quad \frac{L^2}{4T} \quad \text{-->} T \approx \frac{L^2}{4D} \approx \frac{(10^{-5})^2}{4 \times 10^{-16}} = 2.5 \times 10^5 \text{ s} \approx 3 \text{ days} \qquad (4\text{-}7)$$

where

D = diffusion coefficient
T = diffusion time
L = particle diameter
R = particle radius.

Small pseudocolloids, in fluids of low ionic concentrations, should not be able to retain absorbed radionuclides for more than a few days. Very small true colloids may be able to migrate rapidly if fracture flow is occurring; however, more experimental work is needed to determine the importance of true colloid transport. Plans for obtaining the additional information required are outlined in Section 8.3.1.3.

One additional mechanism that might allow transport of some radionuclides are microbes (West and McKinley, 1984). Studies measuring the uptake of radionuclides by bacteria and studies determining the mobility and radionuclide transport capability of bacteria in tuff are detailed in Section 8.3.1.3.

Because natural particulate material in ground water at a repository site may be significant as a means of transport of radionuclides by sorption on the particulate material, it is necessary to measure the ambient concentration of such particles. At Yucca Mountain there are no springs or other accessible sources of flowing ground water. Therefore, well J-13, a water well adjacent to Yucca Mountain, was pumped and the water was sampled for particulates by filtering several hundred liters of water through 0.05

micrometer Nucleopore filters, then examining the filters with a scanning electron microscope. An abundance of material was present on the filters, ranging in size from tens of micrometers in diameter down to less than 0.01 micrometer, the resolving power of the microscope. The composition of individual particles varied considerably, although most contained potassium, aluminum, and silicon as major constituents. Filter samples also were obtained from two other wells at the Nevada Test Site, both drawing from an aquifer in alluvial soil. The results of subsequent filter tests were similar to those from well J-13. Because the samples were derived from water flowing in an artificially created gradient, it can be argued that the particulate content is not that of natural water. However, pumped well water may provide a worst-case situation. Future experimental work is planned to determine whether particulates in well J-13 water can sorb a significant amount of dissolved radioactive material and whether these particulates are readily transported through crushed and fractured tuff. Plans for obtaining the additional information required are outlined in Sections 8.3.1.3.4 and 8.3.1.3.6.

4.1.3.6.2 Gaseous transport

A limited number of radionuclides can form volatile species that are capable of being transported in a moving vapor or gas. Among these are tritium, carbon-14, and iodine-129. In the far field, factors that affect transport in flowing ground water also affect transport in flowing gas, (i.e., the velocity of the gas determines the potential for advective transport). In the absence of flow, diffusion is the only mechanism for transport in the gaseous state. The processes of partitioning of the volatile species between the gaseous, liquid, and solid state and isotopic exchange must also be considered when assessing the impact of gaseous transport.

The probability of gaseous transport will be investigated to determine its applicability to Yucca Mountain. Presently, no work is actively being done on gaseous transport; however, plans for obtaining information required to assess the probability of gaseous transport and the processes of exchange (i.e., gaseous phase and aqueous/solid) are outlined in Section 8.3.1.3.8.

4.1.3.7 Geochemical retardation in the host rock and surrounding units

persion, matrix flow, fracture flow, and equilibrium sorption). More complex geochemical processes, such as speciation, dissolution and precipitation, and colloid formation have only very recently been incorporated into transport models. Plans for refining and improving already developed models, and for developing models that will incorporate all significant processes is outlined in Section 8.3.1.3.7. The development of such models is dependent upon results obtained from Investigations 8.3.1.3.1 through 8.3.1.3.6 and the geohydrology program (Section 8.3.1.2). In turn, the models can be used to interpret results arising from these information needs and to validate the assumption made in constructing the systems models for Information Needs 1.1.4 and 1.6.2; the models may also be useful in establishing the presence of favorable and potentially adverse conditions (Issue 1.8), and making the

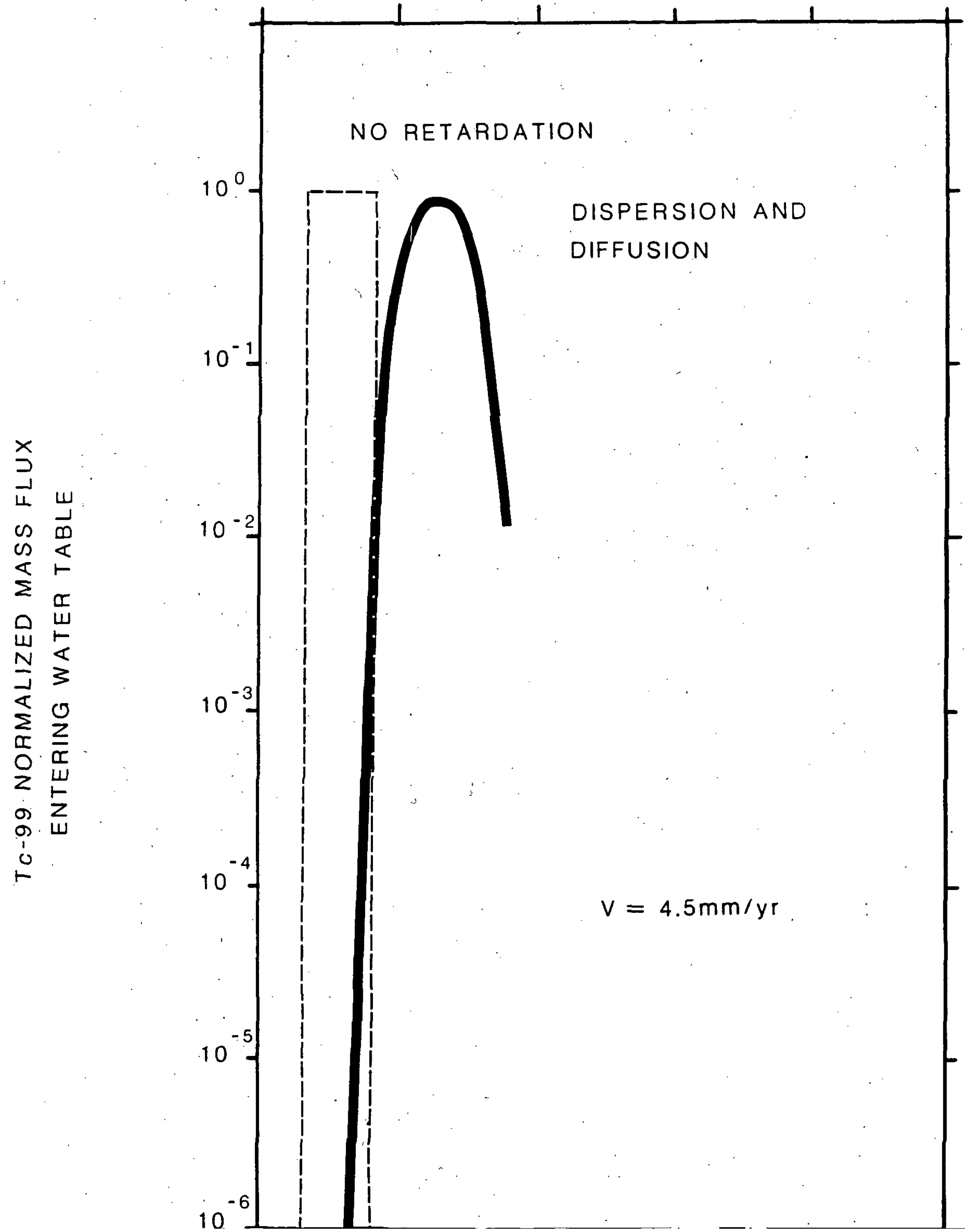
NO RETARDATION
DISPERSION AND DIFFUSION
V = 4.5mm/yr
Tc-99 NORMALIZED MASS FLUX ENTERING WATER TABLE
10^0
10^-1
10^-2
10^-3
10^-4
10^-5
10^-6

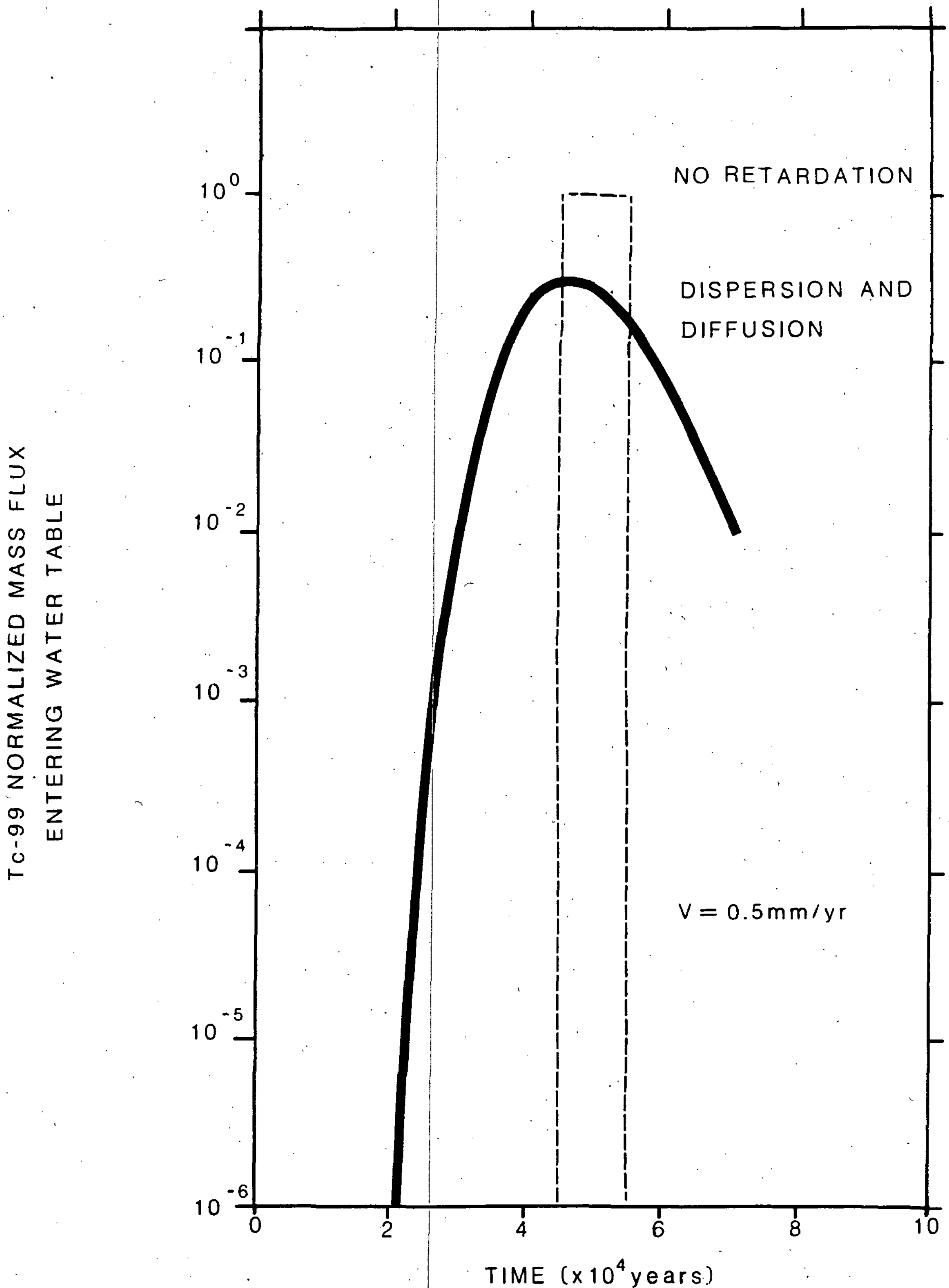

Figure 4-16b. The movement of a 10,000-yr pulse of technetium-99 for V = 0.5 mm/yr. Modified from Vaniman (1987).

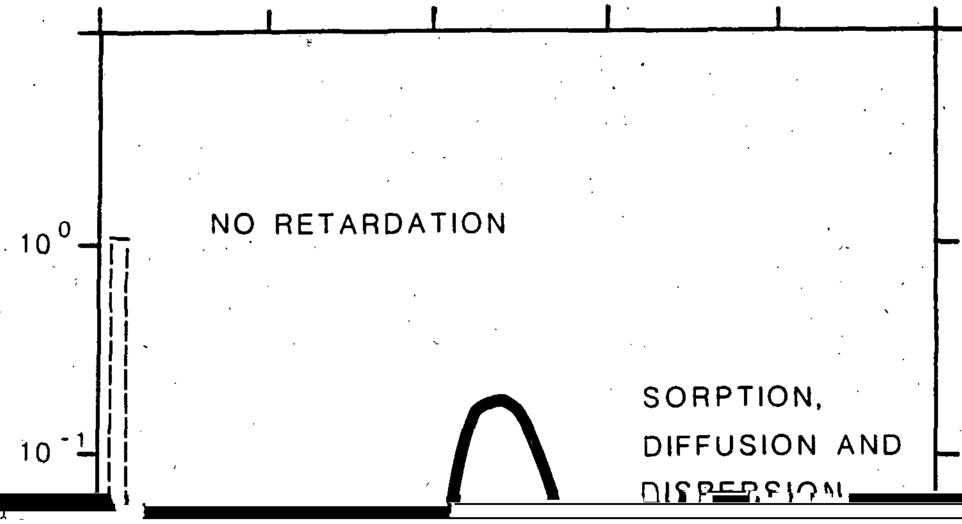
NO RETARDATION
SORPTION,
DIFFUSION AND
10^0
10^-1

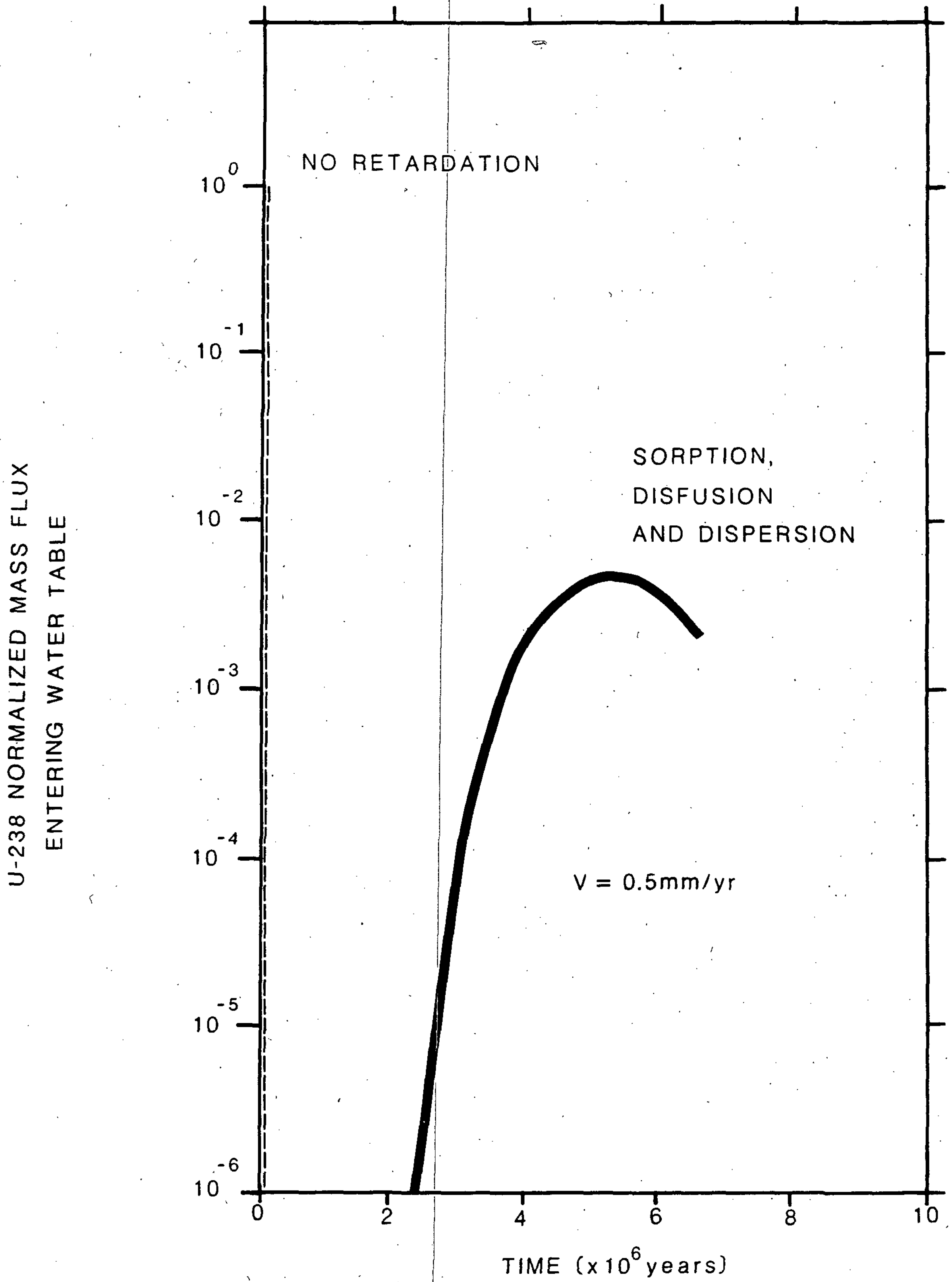

Figure 4-17b. Uranium-238 normalized mass flux entering water table for V = 0.5 mm/yr. Modified from Vaniman (1987).

a significant effect on the transport of sorbing and nonsorbing radionuclides. Therefore, it is extremely important that these processes and their relative parameter values are well-defined. As the processes and their relative parameter values become updated more calculations similar to the examples given above will be done to investigate the sensitivity of radiotently) show that to get a travel time of less than 10,000 yr requires a water flux at least 100 times greater than the present water flux (Travis et al., 1984).

For radionuclide transport through fractures, more information is needed on fracture flow in Yucca Mountain tuffs. For example, additional information is needed to establish whether the recharge water moves vertically through unfractured layers and then enters fractures, or if water moves through fractures as a film on the fracture surface or as a pulse fully saturating the fracture. Film flow would be very much slower than slug flow (Travis et al., 1984). Plans for obtaining this information are outlined in Section 8.3.1.3.6.

Other factors that cannot be evaluated at present because of the lack of data are the connectivity of fractures and the dimensions of fracture apertures. If fractures are present but not connected or intersecting, their impact on flow and transport will be greatly diminished. If fractures are a connected network, the path that a water slug will travel will probably be tortuous and might involve branching into cracks in other directions. In regard to the dimensions of apertures, fracture flow depends on fracture permeability, which varies roughly as the cube of the aperture, a strong sensitivity. Plans for obtaining the required information about fracture aperture and fracture permeability are outlined in Section 8.3.1.3.6, and plans for obtaining such information for a hydrologic model are given in Section 8.3.1.4.

Given fracture flow, the contaminant will diffuse into the pore spaces of the rock. Because of this diffusion into the matrix, the effective flow rate for radionuclides must be modified (Sudicky and Frind, 1982). The [illegible]

fractures. One can then calculate an equivalent retardation value, applicable only when fracture flow is occurring, combining retardation through sorption with retardation through diffusion. The calculated equivalent retardation factors are a factor of 10 to 100 larger than those retardation factors based on sorption alone (Travis et al., 1984).

4.2 GEOCHEMICAL EFFECTS OF WASTE EMPLACEMENT

The thermal pulse from waste emplacement and its effects on water displacements and geochemistry must be characterized for intervals extending tens of meters away from the waste containers emplaced in a repository. Discussions of the interactions within the engineered barrier system are presented in Chapter 7.

This section describes the time-dependent temperature profiles for a reference repository in unsaturated devitrified tuff, with the attendant phenomena of drying near the waste containers and water condensation at boundaries that move inward as the thermal pulse from waste emplacement decays. Also discussed is the possible hydrothermal alteration due to the thermal pulse--a prospect that is not critical to the devitrified host rock but may be important to the hydrous alteration minerals and glasses beneath the host rock. Desiccation and rehydration of the hydrous alteration minerals, as well as other phase transitions that may affect permeability, rock strength, and radionuclide retardation, must be studied as well. Water chemistry as a function of temperature must also be known; therefore, an assessment of thermal effects on unsaturated-zone pore water and on recharge water is important. Finally, this section discusses the thermal dependence of factors important on constraining radionuclide migration--namely, sorption, precipitation, dispersion, diffusion, and advection on unsaturated tuff.

4.2.1 ANTICIPATED THERMAL CONDITIONS RESULTING FROM WASTE EMPLACEMENT

This section discusses the impact of expected thermal conditions resulting from waste emplacement. Waste emplacement leads to heat buildup due to radioactive decay. This heat influences the rate of the waste container degradation, and the compositions of the surrounding tuff due to hydrologic changes.

The magnitude of the effects resulting from the thermal pulse depends on (1) heat content of the waste, (2) rate of decay of the waste, (3) amount of pore water, (4) effective permeability of the tuff, (5) waste emplacement geometry, and (6) presence or absence of venting. These factors are discussed in detail in Section 7.4.1. However, time-temperature calculations described in the sources only extend out to 1 m from the borehole wall.

The following is an example of the type of calculation that can be done to investigate the qualitative behavior of the anticipated thermal conditions resulting from waste emplacement. Preliminary numerical calculations using a flow and transport code (WAFE) that incorporates a thermal component (Travis, 1985) have been made. Using a heat load of 50 kW/acre, Figure 4-18 shows a fluid temperature profile around a 2 by 6 m room after 50 yr. The absolute numbers shown should be considered preliminary because of the uncertainties in the rock property values. However, in these calculations, as heat diffuses away from the source, water vaporizes. The water vapor is then driven outward until it reaches cooler rock and then condenses. Temperatures are buffered by the boiling process because energy is going into vaporizing water rather than raising the rock temperature. Peak temperatures at the wet edge

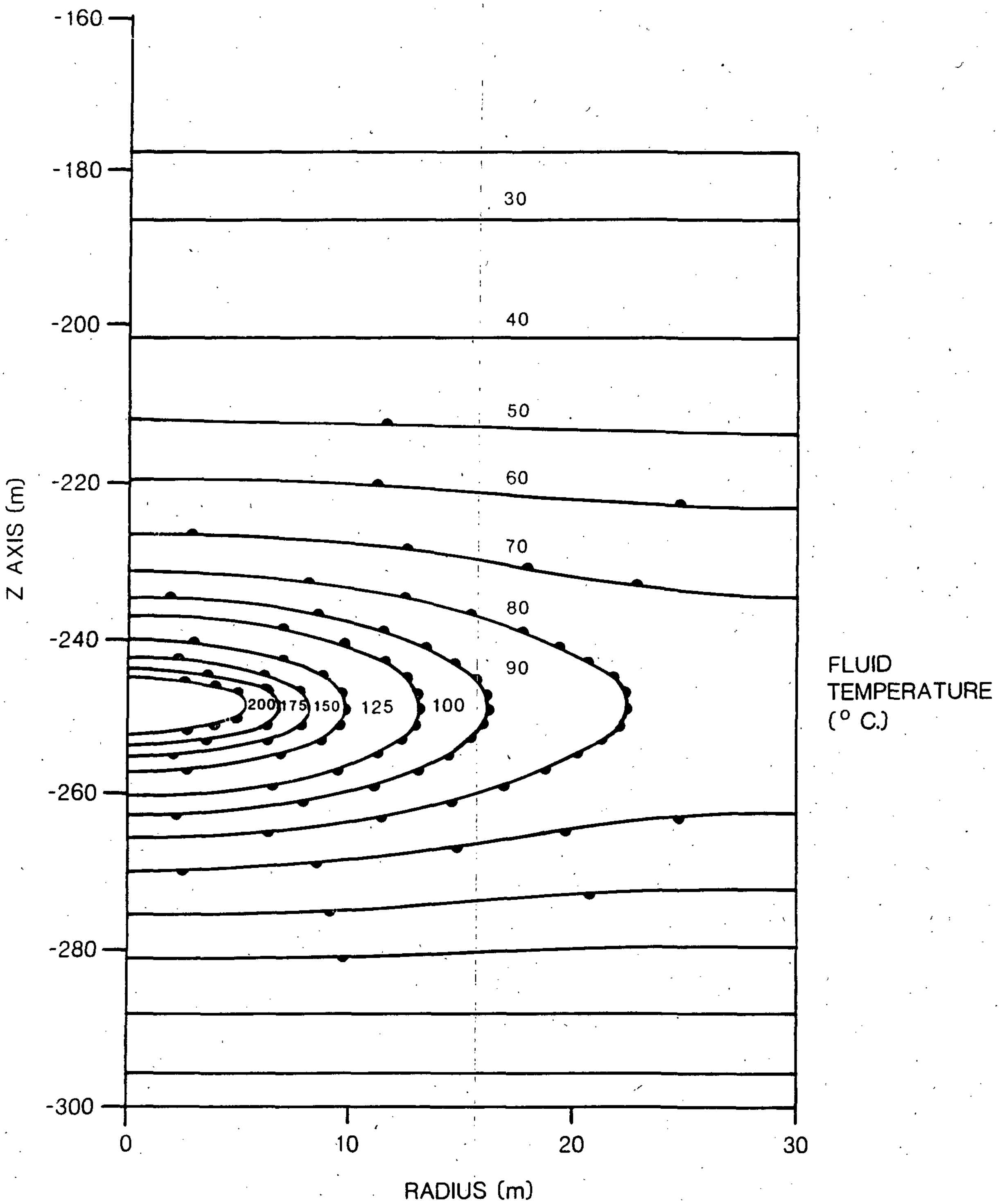

Figure 4-18. Fluid temperature profile showing temperature contours 50 yr after emplacement of a 50 kw/acre heat load using the WAFE code. Dots generated by plotter indicate the direction of the gradient. Modified from Travis et al. (1984)

of the boiling region are only about 140°C, considerably lower than peak waste temperature. After a century or so, temperature and saturation profiles decay back to ambient. A temperature increase of 5°C or more extends to at least 30 m (Travis et al., 1984).

This same heat loading or thermal scenario can in turn influence the rate of breakdown of the waste container. For example, if heat loading were to cause vaporization of pore water near each container, the atmosphere surrounding a container could change from wet air to a dry-steam, oxygen-poor atmosphere, which would affect the degradation of the container. The problem is discussed in Section 7.4.

The presence of fractures in the rock can alter the thermally induced flow patterns and make the interpretation of the effects of anticipated thermal conditions on the natural environment more complicated. Many small cracks will increase the overall permeability, making a convective or circulating flow pattern more likely. However, few large cracks that promote conduction may prevent convective circulation, and more likely provide a path for a fairly rapid movement of water, vapor, and air. Other factors could also be important, such as the thermomechanical behavior of cracks. Heat may close cracks or open them depending on the mechanical properties of the host rock. Plans for obtaining the additional results on these scenarios are outlined in Section 8.3.1.3.7.

icant volume reductions (Bish, 1981; Bish, 1984) may possibly reduce rock strength and alter permeability. Irreversible dehydration of smectites, zeolites, and volcanic glass reduces both volume and cation exchange capacity. Glass devitrification is of particular interest because of the proximity of the host rock to the vitrophyre in the lower Topopah Spring Member and to the nonwelded, nonzeolitized tuffs at the base of the Topopah Spring Member and in the underlying tuffs of Calico Hills in the southern portion of the Yucca Mountain exploration block. Alteration of glass may have four important effects: (1) changing the volume, causing changes in rock property such as permeability; (2) maintaining a high silica activity; (3) raising the pH of acidic water; and (4) forming sorptive secondary phases like smectite and zeolites (Kerrisk, 1983). Finally, the alteration of minerals to less-sorptive phases (i.e., the alteration of clinoptilolite to analcime) can affect the zeolitic rocks influenced by the heat of the repository (Bish et al., 1982; Bish, 1987).

Since mineral reactions at repository temperatures may occur at rates comparable to the isolation period (thousands of years), an understanding of kinetics is also important. Also, because many of the effects of elevated temperatures on hydrous minerals result from mineral dehydration, the effect of the partial pressure of water on the dehydration reactions must be known in order to predict the differences between unsaturated-zone and saturated-zone mineral dehydration. The plans for obtaining information about these processes are outlined in Section 8.3.1.3.

4.2.2.1 Hydrothermal alteration of zeolites

Data on the kinetics of zeolite reactions at slightly elevated temperatures are very limited because of experimental difficulties; reactions occur very slowly at temperatures below 200°C. Hydrothermal experiments have been conducted on zeolitic, vitric, and welded tuff at temperatures of 80 to 180°C (the temperatures necessary to make observable changes in short times) for several weeks to several months (Daniels et al., 1982; Knauss and Beiriger, 1984; Blacic et al., 1986). The results of the experiments pertinent to the near-field environment are discussed in Section 7.4.1.3; some zeolites have been formed during the experiments but the products require further characterization.

Assuming a water composition similar to well J-13 water, the geologic data from the deeper portions of drillholes in Yucca Mountain and the experimental data described by Smyth and Caporuscio (1981) indicate that reaction of clinoptilolite to analcime will occur above 85°C in the tuffaceous beds of Calico Hills, although silica activity may more directly control the reaction than temperature (Section 4.1.1.4).

Although the clinoptilolite-to-analcime reaction is not anticipated in most zeolitic tuffs, experiments in progress suggest that water loss with volume decrease (up to 10 percent) in clinoptilolite will begin below 50°C when the water-vapor pressure is low. The volume loss could occur in the first major zeolite horizon under the thermal influence of the waste emplaced in the repository. The opening of new flow paths in a zeolite horizon barrier is possible, but they will probably expand again and close during rehydration. The effects of temperature on a number of natural clinoptilolites and sodium-, calcium-, and potassium-exchanged clinoptilolites have been examined by x-ray powder diffraction (Bish, 1984). The molar volumes of all clinoptilolites decreased, with sodium-clinoptilolite undergoing the greatest decrease and potassium-clinoptilolite undergoing the least. Calcium-clinoptilolite and the natural clinoptilolite samples underwent intermediate decreases in volume. Most of the volume contraction in most samples occurred on evacuation at room temperature, demonstrating the strong effect of water-vapor pressure upon dehydration. Samples heated under 1-atm water-vapor pressure underwent significantly less volume decrease at a given temperature than those heated in ambient air or in a vacuum. All samples showed the ability to rehydrate upon cooling.

The data of Bish (1984) show that heat effects on volume change of clinoptilolite are strongly related to the exchangeable-cation content. The volumes of natural, mixed sodium-potassium-calcium clinoptilolites in rocks could be reduced in a repository environment, particularly if the clinoptilolites occur in the rock being dehydrated by the thermal pulse. However, tests now in progress suggest that clinoptilolites occurring in partially saturated rocks at temperatures below 100°C should not decrease in volume. Thermogravimetric and differential scanning calorimetric experiments on natural and cation-exchanged clinoptilolites also demonstrate the strong dependence of dehydration on exchangeable-cation composition (Bish, 1985). The results show that clinoptilolites can yield water on heating and rehydrate on cooling if the dehydration process is reversible after long-term heating (more than 1 yr). The volume decreases observed for clinoptilolite were completely reversible over short heating periods (less than 1 wk). However, long-term heating of clinoptilolite can cause modifications, including irreversible collapse and reduction in cation-exchange capacity. Sodium-rich clinoptilolites are most susceptible to large volume reductions and exchange-capacity modifications, and they can alter to a phase analogous to heulandite-B. Further experiments are examining both the dependence of dehydration temperature on water vapor pressure and the possibility of irreversible dehydration at 100°C (Section 8.3.1.3).

4.2.2.2 Hydrothermal alteration of smectites

Although smectites are not as abundant as zeolites, they occur in small amounts in virtually all core samples from Yucca Mountain examined to date (Bish et al., 1982). The smectites are important to radionuclide retardation because they selectively sorb certain cations (cesium, strontium, barium, and some actinides) (Section 4.1.3.3). Bish (1981) reviewed the effects of changes in relative humidity and temperature on smectites and noted that decreases in ambient humidity alone can cause dehydration and large decreases in volume when the ambient humidity drops below 20 to 50 percent. Smectites typically undergo reversible crystal structure collapse with attendant volume decrease at about 100°C with humidities of less than 100 percent. However, Koster van Groos and Guggenheim (1984, 1986) showed for Na- and K-montmorillonite that an increase in water pressure significantly raises the temperature of dehydration and layer collapse. Thus, collapse as a result of dehydration will probably be unimportant except where temperatures are high and the partial pressure of water is low. Smectites will remain in an suspended state along the flow paths in the saturated zone where the clays

4.2.3 CHANGES IN WATER CHEMISTRY DUE TO THE THERMAL PULSE

The heating of fluids in and adjacent to the repository will cause increased reaction with the host rock, changing the compositions of both. Experimental results on the interaction of well J-13 water with crushed and solid samples of devitrified Topopah Spring tuff at 90, 150, and 250°C are discussed in Section 7.4.1.3. Briefly, tests at 150°C for 66 days showed changes from 0.01 to 0.5 parts per million (ppm) for aluminum, from 38 to about 120 ppm for silicon, from 12 to 6 ppm for calcium, from 1.9 to near 0 ppm for magnesium, from 5.1 to 4.4 ppm for potassium, and a pH change from 7.1 to 6.8. The concentrations of sodium ion, fluoride, chloride, nitrate, and sulfate showed no significant changes. The dissolved-carbonate content decreased slightly. These changes were associated with the appearance of secondary phases, including a potassium-rich clay or zeolite; clays rich in magnesium, calcium, and/or iron gibbsite; calcite; and a pure silicon dioxide cooling globules analyzed as pure SiO_2. In addition, greatly increased amounts of clays or other fine grained sheet silicates were deposited on glass edges (examined by scanning electron microscope). The placement of waste containers will lead to the development of a temperature gradient in the surrounding host rock which will induce a solubility gradient. If water also flows, silica will be redistributed and depending on the magnitude and duration of the heat-induced flow, silica may accumulate in cooler regions. This deposition will result in reduced pore size which subsequently will lower permeability. A region of reduced permeability around a waste container will tend to isolate the container from infiltrating water. Thus the infiltrating water will be deflected away from the container, thereby

The scenario described above was qualitatively investigated by a numerical study (Travis and Nuttall, 1987) with the WAFE computer code. The WAFE code (Travis, 1985) can calculate heat and mass transport in porous

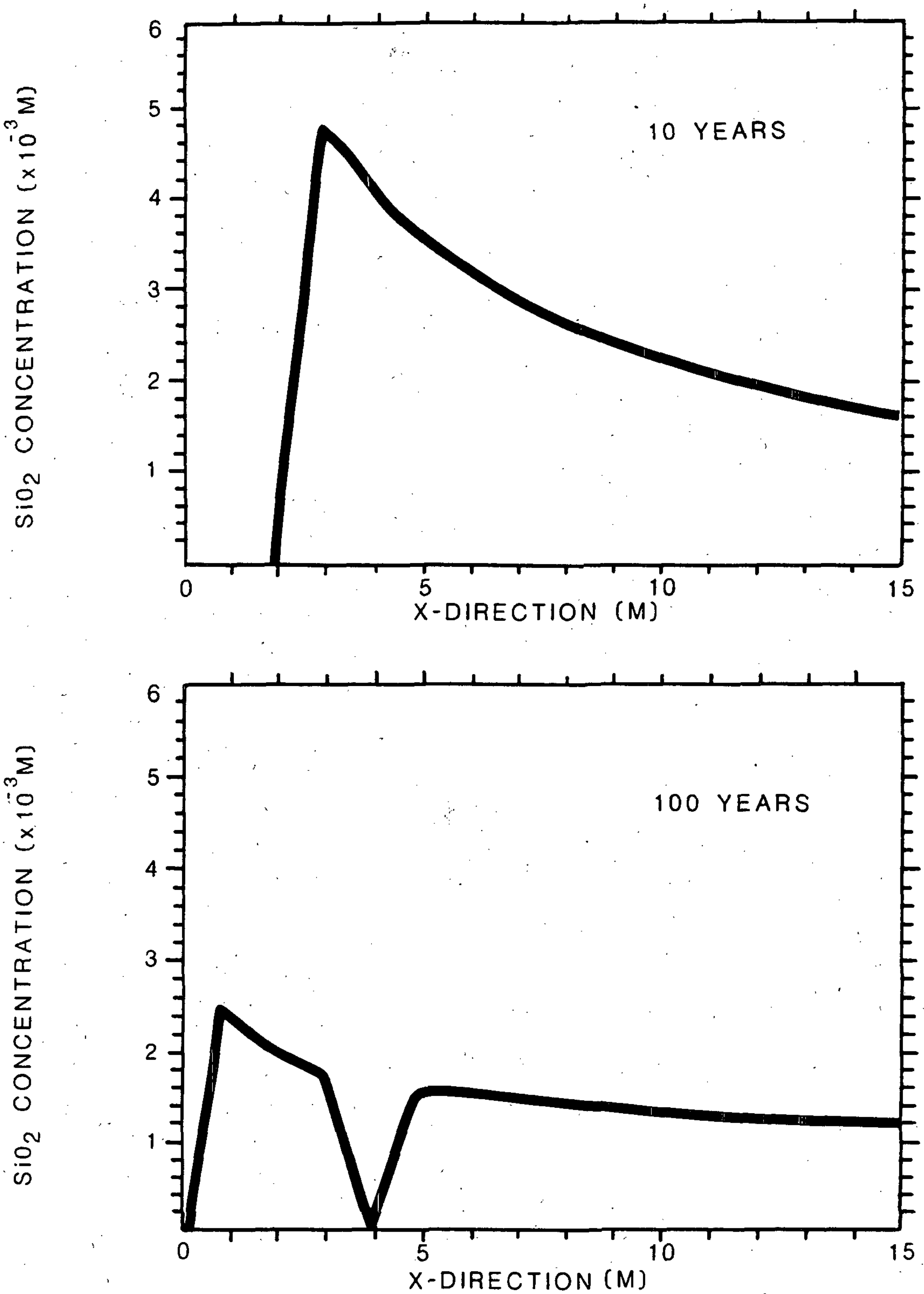

Figure 4-19. Calculated dissolved silicon dioxide distribution at selected times. Modified from Travis and Nuttall (1987).

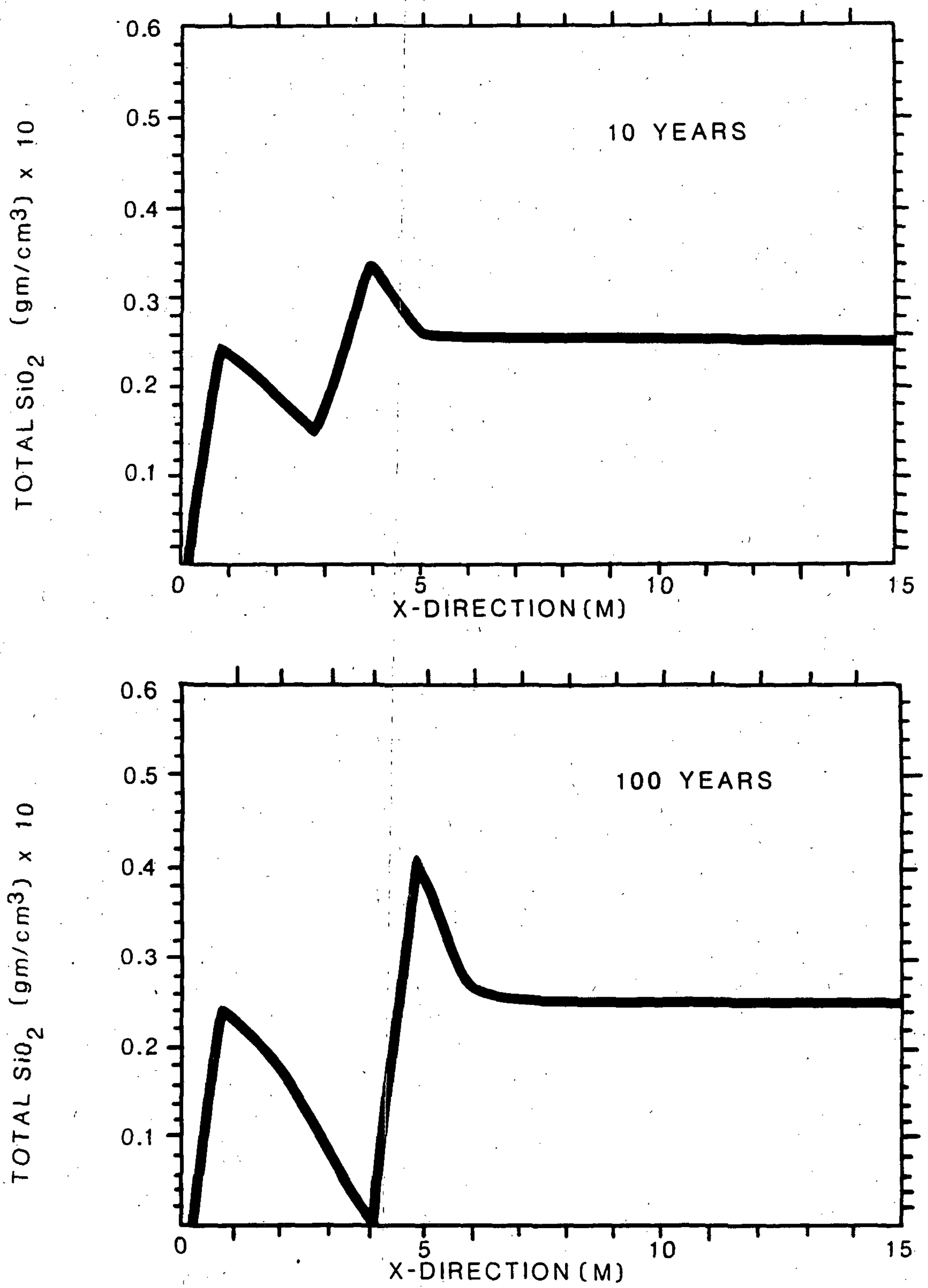

Figure 4-20. Calculated total silicon dioxide (dissolved and precipitated) at selected times. Modified from Travis and Nuttall (1987).

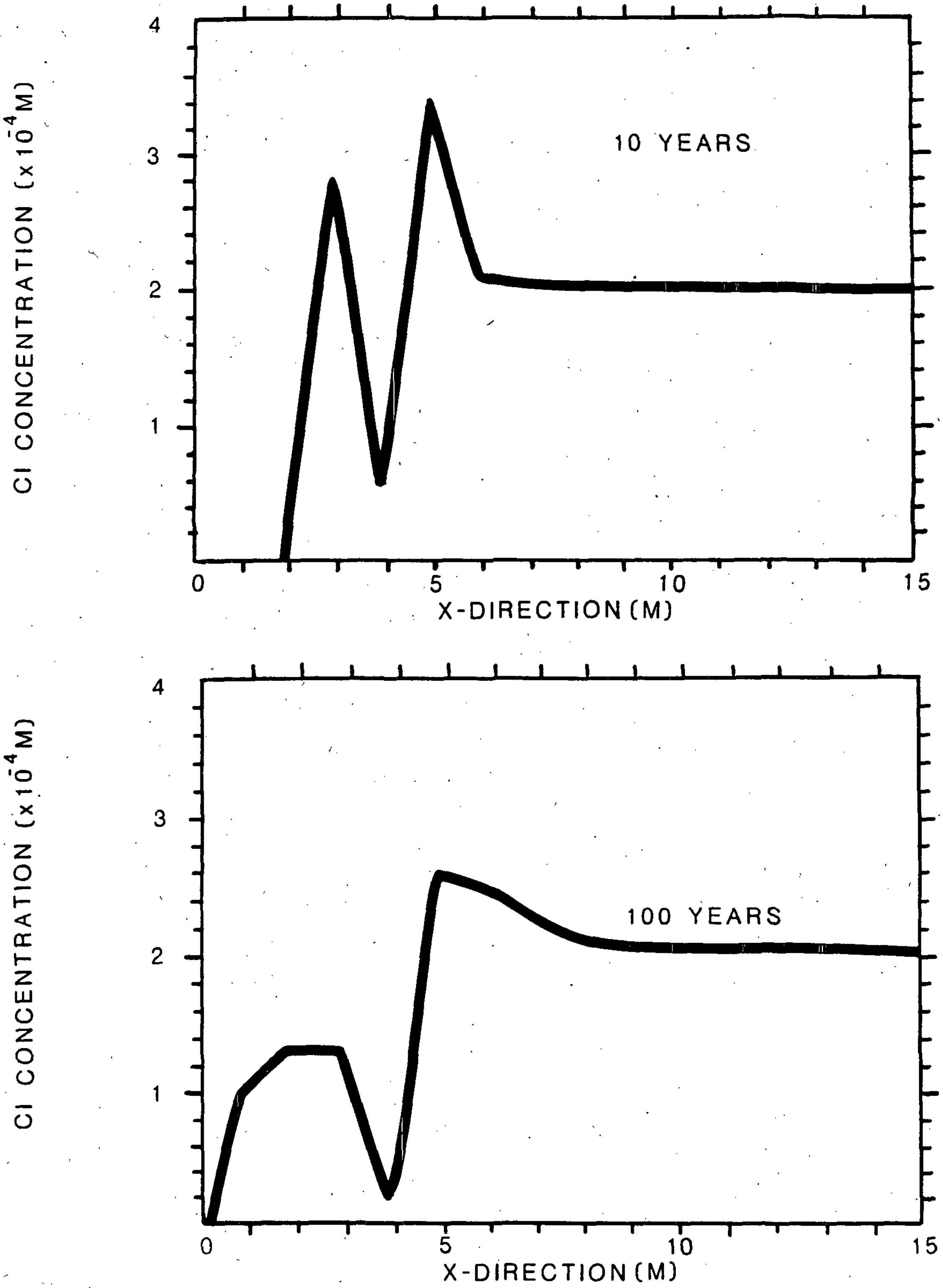

Figure 4-21. Calculated chloride distribution at selected times. Modified from Travis and Nuttall (1987).

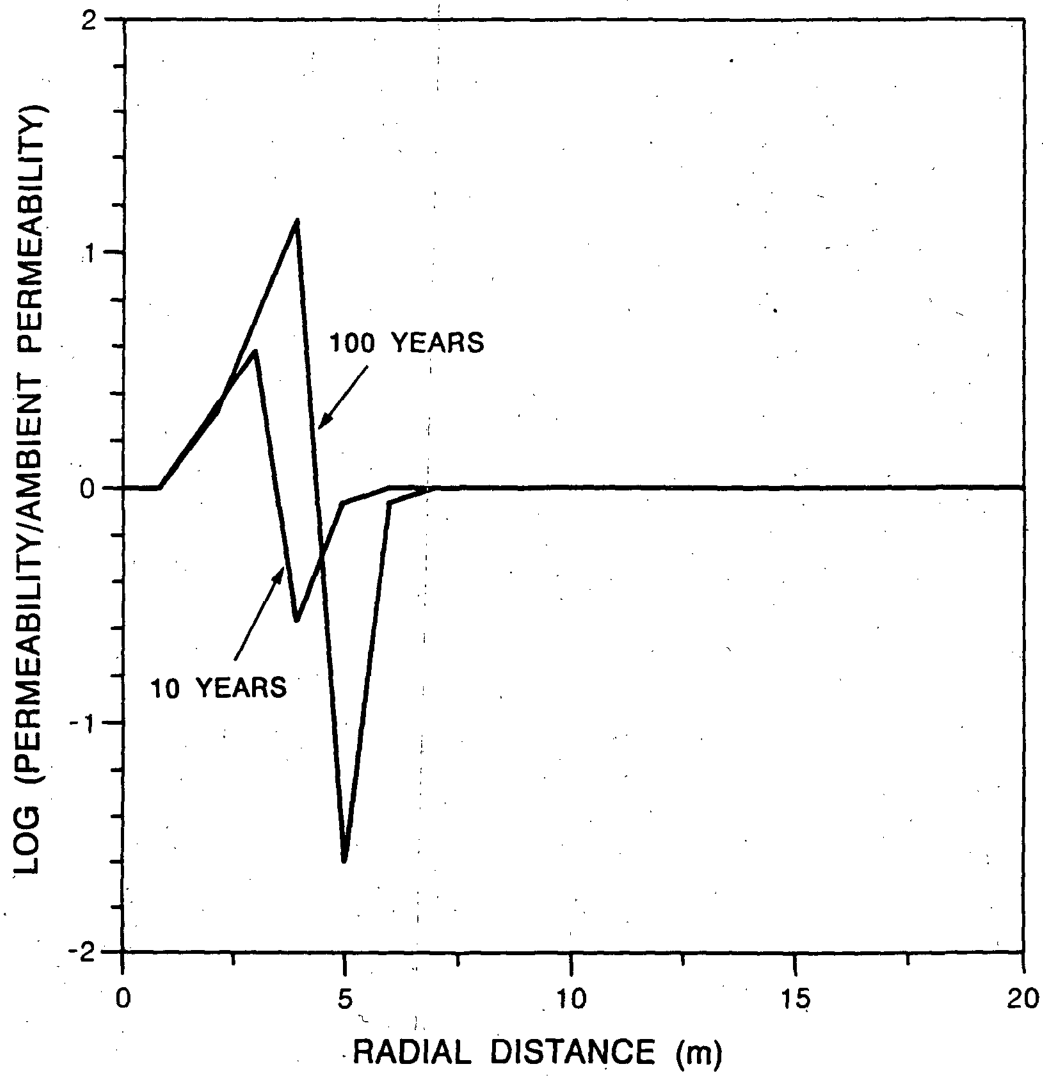

Figure 4-22. Calculated permeability assuming relationships between pore volume and permeability. Modified from Travis and Nuttall (1987).

ring will tend to channel water that had penetrated the low permeability shell, also around the container rather than through it. By reducing the amount of available water, the amount of radionuclides dissolved and transported will be decreased. The exact magnitude of this effect depends on the details of the hydrologic behavior of the host rock, and, in particular, on the presence or absence of fractures.

The numerical calculation of Travis and Nuttall (1987), summarized above, did not treat the full complexity of the water composition and reactions. Instead, the calculations were simplified by considering only silica dissolution, transport, and precipitation. As the potential hydrologic behavior of the Topopah Spring Member is better estimated (Section 8.3.1.2), the information concerning the presence or absence of fractures is obtained (Section 8.3.1.2), and as the ground-water transport models are further developed (Section 8.3.1.3.7), the effects of thermal pulses on radionuclide migration due to all significant changes in transport processes will be further investigated (Section 8.3.1.3.7).

4.3 NATURAL ANALOGS AND RELATED FIELD TESTS

The long period of time over which a repository must provide waste isolation and the large volume of rock present between a repository and the accessible environment pose particularly difficult problems in the prediction and assessment of repository performance. Although laboratory studies provide data on fundamental chemical and physical processes, modeling of the total repository system will require the extrapolation of these data in space and time. However, the study of natural systems possessing one or more features that mimic critical parts of a repository environment may provide additional confidence in the required extrapolations. This section describes natural analogs and related field tests that possess these attributes.

4.3.1 NATURAL ANALOGS

Although there are no natural systems available for study that are totally analogous to a repository environment, the following systems possess features that are pertinent to a repository in tuff: (1) warm and hot springs in tuffaceous rocks, and (2) uranium and thorium ore bodies and their host rocks. Only a small group of potentially analogous sites are discussed in this section.

4.3.1.1 Warm and hot springs

The study of warm and hot springs in tuffaceous rocks provides information about several important aspects of a repository environment in tuffaceous rock including (1) the effect of the thermal pulse on the chemistry of ground water; (2) the effect of heated ground water on the host rock including dissolution and precipitation reactions; (3) the transport of certain elements (e.g., strontium, cesium, uranium, thorium, etc.) found in radioactive waste in a hydrothermal environment; and (4) hydrothermal fluid flow in fractured tuff. In addition, the studies will provide case studies for testing computer codes like EQ3/6.

Warm and hot springs are present in tuffaceous rocks at many locations in the western United States. Several of the locations have been studied in detail, including (1) the geyser basins in Yellowstone National Park (Honda and Muffler, 1970; Thompson et al., 1975; Keith and Muffler, 1978; Keith et al., 1978; Thompson and Yadav, 1979; Bargar and Beeson, 1981; Bargar and Muffler, 1982; Keith et al., 1983; Barger and Beeson 1984a,b); (2) the Valles caldera in northern New Mexico (Goff and Sayer, 1980; Goff et al., 1981; Goff and Grigsby, 1982; Goff et al., 1982; Phillips et al., 1984; Hulen and Nielson, 1985); and (3) the Newberry Volcano in central Oregon (Bargar and Keith, 1984; Keith et al., 1984a,b). Although the Newberry Volcano is not composed of typical silicic ash-flow tuff, it contains intermediate to silicic lavas and tuffs of the type that also occur in and around Yucca Mountain. The results obtained from the studies have been largely empirical and have included (1) descriptions of the petrography and the primary and secondary mineralogy of core and surface samples, (2) chemical analyses of rocks and thermal waters, and (3) temperature profiles.

The warm and hot springs of the geyser basins in the Yellowstone National Park are discussed here because they have been studied in the most detail. The springs emerge from silicic volcanic rocks and volcanogenic sediments that are less than 1 million years old. In fact, the springs are likely surface manifestations of recent igneous activity. The USGS has drilled 13 drillholes (75 to 320 m) to investigate the hydrothermal systems in the Yellowstone National Park. These holes have penetrated volcanogenic sediments (partly glacial), rhyolitic lava flows, volcanic breccias, and various types of silicic tuffs. Because the drillholes are located in parts of the Yellowstone caldera that have been filled in with postcaldera rhyolite flows, ash-flow tuffs are not the dominant rock type encountered (Keith and Muffler, 1978). However, drillholes Y-5 (Keith and Muffler, 1978) and Y-9, Y-12, and Y-11 (Bargar and Muffler, 1982) do contain ash-flow tuffs (part of the Lava Creek Tuff of the Yellowstone Group; Christiansen and Blank, 1972) similar in composition and texture to the tuffs exposed at Yucca Mountain.

The warm and hot springs have altered the Lava Creek Tuff in drillholes Y-5 and Y-11 to a suite of secondary minerals including alpha-cristobalite, beta-cristobalite, quartz, chalcedony, opal, hematite, goethite, pyrite, manganese oxides, clays, zeolites, calcite, gypsum, and other minor phases. Because data are available on the alteration paragenesis, compositions of the secondary minerals, present day temperature profiles, and the compositions of water in the drillholes, the relative stabilities of the secondary mineral assemblages in the Yellowstone drillholes can be derived. In this context, the capability of the EQ3/6 code will be used and tested. Kinetic effects should be apparent in comparisons of the code predictions with the observed mineral assemblages.

Once the dominant chemical controls on the secondary mineral assemblages in the Yellowstone drillholes have been identified, this information can be used to characterize the stability ranges of the secondary minerals (e.g., silica, polymorphs, and zeolites) in Yucca Mountain under ambient conditions as well as in the thermal regime resulting from waste emplacement. In addition, the modeling will result in a better understanding of the effects of the thermal pulse on the chemistry of ground water in the near field. Plans for additional studies are described in Sections 8.3.1.3.1, and 8.3.1.3.3.

4.3.1.2 Uranium and thorium ore deposits and their host rocks

Uranium and thorium ore deposits, are a source of data on the following: (1) the long-term stability of radioactive solids (Naudet, 1978); (2) the long-term release of radionuclides from these solids (Curtis, 1985); (3) the transport of radionuclides under various pH, Eh, temperature, and pressure conditions, ground-water and host rock compositions, and hydrologic regimes (Ruffenach et al., 1980); and (4) the long-term effects of radiolysis (Curtis and Gancarz, 1983). Items 1, 2, and 4 relate to near-field conditions in a repository environment while Item 3 relates to near- and far-field conditions

Table 4-20. Behavior of fission products in industrial reactors and in the Oklo natural reactors[a]

			Industrial reactors		Oklo natural reactors	
Chemical state	Elements	Ionic radius (A)	Retention in the fuel	Localization in the free volume of the cladding	Retention	Migration
Gaseous compounds	Kr	1.8[b]		x		x
	Xe	2.0[b]		x		x
Volatile compounds	I_2	2.5[b]		x		x
	Te	0.60		x	x	
	Cs	1.8		x		x
Oxides insoluble in the matrix	Sr	1.21		x		x
	Ba	1.44		x		x
	Mo	0.73		x		x
Metallic inclusions	Tc	0.72		x	x	
	Ru	0.70		x	x	
	Rh	0.71	x		x	
	Pd	0.70	x		x	
Oxides soluble in the matrix	Y	0.98	x		x	
	Nb	0.72	x		x	
	Zr	0.92	x		x	
	Rare-earths	1.02-1.13	x		x	
	Pb	1.02				
	Th	1.12				
	U	1.08				
	Pu	1.04				

[a]Source: Ruffenach et al. (1980).
[b]Molecular radius (Johnston, 1966).

deposit. Annual release rates cannot be derived for these elements because the timing of the losses cannot be constrained.

The effects of radiolysis in the Oklo ore deposit are discussed by Curtis and Gancarz (1983). The authors calculated the alpha- and beta-particle doses in the critical reaction zones during criticality and the energy imparted to the fluid phase by these particles. The energy caused radiolysis of water and the production of reductants and oxidants. The effect of these reductants and oxidants on the transport of radionuclides within and outside the reactors has been difficult to quantify. Analysis of iron(III)/iron(II) ratios in bulk rock samples from the reactor zones (Branche et al., 1975) indicate that the iron in these zones is generally more reduced than the iron in the host rocks well away from the reactor zones. In fact, iron is most reduced in the samples that show the greatest uranium-235 depletion. This suggests that the reduction of iron in the reactor zones was contemporaneous with the nuclear reactions and not a later supergene phenomenon of secondary enrichment. Curtis and Gancarz (1983) suggest that radiolysis of water resulted in the reduction of iron(III) in the reactor zones and the oxidation of uranium(IV) in uraninite. Furthermore, Curtis and Gancarz suggest that the oxidized uranium was transported out of the critical reaction zones and precipitated through reduction processes in the host rocks immediately outside the zones. The reduction processes likely involved organics or sulfides present in the host rocks. However, if the host rocks around the natural reactor cores had not contained species capable of reducing the oxidized uranium transported out of the cores, the uranium could have been transported much farther from the critical reaction zones. The important point is that even with intensive radiolysis very little of the uranium in the natural reactors was mobilized (several percent --Naudet, 1978).

4.3.1.2.2 Other uranium and thorium deposits

Studies of uranium and thorium deposits that have not undergone a critical reaction phase have provided data on the mobility of various shortlived radionuclides in the uranium and thorium decay series. The deposits may also yield data on the mobility of technetium, neptunium, and plutonium, although no such data have been reported to date. The ore deposits of Alligator Rivers are discussed here because they have been studied in considerable detail. Other deposits that have been investigated are the Colorado Plateau uranium deposits (e.g., Osmond and Cowart, 1981) and the Morro de Ferro thorium deposit in Brazil (Eisenbud et al., 1984).

The Alligator Rivers region of northern Australia is underlain by lower Proterozoic sediments and tuffs that overlie late-Archean granitic complexes. Approximately 1,800 million years ago, these rocks were subjected to regional metamorphism and deformation. After subsequent uplift and some retrograde metamorphism, the rocks were covered by middle-Proterozoic and younger units (Needham and Stuart-Smith, 1980).

The uranium deposits of the Alligator Rivers area are found mainly in the lower Proterozoic Cahill Formation. The formation has a lower member of carbonate rock and carbonaceous schists that is overlain by an upper member composed of mica-quartz schist and gneiss. It was metamorphosed to amphibolite facies and subsequently retrograded to greenschist facies assemblages.

DECEMBER 1988

Because the Alligator Rivers region has a monsoonal climate, deep lateritic weathering profiles with anomalous uranium concentrations overlie the primary ore bodies. The profiles are generally composed of four zones (Airey et al., 1985): (1) a zone of oxidized ferricrete or a ferruginous zone grading into a mottled zone (these zones are unsaturated in the dry season and generally have an oscillating water table at other times--uranium is leached in these zones), (2) a pallid zone from which iron has been leached (some uranium is deposited in this zone--this and the following zones are all permanently saturated), (3) a transition zone between weathered and unweathered rock (conditions are generally oxidizing in the zone with some uranium leaching), and (4) unweathered rock of the Cahill formation.

The Australian Atomic Energy Commission under a contract with the NRC has conducted studies (Airey et. al., 1984, 1985) of radionuclide transport in the rocks, sediments, and waters in and around the Alligator Rivers uranium deposits. The results of the studies include the following: (1) in [illegible] along flow paths from the potential repository at Yucca Mountain. Additionally, although the medium is dominantly tuffaceous alluvium, the reactive surface area is higher and effective porosity lower than is expected for the rocks in and around the exploratory block at Yucca Mountain.

The following information was taken from Hoffman and Daniels (1981). The explosion at the Cambric site was a 0.75-kiloton test fired in May 1965, at a depth of 294 m beneath the water table in tuffaceous alluvium (Figure 4-23). Tests began after the cavity and chimney were predicted to be filled with ground water to the preshot static water level, 73 m above the detonation point. It was assumed that tritium, plutonium, and uranium fission products would be present in the cavity and in the ground water within the cavity and could be used to study possible migration from the cavity.

The field study began with the completion of a satellite well (RNM-2S) 91 m from the Cambric cavity followed by drilling of a reentry well (RNM-1) into the cavity itself. Both solid and liquid samples were taken from well RNM-1 to determine the distribution of radionuclides between the solid material and the ground water. Water was then pumped from the satellite well to induce an artificial gradient sufficient to draw water from the Cambric cavity through the surrounding rocks. Pumping from well RNM-2S began in October 1975. The original pump rate was 1 m^3/min until October 1977 when the pump rate was increased to about 2.3 m^3/min.

The various radionuclides present in water drawn from well RNM-2S reflect the extent of radionuclide migration. Approximately 2 yr after pumping started, significant amounts of tritiated water were found in water from the satellite well, signaling the arrival of water from the Cambric cavity region. By that time, approximately 1.44 million m^3 of water had been pumped from the satellite well. After almost 6 yr of pumping, the tritium concentration in the pumped water reached a maximum. The original amount of tritium produced during the Cambric event was about 6×10^4 curies (Hoffman et al., 1977). By the end of September 1984, slightly more than 3.7×10^4 curies of tritium had been pumped out through well RNM-2S (about 60 percent of the initial inventory). The result of a transport calculation based on Sauty's model for hydrodispersive transfer in aquifers (Sauty, 1980) was presented by Thompson (1985). Travis (1984) has modeled the tritium elution at Cambric using the TRACR3D code. According to Travis (1984), the difference between the calculated and observed breakthrough curves is approximately equal to the margin of error in the input parameters used in the code.

Other radionuclides have also been measured in water from well RNM-2S including chlorine-36, krypton-85, ruthenium-106, and iodine-129. Radionuclides present in the Cambric cavity in cationic form (e.g., strontium-90 and cesium-137) have not been detected to

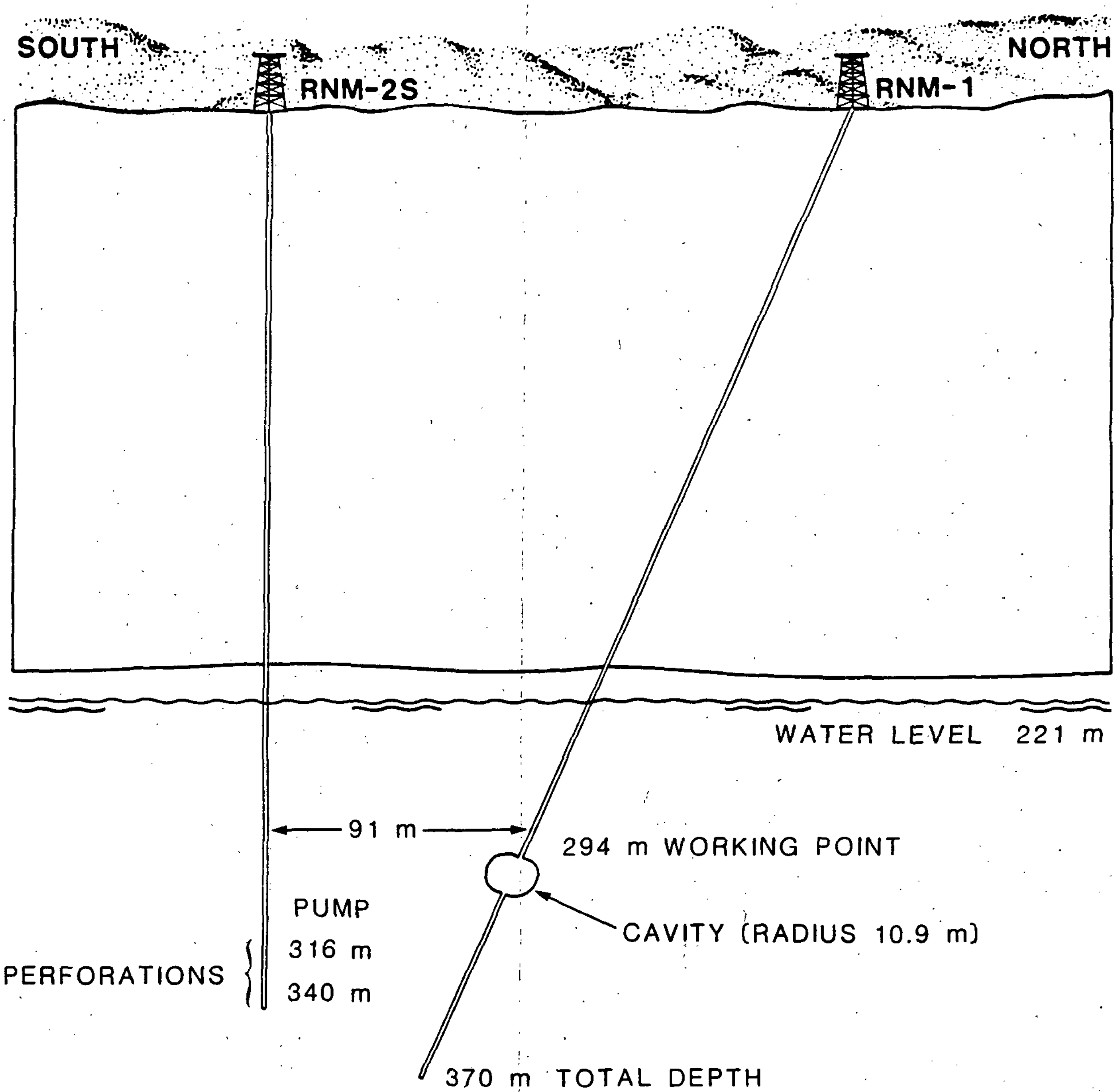

Figure 4-23. Schematic of Cambric explosion cavity and drillholes RNM-1 and RNM-2S. Modified from Hoffman and Daniels (1981).

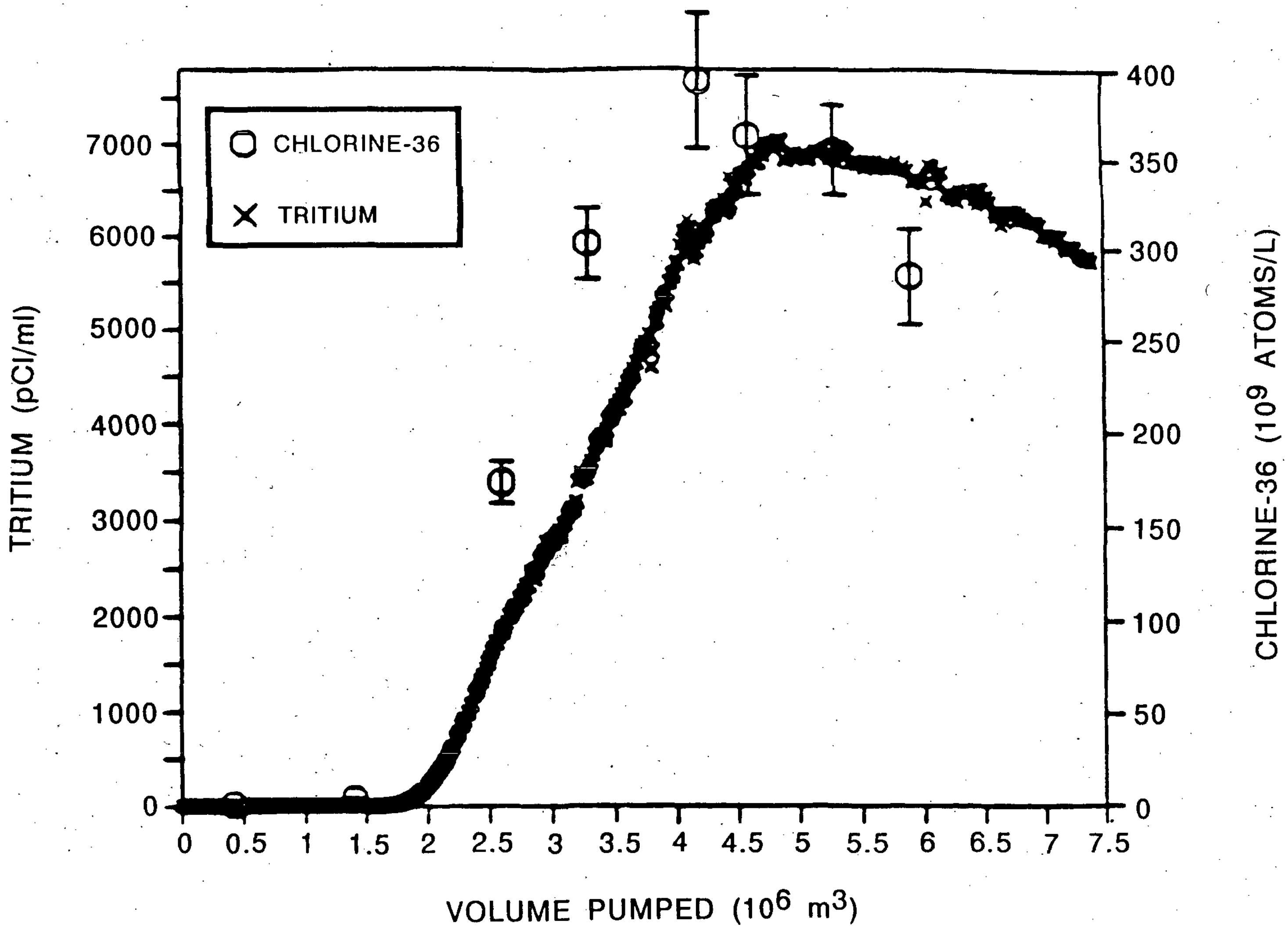

Figure 4-24. Chlorine-36 and tritium concentrations *in well* RNM-2S water. The error bars are the standard deviations for single measurements; they were obtained from the errors associated with measurements and estimated uncertainties for the various parameters entering into the calculation. The estimated uncertainties were propagated in quadrature. Modified from Daniels and Thompson (1984).

Krypton is a noble gas and might be expected to show very little retention in the alluvial aquifer. Although the krypton data show more scatter than the tritium data, the behavior of the elements is correlated. The observations are compatible with the hypothesis that some krypton is sorbed on the alluvium and is therefore retarded relative to water (Thompson, 1985). The fact that the krypton-tritium ratios in well RNM-2S water are lower than the calculated source term ratio of 1.22×10^{-4} while they are higher than consists of an upper 3.6 m of moderately welded, light-brownish-gray tuff underlain by a 3-m-thick layer of reworked tuff and pumice which fills a channel (or cut) in the underlying tuff unit and is separated by a sharp contact zone. The underlying unit consists of 33 m of moderately welded,

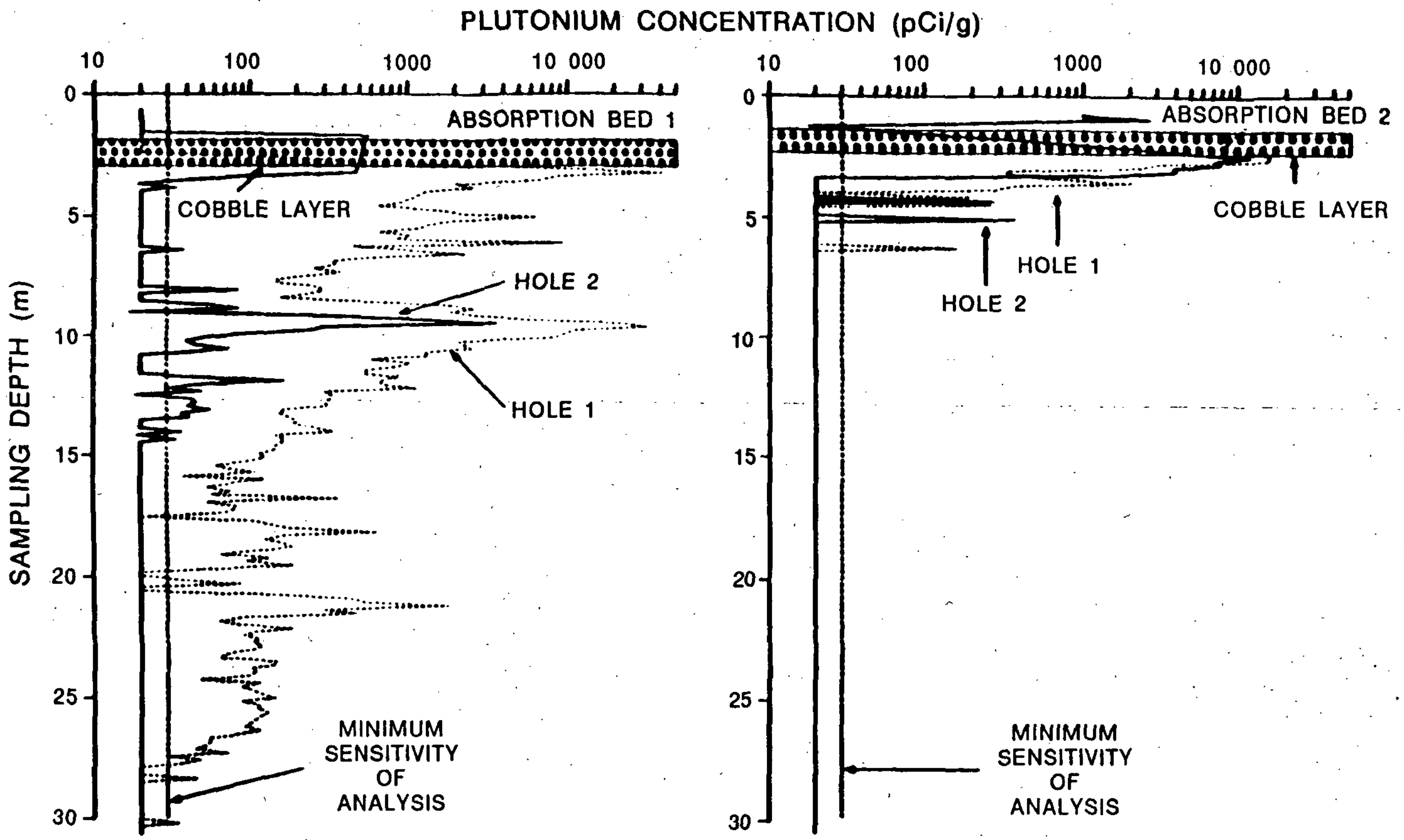

Figure 4-25. Concentration of plutonium as a function of sampling depth for absorption beds 1 and 2 in 1978. Modified from Nyhan et al. (1985).

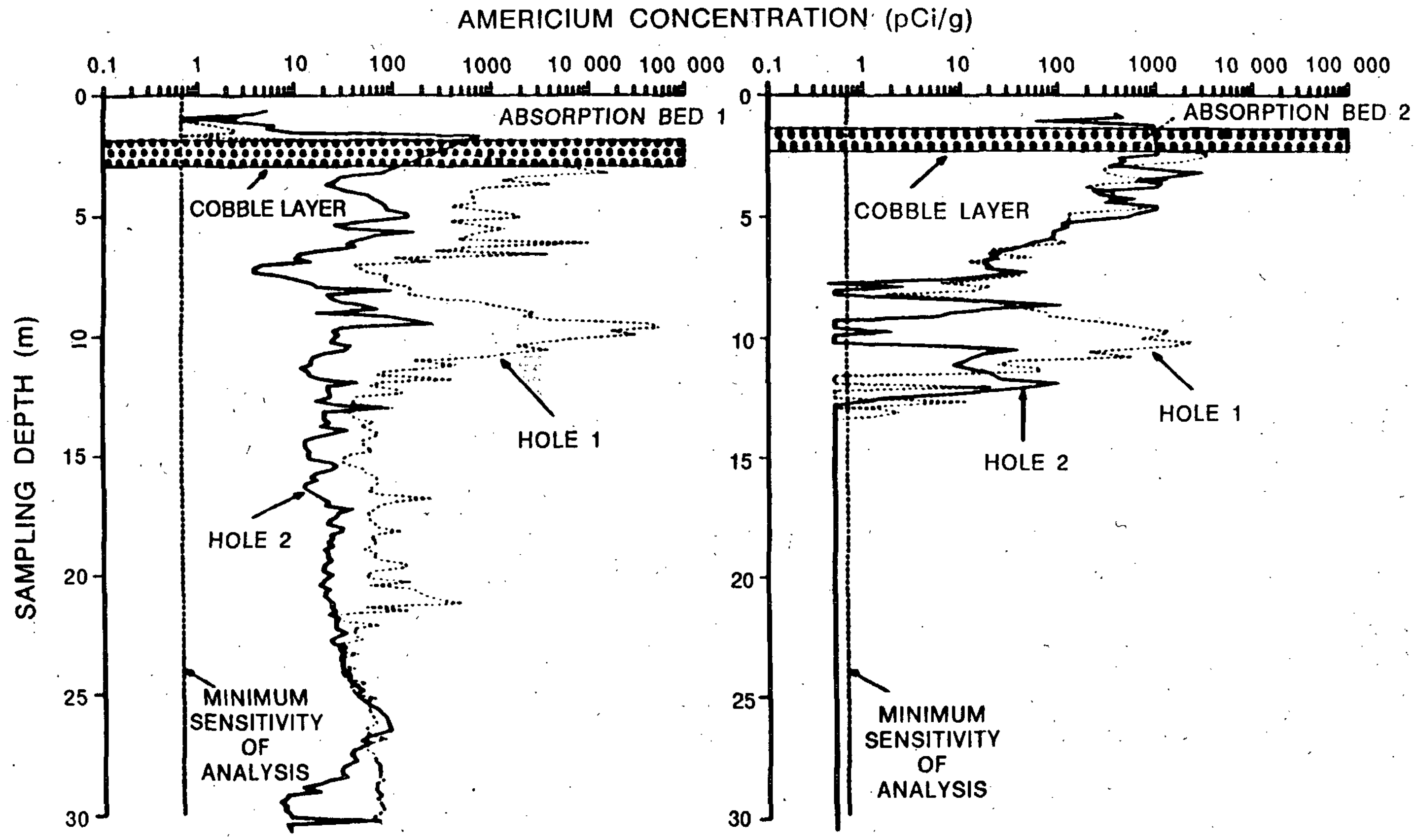

Figure 4-26. Concentration of americium-241 as a function of sampling depth for absorption beds 1 and 2 in 1978. Modified from Nyh 985).

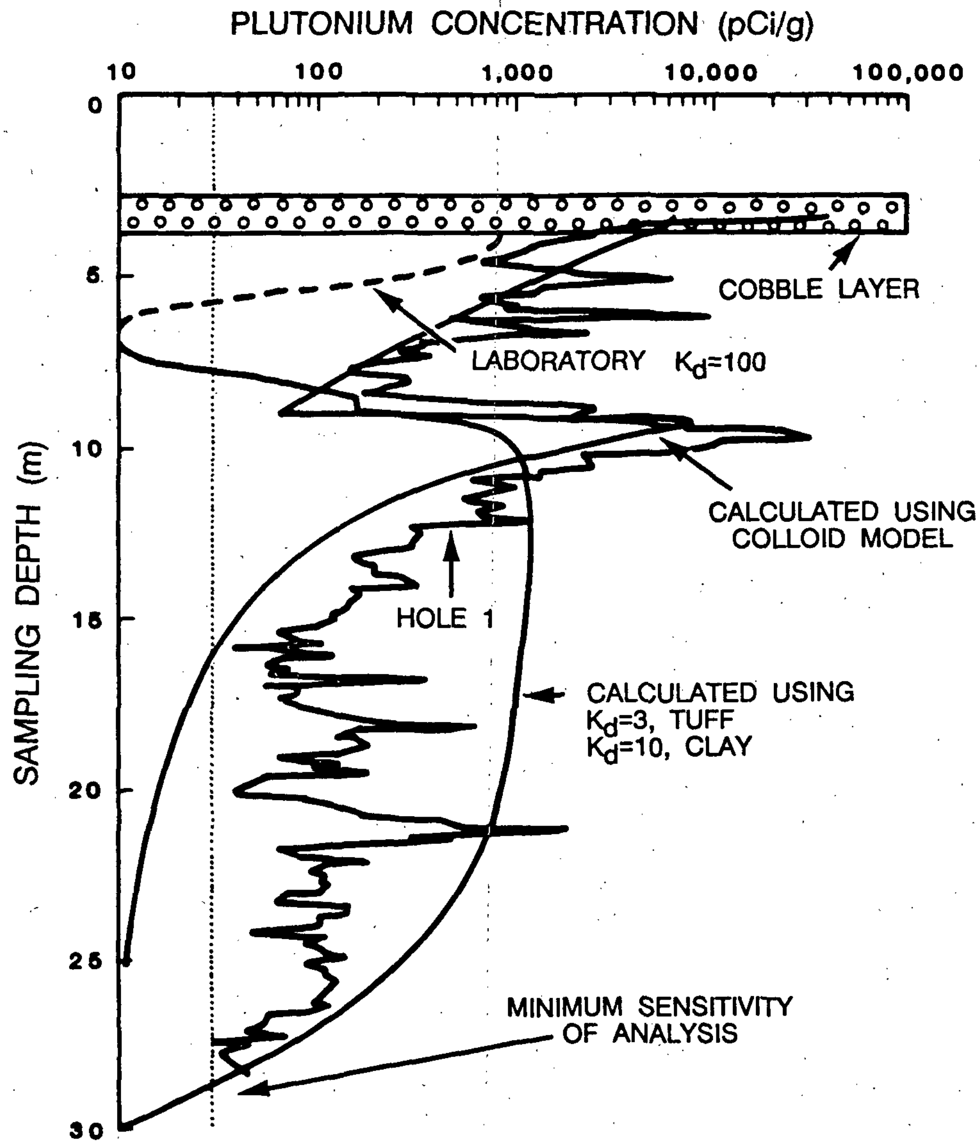

Figure 4-27. The measured and simulated plutonium concentration profiles for the region below bed 1 at the DP West sites. Kd = distribution coefficient. Modified from Nyhan et al. (1985).

4.4 GEOCHEMICAL STABILITY

Man-induced factors that could potentially affect the geochemical stability of the site include mining, exploring for minerals, drilling unrelated to Yucca Mountain Project operations, and withdrawing ground water. Natural changes that could affect the geochemical stability of the site include changes in the water regime as a result of tectonic or climatic variations and the introduction of magmatic fluids into the area. However, natural chemical buffers present in the water and rock help to resist changes in the geochemistry. The geochemical stability of the Topopah Spring tuff can be understood from the data presented in Section 4.1.1; chemical intermay provide a nutrient source for microbes; therefore, the effect of microbial activity on radionuclide migration is being assessed (Section 8.3.1.3.4); and second, the construction of the repository will produce particulates. The sorption and transport of radionuclides by particulates and colloids will also be studied (Section 8.3.1.3.4). Plans for studying the filtration of particulates by Yucca Mountain tuff are discussed in Section 8.3.1.3.6.

4.4.2 POTENTIAL EFFECTS OF NATURAL CHANGES

Natural processes of potential importance for geochemical stability include tectonism and volcanism (Section 1.3), flooding (Section 3.2), glass or mineral alteration that have effects on water composition (Sections 4.1 and 4.2), and climatic changes (Section 5.2). Where appropriate, specific processes that require further study are indicated.

Tectonism, volcanic activity, and structural features have already been treated in terms of possible physical disruption of the repository (Section 1.3.2); the displacement of flow paths by such processes could alter the effectiveness of natural geochemical barriers at the site. Among structural features, faults are important in bounding the exploration block at Yucca Mountain. Because variably mineralized faults may act either to enhance or retard ground-water flow, it is important to know not only what types of faults occur, but also what changes in flow and geochemical retardation might occur as a result of seismic activity and fault movement (Section 1.4). The problem will be addressed among the site characteristics contributing to performance assessment (Section 8.3.5.2.3), based on data obtained from the site geohydrology program (Section 8.3.1.2). The potential effects of igneous intrusion have been evaluated by Link et al. (1982), and the probabilities of volcanic activity have been estimated by Crowe et al. (1982). The post-Miocene hydrothermal activity will have to be considered to be a potential risk at the site. Finally, the possibility of deep-seated spring activity transgressing the repository horizon at some time in the past is being assessed by the study of fault-related mineral deposits (Section 8.3.1.3.2).

The geochemistry (nonhydrothermal) of rock and water interactions at Yucca Mountain involves a number of metastable mineral phases. As such, the chemical rock and water system will change toward more stable assemblages of the lower Topopah Spring vitrophyre; (2) the relatively thick zone of clinoptilolite that occurs in the bedded, nonwelded, and poorly welded tuffs that form the base of the Topopah Spring Member and the underlying tuffs of the Calico Hills, and extends into the top of the Prow Pass Member of the Crater Flat Tuff; (3) the partly welded and bedded tuffs at the base of the Prow Pass Member and at the top of the underlying Bullfrog Member; and (4) the poorly welded and bedded tuffs at the base of the Bullfrog Member compound cooling unit and at the top of the underlying cooling unit within the uppermost Tram Member.

The ground-water chemistry of the site is summarized from the results obtained from the saturated-zone wells on and near Yucca Mountain. Analyses of ground water from the drillholes that penetrate the host rock and surrounding units in the area of the exploration block indicate that they are principally sodium bicarbonate waters with low total dissolved solid content (200 to 400 mg/L). However, water from the carbonate aquifer contains over 1,000 mg/L total dissolved solids. Yucca Mountain ground waters are oxidizing. The dominant cations in the Yucca Mountain ground water are sodium, calcium, potassium, and magnesium with sodium the most abundant, ranging from 65 to 95 percent of the cations present. The concentrations of iron and manganese are generally low. The anionic constituents of the ground water show a relatively uniform distribution in the wells with about 80 percent bicarbonate and the remainder as sulfate and chloride (usually present in nearly equal molar concentrations) and fluoride (in varying concentrations). Overall, only minor variations in ground-water compositions occur in and adjacent to Yucca Mountain. Temporal variations in ground-water composition are also minor. Finally, the water from well J-13 has been chosen as the reference ground water that will represent the ground-water conditions along the transport pathways from the repository to the accessible environment.

The geochemical retardation processes described in Section 4.1.3 include sorption, precipitation, and matrix diffusion. Sorption data have been obtained with samples representative of Yucca Mountain strata. The variables include time, temperature, particle size, oxidation-reduction conditions, element concentration, ground-water composition, and test method (batch, column, or circulating system). The radionuclides investigated were americium, cesium, neptunium, plutonium, uranium, thorium, strontium, technetium, tin, barium, radium, cerium, europium, and selenium. A correlation of sorptive behavior with mineralogy has been identified. Sorption of alkali metals (e.g., cesium) and alkaline earths (strontium, barium, radium) is directly correlated with the presence of minerals with exchangeable cations such as the zeolite clinoptilolite and potentially the smectite clays. Sorption ratios on these minerals vary from 1,000 to more than 10,000 ml/g. The correlation of sorption of cesium, europium, plutonium, and americium with mineralogy exists, but the relation is not as clear as for the alkali metals. However, sorption ratios are high for the elements listed above carbon, cesium, technetium, iodine, tin, zirconium, samarium, and nickel in well J-13 water has been compiled from available measurements and calculations. Diffusion of radionuclides from fracture water into the pore water in the rock matrix is important for retarding the transport of dissolved waste elements through fractures in tuff.

4.5.2 RELATION TO DESIGN

The geochemical characteristics of the backfill materials and the anticipated chemical interactions among the waste container, backfill, ground water, and the host rock under assumed waste emplacement conditions are described in Sections 6.3.3 and 7.4. The geochemical characteristics of the seal material as well as the anticipated chemical interactions among the seal materials, ground water, host rock, and backfill under assumed emplacement conditions are described in Section 6.3.5. Waste container design and geochemical interactions are described in Section 7.4. The mineral stability studies may have an impact on design considering that there is a reported volume change as minerals undergo transitions. This volume change should be assessed in order to determine whether the change is significant to design.

4.5.3 IDENTIFICATION OF INVESTIGATIONS

The investigations under the geochemistry program are listed below and will be discussed in detail in Section 8.3.1.3. Investigations 8.3.1.3.1 (ground water chemistry), 8.3.1.3.2 (mineralogy, petrology and rock chemistry) and 8.3.1.3.3 (stability of minerals and glasses) will provide the base site characterization data on the natural geochemical environment at Yucca Mountain. Investigations 8.3.1.3.4 (radionuclide sorption), 8.3.1.3.5 (radionuclide solubility), 8.3.1.3.6 (radionuclide dispersion, diffusion, and advection), and 8.3.1.3.8 (gaseous radionuclide transport) will investigate the geochemical processes that are acting and may potentially act at Yucca Mountain. Finally, Investigation 8.3.1.3.7 will support the listed investigation and assess the physical/chemical processes through integrated transport calculations. This investigation will synthesize the geochemistry test program data and provide a geochemical/physical model of Yucca Mountain. The investigations are the following:

Investigation 8.3.1.3.1 Water chemistry within the potential emplacement horizon and along potential flow paths

The water chemistry within the saturated zone has been well characterized, but more data are needed for the unsaturated zone (Section 8.3.1.2.2). A model of the ground-water chemistry for Yucca Mountain relating composition to the geologic location along potential pathways is also needed.

The information needed is as follows:

1. Water chemistry of the unsaturated zone.

2. Additional baseline data on naturally occurring radionuclides in Yucca Mountain ground water.

3. Particulate content of Yucca Mountain ground water and collection.

4. More data on the mineralogic controls on Yucca Mountain ground water.

5. Model of the ground-water chemistry at Yucca Mountain.

Investigation 8.3.1.3.2 Mineralogy, petrology, and rock chemistry within the potential emplacement horizon and along potential flow paths

The host rock in the Topopah Spring Member has been described, including the primary phenocryst and vapor-phase constituents. The discussion is found mostly in Chapter 1. Also discussed are the secondary minerals within fractures. The data were assessed for usefulness in indicating stratigraphic position and in characterizing the mineralogy along potential radionuclide travel paths. The chemistry and mineralogy of the surrounding units were detailed including a discussion of the secondary minerals with emphasis on the sorptive zeolites and clays.

More data are still needed to assess (1) how the mineral distributions at Yucca Mountain are going to affect retardation by sorption, (2) what processes account for the minerals found at Yucca Mountain, (3) whether those processes have been completed or are still operating, and (4) how the projected processes would affect a repository at Yucca Mountain. The following list of parameters address these needs:

1. Mineral distributions in bulk rock.
2. Mineral distributions in fractures.
3. Bulk rock chemistry.
4. Fracture chemistry.
5. Mineral origins and alteration history.
6. Mineralogy of transport pathways.

Investigation 8.3.1.3.3 Stability of minerals and glasses

Mineral stability in Yucca Mountain was considered in two ways. The first consideration was whether the present mineral assemblages in Yucca Mountain are stable under present conditions and, if they are not, what mineralogic changes are probable. The presence or absence of clays, cristobalite, glass, and zeolites was studied to assess past thermal gradients. The transformation of cristobalite to quartz was studied in order to understand the evolution of silica activity, which controls the stability of clinoptilolite, a sorbing mineral. The second consideration was what effect repository heating will have on mineral stability, due to both increased temperature and possible dehydration of the rock. The hydrothermal alterations of zeolites, smectites, and rhyolitic glasses were studied to determine alteration products, volume changes, and to understand the kinetics of these mineral reactions. More work is needed to further define the stability of minerals and glasses in every area mentioned previously.

The information needed is as follows:

1. Data on mineral assemblages and temperatures in active hydrothermal systems in vitric tuff.

2. Data on dehydration in smectites, zeolites, and glasses (Section 8.3.1.3.2)

3. Data on the kinetics of silica phase transformations and correlations to aqueous silica activity.

4. Data on the kinetics of transformations in smectites, zeolites, and related tektosilicates.

5. Data for constructing thermodynamic models of clinoptilolite, analcime, and albite.

6. Development of a conceptual model of mineral evolution.

Investigation 8.3.1.3.4 Radionuclide retardation by sorption processes along flow paths to the accessible environment

The retardation process of sorption has been thoroughly considered in this chapter. Sorption as a function of ground-water composition, mineralogy, pH, temperature, oxidation-reduction conditions, sorbing species, and waste element concentrations have been considered. Detail was provided on the analytical techniques used to determine sorptive coefficients and a discussion of the techniques for elucidating dynamic processes and how they are coupled to sorption.

Work must continue on all the previously discussed process parameters in order to assess the interrelationships of water chemistry, mineralogy, solubility, and speciation, and the effect of these processes on the retardation process of sorption in expected and unexpected conditions.

The information needed is as follows:

1. Data on sorption as a function of ground-water composition, mineralogy, and sorbing element concentration.

2. Extension of the sorption data base, specifically sorption coefficients correlated with stratigraphy.

3. Data on sorption on particulates and colloids and its relation to transport.

4. Data on the effects of microbial activity on sorption and the subsequent relation to transport.

Investigation 8.3.1.3.5 Radionuclide retardation by precipitation along flow paths to the accessible environment

Precipitation processes will limit radionuclide transport when the solubility limits of waste elements are exceeded in water as it moves toward the accessible environment. Speciation, defined as the formation of various complexes and oxidation states in the aqueous phase, in turn affects the solubility. This chapter briefly discussed speciation, solubility, radiocolloid formation, and radiolysis, all processes important in understanding concentration limits of elements in solution. The few solubility measurements that have been conducted were discussed along with the modeling work needed to further calculate waste-element solubilities.

To continue the experimental work it is necessary to define the conditions that control solubility (water chemistry, temperature, radiation field) and to define the waste element behavior in order to best understand precipitation processes.

The information needed is as follows:

1. Experimental data on solubility or concentration limits of important waste elements.

2. Experimental data on the ability of waste elements to form natural colloids.

3. Data on, or theoretical understanding of, the sensitivity of solubility limits in controlling parameters. Theory will be developed from speciation measurements and solubility modeling.

4. Solubility calculations.

Investigation 8.3.1.3.6 Radionuclide retardation by dispersive, diffusive, and advective transport processes along flow paths to the accessible environment

The retardation of radionuclides by dispersive, diffusive, and advective processes was discussed in this chapter in relation to the anticipated and unanticipated conditions at Yucca Mountain. The chapter discussed the processes of radionuclide transport (diffusion, fracture flow, anion exclusion, hydrodynamic dispersion, and particulate (colloids or solids) transport. Some of the transport processes retard the rate of radionuclide transport. Matrix diffusion was discussed along with matrix diffusion coupled with fracture flow. Although dispersion is not a transport mechanism, the process also retards radionuclides by channeling (Non-Fickian dispersion) and the broadening effect of heterogeneously distributed material properties. The transport processes are also intimately associated with sorption and with geochemical processes that result in precipitation.

The transport of tracers in geohydrologic systems is not simple and the simplifying assumptions must be tested by laboratory and field experiments to understand fully the relationship of these processes to the retardation of radionuclides. Extensive laboratory work is needed to successfully model the processes.

The information needed is as follows:

1. Data on diffusion processes (advection and no advection).
2. Data on matrix diffusion and its relationship to fracture flow.
3. Data on the relationship of adsorption to these transport processes.
4. Data on sorption kinetics.
5. Data on anion exclusion.
6. Data on colloidal movement and particulate transport.
7. Data on dispersion (hydrodynamic, channeling).

Investigation 8.3.1.3.7 Radionuclide retardation by all processes along flow paths to the accessible environment

The modeling of radionuclide transport requires that chemical reactions of radionuclides occurring between the solid phase (minerals or precipitates) and aqueous phase (fracture or pore water) be coupled with the hydrologic flow and physical processes like diffusion and dispersion. The combination of all processes can be used to assess the retardation of radionuclides.

Because the repository may be in the unsaturated zone, this chapter discussed gaseous transport as a potentially significant mechanism for the transport of volatile radionuclide. Two mechanisms are likely to be effective: (1) isotopic exchange between the gas phase and aqueous phase, and (2) the solubility of the gaseous species in the aqueous phase. No experimental work has been done to date on the geochemical aspects of gaseous transport.

The information needed is as follows:

1. Gaseous species.
2. Gas-phase composition.
3. Physical transport mechanisms and rates.
4. Retardation mechanisms and transport with retardation.
5. Gaseous radionuclide transport calculations.
6. Experimental verification of gaseous transport calculations (gas-transport measurements).

4.5.4 RELATION TO REGULATORY GUIDE 4.17

Regulatory Guide 4.17, Part B, Section 6 (NRC, 1987) provides generic guidance for geochemical topics to be addressed in a site characterization report to the NRC. All of the geochemical topics called for in Regulatory Guide 4.17 are relevant and applicable to the Yucca Mountain site. Most of these are addressed primarily in this chapter, although some are discussed only briefly and with reference to more complete treatments in Chapters 3, 7, and 8 of this document.

 DOE/RW-0199

Nuclear Waste Policy Act
(Section 113)

Site Characterization Plan

Yucca Mountain Site, Nevada Research and Development Area, Nevada

Volume II, Part A

Chapter 4 References

December 1988

U. S. Department of Energy
Office of Civilian Radioactive Waste Management

REFERENCES FOR CHAPTER 4

Airey, P. L., D. Roman, C. Golian, S. Short, T. Nightingale, R. T. Lowson and G. E. Calf, 1984. Radionuclide Migration Around Uranium Ore Bodies - Analogue of Radioactive Waste Repositories, Annual Report, 1982-83, AAEC/C40, Australian Atomic Energy Commission Research Establishment, Lucas Heights Research Laboratories, University of Sydney.

Airey, P. L., D. Roman, C. Golian, S. Short, T. Nightingale, T. Payne, R. T. Lowson and P. Duerden, 1985. Radionuclide Migration Around Uranium Ore Bodies - Analogue of Radioactive Waste Repositories, Annual Report 1983-84, AAEC/C45, Australian Atomic Energy Commission Research Establishment, Lucas Heights Research Laboratories, University of Sydney.

Allard, B., 1983. Actinide Solution Equilibria and Solubilities in Geologic Systems, KBS-TR-83-35, Svensk Karnbransleforsorjning AB/Avdelning KBS, Stockholm, Sweden.

Allard, B., and B. Torstenfelt, 1983. On the Solubility of Technetium in

Bargar, K. E., and M. H. Beeson, 1984a. "Hydrothermal Mineralogy in Research Drill Hole Y-3, Yellowstone National Park, Wyoming," Geothermal Resources Council Transactions, Vol. 8, pp. 111-117.

Bargar, K. E., and M. H. Beeson, 1984b. Hydrothermal Alteration in Research Drill Hole Y-6, Upper Firehole River, Yellowstone National Park, Wyoming, U.S. Geological Survey Professional Paper 1054-B, U.S. Government Printing Office, Washington, D.C.

Bargar, K. E., and T. E. C. Keith, 1984. Hydrothermal Alteration Mineralogy in Newberry 2 Drill Core, Newberry Volcano, Oregon, USGS-OFR-84-92, Open-File Report, U.S. Geological Survey.

Bargar, K. E., and L. J. P. Muffler, 1982. "Hydrothermal Alteration in Research Drill Hole Y-11 from a Vapor-Dominated Geothermal System at Mud Volcano, Yellowstone National Park, Wyoming," Thirty-Third Annual Field Conference, Wyoming Geological Association Guidebook, pp. 139-152.

Bazan, F., and J. Rego, 1985. Parametric Testing of a DWPF Glass, UCRL-53606, Lawrence Livermore National Laboratory, Livermore, Calif.

Benson, L. V., and L. S. Teague, 1980. A Tabulation of Thermodynamic Data for Chemical Reactions Involving 58 Elements Common to Radioactive Waste Package Systems, LBL-11448, Lawrence Berkeley Laboratory, Berkeley, Calif.

Benson, L. V., J. H. Robison, R. K. Blankennagel, and A. E. Ogard, 1983. Chemical Composition of Ground Water and the Locations of Permeable Zones in the Yucca Mountain Area, Nevada, USGS-OFR-83-854, Open-File Report, U.S. Geological Survey.

Bentley, C. B., J. H. Robison, and R. W. Spengler, 1983. Geohydrologic Data for Test Well USW H-5, Yucca Mountain Area, Nye County, Nevada, USGS-OFR-83-853, Open-File Report, U.S. Geological Survey.

Bernkopf, M. F., and J. I. Kim, 1984. Hydrolysereaktionen und Karbonatkomplexierung von Dreiwertigem Americium in Naturlichen Aquatischen System, RCM-02884, Institut fur Radiochemie der Technischen Universitat Munchen, Federal Republic of Germany.

Bidoglio, G., A. De Plano, and A. Chatt, 1983. "Studies on Speciation of Americium, Technecium, and Neptunium in Simulated Vitrified-Waste Leachates," in Scientific Basis for Nuclear Waste Management VI, Materials Research Society Symposia Proceedings, Boston, Massachusetts, November, 1982, G. Brookins (ed.), Vol. 15, North-Holland, Elsevier Science Publishing Co., Inc., New York, pp. 373-382.

Bish, D. L., 1981. Detailed Mineralogical Characterization of the Bullfrog and Tram Members in USW-G1, with Emphasis on Clay Mineralogy, LA-9021-MS, Los Alamos National Laboratory, Los Alamos, N. Mex.

Bish, D. L., 1984. "Effects of Exchangeable Cation Composition on the Thermal Expansion/Contraction of Clinoptilolite," Clays and Clay Minerals, Vol. 32, No. 6, pp. 444-452.

[redacted]CEMBER 1988

[redacted]

Conference on t[redacted]e Occurrence, Properties, an[redacted] Utilization of Neutral

[redacted]

Broxton, D. E., D. T. Vaniman, F. Caporuscio, B. Arney, and G. Heiken, 1982. Detailed Petrographic Descriptions and Microprobe Data for Drill Holes USW-G2 and UE25b-1H, Yucca Mountain, Nevada, LA-9324-MS, Los Alamos National Laboratory, Los Alamos, N. Mex.

Broxton, D. E., R. G. Warren, R. C. Hagan, and G. Luedemann, 1986. Chemistry of Diagenetically Altered Tuffs at a Potential Nuclear Waste Repository, Yucca Mountain, Nye County, Nevada, LA-10802-MS, Los Alamos National Laboratory, Los Alamos, N. Mex.

Bryant, E. A., and D. T. Vaniman (comps.), 1984. Research and Development Related to the Nevada Nuclear Waste Storage Investigations, July 1 - September 30, 1983, LA-10006-PR, Los Alamos National Laboratory, Los Alamos, N. Mex.

Byers, F. M., Jr., 1985. Petrochemical Variation of Topopah Spring Tuff Matrix with Depth (Stratigraphic Level), Drill Hole USW G-4 Yucca

Byers, F. M., Jr., and R. G. Warren, 1983. Revised Volcanic Stratigraphy of Drill Hole J-13, Fortymile Wash, Nevada, Based on Petrographic Modes and Chemistry of Phenocrysts, LA-9652-MS, Los Alamos National Laboratory, Los Alamos, N. Mex.

Byers, F. M., Jr., W. J. Carr, P. P. Orkild, W. D. Quinlivan, and K. A.

Champp, D. R., W. F. Merritt, and J. L. Young, 1982. "Potential for the Rapid Transport of Plutonium in Groundwater as Demonstrated by Core Column Studies," in Scientific Basis for Nuclear Waste Management V, Materials Research Society Symposia Proceedings, Berlin, Germany, June 7-10, 1982, W. Lutze (ed.), Vol. 5, North-Holland, Elsevier Science Publishing Co., Inc., New York, pp. 745-754.

Christiansen, R. L., and H. R. Blank, Jr., 1972. Volcanic Stratigraphy of the Quaternary Rhyolite Plateau in Yellowstone National Park, Geological Survey Professional Paper 729-B, U.S. Geological Survey.

Claassen, H. C., 1973. Water Quality and Physical Characteristics of Nevada Test Site Water-Supply Wells, USGS-474-158, U.S. Geological Survey.

Claassen, H. C., 1985. Sources and Mechanisms of Recharge for Ground Water in the West-Central Amargosa Desert, Nevada--A Geochemical Interpretation, U.S. Geological Survey Professional Paper 712-F, U.S. Government Printing Office, Washington, D.C.

Coles, D. G., and L. D. Ramspott, 1982. "Migration of Ruthenium-106 in a Nevada Test Site Aquifer: Discrepancy Between Field and Laboratory Results," Science, Vol. 215, pp. 1235-1237.

Couture, R. A., 1985. "Rapid Increases in Permeability and Porosity of Bentonite-Sand Mixtures Due to Alteration by Water Vapor," in Scientific Basis for Nuclear Waste Management VIII, Materials Research Society Symposia Proceedings, Boston, Massachusetts, November 26-29, 1984, C. M. Jantzen, J. A. Stone, and R. C. Ewing (eds.), Materials Research Society, Pittsburgh, Penn., pp. 515-522.

Craig, R. W., R. L. Reed, and R. W. Spengler, 1983. Geohydrologic Data for

Curtis, D. B., and A. J. Gancarz, 1983. Radiolysis in Nature: Evidence from the Oklo Natural Reactors, Technical Report 83-10, Svensk Karnbransleforsorjning/Avdelning KBS.

DOE (U.S. Department of Energy), 1986. Final Environmental Assessment: Yucca Mountain Site, Nevada Research and Development Area, Nevada, DOE/RW-0073, Washington, D.C.

Daniels, W. R. (comp.), 1981. Laboratory and Field Studies Related to the Radionuclide Migration Project, October 1, 1979-September 30, 1980, LA-8670-PR, Los Alamos National Laboratory, Los Alamos, N. Mex.

Daniels, W. R., and J. L. Thompson (comps.), 1984. Laboratory and Field Studies Related to the Radionuclide Migration Project, October 1, 1982 - September 30, 1983, LA-10121-PR, Los Alamos National Laboratory, Los Alamos, N. Mex.

Daniels, W. R., K. Wolfsberg, R. S. Rundberg, with others, 1982. Summary Report on the Geochemistry of Yucca Mountain and Environs, J. Heiken (ed.), LA-9328-MS, Los Alamos National Laboratory, Los Alamos, N. Mex.

Daniels, W. R., B. R. Erdal, and D. T. Vaniman (comps.), 1983. Research and Development Related to the Nevada Nuclear Waste Storage Investigations: July 1-September 30, 1982, LA-9577-PR, Los Alamos National Laboratory, Los Alamos, N. Mex.

Drever, J. I., 1982. "Colloid Properties." The Geochemistry of Natural

EPA (U.S. Environmental Protection Agency), 1976. Environmental Monitoring Report for the Nevada Test Site and Other Test Areas Used for Underground Nuclear Detonations, January through December, 1975, EMSL-LV-539-4, Las Vegas, Nev., p. 62.

Eisenbud, M., K. Krauskopf, E. P. Franca, W. Lei, R. Ballad, P. Linsalata, and K. Fujimori, 1984. "Natural Analogues for the Transuranic Actinide

Gayer, K. H., and H. Leider, 1955. "The Solubility of Uranium Trioxide, UO3H2O, in Solutions of Sodium Hydroxide and Perchloric Acid at 25 deg. C," Journal of American Chemical Society, Vol. 77, pp. 1448-1450.

Goff, F. E., and C. O. Grigsby, 1982. "Valles Caldera Geothermal Systems, New Mexico, U.S.A.," Journal of Hydrology, Vol. 56, pp. 119-136.

Goff, F. E., and S. Sayer, 1980. A Geothermal Investigation of Spring and Well Waters of the Los Alamos Region, New Mexico, LA-8326-MS, Los Alamos National Laboratory, Los Alamos, N. Mex.

Goff, F. E., C. O. Grigsby, P. E. Trujillo, Jr., D. Counce, and A. Kron, 1981. "Geology, Water Chemistry and Geothermal Potential of the Jemez Springs Area, Canon de San Diego, New Mexico," Journal of Volcanology and Geothermal Research, Vol. 10, Elsevier Scientific Publishing Co., Amsterdam, pp. 227-244.

Goff, F. E., T. McCormick, P. E. Trujillo, Jr., D. Counce, and C. O. Grigsby, 1982. Geochemical Data for 95 Thermal and Nonthermal Waters of the Valles Caldera - Southern Jemez Mountains Region, New Mexico, LA-9367-OBES, Los Alamos National Laboratory, Los Alamos, N. Mex.

Hay, R. L., 1978. "Geologic Occurrence of Zeolites," Natural Zeolites: Occurrence, Properties, Use, L. B. Sand and F. A. Mompton (eds.), Pergamon Press, New York, pp. 135-143.

Hay, R. L., and R. A. Sheppard, 1977. "Zeolites in Open Hydrologic Systems," Mineralogy and Geology of Natural Zeolites, F. A. Mumpton (ed.), Mineralogical Society of America Short Course Notes, Vol. 4, pp. 93-102.

Heiken, G. H., and M. L. Bevier, 1979. Petrology of Tuff Units from the J-13 Drill Site, Jackass Flats, Nevada, LA-7563-MS, Los Alamos National Laboratory, Los Alamos, N. Mex.

Hoffman, D. C., and W. R. Daniels, 1981. Assessment of the Potential for Radionuclide Migration from a Nuclear Explosion Cavity, LA-UR-81-3181; CONF-811211--1; Los Alamos National Laboratory, Los Alamos, N. Mex.

Hoffman, D. C., R. Stone, and W. W. Dudley, Jr., 1977. Radioactivity in the Underground Environment of the Cambric Nuclear Explosion at the Nevada Test Site, LA-6877-MS, Los Alamos National Laboratory, Los Alamos, N. Mex.

Honda, S., and L. J. P. Muffler, 1970. "Hydrothermal Alteration in Core from Research Drill Hole Y-1, Upper Geyser Basin, Yellowstone National Park, Wyoming," The American Mineralogist, Vol. 55, pp. 1714-1737.

Hulen, J. B., and D. L. Nielson, 1985. "Hydrothermal Alteration in the Baca Geothermal System, Redondo Dome, Valles Caldera, New Mexico," Journal of Geophysical Research.

Isherwood, D., 1985. Application of the Ruthenium and Technetium Thermodynamic Data Bases Used in the EQ3/6 Geochemical Codes, UCRL-53594, Lawrence Livermore National Laboratory, Livermore, Calif.

Johnston, H. S., 1966. Gas Phase Reaction Rate Theory, The Ronald Press Co., New York, pp. 102-103.

Keith, T. E. C., and L. J. P. Muffler, 1978. "Minerals Produced during Cooling and Hydrothermal Alteration of Ash Flow Tuff from Yellowstone Drill Hole Y-5," Journal of Volcanology and Geothermal Research, Vol. 3, pp. 373-402.

Keith, T. E. C., D. E. White, and M. H. Beeson, 1978. Hydrothermal Alteration and Self-Sealing in Y-7 and Y-8 Drill Holes in Northern Part of Upper Geyser Basin, Yellowstone National Park, Wyoming, Geological Survey Professional Paper 1054-A, U.S. Geological Survey.

Keith, T. E. C., J. M. Thompson, and R. E. Mays, 1983. "Selective Concentration of Cesium in Analcime during Hydrothermal Alteration, Yellowstone National Park, Wyoming," Geochimica et Cosmochimica Acta, Vol. 47, pp. 795-804.

Keith, T. E. C., K. E. Bargar, S. S. Howe, W. W. Carothers, and I. Barnes, 1984a. "Mineralogical Studies of the Hydrothermal System in Newberry

Kim, J. I., M. Bernkopf, CH. Lierse, and F. Koppold, 1984b. "Hydrolysis Reactions of Am(III) and Pu(VI) Ions in Near-Neutral Solutions," Geochemical Behavior of Disposed Radioactive Waste, 185th Meeting of the American Chemical Society, Seattle, Wash., March 20-25, 1983, G. S. Barney, J. D. Navratil and W. W. Schulz (eds.), ACS Symposium Series 246, American Chemical Society, Washington, D.C., pp. 115-134.

Kistler, R. W., 1968. "Potassium-Argon Ages of Volcanic Rocks in Nye and Esmeralda Counties," Nevada Test Site, E. B. Eckel (ed.), Geological Society of America Memoir 110, Boulder, Colo., pp. 251-262.

Knauss, K. G., and W. B. Beiriger, 1984. Report on Static Hydrothermal Alteration Studies of Topopah Spring Tuff Wafers in J-13 Water at 150 deg. C, UCRL-53576, Lawrence Livermore National Laboratory, Livermore, Calif.

Koster van Groos, A. F., and S. Guggenheim, 1984. "The Effect of Pressure on the Dehydration Reaction of Interlayer in Na-Montmorillonite (SWy-1)," American Mineralogist, Vol. 69, pp. 872-879.

Koster van Groos, A. F., and S. Guggenheim, 1986. "Dehydration of K-Exchanged Montmorillonite at Elevated Temperatures and Pressures," Clays and Clay Minerals, Vol. 34, No. 3, pp. 281-286.

Krupka, K. M., D. Rai, R. W. Fulton, and R. C. Strickert, 1984. Solubility Data for U(VI) Hydroxide and Np(IV) Hydrous Oxide: Application of MCC-3 Methodology, PNL-SA-12324, Pacific Northwest Laboratory, Richland, Wash.

Lemire, R. J., and P. R. Tremaine, 1980. "Uranium and Plutonium in Equilibria in Aqueous Solutions to 200 deg. C," Journal of Chemical and Engineering Data, Vol. 25, No. 4, pp. 361-370.

Le Page, Y., and G. Donnay, 1976. "Refinement of the Crystal Structure of Low-Quartz," Acta Crystallographica, Vol. B32, pp. 2456-2459.

Levy, S. S., 1984a. Petrology of Samples from Drill Holes USW H-3, H-4 and H-5, Yucca Mountain, Nevada, LA-9706-MS, Los Alamos National Laboratory, Los Alamos, N. Mex.

Levy, S. S., 1984b. "Studies of Altered Vitrophyre for the Protection of Nuclear Waste Repository-Induced Thermal Alteration at Yucca Mountain, Nevada," in Scientific Basis for Nuclear Waste Management VII, Materials Research Society Symposia Proceedings, Boston, Massachusetts, November 1983, G. L. McVay (ed.), Vol. 26, North-Holland, Elsevier Science Publishing Co., Inc., New York, pp. 959-966.

Levy, S. S., 1987. Alteration Products and Processes in the Lower Topopah Spring Member of the Paintbrush Tuff, Yucca Mountain, and Vicinity, Nevada, LA-10677-MS, Los Alamos National Laboratory, Los Alamos, N. Mex.

Lindberg, R. D., and D. D. Runnells, 1984. "Ground Water Redox Reactions: An Analysis of Equilibrium State Applied to Eh Measurements and Geochemical Modeling," Science, Vol. 225, pp. 925-927.

Link, R. L., S. E. Logan, H. S. Ng, F. A. Rockenbach, and K. J. Hong, 1982. Parametric Studies of Radiological Consequences of Basaltic Volcanism, SAND81-2375, Sandia National Laboratories, Albuquerque, N. Mex.

Lipman, P. W., R. L. Christiansen, and J. T. O'Connor, 1966. A Compositionally Zoned Ash-Flow Sheet in Southern Nevada, Geological Survey Professional Paper 525-F, U.S. Geological Survey.

Lundqvist, R., 1982. "Hydrophilic Complexes of the Actinides. I. Carbonates of Trivalent Americium and Europium," Acta Chemica Scandinavica, Vol. A 36, pp. 741-750.

MacEwan, D. M. C., 1972. "Montmorillonite Minerals" The X-ray Identification and Crystal Structures of Clay Minerals, G. Brown (ed.), Chapter IV, Mineralogical Society, London.

Means, J. L., A. S. Maest, and D. A. Crerar, 1983. Organic Geochemistry of Deep Ground Waters and Radionuclide Partitioning Experiments Under Hydrothermal Conditions, ONWI-448, Office of Nuclear Waste Isolation, Battelle Memorial Institute, Columbus, Ohio.

Meyer, R. E., W. D. Arnold, J. G. Blencoe, G. D. O'Kelley, R. I. Case, J. F. Land, and G. K. Jacobs, 1986. Progress in Evaluation of Radionuclide Geochemical Information Developed by DOE High-Level Nuclear Waste Repository Site Projects: Semi-Annual Report for October 1985 - March 1986. NUREG/CR-4708. Vol. 1. No. 1. U.S. Nuclear Regulatory Commission. Washington, D.C.

Miller, L. J., 1958. "The Chemical Environment of Pitchblende," Economic Geology, Vol. 53, pp. 521-545.

Montazer, P., and W. E. Wilson, 1984. Conceptual Hydrologic Model of Flow in the Unsaturated Zone, Yucca Mountain, Nevada, USGS-WRI-84-4345, Water-Resources Investigations Report, U.S. Geological Survey.

Mumpton, F. A., 1960. "Clinoptilolite Redefined" American Mineralogist, Vol. 45, pp. 351-369.

NRC (U.S. Nuclear Regulatory Commission), 1984. Determination of Radionuclide

Neretnieks, I., 1980. "Transport Mechanisms and Rates of Transport of Radionuclides in the Geosphere as Related to the Swedish KBS Concept," in Underground Disposal of Radioactive Wastes, Vol. II, Proceedings of a Symposium, Otaniemi, 2-6 July 1979, IAEA-SM-243/108, International Atomic Energy Agency (IAEA), Vienna, Austria, pp. 315 & 339.

Newton, T. W., and V. L. Rundberg, 1984. "Disproportionation and Polymerization of Plutonium(IV) in Dilute Aqueous Solutions," in Scientific Basis for Nuclear Waste Management VII, Materials Research Society Symposia Proceedings, Boston, Massachusetts, November 1983, G. L. McVay (ed.), Vol. 26, North-Holland, Elsevier Science Publishing, Inc., New York, pp. 867-873.

Nitsche, H., and N. M. Edelstein, 1985. Determination of Solubilities and Complexation of Waste Radionuclides Pertinent to Geologic Disposal at the Nevada Tuff Site, LBL-18900, Lawrence Berkeley Laboratory, Berkeley, Calif.

Nyhan, J. W., B. J. Drennon, W. V. Abeele, M. L. Wheeler, W. D. Purtymun, G. Trujillo, W. J. Herrera, and J. W. Booth, 1985. "Distribution of Plutonium and Americium Beneath a 33-yr-old Liquid Waste Disposal Site," Olofsson, U., B. Allard, K. Andersson, and B. Torstenfelt, 1982b. "Formation and Properties of Americium Colloids in Aqueous Systems," in Scientific Basis for Nuclear Waste Management, Materials Research Society Symposia Proceedings, Boston, Massachusetts, November 1981, S. Topp (ed.), Vol. 6, North-Holland, Elsevier Science Publishing Co., Inc., New York, pp. 191-198.

Olofsson, U., M. Bengtsson, and B. Allard, 1984. "Generation and Transport Properties of Colloidal Tri- and Tetravalent Actinide Species in Geologic Environments," in Scientific Basis for Nuclear Waste Management VII, Materials Research Society Symposia Proceedings, Boston, Massachusetts, November 1983, G. L. McVay (ed.), Vol. 26, North-Holland, Elsevier Science Publishing Co., Inc., New York, pp. 859-866.

Orkild, P. P., 1965. "Paintbrush Tuff and Timber Mountain Tuff of Nye County, Nevada," Changes in Stratigraphic Nomenclature by the U.S. Geological Survey 1964, G. V. Cohee and W. S. West (eds.), U.S. Geological Survey Bulletin 1224-A, U.S. Geological Survey, pp. A44-A51.

Osmond, J. K., and J. B. Cowart, 1981. Uranium-Series Disequilibrium in Ground Water and Core Composite Samples from the San Juan Basin and Copper Mountain Research Sites, Report GJBX 364(81), Department of Geology, Florida State University, Tallahassee.

Peacor, D. R., 1973. "High-Temperature Single-Crystal Study of the Cristobalite Inversion," Zeitschrift fur Kristallographie, Vol. 138, pp. 274-298.

Perkins, B., B. Travis, and G. DePoorter, 1985. Validation of the TRACR3D Code for Soil Water Flow Under Saturated/Unsaturated Conditions in Three Experiments, LA-10263-MS, Los Alamos National Laboratory, Los Alamos, N. Mex.

Phillips, F. M., F. Goff, F. Vautaz, H. W. Bentley, D. Elmore, and H. E. Gove, 1984. "36-Cl as a Tracer in Geothermal Systems: Example from Valles Caldera, New Mexico," Geophysical Research Letters, Vol. 11, No. 12, pp. 1227-1230.

Rai, D., 1984. "Solubility Product of Pu(IV) Hydrous Oxide and Equilibrium Constants of Pu(IV)/Pu(V), Pu(IV)/Pu(VI), and Pu(V)/Pu(VI) Couples," Radiochimica Acta, Vol. 35, pp. 97-106.

Rai, D., and J. L. Ryan, 1982. "Crystallinity and Solubility of Pu(IV) Oxide and Hydrous Oxide in Aged Aqueous Suspensions," Radiochimica Acta, Vol. 30, pp. 213-216.

Rai, D., and J. L. Ryan, 1984. "Solubility Constraint: An Important Consideration in Safety Assessment of Nuclear Waste Disposal," in Scientific Basis for Nuclear Waste Management VII, Materials Research Society Symposia Proceedings, Boston, Massachusetts, November, 1983, G. L. McVay (ed.), Vol. 26, North-Holland, Elsevier Science Publishing Co., Inc., New York, pp. 805-815.

Rai, D., and R. J. Serne, 1978. Solid Phases and Solution Species of Different Elements in Geologic Environments, PNL-2651, Pacific Northwest Laboratory, Richland, Wash.

Sergeyeva, E. I., A. A. Nikitin, I. L. Khodakovskiy, and G. B. Naumov, 1972. "Experimental Investigation of Equilibria in the System UO3-CO2-H2O in 25-200 deg. C Temperature Interval," Geochemistry International, Vol. 9, pp. 900-910.

Shepard, A. O., and H. C. Starkey, 1966. "The Effects of Exchanged Cations on the Thermal Behavior of Heulandite and Clinoptilolite," Papers from the Fourth General Meeting of the International Mineralogical Association, Mineralogical Society of India, pp. 155-158.

Sherry, H. S., 1969. "The Ion Exchange Properties of Zeolites" Advances in [redacted]

Silva, R. J., and H. Nitsche, 1983. "Thermodynamic Properties of Chemical Species of Waste Radionuclides," NRC Nuclear Waste Geochemistry '83, D. H. Alexander and G. F. Birchard (eds.), NUREG/CP-0052, U.S. Nuclear Regulatory Commission, Washington, D.C., pp. 70-93.

Silva, R. J., and H. Nitsche, 1985. "Carbonate Complexation of Pu(IV) in Aqueous Solution," Abstracts of Papers 189th American Chemical Society National Meeting, Miami Beach, Florida, April 28-May 3, 1985, Paper No. 44.

Silva, R. J., and A. W. Yee, 1981. Uranium (VI) Retardation Mechanisms. [redacted]

Thompson, J. M., and S. Yadav, 1979. Chemical Analyses of Waters from Geysers, Hot Springs and Pools in Yellowstone National Park, Wyoming from 1974 to 1978, USGS-OFR-79-704, Open-File Report, U.S. Geological Survey.

Thompson, J. M., T. S. Presser, R. B. Barnes, and D. B. Bird, 1975. Chemical

Walter, G. R., 1982. Theoretical and Experimental Determination of Matrix Diffusion and Related Solute Transport Properties of Fractured Tuffs from the Nevada Test Site, LA-9471-MS, Los Alamos National Laboratory, Los Alamos, N. Mex.

Warren, R. G., F. M. Byers, and F. A. Caporuscio, 1984. Petrography and Mineral Chemistry of Units of the Topopah Spring, Calico Hills and Crater Flat Tuffs, and Older Volcanic Units, with Emphasis on Samples from Drill

National Laboratory, Los Alamos, N. Mex.

West, J. M., and I. G. McKinley, 1984. "The Geomicrobiology of Nuclear Waste Disposal," in Scientific Basis for Nuclear Waste Management VII, Materials Research Society Symposia Proceedings, Boston, Massachusetts, November 1983, G. L. McVay (ed.), Vol. 26, North-Holland, Elsevier Science Publishing Co., New York, pp. 487-494.

White, A. F., and H. C. Claassen, 1979. "Dissolution Kinetics of Silicate Rocks-Application to Solute Modeling," Chemical Modeling in Aqueous Systems: Speciation, Sorption, Solubility, and Kinetics: Chapter 22, ACS Symposium Series, E. A. Jenne (ed.), Vol. 93, American Chemical Society, Washington, D.C., pp. 447-474.

White, A. F., and H. C. Claassen, 1980. "Kinetic Model for the Short-Term Dissolution of a Rhyolitic Glass," Chemical Geology, Vol. 28, pp. 91-109.

White, A. F., H. C. Claassen, and L. V. Benson, 1980. The Effect of

Wolfsberg, K., and D. T. Vaniman, (Comps.), 1984. Research and Development Related to the Nevada Nuclear Waste Storage Investigations, October 1--December 31, 1983, LA-10032-PR, Los Alamos National Laboratory, Los Alamos, N. Mex.

Wolfsberg, K., B. P. Bayhurst, B. M. Crowe, W. R. Daniels, B. R. Erdal, F. O. Lawrence, A. E. Norris, and J. R. Smyth, 1979. Sorption-Desorption Studies on Tuff; I. Initial Studies with Samples from the J-13 Drill Site, Jackass Flats, Nevada, LA-7480-MS, Los Alamos National Laboratory, Los Alamos, N. Mex.

Wolfsberg, K., R. Aguilar, B. Bayhurst, W. Daniels, S. Devilliers, B. Erdal, F. Lawrence, S. Maestas, A. Mitchell, P. Oliver, N. Raybold, R. Rundberg, J. L. Thompson, and E. Vine, 1981. Sorption-Desorption Studies on Tuff: III. A Continuation of Studies with Samples from Jackass Flats and Yucca Mountain, Nevada, LA-8747-MS, Los Alamos National Laboratory, Los Alamos, N. Mex.

Wolfsberg, K., W. R. Daniels, B. R. Erdal, and D. T. Vaniman (comps.), 1982a. Research and Development Related to the Nevada Nuclear Waste Storage Investigations, April 1-June 30, 1982, LA-9484-PR, Los Alamos National Laboratory, Los Alamos, N. Mex.

Wolfsberg, K., W. R. Daniels, D. T. Vaniman, and B. R. Erdal (compilers), 1982b. Research and Development Related to the Nevada Nuclear Waste Storage Investigations, October 1-December 31, 1981, LA-9225-PR, Los Alamos National Laboratory, Los Alamos, N. Mex.

Wolfsberg, K., D. T. Vaniman, and A. E. Ogard, 1983. Research and Development Related to the Nevada Nuclear Waste Storage Investigations, January 1-March 31, 1983, LA-9793-PR, Los Alamos National Laboratory, Los Alamos, N. Mex.

Zielinski, R. A., 1983. Evaluation of Ash-Flow Tuffs as Hosts for Radioactive Waste: Criteria Based on Selective Leaching of Manganese Oxides, USGS-OFR-83-480, Open-File Report, U.S. Geological Survey.

CODES AND REGULATIONS

10 CFR Part 60 (Code of Federal Regulations), 1987. Title 10, "Energy," Part 60, "Disposal of High-Level Radioactive Wastes in Geologic Repositories," U.S. Government Printing Office, Washington, D.C., pp. 627-658.

10 CFR Part 960 (Code of Federal Regulations), 1987. Title 10, "Energy," Part 960, "General Guidelines for the Recommendation of Sites for Nuclear Waste Repositories," U.S. Government Printing Office, Washington, D.C., pp. 518-551.

40 CFR Part 191 (Code of Federal Regulations), 1986. Title 40, "Protection of Environment," Part 191, "Environmental Radiation Protection Standards for Management and Disposal of Spent Nuclear Fuel, High-Level and Transuranic Radioactive Wastes," U.S. Government Printing Office, Washington, D.C., pp. 7-16.

DOE/RW-0199

Nuclear Waste Policy Act
(Section 113)

Site Characterization Plan

Yucca Mountain Site, Nevada Research and Development Area, Nevada

Volume II, Part A

Chapter 5, Climatology and Meteorology

December 1988

U. S. Department of Energy
Office of Civilian Radioactive Waste Management

DECEMBER 1988

Chapter 5

CLIMATOLOGY AND METEOROLOGY

INTRODUCTION

Past, present, and future climatic conditions at Yucca Mountain need to be characterized in order to design and predict the performance of a geologic

The information in this chapter will also be used by the geohydrology, geochemistry, climate, erosion, meteorology, population density, offsite installations, surface characteristics, and preclosure hydrology testing programs. Connections between climatology and meteorology and these issues and testing programs will be identified, and plans for the collection of additional data will be referenced to sections of Chapter 8.

Meteorological data have been collected from monitoring stations operated by the National Weather Service, and at stations on the Nevada Test Site [illegible]

climate are temperature, precipitation, and atmospheric moisture, and to a lesser extent, wind speed and wind direction. Data from a range of elevations are needed to describe the site climate (Figure 5-1). Table 5-1 provides specific information (elevation, period of record, etc.) on each of these stations. Some of the parameters listed in Table 5-1 for the site monitoring program are not specifically related to climate determinations or design considerations but have been included because they will be used in subsequent permitting and licensing activities that are not directly related to site characterization. A plan for environmental monitoring and mitigation will be developed to ensure that site characterization activities will not result in significant adverse environmental impacts. This plan will describe how the site-specific meteorological data will be used in determining impacts associated with site characterization. The meteorological data will also be needed in obtaining permits, as outlined in the environmental regulatory compliance plan (ERCP).

Section 5.1 describes the recent local climate based on temperature, precipitation, upper air, surface winds, atmospheric moisture, and severe weather data collected at the monitoring stations. However, climatic classi-

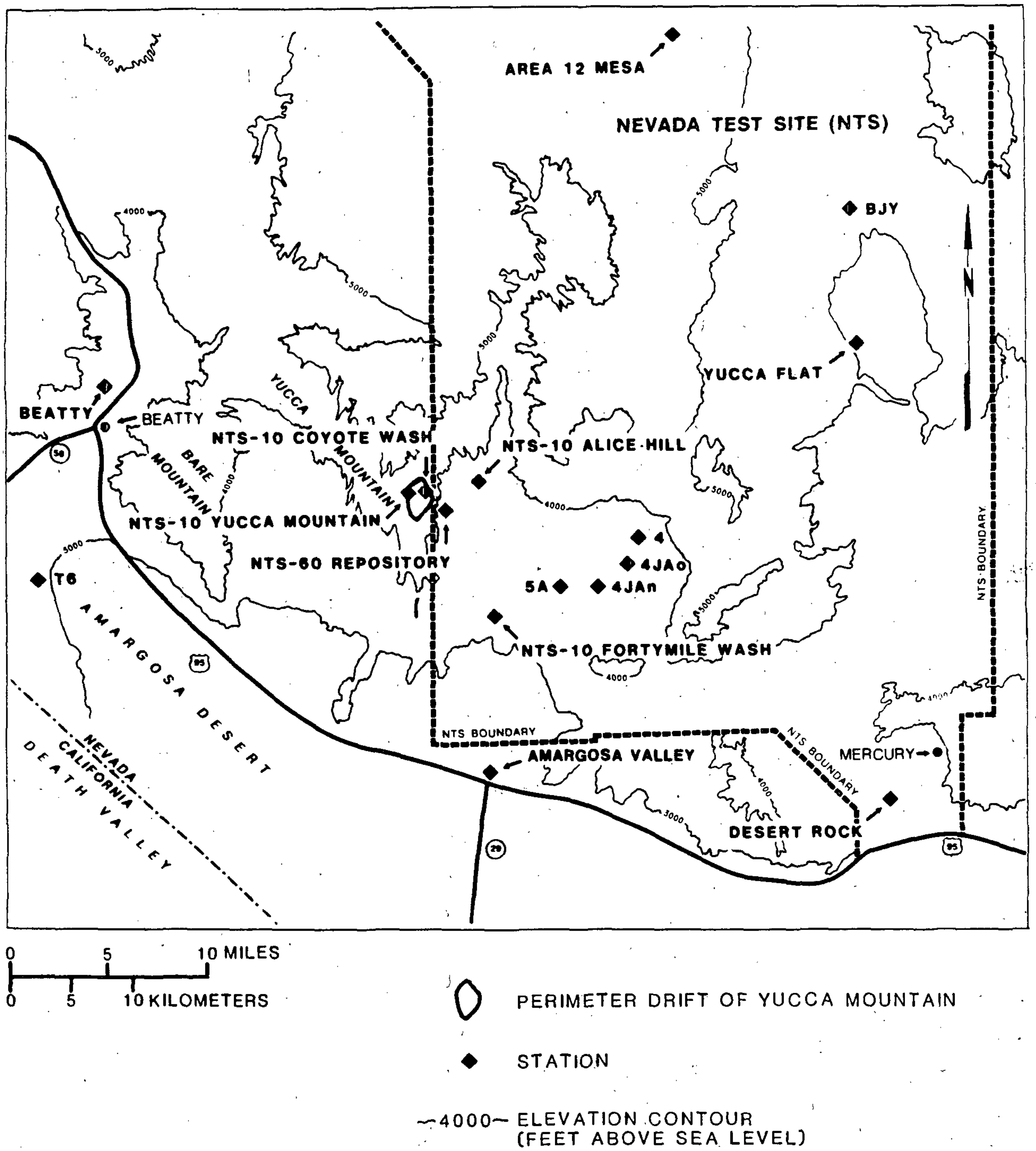

Figure 5-1. Meteorological monitoring stations in the vicinity of Yucca Mountain. Stations NTS-10 Yucca Mountain, NTS-10 Coyote Wash, NTS-10 Alice Hill, NTS-10 Fortymile Wash and NTS-60 Repository are operated as part of the Yucca Mountain Project. Stations at Yucca Flat, Beatty, Desert Rock, and Amargosa Valley are or were operated by the National Weather Service. Stations T6, Area 12 Mesa, BJY, 4, 4JAn, 4JAo, and 5A were or are operated in conjunction with various NTS activities. Stations YA (too close to NTS-60 Repository to be shown on this map) and YR (too close to NTS-10 Yucca Mountain to be shown on this map) were also operated as part of the Yucca Mountain Project.

Table 5-1. Information on meteorological monitoring stations in the vicinity of Yucca Mountain

Station and location[a]	Elevation in meters above MSL[b]	Meteorological parameters	Period of record
Yucca Flat (UCC)[c] 680,875 ft E 803,600 ft N	1,196	Temperature, relative humidity, precipitation at surface	1962-1971
		Wind speed and wind direction at surface	1961-1978
		Wind speed, wind direction, temperature, relative humidity at upper levels	1957-1964
Beatty[c] 481,250 ft E 795,830 ft N	1,006	Temperature, precipitation	1922-1960 1931-1960
BJY[d] 679,100 ft E 842,300 ft N	1,241	Precipitation, wind speed, wind direction	1960-1981 1957-1964
Desert Rock (DRA)[c] 686,719 ft E 682,790 ft N	1,005	Precipitation	1963-1981
4JAn[d] 610,605 ft E 740,840 ft N	1,043	Precipitation	1967-1981
4JAo[d] 617,000 ft E 748,000 ft N	1,100	Precipitation	1957-1967
T6[d] 458,789 ft E 745,662 ft N	992	Precipitation	1958-1964
Area 12 Mesa[d] 631,450 ft E 889,090 ft N	2,280	Wind speed, wind direction	1957-1964
4[d] 620,000 ft E 752,000 ft N	1,138	Wind speed, wind direction	1956-1962

Table 5-1. Information on meteorological monitoring stations in the vicinity of Yucca Mountain (continued)

Station and location[a]	Elevation in meters above MSL[b]	Meteorological parameters	Period of record
5A[d] 599,150 ft E 742,050 ft N	1,111	Wind speed, wind direction	1958-1966
YA (Yucca Alluvial)[e] 569,722 ft E 761,794 ft N	1,128	Precipitation	1983-1984
YR (Yucca Ridge)[e] 559,238 ft E 763,555 ft N	1,469	Precipitation	1983-1984
Amargosa Valley[c] 578,819 ft E 689,580 ft N	817	Temperature	1949-1976
NTS-60 Repository[f] 569,127 ft E 761,795 ft N	1,143	Wind speed, wind direction, standard deviation of wind direction, temperature, temperature difference, net radiation, standard deviation of vertical wind speed, precipitation, dew point	December 1985-present
NTS-10 Yucca Mountain[f] 558,862 ft E 766,434 ft N	1,463	Wind speed, wind direction, standard deviation of wind direction, temperature, relative humidity, precipitation	December 1985-present
NTS-10 Coyote Wash[f] 562,876 ft E 766,195 ft N	1,274	Wind speed, wind direction, standard deviation of wind direction, temperature, relative humidity, precipitation	December 1985-present

Table 5-1. Information on meteorological monitoring stations in the vicinity of Yucca Mountain (continued)

Station and location[a]	Elevation in meters above MSL[b]	Meteorological parameters	Period of record
NTS-10 Alice Hill[f] 576,810 ft E 769,661 ft N	1,234	Wind speed, wind direction, standard deviation of wind direction, temperature, relative humidity, precipitation	December 1985-present
NTS-10 Fortymile Wash[f] 580,882 ft E 733,230 ft N	953	Wind speed, wind direction, standard deviation of wind direction, temperature, relative humidity, precipitation	December 1985-present

[a]All coordinates are based on the Nevada Central grid.
[b]MSL = mean sea level.
[c]Site operated by the National Weather Service.
[d]Site operated in conjunction with various Nevada Test Site activities.
[e]Site previously operated as part of the Yucca Mountain Project.
[f]Site operated as part of the Yucca Mountain meteorological monitoring program.

The data set will consist of seasonal averages of air temperature, relative humidity, cloud cover, surface wind speed, and the type, amount, duration, and intensity of precipitation. Plans for collection of such data are given in Sections 8.3.1.5 and 8.3.1.12. Using these and other data sets as input, potential changes in the rate of infiltration (flux) will be estimated.

To estimate the range and recurrence intervals of future climatic variations and the impact that the variations would have in the vicinity of Yucca Mountain, the nature and potential effects of paleoclimatic variation over the Quaternary Period must be evaluated as required by 10 CFR 960.4-2-4 and 10 CFR 60.122. Because records of Quaternary climate do not exist, climatological proxy data, derived primarily from geologic investigations of past biota and lakes, must be relied upon.

The use of paleobotanic proxy data relies on the fact that climate influences the type and amount of vegetation in an area and also influences the altitudinal range of various types of vegetation. The use of paleohydrologic proxy data is based on the fact that the climate has a significant influence on surface-water systems. In principle, knowledge of past changes in plant distributions and of changes in lake levels and water chemistry will provide the basis for reconstructing the underlying causal climatic variations.

Section 5.2 discusses the availability of published proxy data and describes a general strategy for using these data in the reconstruction of past climatic variations and in the characterization of future climates. The climatic interpretation of the proxy data involves the following steps:

1. Using transfer functions or response surfaces to correlate statistically present-day meteorological data and plant distributions.

2. Obtaining dated records of paleobotanic variations through the analysis of plant macrofossils from pack rat middens and of fossil pollen from cores of lacustrine sediment.

3. Applying the transfer functions, response surfaces, or both to the paleobotanic time series to obtain estimates of past climatic variations.

4. Constructing climatic descriptions (synoptic snapshots) for critical time periods for the region over which the paleobotanic data are available.

5. Validating these climatic reconstructions with information from the paleolimnological data.

6. If possible, subjecting paleoclimatic time series to appropriate forms of spectral or statistical analyses to determine the frequencies of climatic variations.

The paleobotanical and paleolimnological data, and the associated paleoclimatic reconstructions, have three main applications:

1. Documentation. The reconstructions of past climatic variations based on the proxy data will serve to document the extent of past climatic variations in the vicinity of Yucca Mountain. These past climatic variations will illustrate the probable future climatic conditions that may occur under boundary conditions of the climate system similar to those that have occurred in the past.

2. Input to hydrologic studies. The climatic interpretations derived from proxy data will provide information such as estimates of precipitation, temperature, and seasonality for studies on the paleohydrology of the Yucca Mountain region. The relationship(s) established among past climatic variations and the resultant hydrological changes will be used in the prediction of future hydrologic variations.

3. Model validation. Mathematical models must be validated before they can be used to predict future climatic variations or scenarios. In other words, their performance in simulating the climate must be measured under conditions other than those used to formulate or calibrate the models. The paleobotanical and paleolimnological records will provide tests of simulations of past climatic variations.

The future climate model and its assumptions are discussed in Sections 5.2 and 8.3.1.5.1.

The uncertainty associated with data presented in Chapter 5 is primarily related to inherent inaccuracies in measurements and an insufficient number of samples and gaps in the paleoclimatic record. The testing, sampling, and modeling plans discussed in Sections 8.3.1.2, 8.3.1.5, and 8.3.1.12 are structured (1) to reduce these data uncertainties associated with the paleoclimatic and modern meteorological data and (2) to improve modeling of future climate. Uncertainties associated with data presented in this chapter include:

1. Modern meteorological data--the historical records cover only limited time periods and limited areal and elevational ranges.

2. Modern ecological data--the data do not sufficiently cover the necessary elevational and geographic ranges required for developing climate-proxy data calibration equations.

3. Paleoclimatic proxy data--these data are found in very restricted depositional environments and cover limited temporal and spatial ranges. In addition, limited abundance of these proxy data in the Great Basin and especially in the Yucca Mountain area results in gaps in the record, increasing the uncertainty associated with paleoclimatic reconstructions.

4. Age assignments for pack rat middens, lake cores, and pollen samples --radiometric dating techniques introduce uncertainty with increasing age, decreasing sample size, and contamination.

5. Modeling--both global climate models and regional models rely on input in the form of boundary conditions that are either estimated or else provided by other modeling activities that have their own levels of uncertainty. The models contain many assumptions and simplifications that limit their resolution.

These, and any other areas of uncertainty will be reduced through further data collection, additional dating techniques, and model sensitivity studies described in Sections 8.3.1.2, 8.3.1.5, and 8.3.1.12.

5.1 RECENT CLIMATE AND METEOROLOGY

Although a major emphasis throughout the site characterization process will be on assessing the ability of the selected host rock to contain stored wastes, the climate and site-specific meteorology of the Yucca Mountain area can influence some important aspects of repository development. The design and operation of the repository must consider climatic influences to ensure that surface facilities are capable of withstanding expected meteorological conditions (e.g., the design of the ventilation system). The potential for flooding must also be considered in the siting of surface facilities. In addition to these short-term design considerations, defining the existing climatic conditions establishes the basis for comparing the future and past climates with the present climate. Further, establishing the existing climatic conditions and the infiltration rates associated with these conditions is important in evaluating whether climatic variations will affect infiltration rates and subsequent rises or declines in the water table in the Yucca Mountain area. The sections that follow provide both a general description of the climate of the Yucca Mountain area (Section 5.1.1) and discussions of specific atmospheric parameters that are important in establishing the climatic conditions at Yucca Mountain (Sections 5.1.1.1 through 5.1.1.6).

5.1.1 CLIMATE

Long-term site-specific climatological data for Yucca Mountain are not presently available. Five monitoring stations have been established but the period of record is less than 2 yr. Therefore, data from two weather stations near Yucca Mountain that were operated by the National Weather Service (NWS) have been used to provide a general description of the climate in the area (Figure 5-1). One of these stations is located approximately 32 km northeast of the Yucca Mountain site in Yucca Flat, a broad alluvial basin. The other station is near Beatty, Nevada, approximately 24 km west of the Yucca Mountain site. Supplemental information collected at various other locations on the Nevada Test Site covering varying time periods is also available and has been used to describe the climate of the Yucca Mountain site for comparative purposes. A meteorological monitoring program, described in Sections 5.1.3 and 8.3.1.12, will provide site-specific data on the meteorological conditions that are likely to influence site characterization activities or repository development.

The Yucca Mountain site is situated in an area bordering two NWS climatological zones of Nevada: south central and extreme southern (Bowen and Egami, 1983b). The distinction between these two classifications is governed mostly by elevation. Lower elevations in the vicinity of Yucca Mountain experience conditions typical of southwestern desert zones within the United States that are characterized by hot summers, mild winters, and limited amounts of precipitation. Higher elevations have less severe summer temperatures and greater but still limited amounts of precipitation. The general climatological classification of midlatitude desert, in a modified Koeppen system presented in Critchfield (1983), also can be used to describe conditions in and around the Yucca Mountain site. Midlatitude desert areas are far removed from windward coasts and are dominated by tropical and polar air masses. For areas classified as midlatitude desert, summers are dominated by continental tropical air masses and winters are dominated by continental polar air masses. Large annual and diurnal fluctuations in temperature are characteristic of midlatitude desert areas, as is significant variability in precipitation from year to year.

The major air masses affecting the weather of the Yucca Mountain area during winter months originate either over the Pacific Ocean or over polar continental regions. Most of the moisture carried by the Pacific air masses does not reach the Yucca Mountain area because the physical (orographic) lifting effect of the Sierra Nevada forces the air masses to higher elevations as they move eastward, thus cooling the air masses and lowering their ability to hold moisture. The moisture that cannot remain in the vapor phase, due to this cooling, falls as precipitation on the western slopes of the Sierra Nevada. When an air mass has passed the ridge of the mountains, it descends along the eastern slopes and warms again, creating what is called a rain shadow in the lee of the Sierra Nevada (Wallace and Hobbs, 1977). Yucca Mountain and the surrounding areas lie within this shadow. Polar continental air masses bring cold, dry air into the area but are not as common a winter phenomenon as are the Pacific air masses.

A thermally induced area of low pressure is created during the summer months over most desert regions (Wallace and Hobbs, 1977) and prevails over the southwestern United States during summer. Although this thermal low is generally associated with weak cyclonic motion (Huschke, 1959), it brings south to southwesterly winds to the Yucca Mountain area. However, this circulation pattern is essentially nonfrontal. Although summer is generally the driest time of the year, this circulation pattern can bring tropical moisture originating over the Pacific Ocean off the lower coast of California to the area, which in combination with the strong solar insolation during the summer can create thunderstorm activity. Another less frequent summer circulation pattern that brings moisture to the area is a semipermanent subtropical high-pressure system called a Bermuda High (Huschke, 1959). If this system becomes well developed, it can bring moisture from the Gulf of Mexico to the Yucca Mountain area with southeasterly winds, again resulting in thunderstorm activity.

In addition to these synoptic-scale climatic influences, the rugged terrain of the Yucca Mountain area can create micrometeorological variations of a given parameter within relatively short distances. Drainage winds are an example of this phenomenon. These terrain-dependent winds can locally affect wind speed, wind direction, and temperature (Eglinton and Dreicer, 1984), and

are most pronounced under calm (synoptic-scale) conditions during cloudless nights (Huschke, 1959). The ground surface quickly cools under these conditions by radiating its heat into the atmosphere. Air very near the surface

Another example of micrometeorological variations induced by the terrain is the variability in precipitation amounts between stations at different elevations and between those with differing exposure to prevailing storm tracks or occurrences. This issue is dealt with in detail in Sections 8.3.1.2 and 8.3.1.12, which outline plans for a precipitation monitoring network designed to characterize the influence that storm location and precipitation amounts would have on runoff and infiltration.

Table 5-2 provides a general outline of the climatic conditions experienced at Yucca Flat during the 10-yr period from 1962 to 1971 (Bowen and Egami, 1983a). Three important parameters at the Yucca Mountain site that will probably differ from the Yucca Flat summary are temperature minimums, wind speeds, and direction. Also, precipitation amounts are expected to be greater at Yucca Mountain because of its higher elevation (1,463 m at the NTS-10 Yucca Mountain station versus 1,196 m at the Yucca Flat station). These parameters are expected to exhibit terrain influences that will be characterized through analysis of the data collected in the site meteorological monitoring program.

The link between synoptic-scale processes and their effect on site-specific meteorology is not known at this time because the data are not yet available. The multitower monitoring program implemented at Yucca Mountain (Section 8.3.1.12) is designed specifically to collect data that can be used to characterize the relationships between site conditions and regional weather systems. Plans for collecting regional data and establishing this relationship are presented in Section 8.3.1.12. In addition, the monitoring

Table 5-2. Climatological summary for Yucca Flat, Nevada, 1962 to 1971[a] (page 1 of 2)

MONTH	TEMPERATURE[b] (°F) AVERAGES			EXTREMES				DEGREE DAYS (Base 65°)		PRECIPITATION[b,c] (INCHES)							SNOW				
	DAILY MAXIMUM	DAILY MINIMUM	MONTHLY	HIGHEST	YEAR	LOWEST	YEAR	HEATING	COOLING	AVERAGE	GREATEST MONTHLY	YEAR	LEAST MONTHLY	YEAR	GREATEST DAILY	YEAR	AVERAGE	GREATEST MONTHLY	YEAR	GREATEST DAILY	YEAR
JAN	52.1	20.8	36.5	73	1971	-2	1970	877	0	.53	4.02	1969	T	1971#	1.25	1969	0.9	4.3	1962	4.3	1962
FEB	56.7	25.8	41.3	77	1963	5	1971#	662	0	.84	3.55	1969	T	1967#	1.16	1969	1.9	17.4	1969	6.2	1969
MAR	60.9	27.7	44.3	87	1966	9	1969	634	0	.29	.60	1969	.02	1966	.38	1969	2.0	7.5	1969	4.5	1969
APR	67.8	34.4	51.1	89	1962	13	1966	411	1	.45	2.57	1965	T	1962	1.08	1965	0.7	3.0	1964	3.0	1964
MAY	78.9	43.5	61.2	97	1967	25	1967	147	38	.24	1.62	1971	T	1970#	.86	1971	0	T	1964	T	1964
JUN	87.6	49.9	68.8	107	1970	29	1971#	35	154	.21	1.13	1969	T	1971	.45	1969	0	0		0	
JUL	96.1	57.0	76.6	107	1967	40	1964#	0	366	.52	1.34	1966	0	1963	.77	1969	0	0		0	
AUG	95.0	58.1	76.6	107	1970	39	1968	1	368	.34	1.04	1965	0	1962	.35	1971#	0	0		0	
SEP	86.4	46.7	66.5	105	1971	25	1971	51	103	.68	2.38	1969	0	1968#	2.13	1969	0	0		0	
OCT	76.1	36.9	56.5	94	1964+	12	1971	266	9	.13	.45	1969	0	1967#	.42	1969	0	T	1971	T	1971
NOV	61.8	27.6	44.7	82	1962	13	1966	602	0	.71	3.02	1965	0	1962	1.10	1970	0.5	4.8	1964	2.3	1964
DEC	50.7	19.9	35.3	70	1964	-14	1967	914	0	.79	2.66	1965	T	1969#	1.31	1965	2.3	9.9	1971	7.4	1971
ANN	72.5	37.4	54.9	107	AUG 1970#	-14	DEC 1967	4600	1039	5.73	4.02	JAN 1969	0	SEP 1968#	2.13	SEP 1969	8.3	17.4	FEB 1969	7.4	DEC 1971

Table 5-2. Climatological summary for Yucca Flat, Nevada, 1962 to 1971[a] (page 2 of 2)

MONTH	Relative humidity (%), hour (Pacific Standard Time) 04	RH 10	RH 16	RH 22	Wind[b,d] (speeds in mph) average speed	Peak speed	Year	Resultant (dir/sp) 23-02 PST	Resultant (dir/sp) 11-14 PST	Station pressure (inches) averages	Highest	Lowest	(e) Average sky cover sunrise to sunset	Average number of days[f]: sunrise to sunset clear	Partly cloudy	Cloudy	Precipitation .01 inch or more	.10 inch or more	.50 inch or more	1.00 inch or more	1.0 inch or more of snow	Thunderstorms	Temperature maximum 90° F or more	Maximum 32° F or less	Minimum 32° F or less	Minimum 0° F or less
JAN	67	49	35	60	6.6	58	1965	233/0.7	135/2.6	26.10	26.54	25.42	4.9	13	8	10	2	1	*	*	*	*	0	1	29	*
FEB	67	45	32	56	6.9	52	1967	275/1.1	118/2.7	26.05	26.42	25.56	5.0	11	8	9	3	2	*	*	1	0	0	*	23	0
MAR	58	31	23	44	8.4	55	1971	240/1.8	186/4.5	25.99	26.43	25.48	4.8	12	9	10	3	1	0	0	1	1	0	0	24	0
APR	52	27	21	38	9.1	60+	1970#	250/2.2	198/5.1	25.96	26.39	25.50	4.5	13	9	8	3	1	*	*	*	1	0	0	12	0
MAY	46	22	17	31	8.3	60+	1967	260/1.5	179/7.2	25.94	26.39	25.47	4.3	14	11	6	2	1	*	0	0	1	4	0	2	0
JUN	39	19	14	26	7.9	60+	1967	272/1.9	185/8.2	25.92	26.20	25.56	3.0	19	7	4	2	1	0	0	0	2	14	0	*	0
JUL	40	20	15	28	7.5	55	1971	278/0.9	185/12.0	26.00	26.19	25.68	3.0	19	9	3	3	2	*	0	0	4	29	0	0	0
AUG	44	23	16	30	6.7	60+	1968	222/1.5	182/12.0	26.00	26.22	25.71	3.0	20	8	3	3	1	0	0	0	4	27	0	0	0
SEP	43	21	17	32	7.0	52	1970	281/1.3	163/6.4	26.00	26.36	25.56	2.1	22	6	2	2	1	1	*	0	2	11	0	1	0
OCT	46	24	19	36	6.8	60	1971	286/1.3	138/3.7	26.06	26.40	25.52	2.9	20	7	4	1	1	0	0	0	*	2	0	9	0
NOV	61	39	31	52	6.1	51	1970	234/1.2	152/4.1	26.08	26.58	25.64	4.8	13	7	10	3	2	*	*	*	*	0	0	23	0
DEC	68	50	41	64	6.6	53	1970	288/1.9	109/1.0	26.07	26.59	25.49	4.6	14	8	9	3	1	1	*	1	*	0	1	29	1
ANN	53	31	23	41	7.4	60+	APR 1970#	—	—	26.01	26.59	25.42	3.9	190	97	78	30	14	3	1	3	14	87	2	152	1

[a]Source: Bowen and Egami (1983a). Blanks indicate not applicable.
[b]# = most recent of multiple occurrences.
[c]T - trace (amount too small to measure).
[d]Average and peak speeds are for the period December 1964 through May 1969. The directions of the resultant wind are from a summary covering the period December 1964 through May 1969.
[e]Sky cover is expressed in the range from 0 for no clouds to 10 when the sky is completely covered with clouds. Clear, partly cloudy, and cloudy, are defined as average daytime cloudiness of 0-3, 4-7, and 8-10, respectively.
[f]* = one or more occurrences during the period of record but average less than one-half day.

Records of meteorological parameters that together describe the climate of the region include temperature, precipitation, atmospheric moisture, surface wind speed and direction, upper air wind speed and direction, and severe weather phenomena. Each of these variables is discussed in detail in the sections that follow.

5.1.1.1 Temperature

Temperature in the site vicinity varies widely on both a diurnal and annual basis (Quiring, 1968; Eglinton and Dreicer, 1984). Temperature data from the 10-yr climatological summary for Yucca Flat and the 39-yr (1922 to 1960) period of record at Beatty are presented in Table 5-3. These data suggest that Beatty is generally warmer and experiences higher maximum temperatures and less severe minimum temperatures than Yucca Flat. Temperature at the Yucca Mountain site is expected to closely resemble the Yucca Flat data. General temperature cycles and ranges of expected temperature values for the Yucca Mountain site are discussed below.

The lowest temperatures generally occur during the months of November through March. During this period minimum temperatures of ≤32°F (0°C) occur on 85 percent of the days at Yucca Flat and 57 percent of the days at Beatty. On an annual basis, Yucca Flat experiences 152 days (42 percent) with minimum temperatures ≤32°F (0°C) and Beatty experiences 88 days (24 percent) in the same range. The lowest average monthly temperature of 35.3°F (1.8°C) at Yucca Flat occurs in December, which is also the month that has the lowest average daily minimum temperature of 19.9°F (-6.7°C) and the lowest recorded temperature (for the 10-yr summary period) of -14°F (-26°C). Although temperatures below 0°F (-18°C) do occur, they are infrequent and commonly occur on less than 1 percent of the days from November through March. For Beatty, the data suggest that January is the coldest month, averaging 40.6°F (4.8°C) with an average daily minimum of 26.7°F (-2.9°C). However, the lowest temperature recorded at Beatty of 1°F (-17°C) occurred during

Data from Amargosa Valley, Nevada (formerly Lathrop Wells), for the period 1949 to 1976 are presented in Nichols (1986) and are quite similar to data from Beatty and Yucca Flat. The Amargosa Valley monthly minimums occur in January (as at Beatty) with an average daily minimum temperature of 27°F (-3°C). As at Yucca Flat and Beatty, summer temperatures at Amargosa Valley peak in July with an average daily maximum of 99°F (37°C).

Substantial temperature differences between average daily maximum and average daily minimum are characteristic of the area due to high insolation rates and generally low relative humidities. For the data presented in Table 5-3, the Yucca Flat temperature difference between maximum and minimum values of 39.7 Fahrenheit degrees (22.1 Celsius degrees) in September is the most potential is high; a large number of variables influence thunderstorm activities and govern precipitation types, amounts, and intensity, and individual storms generally complete a thunderstorm cycle in about 2 h (Huschke, 1959).

Specific precipitation amounts for the seven stations located in the vicinity of Yucca Mountain that are considered most representative of conditions at the Nevada Test Site are presented in Table 5-4 (Eglinton and Dreicer, 1984). Monthly and annual average and maximum precipitation amounts at these stations are shown in the table. The data cover periods of record ranging from 5 yr at tower T6 to 29 yr at Beatty (see Figure 5-1 for locations).

The maximum 5-yr average precipitation amount of 6.03 in. (153 mm) occurred at tower BJY, and the minimum of these stations was 3.63 in. (92 mm) at tower 4JAo. All the stations follow the characteristic annual precipitation cycle with a winter peak, an early summer minimum, a secondary peak in late summer followed by a secondary minimum in October. This cycle is clearly illustrated in Figure 5-2, which shows precipitation amounts for each month based on the average data presented in Table 5-4. The maximum values

Table 5-4. Monthly and annual average and maximum precipitation for sites in the vicinity of Yucca Mountain[a]

	Precipitation (in.)[b,c]													
	BJY 1,241 mMSL (1960-1981)		Yucca Flat 1,196 mMSL (1962-1971)		Desert Rock 1,005 mMSL (1963-1981)		4JAn 1,043 mMSL (1967-1981)		4JAo 1,100 mMSL (1957-1967)		T6 992 mMSL (1958-1964)		Beatty 1,006 mMSL (1931-1960)	
Month	Avg.	Max.	Avg.	Max.[d]	Avg.	Max.	Avg.	Max.	Avg.	Max.	Avg.	Max.	Avg.	Max.
January	0.76	3.41	0.53	4.02	0.64	2.15	0.63	2.29	0.27	0.62	0.37	0.88	0.60	NA[e]
February	0.87	3.42	0.84	3.60	0.78	2.57	1.08	3.45	0.39	1.01	0.59	1.20	0.70	NA
March	0.73	3.58	0.29	3.50	0.70	3.08	0.83	3.00	0.16	0.35	0.16	0.30	0.48	NA
April	0.34	2.40	0.45	2.70	0.33	1.45	0.18	0.63	0.34	1.91	0.10	0.45	0.47	NA
May	0.33	2.02	0.24	1.62	0.35	1.57	0.31	1.41	0.11	0.28	0.15	0.48	0.23	NA
June	0.21	1.22	0.21	2.66	0.14	0.56	0.13	0.67	0.07	0.26	0.14	0.55	0.09	NA
July	0.48	1.54	0.52	1.87	0.34	1.46	0.35	1.50	0.19	0.48	0.50	2.29	0.20	NA
August	0.45	2.38	0.34	2.52	0.52	1.57	0.31	1.97	0.25	0.71	0.22	0.54	0.20	NA
September	0.53	1.89	0.68	2.38	0.38	2.28	0.28	2.13	0.47	1.68	0.50	1.62	0.19	NA
October	0.36	1.49	0.13	1.69	0.25	1.05	0.32	1.42	0.21	0.63	0.22	0.76	0.30	NA
November	0.50	2.37	0.71	3.02	0.50	2.07	0.33	1.22	0.54	1.67	0.61	1.49	0.43	NA
December	0.57	2.61	0.79	2.66	0.46	2.45	0.33	1.78	0.63	3.03	0.44	1.14	0.58	NA
Annual	6.03	12.13	5.73	14.05	5.39	10.08	5.08	11.62	3.63	8.06	4.00	4.61	4.47	NA

[a]Source: Eglinton and Dreicer (1984). The locations of the monitoring stations are shown on [redacted]

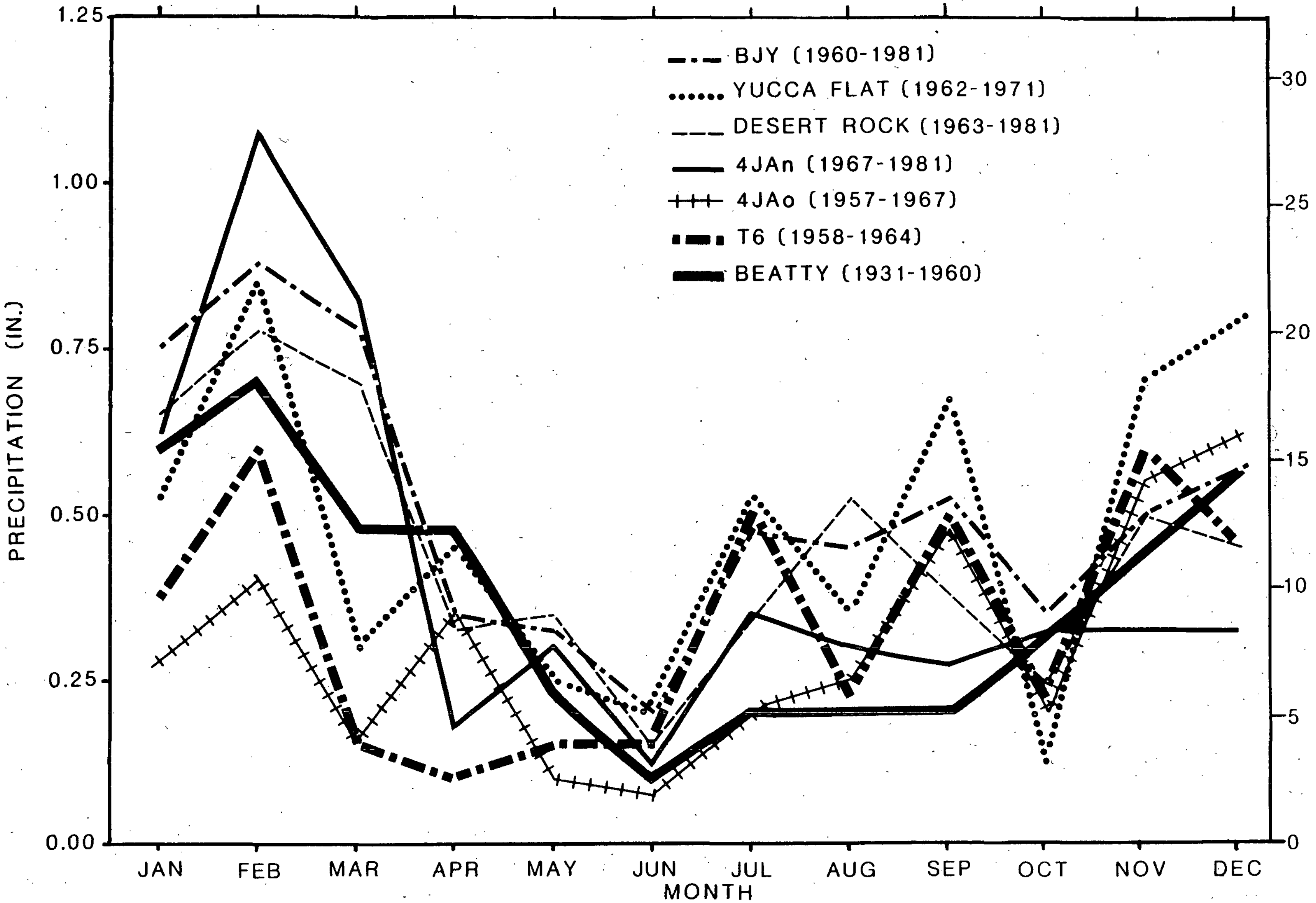

Figure 5-2. Monthly average precipitation (in inches) for stations in the vicinity of Yucca Mountain. Modified from Eglinton and Dreicer (1984).

it is impossible to establish trends or develop corollaries between the short-term data and the long-term conditions at Yucca Mountain. The data are included only as an indicator of the potential thunderstorm-related precipitation. One of the monitoring sites, called Yucca Alluvial (YA), was near the location proposed for the surface facilities, and the other site, called Yucca Ridge (YR), was slightly east of the ridge of Yucca Mountain.

The most significant storm event recorded during the 2-yr period occurred on July 21, 1984. On that date, the YA site recorded a 24-h total precipitation amount of 2.54 in. (64.5 mm), 1.75 in. (44.5 mm) of which fell in 1 h. The YR site registered a similarly significant amount of precipitation of 2.73 in. (69.3 mm) for the 24-h period and an hourly maximum of 1.37 in. (34.8 mm). With a predicted annual average of between 6.30 and 5.70 in. (160 and 145 mm), the individual storm represents a significant and high-intensity event. Several less significant events were recorded during the 2-yr period, in most instances affecting both of the monitoring sites. However, there were occurrences in which one of the sites received precipitation and the other received less, or none at all.

The Yucca Mountain area does receive precipitation in the form of snow, but such occurrences are uncommon (Nichols, 1986). Yucca Flat averages only about 2 in. (50 mm) of snow per month during the winter months. The snow

snowfall recorded at Yucca Flat is 7.4 in. (188 mm), which occurred in December 1971. Snow is not important in terms of overall precipitation amounts but should be considered in the design of the surface facilities.

Because the repository would be located in the unsaturated zone beneath Yucca Mountain, evaluation of the long-term ability of the site to contain stored waste must include a determination of how much of the precipitation falling at the surface infiltrates as potential recharge to the ground water. While thunderstorms are significant events and potentially damaging, they

DECEMBER 1988

[redacted]

DECEMBER 1988

SITE:YUCCA FLAT - SPRING
TOTAL OBS - 12345
% CALMS - 8.8

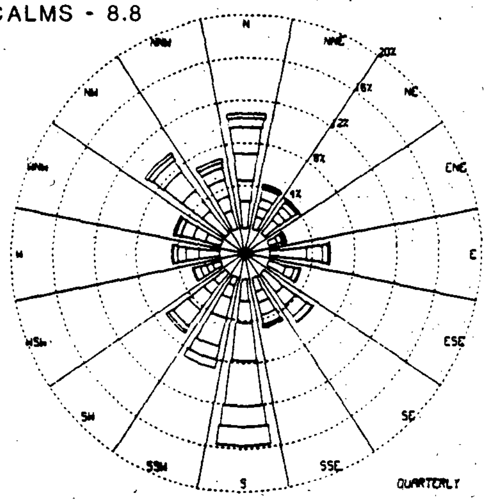

SITE:YUCCA FLAT - SUMMER
TOTAL OBS - 11659
% CALMS - 11.0

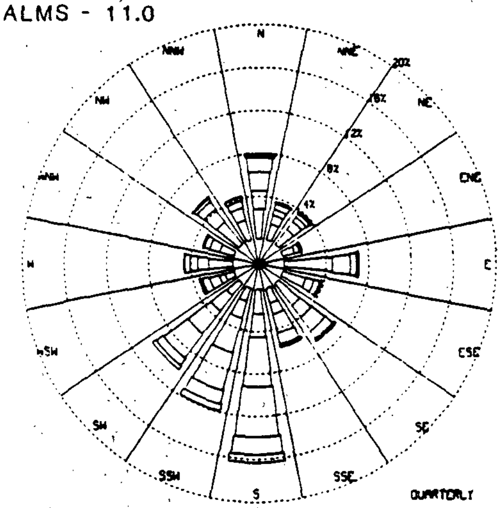

SITE:YUCCA FLAT - ANNUAL
TOTAL OBS - 47620
% CALMS - 13.1

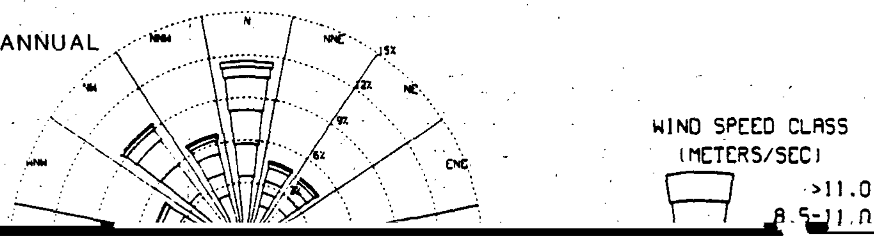

On an annual basis, winds from the south occur somewhat more frequently than winds from the north (14.0 percent from the south versus 11.6 percent from the north). Excluding these two dominant wind flow quadrants, the balance of the annual wind rose exhibits a relatively uniform distribution, somewhat skewed to the northwest and southwest due to the terrain in the vicinity of the Yucca Flat tower.

Wind speeds occurring at Yucca Flat are generally less than 12 mph (5.4 m/s) during all seasons, with generally higher wind speeds occurring in

DECEMBER 1988

SITE:YUCCA FLAT-SPRING
TOTAL OBS - 433
% CALMS - 1.4

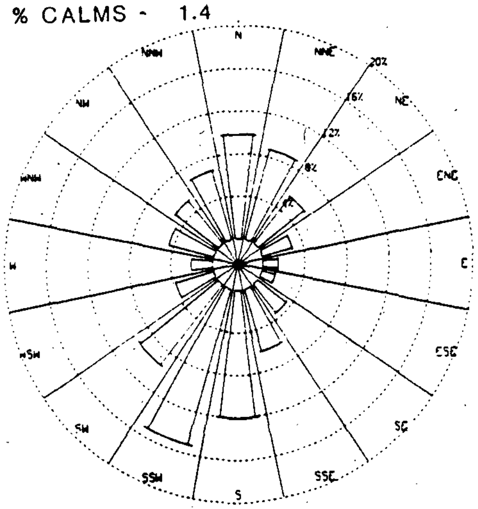

SITE:YUCCA FLAT-SUMMER
TOTAL OBS - 249
% CALMS - 1.2

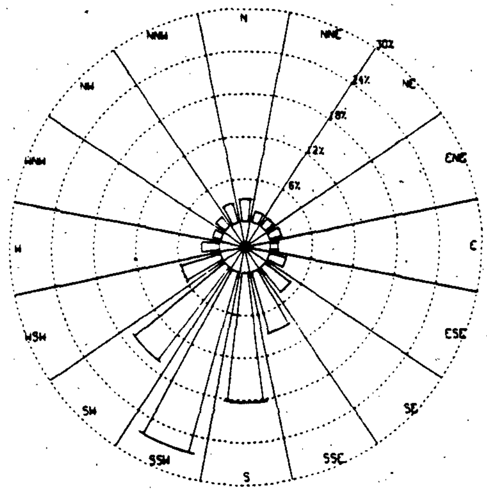

SITE:YUCCA FLAT-ANNUAL
TOTAL OBS - 1922
% CALMS - 1.5

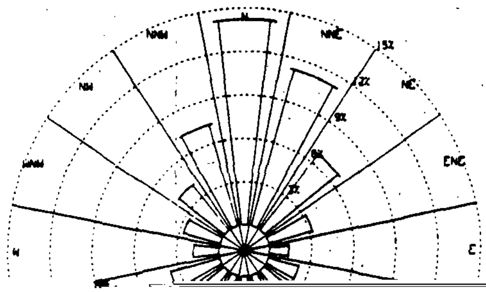

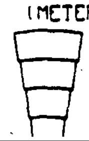

Table 5-6. Yucca Flat upper air data for 5,000 ft (1,524 m) above mean sea level (328 m above ground level)[a]

	Winter		Spring		Summer		Fall		Annual	
Direction[b]	(%)	Avg. speed (m/s)	(%)	Avg. speed (m/s)	(%)	Avg. speed (m/s)	(%)	Avg. speed (m/s)	(%)	Avg. speed (m/s)
N	21.8	5.6	9.8	5.7	3.2	5.9	13.5	6.3	14.2	5.8N
NE	14.9	5.5	8.7	5.1	1.6	4.1	13.1	5.5	11.2	5.4
NE	7.9	5.0	5.6	4.6	1.5	1.5	8.9	4.8	6.7	4.8
ENE	2.9	3.2	2.9	3.5	1.7	0.6	4.9	3.6	3.2	3.4
E	1.5	2.6	1.5	2.0	1.2	1.7	1.3	2.8	1.4	2.4
ESE	1.7	2.0	2.3	2.4	2.5	2.5	2.7	2.8	2.2	2.5
SE	1.9	4.7	3.5	3.2	4.6	3.6	3.6	3.2	3.1	3.1
SSE	3.0	3.6	6.1	5.0	9.0	4.9	5.9	4.6	5.4	4.6
S	6.4	5.0	12.0	7.5	18.3	6.5	12.6	6.4	11.1	6.4
SSW	9.0	5.8	15.1	8.4	26.5	6.9	10.9	7.2	13.2	7.2
SW	6.4	5.4	9.5	7.8	16.5	6.7	6.4	6.7	8.4	6.7
WSW	3.5	4.0	3.8	4.7	5.8	5.0	2.7	4.3	3.6	4.5
W	1.7	3.1	2.0	3.5	2.6	2.8	1.5	3.3	1.8	3.2
WNW	2.4	2.8	4.5	5.9	1.2	3.0	2.3	3.3	2.7	4.1
NW	5.1	4.5	5.3	6.2	1.7	3.3	3.1	3.6	4.1	4.7
NNW	10.6	5.2	6.7	6.2	2.8	3.8	5.9	4.9	7.3	5.3
Calm	1.4	NA[c]	1.4	NA	1.2	NA	1.9	NA	1.5	NA

[a]Calculated from Quiring (1968).
[b]Winds blow from indicated direction.
[c]NA = not applicable.

mean sea level (633 m above ground level) presented in Table 5-7 and shown in

Table 5-7. Yucca Flat upper air data for 6,000 ft (1,829 m) above mean sea level (633 m above ground level)[a]

Direction[b]	Winter (%)	Winter Avg. speed (m/s)	Spring (%)	Spring Avg. speed (m/s)	Summer (%)	Summer Avg. speed (m/s)	Fall (%)	Fall Avg. speed (m/s)	Annual (%)	Annual Avg. speed (m/s)
N	15.3	7.6	7.4	7.8	1.8	6.7	10.8	5.9	10.4	7.1
NNE	17.0	6.8	8.6	5.7	1.6	5.9	14.0	6.6	12.2	6.3
NE	10.7	6.2	6.5	4.7	1.3	4.0	10.2	6.2	8.4	5.7
ENE	4.4	4.6	4.2	3.5	1.1	1.7	5.7	4.8	4.3	4.3
E	1.4	2.2	1.4	1.7	0.6	1.0	1.5	3.5	1.3	2.5
ESE	1.3	2.8	2.1	2.7	1.7	3.4	2.3	3.1	1.8	3.0
SE	1.4	3.0	1.9	3.1	2.9	4.8	3.2	3.6	2.3	3.6
SSE	2.4	4.8	3.6	6.3	7.4	6.0	5.4	5.0	4.2	5.5
S	5.9	7.1	11.9	8.2	21.1	6.8	10.4	7.1	10.6	7.3
SSW	9.8	7.3	19.7	8.3	31.2	7.4	13.7	7.4	16.0	7.6
SW	6.8	6.6	12.4	7.7	18.8	7.1	8.4	6.9	10.1	7.1
WSW	3.6	4.6	4.2	5.1	5.5	5.0	3.0	4.7	3.8	4.8
W	2.9	4.2	1.5	5.8	2.6	4.3	2.2	3.5	2.4	4.2
WNW	3.7	4.2	4.5	6.4	1.0	3.6	2.2	5.2	3.1	5.1
NW	5.4	5.2	4.9	6.5	0.6	3.4	2.4	4.8	3.7	5.5
NNW	8.9	6.3	5.6	6.8	0.9	4.9	4.2	5.0	5.7	6.1
Calm	0.6	NA[c]	0.0	NA	0.0	NA	0.9	NA	0.5	NA

[a]Calculated from Quiring (1968).
[b]Winds blow from indicated direction.
[c]NA = not applicable.

Tornadoes, a possible source of high winds, are considered rare in Nevada but have been observed within a radius of 250 km of Yucca Mountain (Eglinton and Dreicer, 1984). The most severe of these tornadoes was classified as F-0 on the Fujita tornado intensity scale. This scale was developed to classify tornado intensity and maximum wind speed based upon the extent ofresultant damage. An F-0 tornado on this scale is classified as a very weak tornado; it has winds of between 40 and 72 mph (18 and 32 m/s), a path length of less than 1 mi (1.6 km), and a path width of less than 17 yd (16 m) (Ludlum, 1982). Dust devils, which are small whirlwinds containing sand or dust, occur in and around the Yucca Mountain site during the summer months. Dust devils occasionally develop wind velocities in excess of that associated with an F-0 tornado, but they dissipate rapidly (Eglinton and Dreicer, 1984).

Lightning is frequently associated with thunderstorm activity but, because cloud-to-cloud lightning occurs nearly 10 times as frequently as cloud-to-ground lightning, strikes of consequence (i.e., resulting in measurable damage) in Nevada only average 18 per year (Eglinton and Dreicer,

DECEMBER 1988

SITE:YUCCA FLAT-SPRING
TOTAL OBS - 433
% CALMS - 0.0

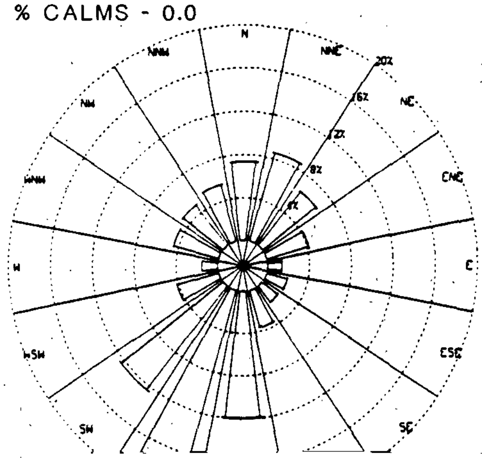

SITE:YUCCA FLAT-SUMMER
TOTAL OBS - 248
% CALMS - 0.0

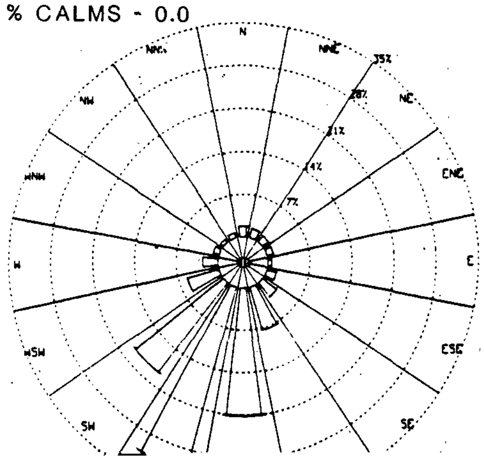

1984). However, the sparse observational network may reflect a somewhat lower frequency of occurrence than actually might be experienced at the Yucca Mountain site.

Hail is a variety of thunderstorm activity that can have quite damaging effects, but only one occurrence is expected annually at Yucca Mountain (Eglinton and Dreicer, 1984).

Obstructions to visibility in the vicinity of Yucca Mountain could temporarily disrupt activities at the proposed repository. The most likely conditions that could obstruct visibility appreciably are sandstorms or fog. The conditions conducive to fog formation occur only about twice a year in this area of Nevada and sandstorms of sufficient magnitude to reduce visibility occur only a small fraction of the time (Eglinton and Dreicer, 1984). More detailed discussions of obstructions to visibility as they relate to safe operation of the repository will be included in the environmental impact statement.

Predictions of severe weather needed in design considerations are generally derived by extrapolating past recorded data. The associated probability of occurrence of an event is then calculated based on the frequency of occurrence of the event during the period of record. Of most importance in designing the surface facilities of the proposed repository at Yucca Mountain are estimates of extreme winds, temperature maximums and minimums, and extreme precipitation events.

Extreme wind speeds and associated probabilities of occurrence have been calculated for the Nevada Test Site and are presented in Table 5-8 (Quiring, 1968). These data are for a fastest mile of wind, which represent an average highest wind velocity as 1 mi of air passes the measurement point. Eglinton and Dreicer (1984) discuss the potential for both straight-line winds and tornadic (cyclic) winds expected to occur at Yucca Mountain. The probability of a tornado strike at Yucca Mountain, given in Eglinton and Dreicer (1984), is approximately 7.5×10^{-4} in any given year. The maximum design wind speeds cited in Eglinton and Dreicer (1984) for the Nevada Test Site are a straight-line wind speed of 94 m/s (210 mph) and a tornadic (cyclic) wind speed of 28 m/s (63 mph). Both phenomena are given as having a probability of 1×10^{-6} of occurring in 1 yr. These extrapolations, however, do not take into account the possibility of climatic change in the future.

The probability of occurrence of extreme temperatures, also given in Eglinton and Dreicer (1984), is shown in Table 5-9. These data are estimated on the basis of measured extreme temperatures but do not account for the influence of climatic change.

Another design consideration is extreme precipitation and the potential for flooding that could occur as a result. Because the flooding potential from short-duration, high-intensity storms is high, 24-h average precipitation amounts (Section 5.1.1.2) are not a realistic indicator of potentially damaging extreme precipitation and subsequent flood events at Yucca Mountain. Both 1- and 24-h maximum precipitation and associated probabilities of occurrence, again based on measured extremes, are given in Table 5-10 (Hershfield,

Table 5-8. Annual extreme wind speed at 30 ft (9.1 m) above ground level and probability of occurrence for Yucca Flat, Nevada[a]

Probability of occurrence in 1 yr	Fastest mile[b] mph	Fastest mile[b] m/s
0.5	48	21
0.2	55	25
0.1	61	27
0.02	75	33
0.01	82	37

[a]Source: Quiring (1968).
[b]Fastest mile is defined as an average highest wind velocity as 1 mi of air passes the measurement point.

Table 5-9. Extreme maximum and minimum temperatures and probability of occurrence for Beatty, Nevada[a]

Probability of occurrence[b] in 1 yr	Temperature (°C) Maximum	Temperature (°C) Minimum
1.0	40.2	-6.6
0.5	42.3	-10.2
0.2	43.6	-12.3
0.1	44.4	-13.7
0.05	45.2	-15.1
0.04	45.5	-15.4
0.02	46.2	-16.8
0.01	47.1	-18.1
0.005	47.8	-19.4
0.002	48.8	-21.2
0.001	49.6	-22.4
0.0001	52.2	-26.8

[a]Source: Eglinton and Dreicer (1984).
[b]These probabilities of occurrence do not reflect potential climatic changes.

Table 5-10. Maximum 1- and 24-h precipitation and probability of occurrence for Yucca Flat[a]

Probability of occurrence in 1 yr	Maximum precipitation 1 h in.	mm	24 h in.	mm
1.0	0.30	7.6	0.75	19.1
0.5	0.40	10.2	1.00	25.4
0.2	0.60	15.2	1.25	31.8
0.1	0.70	17.8	1.50	38.1
0.04	0.80	20.3	1.75	44.5
0.02	0.90	22.9	2.00	50.8
0.01	1.00	25.4	2.25	57.2

[a]Source: Hershfield (1961).

Although this sort of extrapolation of extreme events is useful, more detailed and site-specific data on precipitation are needed. The plan for collecting such data is given in Section 8.3.1.12.

5.1.2 LOCAL AND REGIONAL METEOROLOGY

The meteorological monitoring program (Section 5.1.3) will provide data to be used in characterizing atmospheric dispersion processes. Aside from establishing the link between site meteorology and general (long-term) climatic conditions at the site, the data will be used in satisfying permit requirements and as input to the environmental impact statement. In general, meteorological conditions experienced at the site are expected to be quite similar to those of the stations used in describing the climate. Winds will be governed to a significant extent by the terrain with regard to direction slightly unstable, class D is neutral, class E is slightly stable, and class F is stable. Wind roses for each of these stability classes are shown in Figures 5-6 (A through C) and 5-7 (D through F). The most significant features of the stability distributions are summarized in Table 5-11 and

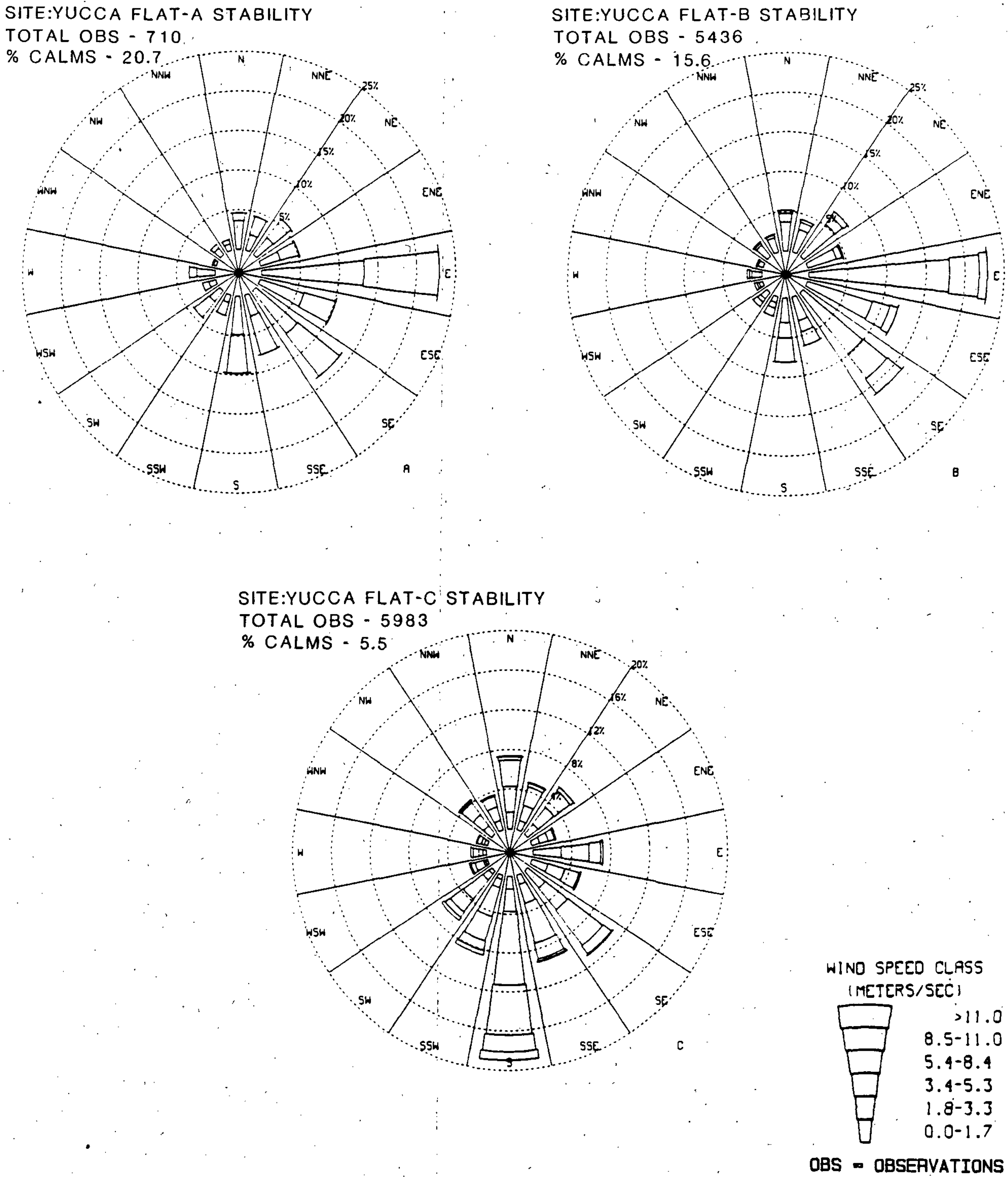

Figure 5-6. Distributions for Pasquill stability classes A, B, and C for Yucca Flat (1961 to 1978). A = extremely unstable, B = unstable, and C = slightly unstable. Note: Scale is not the same for all distribution. Based on data from DOC (1986).

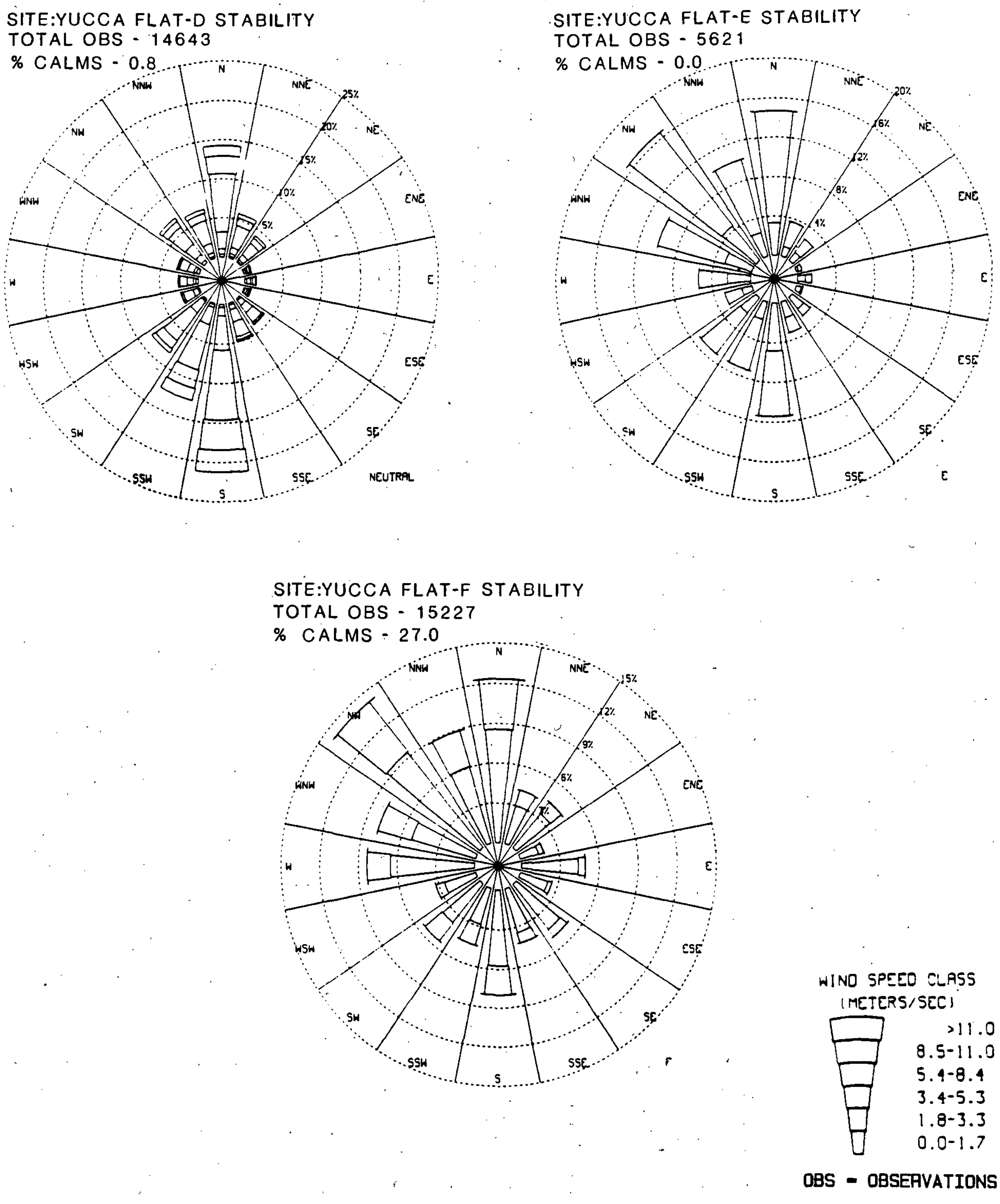

Figure 5-7. Distributions for Pasquill stability classes D, E, and F for Yucca Flat (1961 to 1978). D = neutral, E = slightly stable, and F = stable.

Table 5-11. Yucca Flat Pasquill stability class distributions for the period 1961 to 1978[a]

Stability class[b]	Percentage of total observations	Predominant direction[c]	Percentage of stability class observations	Predominant quadrant[c]	Percentage of stability class observations
A	1.5	E	22.9	E-S	64.5
B	11.4	E	22.9	E-SE	51.0
C	12.6	S	19.0	SE-SSW	47.8
D	30.7	S	21.2	S-SW, N	42.0, 14.2
E	11.8	NW	16.6	WNW-N, S-SW	51.4, 25.8
F	32.0	NW	14.2	W-N	51.7

[a]Source: DOC (1986).
[b]A = extremely unstable, B = unstable, C = slightly unstable, D= neutral, E = slightly stable, F = stable.
[c]Wind blows from indicated direction.

5.1.3 SITE METEOROLOGICAL MEASUREMENT PROGRAM

A monitoring program was operated at Yucca Mountain for approximately 2 yr. It consisted of two 10-m towers instrumented to collect data on temperature, wind speed and direction (3-m and 10-m levels), relative humidity, insolation, ground surface infrared radiation, soil temperature, precipitation, and barometric pressure. The towers were installed to collect preliminary meteorological data and were decommissioned at the end of October 1984. However, most of the data from this program are still being reduced and are not available.

A new, extended monitoring program has been designed to collect data on both synoptic-scale meteorological influences and specific terrain-induced perturbations. The program includes four 10-m towers designated NTS-10 plus an area designation (Yucca Mountain, Coyote Wash, Alice Hill, and Fortymile Wash) and one 60-m tower designated NTS-60 Repository. The locations of the recommended or required to be monitored for regulatory compliance (EPA, 1980). In addition, the hourly average wind speed, wind direction, and temperature data are required as input to dispersion models that will be used in assessing the ambient air quality impacts of the proposed activities. The sigma-theta, vertical wind speed, temperature difference, and net radiation data can all be used to determine atmospheric stability, which is a very important factor in determining ambient impacts through dispersion modeling. The relative humidity and dew point will be used for climatological comparisons, as will the precipitation data. The precipitation data will also be used as input to other studies that will be conducted during site characterization. The other programs are the infiltration studies and the surface water hydrology investigations.

site characterization activities and repository development. A plan for environmental monitoring and mitigation will contain information on those aspects of site characterization that may require air quality data, and the environmental impact statement process will define air monitoring needs with respect to repository development.

5.2 LONG-TERM CLIMATIC ASSESSMENT

An assessment of the long-term climate in the Yucca Mountain area is necessary to resolve several issues. The nature and rates of change in past climates must be understood to allow the prediction of future climate conditions. An understanding of future climate conditions is needed to evaluate the potential effects of climatic change on the location and rates of erosion and on the hydrologic and geochemical characteristics in the vicinity of the Yucca Mountain site. The hydrologic system may be especially susceptible to changes in climate. This section discusses the present understanding of the nature and rates of past climate change and discusses the strategy for developing scenarios for future climatic variations. These scenarios can be used to evaluate anticipated and unanticipated future climate conditions that can be used to assess the potential changes in the hydrologic characteristics in the vicinity of Yucca Mountain (Section 8.3.1.5.2). These estimates of future climate conditions will also be used to determine potential changes in the location and rates of erosion (Section 8.3.1.6.2) at Yucca Mountain.

Paleoclimatic reconstructions discussed in this section focus on the latter part of the Quaternary Period. Figure 5-8 shows the relationship of the geologic time periods discussed in this chapter. The Quaternary Period includes the last 1.6 million years and is subdivided into the Pleistocene Epoch (from 1.6 million to 10,000 yr ago) and the Holocene Epoch (from 10,000 yr ago to the present). Further subdivisions of the Pleistocene Epoch are based on periodic glacial advances and recessions. The most recent of these glacial advances, known in North America as the Wisconsin Stage, is important in the reconstruction of the paleoclimatic history of the Yucca Mountain site because the conditions that accompanied this glacial regime may represent the factors that will affect future hydrologic conditions at the Nevada Test Site, should the Holocene close with a return to a global glacial period. Paleoclimatic investigations must extend back at least to the previous interglacial period (known in North America as the Sangamon) in order to provide a climatic analog for possible future climate states that are warmer than those of today, which could occur in a carbon-dioxide-enhanced world.

Because it is the most recent glacial and pluvial event in the earth's history, the Wisconsin has been intensively studied and is the best understood of the glacial and interglacial stages that make up the Pleistocene. The beginning of the Wisconsin is correlated by Ruddiman and McIntyre (1981) with the 5d-5e boundary of the deep-sea oxygen isotope record, which occurred about 115,000 yr ago. During the late Wisconsin (23,000 to 10,000 yr ago) more than 100 closed basins in the northern and western Great Basin contained lakes (Smith and Street-Perrott, 1983), while in the southern Great Basin, at

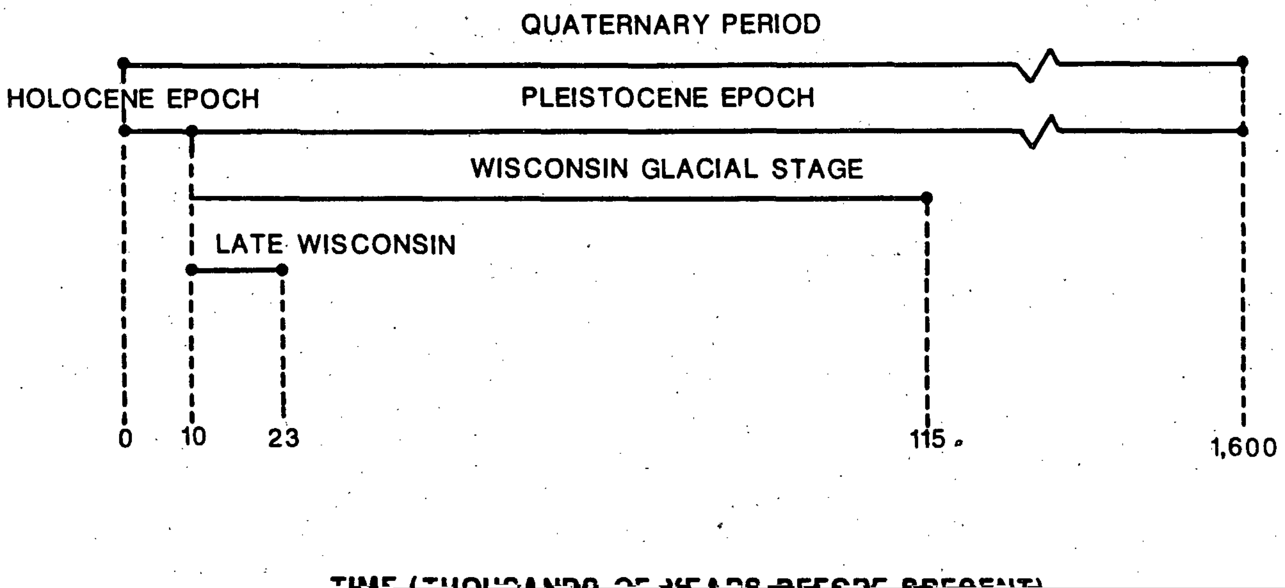
QUATERNARY PERIOD
HOLOCENE EPOCH
PLEISTOCENE EPOCH
WISCONSIN GLACIAL STAGE
LATE WISCONSIN
0
10
23
115
1,600
TIME (THOUSANDS OF YEARS BEFORE PRESENT)

Yucca Mountain, a marked increase in the area of woodland species of vegetation suggests more available moisture and a general decline in temperature (Spaulding and Graumlich, 1986).

In the following sections, climate variation during the Quaternary Period will be discussed. Because past climatic variability is probably the best indicator of future climatic conditions, understanding this climatic variability is important in assessing future climatic variation. Ensuing sections are structured in terms of three principal topics: paleoclimatology (Section 5.2.1), future climate variation (Section 5.2.2), and paleoclimatic variations and their relation to the Yucca Mountain site (Section 5.2.3).

5.2.1 PALEOCLIMATOLOGY

5.2.1.1 Quaternary global paleoclimate

Climate varies on all temporal and spatial scales, ranging from interannual variations at a particular location related to atmospheric circulation anomalies, to the very long period variations at the global scale related to the evolution of the atmosphere and lithosphere (Webb et al., 1985). An understanding of climate variation on the global scale is necessary for the prediction of local climate. This is because climate at any point on the earth's surface is the result of processes that occur over the entire global area.

In assessing the environmental stability of a particular location, the key climatic variations are those that occur on the time scale of centuries to 100,000 yr (Crowley, 1983). During the Quaternary, the principal climatic variations at such time scales have been those associated with the repeated fluctuations between glacial and interglacial conditions.

The glacial cycles of the Quaternary are part of a long period of cooling, commencing in Late Cretaceous time (Lloyd, 1984). During the past 80 million years, global average temperature declined, and first Antarctica and later Greenland, North America, and Europe became glaciated. Glaciation of the northern hemisphere probably began about 3.2 million years ago (Crowley, 1983), with clear evidence about 2.5 million years ago for glaciation on land areas contributing sediments to the North Atlantic (Shackleton et al., 1984).

The global volume of glacial ice has varied continuously throughout the Quaternary, but with characteristic quasi-periodicity correlated with variations of the earth's orbital elements, (i.e., eccentricity (about 100,000 yr), obliquity (about 40,000 yr), and precession (about 20,000 yr) (Hays conditions that might occur in an interglacial to glacial transition (Spaulding, 1983).

At 18,000 yr before present, global average temperatures were lower than at present, and large ice sheets covered parts of North America and Europe (Denton and Hughes, 1981). Consequently, sea levels were lower, exposing much of the continental shelves (Bloom, 1983). Sea surface temperatures as a whole were lower, and extensive sea ice formed in the northern oceans (CLIMAP Project Members, 1981). Eighteen thousand years ago vegetation and the hydrologic cycle differed markedly from those of today (Street-Perrott and Harrison, 1984). The Laurentide ice sheet in eastern North America reached its maximum extent about this time, while the Cordilleran ice sheet in the Northwest approached its maximum by 15,000 yr B.P. (Mayewski et al., 1981; Waitt and Thorson, 1983).

In the North Pacific Ocean adjacent to western North America about 18,000 yr ago, sea-surface temperatures were more than 4 Celsius degrees lower than today over large areas, and oceanic circulation was altered as well (Imbrie et al., 1983). During the last glacial maximum, the average temperature of the atmosphere was a little less than 10 Celsius degrees lower than present temperatures, based on the numerical modeling of Von Neuman (1960). In southern Nevada, average annual temperatures were 6 to 7 Celsius degrees lower than the current average annual temperature (Spaulding, 1985). Experiments with climate simulation models (Section 5.2.2.2) suggest that 18,000 yr ago the expanded ice sheets, extensive sea ice, and colder oceans greatly influenced atmospheric circulation around North America (Gates, 1976b; Kutzbach, 1985; Kutzbach and Wright, 1985; Manabe and Broccoli, 1985). For example, to simulate the climate of 18,000 yr ago, Manabe and Broccoli (1985) used a Geophysical Fluid Dynamics Laboratory general circulation model coupled with a static mixed-layer ocean model (in which the sea surface temperatures were predicted by the model), and Kutzbach and Wright (1985) used the National Center for Atmospheric Research Community Climate Model (NCAR CCM) (in which sea surface temperatures were prescribed using the reconstructions by CLIMAP Project Members, 1981). Both models simulated similar changes in the atmospheric circulation across North America (relative to today) resulting from the imposition in the models of the Laurentide ice sheet, including (1) a split in the jet stream in the upper atmospheric flow, with one weaker branch crossing the continent to the north of the ice sheet, and a second stronger branch crossing the continent from southwest to north-east to the south of the ice (Kutzbach and Wright, 1985); (2) the development of a strong ridge over western North America and a deep trough over eastern North America in the upper atmospheric circulation; and (3) the development of strong anticyclonic circulation at the surface over northern North America. Kutzbach and Wright (1985) describe the general compatibility between the climate simulated by the NCAR CCM and the geologic evidence for 18,000 yr ago in North America. Vegetation patterns in North America at 18,000 yr B.P. differed considerably from those at present, reflecting the great differences between modern and full-glacial regional climates (Spaulding et al., 1983; Kutzbach and Wright, 1985; VanDevender et al., 1987; SCP Section 5.2.1.2.3). Large-scale changes in regional hydrology also

Between 18,000 and 6,000 yr ago, the global ice volume decreased to approximately its present amount, the sea level rose, and the oceans warmed (Kutzbach and Guetter, 1986). Over the same interval the seasonal cycle of solar radiation was amplified (relative to both 18,000 yr ago and today) by the shift in perihelion from January to July, and by changes in the tilt of the axis (Kutzbach, 1981). At 10,000 yr ago, for example, global solar radiation at the top of the atmosphere was about 8 percent greater in summer than today and about 8 percent less in winter (Kutzbach, 1985). Accompanying these changes was an increase in the concentration of carbon dioxide in the atmosphere (Shackleton et al., 1983) in a manner consistent with the changes in global climate during this interval. The amplification of the seasonal cycle of solar radiation has been linked with the intensification of the summer monsoonal circulation of Africa and southern Asia about 9,000 yr B.P. Greater monsoonal precipitation at that time is evidenced by the geologic record of lake-level variations in the tropics (Kutzbach and Street-Perrott, 1985). Similar increases in monsoonal rainfall have been postulated for the Yucca Mountain region (Spaulding and Graumlich, 1986), and this possibility will be examined during site characterization.

Astronomical forcing of climate provides a quasi-periodic physical mechanism for the simulation of past and future climate change. The potential causes of the climatic variations of the Quaternary will be discussed in Section 5.2.2.1 as they pertain to the prediction of future climatic variations. In the following sections, the regional expression of the large-scale climatic variations described above will be reviewed.

5.2.1.2 Quaternary regional paleoclimate

Global paleoclimatology contributes to an understanding of regional and site-scale climatic conditions principally by defining the broad chronology

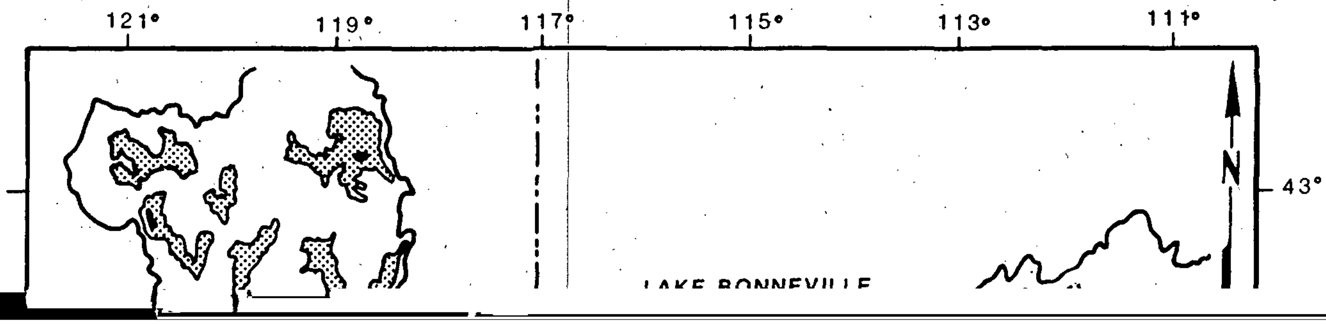
121°
119°
117°
115°
113°
111°
43°
N

3. Provide data for the creation of synoptic snapshots of climate extremes.

These synoptic snapshots of climate and surface hydrology will serve as test scenarios for modeling future climate (Section 8.3.1.5.1).

Hydrologic balance of lake systems

Lake size is a function of a dynamic balance resulting from changes in the magnitudes of water sources and sinks. The principal water sources for a lake are (1) streamflow into the lake, whether as direct runoff from the watershed or as emergence of ground water to stream channels; (2) precipitation on the lake surface; and (3) ground-water discharge directly to the lake. The principal processes by which water leaves a lake are (1) evaporation from the lake surface, (2) streamflow from the lake, and (3) ground-water outflow from the lake.

The paleolakes that persisted as relatively permanent bodies of water, and therefore provide the best preserved and most continuous record, are those that were contained in large drainage basins. Under these conditions ground-water inflow to the basin and ground-water outflow from the lake can be ignored without a significant loss of precision in water-budget calculations. Further, most but not all of the paleolakes of interest in the region occupied closed topographic basins, eliminating streamflow from the lake as a factor and leaving evaporation from the lake surface as the only process by which water leaves the lake.

For a lake and its surrounding large closed drainage area, the mean-annual hydrologic balance for the steady state can be written in terms of total discharge to the lake and evaporation from the lake surface:

$$(E_L)(A_L) = (P_L)(A_L) + D_s + D_g \qquad (5\text{-}1)$$

where

E_L = evaporation rate from lake

A_L = area of lake surface

P_L = precipitation on lake

D_s = stream discharge into the lake

D_g = direct discharge of ground water to lake.

A knowledge of man's impact on the hydrologic balance is necessary for the correction of historical records of streamflow and lake levels (Whitaker, 1971; Stauffer, 1985). Figure 5-10 shows the historical and pristine (corrected) records of fluctuations in the water level of the Great Salt Lake for the period from 1851 to 1984. These corrected records can be subjected

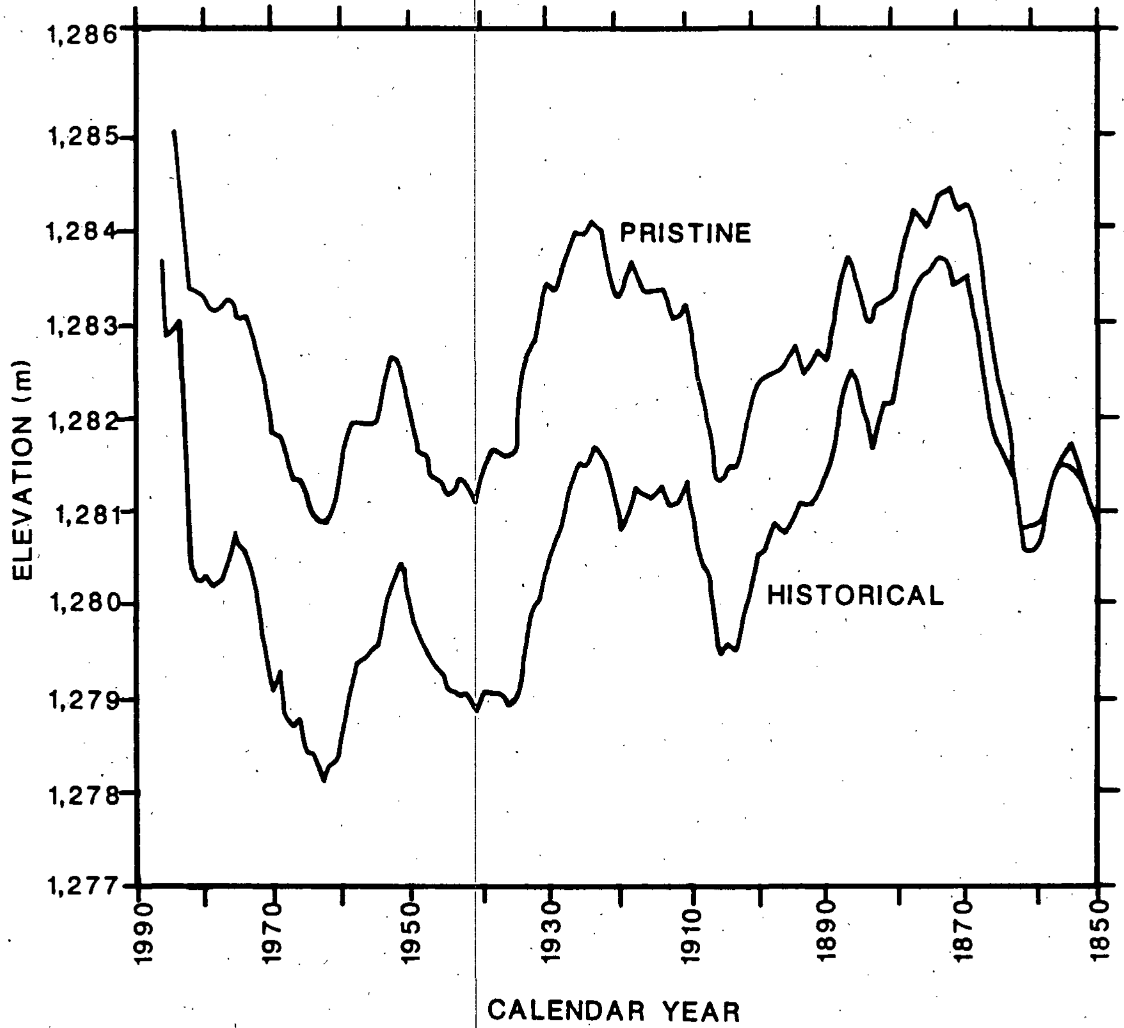

Figure 5-10. Historical and pristine (corrected) records of fluctuations in the level of Great Salt Lake, Utah. Modified from Stauffer (1985).

to spectral analysis to determine the characteristic temporal scales of variation in the hydroclimatological data during the monitored period.

Precipitation and streamflow data

Precipitation data exist for weather stations scattered throughout the western United States (Hershfield, 1961). The data have record lengths of up to 100 yr. Some weather stations located in California and Nevada will be used to provide vegetation-climate calibrations (response surfaces) for

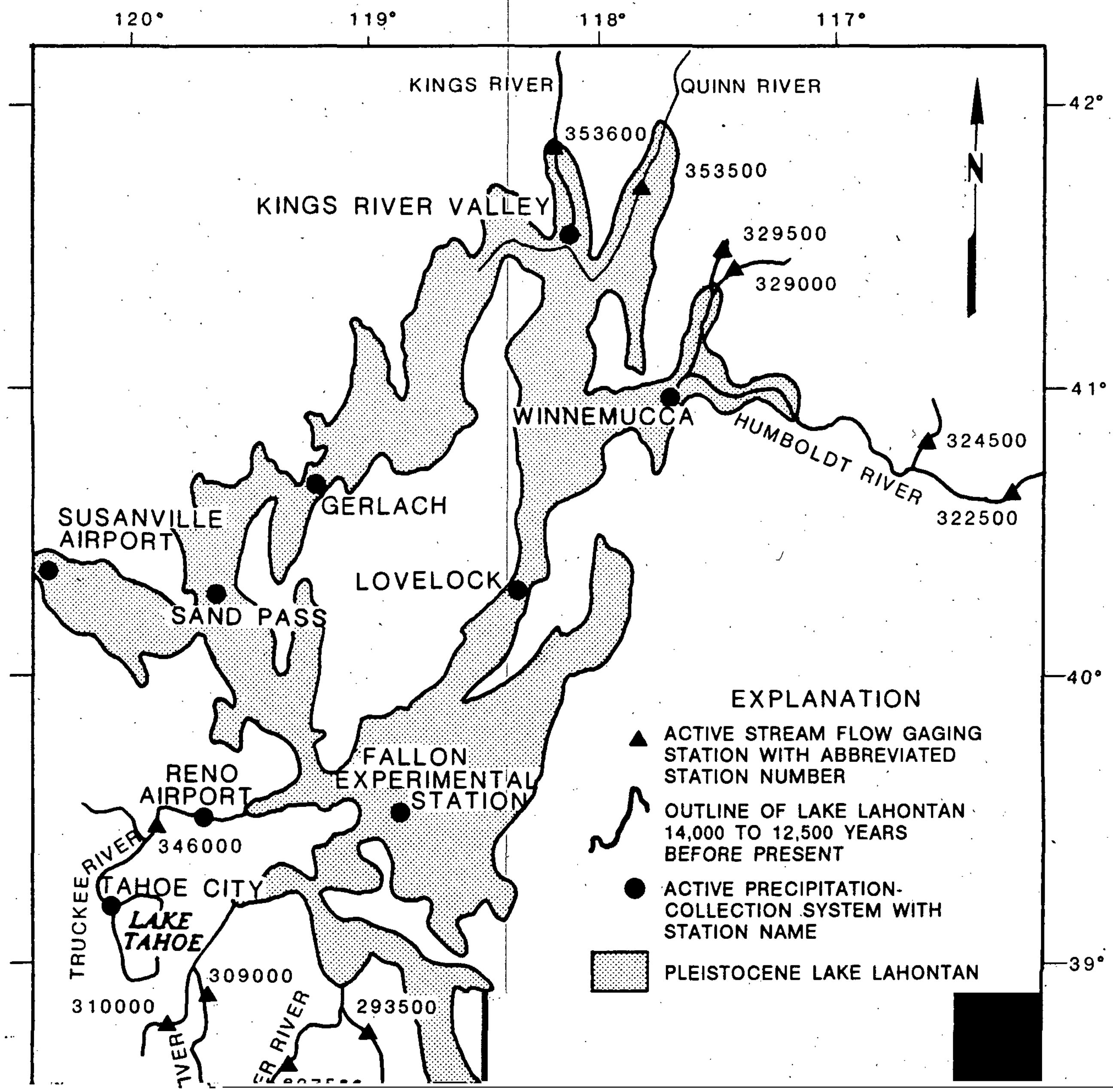
120°
119°
118°
117°
42°
41°
40°
39°
KINGS RIVER
QUINN RIVER
N
353600
353500
KINGS RIVER VALLEY
329500
329000
WINNEMUCCA
HUMBOLDT RIVER
324500
322500
GERLACH
SUSANVILLE AIRPORT
SAND PASS
LOVELOCK
EXPLANATION
ACTIVE STREAM FLOW GAGING STATION WITH ABBREVIATED STATION NUMBER
OUTLINE OF LAKE LAHONTAN 14,000 TO 12,500 YEARS BEFORE PRESENT
ACTIVE PRECIPITATION-COLLECTION SYSTEM WITH STATION NAME
PLEISTOCENE LAKE LAHONTAN
FALLON EXPERIMENTAL STATION
RENO AIRPORT
346000
TRUCKEE RIVER
TAHOE CITY
LAKE TAHOE
309000
310000
293500

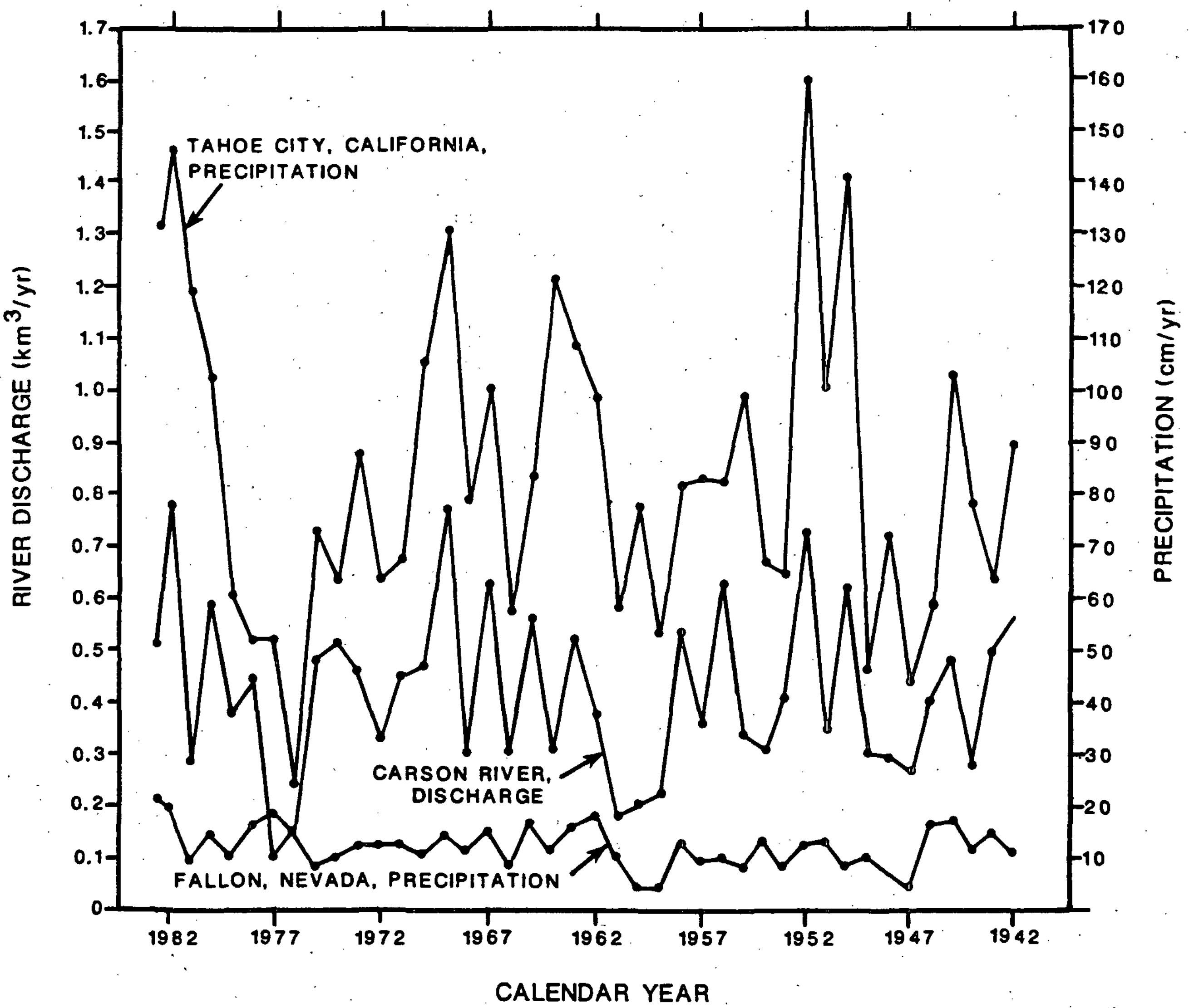
TAHOE CITY, CALIFORNIA, PRECIPITATION
CARSON RIVER, DISCHARGE
FALLON, NEVADA, PRECIPITATION
RIVER DISCHARGE (km³/yr)
PRECIPITATION (cm/yr)
CALENDAR YEAR
1982
1977
1972
1967
1962
1957
1952
1947
1942

Many semiarid areas now produce up to 10 percent runoff and the most arid areas produce less than 5 percent. When viewing either the past or future, however, it is difficult to estimate how much additional precipitation, lowering of temperature, etc., could increase runoff in terms of either percentage or absolute volume. Langbein et al. (1949) constructed an empirical diagram that allows one to estimate runoff variation in nonarid regions caused solely by temperature or precipitation change. The arid end of this diagram suggests that in an area now averaging 5 percent runoff, an 18 Fahrenheit degree (10 Celsius degrees) drop in temperature (weighted according to precipitation) would increase annual runoff by factors ranging from about 3 to 6; in the same area, a 50 percent increase in precipitation could increase runoff by a factor of about 5. Langbein et al. (1949) also notes that drainage areas having similar altitudes and precipitation, but different rock types, exposures, and vegetation, can have runoff percentages that differ by 15 percent or more. Schumm (1965) extends these relations to include areas characterized by 400 mm (15.74 in.) or less precipitation, showing that increasing precipitation by 50 percent or more and decreasing temperatures by about 5 Celsius degrees could increase runoff by factors ranging from about 5 to 20. The total sediment outflow from a watershed is a function of soil resistance, basin topography, and plant cover. The outflow reaches a peak at an effective precipitation of about 300 mm (11.8 in.), trailing off at lower values due to increased vegetation cover that protects against erosion (Knighton, 1984). Further discussion of erosion at Yucca Mountain can be found in Chapter 1 and Section 8.3.1.6.

The study of Meko and Stockton (1984) demonstrates that long-term streamflow records corrected for diversion and consumption can be used to reconstruct synoptic climates for the western United States. The results of also a function of the temperature and the chemical composition of lake water. In some instances, therefore, lake size can be inferred within broad

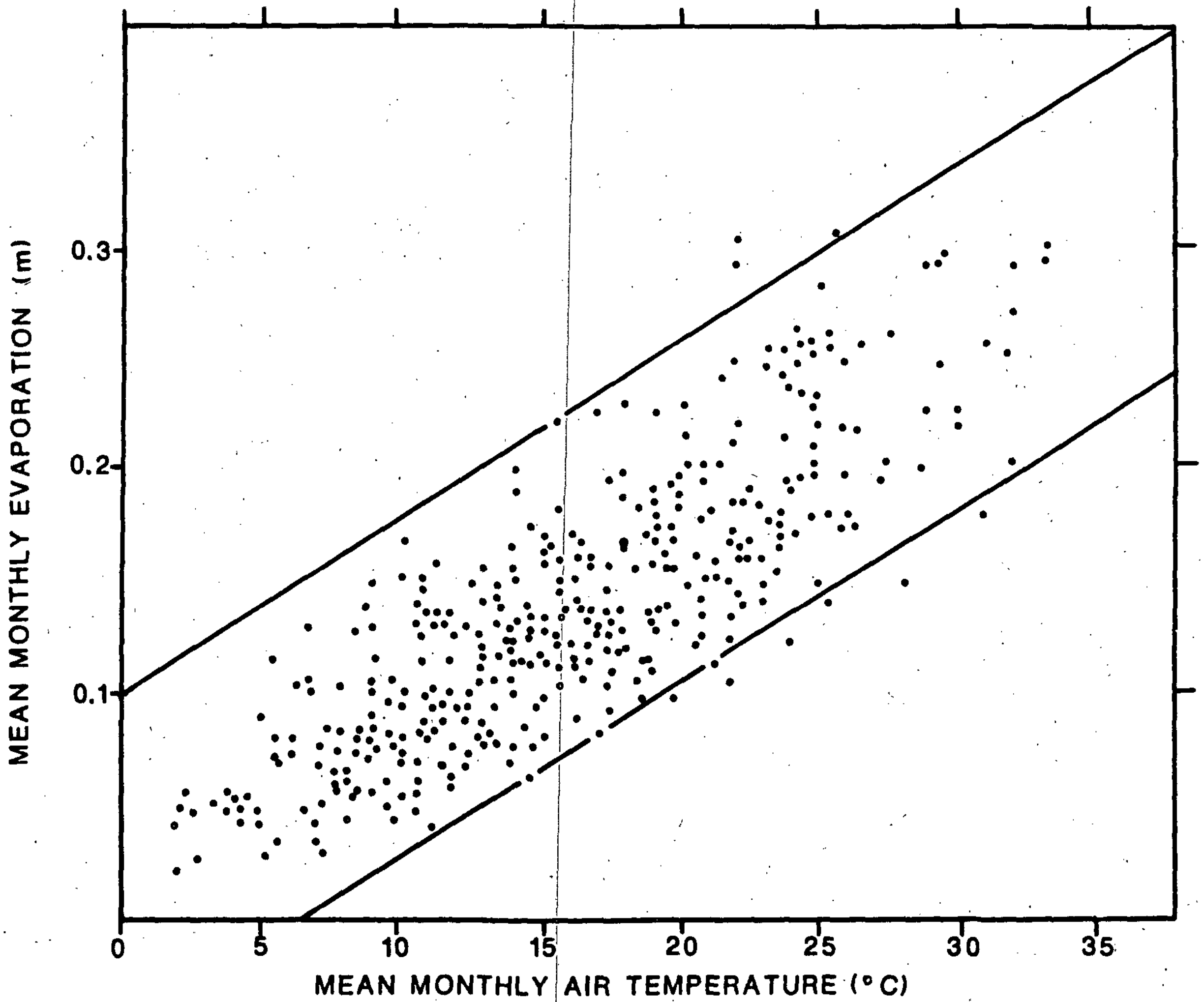

Figure 5-13. Relation of mean monthly evaporation and temperature in the western United States. Modified from Galloway (1970).

temperature, humidity, amount and nature of cloud cover, and amount of heat stored in lakes on evaporation rates. Investigations are also evaluating various other methods (covariance, aerodynamic, Dalton, energy-balance, and combination approaches) for calculating evaporation rates. For calculating the sensitivity of evaporation rate to variation in one or more commonly measured climate parameters, the energy-balance method appears the most promising. Each of the heat terms contained within the energy-balance equation has a theoretical or empirical relation to one or more commonly measured climate parameters. The method is theoretically sound, and when applied to computational periods greater than 1 week, satisfactorily estimates evaporation rates that are nearly the same as those obtained from water budget calculations (USGS, 1954). Historically, the energy-balance method has been the standard to which other evaporation computation methods have been compared. Wind speed does not appear explicitly in equations used in the energy-balance method.

Morton (1986) uses a method of computing evaporation that adjusts the humidity of air passing over a lake for the change that occurs as a result of evaporation from the lake surface. Lake size thus becomes a factor. Using the parameters noted above, plus altitude, depth, salinity, and available evaporation data, Morton (1986) calculates evaporation according to three models and compares them with water budget estimates. He lists monthly evaporation estimates for Winnemucca, Pyramid, and Walker lakes in the Lahontan Basin and for Utah and Great Salt lakes in the Bonneville Basin. Averages of the calculated annual rates using the two methods that include data on lake size differ at most by 7 percent from water-budget estimates; calculations using pan evaporation data without lake-size corrections produce estimates that are 51 to 67 percent greater than water-budget estimates. Therefore, pan evaporation data should be reduced by about 34 to 40 percent in estimating the evaporation from natural lake surfaces.

Using the Pyramid Lake, Nevada, area as a reference lake-climate system, the sensitivity of evaporation rate to change in each of six climate parameters will be investigated: (1) amount of sky cover, (2) type of sky cover, (3) air temperature, (4) water temperature, (5) dew point temperature (humidity), and (6) insolation at the top of the atmosphere.

Using established, empirical relations for components of the energy balance, the response of the calculated evaporation rate to change in the measurable climate parameters allows the following preliminary conclusions (Benson, 1986):

1. Evaporation rate strongly depends on the difference between air temperature and water temperature.

2. The use of insolation values for 12,000 and 18,000 yr ago results in small increases in the calculated rate of evaporation.

3. Relatively large absolute changes in relative humidity result in rather small changes in the calculated rate of evaporation.

4. Change in the fractional distribution and absolute amount of sky cover can bring about a significant reduction in the calculated evaporation rate.

These studies also tentatively demonstrate the fundamental role that reduced evaporation may have played in the creation and maintenance of high-stand closed-basin lakes such as Lake Lahontan. Using precipitation and

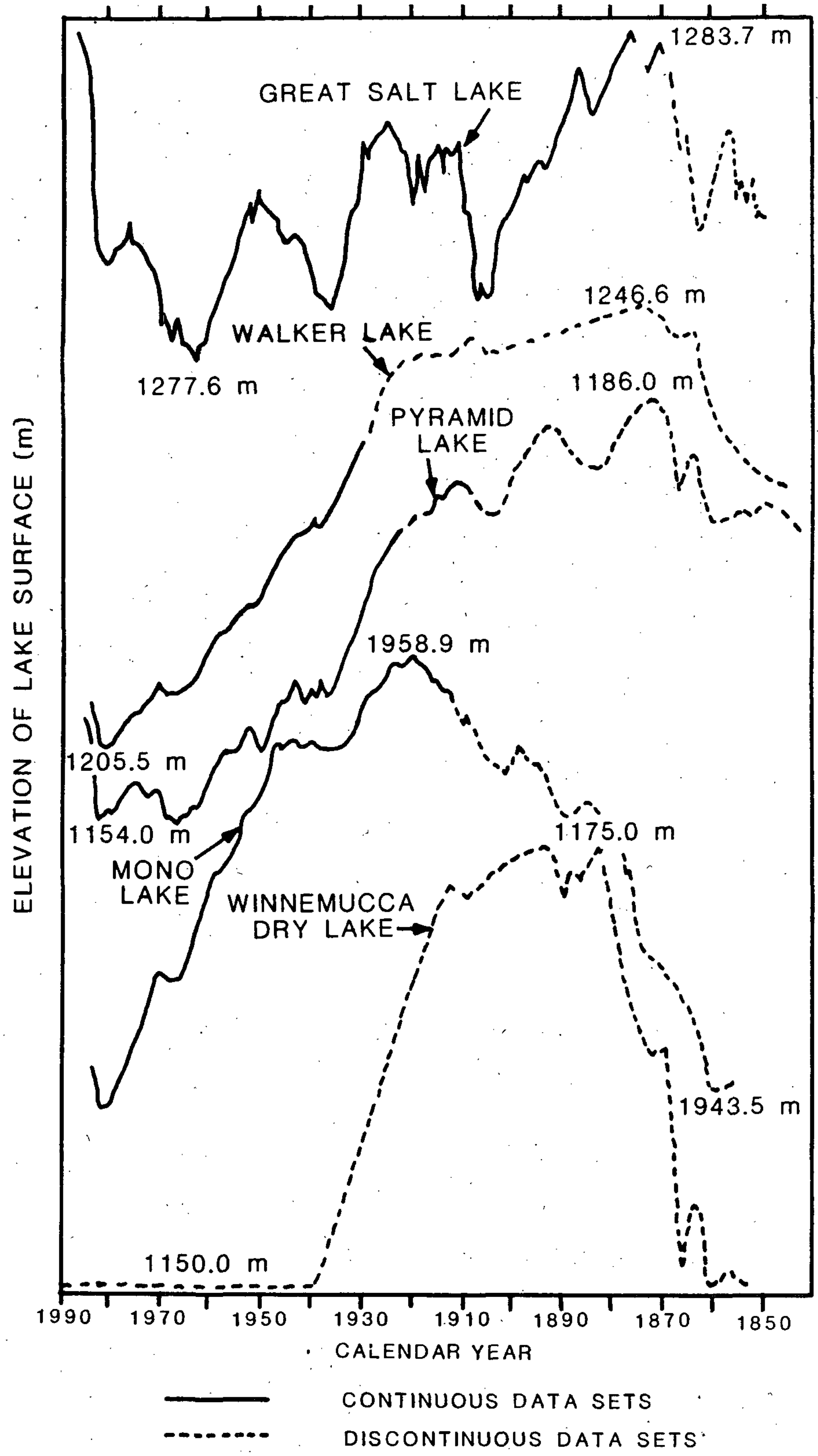

Figure 5-14. Historical fluctuations in the levels of Great Salt, Walker, Pyramid, Mono, and Winnemucca Dry lakes.

2. Provide information on the relationships between climatic variations reconstructed from other proxy data (such as paleobotanical records) and the hydrologic system.

3. Provide data necessary to validate climate models.

Dating of paleolake deposits

A chronology of variation in lake size can be obtained through the use of various methods of dating, including radiocarbon, chlorine-36, tephrachronology, uranium series, and magnetostratigraphy. Low lake levels in some closed basins can be identified by changes in the carbonate mineralogy or by the presence of salt layers, which indicate either desiccation or a shallow, saline lake.

Changes in the level and thus the size of a lake for the past 30,000 yr can often be determined by radiocarbon dating of materials, such as tufa or gastropods, deposited near the air and water interface near the paleoshoreline. Sediment cores recovered from the deepest portion of lake basins contain the remains of microscopic lacustrine plants and animals. Variations in the relative abundances and types of these organisms are a function of lake chemistry and physics and, to some extent, size. By examining the biotic content of cores taken from the deepest part of lake basins, it is

Distribution and age of paleolakes in the Great Basin

The pluvial lake systems in the Great Basin thought to be of Pleistocene age are shown in Figure 5-9. The names and summary hydrographic characteristics of these paleolakes have been given by Mifflin and Wheat (1979).

Only a few of the Great Basin paleolake systems have been sufficiently dated. Nonetheless, most of the radiocarbon dates point toward the existence of lakes in the basins within the last 30,000 yr.

Of the many basins, four of the paleolake systems (Bonneville, Lahontan, Russell, and Searles) have been intensively studied using radiometric dating techniques. Their chronologies for the past 20,000 yr are known well enough for the purpose of model validation. Of these systems, Russell and Searles are close to the Yucca Mountain region and near the same latitude.

Before discussing individual records of lake-level change, it is helpful to consider certain general relations between basinal topography and hydrology that influence the timing of lake-level change. During pluvial maxima, each of the lake systems consisted of a closed basin composed of one or more subbasins, separated from each other by sills (the lowest point on the divide separating adjoining basins or a series of separate basins connected by overflow). Today, some of these subbasins are fed by perennial streams and still contain lakes that rise and fall with changes in climate. Thus, it is the climate in the watershed area of the bordering mountain range that controls surface inflow to a subbasin, not the climate of the basin floor area. The climate of the basin floor area, however, determines the free-surface evaporation rate. The climates of both areas are influenced by the pronounced orographic effect that the Sierra Nevada and other high mountain ranges have on precipitation in the Great Basin (Maxey and Eakin, 1949).

The topography of a basin influences lake-level fluctuations. Lakes in small basins fed by perennial streams will change these levels rapidly in response to changes in moisture storage (influx minus evapotranspiration). Such lake systems are potentially excellent recorders of high-frequency, low-amplitude change in climate on the subregional scale. Lakes that lie in basins with large surface areas fed by perennial streams respond more slowly to changes in moisture storage. Also, the initiation of lake-level rise in a basin that receives surface inflow only when an adjoining basin overflows will lag the onset of lake-level expansion in that adjoining basin by the amount of time it takes the source basin to fill to its sill level. Thus, change in the size (elevation, volume, surface area) of a lake in any particular subbasin or series of basins can be a complicated function of intrabasin climate, extrabasin climate, and basin topography. In settings where adjoining basins coalesce at some level, the combined lakes act as a single body of water responding in an integrated manner to changes in the regional climate.

The records of the four paleolake systems that have been intensively studied are discussed in the following paragraphs.

Lake Bonneville system. Lake Bonneville, located in western Utah (Figure 5-15), had a surface area at its highest stage of about 52,000 km^2, a

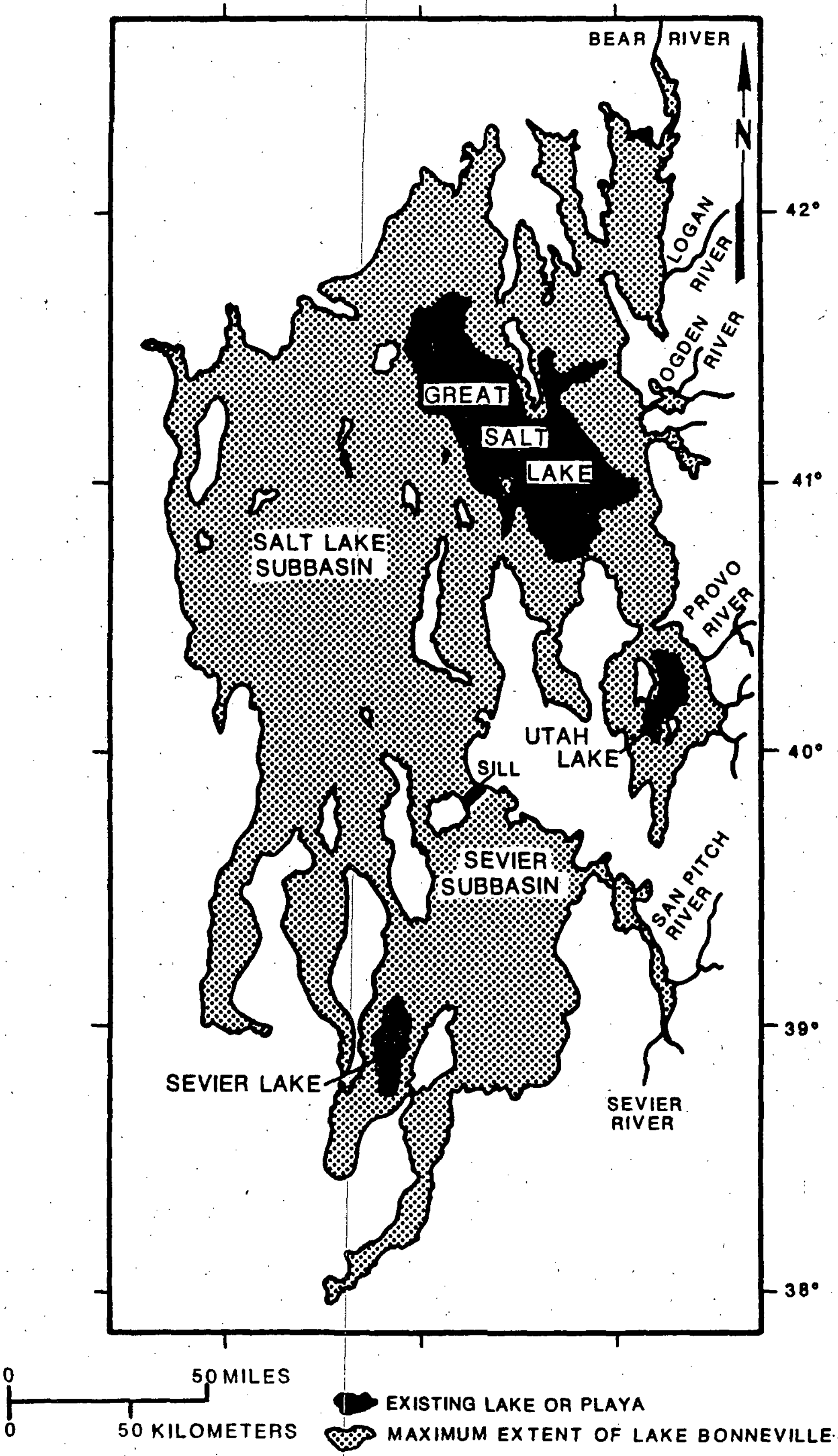

Figure 5-15. Lake Bonneville subbasins. Modified from Morrison (1965).

volume of 7,500 km^3, and a maximum depth of 335 m (Smith and Street-Perrott, 1983); it occupied two main subbasins: Salt Lake subbasin and the Sevier subbasin. Today, runoff contributes about 66 percent, direct precipitation about 31 percent, and ground water about 3 percent of the average influx to Great Salt Lake, the largest present-day manifestation of Lake Bonneville.

Numerous workers have contributed to the knowledge of Lake Bonneville since the classic study of Gilbert (1890). Until recently, the interpretations of Morrison (1965) and Morrison and Frye (1965) were probably cited most frequently, although Eardley et al. (1957), Broecker and Orr (1958), and Broecker and Kaufman (1965) were cited in more complete reviews of the literature. Within the last few years, stratigraphic and chronologic investigations have made extensive use of dating techniques that were not available to earlier studies of Lake Bonneville. These recent studies have given rise to a substantially modified interpretation of fluctuations in the level of Lake Bonneville. The Lake Bonneville chronologies of Currey and Oviatt (1985), Spencer et al. (1984), Scott et al. (1983), and Morrison (1965) are shown together in Figure 5-16. Because of the large distances separating study localities, physically tracing and correlating units is difficult because of disconformities, abrupt facies changes, and similarities in the appearances of deposits from different lake cycles. Scott et al. (1983) relied mainly on analyses of amino acid in shells and radiocarbon dating of wood for correlation, and samples from deposits of uncertain origin were assigned to a specific lake cycle on the basis of the similarity of their alloisoleucine to isoleucine ratios relative to ratios of samples whose relative ages had been determined by other means.

Lake Lahontan system. The Lahontan basin consists of seven subbasins separated by sills of differing altitudes (Figure 5-17). Of the six rivers that terminate in Lahontan subbasins, four (Truckee, Carson, Walker, and Humboldt) presently contribute 96 percent of the total gaged surface inflow (Benson, 1986). The Truckee, Carson, and Walker rivers have their headwaters in the Sierra Nevada, west of the Lahontan basin. The annual flows of these three rivers are highly correlated with each other (Benson, 1986). The Humboldt River has its headwaters in mountain ranges east of the basin. Lake Lahontan, at its highest stage 13,000 yr ago, had a surface area of about 22,300 km^2, a volume of 2,130 km^3 (Benson, 1978), and a maximum depth of 280 m in the Pyramid Lake subbasin (Smith and Street-Perrott, 1983).

The amount of subsurface inflow to present day surface-water bodies in the Lahontan basin is thought to be very small compared with the total amount of water reaching lakes, sinks, and playas in the form of runoff and precipitation (Everett and Rush, 1967). Surface flow accounts for about 85 percent of that total (Benson, 1986).

The first comprehensive study of Lake Lahontan was done by Russell (1885). Broecker and Orr (1958) and Broecker and Kaufman (1965) made the first systematic attempts to assign an absolute time scale to Lake Lahontan history. Morrison and Frye (1965) noted that certain tufa radiocarbon dates were reversed in relation to Morrison's (1964) stratigraphic assignments, which were developed without the benefit of radiocarbon dating. Benson (1978) developed a lake-level chronology for the Pyramid and Walker lake subbasins that used a sample selection procedure that helped to eliminate

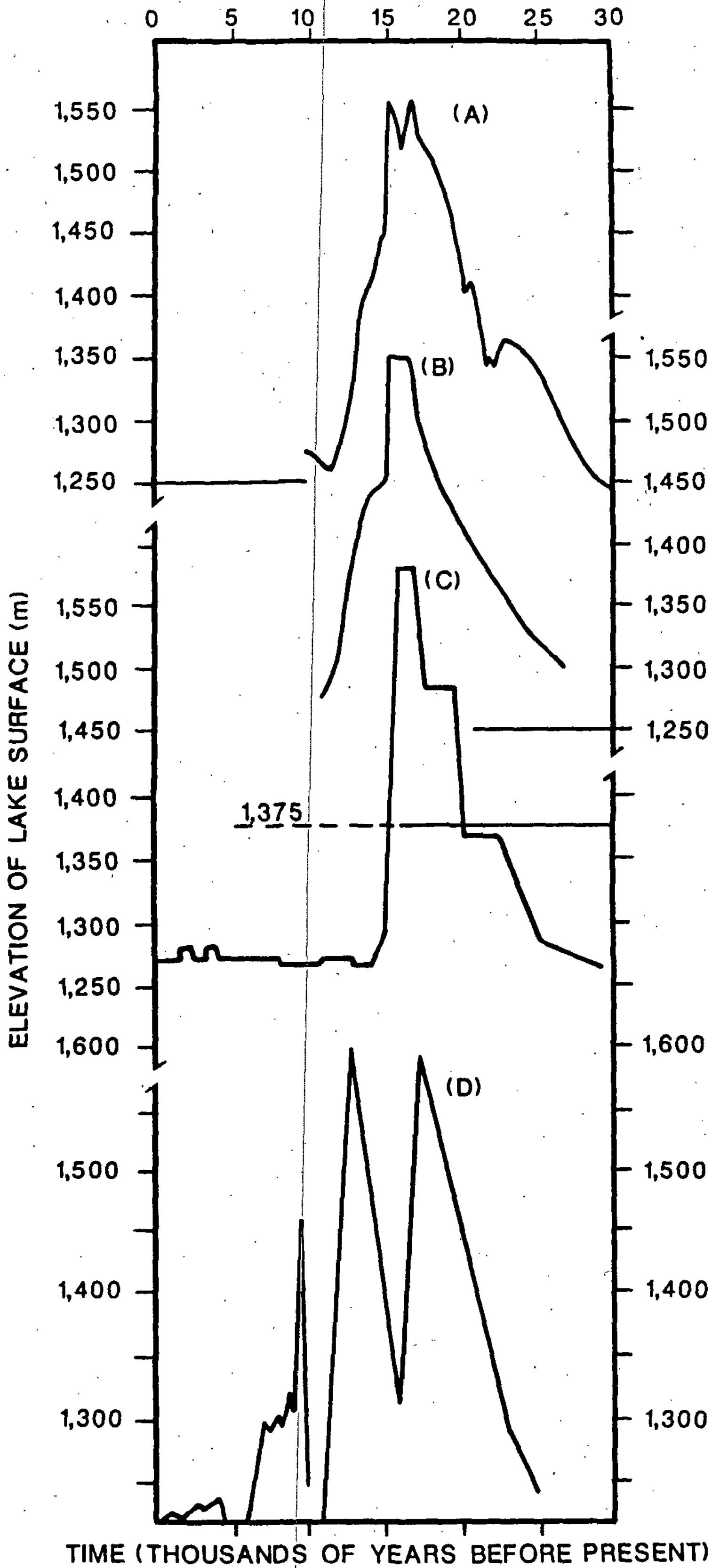

Figure 5-16. The last cycle in the Lake Bonneville Basin as interpreted by (A) Currey and Oviatt (1985), (B) Scott et al. (1983), (C) Spencer et al. (1984), and (D) Morrison (1965).

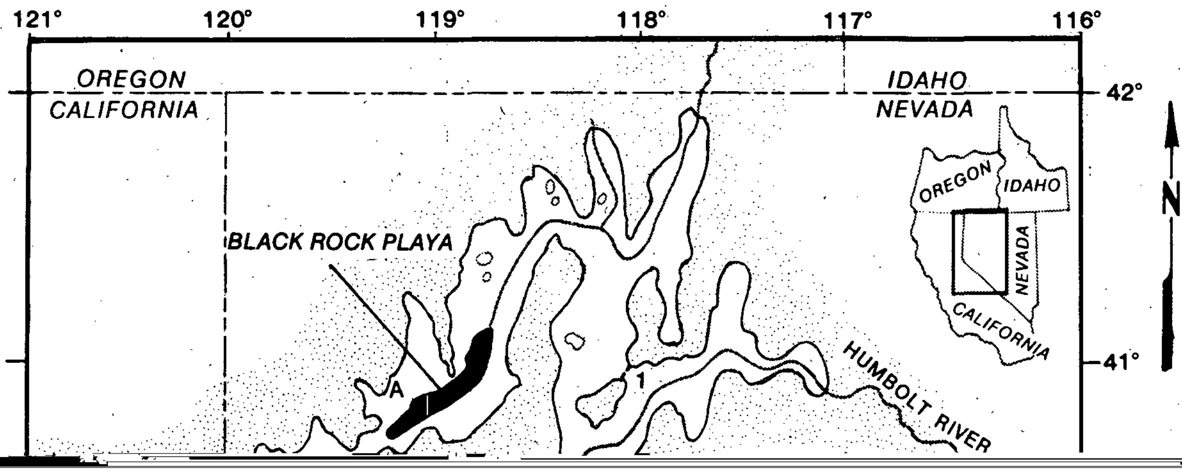
121°
120°
119°
118°
117°
116°
OREGON
CALIFORNIA
IDAHO
NEVADA
42°
41°
BLACK ROCK PLAYA
A
1
HUMBOLT RIVER
OREGON
IDAHO
NEVADA
CALIFORNIA
N

problems caused by the introduction of secondary carbon into tufa samples. Thompson et al. (1986) presented a chronology for the last Pleistocene lake cycle in the central Lahontan Basin, based on radiocarbon dates and tephrachronology. Their data, together with the data of Born (1972) and Benson (1981), have been used to form the Lahontan lake-level chronology of Figure 5-18.

The age of older lacustrine deposits in the Lahontan Basin is not well known. Broecker and Kaufman (1965) dated several samples of gastropod shells and tufa from those deposits. Radiocarbon activities indicated ages in excess of 34,000 yr. Subsequent age determinations on gastropod shells containing less than 5 percent secondary calcite, using the thorium-230/uranium-234 method, resulted in ages near 120,000 yr. These ages are broadly consistent with thorium-230/uranium-234 ages of about 92,000 and older than 100,000 yr on gastropod shells from the Bonneville Basin (Broecker and Kaufman, 1965). Difficulties associated with applying the thorium-230/uranium-234 method to carbonate samples found in closed basin lake systems preclude strict reliance on age dates determined using this method. However, the data are sufficient to suggest the adoption of a working hypothesis that at least two lake cycles occurred more or less synchronously in both the Bonneville and Lahontan lake basins during the time intervals from 120,000 to 90,000 yr ago and from 25,000 to 12,500 yr ago.

<u>Lakes Russell and Searles</u>. The Owens River system in the late Pleistocene consisted of a chain of lakes occupying a succession of basins east of the Sierra Nevada in California (Figures 5-19 and 5-20). The Owens River supplied water to the lakes downstream from its terminus (Gale 1914; Smith, 1979). When Lake Russell in Mono Basin overflowed, its surplus flowed into the headwaters of the Owens River. Only two of the seven lakes in this system, Russell and Searles, have been studied in detail.

Mono Lake and its ancestral Lake Russell lies in a relatively steep-sided basin separated from Adobe Lake and the Owens River drainage by a sill. Because of its morphology, the lake responds in a sensitive manner to changes in water volume and is potentially an excellent recorder of high-frequency, low-amplitude climatic events that take place in its watershed. Lajoie (1963) made a detailed stratigraphic study of the lake sediments, the chronology of which has been supported by radiocarbon dates on ostracodes and tufa and by tephrachronology. Reconstruction of the lake-level history of Lake Russell for the past 20,000 yr is shown in Figure 5-21. The lake-level chronology depicted in Figure 5-21 is noteworthy in that it closely resembles the Lahontan chronology, Figure 5-18.

The other lake in the Owens River system that has been intensively studied is Searles Lake (Smith, 1979; Stuiver and Smith, 1979). During the late Pleistocene, Searles was third in a chain of lakes that received water from the Owens River. When Owens filled to a level of about 60 m, it overflowed into China Lake; when China Lake filled to a depth of 12 m, it overflowed into Searles Lake; and when Searles Lake reached a level of about 200 m, it coalesced with China Lake and overflowed to create a relatively shallow lake in Panamint Valley. During pluvial periods of earlier Pleistocene times, Panamint Lake overflowed into Lake Manly (Death Valley), which was also the terminus of the Mojave and Amargosa rivers (Figure 5-20).

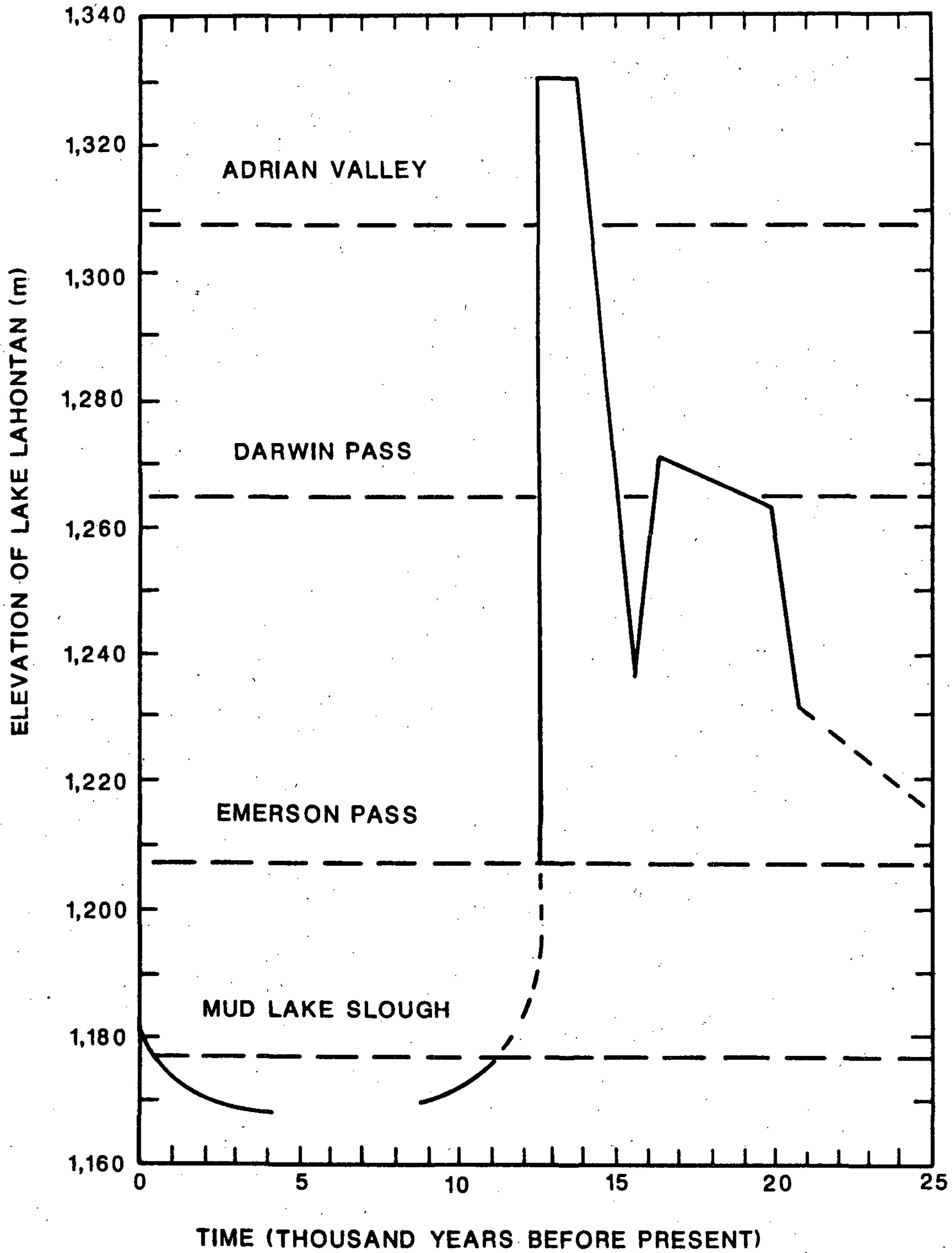

Figure 5-18. Lake Lahontan chronology inferred from data of Born (1972), Benson (1981), and Thompson et al. (1986).

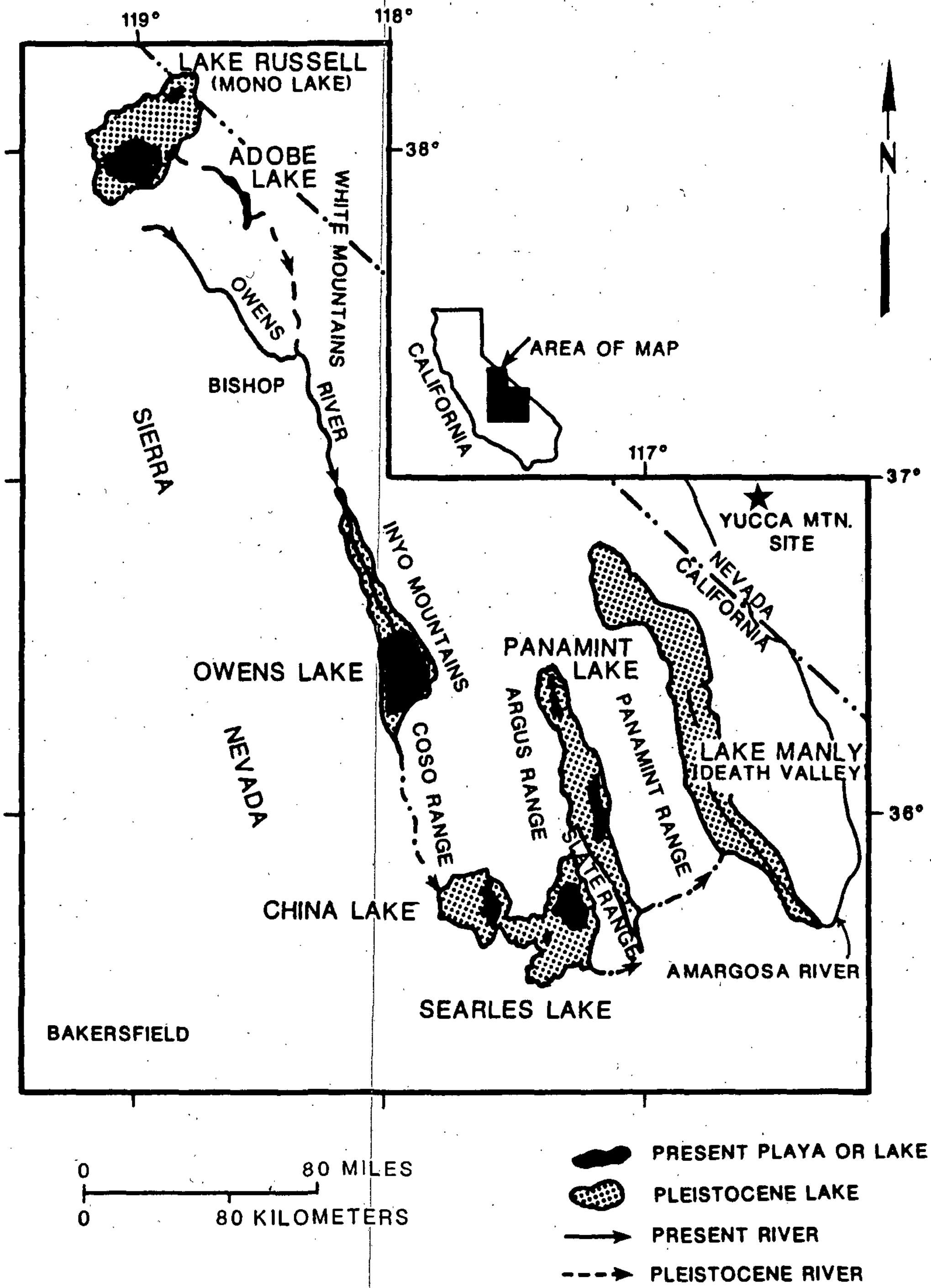

Figure 5-19. Location of lakes in the Owens River system during pluvial periods in the late Pleistocene. Modified from Smith (1979).

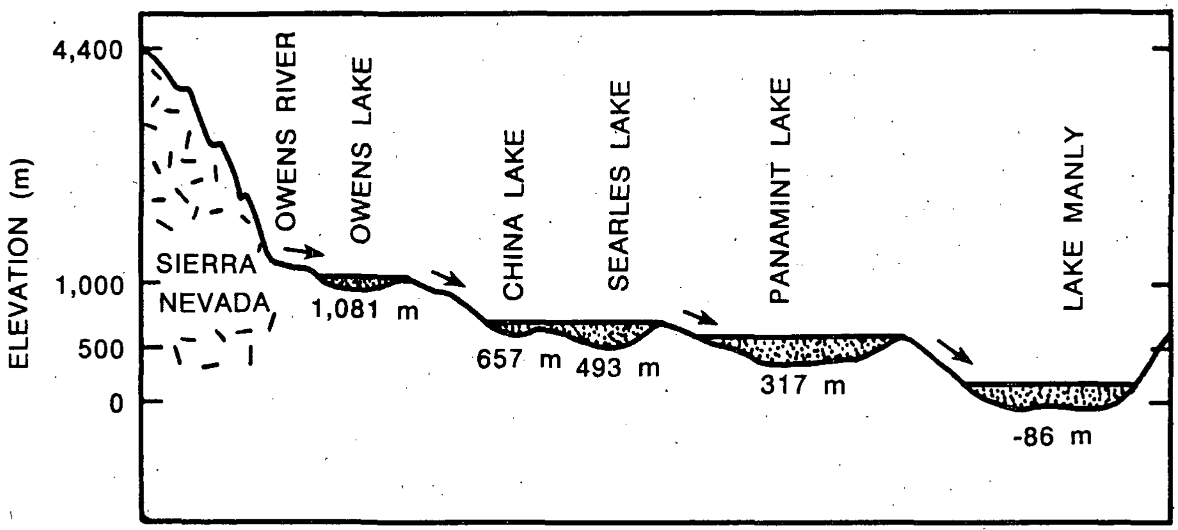

Figure 5-20. Overflow sequence of lakes in the Owens River system. Modified from Gale (1914).

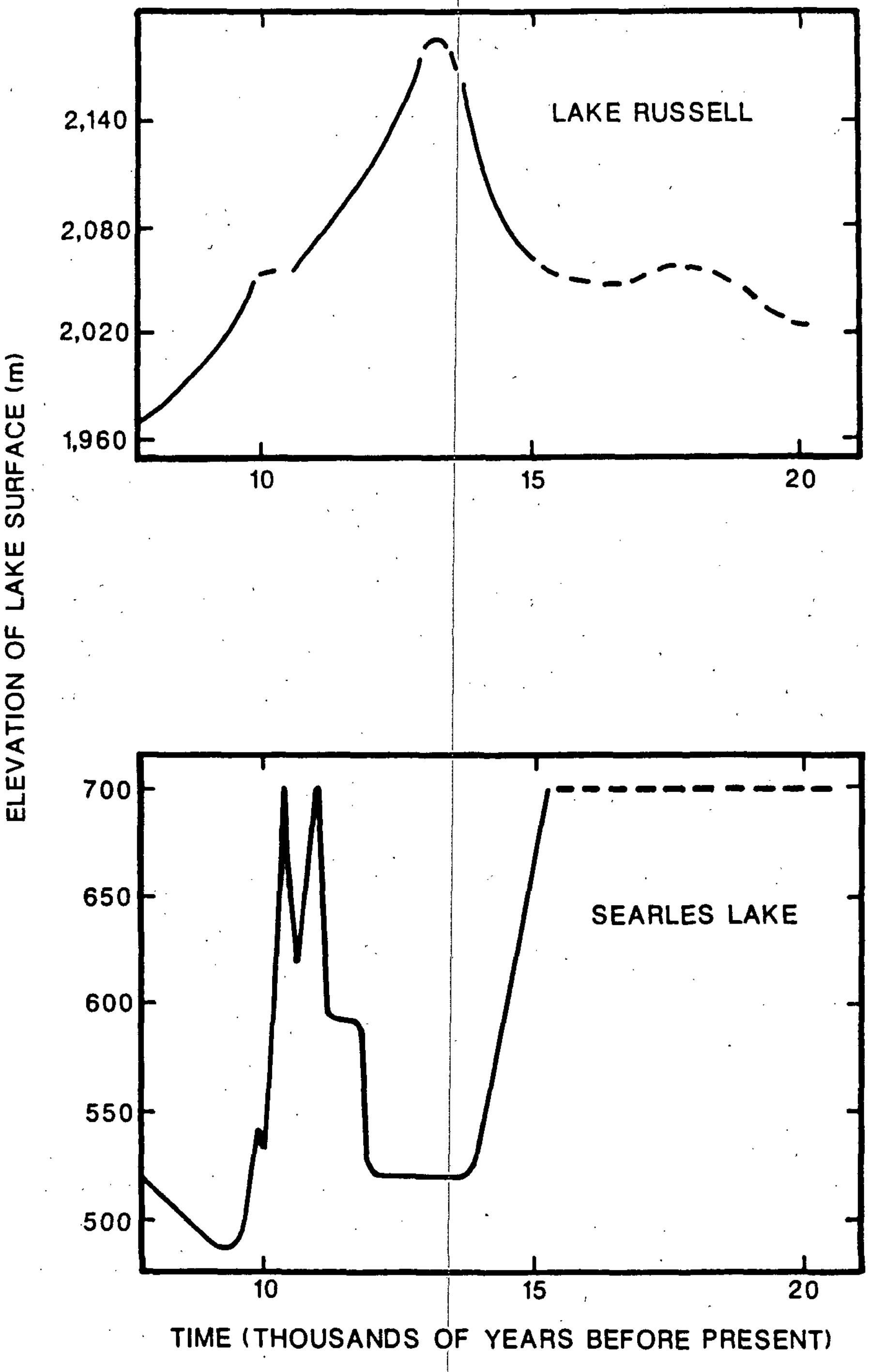

Figure 5-21. Chronologies of lakes in the Russell (Mono) and Searles basins (after Smith and Street-Perrott, 1983, Figure 10-5).

The chronologies of Searles Lake and Lake Russell for the past 20,000 yr are shown in Figure 5-21. The mismatch between the highest stands of Searles Lake and Lake Russell during the time period 20,000 to 11,000 yr ago might be explained in one of the following ways:

1. The data or the data interpretation of one or both of the lake chronologies may be in error.

2. The timing of lake-level fluctuations in the Searles Basin may have been delayed by the cumulative times required for basins upstream in the Owens River system to fill to overflowing or to cease flowing.

3. Both chronologies are basically correct, but there may have been a distinct north-south climate gradient between the watersheds that supply each of the lakes, with each watershed responding to the changing distribution of Pacific sea-surface temperatures in different ways and at different times.

The Searles Lake chronology for the past 30,000 yr, unlike the Russell, Lahontan, and Bonneville chronologies, is based about equally on radiocarbon analyses of samples from both outcropping sediments and core materials, but lacustrine materials of both types carry uncertainties about their carbon-14-based ages. An example from the subsurface record at Searles Lake (Stuiver and Smith, 1979) illustrates the difficulties inherent in all carbon-14 dates from materials deposited in lakes and why differences in chronologies of a few thousand years should not be necessarily viewed as significant. Of the four radiocarbon dates on disseminated organic carbon and wood from the overburden mud (Figure 5-22), Stuiver and Smith (1979) concluded that only the single date on wood was reliable. They reasoned that the unit was deposited in a much smaller lake than were most mud units in this basin, and large areas of older lake beds that contained carbon and carbonate minerals were being eroded, thus contaminating the units being deposited and creating the 3,000-yr discrepancy between the date on wood from this unit (3,520 $\pm$ 190 yr) and the older date on detrital carbon from a nearby horizon. A discrepancy having the same magnitude and direction is found between the dates on wood and organic carbon in a mud layer in the Lower Salt (Figure 5-22).

Figure 5-21 indicates that Lake Russell experienced a high lake cycle beginning at about 15,000 yr ago and ending about 12,000 yr ago. The lake peaked from about 14,000 to 13,000 yr ago and may or may not have spilled. The Searles record (Smith and Street-Perrott, 1983) shows a strong increase in lake size starting at about 12,500 yr ago. While carbon-14 dates from these areas could be in error, they appear to be substantially correct, and the presence of the brief period of high lake stands between about 12,500 and 10,500 yr ago in Searles is suggested by an episode and age assignment supported by extensive stratigraphic and radiometric dating evidence (Smith and Street-Perrott, 1983).

The broad agreement between the Bonneville, Lahontan, and Russell records--disregarding the differences of a few thousand years in peak stages--suggests that they all occupied a zone that shared a similar climatic history. The similarity between historical records from Great Salt, Walker, Pyramid, Mono, and Winnemucca lakes (Figure 5-14) supports this view. The

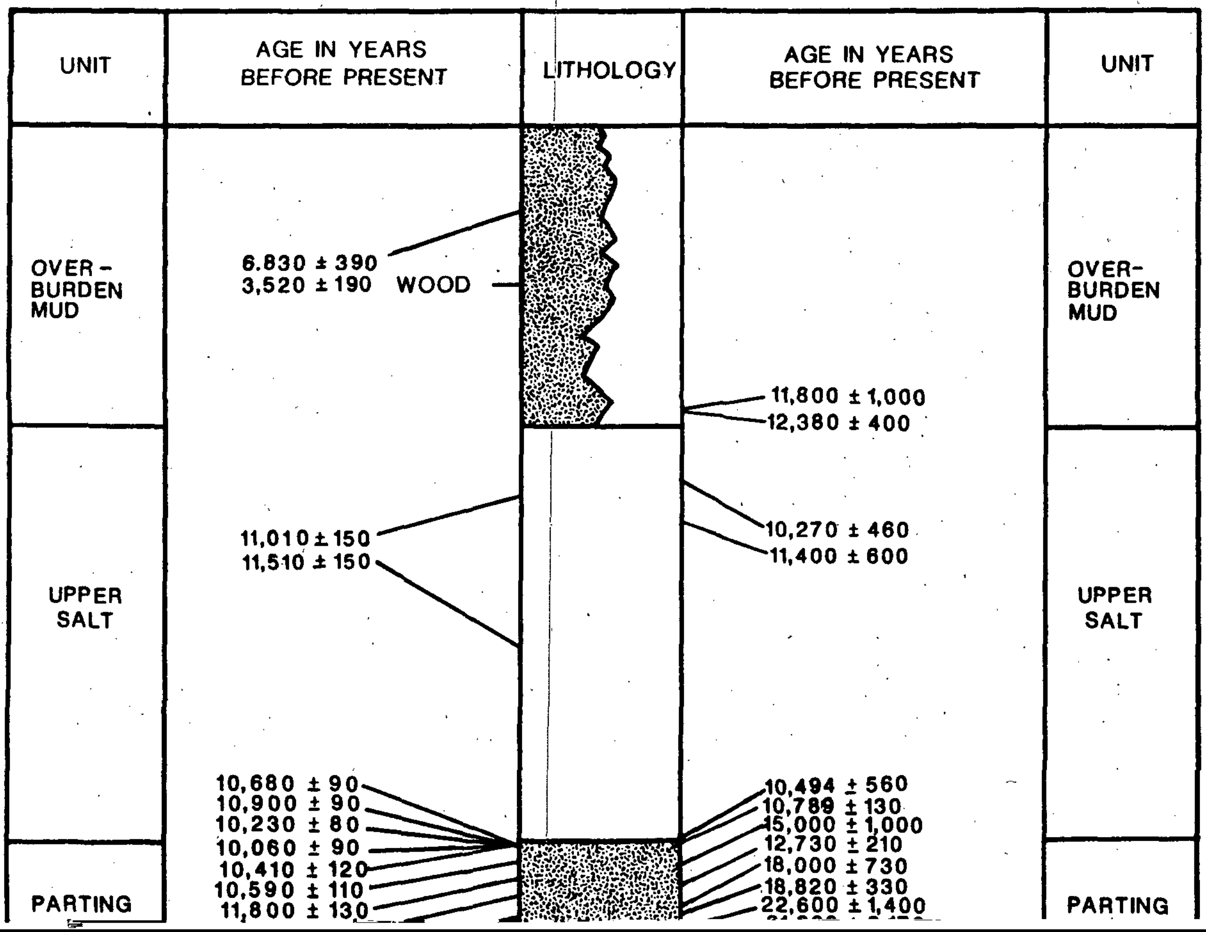
UNIT
AGE IN YEARS BEFORE PRESENT
LITHOLOGY
AGE IN YEARS BEFORE PRESENT
UNIT
OVER-BURDEN MUD
6.830 ± 390
3,520 ± 190 WOOD
11,800 ± 1,000
12,380 ± 400
OVER-BURDEN MUD
UPPER SALT
11,010 ± 150
11,510 ± 150
10,270 ± 460
11,400 ± 600
UPPER SALT
10,680 ± 90
10,900 ± 90
10,230 ± 80
10,060 ± 90
10,410 ± 120
10,590 ± 110
11,800 ± 130
10,494 ± 560
10,789 ± 130
15,000 ± 1,000
12,730 ± 210
18,000 ± 730
18,820 ± 330
22,600 ± 1,400
PARTING
PARTING

strong evidence for a different history for lakes in the Owens River system, derived from Searles Lake, creates doubts as to the comparability that should be expected between the climatic histories of the two regions. The similarities in the latitudes (37 degrees) of the Yucca Mountain site and the segment of the Sierra Nevada that contributed most of the runoff to the Owens River system and Searles Lake supports the notion that the Searles Lake history is the better of the pluvial lake records for the evaluation of future climatic change in the Yucca Mountain area.

Death Valley drainage system. During portions of the Pleistocene, Death Valley received surface water flow from the Owens River system (described previously), surface water from the Mojave River drainage, and surface flow and ground water from the Yucca Mountain region. Because of this latter hydrologic tie to the Nevada Test Site, geologic records from Death Valley are relevant to site characterization activities in paleohydrology, as well as paleoclimatology. Additional discussions are found in Sections 3.7.4.1 and 3.7.4.5.

Because of the poor preservation of shoreline features, relatively little is known about the age and depth of the Pleistocene Lake Manly in

3. A third lacustral episode, during which, the outlet was downcut, occurring between approximately 11,000 and 9,000 yr B.P.

4. A final lacustral episode, estimated to have occurred between approximately 8,500 and 7,500 yr B.P., was of lesser magnitude and did not overflow the outlet.

Further studies by Wells et al. (1984, 1987) provide additional radiocarbon dates that substantiated the late-Pleistocene portion of the chronology presented above, although these authors suggest that due to bedrock control at the outlet, relatively continuous highstand conditions (with only minor fluctuations in level) occurred between 15,500 and 10,500 yr B.P. These authors also question the dating of the lowest and youngest lake stand, and estimate its age to fall between 10,500 and 8,000 yr B.P. and suggest that it was a short-lived phenomenon (less than a few hundred years in duration). Wells et al. (1987) found evidence of larger than modern flood events in the early and middle Holocene and interpreted these deposits as indicative of intensified monsoonal conditions.

Banks of lake sediments up to 68 m thick are present in the Lake Tecopa basin in the Amargosa River drainage, which flows from the Yucca Mountain area to Death Valley (Sheppard and Gude, 1968). These lake beds are estimated to be of no greater than mid-Pleistocene age and were deposited in alkaline saline waters.

Marsh deposits in Southern Nevada. Ground-water-fed marshes and wet meadows present in Southern Nevada during early historical time were greatly expanded in distribution and in areal coverage during late Wisconsin time. Stratigraphic studies at Tule Springs (Haynes, 1967) and Corn Creek Flat and Indian Springs (Quade, 1985) indicate that marshes and associated shallow lakes reached their maximal extent between 30,000 and 15,000 yr B.P. A progressive desiccation of the marsh-lake complexes occurred between 13,500 and 8,000 to 7,200 yr B.P. After this time perennial water was absent, and paleoclimatic conditions responsible for Pleistocene lake high stands also had significant effects on the hydrologic regime of Yucca Mountain.

Summary of paleolacustrine data

Available information indicates the presence of more than one lake cycle in the Great Basin during the past 150,000 yr. The last cycle that occurred during the late Pleistocene is well documented in the Bonneville, Lahontan, Mono, and Searles basins. Older cycles in both the Bonneville and Lahontan basins are less adequately documented (in terms of absolute age determinations), but one cycle may have occurred 115,000 ± 15,000 yr ago. In Searles basin, the nearly continuous existence of perennial bodies of water, over a period extending from 130,000 to 10,000 yr ago, interrupted by only brief periods of salt deposition, is documented by a wealth of subsurface data (Smith, 1979), supplemented by carbon-14 (Stuiver and Smith, 1979) and uranium-series dating (Bischoff et al., 1985). A large number of basins throughout the Great Basin that today are playas or dry lakes contain shoreline evidence of more than one former lake cycle. Radiocarbon analyses of material from these basins indicate that the youngest shoreline probably corresponds to a lake cycle that occurred in the late Pleistocene. The ages of the older shorelines are not known.

5.2.1.2.3 Time series of prehistorical vegetation change

Paleobotanical data provide the most widespread and continuous records surrounding Yucca Mountain as plant macrofossil assemblages from pack rat middens from dry caves and rockshelters and as fossil pollen from lake and marsh sediments. The temporal resolution of the paleoclimatic reconstructions from these data will potentially be limited by the sampling interval for pollen data from lacustrine cores and by the availability of pack rat middens representing the time periods of interest. In the case of palynological data, studies of the pollen content of lake sediments in the Great Basin have had sampling intervals (in temporal terms) of 200 to 1,000 yr (refer to Thompson (1984) for examples). This sampling interval would permit the reconstruction of paleoclimatic fluctuations with a period of 200 to 1,000 yr. The temporal resolution for pack rat midden studies will probably be lower, and it will probably not be possible to confidently reconstruct fluctuations with periods of less than 1,000 yr using pack rat midden data.

Rationale

Studies of past changes in vegetation can be used in the following aspects of paleoclimatology:

1. To determine the nature, range, and frequency of past climatic variability.

2. To provide well-dated paleobotanical time series for the testing and validation of climatic models. These time series provide two types of necessary information:

   a. Long continuous records reflecting low-frequency climatic changes that can be used to reconstruct the slowly varying aspects of climatic change.

   b. A network of sites to test synoptic scale predictions of the more rapidly varying aspects of the models.

Modern vegetation and climate

The sensitivity of plant distributions to geographic and elevational variations in climatic parameters provides a basis for the interpretation of past climatic fluctuations from changes in vegetational records.

The distributions and associations of plant species in the region surrounding Yucca Mountain are greatly influenced by variations in climate, especially temperature and precipitation. For example, the geographic distribution of summer rainfall appears to influence the regional distributions of pinyon pine (*Pinus monophylla*), Utah juniper (*Juniperus osteosperma*), ponderosa pine (*Pinus ponderosa*), and other woodland and montane plants (Houghton et al., 1975). Temperature extremes may also limit the distributions of certain plants. For example, the geographic and elevational

Figure 5-23). In the Great Basin the general progression is from shadscale desert on the hot arid valley bottoms, through sagebrush steppe on bajadas and mountain slopes, pinyon-juniper woodland and upper sagebrush grassland at intermediate elevations, to subalpine conifer forest at or near the mountain summits. An exception to this pattern is found in mountain ranges of the northwest Great Basin, where there is even less summer rainfall. Here, sagebrush dominates the entire elevational range. The mountains of the eastern Great Basin that receive more summer precipitation than ranges farther west support ponderosa pine, douglas fir, and other montane plants at middle elevations.

A similar zonation of plant communities occurs in the Mojave Desert. The valley bottoms in this region are lower, hotter, and drier than those of the Great Basin. Mojave desert scrub communities, usually dominated by creosote bush (Larrea divaricata), joshua tree (Yucca brevifolia), and Mojave yucca (Yucca shidigera), occur in these arid settings.

Dendroclimatology

Past variations in tree-ring widths reflect interannual and even sea-

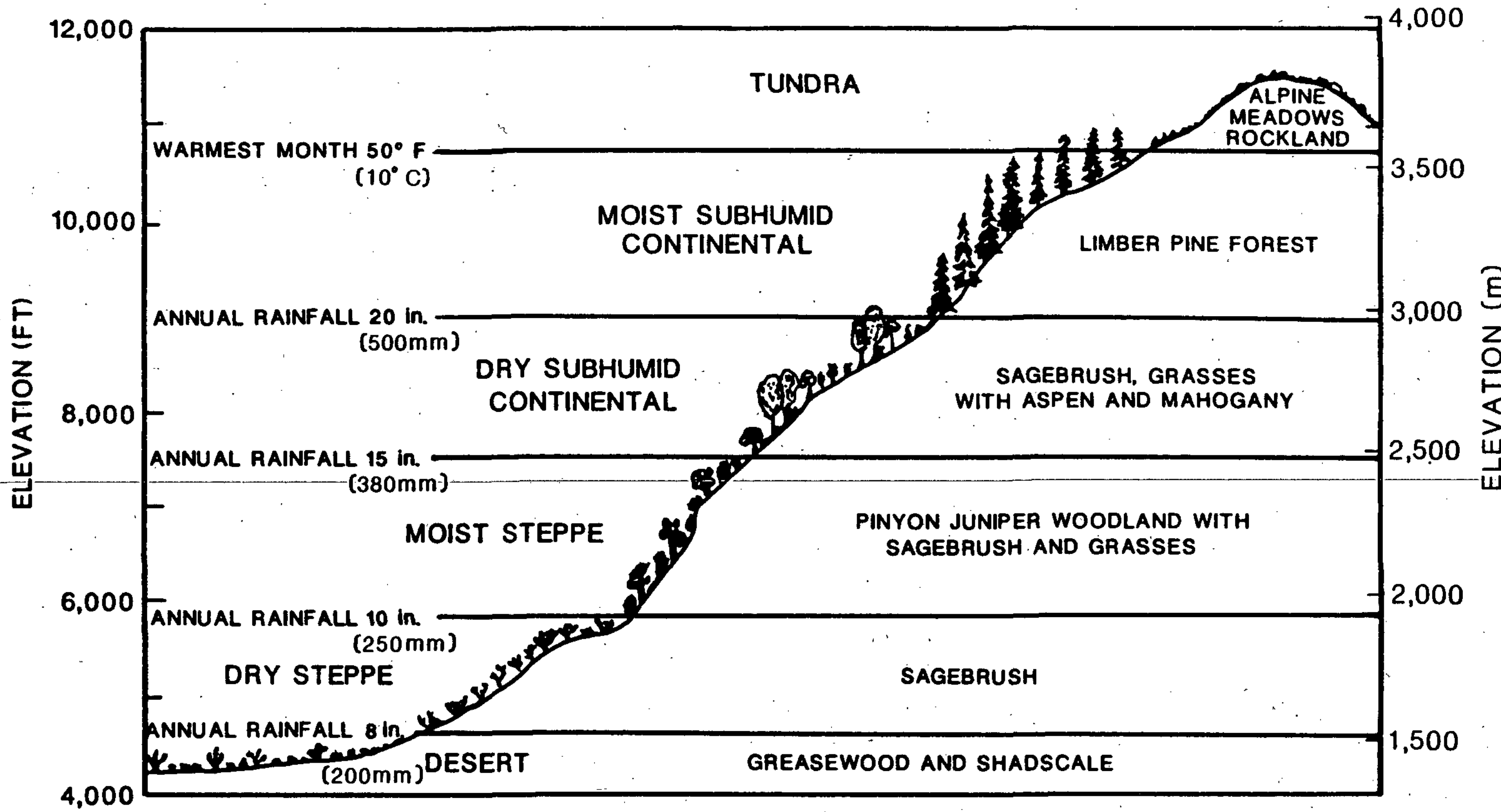

Figure 5-23. Generalized relationships among altitude, precipitation, and the distribution of plant communities for the Great Basin portion of Nevada. Modified from Houghton et al. (1975).

DECEMBER 1988

Palynology and pack rat midden studies

Fossil pollen in stratigraphic deposits have been extensively used in eastern North America and northern Europe to reconstruct fluctuations in temperature and precipitation over the last 15,000 yr (Webb, 1985). The applicability of the method has been somewhat limited by the relative scarcity of bogs and small lakes, the optimal settings for most types of pollen studies. Nevertheless, substantial paleoclimatological insights have been gained from studies of the fossil pollen contained in sediments deposited in

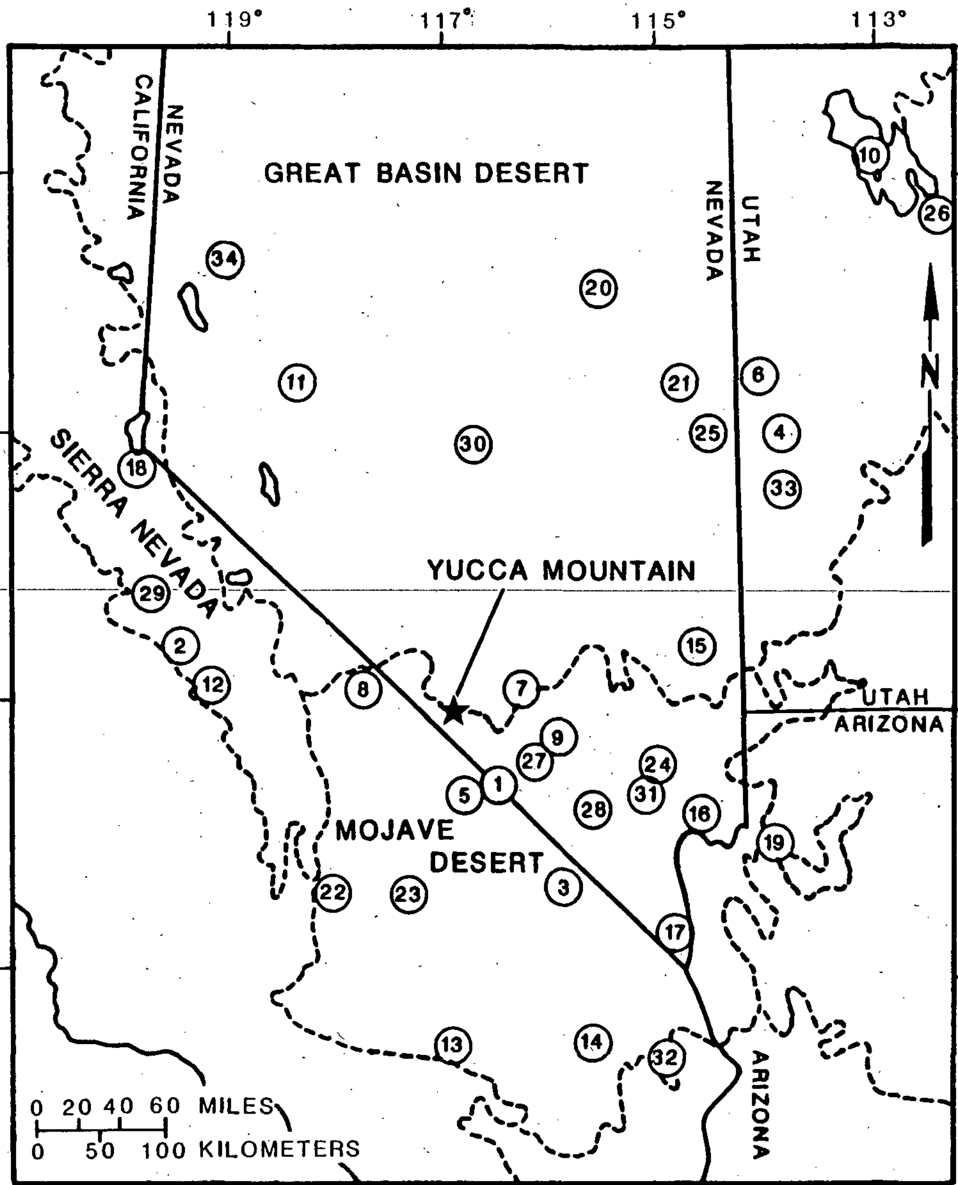

1. AMARGOSA DESERT
2. BALSALM MEADOW
3. CLARK MOUNTAIN
4. CONFUSION RANGE
5. DEATH VALLEY
6. DEEP CREEK RANGE
7. ELEANA RANGE
8. EUREKA VALLEY
9. FRENCHMAN FLAT
10. GREAT SALT LAKE (LAKE BONNEVILLE)
11. HIDDEN CAVE
12. KING'S CANYON
13. LUCERNE VALLEY
14. MARBLE MOUNTAINS
15. MEADOW VALLEY WASH
16. MUDDY MOUNTAINS
17. NEWBERRY MOUNTAINS
18. OSGOOD SWAMP
19. RAMPART CAVE (WESTERN GRAND CANYON)
20. RUBY MARSHES
21. SCHELL CREEK RANGE
22. SCODIE MOUNTAINS
23. LAKE SEARLES
24. SHEEP RANGE
25. SNAKE RANGE
26. SNOWBIRD BOG
27. SPECTER RANGE
28. SPRING RANGE
29. CLEAR LAKE
30. TOQUIMA RANGE
31. TULE SPRINGS
32. TURTLE MOUNTAINS
33. WAH WAH RANGE
34. WINNEMUCCA LAKE

Figure 5-24. Locations of study sites for pollen and pack rat midden investigations discussed in text.

Table 5-12. Summary of palynological and pack rat midden data from the Great Basin, Mojave Desert, and Sierra Nevada with inferred climatic changes (page 1 of 8)

Location[a]	Evidence	Age	Vegetational assemblage	Inferred climatic conditions
		WESTERN GREAT BASIN		
Lake Lahontan basin (11,35)	Pack rat middens	12.1 to 11.5 thousand years ago	Western juniper, sagebrush, and other Great Basin shrubs at lower than modern elevation limits (Thompson et al., 1986).	Semiarid, with dominance of cool-season precipitation and little or no summer precipitation. Summer temperatures cooler than present, but winter temperatures may not have been much colder (Thompson, 1984).
		CENTRAL GREAT BASIN		
Toquima Range (30)	Pollen, pack rat middens	6,000 years ago to present	Early Holocene sagebrush steppe with aspen replaced by pinyon-juniper woodland (Thompson and Hattori, 1983).	Early Holocene assemblages may reflect dry conditions with cooler than modern summer temperatures. Differences between middle Holocene and modern woodland plant associations reflect moisture conditions or higher proportion of summer rainfall (or both) from 6 to 3 thousand years ago.
Ruby Marshes (20)	Pollen	35 to 8 thousand years ago	Expansion of sagebrush steppe in the valleys; reduction of tree cover (Thompson, 1984).	Probably reflects relatively cold and dry conditions with strong predominance of winter precipitation.
		7 to 5 thousand years ago	Expansion of shadscale steppe; establishment of pinyon-juniper woodland.	Suggests warmer and perhaps drier than modern conditions. (Thompson, 1984).

Table 5-12. Summary of palynological and pack rat midden data from the Great Basin, Mojave Desert, and Sierra Nevada with inferred climatic changes (page 2 of 8)

Location[a]	Evidence	Age	Vegetational assemblage	Inferred climatic conditions
		EASTERN GREAT BASIN		
Mountain ranges of east-central Nevada and west-central Utah: Schell Creek (21), Snake (25), Deep Creek (6), Confusion (4), and Wah Wah (33) ranges.	Pollen, pack rat middens	> 40 to 11 thousand years ago (late Wisconsin)	Absence of many woodland plants common in modern assemblage. Occurrence of relatively xeric subalpine conifers, including bristlecone pine (*Pinus longaeva*), limber pine (*Pinus flexilis*), Englemann spruce (*Picea englemanni*), and prostrate juniper (*Juniperis communis*), at elevations as much as 1,000 m below their modern limits (Thompson and Mead, 1982; Thompson, 1984).	Suggests late Wisconsin climate colder than modern, and relatively dry with little summer precipitation.
		11,000 years ago to present	Subalpine conifers (except for limber pine) reduced at low elevation xeric sites. Quaking aspen (*Populus tremuloides*), Rocky Mountain maple (*Acer glabrum*), and other mesophytic montane shrubs increase in abundance. Woodland junipers well established by 7.4 thousand years ago, pinyon-juniper woodland by 6.1 thousand years ago.	Indicates early Holocene climate warmer than late Wisconsin, but still cooler than modern climate. No evidence for major fluctuations in assemblage over last 6.0 thousand years, indicating prevalence of modern climatic conditions during this period.

Table 5.12. Summary of paleoecological and pack rat midden data from the Great Basin, Mojave Desert, and

Table 5-12. Summary of palynological and pack rat midden data from the Great Basin, Mojave Desert, and Sierra Nevada with inferred climatic changes (page 4 of 8)

Location[a]	Evidence	Age	Vegetational assemblage	Inferred climatic conditions
Colorado River Valley: Turtle Mountains (32) Marble Mountains (14)	Pack rat middens	16.9 to 9.9 thousand years ago	Juniper woodlands descended as low as 258 m, persisting as low as 425 m to at least 9.9 thousand years ago (Wells and Berger, 1967; Wells 1983).	Indicates late Wisconsin and early Holocene climates of this region cooler and moister than modern conditions. Trend toward increasing aridity, warmth, or both, began by 14,000 years ago and accelerated after 11,000 years ago.
Newberry Mountains (17) (southernmost Nevada)	Pack rat middens	Late Wisconsin	Descent of pinyon-juniper-oak woodlands to 730-850 m.	Not determined.
Las Vegas Valley: Tule Springs (31)	Pollen	> 30 thousand yr ago to modern	Presence of sagebrush and junipers as low as 700 m (Mehringer, 1967). Sagebrush pollen decreased in abundance after 11,000 years ago, and Mojave Desert vegetation in place by 7,000 years ago.	Wisconsin climate relatively cold and perhaps not much wetter than present, with little summer rainfall. Increase of warmth and aridity before 11,000 years ago, but conditions cooler and wetter than modern until about 9,000 years ago.
Clark Mountain (3), Sheep (24) and Spring (28) Ranges, Muddy Mountains (16)	Pack rat middens	Late Wisconsin	Presence of bristlecone pine and other subalpine plants as low as 1,500 to 1,700 m; pinyon-juniper woodlands below subalpine assemblage, with pinyon pine (<u>Pinus momophylla</u>) as low as 1,600 m and juniper (<u>Juniperus osteosperma</u>) below 1,900 m. Shadscale up to 320 m above present limits (Spaulding, 1981). Woodland plants at low elevations in Sheep Range until at least 9.4 thousand years ago.	Late Wisconsin middens indicate higher than modern precipitation levels (Mehringer and Ferguson, 1969).

Table 5-12. Summary of palynological and pack rat midden data from the Great Basin, Mojave Desert, and Sierra Nevada with inferred climatic changes (page 5 of 8)

Location[a]	Evidence	Age	Vegetational assemblage	Inferred climatic conditions
Amargosa Desert (1)	Pack rat middens	Wisconsin to 9,000 years ago	Modern Mojave desert scrub preceded by mixture of Great Basin, Mojave, and woodland plants during Wisconsin; assemblages ranged from treeless Great Basin desert scrub to juniper to (rare) pinyon pine. Junipers absent by 9.3 thousand years ago, and cacti and other succulents became abundant. Arrival of creosote bush (Larrea divaricata) by 9.3 thousand years ago. Persistence of other plants not present today: Utah agave (Agave Utahensis) and beavertail cactus (Opuntia basilaris).	High abundance of succulents in latest Wisconsin and early Holocene middens may indicate higher than modern summer rainfall levels.
Frenchman Flat (9)	Pack rat middens	40 to 10 thousand years ago	Abundance of juniper and pine between 1,200 and 1,500 m (Wells and Jorgensen, 1964).	Climate significantly less arid than at present (Wells and Jorgensen, 1964).
		10 to 9 thousand years ago	Descent of xerophilous juniper woodlands to 1,100 m (600 m below present woodland limit). Coexistence with desert or semidesert shrubs throughout lowered elevation range (Wells and Berger, 1967).	Climate relatively cooler and not much wetter than present during period of 10 to 9 thousand years ago.

Table 5-12. Summary of palynological and pack rat midden data from the Great Basin, Mojave Desert, and Sierra Nevada with inferred climatic changes (page 6 of 8)

Location[a]	Evidence	Age	Vegetational assemblage	Inferred climatic conditions
Eleana Range (7)	Pack rat middens	17.1 to 13.2 thousand years ago	Limber-pine (*Pinus flexilis*) woodland with Great Basin Desert and woodland shrubs as important understory species.	Later glacial trend toward effectively drier conditions, starting at about 16,000 years ago and well under way at 13,000 years ago. Change to drier climate between 13.2 and 11.7 thousand years ago.
		11.7 to 10.6 thousand years ago	Shift to woodland dominated by juniper, pinyon pine, and prickly pear species present in modern nearby woodland. (Spaulding, 1985).	
Specter Range (27)	Pack rat middens	32 to 18.7 thousand years ago	Middle Wisconsin juniper or juniper-shadscale woodland. Pinyon pine-juniper woodland during Wisconsin maximum. (Spaulding, 1985).	At 30,000 years ago, average annual precipitation higher than present, temperature relatively lower.
		WESTERN MOJAVE DESERT		
Death Valley (5)	Pack rat middens	19.6 to 13.1 thousand years ago 11.2 to 9.1 thousand years ago	Utah juniper grew from 1,200 to 1,500 m below present limits from 19.6 to 13.1 thousand years ago. Lowest elevations from this period have traces of juniper mixed with Joshua tree (*Yucca brevifola*) and Whipple's Yucca (*Yucca whipplei*). Latter not found at present in Death Valley. Junipers absent from lowest elevations by 11.2 thousand	Past occurrence of Whipple's Yucca may reflect very mild winter temperatures and substantial winter rain. Junipers receded from lowest elevations by 11.2 thousand years ago, presaging trend to progressive warmth and aridity from 11.2 to 9.1 thousand years ago.

Table 5-12. Summary of palynological and pack rat midden data from the Great Basin, Mojave Desert, and Sierra Nevada with inferred climatic changes (page 7 of 8)

Location[a]	Evidence	Age	Vegetational assemblage	Inferred climatic conditions
Eureka Valley, CA (8)	Pack rat middens	14.7 to 5.4 thousand years ago	Present creosote bush and shadscale (<u>Atriplex confertifolia</u>) area occupied by Utah juniper and limber pine at 14.7 thousand years ago; also present then were sagebrush, shadscale, and other Great Basin shrubs. Limber pine apparently absent by 10.7 thousand years ago, while juniper continued to persist well below present limits. Woodland species absent by 8.3 thousand years ago. Creosote bush and other modern Mojave Desert species began to appear by 5.4 thousand years ago, and were abundant by 3.9 thousand years ago.	Changes in plant assemblages apparently reflect a trend toward increasing aridity from 10.7 to 5.4 thousand years ago.
Far western and southwestern Mojave Desert: Lucerne Valley (13), Lake Searles (23), Scodie Mountains (22)	Pollen, pack rat middens	Late Wisconsin to 7.8 thousand years ago	Woodland and steppe preceded desert scrub at low elevations during late Wisconsin and early Holocene (Leopold, 1967; Wells and Berger, 1967; Van Devender and Spaulding, 1979). Pinyon-juniper woodland present in Lucerne Valley until at least 11.8 thousand years ago, while juniper persisted below its modern limits until 7.8 thousand years ago. Creosote bush and other modern desert scrub species established by 5.9 thousand years ago.	Late Wisconsin colder than modern conditions; warming and aridification began after 11.8 thousand years ago and reached modern conditions between 7.8 and 5.9 thousand years ago.

Table 5-12. Summary of palynological and pack rat midden data from the Great Basin, Mojave Desert, and Sierra Nevada with inferred climatic changes (page 8 of 8)

Location[a]	Evidence	Age	Vegetational assemblage	Inferred climatic conditions
		SIERRA NEVADA		
Sierra Nevada: Osgood Swamp (18), Clear Lake (29), Balsam Meadows (2)	Pollen	Late Wisconsin	Sierran montane forests restricted in distribution; replaced in modern time by sagebrush and other steppe species in association with scattered pines and perhaps junipers (Adam, 1967; Davis et al., 1985).	Climate passed from glacial conditions into warmer postglacial conditions about 10,000 years ago and cooling within the last 2,900 years (Adam, 1967).
		10.5 thousand years ago to present	Steppe replaced by forest by 10.5 to 9.5 thousand years ago at Osgood Swamp and Swamp Lake, while it may have persisted as late as 7.0 thousand years ago at Balsam Meadows (Davis et al., 1985). Pine forests were more widespread than today in the Sierra Nevada from 7.0 to 3.0 thousand years ago (Davis et al., 1985).	Dry from 10 to 7 thousand years ago and cool and moister from 3,000 years ago to present (Davis et al., 1985).
Kings Canyon (12)	Pack rat middens	45 to 12.5 thousand years ago	Modern oak and chaparral vegetation preceded by more xerophytic and cold-adapted species, including single-needle pinyon pine (*Pinus monophylla*), western juniper, and ponderosa pine (*Pinus ponderosa*) (Cole, 1983).	Pleistocene conditions in southern Sierra Nevada were colder and drier than today. Precipitation during the late Wisconsin not much greater than at present (Cole, 1983).

[a]Numbers in parentheses following location names correspond to those on Figure 5-24.

Table 5-13 is a compilation of vegetative cover and inferred climatic conditions in the Yucca Mountain area over the past 45,000 yr. It illustrates a correlation between variation of species with elevation over time and variation in temperature and precipitation.

The climatic inferences presented in Table 5-13 are slightly different from those discussed in Table 5-12 for some of the site locations. These differences are due to slightly different interpretations by the various workers. As more data are collected during site characterization, these differences are expected to be reduced.

Summary of paleovegetation changes

During the Wisconsin glacial period, greater than 40,000 to 11,000 yr ago, sagebrush steppe ranged over larger elevation and area than today in the Great Basin. It expanded into the Sierra Nevada and Wasatch mountains and descended southward into the modern Mojave Desert. Shadscale and other xerophytic steppe plants were common in this regime, particularly in the Mojave region. The modern Sierran forests, Great Basin pinyon-juniper woodlands, and southwestern ponderosa pine forests were absent or restricted

Table 5-13. Vegetative cover and inferred climatic regime of the Yucca Mountain region[a]

Yr B.P.[b]	Vegetation: Lower elevations (790-1200 m[c])	Vegetation: Intermediate elevations (1200-1800 m)	Vegetation: Higher elevations (1800-2100 m)	Temperature (°) (compared to modern): Winter	Temperature: Summer	Temperature: Annual	Precipitation (% change from modern): Winter	Precipitation: Summer	Precipitation: Annual	Remarks
5.000	Modern desert scrub	Modern desert scrub	Woodland	--[d]	--	--	--	--	--	Minor fluctuations.
10,000	Amargosa: Utah agave, juniper creosote	Desert scrub expansion	Woodland dominated by juniper, pinyon pine, prickly pear	-1 to -2	+1 to +2	0	0	+50	+10 to +20	Trend toward drier conditions and increasing temperatures.
18,000	Specter Range: pinyon-juniper woodland	Sheep Range: transition to subalpine-conifer woodland	Sheep Range: subalpine conifer woodland	-6	-7 to -8	-6 to -7	+60 to +70	-40 to -50	+30 to +40	Global glacial maximum at 18,000 ± 3,000 yr B.P.
30,000	Specter Range: open juniper-shad scale woodland	Sheep Range: Utah juniper	Sheep Range: juniper woodland with prickly pear, sage, mountain mahogany	--	--	-3 to -6	--	--	+10 to +25	
37,800	No record	No record	Eleana Range: subalpine conifer woodland	--	--	-5	--	--	+20	Cooling trend.
38,700	No record	No record	Increase in juniper decline of steppe shrubs	--	--	-1 to -2	+25 to +50	-40	+10 to +20	
45,000	No record	Sheep Range: juniper woodland	Eleana Range: open juniper woodland	-2 to -3	--	-1 to -3	+20	-60	0	Seasonality of rainfall different, but annual [illegible] the same.

[a]Spaulding (1983) and Spaulding et al. (1984).
[b]B.P. = before present.
[c]m = meter(s).
[d]-- No data.

DECEMBER 1988

Paleoclimatic applications of paleobotanical data

The interpretation of palynological and pack rat midden records in climatic terms requires information on the modern relationships between vegetation and climate. Given such relationships, under certain assumptions it is possible to infer the nature of the climatic variations responsible for the vegetation changes recorded by the fossil evidence. The general assumption underlying the drawing of these inferences is "that past temporal changes in the abundances of a set of pollen types reflect climatic changes equivalent to those responsible for spatial variation in the abundances of the same taxa on the contemporary landscape" (Howe and Webb, 1983). This general assumption can be expanded to more-specific ecological and statistical assumptions.

The specific ecological assumptions are as follows (Bartlein et al., 1984):

1. The modern vegetation data are in equilibrium with the modern climate at the temporal and spatial scales of interest. Given this assumption, the modern vegetation will adequately reflect the modern climate.

2. The variations in the paleoecological record being interpreted are ultimately attributable to climatic variations.

It is not possible to test either assumption in practice, but by proper selection of the temporal and spatial scales of interest, violations of the assumptions can be minimized (Prentice, 1983). The scales of interest for the Yucca Mountain repository will imply an assumption that the modern vegetation-climate relationships can be extrapolated back through Quaternary time over the Great Basin.

The specific statistical assumptions are (1) the statistical model used is specified correctly and (2) the parameters of that model are estimated in an appropriate fashion.

Two data bases are thus required for paleoclimatic reconstruction: (1) a data base of modern combined vegetation and climatic data and (2) a data base of fossil vegetation data. The first data base is used to construct baseline relationships between vegetation and climate to determine, for example, the environmental requirements of individual taxa. The relationships are then applied to the fossil data, either to interpret them in climatic terms, or to permit comparison of the observed fossil record with that simulated by differing paleoclimatic scenarios.

Relationships between modern vegetation and climate are also required for the paleobotanic validation of climate simulation models (Webb, 1980). To judge the ability of a model to correctly simulate the past climate, modern vegetation-climate relationships are used to transform model simulations of past climates into estimates of past vegetation, which can then be compared with the observed fossil record (Webb, 1980). The collection and the both climatic reconstruction and the validation of climate models that may be applied for predicting future climates.

It is possible to construct relationships between modern climate and vegetation in both a qualitative and a quantitative fashion. The following sections discuss these two methods. Both methods rest on the two basic ecological assumptions listed previously.

Qualitative relationships. Thus far, paleoclimatic estimates from vege-

The transfer function approach usually makes use of a multiple regression analysis to construct a relationship between a particular climate variable and a number of predictor variables--generally, the percentages of individual pollen types (Webb, 1980; Bartlein et al., 1984). In practice, a data set of paired observations of modern surface pollen samples and climate is required for calibration of the multiple regression equation. The resulting equation is then applied to fossil pollen data to interpret them in climatic terms.

Several statistical assumptions (in addition to the basic assumptions described earlier) underlie the application of regression analysis; these are described by Howe and Webb (1983) and Bartlein and Webb (1985). Comparisons among some of the different approaches to constructing the statistical relationships have been described by Kay and Andrews (1983). Strategies for identifying and minimizing the sources of uncertainty in the paleoclimatic estimates are given in Bartlein et al. (1984) and Bartlein and Webb (1985). Bartlein and Webb (1985) show how to determine the applicability of the methods in time and space.

In the response function approach, the relative abundance or probability

suggested that lake-level reconstructions provide evidence for increased rainfall with a more moderate decrease in mean annual temperatures. Benson (1981) modeled the lake budget for Pleistocene Lake Lahontan in western Nevada and concluded that a reduction in mean annual temperature, coupled with an increase in sky cover, were needed to create and maintain these lakes. Smith and Street-Perrott (1983) calculated streamflow volumes that would offset the estimated evaporation from the maximum cumulative areas of late-Pleistocene lakes in the Owens River system (1,863 km^2), and found inflow volumes to be in the range of 4.9 to 3.4 times present volumes, depending on whether a 5 or 10 Celsius degree lowering of temperatures was assumed. Van Devender and Spaulding (1979) interpreted pack rat midden data as reflecting late-Wisconsin climates characterized by increased precipitation, cool summers, and mild winters. Spaulding (1985) presents evidence that the pack rat midden data from southern Nevada indicates temperatures about 7 Celsius degrees below modern mean annual temperature and more abundant winter rainfall. Wells (1979) interpreted pack rat midden from the late Wisconsin as reflecting increased summer rainfall, with little reduction in mean annual temperature.

Opinions on Holocene climates are equally diverse. Antevs (1948), largely on the basis of studies in the northern Great Basin, argued that the middle Holocene was characterized by hot and dry conditions across the entire western United States. Martin (1963) hypothesized that this was instead a period of enhanced monsoonal summer precipitation throughout much of the can be expected in the future. For example, the repeated fluctuations between glacial and interglacial climates during the Quaternary appear to have occurred mainly in response to changes in the seasonal and latitudinal receipt of solar radiation, as determined primarily by variations of the earth's orbital elements (Hays et al., 1976). Since the orbital variations will continue in the future, it is likely that the present interglacial climate will eventually give way to another glacial one.

Deciding whether such variations can significantly affect a repository

The state of the climate system at any given time can be described by a large and varied set of climate variables that are observed over temporal scales ranging from 10 yr (in the case of annual values of standard meteorological variables) to 10 million years (the position of the continents), and over spatial scales from local to global. Individual variables can be classified (Saltzman, 1985) as those that describe (1) the boundary conditions or external controls; (2) the slowly varying components, such as the ice sheets and deep oceans; and (3) the fast-response components, such as the atmosphere.

Boundary conditions include those variables that influence the climate system, but in turn are not influenced by it (Imbrie, 1985). The boundary conditions thus include the incoming solar radiation, the position and size of the continents, and inputs of dust and aerosols from volcanic eruptions, and the inputs of dust and carbon dioxide from human activities.

Depending on the particular temporal and spatial scale of the climatic variation under consideration, additional components of the climate system can be added to the list of boundary conditions. At the scale of 10,000 to 1 million years, the size (volume, area, and elevation) of the ice sheets and the temperature of the oceans are internal variables of the climate system that respond to the orbital variations. At shorter time scales (i.e., shorter than 10,000 yr), the ice sheets and ocean may be regarded as external controls because their response times are 10,000 yr or longer. At short time scales, the preindustrial concentration of carbon dioxide in the atmosphere

(3) resonant interactions that are a combination of the two. Climatic variations thus have two ultimate sources: the external controls of the climate system (or boundary conditions) and the climate system itself.

The specific response of the climate system to changes in its external controls (forced variations) depends on both the nature of the variations in the controls and the state of the climate system itself (Imbrie, 1985). For example, a constant change in solar radiation inputs will likely produce different responses depending on the presence or absence of continental ice sheets (Kutzbach and Guetter, 1984).

Free variations of the climate system can arise from the existence of many pathways for the flow of mass and energy within the climate system, and hence from the existence of many feedback mechanisms. It is not unlikely that significant variations in global climate could be generated by such feedback even under fixed boundary conditions. For example, Saltzman and Sutera (1984) described a climate model that considers the continental ice mass, the marine ice mass, and temperature of the ocean. With no external forcing, the model generated a variation of the ice and ocean with many characteristics of the geologic record, for instance, a dominant period of variation of about 100,000 yr. Such free oscillations of the climate system have been obtained using a number of different climate models (Saltzman, 1985). However, the phase relationships between the continental ice mass and ocean temperature in the model were not consistent with those observable in the real climate system. When the model was forced with realistic variations of solar radiation (such as those produced by the orbital variations), the correct relationships among the variables were obtained (Saltzman et al., 1984). This latter result provides an example of climatic variations produced by resonant interactions between forced and free variations of the climate system represented by the model.

The existence of temporal and spatial hierarchies in both the components of the climate system and also the sources of the climatic variations makes it difficult to assign past climatic change at a particular location to a specific ultimate cause, and consequently difficult to predict future changes. For example, variations of the fast-response components may be generated by variations of the slowly varying components (and by internal variations), and in turn, variations of the slowly varying components may be generated by variations of the boundary conditions (and by internal variations).

Similarly, local climate variations of the kind, for example, that make one winter different from the last, are embedded in hemispheric-scale circulation anomalies (Namias, 1975). Moreover, local variations are indeterminate with respect to larger scale variations. The climate of a particular location has two components: (1) a locational component, governed mainly by the latitude of the place and its position on the continent, which determines the mean values of temperature and precipitation and (2) an advective component, governed by the location of the place relative to the traveling weather systems, which determines the day-to-day variations of the weather. Thus, a variety of atmospheric circulation patterns could be envisaged that would lead to the same local climate variations.

Each level of the temporal and spatial hierarchy contributes additional uncertainty about the ultimate causes of past climate variations at a particular place, and the likely consequences of future variations in the controls, 100,000 yr is not well known. Past estimates of volcanic loadings might be made stochastically, based on past summaries of volcanic-loading estimates such as those given by Hirschboeck (1980). The prediction of future loadings from natural (e.g., volcanos, wind erosion) and human-induced (desertification) sources is not likely to be easily implemented. Similarly, the source of past variations of the concentration of carbon dioxide in the atmosphere is not clear at present (Shackleton et al., 1983), and so this variable too may be inherently unpredictable, although it is clear that the concentration of carbon dioxide due to human activities will continue to increase at least into the next century.

While the specific course of future variations of climatic variables may not be predictable, the range of their past variations as deduced from the paleoclimatic record can serve to limit the range of variations expectable in the future.

5.2.2.3.2 Prediction of slowly varying components

The prediction of the slowly varying components of the climate system, such as the global volume of glacial ice and deep ocean temperature, will require the application of models from the statistical-dynamical family of climate models. Saltzman (1985) recognizes two groups of models of the slowly varying components: (1) a quasi-deductive group of models that derives models of, for example, the ice sheets from basic physical principles and (2) an inductive group of models that derives models consistent with observed paleoclimatic records that are required to be only physically reasonable. In other words, the first group proceeds from physical principles to a model of observed paleoclimatic variations, while the second starts with the geologic record and derives a physically reasonable model based on it. The distinction between the two groups arises from the inability of

Estimates of ice sheet geometry can be produced with numerical computer models based upon a solution of the two-dimensional, time varying, ice flow law. Examples of such models are now in existence. One has been applied to the reconstruction of the dynamics of the Laurentide ice sheet for the last 100,000 yr (Budd and Smith, 1981) and was based on orbitally induced variations of insolation over the ice sheet. Other reconstructions of continen-

An important element of general circulation models in need of further development is the manner in which the oceans are treated. In most paleoclimatic applications, ocean surface temperatures were prescribed, fixed at the CLIMAP Project Members (1981) values for 18,000 yr ago, for example. In Manabe and Broccoli (1985) a mixed-layer ocean was used, but such a model basis, and lack of explicit physics, may limit the usefulness of the statistical models when extrapolation is required, as it is for both paleoclimatic simulations or future climate predictions.

The second model-based approach for the spatial disaggregation of general circulation model simulations makes use of mesoscale meteorological models (Anthes, 1983). Mesoscale meteorological models like general circulation models attempt to explicitly represent the physical processes that govern atmospheric circulation and the surface energy and hydrologic balances. The spatial resolution of regional mesoscale models is generally much finer than that of general circulation models and the representation of the surface energy and hydrologic balances is usually more detailed, as is the representation of topography. In practice, mesoscale meteorological models could be used to spatially disaggregate the output of a general circulation model. This could be accomplished by using the general circulation models output to initialize the mesoscale meteorological model, in much the same way that widely distributed meteorological observations are used to initialize standard numerical weather prediction models. The greater topographic detail, and more realistic representation of the surface processes in the mesoscale meteorological models, permit the simulation of regional and local-scale snapshots of climate variables consistent with the larger-scale patterns of those variables simulated by a general circulation model. One limitation of mesoscale meteorological models, however, is that they use the broadly defined boundary conditions of the general circulation model. If there are assumptions and approximations made in developing these boundary conditions, these assumptions are transferred to the mesoscale meteorological models.

Like general circulation models, mesoscale meteorological models require considerable computing resources. This disadvantage is somewhat outweighed, however, by the physical basis of the models, which should make them more robust than the empirically based models when applied in the context of either paleoclimatic reconstruction or climatic prediction.

In making a choice between using a general circulation model-mesoscale meteorological model approach versus an empirically based approach, these factors as well as others (e.g., amount of data available and requirements made by the hydrologic investigators) need to be considered. This consideration is discussed briefly in Section 8.3.1.5.1 and will be a continuing process throughout site characterization.

5.2.2.3.5 Model validation

An important step in the overall modeling effort will be to measure the performance of the model in order to estimate the uncertainties inherent in the eventual climate predictions. The standard criterion used is how well a model simulates the modern climate. While such measures are useful, the danger always exists that a model may be tuned to perform well with respect to the modern climate.

In the hierarchy of climate simulation methods just described, there are two important sources of uncertainty. The first arises in the simulation, on the basis of boundary conditions, of the slowly varying components, and in turn, simulations of the fast-response components of the climate system. The second source of uncertainty arises in the spatial disaggregation of the fast-response components. These uncertainties may be posed as two questions. As the boundary conditions and slowly varying components evolve through time, will the snapshots simulated by the models of the fast-response components adequately track the actual climate? At a specific time, will the spatial patterns of climate be adequately portrayed by the approach used to disaggregate the simulations of the fast-response components? The paleoclimatic record, containing as it does the output of the ideal climate model, can provide the answers to these questions.

Two model validation exercises can be envisaged, one involving long time series of paleoclimatic data at key locations, and the second using dense networks of data at key times. The first exercise would test the ability of the model to track the actual climate as the boundary conditions and slowly varying components change over the next 100,000 yr. Ideally, continuous paleoclimatic records from key locations extending back to the previous interglacial would be used in this exercise. The second exercise would test the ability of the model to simulate correctly the spatial patterns of climatic variations at an appropriate scale. For this exercise, paleoclimatic evidence will be collected to describe spatial patterns of climatic variations at such key times as the full-glacial, late-glacial, early Holocene, etc. For both exercises, methods such as those described in Section 5.2.1.2.2 would be used to transform the model output into simulations of the various paleoclimatic indicators that would then be compared with the observed fossil record. Plans for investigations to develop and validate climate models to satisfy the needs just discussed are specified in Section 8.3.1.5.1.

The individual elements of this procedure for predicting future climates follow the hierarchical nature of climatic variations in a particular region--from global-scale variations of boundary conditions and the slowly varying components of the climate system, to regional-scale variations of the fast-response components. While individual climate simulation models applicable to this approach exist, no comprehensive attempt at predicting future climatic variations has yet been made. For this reason, model validation experiments must be carried out to judge the reliability of the predictions. In addition to providing insight into the nature and extent of past climatic variations, the paleoclimatic record provides the information required for the climate model validation exercises. The use of paleoclimatic data for these purposes involves three broad tasks:

1. A data collection task in which the necessary paleoclimatic data, both geologic and biologic, are collected over appropriate networks where possible (i.e., long records at key locations and dense networks at key times).

2. A modeling task in which relationships are developed to link the various climatic indicators to their climatic controls (e.g., lake hydrologic models (Benson, 1986) and modern vegetation-climate relationships (Bartlein et al., 1986)).

3. An interpretation task in which (1) the geologic or paleoecologic record is interpreted in climatic terms, (2) the nature of past climatic variations is inferred, and (3) the observed paleoclimatic record is compared with that generated by climate-simulation models.

Successful completion of these three tasks is required to document the range of climate variations experienced in the past, to simulate probable future variations, and to provide input for estimating the impact of the effect of those variations on the surface and ground-water systems in the vicinity of Yucca Mountain.

5.2.3 SITE PALEOCLIMATIC INVESTIGATIONS

Historical and prehistorical climatic, limnologic, hydrologic, and vegetational data obtained from near Yucca Mountain and the surrounding region will be used to increase and supplement the paleoclimatic data base used for characterization of the Yucca Mountain site. Detailed plans designed to obtain these data are presented in Section 8.3.1.5.1 for the following activities.

5.2.3.1 Synoptic characterization of regional climate

Historical meteorological data from the Great Basin will be compiled and summarized to provide synoptic-scale information. These data will be used in calibration activities for vegetation-climate and lake-climate models, as well as in the development of a regional climate model. Information on the stable isotope "signatures" from dated ground water and from modern precipitation networks will be obtained from the geohydrology (Section 8.3.1.2) and sedimentolgical changes recorded in these cores will provide dated time series of (1) changes in size, chemistry, and productivity of lakes and (2) wet phases in now-dry playas and marshes.

5.2.3.4 Development, validation, and application of a generalized model of late-Quaternary climatic variations to predict future climate change at the Yucca Mountain site

A generalized model of late-Quaternary climatic variations in the southern Great Basin will be developed, upon which estimates of the range of future climatic conditions can be based. This generalized model has two elements: (1) the reconstruction of past climatic variations to illustrate the range of potential regional climatic variations and (2) the development of climate simulation models to estimate the response of the regional climate to future changes in the boundary conditions. Reconstruction of past climatic variations will be based on the paleoecological record (pollen and plant macrofossil), supplemented by paleohydrologic, sedimentologic, and geomorphic or February. Precipitation is also generated in the area by summer thunderstorm activity, representing a secondary monthly average peak in July or August. Despite the existence of this well-defined annual cycle, precipitation averages only about 150 mm/yr. Winds from the north dominate during fall, winter, and into early spring, but shift to predominately south to southwesterly in late spring and early summer. Terrain influences somewhat disrupt this annual average cycle, with upgradient winds occurring during daylight hours in almost all months.

Meteorological data are also needed as input to infiltration studies and rainfall-runoff modeling. The existing data set is not site specific enough for these investigations, and does not provide detailed information on precipitation intensity, temporal, or areal variability that is necessary for hydrologic investigations (see Chapter 3 and Section 8.3.1.2 for more on hydrologic studies). Therefore, a site monitoring program that will provide [illegible] portion of the Great Basin. Moreover, the relationship between increased [redacted] data for the region during the past 50 yr are of fair quality and are probably sufficient for modeling applications. Lake-level and vegetational time-series data exist for a limited number of sites in the northern and western parts of the region for approximately the past 20,000 yr, but they are insufficient in the southern Great Basin, particularly in the vicinity of Yucca Mountain. Vegetational, hydrologic, and geologic time-series data are poor to inadequate for times before 20,000 yr ago; the acquisition of this older time-series data will be necessary for future climate modeling efforts.

climatic variations (Tables 8.3.1.5-3, 8.3.1.5-4). A second empirical approach to climate modeling also will be used. Empirical modeling will be done on a regional scale (Southern Great Basin), and it will involve an evaluation of alternative hypotheses regarding the nature of Quaternary paleoclimate variations (Table 8.3.1.5-5). The paleoclimate variations will be used to extrapolate future climatic trends, and they will also provide a data base for validating the regional numerical model simulations.

Underlying these planned and ongoing studies and, indeed, all paleoclimatic studies in southern Nevada generally and at the Yucca Mountain site specifically, is the need for integrating results and interpretations to produce a coherent picture of paleoenvironmental change. The interpretive, integrative, and data gathering processes must all equally progress in time because the insights gained by this effort will direct future research most efficiently.

5.3.4 RELATION TO REGULATORY GUIDE 4.17

A comparison of the information in Chapter 5 with Regulatory Guide 4.17 (NRC, 1987) shows that none of the information required by the guide has been omitted from Chapter 5, but the chapter does include additional information as follows:

1. An introduction that discusses the general information included in the chapter.

2. A summary (Section 5.3) that provides a link between the data presented in the chapter and the plans described in Chapter 8.

DOE/RW-0199

Nuclear Waste Policy Act
(Section 113)

Site Characterization Plan

Yucca Mountain Site, Nevada Research and Development Area, Nevada

Volume II, Part A

Chapter 5 References

December 1988

U. S. Department of Energy
Office of Civilian Radioactive Waste Management

REFERENCES FOR CHAPTER 5

Adam, D. P., 1967. "Late-Pleistocene and Recent Palynology in the Central Sierra Nevada, California," Quaternary Paleoecology, E. J. Cushing and H. E. Wright, Jr. (eds.), Yale University Press, New Haven, Conn., pp. 275-301.

Antevs, E., 1948. "Climatic Changes and Pre-White Man," The Great Basin, with Emphasis on Glacial and Postglacial Times, Bulletin of the University of Utah, Vol. 38, No. 20, pp. 168-191.

Anthes, R. A., 1983. "Regional Models of the Atmosphere in Middle Latitudes," Monthly Weather Review, Vol. 111, pp. 1306-1335.

Arnow, T., 1984. Water-Level and Water Quality Changes in Great Salt Lake, Utah, 1847-1983, Geological Survey Circular 913, Alexandria, Va.

Atwater, B. F., D. P. Adam, J. P. Bradbury, R. M. Forester, R. K. Mark, W. R. Lettis, G. R. Fischer, K. W. Gobalet, and S. W. Robinson, 1986. "A Fan Dam for Tulare Lake, California, and Implications for the Wisconsin Glacial History of the Sierra Nevada," Geological Society of America Bulletin, Vol. 97, pp. 97-109.

Bartlein, P. J., 1982. "Streamflow Anomaly Patterns in the U.S.A. and Southern Canada - 1951 - 1970," Journal of Hydrology, Vol. 57, Elsevier Scientific Publishing Co., Amsterdam, pp. 49-63.

Bartlein, P. J., and T. Webb, III, 1985. "Mean July Temperature at 6,000 Yr B.P. in Eastern North America: Regression Equations for Estimates from Fossil-Pollen Data," Climatic Change in Canada 5: Critical Periods in the Quaternary Climatic History of Northern North America, C. R. Harington (ed.), pp. 301-342.

Bartlein, P. J., T. Webb, III, and E. Fleri, 1984. "Holocene Climatic Change in the Northern Midwest: Pollen-Derived Estimates," Quaternary Research, Vol. 22, pp. 361-374.

Bartlein, P. J., I. C. Prentice, T. Webb, III, 1986. "Climatic Response Surfaces from Pollen Data for Some Eastern North American Taxa," Journal of Biogeography, Vol. 13, pp. 35-57.

Benson, L. V., 1978. "Fluctuation in the Level of Pluvial Lake Lahontan during the Last 40,000 Years," Quaternary Research, Vol. 9, pp. 300-318.

Benson, L. V., 1981. "Paleoclimatic Significance of Lake-Level Fluctuations in the Lahontan Basin," Quarternary Research, Vol. 16, pp. 390-403.

Benson, L. V., 1986. The Sensitivity of Evaporation Rate to Climate Change--Results of an Energy-Balance Approach, USGS-WRI-86-4148, Water-Resources Investigations Report, U.S. Geological Survey.

Benson, L. V., and P. W. McKinley, 1985. Chemical Composition of Ground Water in the Yucca Mountain Area, Nevada, 1971-84, USGS-OFR-85-484, Open-File Report, U.S. Geological Survey.

Benson, L. V., and M. D. Mifflin, 1986. Reconnaissance Bathymetry of Basins Occupied by Pleistocene Lake Lahontan, Nevada and California, USGS-WRI-85-4262, Water-Resources Investigations Report, U.S. Geological Survey.

Benson, L. V., and R. S. Thompson, 1987. The Physical Record of Lakes in the Great Basin, North America and Adjacent Oceans during the Last Deglaciation, W. F. Ruddiman and H. E. Wright, Jr. (eds.), Vol. K-3, Chapter 11, Geological Society of America, Boulder, Colo., pp. 241-260.

Benson, L. V., J. H. Robison, R. K. Blankennagel, and A. E. Ogard, 1983. Chemical Composition of Ground Water and the Locations of Permeable Zones in the Yucca Mountain Area, Nevada, USGS-OFR-83-854, Open-File Report, U.S. Geological Survey.

Bischoff, J. L., R. J. Rosenbauer, and G. I. Smith, 1985. "Uranium-Series Dating of Sediments from Searles Lake: Differences Between Continental and Marine Climate Records," Science, Vol. 227, pp. 1222-1224.

Blackwelder, E., 1931. "Pleistocene Glaciation in the Sierra Nevada and Basin Ranges," Bulletin of the Geological Society of America, Vol. 42, pp. 865-922.

Blaney, H. F., 1957. "Evaporation Study at Silver Lake in the Mojave Desert, California," Transactions, American Geophysical Union, Vol. 38, No. 2, pp. 209-215.

Bloom, A. L., 1983. "Sea Level and Coastal Morphology of the United States Through the Late Wisconsin Glacial Maximum," Late-Quaternary Environments of the United States, Volume 1, The Late Pleistocene, S. C. Porter (ed.), Chapter 11, University of Minnesota Press, Minneapolis, pp. 215-229.

Born, S. M., 1972. Late Quaternary History, Deltaic Sedimentation, and Mudlump Formation at Pyramid Lake, Nevada, Center for Water Resources Research, Desert Research Institute, University of Nevada System.

Bowen, J. L., and R. T. Egami, 1983. Atmospheric Overview for the Nevada Nuclear Waste Storage Investigations, Nevada Test Site, Nye County, Nevada, NVO-269, Nevada Operations Office, U.S. Department of Energy, Las Vegas, Nev.

Brakenridge, G. R., 1978. "Evidence for a Cold, Dry Full-Glacial Climate in the American Southwest," Quaternary Research, Vol. 9, pp. 22-40.

Broecker, W. S., and A. Kaufman, 1965. "Radiocarbon Chronology of Lake

Brubaker, L. B., and E. R. Cook, 1983. "Tree-Ring Studies of Holocene Environments," Late Quaternary Environments of the United States, Volume II, The Holocene, H. E. Wright, Jr. (ed.), University of Minnesota Press, Minneapolis, pp. 222-235.

Currey, D. R., and C. G. Oviatt, 1985. "Durations, Average Rates, and Probable Causes of Lake Bonneville Expansions, Stillstands, and Contractions during the Last Deep-Lake Cycle, 32,000 to 10,000 Years Ago," Problems of and Prospects for Predicting Great Salt Lake Levels, P. A. Kay and H. F. Diaz (eds.), Center for Public Affairs and Administration, University of Utah.

DOC (U.S. Department of Commerce), 1986. Monthly and Annual Wind Distribution by Pasquill Stability Classes, Star Program, 6 Classes, Job No. 01775, National Climatic Data Center, Federal Building, Asheville, N.C.

Davis, J. O., R. Elston, and G. Townsend, 1976. "Coastal Geomorphology of the South Shore of Lake Tahoe: Suggestion of an Altithermal Lowstand," Holocene Environmental Change in the Great Basin, R. Elston (ed.), Nevada Archeological Survey Research Paper No. 6, pp. 41-65.

Davis, O. K., R. S. Anderson, P. L. Fall, M. K. O'Rourke, and R. S. Thompson, 1985. "Palynological Evidence for Early Holocene Aridity in the Southern Sierra Nevada, California," Quaternary Research, Vol. 24, pp. 322-332.

Denton, G. H., and T. J. Hughes, 1981. The Last Great Ice Sheets, J. Wiley & Sons, New York, 484 p.

Dohrenwend, J. C., 1984. "Nivation Landforms in the Western Great Basin and Their Paleoclimatic Significance," Quaternary Research, Vol. 22, pp. 275-288.

Dorn, R. I., M. J. DeNiro, and H. O. Aije, 1987. "Isotopic Evidence for Climatic Influence on Alluvial-Fan Development in Death Valley, California," Geology, Vol. 15, pp. 108-110.

EPA (U.S. Environmental Protection Agency), 1980. Ambient Monitoring Guidelines for Prevention of Significant Deterioration (PSD), EPA-450/4-80-012, Office of Air Quality Planning and Standards, Research Triangle Park, N.C.

Eardley, A. J., V. Gvosdetsky, and R. E. Marsell, 1957. "Hydrology of Lake Bonneville and Sediments and Soils of Its Basin," Bulletin of the Geological Society of America, Vol. 68, pp. 1141-1201.

Eglinton, T. W., and R. J. Dreiger, 1984. Meteorological Design Parameters

Gale, H. S., 1914. "Salines in the Owens, Searles, and Panamint Basins, Southeastern California," Contributions to Economic Geology, Part I.--Metals and Nonmetals Except Fuels, Geological Survey Bulletin 580, U.S. Government Printing Office, Washington, D.C., pp. 251-323.

Galloway, R. W., 1970. "The Full-Glacial Climate in the Southwestern United States," Association of American Geographers Annual, Vol. 60, pp. 245-256.

Gates, W. L., 1976a. "Modeling the Ice-Age Climate," Science, Vol. 191, pp. 1138-1144.

Gates, W. L., 1976b. "The Numerical Simulation of Ice-Age Climate with a Global General Circulation Model," Journal of the Atmosperic Sciences, Vol. 33, pp. 1844-1873.

Gates, W. L., 1985. "Modeling as a Means of Studying the Climate System," Projecting the Climatic Effects of Increasing Carbon Dioxide, M. C. MacCracken, and F. M. Luther (eds.), DOE/ER-0237, U.S. Department of Energy, Washington, D.C., pp. 59-79.

Gilbert, G. K., 1890. "Lake Bonneville," U.S. Geological Survey Monograph 1, U.S. Geological Survey, Washington, D.C., 438 p.

Harding, S. T., 1965. Recent Variations in the Water Supply of the Western Great Basin, Archives Series Report No. 16, Water Resources Center Archives, University of California, Berkeley, pp. 99, 107, 145, 159.

Haynes, C. V., 1967. "Quaternary Geology of the Tule Springs Area, Clark County, Nevada," Pleistocene Studies in Southern Nevada, H. M. Wormington and D. Ellis (eds.), Nevada State Museum Anthropological Papers No. 13, Carson City, Nev., pp. 15-104.

Hays, J. D., J. Imbrie, and N. J. Shackleton, 1976. Variations in the Earth's Orbit: Pacemaker of the Ice Ages, Science, Vol. 194, No. 4270, pp. 1121-1132.

Hershfield, B. M., 1961. Rainfall Frequency Atlas of the United States for Durations from 30 Minutes to 24 Hours and Return Periods from 1 to 100 Years, U.S. Weather Bureau Technical Paper No. 40, Department of Commerce, Washington, D.C.

Hirschboeck, K. K., 1980. "A New Worldwide Chronology of Volcanic Eruptions," Palaeogeography, Palaeoclimatology, Palaeoecology, Vol. 29, pp. 223-241.

Hooke, R. L., 1972. "Geomorphic Evidence for Late-Wisconsin and Holocene Tectonic Deformation, Death Valley, California," Geological Society of America Bulletin, Vol. 83, No. 7, pp. 2073-2098.

Houghton, J. G., C. M. Sakamoto, and R. O. Gifford, 1975. Nevada's Weather and Climate, Nevada Bureau of Mines & Geology Special Publication Number 2, Mackay School of Mines, University of Nevada, Reno.

Howe, S., and T. Webb, III, 1983. "Calibrating Pollen Data in Climatic Terms: Improving the Methods," Quarternary Science Reviews, Vol. 2, pp. 17-51.

Hughes, T. J., G. H. Denton, B. G. Andersen, D. H. Schilling, J. L. Fastook, C. S. Lingle, 1981. "The Last Great Ice Sheets: A Global View," The Last Great Ice Sheets, G. H. Denton and T. J. Hughes (eds.), John Wiley & Sons, New York, pp. 263-317.

Hunt, C. B., and D. R. Mabey, 1966. Stratigraphy and Structure, Death Valley, California, General Geology of Death Valley, California, U.S. Geological Survey Professional Paper 494-A, U.S. Goverment Printing Office, Washington, D.C.

Huschke, R. E. (ed.), 1959. Glossary of Meteorology, American Meteorological Society, Boston, Mass., pp. 581-582.

Imbrie, J., 1985. "A Theoretical Framework for the Pleistocene Ice Ages," Journal of the Geological Society of London, Vol. 142, Northern Ireland, pp. 417-432.

Imbrie, J., and J. Z. Imbrie, 1980. "Modeling the Climatic Response to Orbital Variations," Science, Vol. 207, pp. 943-953.

Imbrie, J., A. McIntyre, and T. C. Moore, Jr., 1983. "The Ocean Around North America at the Last Glacial Maximum," Late Quaternary Environments of the United States, The Pleistocene, S. C. Porter (ed.), Vol. I, Chapter 12, University of Minnesota Press, Minneapolis, pp. 230-236.

Imbrie, J. H., J. D. Hays, D. G. Martinson, A. McIntyre, A. C. Mix, J. J. Morely, N. G. Pisias, W. L. Prell, and N. J. Shackleton, 1984. "The Orbital Theory of Pleistocene Climate: Support from a Revised Chronology of the Marine 18-0 Record," Milankovitch and Climates, Part 1, A. Berger, J. Imbrie, J. Hays, G. Kukla, and B. Saltzman (eds.), D. Reidel Publishing Co., Boston, Mass., pp. 269-305.

Kay, P. A., and J. T. Andrews, 1983. "Re-evaluation of Pollen-Climate Transfer Functions in Keewatin, Northern Canada," Annals, Association of American Geographers, Vol. 73, pp. 550-559.

Kutzbach, J. E., and P. J. Guetter, 1986. "The Influence of Changing Orbital Parameters and Surface Boundary Conditions on Climate Simulations for the Past 18,000 Years," Journal of the Atmospheric Sciences, Vol. 43, No. 16, pp. 1726-1759.

Kutzbach, J. E., and F. A. Street-Perrott, 1985. "Milankovitch Forcing of Fluctuations in the Level of Tropical Lakes from 18 to 0 kyr BP," Nature, Vol. 317, pp. 130-134.

Kutzbach, J. E., and H. E. Wright, Jr., 1985. "Simulation of the Climate of 18,000 Years BP: Results for the North American/North Atlantic/European Sector and Comparison with the Geologic Record of North America," Quaternary Science Reviews, Vol. 4, pp. 147-187.

Lajoie, K. R., 1963. Late Quaternary Stratigraphy and Geologic History of

Manabe, S., and A. J. Broccoli, 1985. "The Influence of Continental Ice Sheets on the Climate of an Ice Age," Journal of Geophysical Research, Vol. 90, No. D1, pp. 2167-2190.

Manabe, S., and D. G. Hahn, 1977. "Simulation of the Tropical Climate of an Ice Age," Journal of Geophysical Research, Vol. 82, No. 27, pp. 3889-3911.

Manabe, S., and R. T. Wetherald, 1985. "CO2 and Hydrology," Advances in Geophysics, Vol. 28A, pp. 131-157.

Martin, P. S., 1963. The Last 10,000 Years - A Fossil Pollen Record of the American Southwest, University of Arizona Press, Tucson, 87 p.

Mason, D. T., 1967. "Limnology of Mono Lake, California," University of [illegible]
Press, Berkeley, and Los Angeles, 110 p.

Maxey, G. B., and T. E. Eakin, 1949. Ground Water in White River Valley, White Pine, Nye, and Lincoln Counties, Nevada, Water Resources Bulletin No. 8, State of Nevada, Office of the State Engineer, Carson City.

Mayewski, P. A., G. H. Denton, and T. J. Hughes, 1981. "Late Wisconsin Ice Sheets of North America," The Last Great Ice Sheets, G. H. Denton and T. J. Hughes (ed.), Chapter 2, John Wiley & Sons, New York, pp. 132-158.

Meehl, G. A., 1984. "Modeling the Earth's Climate," Climatic Change, Vol. 6, pp. 259-286.

Mehringer, P. J., Jr., 1967. "Pollen Analysis of the Tule Springs Area, Nevada," Nevada State Museum Anthropological Papers, No. 13, pp. 130-200.

Mehringer, P. J., Jr., and C. W. Ferguson, 1969. "Pluvial Occurrence of Bristlecone Pine (Pinus Aristata) in a Mohave Desert Mountain Range," Journal of the Arizona Academy of Science, Vol. 5, No. 4, pp. 284-292.

Mehringer, P. J., Jr., and C. N. Warren, 1976. "Marsh, Dune and Archaeological Chronology, Ash Meadows, Amargosa Desert, Nevada," Holocene

Morrison, R. B., and J. C. Frye, 1965. Correlation of the Middle and Late Quaternary Successions of the Lake Lahontan, Lake Bonneville, Rocky Mountain (Wasatch Range), Southern Great Plains, and Eastern Midwest Areas, Nevada Bureau of Mines, Report No. 9, University of Nevada, Reno, 45 p.

Morton, F. I., 1986. "Practical Estimates of Lake Evaporation," Journal of Climate and Applied Meteorology, Vol. 25, pp. 371-387.

NRC (U.S. Nuclear Regulatory Commission), 1987. Standard Format and Content of Site Characterization Plans for High-Level-Waste Geological Repositories, Regulatory Guide 4.17, Washington, D.C.

Namias, J., 1975. "Remarks on the Potential for Long-Range Forecasting," pp. 242-251.

Nichols, W. D., 1986. Geohydrology of the Unsaturated Zone at the Burial Site for Low-Level Radioactive Waste Near Beatty, Nye County, Nevada, USGS-OFR-85-198, Open-File Report, U.S. Geological Survey.

Oerlemans, J., 1982. "Glacial Cycles and Ice-Sheet Modelling," Climatic Change, Vol. 4, pp. 353-374.

Russell, I. C., 1885. Geological History of Lake Lahontan, a Quaternary Lake of Northwestern Nevada, U.S. Geological Survey Monograph Volume XI, Government Printing Office, Washington, D.C.

SAIC (Science Applications International Corporation), 1985. Meteorological Monitoring Plan for the Nevada Nuclear Waste Storage Investigations Project, Yucca Mountain Site, DOE/NV/10270-5, Las Vegas, Nev.

Saltzman, B., 1985. "Paleoclimatic Modeling," Chapter 8, pp. 341-396.

Saltzman, B., and A. Sutera, 1984. "A Model of the Internal Feedback System Involved in Late Quaternary Climatic Variations," Journal of the Atmospheric Science, Vol. 41, No. 5, pp. 736-745.

Saltzman, B., A. R. Hansen, and K. A. Maasch, 1984. "The Late Quaternary Glaciations as the Response of a Three-Component Feedback System to Earth-Orbital Forcing," Journal of the Atmospheric Sciences, Vol. 41, No. 23, pp. 3380-3389.

Schlesinger, M. E., 1984. "Climate Model Simulations of C02-Induced Climatic Change," Advances in Geophysics, Vol. 26, pp. 141-235.

Schneider, S. H., and R. E. Dickinson, 1974. "Climate Modeling," Reviews of Geophysics and Space Physics, Vol. 12, No. 3, pp. 447-493.

Schumm, S. A., 1965. "Quaternary Paleohydrology," The Quaternary of the United States, H. E. Wright, Jr., and D. G. Frey (eds.), Princeton University Press, Princeton, New Jersey, pp. 783-794.

Scott, W. E., W. D. McCoy, R. R. Shroba, and M. Rubin, 1983. "Reinterpretation of the Exposed Record of the Last Two Cycles of Lake Bonneville, Western United States," Quaternary Research, Vol. 20, pp. 261-285.

Shackleton, N. J., M. A. Hall, J. Line, and C. Shuxi, 1983. "Carbon Isotope Data in Core V19-30 Confirm Reduced Carbon Dioxide Concentration in the Ice Age Atmosphere," Nature, Vol. 306, pp. 319-322.

Shackleton, N., J. Bachman, H. Zimmerman, D. Kent, M. Hall, D. Roberts, D. Schnitker, with others, 1984. "Oxygen Isotope Calibration of the Onset of Ice-Rafting and History of Glaciation in the North Atlantic Region," Nature, Vol. 307, pp. 620-623.

Sharp, R. P., 1938. "Pleistocene Glaciation in the Ruby-East Humboldt Range, Northeastern Nevada," Journal of Geomorphology, pp. 296-323.

Sheppard, R. A., and A. J. Gude, 3rd, 1968. Distribution and Genesis of Authigenic Silicate Minerals in Tuffs of Pleistocene Lake Tecopa, Inyo County, California, Geological Survey Professional Paper 579, U.S. Government Printing Office, Washington, D.C.

Smith, G. I., 1979. Subsurface Stratigraphy and Geochemistry of Late Quaternary Evaporites, Searles Lake, California, Geological Survey Professional Paper 1043, U.S. Geological Survey, 130 p.

Smith, G. I., and W. P. Pratt, 1957. Core Logs from Owens, China, Searles, and Panamint Basins, California, Geological Survey Bulletin 1045-A, U.S. Government Printing Office, Washington, D.C.

Smith, G. I., and F. A. Street-Perrott, 1983. "Pluvial Lakes of the Western United States," Late-Quaternary Environments of the United States, Volume I, The Late Pleistocene, S. C. Porter (ed.), University of Minnesota Press, Minneapolis, pp. 190-212.

Snyder, C. T., and W. B. Langbein, 1962. "The Pleistocene Lake in Spring Valley, Nevada, and Its Climatic Implications," Journal of Geophysical Resources, Vol. 67, No. 6, pp. 2385-2394.

Solomon, A. M., and T. Webb, III, 1985. "Computer-aided Reconstruction of Late-Quaternary Landscape Dynamics," Annual Review of Ecology Systematics, Vol. 16, pp. 63-84.

Spaulding, W. G., 1981. The Late Quaternary Vegetation of a Southern Nevada Mountain Range, Ph.D. dissertation, University of Arizona, Department of Geosciences, Tuscon, 271 p.

Spaulding, W. G., 1983. Vegetation and Climates of the Last 45,000 Years in the Vicinity of the Nevada Test Site, South-Central Nevada, USGS-OFR-83-535, Open-File Report, U.S. Geological Survey.

Spaulding, W. G., 1985. Vegetation and Climates of the Last 45,000 Years in the Nevada Test Site and Vicinity, U.S. Geological Survey Professional Paper 1329, U.S. Government Printing Office, Washington, D.C.

Spaulding, W. G., and L. J. Graumlich, 1986. "The Last Pluvial Climatic Episodes in the Deserts of Southwestern North America," Nature, Vol. 320, pp. 441-444.

Spaulding, W. G., E. B. Leopold, and T. R. Van Devender, 1983. "The Late Wisconsin Paleoecology of the American Southwest," Late-Quaternary Environments of the United States, Volume I, The Late Pleistocene, S. C.

Street-Perrott, F. A., and S. P. Harrison, 1984. "Temporal Variations in Lake Levels Since 30,000 Yr BP - An Index of the Global Hydrological Cycle," Geophysical Monograph, Vol. 29, pp. 118-129.

Stuiver, M., and G. I. Smith, 1979. "Radiocarbon Ages of Stratigraphic Units," Subsurface Stratigraphy and Geochemistry of Late Quaternary Evaporites, Searles Lake, California, G. I. Smith (ed.), Geological [illegible]

Van Devender, T. R., R. S. Thompson, and J. L. Betancourt, 1987. "Vegetation History of the Deserts of Southwestern North America: The Nature and Timing of the Late Wisconsin - Holocene Transition," North America and Adjacent Oceans during the Last Deglaciation, W. F. Ruddiman and H. E. Wright, Jr. (eds.), Geological Society of America, Boulder, Colo., pp. 1-56.

Von Neumann, J., 1960. "Some Remarks on the Problem of Forecasting Climatic Fluctuations," Dynamics of Climate, R. L. Pfeffer (ed.), Pergamon Press, New York, pp. 9-11.

Waitt, R. B., Jr., and R. M. Thorson, 1983. "The Cordilleran Ice Sheet in Washington, Idaho, and Montana," Late Quaternary Environments of the United States, Vol. I, Chapter 3, pp. 53-70.

Wallace, J. M., and P. V. Hobbs, 1977. Atmospheric Science: An Introductory Survey, Academic Press, New York, pp. 71-81.

Wang, W. -C., D. J. Wuebbles, W. M. Washington, R. G. Isaacs, and G. Molnar, 1986. "Trace Gases and Other Potential Perturbations to Global Climate," Reviews of Geophysics, Vol. 24, No. 1, pp. 110-140.

Wayne, W. J., 1984. "Glacial Chronology of the Ruby Mountains - East Humboldt Range, Nevada," Quaternary Research, Vol. 21, pp. 286-303.

Weast, R. C. (ed.), 1972. Handbook of Chemistry and Physics, 53rd Edition, The Chemical Rubber Co., Cleveland, Ohio, p. E-39.

Webb, T., III, 1980. "The Reconstruction of Climatic Sequences from Botanical Data," Journal of Interdisciplinary History, Vol. 4, pp. 749-772.

Webb, T., III, 1985. "Holocene Palynology and Climate," Paleoclimatic Analysis and Modeling, A. D. Hecht (ed.), John Wiley & Sons, New York, pp. 163-195.

Webb, T., III, and R. A. Bryson, 1972. "Late- and Postglacial Climatic Change in the Northern Midwest, USA: Quantitative Estimates Derived from Fossil Pollen Spectra by Multivariate Statistical Analysis," Quaternary Research, Vol. 2, pp. 70-115.

Webb, T., III, J. Kutzbach, and F. A. Street-Perrott, 1985. "20,000 Years of Global Climatic Change: Paleoclimatic Research Plan," pp. 182-218.

Wells, P. V., 1979. "An Equable Glaciopluvial in the West: Pleniglacial Evidence of Increased Precipitation on a Gradient from the Great Basin to the Sonoran and Chihuahuan Deserts," Quaternary Research, Vol. 12, pp. 311-325.

Wells, P. V., 1983. "Paleobiogeography of Montane Islands in the Great Basin Since the Last Glaciopluvial," Ecological Monographs, Vol. 53(4), pp. 341-382.

Wells, P. V., and R. Berger, 1967. "Late Pleistocene History of Coniferous Woodland in the Mohave Desert," Science, Vol. 155, pp. 1640-1647.

Wells, P. V., and C. D. Jorgensen, 1964. "Pleistocene Wood Rat Middens and Climatic Change in Mohave Desert: A Record of Junifer Woodlands," Science, Vol. 143, pp. 1171-1174.

Wells, S. G., L. D. McFadden, T. F. Bullard, B. F. Feilberg, R. L. Ford, J. P. Grimm, J. R. Miller, S. M. Orbock, J. D. Pickle, and J. C. Dohrenwend, 1984. "Late Quaternary Geomorphic History of the Silver Lake Area, Eastern Mojave Desert, California: An Example of the Influence of Climatic Change on Desert Piedmonts," pp. 122-136.

Wells, S. G., L. D. McFadden, and J. C. Dohrenwend, 1987. "Influence of Late Quaternary Climatic Changes on Geomorphic and Pedogenic Processes on a Desert Piedmont, Eastern Mojave Desert, California," Quaternary Research, Vol. 27, pp. 130-146.

Whitaker, G. L., 1971. "Changes in the Elevation of Great Salt Lake Caused by Man's Activities in the Drainage Basin," Geological Survey Research 1971, U.S. Geological Survey Professional Paper 750-D, U.S. Governmant Printing Office, Washington, D.C. pp. D187-D189.

Williams, J., R. G. Barry, and W. M. Washington, 1974. "Simulation of the Atmospheric Circulation Using the NCAR Global Circulation Model with Ice Age Boundary Conditions," Journal of Applied Meteorology, Vol. 13, No. 13, pp. 305-317.

CODES AND REGULATIONS

10 CFR Part 60 (Code of Federal Regulations), 1987. Title 10, "Energy," Part 60, "Disposal of High-Level Radioactive Wastes in Geologic Repositories," U.S. Government Printing Office, Washington, D.C., pp. 627-658.

10 CFR Part 960 (Code of Federal Regulations), 1987. Title 10, "Energy," Part 960, "General Guidelines for the Recommendation of Sites for Nuclear Waste Repositories," U.S. Government Printing Office, Washington, D.C., pp. 518-551.